Coordination Chemistry

Organometallic Chemistry

Edited by Hiroshi Nakazawa and Julian Koe

Organometallic Chemistry

Coordination Chemistry Fundamentals Series

Series editors:
Makoto Fujita, *The University of Tokyo, Japan*
Naohito Ishikawa, *Osaka University, Japan*
Osamu Ishitani, *Tokyo Institute of Technology, Japan*
Hideki Masuda, *Nagoya Institute of Technology, Japan and Aichi Institute of Technology, Japan*
Hiroshi Nakazawa, *Osaka City University, Japan*
Hiroki Oshio, *The University of Tsukuba, Japan*
Toshio Yamaguchi, *Fukuoka University, Japan*

Titles in the series:
1: Organometallic Chemistry

How to obtain future titles on publication:
A standing order plan is available for this series. A standing order will bring delivery of each new volume immediately on publication.

For further information please contact:
Book Sales Department, Royal Society of Chemistry, Thomas Graham House, Science Park, Milton Road, Cambridge, CB4 0WF, UK
Telephone: +44 (0)1223 420066, Fax: +44 (0)1223 420247
Email: booksales@rsc.org
Visit our website at www.rsc.org/books

Organometallic Chemistry

Edited by

Hiroshi Nakazawa
Osaka City University, Japan
Email: nakazawa@sci.osaka-cu.ac.jp

and

Julian Koe
International Christian University, Japan
Email: koe@icu.ac.jp

ROYAL SOCIETY OF CHEMISTRY

Preface

This book is intended for use by middle to final year chemistry students in undergraduate courses in organometallic chemistry. It is based on the book written in Japanese named "有機金属化学" (Yuki-kinzoku kagaku = Organometallic Chemistry), one of a series of works on coordination chemistry organized by the Japan Society of Coordination Chemistry. The Japanese language version of the book has been used as a textbook of organometallic chemistry in Japan since 2010 and has a good reputation. It has now been decided that the Royal Society of Chemistry will publish several books from this series in English, and this book is the first in the series.

The book consists of two sections; Section 1: Basics and Section 2: Advanced. The former covers fundamental aspects of organometallic chemistry, preparing readers for understanding the more advanced topics in the latter. Readers will thus grasp both the basics and the cutting edge of the field. In the basic part, the fundamental reaction patterns concerning bonds between transition metals and carbon atoms are described, including also how these are combined to establish effective catalytic cycles. To understand the basics and make use of the knowledge, it is most effective to solve problems, so the book contains a number of practice questions and gives appropriate answers to deepen the reader's understanding. In the advanced part, the chemistry concerning bonding between transition metals and main group elements other than C, such as M–Si, M–N, M–P, M–O and M–S covalent bonds is described and the origin of the differences to the M–C case is discussed. Since there are few textbooks that systematically describe the bonding between transition metals and main group elements other than C, this book is both unique and useful in this respect.

Chapters 1 to 7 of Section 1 and Chapter 13 (solutions to problems) were prepared by H. Nakazawa. In Section 2, the contributors were Chapter 8:

Author Biography

Yasuro Kawano was born in Sapporo city. He received his PhD degree in 1993 from Tohoku University. Since 1994, he has pursued his career as an assistant professor and an associate professor at the University of Tokyo. His research field is coordination chemistry, in particular, silicon–metal chemistry and boron–metal chemistry. At present, he works as a lecturer at several universities.

Julian Koe received his PhD from the University of Exeter in 1989 and subsequently carried out post-doctoral research as a JSPS fellow at Tohoku University, a Royal Society Return Fellow at Exeter, a Toshiba Fellow, a Research Associate at the University of Madison-Wisconsin and a Research Fellow at NTT Basic Research Labs, before taking up an academic position at International Christian University, Tokyo. He has been a full professor since 2010. His research interests are in organosilicon materials and the stereodynamics of transition metal complexes.

Hiroyuki Matsuzaka He received his PhD degree in 1988 from The University of Tokyo. After a postdoctoral research fellowship at The Pennsylvania State University, he became a research associate at The University of Tokyo in 1989. He moved to Tokyo Metropolitan University as an Associate Professor in 1995. Since 2001, he has been a full professor at Osaka Prefecture University. His research interests focus on organometallic chemistry and homogeneous catalysis, especially on the synthesis and reactivity of organometallic clusters.

Tsutomu Mizuta He received his PhD degree in 1991 from Hiroshima University. He joined Hiroshima University as an assistant professor and was promoted to an associate professor in 2002 and a full professor in 2011. His research field is coordination chemistry, organometallic chemistry, and nanocluster chemistry.

Hiroshi Nakazawa He received a PhD degree in 1981 from Hiroshima University. After postdoctoral research fellowships at the Tokyo Institute of Technology and the University of Utah, he became a research associate at Hiroshima University in 1984. He was promoted to full professor at Osaka City University in 2002. His research field is coordination chemistry, organometallic chemistry, and catalytic chemistry.

Masaaki Okazaki He received his PhD degree in 1997 from Tohoku University under the supervision of Prof. Hiroshi Ogino and was promoted

to a research associate. In, 2004, he moved to Kyoto University as an associate professor to work with prof. Fumiyuki Ozawa. In 2009, he was appointed to his current position as a full professor of Hirosaki University. His research interest is in the area of the synthesis, structure, and reactivity of oraganotransition metal complexes and clusters.

Kohtaro Osakada He graduated from Tokyo University in 1982. He was appointed as an assistant professor of Tokyo Institute of Technology, and then promoted to associate professor in 1989, and professor in 1999. He stayed at the University of North Carolina, Chapel Hill as a visiting fellow from 1995 to 1996. His research covers organometallic chemistry, polymer synthesis, and supramolecular chemistry.

Keiji Ueno He received his PhD degree in 1988 from Tohoku University. After graduation, he became an assistant professor at Tohoku University in 1988. From 1992 to 1993, he worked at Massachusetts Institute of Technology as an overseas research fellow of MEXT. He was promoted to a full professor at Gunma University in 2004. His research field is coordination chemistry, organometallic chemistry, and organoelement chemistry.

Prof. Ueno very sadly passed away soon after completing his chapter. He is greatly missed and will be remembered for his warmth and great contributions to chemistry. We all pray for his soul.

Contents

Section 2: Advanced

Chapter 8 Chemistry of Transition Metal Complexes with Group 14 Elements: Transition Metal Complexes with Silicon, a Heavier Carbon Group Element

Hiroshi Nakazawa

Chapter 9 Chemistry of Transition Metal Complexes with Group 13 Elements: Transition Metal Complexes with Lewis Acidic Ligands

Yasuro Kawano and Keiji Ueno

Chapter 13 Problem Solutions

Hiroshi Nakazawa

Appendix

Subject Index

Section 1: Basics

Chapter 1

What is Organometallic Chemistry

Hiroshi Nakazawa[a]

[a] Osaka City University Osaka, Japan
Email: nakazawa@sci.osaka-cu.ac.jp

1.1   Organic Chemistry and Inorganic Chemistry

The development of chemistry has been impressive and many of the recent exciting advances have occurred at the interface of the traditional fields, resulting in the blurring of the areas of organic and inorganic chemistry. However, during the period when chemistry was developing, a distinction was made between compounds that were synthesized by living things and those that were not, leading to the branching of the science. The former and latter were termed respectively organic and inorganic chemistry. However, following Friedrich Wöhler's preparation of urea (an organic compound) artificially in 1828, it became possible to synthesize by human endeavor compounds which hitherto had been thought to be preparable only by biological systems. Along with that, the original meaning of "organic compounds" was lost, and the field has now become established in terms of carbon-centered chemistry, though the term is still used even today. Thus, the ideas that one 2s orbital and three 2p orbitals play important roles in organic chemistry and that the number of valence electrons around a carbon atom is eight, as embodied in the octet rule, are valid. In addition, sp^3, sp^2, and sp hybridizations reasonably explain the geometries around the carbon atom, such as tetrahedral, trigonal planar and linear. In contrast, inorganic chemistry became a general term referring to all chemical compounds except organic compounds. Thus, the elements included under "inorganic chemistry" comprise almost all the elements of the periodic table, and the orbitals used in discussing their bonding and properties include additionally

d and f orbitals, thus leading to many compounds that do not obey the octet rule.

1.2   Coordination Chemistry

Among inorganic compounds, those containing transition metal atoms are especially complicated in terms of composition and structure. Compared to organic chemistry in which carbon may be considered to have 4 hands for making bonds, transition metals show variable numbers of bonding hands – from 1 to 10 – and thus seem complicated in comparison. The term "complex" in transition metal complex is derived from "complicated".

In the late 19th century, many complicated compounds involving a transition metal (transition metal complexes) were prepared and isolated. It was fortunate for transition metal chemistry that most of those complexes were colored. Even in the late 19th century, when spectroscopy was not yet popular, just by looking at the colors of the synthesized compounds, it could be judged whether they were the same or different. For example, the material represented by the composition $CoCl_3(NH_3)_6$ appears yellow, violet, green and purple depending on the synthetic method. It was apparent that different compounds could still have the same composition. This could not be explained by the common sense of organic chemistry at that time.

It was Alfred Werner who showed how to explain such a complicated compound reasonably. He started from the common sense of the time that "each element has a fixed valence" and introduced the idea that "the element can take different valences". For example, cuprous chloride (CuCl) and cupric chloride ($CuCl_2$) are both possible forms of copper chloride. Until then, it was thought that copper had 2 bonding hands, and thus $CuCl_2$ was represented as Cl–Cu–Cl and CuCl as Cl–Cu–Cu–Cl. Werner, on the other hand, suggested that Cu in CuCl had 1 bonding hand and so the compound should be represented as Cu–Cl, and Cu in $CuCl_2$ had 2 bonding hands and should be shown as Cl–Cu–Cl. Looking at the compound formulated as $CoCl_3(NH_3)_6$ shown above, there are 9 atoms (Cl) or groups of atoms (NH_3) other than Co. Co is considered to have 6 bonding hands, so the remaining 3 atoms or groups of atoms have no bonds with Co. An atom or group of atoms directly bonded to a metal is called a "ligand". Werner's sharp insight revealed a spatially clear image of these 6 ligands and provided for a discussion of stereochemistry. Co is placed at the origin of

the orthogonal coordinate system and six atoms (groups of atoms) are arranged in the directions of the *x, -x, y, -y, z,* and *-z* axes to form an octahedral molecular structure (Figure 1.1). Figure 1.2 shows the possible arrangements of $CoCl_3(NH_3)_6$. Considering the stereochemistry of an octahedral structure, it is possible to explain the existence of geometric isomers, such as *trans* and *cis,* in this complex, and thus that compounds of different color can be formed despite having the same composition.
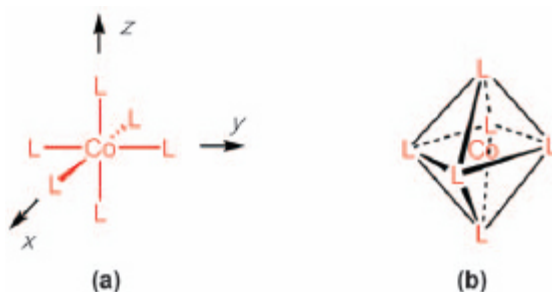
Figure 1.1   (a) Configuration of CoL_6. (b) When connecting the six ligands (L) surrounding Co, it becomes an octahedron. There are no actual bonds between L and L.
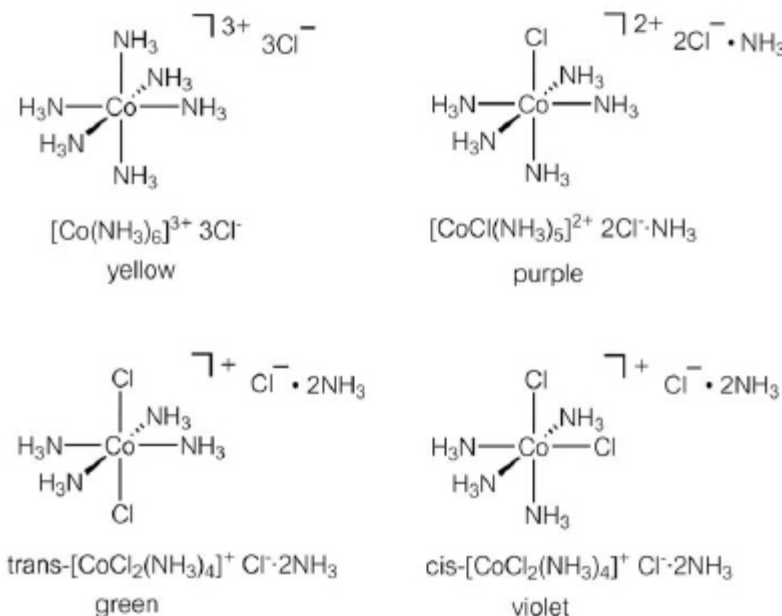
Figure 1.2   Structures and colors of complexes formulated as $CoCl_3(NH_3)_6$.

[PtCl$_2$(NH$_3$)$_2$] has two isomers. If Pt takes a planar square structure, it can be understood that *trans* and *cis* isomers exist (Figure 1.3). *cis*-[PtCl$_2$(NH$_3$)$_2$] is known as *cisplatin* and is effective as an anticancer drug.
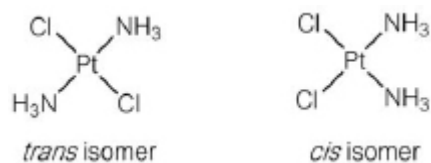
Figure 1.3   Two isomers of square planar [PtCl$_2$(NH$_3$)$_2$].

It was in 1893 that Werner proposed his revolutionary coordination theory. He was just 27 years old at the time. The chemical establishment of the time found his proposals hard to accept. However, the validity of Werner's coordination theory was proved by the accumulation of experimental results, and for this achievement, Werner was awarded the Nobel Prize in chemistry in 1913.

In coordination chemistry, the bond between metal and ligand is considered as follows. The ligand donates a lone pair of electrons to the empty d orbital of the transition metal to form a bond. The bond formed in this way is called a dative (or coordinate) bond. That is, the transition metal, as an electron pair acceptor, is a Lewis acid and the ligand, as an electron pair donor, is a Lewis base (Figure 1.4). This is the basis for considering bonding in transition metal complexes.
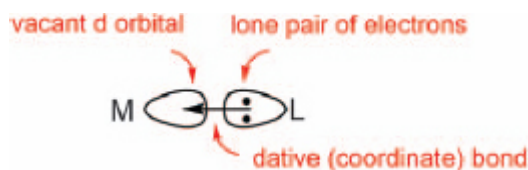
Figure 1.4   Dative (coordinate) bond of a transition metal complex.

1.3   Organometallic Chemistry

From the dawn of the study of chemistry, organic and inorganic chemistry developed independently due to the differences in the compounds handled, and with the advent of Werner's research, a new field called "complex

chemistry" was born in inorganic chemistry. As noted above, a transition metal complex consists of a transition metal and coordinating ligands. The coordinating atom in the ligand has at least one pair of electrons available for donation, such as a nitrogen atom, oxygen atom or other atom, and forms a dative covalent bond with the transition metal using the lone pair of electrons. Although NH_3 and H_2O are typical inorganic molecules, such ligands are rather rare, and many ligands contain organic groups bound to the coordinating N, O, *etc*. atoms. Amino acids and porphyrins are good examples. When attempting to impart functions such as color, redox properties, catalytic ability *etc*. to the complex, the ligand should be designed appropriately. Of course, knowledge of organic chemistry is required. In that sense, complex chemistry can be said to be a hybrid of both inorganic and organic chemistry. In the middle of the 20th century, a new field situated right between inorganic and organic chemistry was born. This is "organometallic chemistry". Compounds bearing a bond between an organic group, such as a methyl or phenyl group, and a transition metal emerged. From the viewpoint of the transition metal, this compound is a complex in which the ligand is an organic group such as a methyl or a phenyl group. On the other hand, when viewed from an organic perspective, it is an organic substance in which one of the carbon substituents is a transition metal. A compound having a bond between a transition metal (M) and a carbon (C) is an organometallic complex, and the research field to handle this is organometallic chemistry (Figure 1.5). In addition to being formally intermediate between organic and inorganic chemistry, organometallic chemistry also provides a point of contact for a discussion of chemical bonding from organic and inorganic points of view. In organic chemistry the C–C bond is undoubtedly a covalent bond. Thus, from an organic point of view, a compound in which one C is replaced by M giving M–C is considered to contain a covalent M–C bond. On the other hand, in complex chemistry, the M–C bond in M-CH_3, for example, is considered to be constructed by the donation of a lone pair of electrons on the carbon of the methyl anion (:CH_3^-) to an empty d orbital of the metal. Thus, the M–C bond is considered to be a dative covalent (or coordinate) bond.
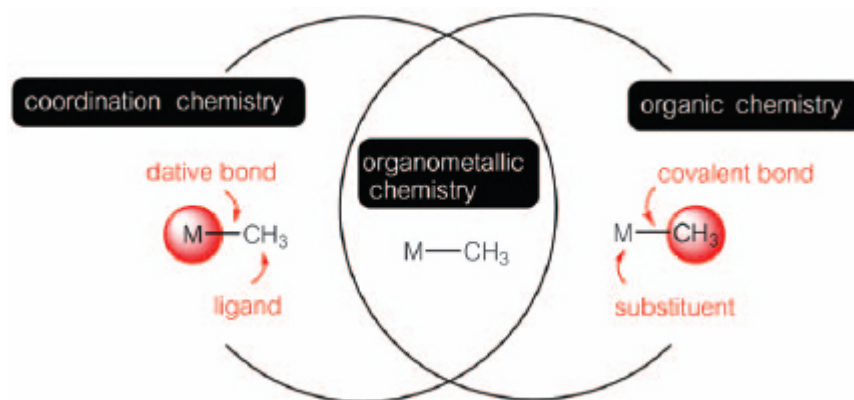
Figure 1.5   M-CH$_3$ complex.

The field of organometallic chemistry developed rapidly and is still developing, as it offers much novel and unique chemistry, especially as regards structure, bonding and reactivity, and it is not merely an area halfway between complex chemistry and organic chemistry. In this part of this book, we will explain the fundamentals of organometallic chemistry.

Regarding organometallic chemistry, a number of books have already been published. Some of them are listed below.[1–6]

References

1. A. Yamamoto, *Organotransition Metal Chemistry*, Wiley-Interscience Publication, 1986.
2. A. W. Parkins and R. C. Poller, *An Introduction to Organometallic Chemistry*, Macmillan Education LTD, 1986.
3. Ch. Elschenbroich and A. Salzer, *Organometallics. A Concise Introduction*, VCH, 2nd edn, 1992.
4. A. F. Hill, *Organotransition Metal Chemistry*, Wiley-Interscience, 2002.
5. R. H. Crabtree, *The Organometallic Chemistry of the Transition Metals*, Wiley, 5th edn, 2009.
6. R. Whyman, *Applied Organometallic Chemistry and Catalysis*, Oxford University Press, 2001.

Chapter 2

Basic Concepts Relating to Organometallic Complexes

Hiroshi Nakazawa[a]

[a] Osaka City University Japan
nakazawa@sci.osaka-cu.ac.jp

2.1   Introduction

Electron counting is strictly a formalism. Nevertheless, in accounting for the structure, properties and reactivity of metal complexes it is useful to be able to count the electrons and consider to which atoms and in what kinds of bonds they may be assigned. In organic chemistry, the octet rule is very useful. This states that when a carbon atom forms bonds with other atoms to build up a molecule, the valence electron count around the carbon becomes 8. The number 8 arises due to electrons filling the 2s and three 2p orbitals (giving a total of 8 electrons) to afford the same stable electronic structure as one of the noble gases (in this case, neon).

2.2   EAN Rule

When dealing with organometallic complexes, the *effective atomic number* (EAN) rule may be used. This rule expresses the idea that combining the number of electrons possessed by the metal in the complex and the number of electrons donated from the ligands to the metal, the total number becomes the number of electrons of one of the noble gases (18 in Ar, 36 in Kr, 54 in Xe, and 86 in Rn). The EAN rule is explained in more detail below with two complexes as examples.

   $[Co(NH_3)_6]^{3+}$ complex
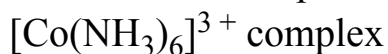
Co in this complex has a $3+$ charge and is thus in oxidation state $+3$, so the metal has 24 electrons. In addition, each NH_3 of the ligand donates a lone pair of electrons (2e) from the nitrogen to the Co. Therefore, the total number of electrons is as follows:

$$\begin{array}{ccc} \text{Co(III)} & & 6\,NH_3 \\ 24 & + & 6 \times 2 = 36 \text{ (same as electron count of Kr)} \end{array}$$

$[Pd(PPh_3)_4]$ complex

As the Pd in this complex is zero valent, the metal has 46 electrons. The ligand PPh_3 (a type of compound called a "phosphine") donates the lone pair of electrons on P to Pd.[1] Therefore, the total number of electrons is as follows:

$$\begin{array}{ccc} \text{Pd(0)} & & 4\,PPh_3 \\ 46 & + & 4 \times 2 = 54 \text{ (same as electron count of Xe)} \end{array}$$

2.3 Eighteen Electron Rule (18e Rule)

In the EAN rule, all of the electrons at the transition metal are counted, including core electrons. However, when considering the stability and reactivity of complexes, it is more important to consider the electrons in the outermost (valence) shell of the transition metal, that is, the electrons in the d orbitals (the electrons in the inner orbitals are not particularly important). The sum of the d electron number of the metal and the number of electrons donated from the ligands is called the total valence electron count, and the 18 electron rule (hereafter the 18e rule) states that the total valence electron count becomes 18. The 18e rule is thus essentially the same as the EAN rule, but more convenient because it does not require checking against the number of noble gas electrons (18, 36, 54, and 86), and for metals, it is only necessary to count d electrons. Let us examine whether the two complexes shown above follow the 18e rule.

$[Co(NH_3)_6]^{3+}$ complex

As Co is trivalent, it has 6 d electrons. Therefore, the total valence electron count is as follows:

$$Co(III) \quad 6 \, NH_3$$
$$6 \quad + \quad 6 \times 2 \quad = \quad 18$$

[Pd(PPh$_3$)$_4$] complex

As Pd is zero valent, it has 10 d electrons, resulting in the following total valence electron count:

$$Pd(0) \quad 4 \, PPh_3$$
$$10 \quad + \quad 4 \times 2 \quad = \quad 18$$

When organometallic complexes are considered, the total valence electron count around the metal in the complex is important. First of all, it is important to master how to count the electrons. The next section will explain electron counting.

2.4 Electron Counting

In order to determine the total valence electron count around a metal, the number of d electrons and the number of electrons donated from the ligands are counted. There are principally two ways.

> Method (A): determine the number of d electrons by considering the oxidation number of the metal.
> Method (B): determine the number of d electrons by considering the metal as zero valent and by also considering the total charge of the complex

We explain this further with the same example used above of $[Co(NH_3)_6]^{3+}$.

In Method (A) the Co is trivalent, so the metal d electron count is 6. The ligands together donate 12 electrons. The total valence electron count is thus 18.

In Method (B), the Co is considered to be zero valent, so the d electron count is 9, although the total charge must still be considered. The Co is tentatively assigned as zero valent, but in fact it is trivalent, so three electrons must be removed, as follows:

$$Co(0) \quad 6 \, NH_3 \quad total \; charge$$
$$9 \quad + \quad 6 \times 2 \quad - \quad 3 \quad = \quad 18$$

If the oxidation number of the metal is uniquely determined, Method A is easy to understand and apply. However, as will be mentioned later, it is sometimes difficult to determine the oxidation number of the metal in an organometallic complex. Method B avoids this potential difficulty, because the electrons can be counted without considering the oxidation number of the transition metal, and is described below in more detail. In order to evaluate the total valence electron count around the transition metal of the complex, the following three items must be considered: the transition metal, the ligand, and the total charge of the complex.

2.4.1 Transition Metal

First, the number of d electrons must be ascertained, assuming that the given transition metal is zero valent (oxidation number is zero). Table 2.1 shows transition metals of the Periodic Table and their Group number. When the metal is zero valent, the number of d electrons equals the group number of the element.[2] For example, the d electron count of Ti is 4, that of V is 5,[3] and that of Ru is 8.[4]

Table 2.1 Transition metal section of the periodic table.

3	4	5	6	7	8	9	10
Sc	Ti	V	Cr	Mn	Fe	Co	Ni
Y	Zr	Nb	Mo	Tc	Ru	Rh	Pd
La	Hf	Ta	W	Re	Os	Ir	Pt

2.4.2 Ligand

While it is sufficient and relatively simple to recall the position of a transition metal among the 24 transition metals in the Periodic Table, it is rather more challenging to remember how many electrons are donated by each ligand due to the numerous ligand types. However, once the concepts presented below are understood, there is no need to remember individual ligands.

(1) **One-electron (1e) donor ligand (a ligand which is considered to donate one electron to a metal)**
A group (or a radical) in organic chemistry serves as a 1e donor ligand. Some examples are shown: hydride (–H), alkyl (–CH_3, –C_2H_5 *etc.*), aryl (–C_6H_5 *etc.*), halogeno (–F, –Cl, *etc.*), alkoxy (–OMe, –OEt, *etc.*), vinyl (–CH=CH_2, *etc.*), acyl (–C(O)Me, –C(O)Et, *etc.*), amide (–NMe_2, *etc.*), and phosphide (–PMe_2, *etc.*). In addition, a transition metal fragment with an M–M single bond serves as a 1e donor. [$(CO)_5Mn–Mn(CO)_5$] is an example. The $Mn(CO)_5$

fragment is a part of a transition metal complex and is also a ligand of the other Mn. In the case of a complex having an M–M single bond, each metal fragment can be considered as a 1e donor ligand to the other fragment. These ligands serving as 1e donors are said to have a σ-bond with the metal.[5]

(2) **Two-electron (2e) donor ligand (a ligand which is considered to donate two electrons to a metal)**

Such a ligand is not itself a group (or a radical) but rather a neutral molecule. These ligands are roughly classified into those coordinated *via* a lone pair of electrons and those coordinated *via* π electrons. Examples are shown below.

1) Ligands coordinated *via* a lone pair of electrons:

Amines (NH_3, NMe_3, *etc.*), phosphines (PMe_3, PPh_3, *etc.*), ethers (OMe_2, OEt_2, *etc.*), carbonyl (CO), carbene or alkylidene ($:CH_2$, $:CMe_2$, *etc.*).

2) Ligands coordinated *via* π electrons:

Alkenes (CH_2=CH_2, CH_2=CHMe, *etc.*; *e.g.* the two π electrons of a C=C double bond are donated to the metal. This will be discussed in detail in Section 3.2.3), and alkynes (HC≡CH, PhC≡CPh, *etc.*).

3) A transition metal fragment bonded to another transition metal through an M=M double bond:

In cases with an M=M double bond, each metal fragment counts as a 2e donor ligand to the other fragment.

(3) **Three-electron (3e) donor ligand (a ligand which is considered to donate three electrons to a metal)**

An important 3e donor ligand in organometallic chemistry is the π allyl ligand (Figure 2.1). The allyl group is $-CH_2-CH=CH_2$. It is a 1e donor ligand like an alkyl group if it coordinates to a metal only with the left hand side terminal carbon (Figure 2.1(a)). When, in addition to this 1e donation, the π-bonding electrons between C^2–C^3 are also donated to the metal, two more electrons are added, affording a 3e donor ligand (Figure 2.1(b)). For clarity, 1e donation is represented by a single line and two electron donation by an arrow in this section. As an allyl group has a 1e donating portion and a 2e donating portion to the metal, it serves as a 3e donor ligand. A characteristic of the allyl ligand is that it is symmetric. In (b), the C^1 carbon donates one electron and two electrons are donated from the C^2=C^3 π bond. However, when describing it as shown in (c), the C^3 carbon donates one electron and the C^1=C^2 π bond donates two electrons. Since (b) and (c) are resonance hybrids, it is appropriate to draw the 3e donation as (d). In this case, the single line does not represent a 1e donor because it is not attached to one particular atom. The metal is situated above the C^1–C^2–C^3 plane and the allyl ligand donates three electrons as a whole.

The allyl ligand functions both as a 1e donor ligand as in Figure 2.1(a) and as a 3e donor ligand as in (d). The Greek symbol eta "η" is used to indicate the type of coordination. This represents the number of carbons bonded to the metal and (d) is represented by $η^3$-C_3H_5. $η^3$ is pronounced as "eta-three" and sometimes referred to as "hapto-three".[6] (a) and (d) are distinguished as σ-allyl and π-allyl complexes respectively, because only a σ bond between the allyl ligand and the metal exists in (a), whereas the electrons of the π bond are also involved in bonding in (d).

Amides and phosphides are other ligands that can function as both 1e and 3e donors (Figure 2.2). These ligands are introduced as 1e donor ligands in Figure 2.2(a) and (c). As these ligands have a lone pair of electrons on the nitrogen and on the phosphorus donor atoms, the hybridization around the N and P atoms can change from four sp^3 orbitals to three sp^2 and one p orbitals, and 2e in the p orbital are donated to M through π interaction (Figure 2.2(b) and (d))

resulting in the formation of 3e donor ligands. In order to use the lone pair of electrons in coordination, the hybridization of N and P changes from sp^3 to sp^2, so that the geometry around N and P changes from a trigonal pyramidal to a trigonal planar structure. Thus, if bond angle information around N and P are obtained by X-ray structure analysis, it can be ascertained whether the ligand is functioning as a 1e donor ligand or a 3e donor ligand.

In complexes with an M–M triple bond, each M acts as a 3e donor ligand to the other metal.

(4) **Four-electron (4e) donor ligand**

As described above, the η^3-allyl ligand is considered to consist of a 1e donor part and a 2e donor part. The ligands in (4)–(7) described below will basically be a combination of a 1e donor part and a 2e donor part or more than two 2e donor parts. 1,3-Butadiene and 1,5-cyclooctadiene (cod) can be mentioned as examples of 4e donor ligands (Figure 2.3). In both cases, two olefin functions coordinate to the metal, and thus they act as 4e donor ligands. As an alkyne has two π bonds, it may act as either a 2e donor or a 4e donor and care must be exercised when considering complexes with an alkyne ligand.

(5) **Five-electron (5e) donor ligand**

The cyclopentadienyl ligand, Cp (C_5H_5), is one of the most important ligands for organometallic complexes (Figure 2.4). Ferrocene is a compound in which two cyclopentadienyl ligands are η^5 bonded to iron. Figure 2.4(a) shows an η^1-complex. In addition to the σ bond, the two olefin functions in (a) can coordinate to M, resulting in the formation of an η^5-complex (Figure 2.4(b)). Five structural formulae from (b) to (f) are conceivable, depending on the positional relationship of the carbons in the C=C double bonds and the σ bond. As these structures ((b) to (f)) are all resonance hybrids, it is usually shown as depicted in (g) in which the ligand is written as η^5-C_5H_5 or simply Cp. See below for further details on the bonding modes of this important ligand.

(6) **Six-electron (6e) donor ligand**

Benzene appears frequently as a ligand in organometallic chemistry (Figure 2.5). Having formally three C=C double bonds, it can behave as a 6e donor ligand. Although the two resonance forms (a) and (b) can be written depending on the positions of the double bonds, it is often written as in (c), just as in organic chemistry.

(7) **Ligands requiring particular attention**

The 1e to 6e donor ligands frequently appearing in organometallic chemistry are shown above. If these are kept in mind, it is simple to predict, in most cases, how many electrons a given ligand donates to a metal. Here, we describe ligands that require attention when performing electron counting.

1) **Carbonyl ligand (Figure 2.6)**

"Carbonyl" in organic chemistry refers to the C=O functional group that is found in, for example, aldehydes and ketones (Figure 2.6(a)). In contrast, "carbonyl" in transition metal complex chemistry refers to a carbon monoxide ligand (b). The molecule has a triple bond between C and O, and each atom has a lone pair of electrons. As the lone pair of electrons on C is more basic than that on O, the CO molecule coordinates to a transition metal *via* the carbon side (c). A carbonyl coordinating as in (c) is called a "terminal carbonyl" and functions as a 2e donor ligand. In contrast, a carbonyl ligand may also bridge two metals (d). In this mode it is called a "bridging carbonyl". The bridging carbonyl donates two electrons in total: one to each metal. This corresponds to the case where the two substituents on the carbonyl carbon of (a) are replaced by transition metals, so these are considered to be M–C σ bonds.

2) **Cyclopentadienyl ligand (Figure 2.7)**

This widely used and important ligand was introduced in the section above. Since this ligand has one σ bond and two olefin moieties, it can coordinate to a transition metal as either a 1e, a 3e, or a 5e donor ligand. There are many complexes of type (c), but complexes of type

(a) are also known. Complexes of type (b) can be thought of as intermediates, but few are known as stable complexes. It is necessary to judge appropriately the type of coordination.

3) **Benzene ligand (Figure 2.8)**

Since benzene has three olefin moieties, it can coordinate to a metal as either a 2e, 4e, or 6e donor ligand.

1) **Alkyne ligand (Figure 2.9)**

As alkynes have two π bonds, it is possible to donate two electrons, as in Figure 2.9 (a) or four electrons as in (b) to a transition metal. Alkyne-bridged complexes are also known in which the two different π electron clouds of the alkyne ligand are donated to two different metals (c).

5) **Halogeno ligand (Figure 2.10)**

It was mentioned in Section 2.3.2 (1) that a chloro ligand, for example, functions as a 1e donor ligand (Figure 2.10(a)). However, as it has three lone pairs of electrons, these lone pairs may also coordinate to a transition metal. The three lone pairs are not oriented towards the metal side, but many complexes exist in which one lone pair of electrons participates in coordination in addition to the M–Cl bond and thus the chloro ligand can be considered as a 3e donor ligand (b) since, in these cases, in addition to the σbond, the ligands are π donors. In the case of amide or phosphide ligands, it is easily judged from its structure whether it coordinates as a 1e or a 3e donor ligand. However, as a halogeno ligand has no other substituent, it can be quite difficult to judge the coordination mode. The halogeno ligand can also serve as a bridging ligand, as in (c). In this case, it makes a σ bond with one metal, donating one electron, and donates two electrons using one of the lone pairs of electrons to the other metal. Particularly in the case of (d), the lengths of the four M–Cl bonds are all the same, so that there is no difference between 1e and 2e donation. However, when counting the electrons of a bridging halogeno ligand, one bond is considered to consist of one halogeno and one metal electron, while the other is considered to consist of two donated halogeno electrons (d).
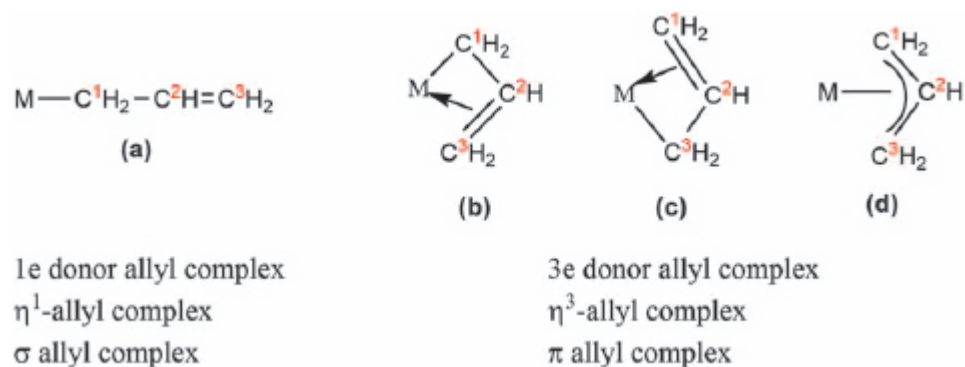
Figure 2.1 Allyl complex.
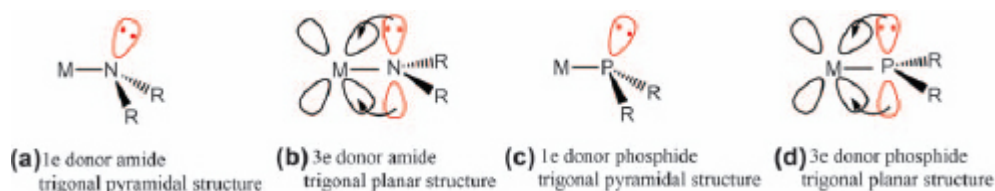
Figure 2.2 Transition metal complexes with an amide or phosphide ligand.

η^4-1,3-butadiene complex η^2,η^2-1,5-cyclooctadiene complex
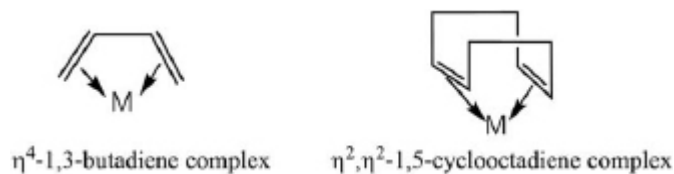
Figure 2.3   4e donor diene complexes.

(a)   (b)   (c)   (d)   (e)   (f)   (g)
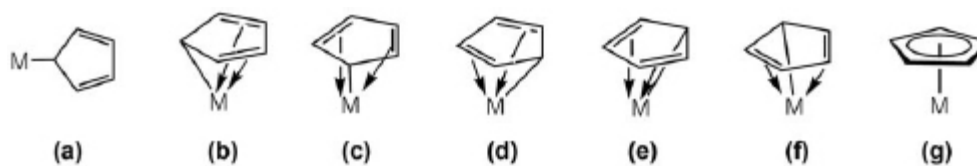
Figure 2.4   Bonding modes in cyclopentadienyl complexes.

(a)   (b)   (c)
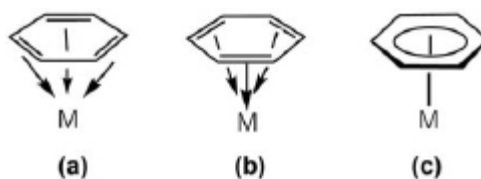
Figure 2.5   Benzene-coordinated complex.

(a) carbonyl group   (b) carbonyl ligand   (c) terminal carbonyl ligand   (d) bridging carbonyl ligand
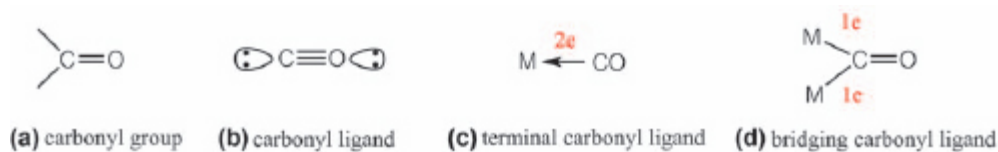
Figure 2.6   Carbonyl group and carbonyl ligand.

(a) 1e donor   (b) 3e donor   (c) 5e donor
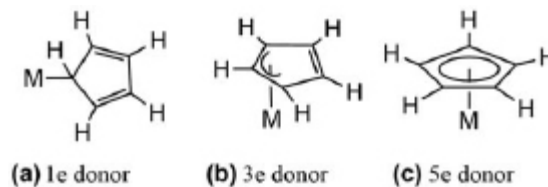
Figure 2.7   Complexes with cyclopentadienyl ligand. For better understanding, all hydrogen atoms on the Cp are shown here.

(a) 2e donor   (b) 4e donor   (c) 6e donor
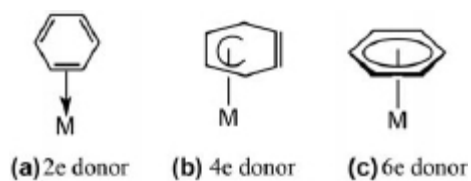
Figure 2.8   Complexes with a benzene ligand.

(a) 2e donor   **(b)** 4e donor   **(c)** bridging 4e donor
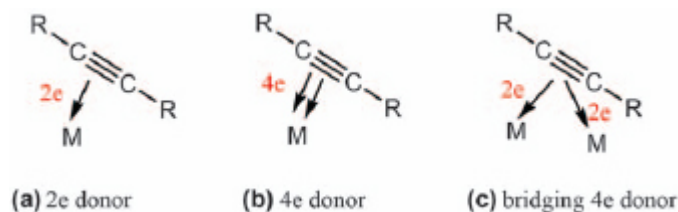
Figure 2.9   Complexes with an alkyne ligand.

(a) 1e donor   **(b)** 3e donor   **(c)** bridging ligand   **(d)** bridging ligand
$(\mu\text{-Cl})M_2$ $(\mu\text{-Cl})_2M_2$
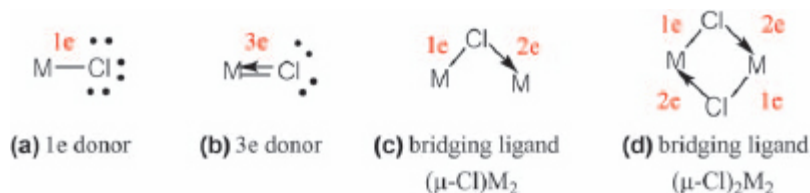
Figure 2.10   Complexes with halogeno ligands.
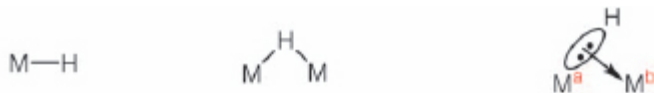
Figure 2.11   Complexes with hydride.

When a ligand bridges two or more metals, the symbol "μ" (mu) is used. It is expressed as $(\mu\text{-Cl})M_2$ in the case of (c) above, and as $(\mu\text{-Cl})_2M_2$ in the case of (d).

6) **Hydride ligand (Figure 2.11)**

Since H has only one electron, it is unlikely to be thought of other than as a terminal hydride ligand (a 1e donor ligand, Figure 2.11(a)), but many bridging hydride complexes have been reported (b). How is the electron counting in this case best considered? When bonding to one metal (M^a in (c)) it acts as a normal terminal hydride, but when also bonding to another metal (M^b in (c)) the σ bonding electrons between M^a and H (two electrons) are shared with the other metal. When M^a and M^b are the same, it is impossible to distinguish to which metal one electron is donated and to which metal two electrons are donated. It is best considered that it functions as a ligand donating three electrons in total.

2.4.3   Total Charge of the Complex

In Section 2.3.1, the d electrons in the central metal were counted assuming the metal to be zerovalent. Adjustment needs to be made in the cases of charged complex ions by considering the total charge. If the charge of the complex as a whole is 1 + , *i.e.* it is a monovalent cationic complex, 1 is subtracted since the number of electrons is one less than that considered for the zero valent case. If it is a divalent cation, 2 is subtracted. Conversely, if

it is a monovalent anionic complex, 1 is added, and if it is divalent anionic, 2 is added.

2.4.4 Importance of Electron Counting

Examining whether a given complex obeys the 18e rule is helpful in considering the reactivity or the catalytic cycle of the complex. For this purpose it is important for various complexes that the total valence electron number around the transition metal (the number of d electrons of the transition metal and that donated from the ligand) can be simply calculated.

A complex satisfying the 18e rule is called "a coordinatively saturated complex", and a complex in which the total valence electron number is less than 18 is called "a coordinatively unsaturated complex".

The following problems should be answered in order to become familiar with electron counting.

Problem 1. According to the worked example, calculate the total number of valence electrons around the transition metals in the following complexes. Here, Cp stands for η^5-C_5H_5.

Example: $[Ni(CO)_4]$,   Answer: $10(Ni) + 2(CO) \times 4 = 18$

1) $[Cr(CO)_6]$
2) $[CpFe(CO)_2Me]$
3) $[Mo(C_6H_6)_2]$
4) $[(CO)_5Mn–Mn(CO)_5]$
5) $[Fe(CO)_3(PPh_3)_2]$
6) $[Fe(H)_2(CO)_4]$
7) $[Co(CN)_2(CO)(PEt_3)_2]^-$
8) $[Pt(C_2H_4)Cl_3]^-$
9) $[CpFe(CO)_2(PMe_3)]^+$
10) $[(\eta^5$-$C_5H_5)(\eta^1$-$C_5H_5)Ru(CO)_2]$
11) $[Ni(Ph)_2(PPh_3)_2]$
12) $[CpOs(\eta^3$-$C_3H_5)(CO)]$
13) $[Cp_2Mo(C_2H_2)]$
14) $[Pd(PEt_3)_2(OMe)_2]$
15) $[(\eta^3$-$C_3H_5)Pd(\mu$-$Cl)_2Pd(\eta^3$-$C_3H_5)]$
16) $[Mn(CO)_5\{C(O)Me\}]$

In order to appreciate fully the nature of organometallic complexes, it is best to actually synthesize them, but often particular experimental

equipment and techniques are necessary due to their often reactive nature. It is thus useful to solve the following problems in order to become familiar with organometallic complexes.

Problem 2. What is the simplest complex consisting of the transition metal and ligand(s) shown that satisfies the 18e rule? Here too, Cp stands for η^5-C_5H_5.

1) Ni, CO
2) Co, Cp, CO
3) Mn, CO
4) Fe, Cp, CO
5) Re, CO, H

2.5   Formal Oxidation Number and d Electron Number

2.5.1   Formal Oxidation Number

The oxidation number of the central metal is an important factor in considering the properties of a metal complex. The oxidation numbers for Werner-type complexes can be readily determined. For example, considering $[CoCl(NH_3)_5]^{2+}$, since Cl is an anionic ligand and NH_3 is a neutral ligand, the cobalt is trivalent. Similarly, the chromium in $[Cr(NH_3)_6]^{2+}$ is divalent. There is no difficulty in the case of these complexes. In contrast, however, it is difficult to determine the oxidation number of the central metal in an organometallic complex. Consider, for example, the Pd complexes shown in Figure 2.12. When considering the methyl group of the complex in (a) as an anionic ligand, the oxidation number of Pd is +2. In the complex in (b), as both PPh_3 and ethylene are neutral ligands, the oxidation number of the Pd is 0. This complex can be regarded as a complex in which ethylene is coordinated by its π electrons, but it can also be seen as a three-membered ring complex containing Pd as shown in (c). From this perspective, the Pd is coordinated by the two linked alkyl groups, so that it becomes a complex with two anionic ligating groups, and the oxidation number of the Pd is thus +2. Although (b) and (c) are the same complex, the oxidation number depends on how the structure

is drawn. Actually, it is quite difficult to write the structures of these types of complex, because the bond character changes depending on the substituents on the Pd and the olefin.
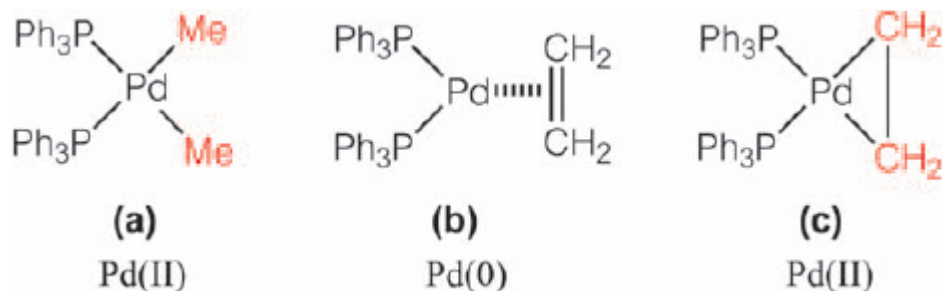
Figure 2.12   Oxidation number of Pd.

As we have seen, it can be difficult to determine the oxidation number of metals in organometallic complexes, and the IUPAC nomenclature committee has stated that for organometallic complexes the oxidation number of the central metal should not be specified.[1]

For organometallic complexes, then, is there any merit to the concept of oxidation number? The answer is YES. The oxidation number determined according to certain rules is very helpful for considering the nature and reactivity of the complex. The oxidation number determined according to this "certain rule" is called the "formal oxidation number" and is described below.

2.5.2   How to Determine the Formal Oxidation Number

To determine the formal oxidation number, all ligands around the central metal are removed from the metal with closed shell electron configurations. The charge remaining on the metal is called the "formal oxidation number".

Considering the complex in Figure 2.12(a), the 2 electrons between Pd and P are allocated to P and PPh_3 is removed from Pd. By doing so, the phosphorus atom can keep a closed shell structure (satisfying the octet rule). When removing Me, the two electrons between Pd and C in the Me are allocated to the carbon in order to keep the closed shell structure of the methyl carbon, that is, it is removed as Me^-. As a result, Pd becomes Pd^+. In this way, the formal oxidation number of Pd in (a) is +2.

In general, a 1e donor ligand increases the formal oxidation number of the central metal by one, and a 2e donor ligand does not change the formal oxidation number of the central metal. A metal–metal bond does not change the formal oxidation number. Ligands serving as three or more electron donor ligands basically consist of 1e and 2e donor parts. The formal oxidation number can therefore be derived based on this. For example, a 3e donor allyl ligand can be divided into a 1e donor alkyl moiety and a 2e donor olefin moiety. Thus, one allyl ligand effectively increases the formal oxidation number by one. Likewise, the η^5-C_5H_5 ligand will also increase the formal oxidation number by one. The total charge of the complex is considered to be attributed to the central metal. That is, a 1 + charge increases the oxidation number of the central metal by 1, and a 1 − charge decreases the oxidation number by 1.

To become familiar with the calculation of formal oxidation numbers, consider examples 1) to 4) of Problem 1.

1) $[Cr(CO)_6]$: As CO is a 2e donor ligand, no matter how many CO ligands are coordinated, there is no change in the formal oxidation number. Therefore, the formal oxidation number of the Cr is zero.

2) $[Cp(CO)_2FeMe]$: The Cp and Me ligands each increase the oxidation number by 1, so the formal oxidation number of the Fe is +2.

3) $[Mo(C_6H_6)_2]$: As the C_6H_6 (benzene) ligand is considered to coordinate *via* the πelectrons of the olefin, it does not affect the formal oxidation number, and the formal oxidation number of Mo is zero.

4) $[(CO)_5Mn–Mn(CO)_5]$: Since the CO ligand and the metal–metal bond do not influence the formal oxidation number, the formal oxidation number of the Mn is zero.

Problem 3. Determine the formal oxidation number of the central metal for the complexes 5) to 16) in Problem 1.

2.5.3 d Electron Number (d Electron Count)

When the oxidation number of the metal is obtained (although it is formal), the d electron number of the metal can also be determined. When the transition metal is zero valent, the number of the group corresponds directly to the d electron number, so calculation is simple.

For example, the d electron count in the central metals of the complexes of 1) to 4) shown in Problem 1 are as follows:

1) $[Cr(CO)_6]$: The formal oxidation number of Cr is zero and since Cr is in Group 6, the d electron number is 6 (d^6 electron configuration).

2) $[Cp(CO)_2FeMe]$: Since Fe is a Group 8 transition metal, the electron configuration would be d^8 for Fe(0), but as this complex is Fe(ii), it is d^6 and the d electron count is thus 6.

3) $[Mo(C_6H_6)_2]$: Since this complex is d^6 Mo(0), the d electron count is thus 6.

4) $[(CO)_5Mn–Mn(CO)_5]$: Since the formal oxidation number of Mn is zero, the electron configuration is d^5 and the d electron count is thus 5.

Problem 4. Determine the d electron count of the central metal for the complexes of (5) to (16) shown in Problem 1.

2.6 Bond Order in Metal–Metal Bonds between Transition Metals

The central metals of organometallic complexes usually follow the 18e rule. If this rule is also observed in multinuclear complexes, it is possible to predict how many metal–metal bonds are present.

Firstly as an example, consider $[Cp(CO)Fe(\mu\text{-}CO)_2Fe(CO)Cp]$, a binuclear iron complex. As the complex has two bridging CO ligands between the two iron atoms, the structure shown in Figure 2.13(a) can initially be drawn. However, it is not apparent from the chemical formula whether the complex has an Fe–Fe bond or not. If there is a single bond between the two iron atoms, it should be drawn as in (b).

(a) without Fe-Fe bond   (b) with Fe-Fe bond
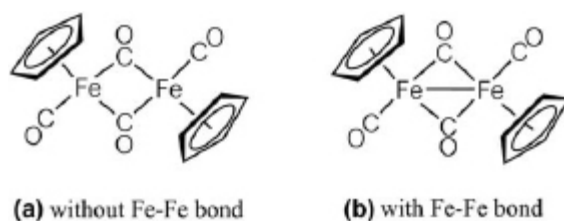
Figure 2.13 $[Cp(CO)Fe(\mu\text{-}CO)_2Fe(CO)Cp]$ complex.

The total valence electron number around each iron is 17 in (a), but 18 in (b). In order to satisfy the 18e rule it is clear that a single bond between the two iron atoms is necessary.

Consider this more generally. First, electrons donated from all ligands and the d electrons of all metals are added. In the case of $[Cp(CO)Fe(\mu\text{-}$

CO)₂Fe(CO)Cp], the calculation is as follows, from the left: 5 (Cp) + 2 (CO) + 8 (Fe) + 2 (μ-CO) × 2 + 8 (Fe) + 2 (CO) + 5 (Cp) = 34. However, if each iron is to satisfy the 18e rule, the sum of the total valence electron numbers around each iron should be 36 (=18 × 2), since this is a binuclear complex. Where did the difference of two electrons (36–34) arise? The discrepancy arises because electrons used in metal–metal bonds were not included in the first calculation. If there is one metal–metal bond, two electrons are utilized there. Thus, the metal–metal bond order is obtained by dividing the value of the difference between the apparent calculated electron number in the absence of a metal–metal bond (in this case, 34) from the theoretical value assuming each metal obeys the 18e rule (36 in this complex) by two. The metal–metal bond order in the given complex is thus 1, *i.e.* the complex has an Fe–Fe single bond. The X-ray structure of this complex revealed that the distance between the two iron atoms was in the range expected for an Fe–Fe single bond.[2] This methodology can be applied to various multinuclear organometallic complexes.

Consider [Cp(CO)₂Mo]₂. The sum of the numbers of electrons derived from all ligands and the d electrons from both Mo atoms is obtained as follows: {5(Cp) + 2(CO) × 2 + 6(Mo)} × 2 = 30. As this complex is also binuclear, there should be 36 electrons, so (36 − 30)/2 = 3, which indicates that there is a molybdenum–molybdenum triple bond.[3] This complex is drawn in Figure 2.14. It is a famous example of a complex with a metal–metal triple bond.
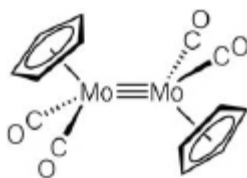
Figure 2.14   Triply bonded [Cp(CO)₂Mo]₂ complex.

Next, consider the trinuclear complex, [Ru₃(CO)₁₂]. Electron counting for the ligand and metal appearing in the formula leads to a count of 8 (Ru) × 3 + 2 (CO) × 12 = 48 electrons. If each Ru satisfies the 18e rule, there should be 18 × 3 = 54 electrons. It is thus apparent that 6 electrons (=54 −

48) are used in Ru–Ru bonding, leading to the existence of 6/2 = 3 Ru–Ru bonds.[7]

Since $[Ru_3(CO)_{12}]$ is predicted to have three Ru–Ru bonds, let us consider the structure of the complex. There are three possibilities: the molecule has (a) three Ru–Ru single bonds, (b) one single bond and one Ru=Ru double bond, (c) one Ru≡Ru triple bond. The calculation above does not indicate the connectivity of the metals. In order to satisfy the condition of (a), a triangle is formed with three Ru atoms at the vertices, and if twelve CO ligands are coordinated so that each Ru satisfies the 18e rule, the structure shown in Figure 2.15 (a) results. In the case of (b), a skeleton structure of Ru=Ru–Ru is expected. In order to satisfy the 18-electron rule by coordinating 12 COs to each Ru, either Ru^-–Ru^+ must be present, as shown in (b), or CO bridging must exist, as shown in (b'). In the case of (c), bridging CO is required. The structures of (b), (b') and (c) cannot be ruled out, but it can be predicted that (a) having the highest symmetry is the most reasonable structure. Single crystal X-ray diffraction experiments showed that the complex indeed adopts structure (a).[4]
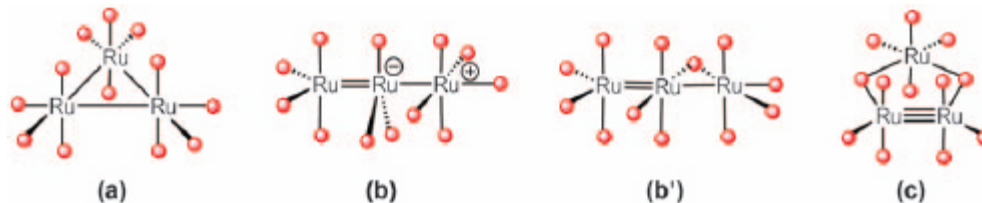
Figure 2.15 Structures of $[Ru_3(CO)_{12}]$ (red spheres indicate CO ligands).

Thus, assuming that each transition metal atom in a multinuclear complex satisfies the 18e rule, the metal–metal bond order can be predicted from the molecular formula, and furthermore the three-dimensional structure of the complex can be conjectured by using some chemical "common sense".

Problem 5. For the following complexes, estimate the metal–metal bond order and the geometrical structure. Here, Cp* stands for η^5-C_5Me_5.

1) $[\mu\text{-CO-}\{(\eta^4\text{-}C_4H_4)Fe(CO)\}_2]$
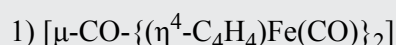
2) [μ-CMe$_2$-{Cp*Rh(CO)}$_2$]
3) [μ-CO-μ-CMe$_2$-{Cp*Rh}$_2$]
4) [(μ-Br)$_2$-{Mn(CO)$_4$}$_2$]
5) [μ-Cl-μ-CH$_2$-{Os$_3$(CO)$_{10}$}]$^-$

2.7   Structures of Organometallic Complexes

Transition metals combine with various atoms and molecules to form transition metal complexes. The structure of the complex is determined by the relative positional relationship of the ligands around the metal. The main factor determining the structure is steric repulsion between the ligands, and the ligands are arranged so as to minimize this. Another factor is which d orbital the metal uses for binding to the ligand. Figure 2.16 shows the typical relationship between coordination number (CN) and geometrical structure.

| CN = 2 | CN = 3 | CN = 4 | | CN = 5 | CN = 6 |

linear   trigonal   tetrahedral   square-planar   trigonal-bipyramidal   octahedral
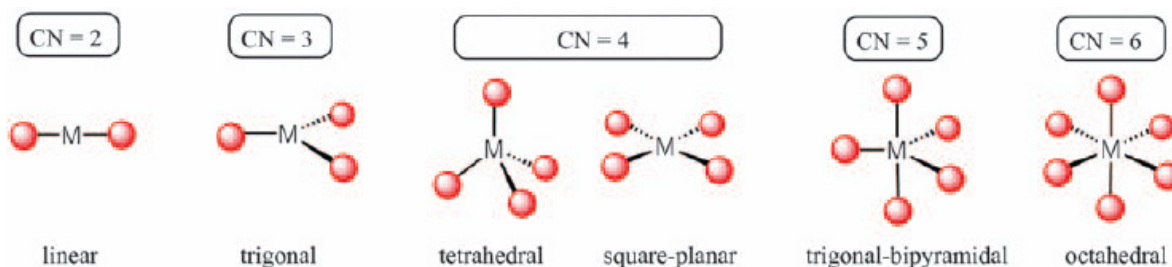
Figure 2.16   Relationship between coordination number (CN) and geometrical structure.

Most of the structures shown in Figure 2.16 can be expected when considering mutual steric repulsion between the ligands. Most complexes having a coordination number of 4 prefer a tetrahedral structure. However, some of them take square planar structures depending on the number of d electrons in the metal, so care must be exercised. This will be described in detail in Section 3.4.

Ligands such as halogen atoms, and molecules such as amines and phosphines, occupy one coordination site and are said to be monodentate. Ethylenediamine (H$_2$NCH$_2$CH$_2$NH$_2$), however, has two amine functions and can act as a bidentate ligand. The number of coordination sites occupied by these ligands is easy to understand. However, in organometallic complexes bearing organic molecules or organic groups as

ligands, it is often difficult to identify how many coordination sites the ligand occupies.

For example, in the case of the η^3-allyl ligand, supposing it coordinates as shown in Figure 2.1(b) and (c), the alkyl moiety occupies one coordination site and the olefin moiety occupies another site. Thus, the η^3-allyl ligand acts as a bidentate ligand. When considering the allyl ligand as in (d), however, the ligand is described as CH_2–CH–CH_2, donates three electrons to a metal and occupies one coordination site. Similarly for the η^5-C_5H_5 (Cp) ligand, it becomes a tridentate ligand when considered as (b)–(f) in Figure 2.4, or a monodentate ligand when considered as (g) in Figure 2.4.

Thus, depending on how many coordination sites the ligand occupies, the structure of the complex will change. Let us consider this further, with [CpFe(CO)$_2$Me] as an example. This complex has the structure shown in Figure 2.17(a). If one considers that Cp is a monodentate ligand, in other words, Cp occupies one coordination site, this complex can be regarded as having a tetrahedral structure. On the other hand, if one considers that a Cp ligand coordinates through one alkyl and two olefin moieties, it becomes a tridentate ligand, and the complex is thus hexacoordinate and octahedral. It is somewhat confusing if the description of the structure changes depending on the viewpoint of how many coordination sites the ligand occupies. One useful indicator as to structural type may be the bond angles: the Me–Fe–CO or OC–Fe–CO bond angles should be close to 109.5° for a tetrahedral structure, whereas for an octahedral complex they are expected to be close to 90°. X-ray structural analysis of a similar complex has been reported, and these angles are almost 90°.[5] Therefore, the bond angles suggest an octahedral structure for the complex. Many chemists, however, have described this complex as tetrahedral. Is there any alternative to describing the complex as tetrahedral or octahedral? In fact, this complex resembles the shape of a piano stool (see Figure 2.17(b); nowadays it seems rather old-fashioned!) and the term "piano stool complex" is used in academic papers.
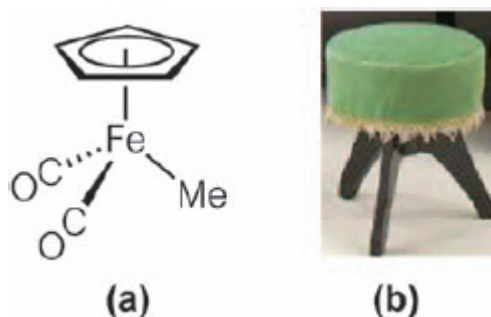
Figure 2.17 (a) Structure of [CpFe(CO)$_2$Me]. (b) Piano stool.

As mentioned above, it is sometimes difficult to describe the structure of organometallic complexes. This is attributed to the difficulty in unambiguously determining how many coordination sites the ligand occupies, and is a common characteristic of organometallic complexes. The important point is not how to express the structure of the complex, but whether you can imagine the structure three dimensionally.

References

1. N. G. Connelly, T. Damhus, R. M. Hartshorn and A. T. Hutton, *Nomenclature of Inorganic Chemistry IUPAC Recommendations 2005*, RSC Publishing, 2005.
2. R. F. Bryan and P. T. Greene, *J. Chem. Soc. A*, 1970, 3064.
3. R. J. Klingler, W. Butler and M. D. Curtis, *J. Am. Chem. Soc.*, 1975, **97**, 3535.
4. M. R. Churchill, F. J. Hollander and J. P. Hutchinson, *Inorg. Chem.*, 1977, **16**, 2655.
5. M. J. Bennett, Jr.F. A. CottonA. DavisonJ. W. FallerS. J. Lippard and S. M. Morehouse, *J. Am. Chem. Soc.*, 1966, **88**, 4371.

---

[1] Phosphines (PR$_3$) are used more often than amines (NR$_3$) in organometallic chemistry. P is a Group 15 element in the Periodic Table located below N. When donating electrons to metals as ligands, NR$_3$ and PR$_3$ can be considered in the same way.

[2] There is one point to be aware of here. For example, the electron configuration of Fe is described as $1s^2 2s^2 2p^6 3s^2 3p^6 4s^2 3d^6$. Since the energy level is lower for the 4s orbital than for the 3d orbitals, electrons enter first into the 4s orbital and then into the 3d orbitals, affording the above electron configuration. However, the energy levels of 4s and 3d are subtle. The energy level of the 4s orbital is lower when it is in the atomic state, but when Fe forms a complex, the 3d orbitals become lower than the 4s orbital in energy. Therefore, the electron configuration of a zero valent iron complex is $1s^2 2s^2 2p^6 3s^2 3p^6 3d^8$, and the d electron number is 8 instead of 6. The same is true for other transition metals, and the number of d electrons in zero valent transition metal complexes coincides with the group number in the periodic table.

3 This is easy to memorize because V corresponds to 5 in Roman numerals.

4 In order to obtain the number of d electrons of a transition metal, it is sufficient to recall the Periodic Table. This is not as difficult as it might at first seem, since there are only 24 transition elements in the transition metal section of the Periodic Table. It should be noted that M(i), M(ii), and M(iii) for Group 11 elements and M(ii) for Group 12 elements in the Periodic Table are also often treated as transition metals.

5 When considering the bond of M–CH_3, for example, we here assume that M· and ·CH_3 combine to form an M–CH_3 bond. Thus it is considered that the methyl group donates one electron to the metal, corresponding to Method (B) mentioned above, forming a shared electron pair covalent bond. On the other hand, it can be considered that M–CH_3 consists of $[M]^+$ and $[:CH_3]^-$, and that the $[:CH_3]^-$ ligand donates two electrons to the metal *via* a dative bond, corresponding to Method (A) mentioned above. By this approach, all of the above 1e donor ligands should be considered as 2e donor ligands. The difficulty of how to treat these ligands when counting electrons is due to how the M–C bond is considered. Since the actual bond has properties intermediate between the two, both are "extreme". Whichever method is used, the final conclusion is the same, but one should avoid confusing them in one textbook or paper. This book treats the above ligands as 1e donor ligands, *i.e.* employs Method (B).

6 The η notation is used when multiple carbons are bonded to a transition metal, so η^1 is not normally used. However, as shown in Figure 2.1(a), when it is wished to emphasize that it is a 1e donor ligand, it may be written η^1-C_3H_5.

7 Care should be taken not to divide the total of 6 electrons by 3 (for the 3 Ru atoms), thus obtaining the erroneous result of two Ru–Ru bonds. The 6 electrons should of course be divided by 2 (for the number of electrons per M–M bond).

Chapter 3

Bonds in Organometallic Complexes

Hiroshi Nakazawa[a]

[a] Osaka City University Osaka, Japan
Email: nakazawa@sci.osaka-cu.ac.jp

3.1   σ-Bonds between Transition Metals and Carbon

Since a transition metal methyl complex corresponds to a compound in which one hydrogen atom of methane is replaced by a transition metal (M), the M–C bond is considered to be a covalent bond or σ-bond. To understand the properties and reactivity of organometallic complexes, it is important to understand the character of M–C σ-bonds in transition metal alkyl complexes.

How is the σ-bond between a transition metal and carbon polarized? When considering a C–Cl bond, for example, since Cl is more electronegative than C, it is expected to be polarized $C^{\delta +}$–$Cl^{\delta -}$. M–C bonds may be considered in a similar way. A table of Allred–Rochow electronegativities is given in the Appendix. The electronegativity of carbon is given as 2.5. For transition metals, the electronegativity values are between 1.1 and 1.8, showing that all transition metals have lower electronegativity than carbon. Thus in any complex L_nM–CR_3, it is almost certain that the polarization of the M–C bond is $M^{\delta +}$–$C^{\delta -}$, regardless of the identity of M, the kind of ligand L and the substituent R.

The strength of the M–C bond varies depending on the other carbon substituents. Empirically, the M–C bond is stronger in a CF_3 complex than in a CH_3 complex. Generally, the stronger the electron-withdrawing property of the carbon substituents, the stronger the M–C bond. That is, the strength of the M–C bond increases in the following order:

$$M-{}^tBu < M-{}^nBu < M-Et < M-Me < M-Ph < M-CF_3$$
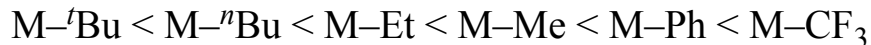
What factors are behind this ordering? The energy of the M–C bond corresponds to the energy required for radical cleavage of the bond. Since the M–C bond is inherently polarized $M^{\delta+}-C^{\delta-}$ as mentioned above, if the substituent of C is an electron-donating group (for example, CH_3), electron density on the C is pushed back towards M, reducing the polarization so that radical cleavage occurs more easily. On the other hand, if the substituent is an electron-withdrawing group (for example, CF_3), electron density on the C decreases, resulting in greater removal of electron density from M, which increases $M^{\delta+}-C^{\delta-}$ polarization, leading to higher energy radical cleavage of the M–C bond, and greater M–C bond stability (Figure 3.1). In fact, in thermal reactions of transition metal alkyl complexes, products are often generated which are considered to result from radical cleavage, although the M–C bonds are polarized $M^{\delta+}-C^{\delta-}$.
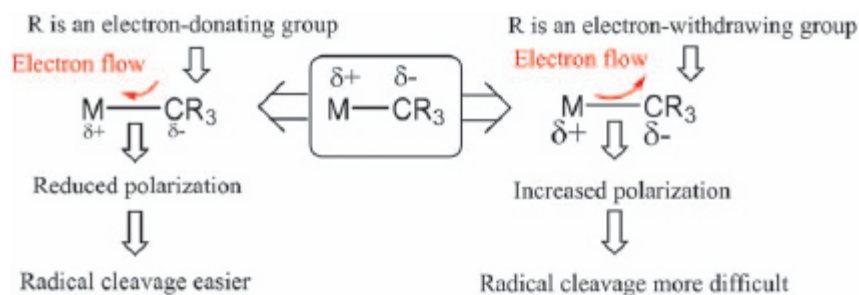
Figure 3.1 Trends in M–C bond strengths.

3.2 π-Bonds between Transition Metals and Carbon

3.2.1 π-Bond

This section describes π-bonds between transition metals and carbon. First, the difference between σ- and π-bonds is clarified.

Generally, when two atoms approach each other from infinity and make a bond to form a molecule, new molecular orbitals are created. The molecular orbitals are made by linear combination of the atomic orbitals of each atom. Regarding a bonding molecular orbital, it is formed by combining two atomic orbitals of the same symmetry (wave function sign). Although one

or more mirror planes containing the bond axis may exist in the bonding molecular orbital thus formed, it is important whether the sign of the orbital changes (reverses) by this mirror operation. A bond without such a mirror plane is referred to as a "σ-bond", and a bond in which there is one mirror plane is a "π-bond".

Consider the C–C bond of ethylene as an example (Figure 3.2). First, to make a σ-bond, the sp^2 hybridized orbital of one carbon atom approaches the sp^2 hybridized orbital of the other carbon. Although there are numerous mirror planes including the bond axis (in this case, the C–C bond) in the molecular orbital thus formed, the sign of the orbital does not change (does not invert), even if the mirror operation is performed for all the mirror planes. A bond like this with a bonding orbital whose sign does not change by mirror plane manipulation is called a "σ-bond". Next, consider a π-bond. To make this bond, the non-hybridized p orbital of one carbon (if the C–C bond axis is the z-axis, p_x and p_y orbitals can be considered, but here we consider the p_x orbital) is brought close to the non-hybridized p orbital of the other carbon. There are two mirror planes containing the bond axis in the molecular orbital (xz plane and yz plane). The sign of the orbital does not change by reflection in the xz plane. However, mirror operation of the yz plane causes the sign of the orbital to reverse (become inverted). A bond like this, with one mirror plane reversing the sign of the molecular orbital, is called a "π-bond".

C-C σ-bonding molecular orbital formed by overlap of two sp^2 hybridized orbitals of adjacent C atoms

C-C π-bonding molecular orbital formed by overlap of two p_x orbitals of adjacent C atoms
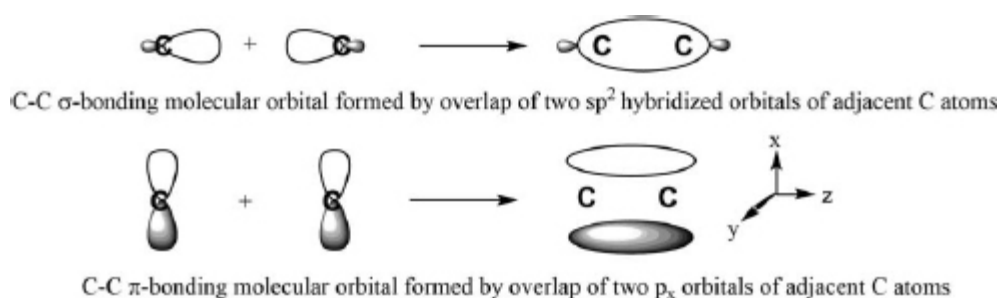
Figure 3.2   C–C σ-bond (top) and π-bond (bottom) of ethylene.

In addition, a δ-bond, which may be found between transition metals in complexes but not in organic chemistry, is explained. A bond with two mirror planes reversing the sign of the molecular orbital is called a "δ-bond". Such a bond arises from the "face-to-face" overlap of d orbitals as

shown in Figure 3.3, and both the *xz* plane and the *yz* plane are such mirror planes.

Figure 3.3   δ-Bond formed by overlap of d orbitals.

3.2.2   Metal–carbonyl Bond

Carbon monoxide is a very important ligand in organometallic chemistry. As mentioned before, when carbon monoxide coordinates to a transition metal, almost without exception, it is the carbon atom that binds to the metal. Figure 3.4(a) shows how a lone pair of electrons on the carbon in CO and an empty d orbital of a transition metal form a bond. When taking coordinate axes as shown in the figure, a lone pair of electrons on the carbon of the CO donates to the empty $d_{x^2-y^2}$ orbital. This bond is a σ-donor bond since there is no mirror plane reversing the sign of the bonding molecular orbital.
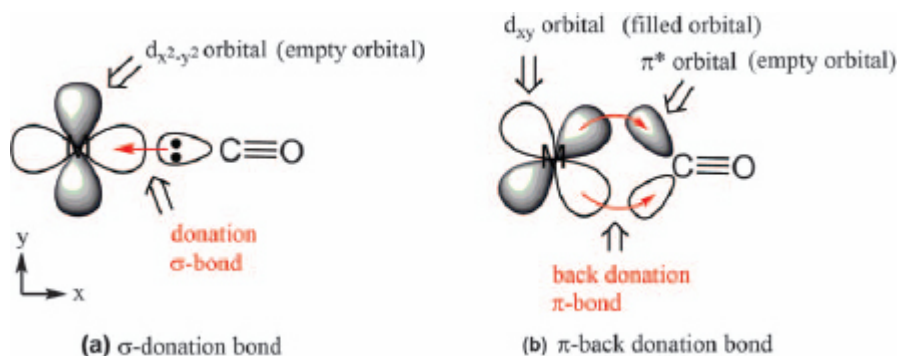
Figure 3.4   Bond between a transition metal and carbonyl.

Since carbon monoxide has two π-bonds between C and O, there are also π*anti-bonding orbitals, which are empty. When CO approaches along the *x*-axis and forms a σ-bond, the π* (p_y) orbital of CO can overlap with the d_{xy} orbital of the transition metal, since the symmetries are also correct (Figure 3.4(b)). When electrons are contained in this d_{xy} orbital, on forming

the M–CO bond, electron density flows from the metal d_{xy} orbital into the π^* (p_y) orbital of the carbonyl ligand. Usually, electron density flows from ligand to metal, but in this case the flow of electrons is reversed, so it is called "back-donation". Since there is one mirror plane reversing the sign of the bonding orbital, this is a π-bond. The electron density flow and this bond are sometimes referred to as π-back-donation and a π-back-donation bond, respectively, for expressing both features. Together the combination of σ-donation and π-back-donation is referred to as "synergic bonding".

3.2.3 Metal–olefin Bond

Olefins are also important ligands for organometallic complexes. Olefins coordinate to a transition metal by 2e-donation from the π bonding orbital of the C=C double bond. Further information about this bond is described below.

In olefins, the two carbons in the C=C double bond and the four C substituents are in the same plane. Olefin π electrons exist above and below the plane. Donation of these π electrons to an empty d orbital of a transition metal produces a bond. For the coordinate system shown in Figure 3.5, the olefin π electrons are donated to the empty $d_{x^2-y^2}$ orbital (a). Since there is no mirror plane reversing the sign of the bonding orbital, this is a σ-bond.[1]
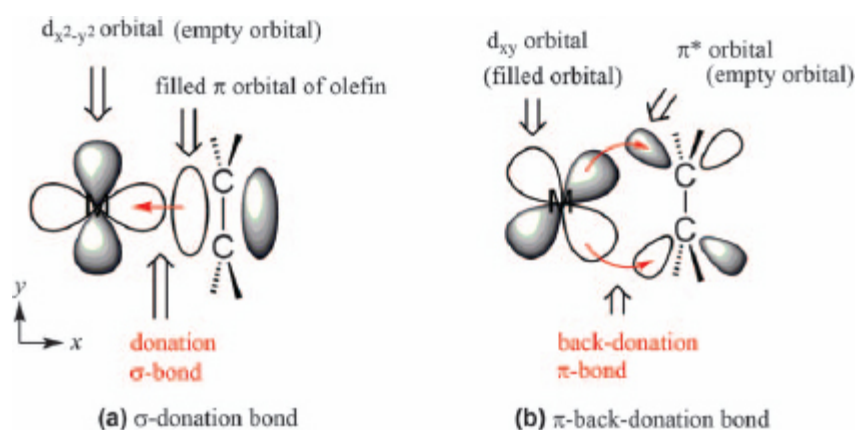
Figure 3.5   Bond between a transition metal and olefin (DCD model).

When a σ-bond is formed as shown in Figure 3.5(a), the π^* orbital of the olefin is correctly aligned to overlap with the d_{xy} orbital of the transition metal considering both orientation and symmetry. Additionally, if the metal

d_{xy} orbital contains electrons, electron density may flow into the π^* orbital of the olefin (Figure 3.5(b)). In this case, since there is one mirror plane (xz plane) reversing the sign of the bonding orbital, this is a π-bond. This bond is also referred to as a π-back-donation bond. Dewar, Chatt and Duncanson demonstrated that olefin-to-metal coordination is composed of both σ-donation and π-back-donation components. Appropriately, this bonding model is called the Dewar–Chatt–Duncanson (DCD) model.

3.3   Theoretical Considerations

Most organometallic compounds obey the 18e rule. This is not an empirical rule, but there are good reasons for it. In order to understand the reasons, it is necessary to understand the application of molecular orbital theory to transition metal complexes.[1] Crystal field theory explains in a clear and simple way how the transition metal d orbital energies split when ligands (considered as point charges) approach the metal to form a complex. However, while sufficient for understanding Werner-type (ionic) complexes, it is insufficient for understanding organometallic complexes, due to the substantial covalent character. Ligand field theory therefore emerged, combining molecular orbital and crystal field theory concepts, while remaining relatively simple. According to this theory, it is possible to understand why organometallic complexes follow the 18-electron rule. In this section, crystal field theory, and its successor, ligand field theory, are described.

3.3.1   Crystal Field Theory

A transition metal has five d orbitals, the designations and shapes of which are shown in Figure 3.6. Three of the orbitals (d_{xy}, d_{xz} and d_{yz}) can be arranged to point between the axes and two point along the axes ($d_{x^2-y^2}$ and d_{z^2}). These five d orbitals have the same energy (they are degenerate) when the metal atom exists alone (it does not form a complex). Next, let us consider how the d orbital energies split when ligands are bonded to a transition metal to form a complex. The splitting pattern of the d orbitals depends on how many ligands coordinate and their geometric arrangement around the transition metal. The splitting pattern of the d orbitals will be explained using the example of an octahedral complex, since this is easy to imagine in three dimensions.
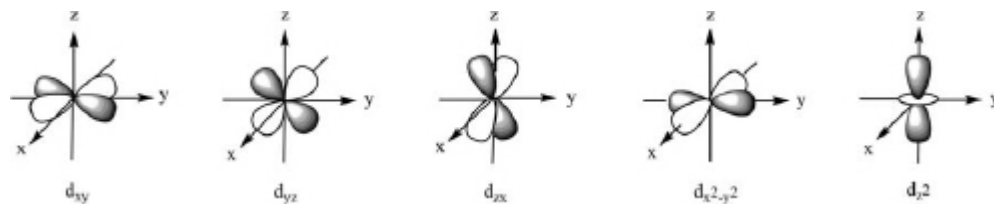
Figure 3.6   The five d orbitals.

To create an octahedral complex, a transition metal is placed at the origin and six point charges (ligands) are placed in the $+$ and $-$ directions of each coordinate axis, with a filled orbital pointing towards the metal. Various molecules and ions serve as ligands, but considering the essence of a ligand, it means that a ligand donates a lone pair of electrons to a metal d orbital. Thus, in crystal field theory, a ligand is simplified and considered as a point negative charge. Furthermore, only the charge effect is considered without considering the steric viewpoint. In that sense, an octahedral complex can be expressed as a symmetric arrangement of six point charges on the coordinate axes around the origin. A step by step consideration of how the d orbitals split is shown in Figure 3.7.
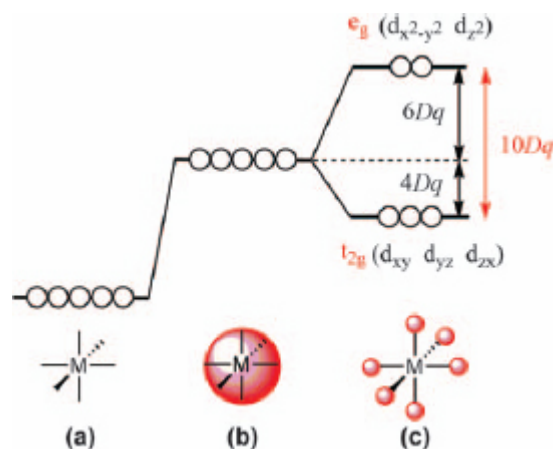
Figure 3.7   Splitting of metal d orbitals in (a) zero, (b) spherical, and (c) octahedral crystal fields.

Figure 3.7(a) shows the case where the metal exists alone (in the absence of any field), and the five d orbitals are degenerate. Figure 3.7(b) shows the case where six point charges exist around the metal in a spherically symmetrical arrangement so that the orbitals are still degenerate. Their energies, however, have increased due to approach by the ligand negative

charges and the resulting increased repulsion. Figure 3.7(c) shows the case where the six negative charges are localized into the plus and minus directions on each axis to form an octahedral complex. In this case, the lobes of the $d_{x^2-y^2}$ and d_{z^2} orbitals extend toward the ligands along each axis and their energies rise accordingly, and in equal amounts. In contrast, since the lobes of the d_{xy}, d_{yz} and d_{zx} orbitals point between the axes, and thus not at, but between the ligands, their energies are reduced, by the same extent, since the ligand charges and d_{xy}, d_{yz} and d_{zx} orbitals are further apart. These three lower energy orbitals constitute the t_{2g} set of orbitals, and the two higher energy orbitals constitute the e_g set, and the energy difference between them is known as the crystal field splitting parameter, denoted as $10Dq$ or Δ_o, (where the subscript o refers to the octahedral geometry). Although both Dq and Δ notations can be seen in texts, only the Dq notation is used below for simplicity. The total energy of the states shown in (b) and (c) is the same since the amount and proximity of the charges is the same, and only their localization changes. In (c), occupation of one of the t_{2g} orbitals by one electron thus results in stabilization relative to (b) with one electron due to the crystal field splitting. This stabilization is called the crystal field stabilization energy (CFSE), and has the value of $-4Dq$ per electron. If all the t_{2g} orbitals are fully occupied (six electrons in total) the CFSE is $-24Dq$. Of course, electrons placed in the higher energy e_g orbitals will result in destabilization of $+6Dq$ per electron. Thus for fully occupied d orbitals, the stabilizing CFSE is $-24Dq$ for the six electrons in the t_{2g} set and $+24Dq$ for the four electrons in the e_g set, giving a total of zero (due to summing over the coordination sphere).

As noted above, in an octahedral crystal field, the five d orbitals are divided into a triply degenerate t_{2g} set and a doubly degenerate e_g set of orbitals. If an electron in one of the t_{2g} orbitals absorbs energy corresponding to the crystal field splitting ($10Dq$) it may be promoted to an upper e_g orbital if there is a vacancy. This transition is termed a d–d transition, because an electron transitions from one d orbital to another. Electronic transitions are also subject to certain rules called selection rules, which govern whether or not they are allowed. In many complexes, the d–d transition energy (which is the crystal field splitting energy, $10Dq$) corresponds to the energy of visible light. The observed color of the

transition metal complex is the complementary color of the absorbed visible light. For example, when a complex absorbs red light, the complex appears to be bluish green. Since the energy of the d–d transition changes according to the structure and geometry of the complex, the wavelength of the visible light absorbed, and thus the observed color, also depends on those factors. This is the reason that transition metal complexes exhibit various colors.

Let us consider how electrons are arranged in d orbitals subject to crystal field splitting. For a d^3 complex, such as Cr(iii), one electron is placed in each of the three orbitals of the t_{2g} set, obeying the Aufbau, Hund and Pauli rules. In the case of a d^4 complex also obeying the rules, the fourth electron pairs in one of the already half occupied t_{2g} orbitals, affording a low spin complex (Figure 3.8(a)). To effect this pairing, however, requires energy, known as the pairing energy, P, in order to overcome the repulsive force resulting from placing two electrons in the same region of space. However, instead of entering a t_{2g} orbital, if the energy cost ($10Dq$) of using one of the higher energy e_g orbitals is less than the energetic cost of pairing the electrons in the t_{2g} (P) the fourth electron may "disobey" the Aufbau rule for the reason that the overall energy cost is lower, and enter an e_g orbital (Figure 3.8), maximizing the stabilizing exchange energy arising due to having parallel unpaired electron spins. Such a complex is called a high spin complex (Figure 3.8(b)). Since the number of unpaired electrons differs between low and high spin states, we can determine which state is actually adopted by measuring the magnetic properties of the complex. For d^1 to d^3 and d^8 to d^{10} complexes, there is only one possibility for the final electron, so the question of high spin or low spin does not arise. For d^4 to d^7 complexes, however, two possible spin states exist: low spin and high spin.
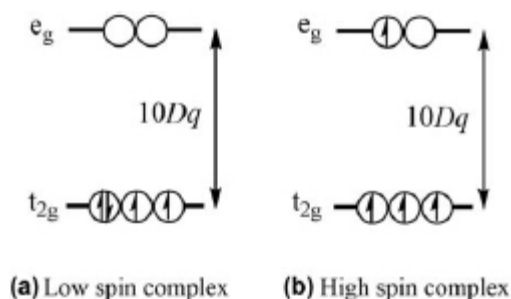

(a) Low spin complex   (b) High spin complex

Figure 3.8   Low spin and high spin for a d^4 complex.

The size of 10Dq thus affects the color, magnetism and reactivity of metal complexes. Factors affecting the size of 10Dq are described below.

   (1) **Central metal**
   10Dq depends on the transition metal. 10Dq increases by about 50% for each element down a group.
   (2) **Oxidation number of the central metal**
   As the oxidation number of the central metal increases, the metal becomes more electron deficient and thus attracts the ligands more strongly. The closer proximity of the ligands to the metal results in greater ligand–d orbital interaction, which in turn increases the crystal field splitting energy.
   (3) **Number of ligands and geometry**
   The crystal field splitting pattern and the magnitude of the splitting of the d orbital energies depend on the number of ligands and the geometry of the metal complex. The example of a hexacoordinate octahedral complex was described above due to its ready visualization. It should be noted that complexes with other geometries, such as tetrahedral or square-planar ML_4, have different d orbital splitting patterns. See Figure 3.14 for square-planar complexes and Figure 3.15 for tetrahedral complexes.
   (4) **Ligand type**
   10Dq also depends inherently on the type of ligand. Ryutaro Tsuchida found that a ligand enhancing d–d splitting in one complex similarly enhances d–d splitting in other complexes. Ligands can be arranged in order of their effect on the d–d transition energy in the "spectrochemical series". Common ligands are listed below in order of decreasing crystal field splitting effect:

$$CO > CN^- > PPh_3 > NO_2^- > NH_3 > CH_3CN > H_2O > OH^- > F^- > Cl^- > Br^- > I^-$$
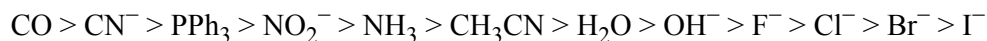
3.3.2   Ligand Field Theory (LFT)

Crystal field theory, introduced above, is very useful for understanding the d orbital splittings of transition metal complexes. However, there are many observations that cannot be explained by this theory. For example, although a CO ligand is a neutral molecule with no charge and little polarization, it is located at the top of the spectrochemical series. This cannot be explained by CFT. This is because a ligand is considered as a point charge in CFT, and π-back-donation from the metal to the CO ligand has not been considered at all. There are many organometallic transition metal complexes in which π-back-donation is important, and for which CFT cannot provide a suitable explanation. "Ligand field theory (LFT)" was thus developed to address these issues, allowing ligands to be treated as more than simple point charges and bonding as not just a simple electrostatic interaction by

incorporating ideas from molecular orbital theory. In this theory, π-back-donation is also considered. LFT is described below.

Again, an octahedral complex, ML_6 is taken as an example because it is easier to visualize in three dimensions. The molecular orbitals of a complex are basically constructed from orbitals derived from the transition metal (M) and ligands (L). However, instead of considering each M–L orbital overlap individually, it is conceptually much simpler to consider orbitals composed of a combination of the metal orbitals (nd, $(n + 1)$s and $(n + 1)$p orbitals) and the orbitals of the group of six ligands arranged octahedrally (ligand group orbitals or symmetry-adapted linear combinations (SALCs)). In order for two orbitals to form a molecular orbital, the symmetry needs to be matched. When considering the molecular orbitals of diatomic molecules, it is possible to judge whether orbital symmetry matches or not by drawing the shapes of the corresponding atomic orbitals, but considering a metal and six ligands, it is more difficult to judge this, so group theory will be used. For details of group theory, the reader should refer to a specialized book; here, only the results will be used. The group orbitals consisting of the six ligands arranged octahedrally (no metal atom yet at the center) are represented by the irreducible representations a_{1g}, e_g and t_{1u}. Here, a, e, and t signify zero degeneracy, double degeneracy and triple degeneracy, respectively. Six ligand group orbitals, $1(a_{1g}) + 2(e_g) + 3(t_{1u})$, are thus generated from the six ligands. For the transition metal, the d orbitals are expressed by the irreducible representations of e_g and t_{2g} for the nd orbitals, the $(n + 1)$s orbital is expressed by a_{1g}, and the $(n + 1)$p orbital is expressed by t_{1u}. Symmetry matching when making molecular orbitals corresponds to having matching irreducible representations.

Since there are orbitals with irreducible representations of a_{1g}, t_{1u}, and e_g for both the metal and ligand group, molecular orbitals for ML_6 can be formed (Figure 3.9). The ligand group orbitals have no orbital with the t_{2g} irreducible representation, so the t_{2g} orbital on the metal side does not form a molecular orbital and remains non-bonding. Regarding the energy levels, information cannot be obtained from the discussion of symmetry using group theory, so the energy levels shown in Figure 3.9 are based on experimental data.
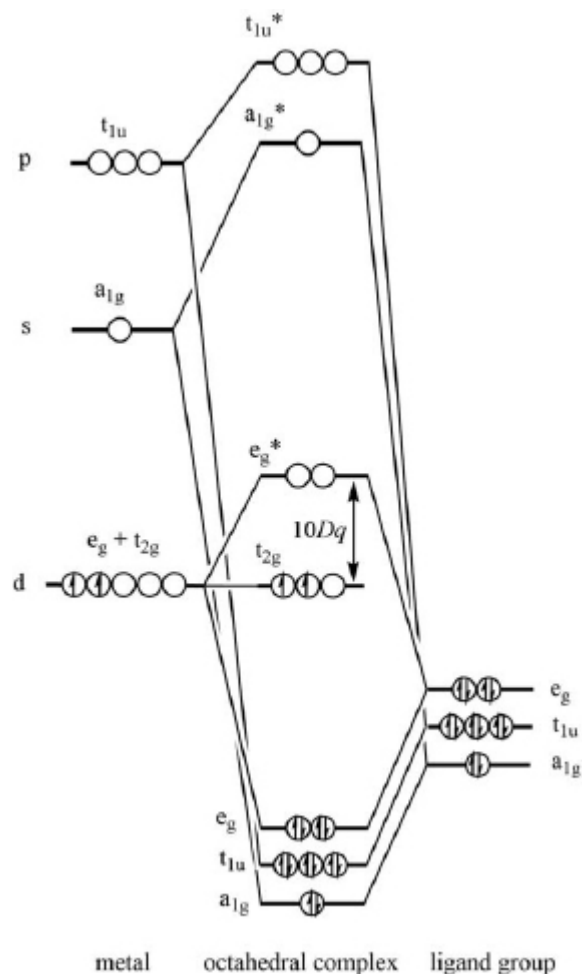
Figure 3.9   Molecular orbitals of an octahedral d^2 complex.

Since a ligand usually donates a lone pair of electrons to a metal, for an octahedral complex, a total of twelve electrons are donated from the six ligands. These electrons, together with the electrons already in the metal d orbitals, constitute the total set of electrons to be assigned to the ML_6 molecular orbitals. Considering a d^2 complex, fourteen electrons are placed in the molecular orbitals according to the Aufbau, Hund and Pauli conditions: two electrons in the a_{1g}, six in the t_{1u}, four in the e_g, and two in the t_{2g} orbitals. It is essentially meaningless to argue whether the electrons in the t_{2g} orbital, for example, are electrons "originally in the ligand" or "from the metal d orbitals". However, for convenience, it may be easier to consider that the electrons in the ligands enter the bonding molecular orbitals (a_{1g}, t_{1u}, and e_g orbitals) and the metal d electrons occupy the t_{2g}

orbital (this latter aspect corresponds to the CFT situation). The transition from HOMO to LUMO is a transition from t_{2g} to e_g^*, which corresponds to $10Dq$. The crystal field and ligand field theories thus correlate well so far.

Some of the differences between CFT and LFT will now be addressed. One difference concerns the fact that in CFT, d electrons in the t_{2g} orbital result in crystal field stabilization energy, but in LFT, since the t_{2g} orbital is a non-bonding orbital, there is no energy gain or loss on placing electrons there.

A second difference concerns π-back-donation, which cannot be rationalized using CFT. Consider the t_{2g} and e_g orbitals occupied by the metal d electrons. The t_{2g} set consists of the d_{xy}, d_{yz}, and d_{zx} orbitals. The e_g^* orbital is the anti-bonding molecular orbital constructed from the metal $d_{x^2-y^2}$ and d_{z^2} orbitals and ligand group orbitals with e_g symmetry. Since the e_g^* orbital is energetically close to the metal $d_{x^2-y^2}$ and d_{z^2} orbitals, it is considered to be mainly composed of the $d_{x^2-y^2}$ and d_{z^2} orbitals. Consider the interaction of the d_{yz} orbital, for example, in the t_{2g} set with a CO ligand located on the y axis (Figure 3.10). The symmetry of the d_{yz} orbital does not match with that of the lone pair of electrons on the carbon of a CO ligand located on the y axis (left side in Figure 3.10), but it does match with that of the π^* orbitals of the CO ligand (right side in Figure 3.10). Similarly, CO ligands on the x and z axes can π-interact with the d_{xy} and d_{yz} orbitals of the metal, respectively, to give new bonding t_{2g} and anti-bonding t_{2g}^* orbitals. This situation is shown in Figure 3.11. The π^* orbital of CO (constructed by the out of phase interaction of the carbon monoxide C and O p_y orbitals) is an anti-bonding orbital, so the energy level is high. The symmetry of the ligand group π^* orbitals of the CO ligands is t_{2g}. When the metal t_{2g} set (d_{xy}, d_{yz}, d_{zx}) makes molecular orbitals with the ligand t_{2g} set (the ligand group π^* orbitals of the CO ligands), the energy of the bonding t_{2g} orbitals in which the electrons are accommodated is lower than before making the molecular orbitals. $10Dq$ therefore increases. This is the reason why the CO ligand, despite being a neutral molecule with little polarity, is located at the top of the spectrochemical series.

d_{yz} orbital and σ orbital of C.
Symmetry does not match.

d_{yz} orbital and π^* orbital of CO.

Since symmetry matches,
molecular orbital is formed.
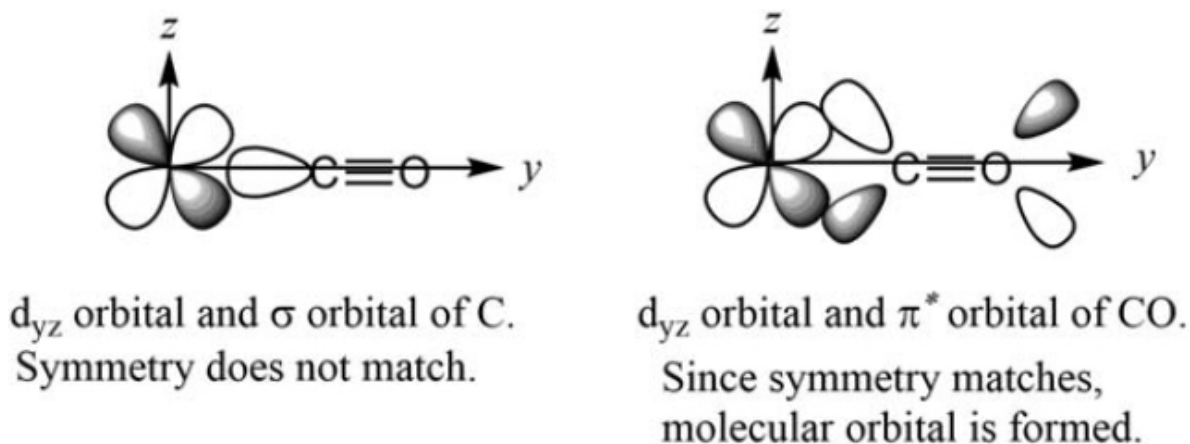
Figure 3.10 Overlap of metal d_{yz} and CO ligand orbitals.
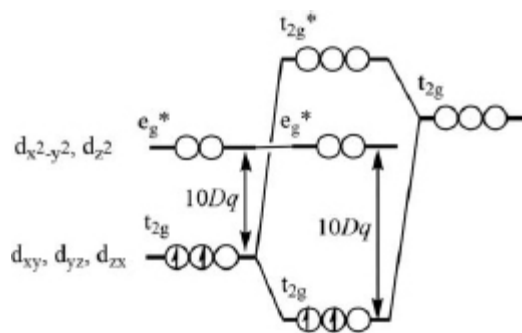
Figure 3.11 Octahedral ligand field splitting of metal d orbitals including π-back-donation.

Next, consider a ligand with filled π symmetry orbitals, such as a halogen (Figure 3.12). The energy level of the π symmetry orbital is lower because it is filled with electrons. When the ligand π orbital and the t_{2g} orbital of the metal form a molecular orbital, d electrons must enter the higher energy, anti-bonding molecular orbitals created (t_{2g}^* orbitals) since the bonding t_{2g} orbitals are already occupied (by ligand electrons). As a result, $10Dq$ decreases (Figure 3.13), which is why π-donating ligands such as halogens are lower in the spectrochemical series.
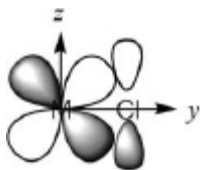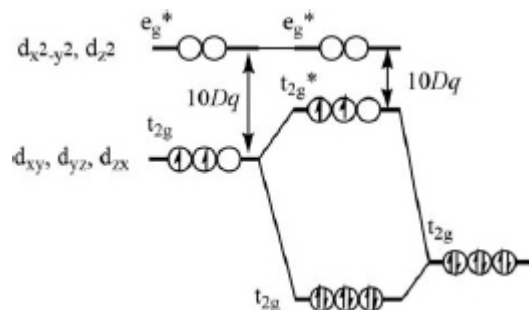
Figure 3.13 Octahedral ligand field splitting of a metal d orbital including π-donation.

Ligand field theory can be summarized as follows. In the cases of complexes with ligands that have σ-interaction with a transition metal, but do not have π-interactions (such as amines), the molecular orbital diagram shown in Figure 3.9 is adopted. The d orbitals of the metal comprise a bonding e_g set, an anti-bonding e_g* set and a non-bonding t_{2g} set, and the metal d electrons are accommodated in the t_{2g} and e_g* orbitals. The energy gap between these two sets of orbitals corresponds to $10Dq$. In the cases of complexes with ligands that accept electron density from the metal by π-back-donation (π-acid ligands, such as carbonyl), the empty t_{2g} ligand group orbital (SALC), and the metal t_{2g} orbital overlap, forming complex molecular orbitals with new bonding t_{2g} and antibonding t_{2g}* orbitals (Figure 3.11). In this case, since the metal d electrons are accommodated in the t_{2g} and e_g* orbitals, $10Dq$ becomes larger. In the cases of complexes with ligands that donate π electrons (π-basic, such as halogens), the filled t_{2g} ligand group orbital set and the metal t_{2g} set in the complex combine to form new t_{2g} and t_{2g}* molecular orbitals (Figure 3.13). In this case, since the metal d electrons are accommodated in the t_{2g}* and e_g* orbital sets, $10Dq$ becomes smaller.

3.3.3 Reason for the Establishment of the 18e Rule

Most organometallic complexes follow the 18e rule, although there are many transition metal complexes that do not. All of the complexes shown in Table 3.1 actually exist, though there are many for which the total valence electron number is not 18. These complexes can be divided into three

groups. Complexes in Group 1 contain metals in the first transition metal series and do not have a π-back-donating ligand. Most of these complexes do not follow the 18e rule and their total valence electron numbers are between 12 and 22. Complexes in Group 2 have metals in the second or the third transition metal series and also have no π-back-donating ligand. These complexes do not obey the 18e rule, but none has more than eighteen valence electrons in total. All the complexes in Group 3 follow the 18e rule and contain a π-back-donating ligand.

Table 3.1   Total valence electron number of various complexes.

Group 1		Group 2		Group 3	
$[VCl_6]^{2-}$	13	$[WCl_6]^-$	13	$[Fe(CO)_5]$	18
$[Fe(OH_2)_6]^{2+}$	18	$[PtF_6]$	16	$[Co(CO)_4]^-$	18
$[Ni(en)_3]^{2+}$	20	$[OsCl_6]^{2-}$	16	$[HMn(CO)_5]$	18
$[Cu(NH_3)_6]^{2+}$	21	$[ZrF_6]^{2-}$	12	$[V(CO)_6]^-$	18
$[Zn(en)_3]^{2+}$	22	$[PtCl_4]^{2-}$	16	$[Mo(CO)_3(PPh_3)_3]$	18
$[TiF_6]^{2-}$	12			$[CoMe(CO)_4]$	18
$[Co(OH_2)_6]^{2+}$	19				

en = $H_2NCH_2CH_2NH_2$

Consider the characteristics of these complexes from the perspective of ligand field theory. Since the complexes in Group 1 have only σ- or π-donor ligands, the molecular orbitals shown in Figure 3.9 or Figure 3.13 are used. Furthermore, since these are first row transition metal complexes, $10Dq$ is relatively small. Looking at Figure 3.9, since a_{1g}, t_{1u}, and e_g are bonding molecular orbitals, occupation by electrons results in stabilization. In other words, at least twelve electrons should be accommodated. If the t_{2g} set is additionally occupied, since it is a non-bonding orbital, the system is neither stabilized nor destabilized, and a total of eighteen metal and ligand electrons can be accommodated. However if still more electrons are to be accommodated, up to a total of twenty-two, they must enter the anti-bonding e_g* orbitals above the t_{2g} orbitals, resulting in destabilization. The degree of destabilization (magnitude of $10Dq$) is relatively small, so it is also possible for electrons to enter these orbitals. At still higher energy yet is the $a_{1g}*$ orbital and occupation of this would cause considerable destabilization of the system, and stable examples of such complexes do not

exist. The total valence electron count of complexes classified as Group 1 is thus between twelve and twenty-two.

Complexes in Group 2 contain second or the third row transition metals. $10Dq$ is thus relatively large (see above) so that if electrons were to enter the e_g^* orbitals, destabilization of the whole system would occur. Group 2 complexes are those in which the metal t_{2g} orbitals (non-bonding) accept electrons, and thus the total valence electron number is between 12 and 18.

Complexes in Group 3 show the d orbital splitting pattern shown in Figure 3.11, so that occupation of the t_{2g} orbitals results in stabilization. Therefore, the total valence electron number is thus 18. This is why many organometallic complexes fulfill the 18-electron rule: they contain ligands that accept electron density from the metal by π-back-donation.

Up to this point, the theories have been explained using the example of octahedral complexes, since these are conceptually easy to understand. The theories of course also apply to complexes with other geometries. When the three-dimensional structure is changed, the ligand group orbitals (SALCs) also change and the resulting molecular orbitals change. However, in any complex, equal numbers of bonding and anti-bonding molecular orbitals are formed and orbitals that are neither will be non-bonding orbitals.

Let us consider whether the 18e rule can be applied generally to ML_n complexes. Since there are n ligands, there are n ligand group orbitals with σ symmetry. It is necessary to verify in each case whether these ligand group orbitals match the symmetry of the orbitals prepared on the metal side, but in fact, suitable symmetries can be found in all cases. Thus, in an ML_n complex, n bonding molecular orbitals and n anti-bonding orbitals are formed. On the metal side, a total of nine orbitals (five d and in the next row down, one s and three p orbitals) are available for making molecular orbitals. The number of orbitals which thus do not form molecular orbitals with the ligand group orbitals is 9-n (non-bonding orbitals). So far, only σ donor bonds are considered. If π-back-donation is considered, the orbitals that are non-bonding in the σ-only case will form bonding and anti-bonding molecular orbitals for any number of n, so that π-back-donation results in 9-n stabilized orbitals. Thus, if electrons are accommodated in n orbitals stabilized by σ bonds and 9-n orbitals stabilized by π-back-donation bonds, the system is stabilized as a whole. Since two electrons enter each orbital,

the total number of valence electrons in orbitals is given by $\{n + (9–n)\} \times 2 = 18$, and in general the 18-electron rule holds for ML_n complexes.

3.4 Reason Why a Four-coordinate d⁸ Complex Adopts a Square-planar Structure

The structures of the complexes were described in Section 2.6. When the coordination number is decided, the basic structure is determined. However, in the case of a four-coordinate complex, it was noted that there are two structural possibilities: tetrahedral and square-planar. Although a tetrahedral structure is more favorable sterically, in the case of a d^8 complex, electronic effects outweigh the steric, so that a square-planar structure is adopted. The manner in which the electronic effect works is shown in Figure 3.14.
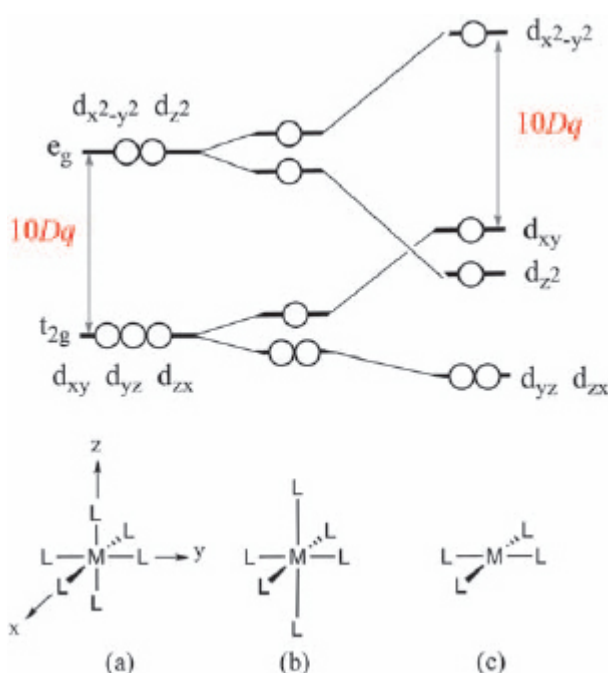

Figure 3.14 (a) Octahedral complex, (b) tetragonally distorted state (bonds to z axis ligands stretched), and (c) square-planar (the bonds to z axis ligands are infinitely long).

To consider the metal d orbital splitting in a square-planar complex, it is easiest to start from an octahedral complex. As described above in both CFT and LFT, for an octahedral complex, the d orbitals split into the lower energy triply degenerate t_{2g} set and the higher energy doubly degenerate e_g

(e_g^* in ligand field theory) set (Figure 3.14(a)). If the two ligands on the z axis of this octahedral complex are then moved slightly away from the metal, the d orbitals with a component in the z direction (d_{yz}, d_{zx}, d_{z^2}) decrease in energy, while the remaining d orbitals (d_{xy}, $d_{x^2-y^2}$) increase in energy (Figure 3.14(b)). If these two ligands on the z axis are then further displaced to an infinite distance, a square-planar complex results (Figure 3.14(c)). The d_{yz}, d_{zx}, and d_{z^2} orbitals are further stabilized and the d_{xy} and $d_{x^2-y^2}$ orbitals rise further, eventually resulting in reversal of the d_{xy} and d_{z^2} energy levels. Since the d_{xy} and $d_{x^2-y^2}$ orbitals are equally affected by the ligands on the z axis, the energy difference between them remains at $10Dq$. Thus, a square-planar complex has the doubly degenerate d_{yz} and d_{zx} orbitals at the lowest energy level, followed by the d_{z^2}, then the d_{xy} and finally, at the highest level, the $d_{x^2-y^2}$ orbital. Since the $d_{x^2-y^2}$ orbital is considerably higher than the other four d orbitals, d^8 complexes, in which the $d_{x^2-y^2}$ orbital is vacant, are quite stable.

The other geometry for a four-coordinate complex is the tetrahedral structure. The d orbital splitting pattern is shown in Figure 3.15. Although the reason for the splitting pattern is omitted, the following points should be noted: (i) the orbitals of a tetrahedral complex split into doubly degenerate and triply degenerate orbital sets reversed in energy order in comparison to the octahedral case, and (ii) the splitting value ($10Dq$) for a tetrahedral complex is 4/9 that for an octahedral complex (assuming that the difference is due solely to the difference in number and geometry of the ligands).
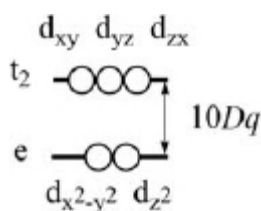

Figure 3.15   d orbital splitting in a tetrahedral complex.

Thus, considering steric repulsion between four ligands, a tetrahedral geometry is favored; however, for d^8 complexes, a square-planar structure is electronically advantageous. Since a square-planar complex has four

ligands, four bonding and four anti-bonding molecular orbitals are formed from four ligand group orbitals and appropriate transition metal d, s, and p orbitals. The bonding molecular orbitals accept eight electrons and the low-lying four d orbitals of the transition metal (see Figure 3.14(c)) can be considered to accommodate the eight metal electrons to form a stable complex. This is the reason why four coordinate d^8 complexes are 16-electron complexes and adopt square-planar geometries.

> **Problem 6.** BF_4^-, $[FeCl_4]^-$, and $[NiBr_4]^{2-}$ adopt tetrahedral rather than square-planar geometries. Explain why.

References

1. D. M. P. Mingos, *J. Organomet. Chem.*, 2001, **635**, 1.

---

[1] This bond may be misunderstood to be a π-bond since it forms a bond with a transition metal using the π electrons of an olefin. Clear understanding of the definitions of σ- and π-bonds avoids such confusion.

Chapter 4

Carbonyl, Olefin and Phosphine Complexes

Hiroshi Nakazawa[a]

[a] Osaka City University Osaka, Japan
Email: nakazawa@sci.osaka-cu.ac.jp

4.1 Introduction

Carbonyl, olefins, and phosphines are fundamental ligands in organometallic complex chemistry. Complexes containing these ligands are discussed in detail in this chapter.

4.2 Carbonyl Complexes

The bonding in transition metal complexes with carbonyl ligands was discussed in Section 3.2.2. This situation is shown again in Figure 4.1(a). The bond between a transition metal (M) and a carbonyl ligand (CO) consists of both a σ-donor bond, which is formed by donation of a lone pair of electrons on the carbon of the CO to an empty d orbital of the transition metal, and π-back-donation from a filled metal d orbital to an empty π* orbital of the CO. Looking only at the M–CO bond, these directionally opposite interactions in a "give and take" relationship of electron density, are referred to as "synergic bonding". On the other hand, the M–CO bond strength of the complex represented by L_nM–CO also depends on the influence of the ligands (L) other than CO bound to M. When L is electron-donating, then the electron density of M increases, so that π-back-donation to CO increases and the CO σ-donation contribution decreases. Conversely, when L is electron-withdrawing, the electron density of M decreases, so

that σ-donation increases and π-back-donation decreases. In fact, as the former complexes have stronger M–CO bonds, the π-back-donation component has a significantly greater effect than the σ-donation component in an M–CO bond. Put simply, the stronger the π-back-donation, the stronger the M–CO bond.
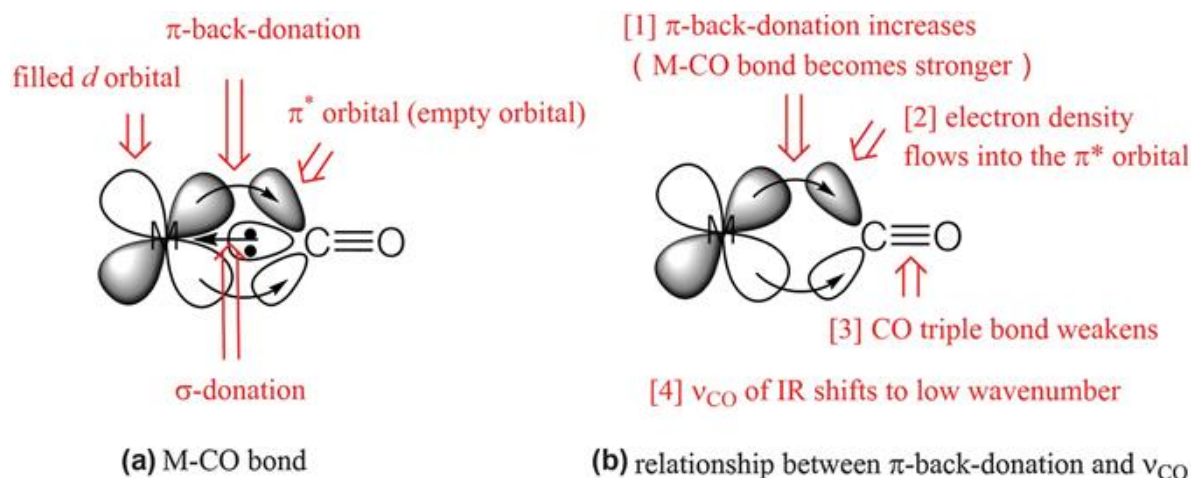

Figure 4.1   Bond between a transition metal and a carbonyl ligand.

The wavenumber of the stretching vibration of the C≡O bond (v_{CO}) in the infrared absorption spectrum of a transition metal carbonyl complex is a very useful indicator of the strength of the M–CO bond. The change of v_{CO} as the π-back-donation increases is illustrated in Figure 4.1(b).

The following statements in [1] to [4] correspond to the numbers in Figure 4.1.

[1] π-back-donation from a filled metal d orbital to an empty π* orbital of CO increases.
[2] The flow of electron density into the π* orbital increases.
[3] Since the π* orbital is an anti-bonding orbital of the CO triple bond, the flow of electron density into it results in weakening of the CO triple bond.
[4] The wavenumber of the stretching vibration (v_{CO}) of the CO bond in the IR spectrum is proportional to the square root of the strength of the CO bond. As the CO bond weakens, v_{CO} shifts to lower wavenumbers, so v_{CO} will be observed at a lower wavenumber as π-back-donation increases.

If the relationship described above is understood, it is possible to estimate the relative strength of the M–CO bond from the v_{CO} value among similar carbonyl complexes.

Three d^6 hexacarbonyl complexes are shown in Table 4.1. It is apparent that the v_{CO} values of the cationic complex, the neutral complex, and the anionic complex are shifted to lower wavenumbers relative to free CO, in this order. This observation can be interpreted as an indicator of the relative electron densities on the transition metal, which also increase in this order, with greatest π-back-donation from M to CO in the case of the metal with the greatest electron density ($[V(CO)_6]^-$). Table 4.2 shows the v_{CO} values of tetracarbonyl d^{10} complexes. In these cases too, as the electron density of the central metal increases, the v_{CO} value shifts to lower wavenumber, and it is expected that the strength of the M–CO bond is in the order $[Fe(CO)_4]^{2-} > [Co(CO)_4]^- > [Ni(CO)_4]$.

Table 4.1 v_{CO} values for $[M(CO)_6]$.

Complex	v_{CO}/cm^{-1}
$[Mn(CO)_6]^+$	2090
$[Cr(CO)_6]$	2000
$[V(CO)_6]^-$	1860

Table 4.2 v_{CO} values for $[M(CO)_4]$.

Complex	v_{CO}/cm^{-1}
$[Ni(CO)_4]$	2060
$[Co(CO)_4]^-$	1890
$[Fe(CO)_4]^{2-}$	1790

As noted above, since the M–CO bond strength in a carbonyl complex is mainly determined by the degree of π-back-donation from the transition metal to the carbonyl ligand, it should also be possible to predict approximately the v_{CO} wavenumber in a carbonyl complex. The following three items should be considered, in this order:

(1) The charge of the complex
The larger the negative charge, the greater the electron density of the central metal and the greater the π-back-donation to the carbonyl ligand, so the v_{CO} wavenumber shifts to a lower value.
(2) The number of d electrons of the central metal
As the number of d electrons increases, the electron density at the central metal increases and the possibility of π-back-donation to the carbonyl ligand increases, resulting also in a shift of v_{CO} wavenumber to a lower value.
(3) Electron-donating ability (Lewis basicity) of other ligands

As the number of electron-donating ligands in the complex increases or the electron donating ability of a ligand increases, the electron density of the central metal increases and the π-back-donation to the carbonyl ligand increases, also resulting in a shift of v_{CO} wavenumber to a lower value.
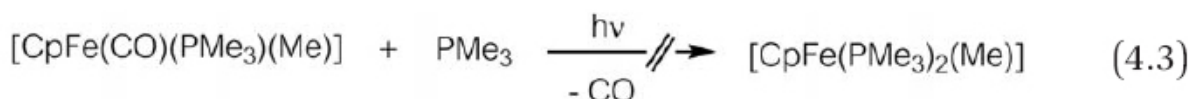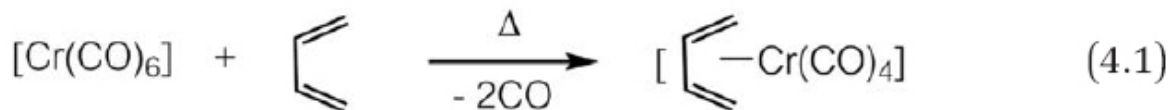
Thus, even if the number of d electrons on the central metal is small, but the negative charge of the whole complex is large, the latter factor will predominate, and a relatively low wavenumber for v_{CO} in the complex is to be expected.

It should be noted here that this relationship holds only when similar complexes are compared. Comparing v_{CO} values between complexes that are not very similar may lead to incorrect predictions. For example, simply comparing the v_{CO} values of the d^6 complex $[Cr(CO)_6]$ and $[Ni(CO)_4]$, which is a d^{10} complex, it might be thought that the v_{CO} value in $[Ni(CO)_4]$ should be the lower, since Ni has more d electrons and thus greater electron density. However, as Tables 4.1 and 4.2 show, the v_{CO} value for $[Ni(CO)_4]$ (2010 cm^{-1}) is higher than that for $[Cr(CO)_6]$ (2000 cm^{-1}). This is because the v_{CO} values of rather dissimilar complexes were compared. Thus, although the v_{CO} values in the IR spectra of carbonyl complexes provide useful information about the M–CO bond strength, caution needs to be exercised, particularly when comparing complexes with significant differences.

Box 4.1 Problem 7. Which complex is more likely to have the lower IR v_{CO} value?

(1) $[W(CO)_5Cl]^-$	or	$[Re(CO)_5Cl]$
(2) $[Fe(CO)_5]$	or	$[Fe(CO)_4Br_2]$
(3) $[Mo(CO)_6]$	or	$[Mo(CO)_4(PPh_3)_2]$
(4) $[Mo(CO)_4(PMe_3)_2]$	or	$[Mo(CO)_4(PPh_3)_2]$
$[CpFe(CO)_2Br]$	or	$[CpFe(CO)_2]^-$

Since a carbonyl ligand dissociates relatively easily from the central metal by heating or UV irradiation, in the presence of other ligands, a carbonyl ligand may be readily substituted. Some examples are shown below.

$$[Cr(CO)_6] \; + \; \text{(butadiene)} \; \xrightarrow[-2CO]{\Delta} \; [\text{(butadiene)}{-}Cr(CO)_4] \qquad (4.1)$$

$$[CpFe(CO)_2(Me)] + PMe_3 \xrightarrow[-CO]{h\nu} [CpFe(CO)(PMe_3)(Me)] \qquad (4.2)$$

$$[CpFe(CO)(PMe_3)(Me)] \; + \; PMe_3 \; \xrightarrow[-CO]{h\nu} \!\!\!/\!\!\!\!\rightarrow \; [CpFe(PMe_3)_2(Me)] \qquad (4.3)$$

Since a carbonyl ligand is a good acceptor of π-back-donated electron density (a strong π-acid ligand), the π-acidity of a ligand newly introduced by substitution of a carbonyl ligand is often weaker than that of the carbonyl ligand. Thus, as the carbonyl ligands are replaced by other ligands, the remaining carbonyl ligand receives a greater amount of π-back-donated electron density and its M–CO bond becomes stronger. That is, as the number of remaining carbonyl ligands decreases, their ease of substitution decreases, and it is found generally that substitution of the last carbonyl ligand rarely occurs (see eqn (4.3)).

Organometallic complexes with both carbonyl and alkyl ligands exhibit CO insertion reactions, which is one of the characteristic reactions of organometallic compounds. This reaction will be discussed in detail in Section 6.4.1.

4.3 Olefin Complexes

The bonding pattern of transition metal complexes with olefins as ligands was discussed in Section 3.2.2. This situation is shown again in Figure 4.2. The bond between a transition metal (M) and olefin consists of both a σ-donor bond, which is formed by donation of π electron density from the C=C double bond to an empty d orbital of the transition metal, and π-back-donation from a filled d orbital of the transition metal to an empty π* orbital of the C=C double bond (DCD: Dewar–Chatt–Duncanson model).
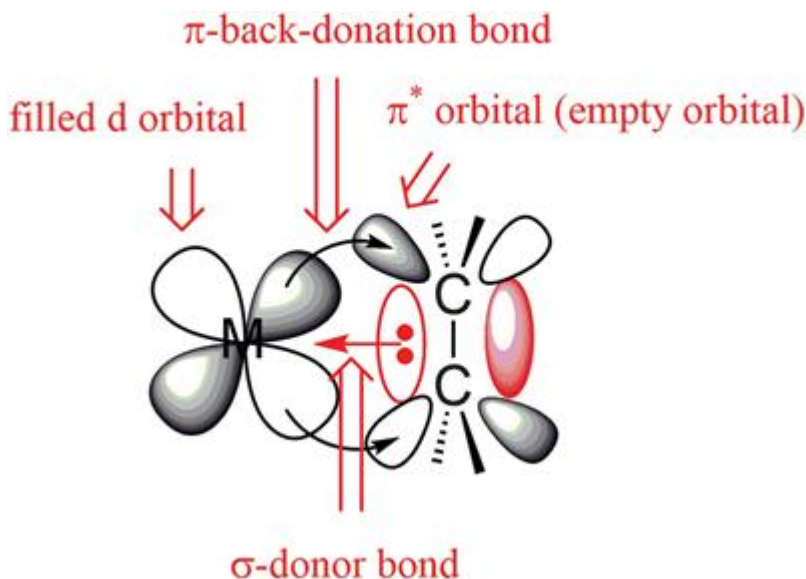
π-back-donation bond

filled d orbital   π* orbital (empty orbital)

σ-donor bond

Figure 4.2   Bond between a transition metal and olefin (DCD model) (for clarity, the metal orbital receiving σ-donated electron density from the alkene double bond is not shown).

The coordination of carbonyl and olefin ligands is similar in the sense that the coordination consists of both σ-donation and π-back-donation. In the case of a carbonyl ligand, the contribution of the π-back-donation is much greater than that of the σ-donation. In the case of an olefin ligand, the importance of σ-donation and π-back-donation depends on the oxidation state of the transition metal, the other ligands on the metal, the character of the olefin substituents, and other factors.

Consider a simple molecular orbital (MO) description of olefin coordination to a metal. Although σ-donation and π-back-donation occur at the same time, they will be addressed separately for convenience. Figure 4.3(a) shows the MOs concerned with σ-donation. Since the π orbital of the olefin is filled with electrons, it is at lower energy than the empty $d_{x^2-y^2}$ metal orbital. Figure 4.3(b) shows how π-back-donation occurs. Since the π* orbital of the olefin is an anti-bonding orbital, it is empty and of high energy. Figure 4.3(c) is a combination of (a) and (b). On the transition metal side, the d_{xy} orbital has the highest energy among orbitals with electrons (highest occupied molecular orbital, HOMO). The $d_{x^2-y^2}$ orbital is the lowest energy orbital among those without electrons (lowest unoccupied molecular orbital, LUMO). On the olefin side, the π orbital is the HOMO and the π* orbital is the LUMO.
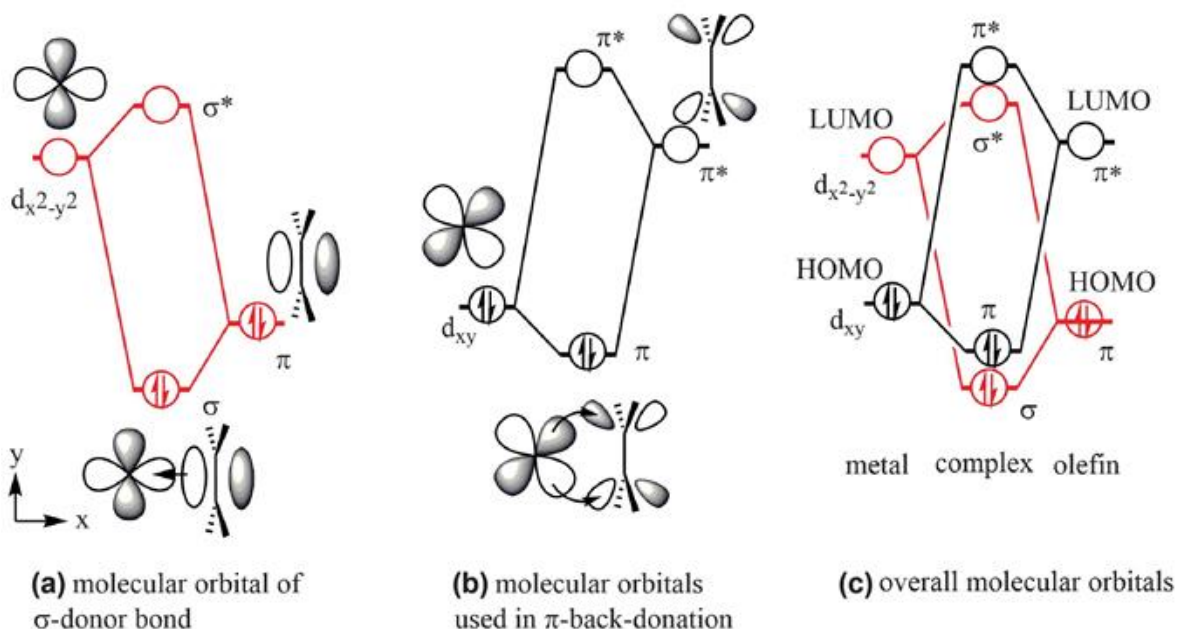
(a) molecular orbital of σ-donor bond

(b) molecular orbitals used in π-back-donation

(c) overall molecular orbitals

Figure 4.3 Schematic diagram of molecular orbitals of transition metal–olefin complexes.

At this point some simple rules for constructing molecular orbitals (see Figure 4.4) are reviewed. When orbitals **a** and **b** interact with each other to generate the bonding MO, **c**, and the anti-bonding, MO, **c***, it is essential that the symmetries of orbitals **a** and **b** are appropriate. Next, the closer the energy levels of orbitals **a** and **b**, the greater the stabilization of the bonding MO, **c**, and at the same time, the greater the destabilization of the anti-bonding MO, **c***. Since electrons usually enter only the bonding MO, the greatest stabilization is achieved by forming the MO **c** when **a** and **b** are close in energy.

Energy levels of **a** and **b** are close; stabilization on forming bonding MO **c** is large.

Energy levels of **a** and **b** are significantly different; stabilization on forming bonding MO **c** is small.
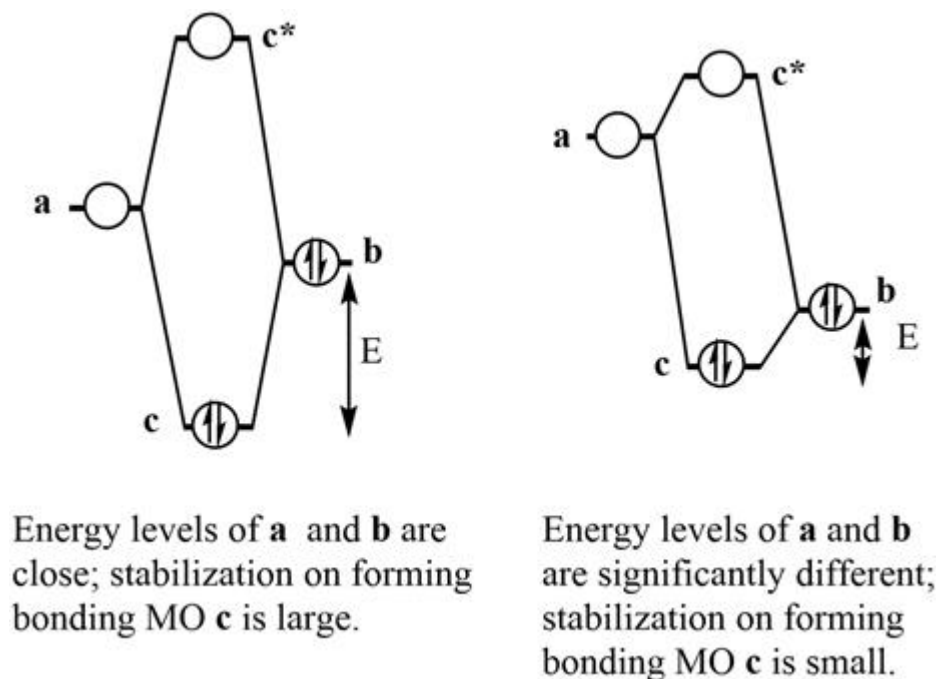
Figure 4.4   Comparison of MOs for different relative energies of **a** and **b**.

Consider Figure 4.3. Referring to the σ-donor bond (a), as the energy level of the π-orbital of the olefin rises, it approaches that of the metal $d_{x^2-y^2}$ partner orbital. That is, the higher the π-orbital energy of the olefin, the greater the importance of the σ-donor bond in stabilizing the complex. Considering the situation from the perspective of the transition metal, the lower the energy of the LUMO (the $d_{x^2-y^2}$ orbital in this case), the greater the stabilization afforded by the σ-donor bond. Next, consider the π-back-donation (Figure 4.3(b)). The lower the energy of the olefin π* orbital and the higher the energy of the HOMO (the metal d_{xy} orbital in this case), the smaller the separation between their energies becomes. As a result, the stabilization on forming the molecular orbitals increases. Thus, in this case, π-back-donation is important in stabilizing the complex. Various factors influencing the relative contributions of σ-donation and π-back-donation in the metal–olefin bond are considered next.

4.3.1   Change in Oxidation State of the Metal

Increasing the oxidation number of the metal means decreasing the number of metal d electrons. Consider the removal of two metal d electrons,

resulting in an increase in the oxidation number by 2. Since the electrons lost are those highest in energy (*i.e.* the electrons in the HOMO), the former HOMO becomes the new LUMO after oxidation. That is, the energies of both the HOMO and LUMO decrease on oxidation. As explained in the preceding section, the lowering of the LUMO energy leads to an increase in the influence of the σ-donor bond, while lowering the energy of the HOMO leads to a decrease in the influence of the π-back-donation bond. More intuitively, if the central metal is oxidized by removal of electrons, it becomes more electron-deficient, so the σ-donation factor becomes more important in transferring electron density to the metal. At the same time, π-back-donation of electron density from the metal to the ligand becomes less favorable. Thus, σ-donation dominates in olefin complexes of Fe(iii), Ni(ii), Pd(ii), and Pt(ii), while π-back-donation dominates in those of Fe(0), Ni(0), Pd(0), and Pt(0).

4.3.2   Substituents on the Olefin

The introduction of electron-donating groups on the olefin carbons leads to an electron-rich olefin, which favors σ-donation of the olefin π-electrons to the metal. On the other hand, the introduction of electron-withdrawing groups on the olefin carbons results in an electron-deficient olefin, which is consequently a weaker σ-donor, but better at receiving electron density from the metal by π-back-donation.

4.3.3   Fluxionality: Olefin Rotational Motion

In some transition metal–olefin complexes, the olefin is observed to rotate about the olefin centroid–metal axis (Figure 4.5). This fluxionality is sometimes called "propeller-like rotational motion". Whether such motion occurs or not is strongly related to the character of the metal–olefin bond. In complexes in which σ-donation is dominant, there is no particular electronic disadvantage to rotating the olefin. On the other hand, in complexes in which π-back-donation dominates, as the olefin rotates, the overlap between the π* orbital of the olefin and the d orbital of the metal decreases and is minimized when rotated 45°. Further rotation leads to better overlap with another metal d orbital, and the system stabilizes again. Rotational motion of olefin ligands is thus less likely in complexes where π-back-donation is important, since rotation occurs *via* an energetically unstable state.

Figure 4.5　Olefin rotational motion (propeller-like rotational motion).

4.3.4　C=C Double Bond Length of the Olefin

The C=C double bond lengths of olefins coordinated to metals show some interesting tendencies. In metal–olefin complexes in which σ-donation is dominant, the C=C double bond distance is slightly longer than that when not coordinated to a metal, but its elongation is only around 0.02 Å. On the other hand, in olefin complexes where π-back-donation is predominant, coordination results in elongation of the C=C double bond by up to around 0.15 Å. This can be interpreted as follows: in the σ-donation dominant case, electron density in the olefin double bond decreases somewhat upon donation to the metal, and so some weakening and lengthening of the C=C double bond is observed. However, in the π-back-donation dominant case, π-back-donation of electron density from the metal results in population of the olefin π* antibonding orbital, which results in significant weakening and lengthening of the C=C double bond.

4.3.5　Bent Back Angle of the Olefin

In a free (non-coordinated) olefin, the two carbon atoms of the C=C double bond and their four substituents are in the same plane. However, upon coordination to a metal, the four substituents bend back, away from the metal (Figure 4.6). This warping angle is called the *bent back angle* (θ). θ depends strongly on the character of the metal-olefin bond. In a complex in which σ-donation is predominant, θ is about 15°, but in a complex in which

π-back-donation is predominant, θ is about 35°. When the flow of electron density from metal to olefin by π-back-donation is extremely large, it amounts to the formation of a single bond between the metal and each olefinic carbon, generating, in effect, an M–C–C three-membered ring compound. In such compounds, the olefinic carbons are closer to the sp^3 hybridized state rather than the usual alkene hybridization of sp^2. This rehybridization accounts for the large value of θ.
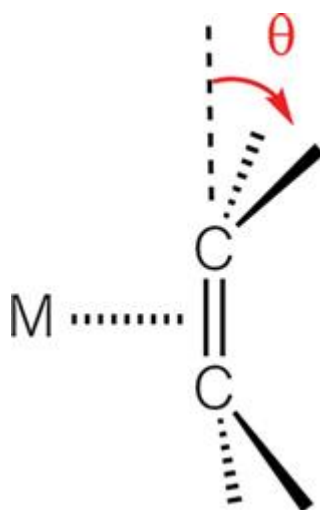

Figure 4.6   Bent back angle (°) (θ) of an olefin.

As described above, a metal-olefin bond comprises σ-donor and π-back-donor components. The relative contribution of these components depends on the oxidation number of the central metal, the types of other ligands, and the substituents of the olefin, and these factors in turn affect the C=C bond distance of the coordinated olefin, the bent back angle of the olefin substituents and the facility of rotational motion of the olefin. These points are summarized in Table 4.3.

Table 4.3   Complexes containing a metal–olefin bond.

	Complex in which σ-donation is predominant	Complex in which π-back-donation is predominant
LUMO level of the metal	The lower, the better	No direct effect
HOMO level of the metal	No direct effect	The higher, the better
LUMO level of the olefin	No direct effect	The lower, the better

HOMO level of the olefin	The higher, the better	No direct effect
Oxidation state of the metal	The higher, the better	The lower, the better
Substituent of the olefin	Electron-donating group	Electron-withdrawing group
Olefin rotational motion	Free rotation	Large rotation barrier
C=C bond distance	Small elongation	Large elongation
Bent back angle (θ) of the olefin	Small (*ca.* 15°)	Large (*ca.* 35°)

4.4 Phosphine Complexes

Phosphines (trivalent phosphorus compounds, PR_3) are widely used as 2e donor ligands in organometallic chemistry. The substituents (R) of phosphines are often alkyl or aryl groups. PMe_3 is trimethylphosphine; PPh_3 is triphenylphosphine; PH_3 is called phosphine (this latter compound is highly toxic and reactive, so it is rarely used as a ligand). Compounds with an oxygen atom between the phosphorus and the rest of the substituent group are also useful ligands. $PR_2(OR)$ are phosphinites, $PR(OR)_2$ are phosphonites, and $P(OR)_3$ are phosphites. Although the naming of such phosphorus compounds is complicated for historical reasons, these are all trivalent phosphorus compounds and coordinate to transition metals using the lone pair of electrons on the phosphorus, like phosphines. One of the main reasons for their widespread use as ligands is that their basicity and bulkiness can be tuned by suitable choice of substituents.

Amines (NR_3) are similar to phosphines in electronic structure and geometry and are also used as ligands. Although both amines and phosphines adopt trigonal pyramidal structures, their bond angles are significantly different. Comparing the bond angles in NH_3 and PH_3, where the influence of the steric bulkiness of the substituents is negligible, the H–N–H angle is 107° whereas the H–P–H angle is 94° (Figure 4.7). Since the nitrogen of NH_3 is sp^3 hybridized, the bond angles around the nitrogen should ideally be 109.5°, but due to the strong electrostatic repulsion between the lone pair of electrons on the nitrogen and the N–H bonding electron pairs, the H–N–H angles become slightly smaller. The bond angle of H–P–H, however, should be considered as being slightly larger than 90° as opposed to deviating from 109.5°. In other words, phosphorus in

phosphine is not sp^3 hybridized, and the P–H bonds are mainly constructed using the phosphorus p-orbitals. As a result, the bond angle is close to 90°. The reason for the non-hybridization is the increasing energy difference between the valence shell s and p orbitals as a Group is descended, which reduces the possibility of hybridization.
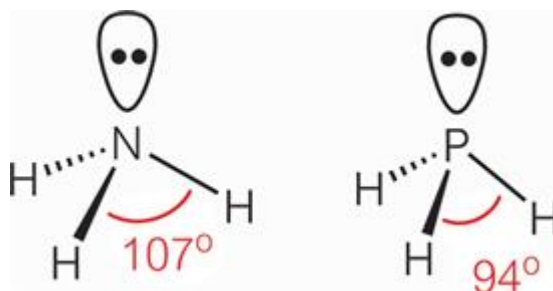

Figure 4.7   Structure of NH$_3$ and PH$_3$.

Phosphines are more commonly used as supporting ligands (ancillary ligands) in organometallic complexes than amines. A supporting ligand is a ligand that does not directly participate in the reaction, but nevertheless influences the reaction through electronic and steric effects resulting from coordination to the central metal. From the view point of HSAB (hard and soft acids and bases) concepts, phosphines are softer bases than amines. Since the central metals in organometallic complexes are relatively softer acids, phosphines are more compatible as ligands.

A major difference between amines and phosphines is their inversion behavior. While amines readily undergo pyramidal atomic inversion of the configuration at room temperature, passing through a transition state with trigonal planar geometry, phosphines hardly undergo inversion (Figure 4.8). Since the bond angles in phosphines are smaller than those in amines, phosphines require a greater structural change and thus greater activation energy to attain the transition state (the pyramidal atomic, *i.e.* stereochemical, inversion barrier is 126–146 kJ mol^{-1}). If all the substituents in an amine or phosphine are different, the compounds are chiral. Whereas chiral amines often readily racemize at room temperature due to their facile inversion of configuration, phosphines usually preserve their configurations. Because of this, optically active phosphines can be utilized and are very useful as chiral centers in organometallic complexes.
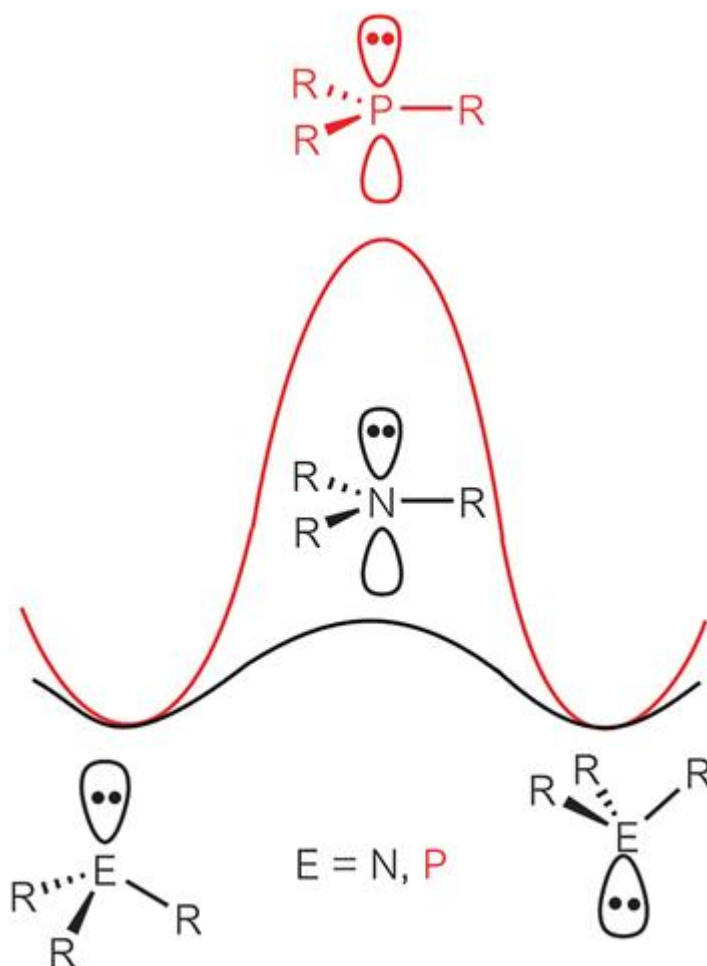
Figure 4.8   Relative inversion barrier energies in amines and phosphines.

Amines are typical σ-donor ligands since they coordinate to a transition metal using the nitrogen lone pair of electrons. Phosphines are also σ-donor ligands, but they are able to accept some π-back-donation from a transition metal. The N–C bond of an alkylamine is generated by forming a molecular orbital from the atomic orbitals of N and C. Since both N and C are elements in the second row of the periodic table, their atomic orbital energies and sizes are similar, so that the σ bonding molecular orbital is significantly stabilized and the σ* antibonding molecular orbital is significantly destabilized. On the other hand, since P is in the third period, the energy and size difference between the P and C atomic orbitals is much greater, leading to much poorer overlap. The σ* antibonding molecular orbital generated when a P–C bond is formed is thus rather lower in energy than the σ* orbital of an N–C bond (Figure 4.9). When an amine or

phosphine coordinates to a transition metal, the σ* orbital of an N–C or P–C bond has suitable symmetry and orientation for overlap with some of the metal d orbitals. Since the energy of the P–C σ* orbital is close to that of the metal d orbitals, π-back-donation is possible (Figure 4.10). However, since the N–C σ* orbital is at much higher energy, π-back-donation to it from the metal is negligible.
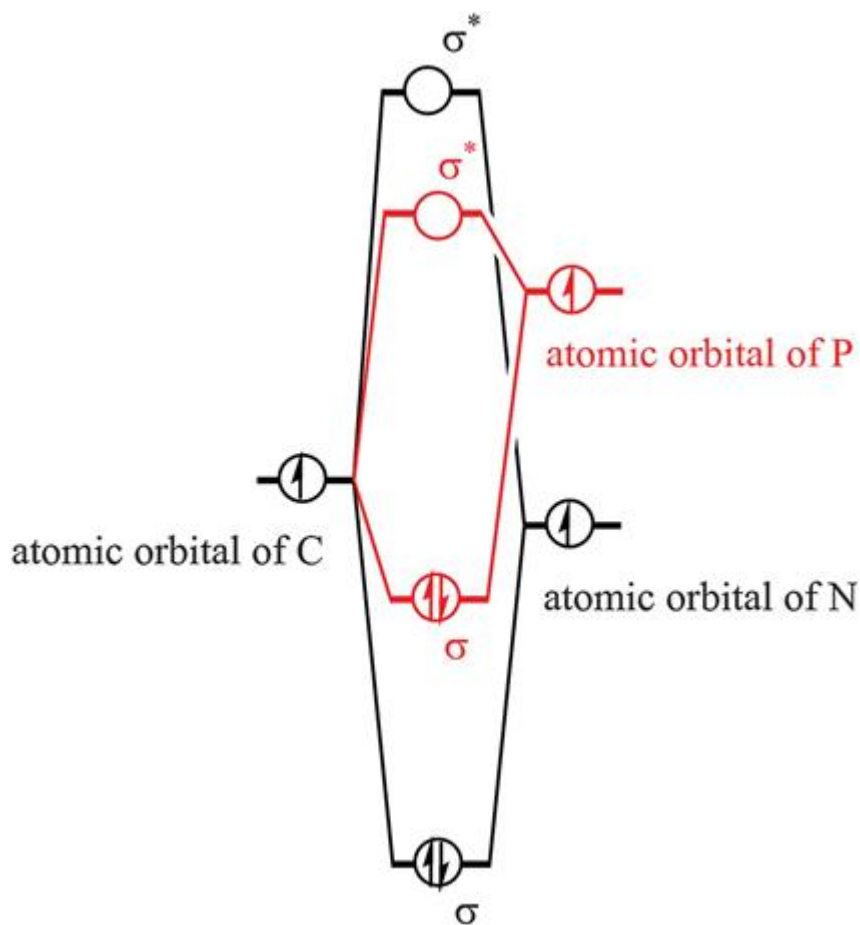
Figure 4.9   Comparison of MO diagram for N–C and P–C bonds.
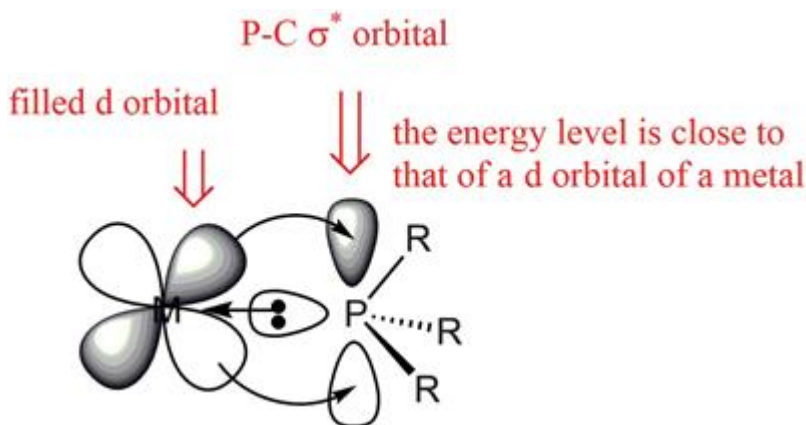
Figure 4.10 π-Back-donation from a transition metal to phosphine.[1]

    Significant substituent-dependent effects on the π-acceptor ability of phosphines are also evident. As E in P–E changes from C to N, O and F, the electronegativity of E increases and the energy of the E atomic orbital used in making the bond decreases. The energy of the P–E σ* orbital thus decreases in this order (Figure 4.11) resulting in increased ability to accept π-back-donated electron density from the metal, to the extent that PF_3 has similar π-acceptor ability to the CO ligand, although it is a phosphorus compound.
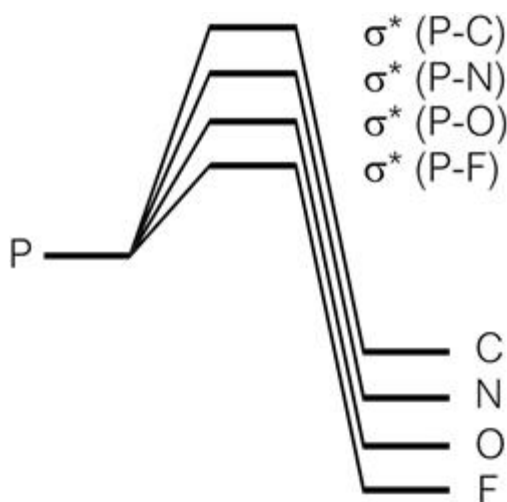
Figure 4.11 Relative energies of σ* orbitals of the P–E bond (E = C, N, O, or F).

Similarly to the phosphines, when the coordinating atom is an element in the third period or lower, it is important to consider the σ* orbital as an acceptor of π-back-donated electron density from the metal.

As noted above, phosphines are useful supporting ligands in organometallic chemistry since the electronic state and steric environment of the central metal can be appropriately tuned by changing the kind of phosphine. These points are now examined in greater detail. The electronic influence of a phosphine on the metal reflects the basicity of the phosphine. Essentially, the basicity of a phosphine increases with the electron-donating ability of its substituents (usually organic groups). When phosphines PR_3 are arranged in order of decreasing basicity, the following order is found, which is in good agreement with the electron-donating ability of the R group in organic chemistry:R = t-Bu > n-Bu > Et > Me > Ph > H > OPh > Cl

Tolman considered the steric effects of phosphine coordination to a metal in detail, proposing the concept of *cone angle*[1] which permits quantitative consideration of the steric factor. Tolman's concept considers the volume of space occupied when a phosphine coordinates to a transition metal, taking into account the van der Waals radius of the phosphine, and the cone angle is taken as the angle subtended by the ligand assembly at the metal atom. In the case of a phosphine coordinated to a nickel atom, the Ni–P bond distance is typically around 2.28 Å (Figure 4.12). A cone of angle θ with the Ni atom at the apex can be drawn. The θ values of representative phosphines are shown in Table 4.4. If the substituents are different, distorted cones are formed, but since the phosphine rotates about the Ni–P axis, it is considered that the steric effects of the substituents are also averaged, and the cone angle may thus be represented by the average value. For example, in the case of $PMePh_2$, the contribution of PMe_3 ($\theta = 118°$) is 1/3 and the contribution of PPh_3 ($\theta = 145°$) is 2/3, such that θ for $PMePh_2$ is calculated as $118° \times 1/3 + 145° \times 2/3 = 136°$.
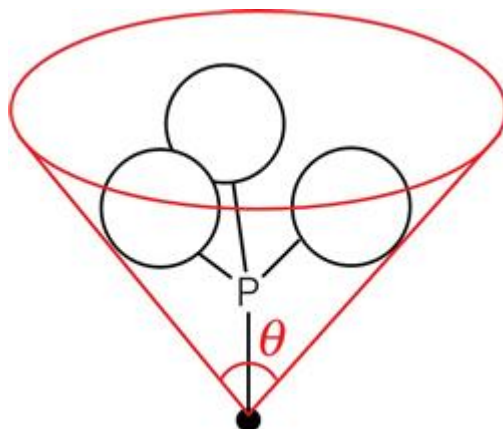
Figure 4.12 Tolman's cone angle θ.

Table 4.4 Tolman's cone angle.

Phosphine	θ (°)
PMe$_3$	118
PEt$_3$	132
PMePh$_2$	136
PPh$_3$	145
P(i-Pr)$_3$	160
P(t-Bu)$_3$	182
P(mesityl)$_3$[a]	212

[a] Mesityl = 2,4,6-trimethylphenyl.

The θ of P(mesityl)$_3$ is 212°, which means that over half of the coordination sphere of the central metal is covered (and thus sterically protected) by coordination of only one P(mesityl)$_3$ ligand.

Box 4.2 Problem 8. When $[CoBr_2(CO)L_2]$ is dissolved in solution, an equilibrium is established between coordinated and free CO species in the solvent, as shown in eqn (4.4). The equilibrium constant (K_d) depends greatly on the identity of the phosphine (L). Explain the trend in equilibrium constants among these complexes by using the IR (v_{CO}) of the starting complexes and the cone angles (θ) of the phosphines shown in Table 4.5.

$$[CoBr_2(CO)L_2] \overset{k_d}{\rightleftharpoons} [CoBr_2L_2] + CO \qquad (4.4)$$
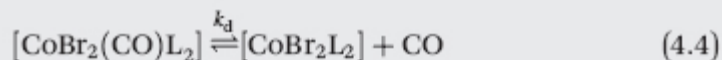
Table 4.5   Parameters of K_d, v_{CO}, and θ in eqn (4.4).

Run	L	K_d	v_{CO} (cm^{-1})	θ (°)
1	PEt$_3$	1.0	1985	132
2	P(n-Bu)$_3$	1.1	1980	135
3	PEt$_2$Ph	2.5	1990	135
4	PEtPh$_2$	24.2	1990	140
5	PPh$_3$	750.0	1995	145

References

1. (a) C. A. Tolman, *Chem. Rev.*, 1977, **77**, 313; (b) K. A. Bunten, L. Z. Chen, A. L. Fernandez and A. J. Poe, *Coord. Chem. Rev*, 2002, **233**, 41.
2. M. Gerloch and G. Woolley, The Functional Group in Ligand–Field Studies: the Empirical and Theoretical Status of the Angular Overlap Model, in *Progress in Inorganic Chemistry*, ed. S. J. Lippard, Wiley, New York, 1984, **vol. 31**, pp. 371–446.

1

The P–C σ* orbital shown in this figure is not located on the opposite side of the P–C σ bond, so that at first glance it does not look like the antibonding orbital of the P–R bond in PR$_3$. However, according to the molecular orbital method, the combined group σ* orbitals have the geometry shown. Consider, for example, PH$_3$: the molecular orbitals of the group include three H 1s orbitals and one 3s and three 3p orbitals of P. Two of the resulting antibonding orbitals are similar to p orbitals in shape and point in directions perpendicular to the axis connecting the P atom center and the orbital of the lone pair of electrons. These orbitals thus overlap well with one of the M d orbitals, and π-back-donation occurs. (For further details, refer to ref. [2].).

Chapter 5

Carbene Complexes — Complexes with M=C Double Bonds

Hiroshi Nakazawa[a]

[a] Osaka City University Osaka, Japan
Email: nakazawa@sci.osaka-cu.ac.jp

5.1 History of Carbene Complexes

Compounds having multiple bonds between elements are important for understanding the fundamentals of chemistry and also noteworthy from the point of view of substance conversion, as these multiple bond moieties are highly reactive.

The term "carbene" is applied to organic compounds described as CR_2. A transition metal complex having this as a ligand is referred to as a "carbene complex", and may be written $M=CR_2$ with a double bond between M and C. A transition metal complex with a triple bond between M and C ($M\equiv CR$) is referred to as a "carbyne complex".

The first carbene complex was prepared by Chugaev in 1925. He reported the preparation of the compound shown in Figure 5.1(a),[1] but 45 years later it was found that this compound was actually the carbene complex shown in Figure 5.1(b).[2]
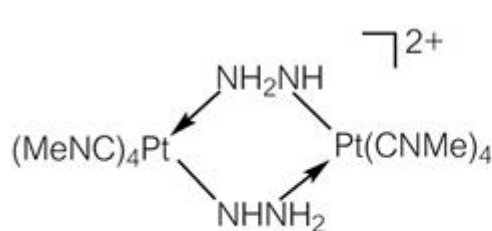
(a) Structure reported in 1925   **(b)** Structure reported in 1970
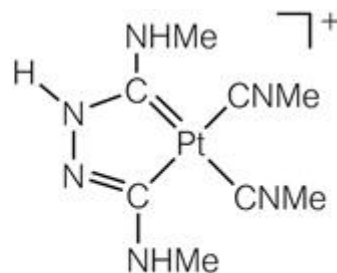
Figure 5.1   First carbene complex.

The first report of carbene complexes was by E. O. Fischer in 1964. He prepared a tungsten carbene complex according to the reaction shown in eqn (5.1).[3] After that, he studied carbene complexes most energetically, leaving a great footprint in this area. It can be said that he is the founder of the research field of carbene complex chemistry.
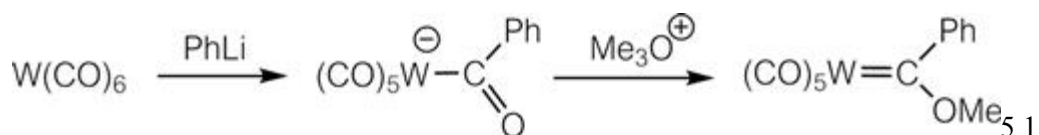
The carbene complexes prepared by Fischer have an atom other than carbon or hydrogen (*i.e.* a heteroatom) on the carbene carbon, as shown in Figure 5.2(a). Most of these carbene complexes are readily prepared and relatively stable. On the other hand, carbene complexes without heteroatoms on the carbene carbon (Figure 5.2(b)) are very unstable. It thus took 10 years from Fischer's first report of a carbene complex until such compounds were made, firstly by Schrock in 1974.[4] The synthetic route is shown in eqn (5.2).

5.2

(X = heteroatom)

(a) Fischer carbene complex　　**(b)** Schrock carbene complex
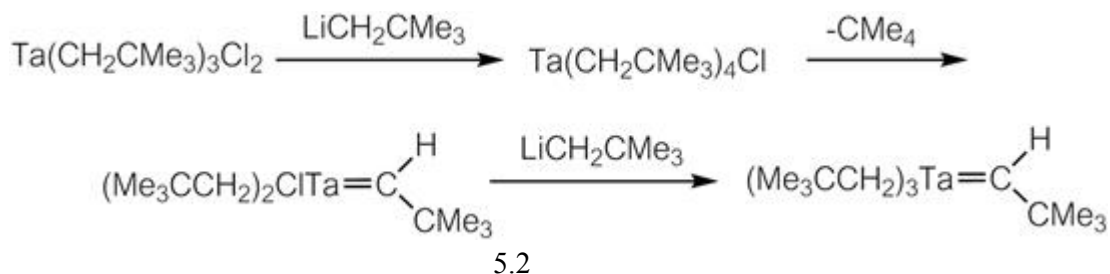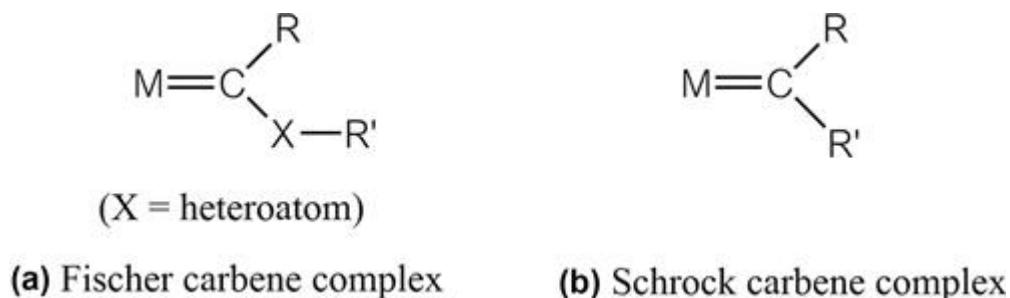
Figure 5.2　　Fischer and Schrock carbene complexes.

There is a large difference in stability and reactivity between complexes with and without heteroatoms on the carbene carbon. They are thus frequently distinguished by referring to the former as Fischer carbene complexes and to the latter as Schrock carbene complexes (which may also be called alkylidene complexes). Section 5.2 describes the features of these carbene complexes.

5.2　Properties of Carbene Complexes

A carbene, CR_2, is a molecule containing a neutral divalent carbon atom with two substituents and two unshared (*i.e.* non-bonded) valence electrons, and it is thus sp^2 hybridized. Depending on the arrangement of the electrons, the carbene may be described as being a singlet or a triplet. A singlet carbene is one in which the two electrons are paired (Figure 5.3(a)). A triplet carbene contains one electron in one of the sp^2 hybrid orbitals and the other electron in the non-hybridized p orbital (Figure 5.3(b)). Since both types of carbene have six valence electrons, they cannot obey the octet rule. Singlet carbenes are highly electrophilic due to the vacant p orbital.

(a) Singlet carbene　　　　**(b)** triplet carbene

(C: sp^2 hybridization, valence electron number: 6)
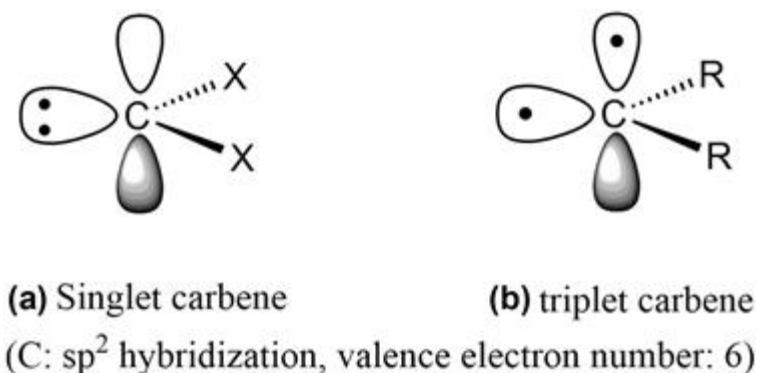
Figure 5.3   Singlet and triplet carbenes.

Fischer carbene complexes are considered to contain singlet carbenes coordinated to metals. When a singlet carbene acts as a ligand toward a transition metal, the lone pair of electrons in the carbene sp^2 orbital is donated to an empty metal d orbital. Concomitantly, the empty p orbital on the carbene carbon accepts electron density back-donated from a filled metal d orbital ($p\pi$–$d\pi$ interaction) (Figure 5.4).
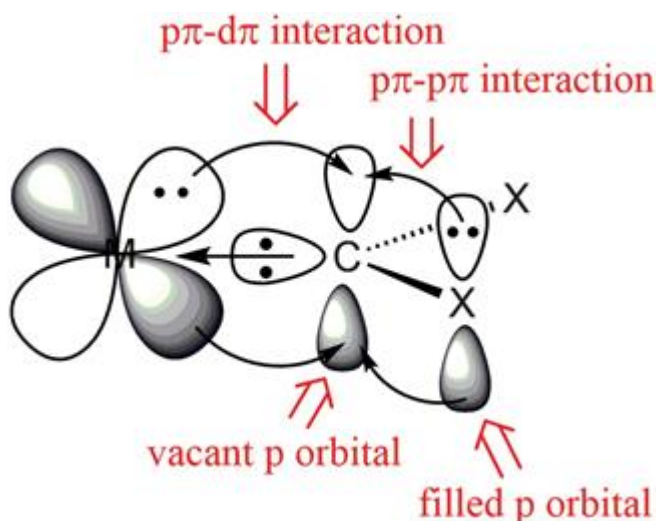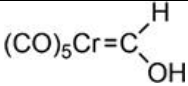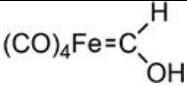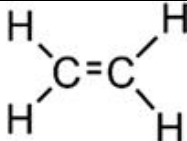
Figure 5.4   Fischer carbene complex (vacant M d orbital omitted for clarity).

This bond is similar to that between a transition metal and CO in the sense that the bonds in both complexes comprise σ donation and π back-donation. However, the orbitals that accept the electron density back-donated from the metal are different: in a carbonyl complex, a π^* orbital of the CO triple bond is used, whereas in a carbene complex, the empty p orbital of the singlet carbene carbon is used. When a substituent atom on the carbene carbon is a heteroatom such as N or O, a lone pair of electrons on the heteroatom may interact with the empty p orbital on the carbene carbon ($p\pi$–$p\pi$ interaction), stabilizing it by transferring some electron density. The reason for the relative stability of a Fischer carbene complex stems not only from the M–C $p\pi$–$d\pi$ interaction, but also from the X–C $p\pi$–$p\pi$ interaction between the carbene carbon and the heteroatom attached to it. N is an effective stabilizing heteroatom in Fischer carbene complexes, and the stability decreases in the order N $\gg$ Se > S > O.

It may be asked whether the pπ–dπ or the pπ–pπ interactions play the more important role in stabilizing a Fischer carbene complex. To answer simply, the pπ–pπ interaction is more important. The results of theoretical calculations relating to M=C (M = Cr, Fe) and C=C bonds are shown in Table 5.1.[5] The bond distances for Cr=C and Fe=C are expected to be around 2.00 Å, in good agreement with the observed value for [(CO)$_5$Cr=CPh(OMe)] of 2.04 Å. The bond energies of Cr=C and Fe=C are 185.8 and 154.0 kJ mol^{-1}, respectively, being much lower than that of the C=C double bonds in olefins, which are typically around 610 kJ mol^{-1}. The rotational energy barriers of Cr=C and Fe=C are 1.7 and 12.1 kJ mol^{-1}, respectively. These values are much smaller than that for C=C (272.0 kJ mol^{-1}), and are actually close to that of the C–C single bond in CH$_3$–CH$_3$ (12.6 kJ mol^{-1}). These results suggest that the M=C bond in a Fischer carbene complex approximates a C–C single bond rather than a double bond.

Table 5.1   Theoretical calculations of Fischer carbene complexes.

M=C	(CO)$_5$Cr=C(H)(OH)	(CO)$_4$Fe=C(H)(OH)	H$_2$C=CH$_2$
Bond distance	2.00 Å	2.00 Å	1.34 Å
Bond energy	186 kJ mol^{-1}	154 kJ mol^{-1}	502 kJ mol^{-1}
Rotational barrier	1.7 kJ mol^{-1}	12 kJ mol^{-1}	272 kJ mol^{-1}

In contrast, significant multiple bond character is observed between the carbene carbon and the heteroatom. The carbene C–O bond distance in [(CO)$_5$Cr=CPh(OMe)] mentioned above is 1.33 Å, which is between the distances of normal C–O single (1.43 Å) and C=O double (1.23 Å) bonds (Figure 5.5). In addition, the rotational barrier energy of the C–O bonds in M=C(OR)$_2$ complexes is from 41.8 to 58.6 kJ mol^{-1}, and *syn* and *anti* forms are separately observed in the NMR spectrum at low temperature (Figure 5.6).
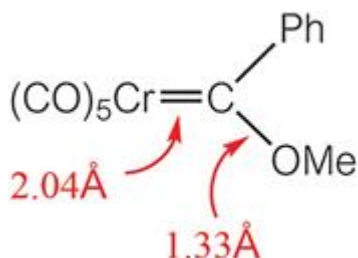
Figure 5.5   Fischer carbene chromium complex.

Figure 5.6   *Syn/anti* structure of a Fischer carbene complex.

The character of the M–C bond noted above for the Fischer carbene complexes of Cr and Fe also applies to other Fischer complexes. Thus, although a double bond is drawn between a transition metal and a carbene carbon, the π bond character in the M–C bond is actually small and it rotates almost freely. In contrast, there is considerable π bond character between the carbene carbon and the heteroatom, and rotation is restricted to some extent (Figure 5.7 and Figure 5.8(c)).
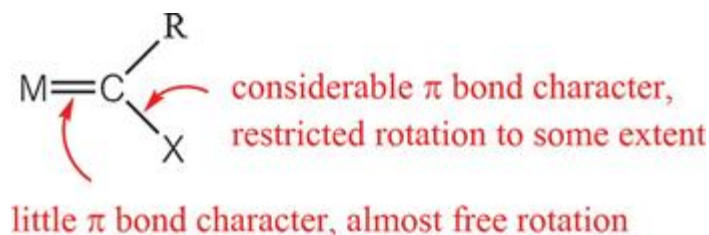
Figure 5.7   Character of Fischer carbene complexes.
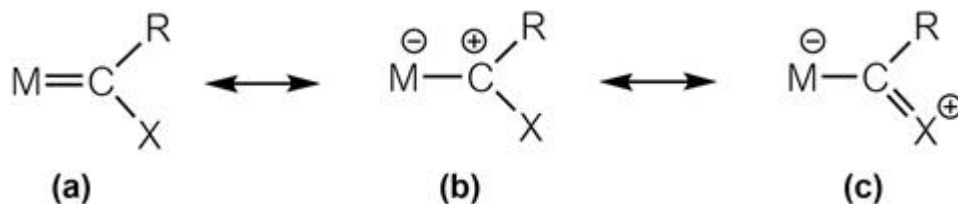
Figure 5.8   Resonance forms of Fischer carbene complexes (X indicates a heteroatom with a lone pair of electrons).

Since Schrock carbene complexes have no heteroatoms on the carbene carbon, the electron-deficient carbene carbon accepts π back-donated electron density from the transition metal d orbitals only. Most Schrock carbene complexes are thus unstable. However, the degree of π back-donation from the transition metal is large.

> **Problem 9.** The rotational barrier energies for methylidene complexes, $M=CH_2$, have been reported as follows. Explain the relative magnitudes of these values.
>
> 1) $[Cp(CO)_2(PPh_3)Mo=CH_2]^+$ < 25 KJ mol^{-1}
> 2) $[Cp(CO)_2(PPh_3)W=CH_2]^+$ 35 KJ mol^{-1}
> 3) $[Cp(CO)_2(PEt_3)W=CH_2]^+$ 38 KJ mol^{-1}

5.3   Reactivity of Carbene Complexes

Fischer and Schrock carbene complexes show very different reactivity. The carbene carbon in Fischer carbene complexes is electrophilic, whereas that in Schrock carbene complexes is nucleophilic.

Resonance forms for a Fischer carbene complex are drawn in Figure 5.8. The bond between M and the carbene carbon is usually drawn as a double bond, as in (a) M=C, but polarization with negative partial charge on the metal and positive partial charge on the carbene carbon exists to a considerable extent, as in (b). If π donation from the heteroatom on the carbene carbon is included, the form shown in (c) can be drawn. Actual carbene complexes have structures resulting from a combination of these resonance hybrids.

Fischer carbene complexes are considered to be constructed from a singlet carbene and a transition metal (Figure 5.4). Since the carbene carbon is inherently electron-deficient, it accepts π electron density from the transition metal. However, this is insufficient to cancel the electron-deficiency, so the carbene carbon still shows electrophilicity despite its interaction with the transition metal.

Evidence that the carbene carbon is positively polarized includes:

1) The carbene carbon is observed at very low magnetic field in the ^{13}C NMR spectrum. For example, the carbene carbon in $[(CO)_5Cr=CPh(OMe)]$ is observed at 315 ppm.

2) The molecular dipole moment is relatively large: for $[(CO)_5Cr=CPh(OMe)]$ it is 5 Debye.

3) Hydrogen atoms on a carbon atom α to the carbene carbon are acidic, and the reaction shown in Figure 5.9 takes place.

4) On reaction with a Lewis base, formation of a betaine complex or substituent exchange on the carbene carbon can occur (Figure 5.10). It is considered that these are due to the electrophilicity of the carbene carbon.
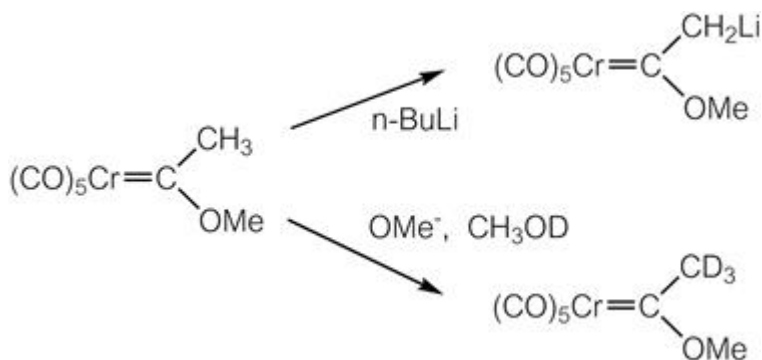
Figure 5.9   Acidity of hydrogen on the carbon α to the carbene carbon.
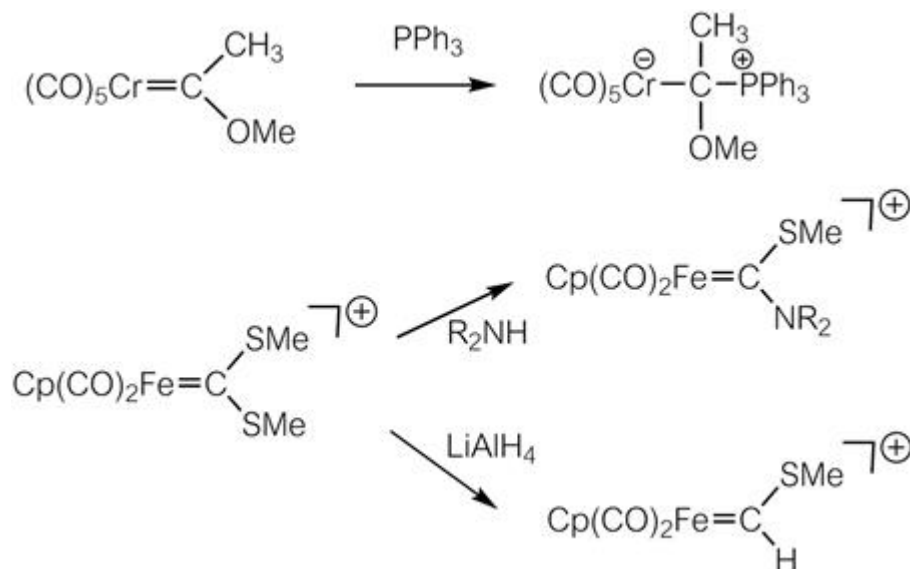
Figure 5.10 Reactions resulting from electrophilicity of Fischer carbene complexes.

Schrock carbene complexes, on the other hand, exhibit reactivity consistent with the polarization $M^{\delta+}=C^{\delta-}$ (Figure 5.11). These carbene complexes react with ketones to give olefins, similar to Wittig reagents ($R_3P=CR_2$). Since the Wittig reagent is considered to be polarized $R_3P^{\delta+}=C^{\delta-}R_2$, it is suggested that the Schrock carbene complex is also polarized $M^{\delta+}=C^{\delta-}$.
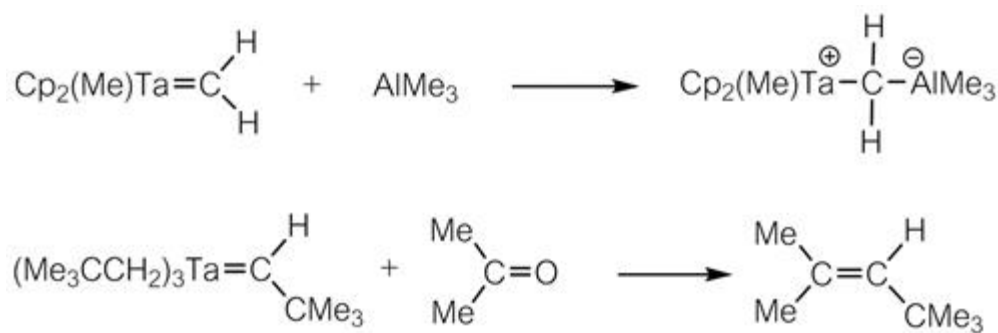
Figure 5.11 Reactions occurring due to the nucleophilicity of Schrock carbene complexes.

Various Fischer and Schrock carbene complexes have been synthesized and the characteristics of each complex have been clarified. Most Fischer carbene complexes contain late transition metals with low formal oxidation

numbers, from 0 to 2. In addition, the metals have π-accepting supporting ligands, such as carbonyl ligands. In contrast, most Schrock carbene complexes contain early transition metals with high formal oxidation states of 4 or 5, and they do not have π-accepting supporting ligands. These features are summarized in Table 5.2.

Table 5.2 Features of Fischer and Schrock carbene complexes.

$L_nM=CR_2$	Fischer carbene complex	Schrock carbene complex
Central metal (M)	Late transition metal	Early transition metal
Oxidation state of M	Low	High
Supporting ligands (L)	π acceptors (such as CO)	Not π acceptors (such as alkyl)
Substituents on carbine C (R)	π donating (such as OR, NR$_2$)	Not π donating (such as alkyl)
Reactivity of carbine C	Electrophilic	Nucleophilic
Polarization of M=C	$M^{\delta-}=C^{\delta+}$	$M^{\delta+}=C^{\delta-}$

Thus, in Fischer carbene complexes, the metal is usually a late transition metal in a low oxidation state (*i.e.* electron-rich) and the carbene carbon is electrophilic, while in Schrock carbene complexes, the metal is usually an early transition metal in a high oxidation state (*i.e.* electron-poor) and the carbene carbon is nucleophilic. At first glance this may appear strange. However, if a Fischer carbene complex is considered as a complex in which a singlet carbene coordinates to a metal (Figure 5.4) and a Schrock carbene complex is considered to be a complex in which a triplet carbene coordinates to a metal (Figure 5.12), then it can be rationally interpreted. In the triplet carbene, one electron is contained in one of the sp^2 hybrid orbitals and the other is contained in the non-hybridized p orbital (Figure 5.3(b)). These two unpaired electrons combine with two unpaired electrons in metal d orbitals to form one σ bond and one π bond (Figure 5.12(a)). This bond formation is similar to that in Figure 5.12(b) when a triplet carbene dimerizes to form an olefin. Since the electronegativity of carbon is greater than that of transition metals, both the σ-bonded and π-bonded electron pairs in a Schrock carbene complex are localized more towards the carbon side, resulting in a δ$^-$ polarized C and nucleophilicity.

π bond

σ bond

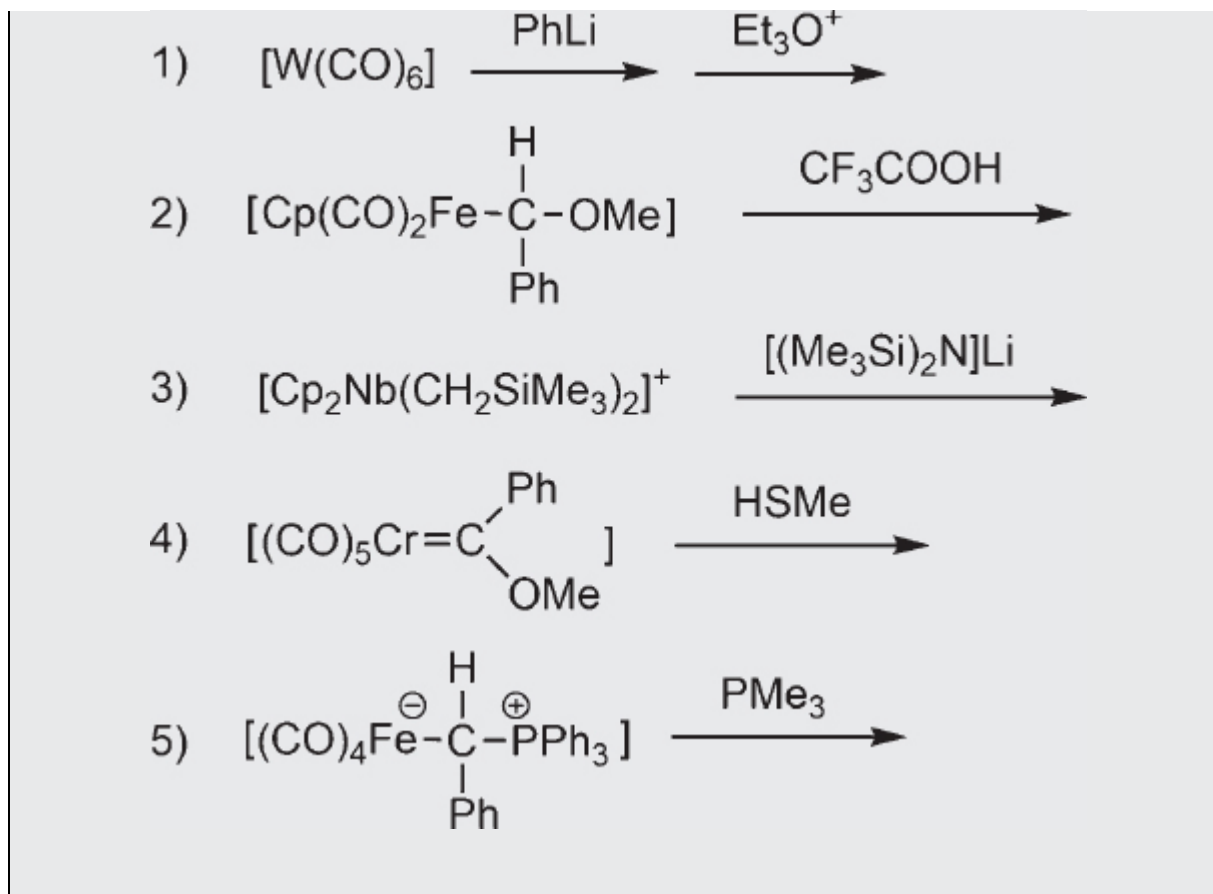**(a)** Schrock carbene complex

π bond

σ bond
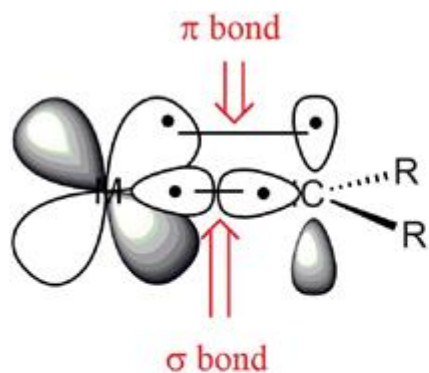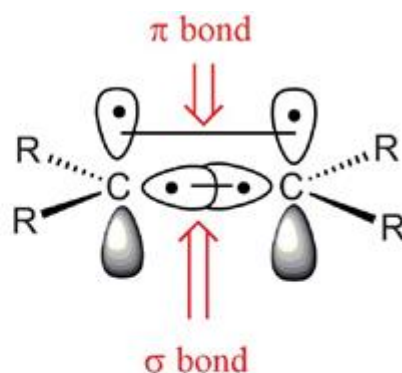
(b) olefin formation by
dimerization of triplet carbene

Figure 5.12   Triplet carbene in a Schrock carbene complex and analogous consideration for ethylene.

A Schrock carbene complex can also be considered as a Fischer carbene complex in which π back-donation from the metal to the carbene ligand (pπ–dπ interaction) is extremely large. Since the electronegativities of early transition metals are lower than those of late transition metals, π back-donation is more likely to occur in an early transition metal. Therefore, Schrock carbene complexes are often found for early transition metals. In a complex having a π-accepting supporting ligand such as CO, π back-donation to the carbene ligand is inhibited. Schrock carbene complexes thus tend to have non-π-accepting supporting ligands, such as alkyl groups. As a result, the formal oxidation number of the metal in a Schrock carbene complex inevitably increases.[1]

Problem 10. Predict the products in the following reactions:

1) $[W(CO)_6]$ $\xrightarrow{\text{PhLi}}$ $\xrightarrow{\text{Et}_3\text{O}^+}$

2) $[Cp(CO)_2Fe-\overset{\displaystyle H}{\underset{\displaystyle Ph}{\overset{|}{\underset{|}{C}}}-OMe]}$ $\xrightarrow{\text{CF}_3\text{COOH}}$

3) $[Cp_2Nb(CH_2SiMe_3)_2]^+$ $\xrightarrow{[(Me_3Si)_2N]Li}$

4) $[(CO)_5Cr=C\overset{\displaystyle Ph}{\underset{\displaystyle OMe}{}}\ ]$ $\xrightarrow{\text{HSMe}}$

5) $[(CO)_4\overset{\ominus}{Fe}-\overset{\displaystyle H}{\underset{\displaystyle Ph}{\overset{|}{\underset{|}{C}}}-\overset{\oplus}{P}Ph_3}\ ]$ $\xrightarrow{\text{PMe}_3}$

References

1. L. Chugaev, M. Skanavy-Grigorieva and A. Posniak, *Z. Anorg. Allg. Chem.*, 1925, **148**, 37.
2. A. Burke, A. L. Balch and J. H. Enemark, *J. Am. Chem. Soc.*, 1970, **92**, 2555.
3. E. O. Fischer and A. Maasböl, *Angew. Chem., Int. Ed. Engl.*, 1964, **3**, 580.
4. R. R. Schrock, *J. Am. Chem. Soc.*, 1974, **96**, 6796.
5. H. Nakatsuji, J. Ushio, S. Han and T. Yonezawa, *J. Am. Chem. Soc.*, 1983, **105**, 426.

---

1 The formal oxidation number of the central metal differs between Fischer and Schrock carbene complexes. In a Fischer carbene complex, a singlet carbene bonds to a transition metal. The bond thus comprises the σ donation of the carbene lone pair of electrons to the metal and π back-donation from the metal to the carbene ligand, as in the coordination bond of CO to a metal. Coordination of a Fischer carbene thus does not change the formal oxidation number of the metal. On the other hand, a Schrock carbene complex involves coordination of a triplet carbene to a metal. Removal of the carbene portion as $CR_2{}^{2-}$ to maintain ligand electron octets then results in an increase of the oxidation number of the central metal by two. When it is difficult to determine whether a carbene complex contains a Fischer-type or Schrock-type carbene, the formal oxidation number of the central metal will be unclear. Therefore, in general, metal formal oxidation numbers are not discussed in depth in carbene complexes.

Chapter 6

Basic Reactions of Organometallic Complexes

Hiroshi Nakazawa[a]

[a] Osaka City University Osaka, Japan
Email: nakazawa@sci.osaka-cu.ac.jp

6.1 Introduction

When a transition metal-coordinated ligand, considered as donating two electrons (a 2e donor ligand, see Section 2.4.2), dissociates from the metal, the ligand itself does not change (*e.g.* neutral molecules such as NH_3 and CO). For such a ligand, dissociation and replacement by another 2e donor ligand are typical reactions in coordination chemistry. In contrast, for organometallic compounds, there are several characteristic reactions and most of them involve 1e donor ligand(s). Understanding these reactions is very important to master organometallic chemistry. This chapter will explain several basic reactions among many characteristic reactions of organometallic complexes.

6.2 Oxidative Addition

Oxidative addition refers to the reaction in which a compound (A–B) having a covalent bond between A and B reacts with a transition metal fragment described as L_nM (L generally stands for a supporting ligand) to give $L_nM(A)(B)$ with two ligands A and B. The general formula is expressed by eqn (6.1). Since this reaction is formally reversible, it may be written as an equilibrium. The reverse reaction is referred to as reductive elimination and will be discussed in Section 6.3.

$$L_nM \quad + \quad A\text{-}B \quad \xrightarrow[\left(\text{reductive elimination}\right)]{\text{oxidative addition}} \quad L_nM \overset{A}{\underset{B}{\diagup}} \qquad (6.1)$$
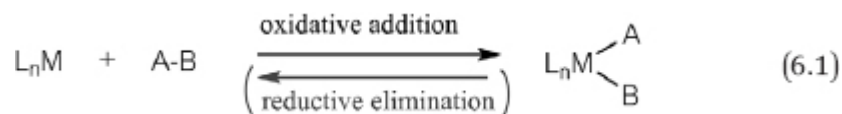
Oxidative addition leads to an increase in the coordination number of the central metal by 2 and increase of the formal oxidation number by 2. The central metal is oxidized, but this is the case when thinking about *formal* oxidation number, so it is called *oxidative* addition rather than *oxidation* addition. Since it is difficult to imagine a real reaction from the general formula, a typical example is given below.

6.2.1 Vaska's Complex

trans-[IrCl(CO)(PPh$_3$)$_2$] is called Vaska's complex after its discoverer.[1] This complex is intriguing as it exhibits various reactivities towards different compounds. In particular, investigations using this complex have afforded much knowledge about oxidative addition.

Vaska's complex contains iridium in formal oxidation number 1, has eight d electrons and is a 16e species. The complex therefore adopts a square planar structure (see Section 3.4). In the reaction of MeI with this complex, the C–I portion undergoes oxidative addition to the Ir center to form *trans*-[IrCl(Me)(CO)(PPh$_3$)$_2$] (Figure 6.1). In general, the C–X moiety in alkyl halides (RX) is susceptible to oxidative addition to 16e complexes. The R and X ligands are situated *trans* to each other in the product. Investigations using an optically active alkyl halide revealed that inversion of chirality at the alkyl carbon α to X occurred. Based on this observation, it is proposed that the Ir moiety of Vaska's complex nucleophilically attacks the α carbon of the alkyl halide in an S_N2-type step and the liberated X$^-$ then coordinates to the Ir on the opposite side to the alkyl ligand to form a *trans* complex. In the case of acyl halides (RC(O)X), oxidative addition occurs in the C–X moiety to form the corresponding *trans*-[IrCl(X)(C(O)R)(CO)(PPh$_3$)$_2$]. The product stereochemistry is not always *trans*, though, and depends on the nature of the adding species.
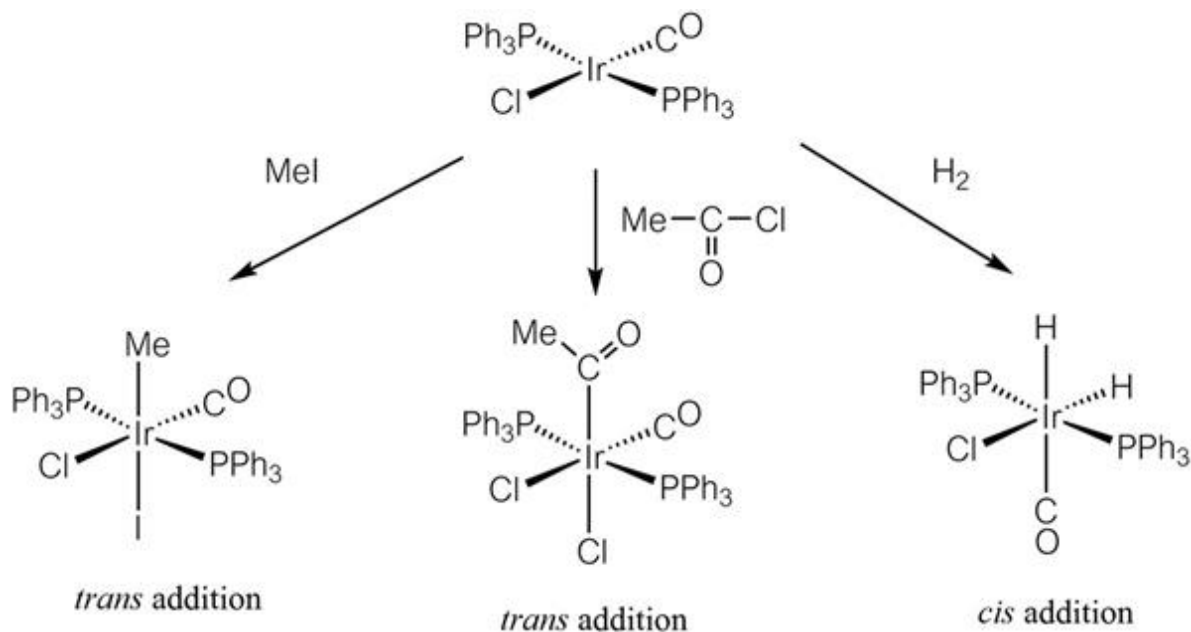
Figure 6.1   Reactivity of Vaska's complex.

One of the features of Vaska's complex is that it undergoes oxidative addition by a hydrogen molecule. The H–H bond energy is very large (430 kJ mol^{-1}). H_2 adds to Vaska's complex to form a dihydride complex in a "concerted" reaction, which provides a lower energy route as it is not necessary first to break the H–H bond and then to generate two Ir–H bonds. The H_2 molecule approaches Ir as shown in Figure 6.2 and H–H bond breaking proceeds with simultaneous formation of two Ir–H bonds. For this reason, H_2 molecules can oxidatively add to Ir with lower activation energy to form a dihydride complex and as a result, the two hydride ligands are located next to each other (*cis* addition).
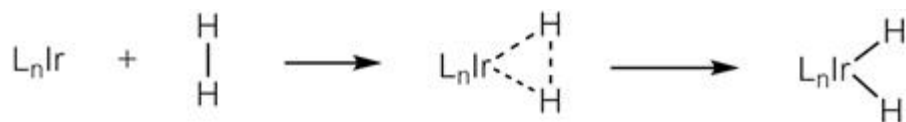
Figure 6.2   Concerted oxidative addition of H–H to Vaska's complex.

6.2.2   C–H Bond Activation

Some bonds not normally considered reactive may nevertheless undergo oxidative addition to transition metals. Figure 6.3 shows an example of such a C–H bond cleavage reaction. The starting Re complex is an 18e species and stable, but it undergoes photolysis with the ejection of a PMe_3 ligand to form a very unstable 16e complex, $[CpRe(PMe_3)_2]$. This complex can activate the C–H bonds in benzene or methane to give the corresponding C–H oxidative addition products, which are stable 18e species.
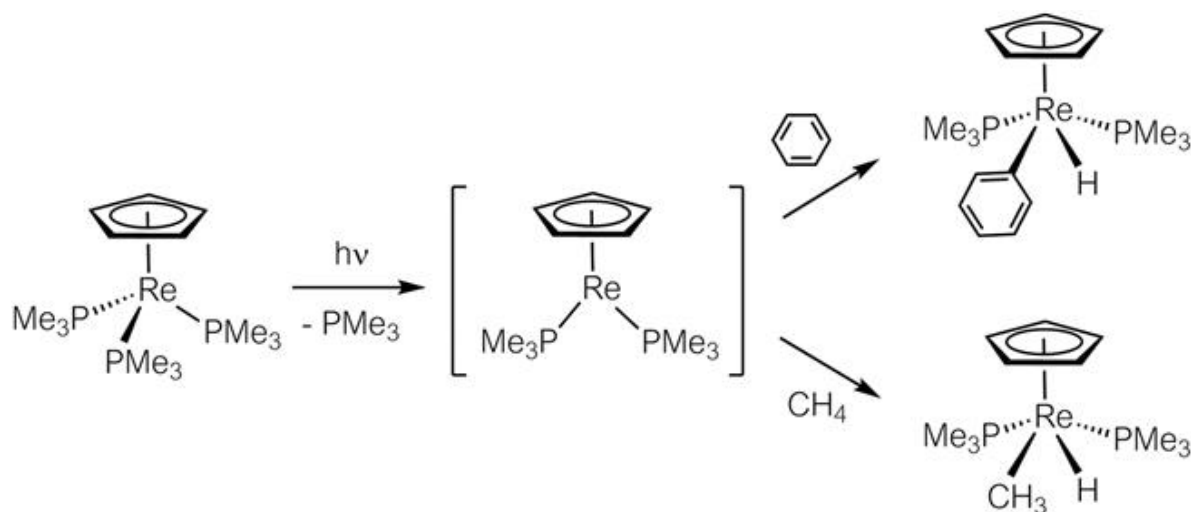
Figure 6.3   C–H bond activation reaction.

6.2.3   Orthometallation

$[IrCl(PPh_3)_3]$ is similar to Vaska's complex and also a 16e complex. When some energy (heat) is given to the complex, it changes to a six-coordinate complex (Figure 6.4). At first glance, it looks like a complicated reaction, but it is in fact an intramolecular oxidative addition of a C–H bond. In general, 16e complexes undergo oxidative addition to form thermodynamically stable 18e complexes if appropriate reagents are present. As the starting compound in Figure 6.4 is a 16e, four-coordinate d^8 complex, it is stable to some extent. If a compound having a bond that is likely to be activated is present in the system and further energy is added (in this case, by heating), the activation barrier can be overcome and oxidative addition occurs. However, in the absence of an appropriate reagent, the C–H bond of a phenyl group in one of its own PPh_3 ligands is activated, leading to *cis* oxidative addition of the stereochemically favored *ortho* C–H

bond. Such a reaction, in which the C–H bond is at the *ortho* position of a coordinated phosphine having a phenyl substituent, is known as orthometallation.
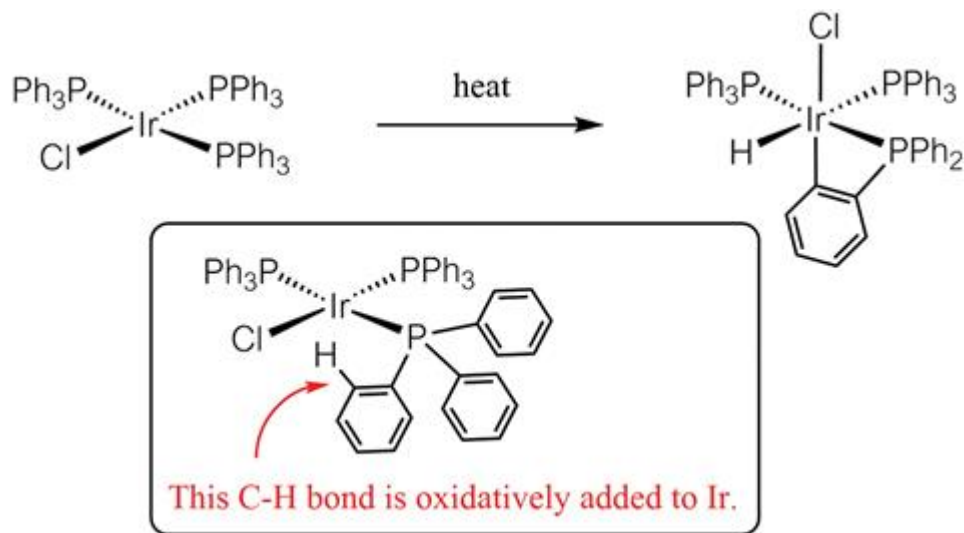
Figure 6.4   Orthometallation reaction.

6.2.4   Ease of Oxidative Addition

Oxidative addition results in an increase of the coordination number of the central metal by 2, increase of the formal oxidation number by 2, and increase of the valence electron number around the metal by 2. In general, regarding oxidative addition reactions, it can be said that:

 (1) A complex having 16 or fewer valence electrons undergoes the reaction. 18e complexes do not undergo oxidative addition to form 20e complexes.
 (2) Since the oxidation number increases by 2 when the reaction occurs, the reaction is more likely to occur for starting materials in which the metal has a lower oxidation number. For example, in the case of a transition metal complex with eight d electrons, when the bound ligands are the same, the reactivity is in the order of Fe(0) > Co(i) > Ni(ii).
 (3) The reaction is more likely to occur for complexes bearing electron-donating supporting ligand(s).
 (4) The reaction is more favorable for transition metals lower in the periodic table. For example, in the case of Group 9 transition metals, the reactivity order is Ir > Rh > Co. This is because the heavier transition metal better stabilizes the oxidatively added complex.
 (5) In all cases, steric effects are important. Even if the conditions described above are satisfied, the reaction will not occur if there is sterically no space for two ligands to be added.

Problem 11. Which complex shows greater reactivity towards oxidative addition of H_2? Here, *dppe* and *dmpe* stand for $Ph_2PCH_2CH_2PPh_2$ and $Me_2PCH_2CH_2PMe_2$, respectively.

1)	$[Co(dppe)_2]^+$	or	$[Ir(dppe)_2]^+$
2)	$[RhCl(PPh_3)_3]$	or	*trans*-$[RhCl(CO)(PPh_3)_2]$
3)	*trans*-$[IrCl(CO)(PPh_3)_2]$	or	*trans*-$[RhCl(CO)(PPh_3)_2]$
4)	*trans*-$[IrCl(CO)(PPh_3)_2]$	or	*trans*-$[IrBr(CO)(PPh_3)_2]$
5)	$[Rh(dppe)_2]^+$	or	$[Rh(dmpe)_2]^+$
6)	*trans*-$[IrCl(CO)(PPh_3)_2]$	or	*trans*-$[PtCl(CO)(PPh_3)_2]^+$
7)	$[Os(CO)_5]$	or	*trans*-$[Os(PPh_3)_2(CO)_3]$

6.3 Reductive Elimination

Reductive elimination (eqn (6.2)) corresponds to the reverse of oxidative addition discussed above. In general, this reaction occurs when two metal-bound ligands, A and B, become directly bonded to each other within the metal coordination sphere and an A–B molecule is released with concomitant reduction of the metal. Reductive elimination is thus a bond forming reaction, and is especially useful in C–C bond formation. Reductive elimination leads to a decrease of the coordination number of the central metal by 2, a decrease in the formal oxidation number by 2 and decrease of the metal valence electron number by 2. The central metal is *formally* reduced in this reaction, so it is called *reductive* (but not *reduction*) elimination.

$$L_nM\underset{B}{\overset{A}{<}} \quad \xrightarrow{\text{reductive elimination}} \quad L_nM \quad + \quad A\text{-}B \qquad (6.2)$$
$$\left(\xleftarrow{\text{oxidative addition}}\right)$$
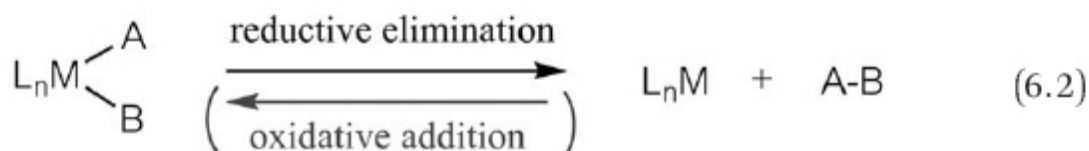
6.3.1 Reductive Elimination in *cis*-$[MR_2L_2]$ (L = Phosphine, M = Ni, Pd, Pt)

Heating *cis*-$[PdMe_2(PPh_3)_2]$ in solution forms ethane by reductive elimination of the two methyl ligands (eqn (6.3)). One of the products, $[Pd(PPh_3)_2]$, cannot be isolated due to its high reactivity. However, it is

considered to be formed in the reaction, despite its short lifetime. It is therefore denoted as "Pd(PPh$_3$)$_2$" in this equation. The Pd is reduced from oxidation state 2 to 0 and the valence electron count is reduced from 16 to 14.

$$Ph_3P \diagdown \diagup Me \qquad \xrightarrow{\text{heat}} \qquad \text{"Pd(PPh}_3\text{)}_2\text{"} \quad + \quad Me\text{-}Me \qquad\qquad (6.3)$$
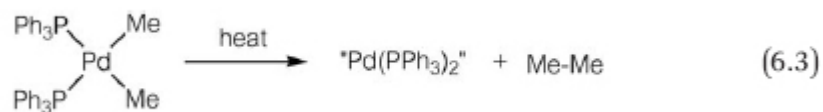
Reductive elimination takes place not only between alkyl ligands but essentially between any two 1e donor ligands. Comparison of the ease of reductive elimination between two hydrides, two methyl ligands and a hydride and a methyl ligand revealed an order of decreasing reactivity of $[M(H)_2L_2] > [M(H)(Me)L_2] > [M(Me)_2L_2]$. The key factors are:

1) Product stability difference
2) Bond directionality

Concerning (1), the reactivity trend reflects the energies of the bonds to be generated *viz.* 430 kJ mol^{-1} for H–H, 410 kJ mol^{-1} for C–H and 347 kJ mol^{-1} for C–C, with reductive elimination of hydrides thus being most favorable.

Concerning (2), a hydride ligand bonds with a metal using its 1s orbital, and also uses this orbital in the reductively eliminated H–H bond. The 1s orbital is spherical and has no directionality; thus, when two hydride ligands approach each other to make a new H–H bond, the 1s orbitals in the two hydride ligands do not need to change their relative orientation.[1] On the other hand, the carbon in a methyl group is sp^3 hybridized. Therefore, when a new C–C bond is formed, it is necessary to change the direction of the sp^3 orbital from its direction pointing to the central metal to the direction of the other methyl group. This requires energy. Generally, a hybridized orbital with greater p character has greater directionality, and consequently requires greater energy to change orientation. It is thus expected that reductive elimination is more favorable for sp^2 hybridized phenyl groups than for sp^3 hybridized alkyl groups, as is experimentally observed.

The identity of the central metal also affects the susceptibility towards reductive elimination. It is difficult to compare metals in different groups in

the periodic table, but clear trends are evident for comparisons in the same group. Ethane is reductively eliminated from $[M(Me)_2L_2]$ (M = Ni, Pd, Pt) in the order of $[Ni(Me)_2L_2] > [Pd(Me)_2L_2] > [Pt(Me)_2L_2]$. This is because, in the same group of the periodic table, the heavier the metal, the more stable the M–C bond, the more difficult its cleavage, and consequently the less favorable the reductive elimination.

6.3.2 Ease of Reductive Elimination

Reductive elimination of two alkyl ligands in a transition metal complex produces a molecule with a C–C bond. Since a transition metal–carbon (M–C) bond is generally polarized $M^{\delta+}–C^{\delta-}$ (see Section 3.1), the coupling of two negatively polarized alkyl ligands will result in electrostatic repulsion. Thus, complexes in which the polarization is weaker are more likely to undergo reductive elimination. The following points can be noted:

1) The more electron-withdrawing (*i.e.* the less electron-donating) the supporting ligands (L) coordinated to the metal, the easier the reductive elimination.

This can be understood as follows. Assume that the L–M–C part is polarized $L–M^{10\alpha+}–C^{10\alpha-}$ (corresponding to $M^{\delta+}–C^{\delta-}$). From this state, the electron-withdrawing property of the L is increased from 0 to $5\alpha-$. As a result, the electron density of M decreases by $5\alpha-$, and the polarization becomes $L^{5\alpha-}–M^{15\alpha+}–C^{10\alpha-}$. However, M with now reduced electron density receives some electron density from the attached alkyl carbon. It is not possible to say how much electron density will be transferred from C to M, but assuming for simplicity that the same amount of electron density ($5\alpha-$) is transferred, the polarization will then become $L^{5\alpha-}–M^{10\alpha+}–C^{5\alpha-}$. Therefore, by making the supporting ligand L more electron-withdrawing, the M–C polarization is reduced from $M^{10\alpha+}–C^{10\alpha-}$ to $M^{10\alpha+}–C^{5\alpha-}$ and reductive elimination between the alkyl groups is then more likely.

2) The more electron-donating the substituents of the alkyl carbon, the easier the reductive elimination.

This is also easy to understand when considered as follows. Assume that the M–C–R part (R is a substituent of the carbon coordinating to the metal) is polarized as $M^{10\alpha+}–C^{10\alpha-}–R$. Next, consider the case where the electron-donating ability of R increases. If 5α-electron density is donated from R to C, the polarization becomes $M^{10\alpha+}–C^{15\alpha-}–R^{5\alpha+}$. However, C with increased electron density transfers some electron density to M. Again, assuming that the same amount of electron density ($5\alpha-$) is transferred, the polarization will become $M^{5\alpha+}–C^{10\alpha-}–R^{5\alpha+}$. Therefore, by making the substituents on C more electron-donating, the M–C polarization is reduced from $M^{10\alpha+}–C^{10\alpha-}$ to $M^{5\alpha+}–C^{10\alpha-}$, consequently facilitating reductive elimination between the alkyl groups.

3) The longer the chain of an alkyl ligand, the more facile the reaction. The direct reason is not the length of the alkyl group *per se*, but rather the increased electron-donating ability of the longer chain, so that the polarization of $M^{\delta+}–C^{\delta-}$ is reduced, thus favoring reductive elimination.

6.3.3 Effects of Additives on Reductive Elimination

Heating cis-[Pd(Me)$_2$(PR$_3$)$_2$] in solution results in the reductive elimination of ethane. The addition of phosphine to this system, however, suppresses the ethane formation. In contrast, addition of acrylonitrile to [Ni(Me)$_2$(bpy)] enhances the reductive elimination of ethane. How may these seemingly contradictory experimental results be interpreted?

There is a route to form ethane directly from cis-[Pd(Me)$_2$(PR$_3$)$_2$] by reductive elimination. However, an alternative route also exists in which one phosphine dissociates from cis-[Pd(Me)$_2$(PR$_3$)$_2$] to give [Pd(Me)$_2$(PR$_3$)], from which ethane is then reductively eliminated. The latter reaction path is favored, since it is considered that the dissociation of a phosphine reduces the electron density on Pd and hence also reduces the Pd$^{\delta +}$–C$^{\delta -}$ polarization, facilitating coupling between the two methyl groups (eqn (6.4)). Since addition of phosphine to this system suppresses the dissociation of a phosphine, reductive elimination is inhibited.

$$\text{(6.4)}$$
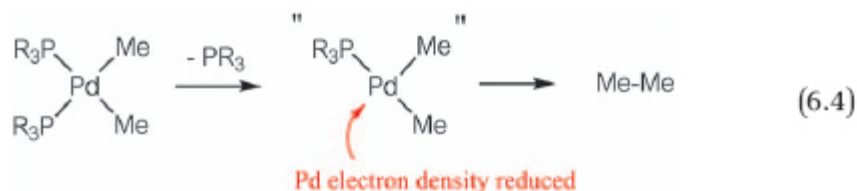
[Ni(Me)$_2$(bpy)] is a 16e complex. When acrylonitrile, H$_2$C=C(H)CN, is present in this system, it coordinates to the Ni using its C=C double bond portion. Since the CN group is strongly electron-withdrawing, acrylonitrile receives a greater amount of electron density by π-back-donation than it donates in σ-donation (see Section 4.3). The electron density on Ni thus decreases as a result of the coordination of acrylonitrile (eqn (6.5)), reducing the degree of polarization in Ni$^{\delta +}$–C$^{\delta -}$, and promoting coupling between the methyl ligands. Additives that seem to have opposite effects can be rationally interpreted if their actions are well understood.

π-back-donation is dominant

electron density on Ni decreases

(6.5)
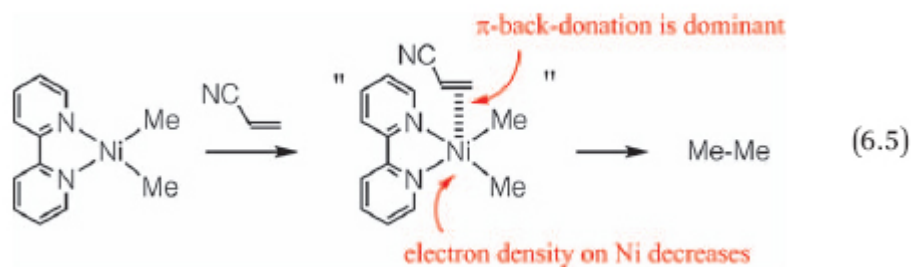
6.3.4 Concerted Reductive Elimination

Reductive elimination was examined for metals with optically active alkyl ligands and it was found that the stereochemistry of the carbon was maintained (eqn (6.6)).

(6.6)
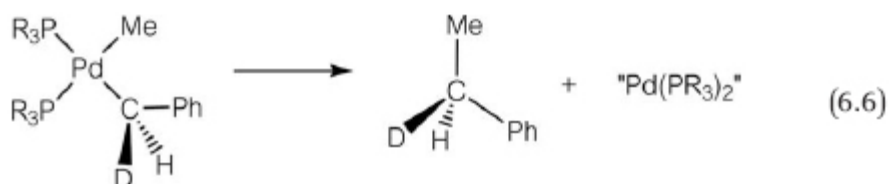
Analysis of the product in the reductive elimination of propane from a square planar gold complex, *trans*-[Au(PR$_3$)(Me)$_2$(Et)] with three alkyl ligands, revealed the formation of propane and no formation of ethane (eqn (6.7)).

Me−Et + "Au(PR$_3$)Me" (6.7)

(no formation of Me-Me)

From the above results, reductive elimination may be considered as a reaction in which the cleavage of two metal–ligand bonds takes place with simultaneous bond formation between two adjacent (*cis*) ligands. The reaction is thus a concerted reaction.

Problem 12. Answer the following questions about the reactions shown below. Here, L is a phosphine.

1) [CpRh(CO)$_2$] + CF$_3$CF$_2$I $\xrightarrow{\text{30 °C}}$

2) [IrCl(PPh$_3$)$_3$] $\xrightarrow{\text{heat}}$

3) [Cp*Ir(CO)$_2$] $\xrightarrow{h\nu, \text{ in neopentane}}$

4) [Cp$_2$W(Me)(H)] $\xrightarrow{h\nu, \text{ in benzene}}$

5) [IrCl(PPh$_2$Me)$_2$(CO)] + CF$_3$I $\xrightarrow{\text{25 °C, 30 min}}$

6) [IrBr(CO)(dppe)] + Et$_3$SiH $\longrightarrow$

7) [CpRe(CO)$_3$] + Br$_2$ $\longrightarrow$

8) [Cp*Ir(H)$_2$(PMe$_3$)] $\xrightarrow{h\nu, \text{ in } n\text{-pentane}}$ four Ir complexes

(1) Reaction a) is faster than that of b). Why?
(1) Reaction c) proceeds on heating, whereas reaction d) does not. Why?

Problem 13. What transition metal complexes are formed in the following reactions?

1) [CpRh(CO)$_2$] + CF$_3$CF$_2$I $\xrightarrow{\text{30 °C}}$

2) [IrCl(PPh$_3$)$_3$] $\xrightarrow{\text{heat}}$

3) [Cp*Ir(CO)$_2$] $\xrightarrow{h\nu, \text{ in neopentane}}$

4) [Cp$_2$W(Me)(H)] $\xrightarrow{h\nu, \text{ in benzene}}$

5) [IrCl(PPh$_2$Me)$_2$(CO)] + CF$_3$I $\xrightarrow{\text{25 °C, 30 min}}$

6) [IrBr(CO)(dppe)] + Et$_3$SiH $\longrightarrow$

7) [CpRe(CO)$_3$] + Br$_2$ $\longrightarrow$

8) [Cp*Ir(H)$_2$(PMe$_3$)] $\xrightarrow{h\nu, \text{ in } n\text{-pentane}}$ four Ir complexes

> **Problem 14.** Predict the reaction pathway of the following reaction.
> $[Rh(CH_3)(PPh_3)_3] + D_2 \rightarrow [Rh(D)\{PPh_2(C_6H_4D)\}(PPh_3)_2] + CH_4$

6.4 Insertion

For a transition metal complex having, for example, hydride, alkyl or aryl ligands, other molecules may insert into the M–H or M–C bond (eqn (6.8)). Here, two typical types of insertion reactions, those of CO and olefins, are described.

$$[L_nM-R] + X \rightarrow [L_nM-X-R] \qquad (6.8)$$
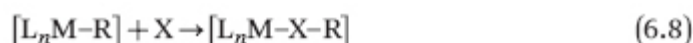
6.4.1 CO Insertion

When a transition metal bears a carbonyl ligand and an alkyl, R (or hydride or aryl) ligand, the CO ligand may insert into the M–R bond to give an acyl complex (Figure 6.5). This is termed CO insertion or carbonylation and it is reversible. The reverse reaction is called CO deinsertion or decarbonylation.
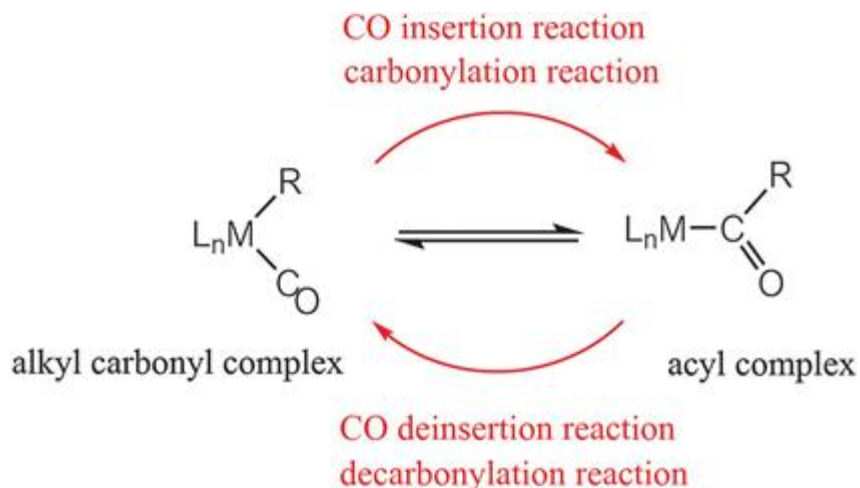
Figure 6.5 CO insertion.

An example is the following. When $[Mn(Me)(CO)_5]$ is dissolved in a solvent under pressure of CO, the insertion product $[Mn\{C(O)R\}(CO)_5]$ is formed. Since CO pressure drives the conversion of the methyl complex to the acyl complex, it may appear that the added CO inserts into the Mn–Me

bond. However, experiments using CO labeled with ^{13}C revealed that the inserted CO was originally one of the terminal CO ligands and that the added CO became a terminal CO ligand (eqn (6.9)).[2]

$$[Mn(Me)(CO)_5] + {}^{13}CO \rightarrow [Mn\{C(O)Me\}(CO)_4({}^{13}CO)] \qquad (6.9)$$
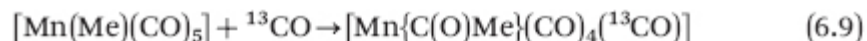
CO insertion is considered to proceed according to the following mechanism. One of the CO ligands originally coordinated to Mn inserts into the Mn–Me bond to form an acetyl complex. Although this is an equilibrium reaction, it is largely shifted to the left because the acetyl complex is a 16e species, typically making detection of the acetyl complex difficult. If the added CO coordinates to the acetyl complex, a stable 18e complex is formed, so that the acetyl complex becomes isolable. The added CO is not directly used for the insertion (except to the extent that the reversibility of the reaction results in scrambling of the CO groups), but is used as a 2e donor ligand to stabilize the 16e species. Addition of other 2e donor ligands also stabilizes the acetyl complex: addition of PPh$_3$ to [Mn(Me)(CO)$_5$] resulted in the isolation of [Mn\{C(O)Me\}(CO)$_4$(PPh$_3$)] (Figure 6.6).
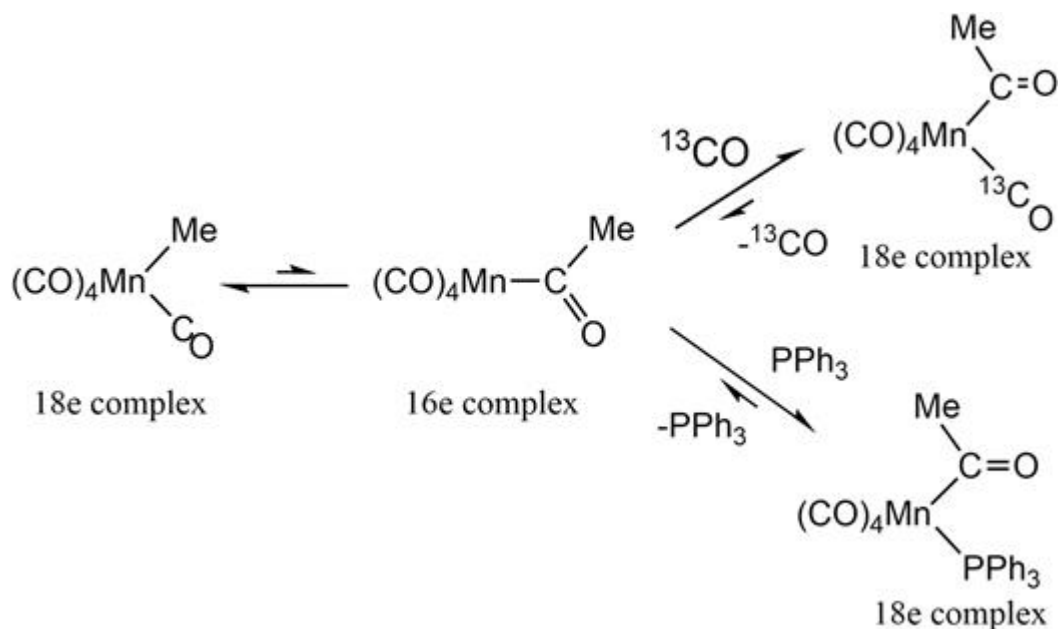
Figure 6.6   Terminal CO insertion into a Mn–Me bond.

Concerning the structure of the acyl complex, there are two possibilities for the location of the acyl group: either in the position where R originally existed or in the position where the CO existed as a terminal ligand. The former case may be considered as the literal insertion of CO into the M–R bond, while the latter case corresponds to migration of the alkyl to a terminal CO. Although a detailed explanation is omitted for reasons of space, it has been confirmed that the reaction proceeds *via* alkyl migration, so it is thus more precise to say that it is an alkyl migration, rather than a CO insertion.[2] However, since an acyl complex is formed from an alkyl complex, the term "CO insertion" is often used. There are also reaction systems in which it is not always clear whether CO insertion or alkyl migration occurs, in which case the term "migratory insertion" may be used.

Studies focusing on the configuration of the alkyl groups have also been reported. CO insertion in an iron complex has been reported to proceed with retention of the carbon configuration (eqn (6.10)), indicating a concerted mechanism to form the C–C bond from the alkyl and carbonyl carbon atoms.[3,4]

$$(6.10)$$
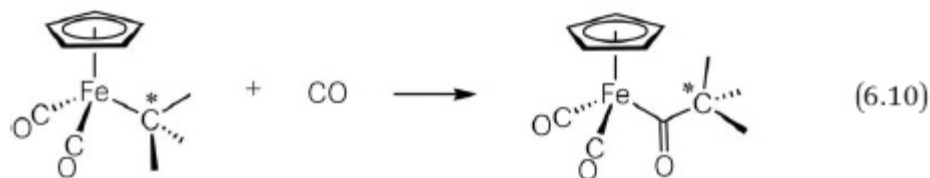
Studies focusing on the metal atom stereochemistry have been reported for iron complexes (eqn (6.11)). Since the iron atom in the starting complex is a chiral center, the starting complex was optically resolved and then reacted with CO. The optical purity of the product was then examined. In the case of this iron complex, it was found from isotope labeling experiments that the externally added carbonyl became the terminal carbonyl ligand of the product. The stereochemistry around the iron and whether CO insertion or alkyl migration occurs depends strongly on the solvent used. When $MeNO_2$ or $EtNO_2$ were used as solvents, an alkyl migration reaction occurred and high stereoselectivity around the iron was observed. On the other hand, when MeCN was used, alkyl migration occurred, but with considerable racemization at the iron atom. In HMPA

(P(NMe$_2$)$_3$), DMSO (Me$_2$SO), and DMF (Me$_2$NCHO), the reaction was of the CO insertion type (as opposed to alkyl migration) and was accompanied by considerable loss of optical activity.[3]

$$(6.11)$$
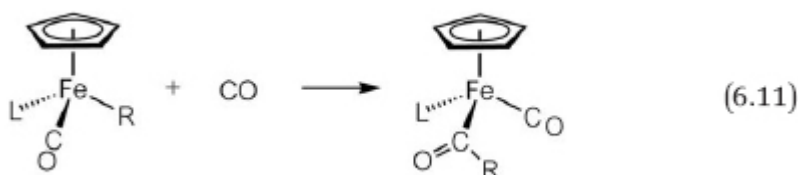
Let us consider simple CO insertion. This is the concerted reaction without ligand dissociation (eqn (6.12)) and M–R and M–CO bond cleavage is accompanied by M–C(O)R and MC(O)–R bond formation and conversion of the CO triple bond into a CO double bond. The ease of CO insertion depends on the energies of these steps. Although the bond energies change according to the identities of M, R and L, it is known that the M–R bond energy has a great influence on the overall reaction and that CO insertion is favored in complexes in which the M–R bond is more easily broken.

$$(6.12)$$
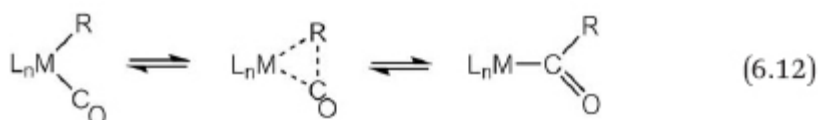
Considering the trends of M–C bond strengths described in Section 3.1, CO insertion is favored in complexes bearing an alkyl group containing an electron-donating substituent and less likely to occur in complexes in which the alkyl group contains electron-withdrawing substituents.

Problem 15. For the following complexes and reaction conditions, explain which reaction is most likely to occur.

1) [CpM(Me)(CO)$_3$] + PPh$_3$ $\longrightarrow$ [CpM{C(O)Me}(CO)$_2$(PPh$_3$)]

     M = Cr, Mo, W

2) [CpMo(R)(CO)$_3$] + CO $\longrightarrow$ [CpMo{C(O)R}(CO)$_3$]

     R = CH$_3$, CF$_3$

3) [CpFe(Me)(CO)$_2$] + PPh$_3$ $\longrightarrow$ [CpFe{C(O)Me}(CO)(PPh$_3$)]

     in THF and in benzene

4) [FeR(CO)$_4$]$^-$ + PMe$_3$ $\longrightarrow$ [Fe{C(O)R}(CO$_3$)(PMe$_3$)]$^-$

     R = Et, Ph

5) [Mn(Me)(CO)$_5$] + CO $\longrightarrow$ [Mn{C(O)Me}(CO)$_5$]

     in the presence and absence of AlBr$_3$
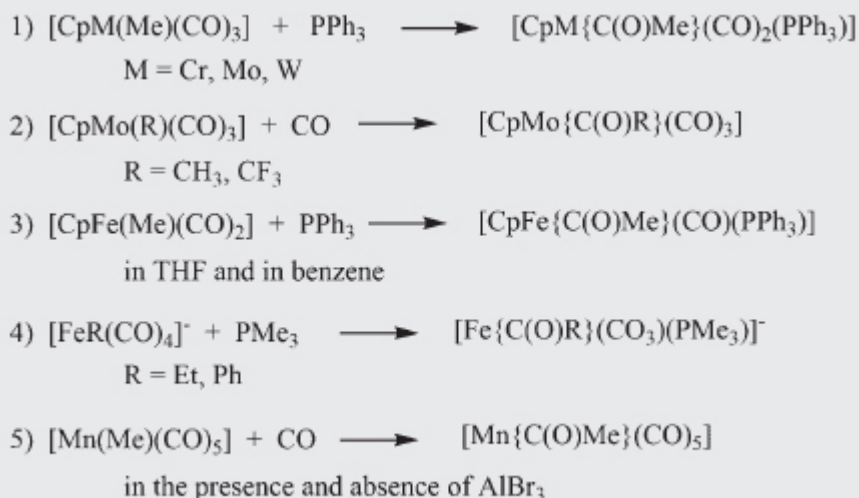
6.4.2 Olefin Insertion

A transition metal complex with a hydride ligand (L$_n$M–H) reacts reversibly with ethylene forming an ethyl complex (L$_n$M–CH$_2$CH$_3$). The reverse reaction is called "β hydride elimination", which will be mentioned in Section 6.4.3.

A closer look at ethylene insertion in the hydride complex reveals that ethylene does not insert directly into the M–H bond, but firstly coordinates to the metal using its π electrons (Figure 6.7(a)). Then, in a concerted reaction, the original M–H bond and the C=C double bond break with simultaneous formation of a new M–C σ bond and C–H bond (Figure 6.7(b)). Overall, an M–H bond is cleaved, a C=C double bond is converted into a C–C single bond, and new M–C and C–H bonds are formed to give an ethyl complex.
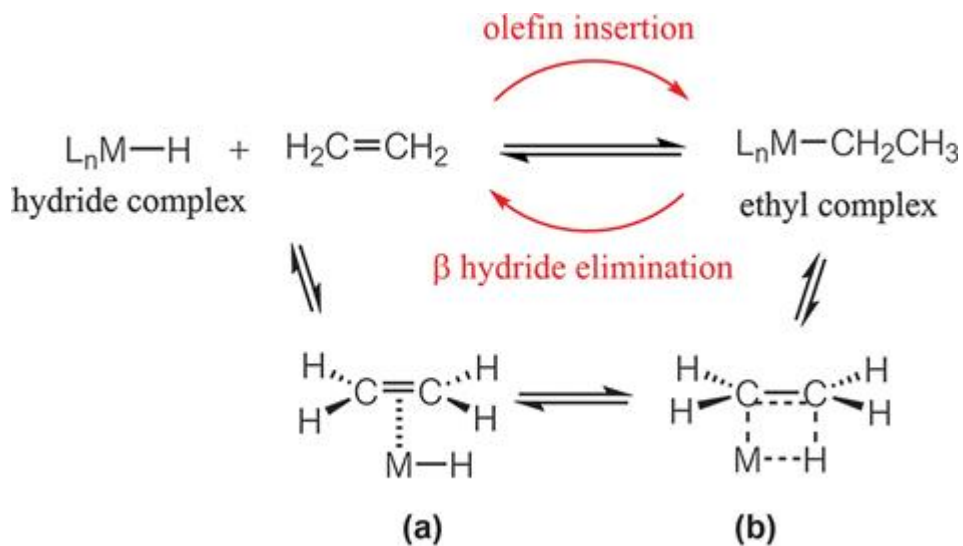
Figure 6.7   Olefin insertion into a hydride complex and β hydride elimination.

The following two points are important in this reaction:

1) From the perspective of the hydride complex, the reaction is the insertion of an olefin into the M–H bond. From the perspective of the olefin, the reaction is addition of M–H across the C=C double bond. Because the reaction proceeds in a concerted mechanism *via* transition state (b), M and H add *cis* to the same side of the C=C double bond.

2) In order for the reaction to occur, it is necessary that the olefin first π-coordinates to the metal as shown in (a). If the starting hydride complex is an 18e species, olefin coordination to the complex would form a 20e species, and so olefin insertion is unfavorable. In contrast, if the starting hydride complex is a 16e species, the complex (a) is an 18e species, so olefin insertion and formation of an ethyl complex are expected to proceed smoothly.

Not only metal–hydrogen bonds, but also metal–alkyl bonds undergo olefin insertion (Figure 6.8). Such reactions are also reversible, termed "β alkyl elimination". This reaction will be discussed in Section 6.4.3.
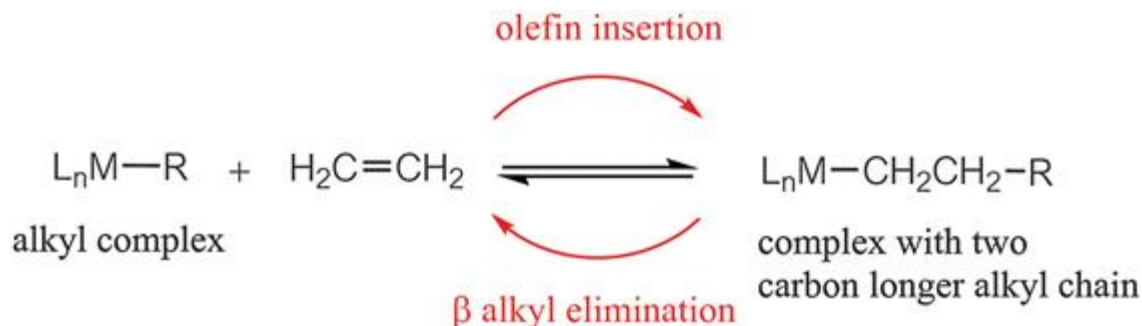
Figure 6.8   Olefin insertion into an alkyl complex and β alkyl elimination.

Since olefins insert into alkyl complexes in addition to hydride complexes, such reactions are highly useful. When ethylene inserts into a hydride complex, an ethyl complex is formed and this may undergo ethylene insertion to form the butyl complex, which in turn may undergo insertion to form the hexyl complex. Thus, since olefins can continuously insert into alkyl complexes, olefins can be polymerized in the coordination spheres of transition metals (Figure 6.9).

$$L_nM-H \xrightarrow{C_2H_4} L_nM-CH_2CH_2-H \xrightarrow{C_2H_4} L_nM\left(CH_2CH_2\right)_{\frac{1}{2}}H \xrightarrow{C_2H_4} L_nM\left(CH_2CH_2\right)_{\frac{1}{n}}H$$
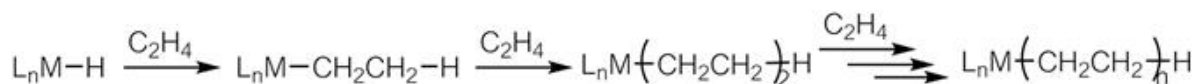
Figure 6.9   Continuous insertion of olefins.

Let's think whether olefins insert more easily into M–H or M–C bonds. Considering the bond energies of M–H and M–C in the starting complexes and of C–H and C–C in the products, olefins are more likely to insert into the M–C bond thermodynamically. However, since insertion into M–C is sterically less favorable than into M–H, olefin insertion into M–H is more likely to occur kinetically. Furthermore, from the viewpoint of the orbital directionality of H in M–H and that of C in M–C, olefins are more likely to insert into the M–H bond. Although it is necessary to consider the above comprehensively, experimentally it is found that olefins insert more easily into M–H than M–C.

Activation energies for olefin insertion into M–H and M–C bonds have been reported for the reactions shown in eqn (6.13). The activation energy for ethylene insertion in both the Co and Rh complexes is 25 to 43 kJ mol^{-1} larger in the M–Et complex than in the M–H complex (Table 6.1).[5] In other words, insertion into the M–H bond is 10^6 to 10^8 times faster than insertion into the M–Et bond.

$$(6.13)$$

M = Co, Rh
R = H, Et
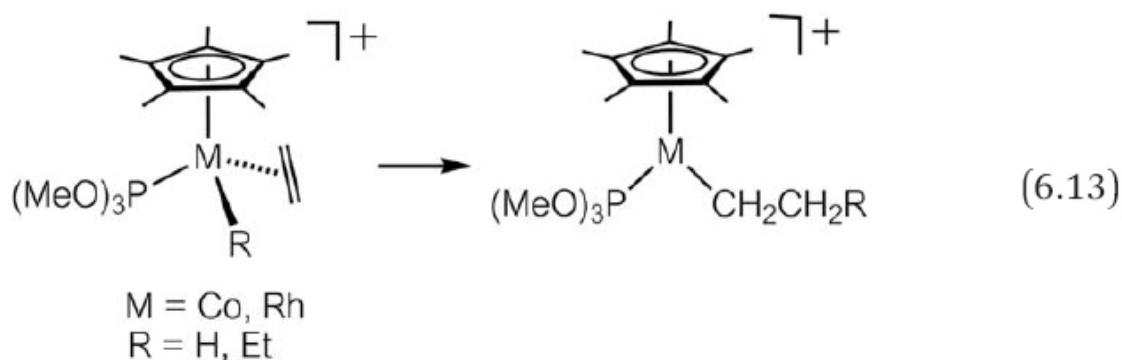
Table 6.1 Comparison of the activation energies of the reactions in eqn (6.13) (kJ mol^{-1}).

M	R = H	R = Et	Difference
Co	25–33	60	25–33
Rh	51	94	43

Olefins other than ethylene, such as propene and styrene, can also insert if it is sterically feasible.

Alkynes may also insert into M–H and M–C bonds similar to olefins. In this case too, *cis* addition occurs (Figure 6.10).
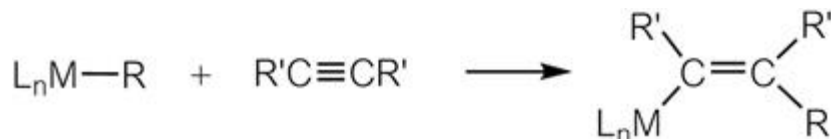
Figure 6.10 Alkyne insertion.

Problem 16. Predict the products in these reactions:

1) $[Cp_2Mo(H)(C_2H_4)]^+ + PPh_3 \rightarrow$
2) $[Pt(H)(OCMe_3)(PEt_3)_2] + C_2H_4 \rightarrow$

6.4.3 β Hydride and β Alkyl Elimination Reactions

The reverse reactions of olefin insertion into M–H and M–C bonds are β hydride elimination and β alkyl elimination, respectively. These are sometimes referred to as β hydride abstraction and β alkyl abstraction. Consider Figure 6.11.
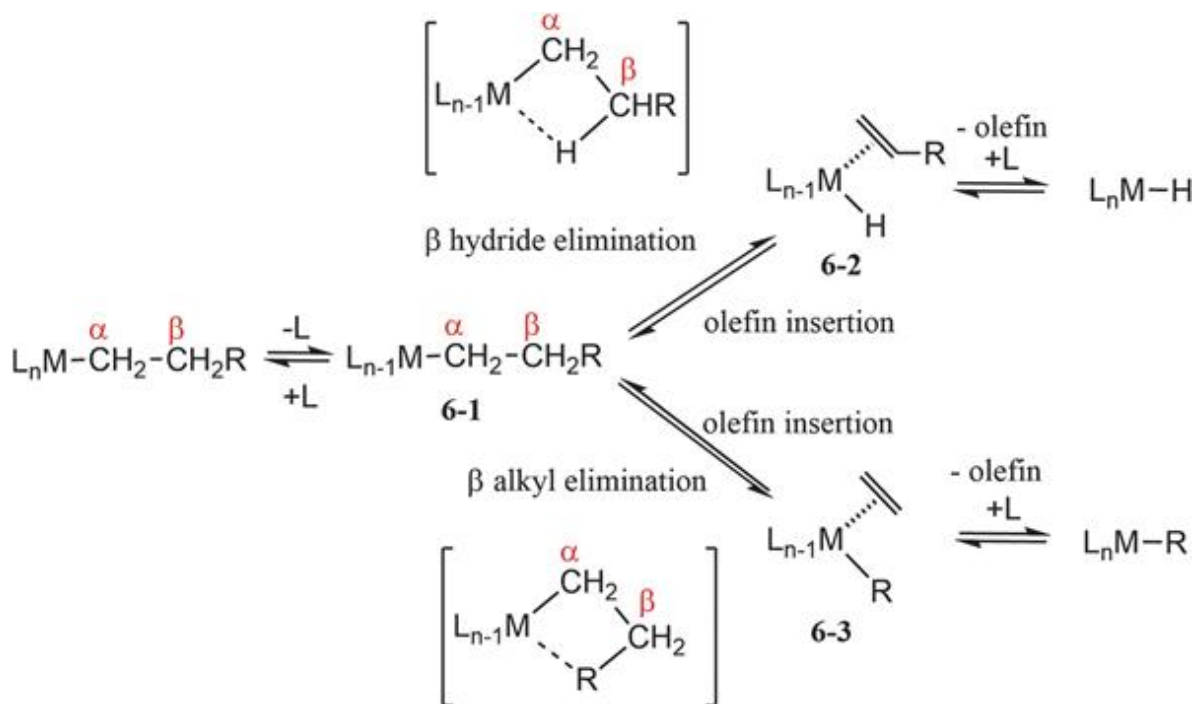
Figure 6.11 β Hydride elimination and β alkyl elimination.

The carbon directly bonded to the metal is called the α carbon, and the carbon next to it is called the β carbon. The β carbon of **6-1** has two hydrogens (β hydrogens) and an alkyl group (β alkyl). Thus, either β hydride elimination or β alkyl elimination may occur. Substituents in the β position are likely to be eliminated (to migrate to the central metal) because they can be sterically located near the metal. It is also important for M–$^{\alpha}$C–$^{\beta}$C–H/R to be coplanar in order for elimination (migration) to occur. In fact, β hydride elimination is overwhelmingly more favorable than β alkyl elimination because H is much less bulky and the orbital used for migration of H has much lower directionality than that of an alkyl group. The β hydride and alkyl elimination reactions of **6-1** form **6-2** and **6-3**, respectively, as shown in Figure 6.11. The olefin in the product may readily be substituted by another coexisting ligand. Conversion of **6-1** into **6-2** or **6-3** increases the total valence electron count by 2. Therefore, the complex (in this case **6-1**) undergoing elimination needs to have a valence electron count of 16 or less. Usually, a 2e donor ligand L first dissociates from the 18e complex [$L_nM(CH_2CH_2R)$] to give [$L_{n-1}M(CH_2CH_2R)$], and then the

β hydride or alkyl is eliminated. After that, the coordinating olefin is replaced by a dissociated L to give L_nMH or L_nMR.

Just prior to elimination, the β hydrogen approaches and then interacts with the metal, as shown in Figure 6.11. Depending on the system, the complex at this point may be isolable. Figure 6.12 shows an example of such a complex for which X-ray structural analysis showed one of the methyl β hydrogens in the ethyl ligand located very close to Ti. This type of interaction between a transition metal and a H atom bonded to another group is called an "agostic interaction". In a typical β hydride elimination, some electron density from the C–H bond is donated to the metal and d electron density of the metal is back-donated to the anti-bonding orbital of the C–H bond weakening the C–H bond and leading to cleavage. However, since the central metal of the complex shown in Figure 6.12 is Ti(iv), there are no d electrons for π-back donation. This is considered to be the reason that an agostic interaction was observed instead of the β hydride elimination.
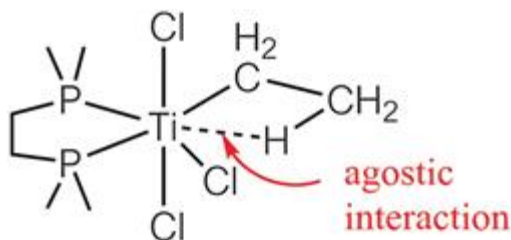
Figure 6.12 Complex with agostic interaction.

Although rare, in a complex having no hydrogen at the β position, hydrogen at the α position may be eliminated. Eqn (5.2) is an example of this in which α hydride elimination leads to a hydride carbene complex.

Problem 17. The reaction to form 1-butene from the metallacycle complex shown below is much slower than the reaction to form 1-butene from *trans*-[Pt(n-Bu)$_2$L$_2$] (L = phosphine). Explain why.
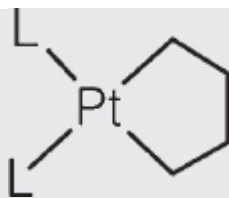
Problem 18. Reaction of **6-4** with AgBF$_4$ produced **6-5**. When **6-5** was heated, the formation of **6-6** was observed, resulting in a 1 : 1 ratio of **6-5** to **6-6**. Explain the mechanism of formation of **6-6** from **6-5**.

6-4   6-5   6-6
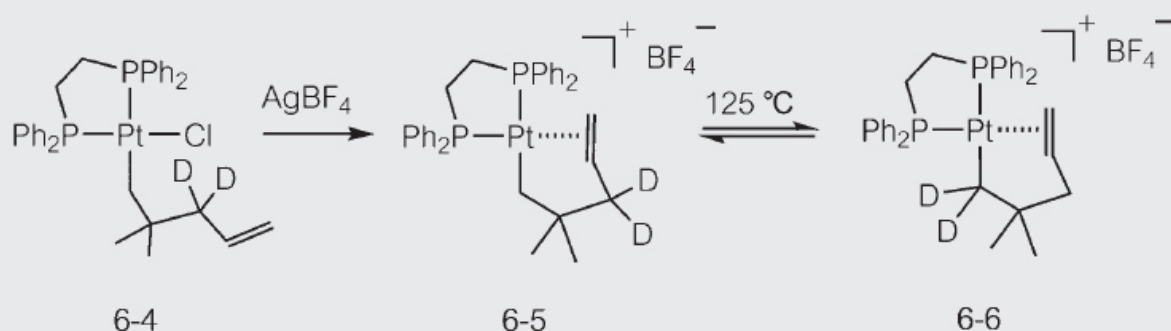
Problem 19. For [PdEt$_2$L$_2$] (L = phosphine), reactions of the *trans* and *cis* complexes with CO lead to different products, as shown below. What reaction mechanism rationally explains this difference? (Hint: in both complexes, dissociation of L takes place first, followed by coordination of CO at the vacant site. During the reactions, the stereochemistry of the metal is maintained and isomerization does not occur.)
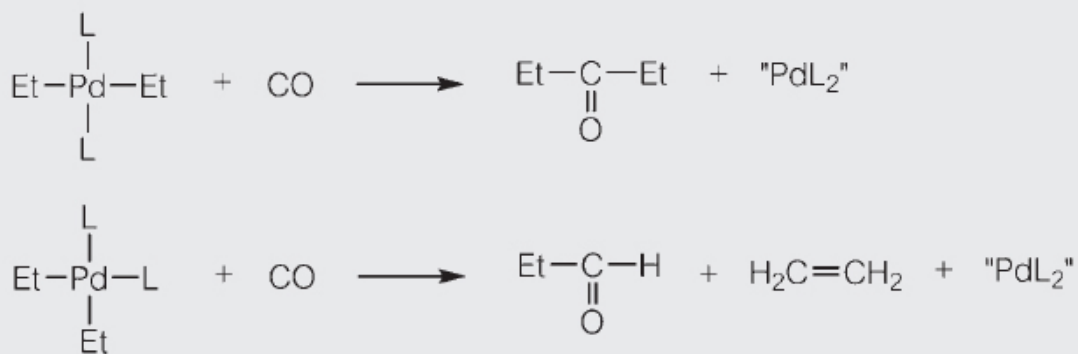
Problem 20. Predict the mechanism of the reactions below.
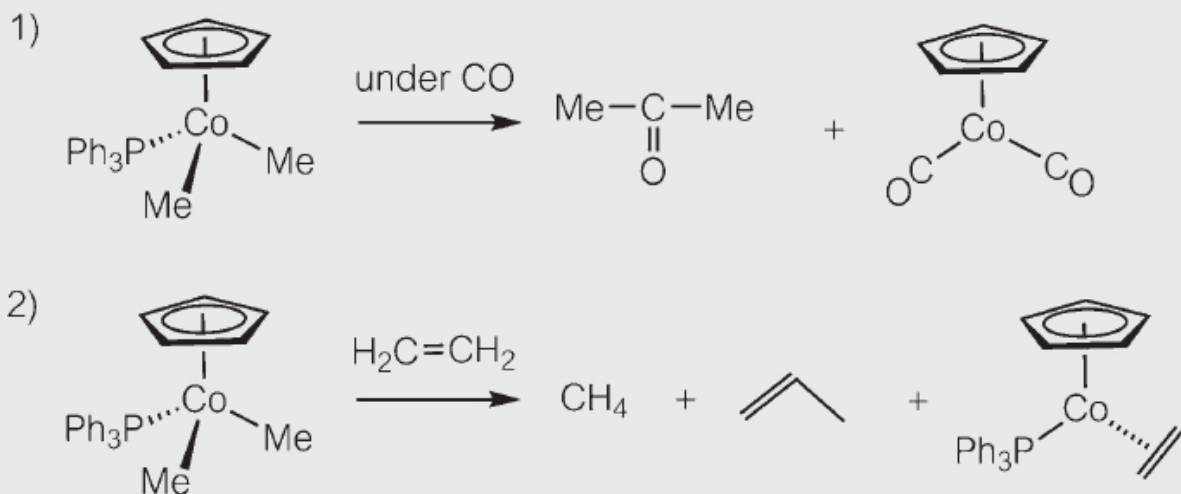
References

1. L. Vaska and J. W. DiLuzio, *J. Am. Chem. Soc.*, 1961, **83**, 2748.
2. K. Noack and F. Calderazzo, *J. Organomet. Chem.*, 1967, **10**, 101.
3. T. C. Flood, K. D. Campbell, H. H. Downs and S. Nakanishi, *Organometallics*, 1983, **2**, 1590.
4. T. C. Flood and K. D. Campbell, *J. Am. Chem. Soc.*, 1984, **106**, 2853.
5. L. Luna, P. S. White, M. Brookhart and J. L. Templeton, *J. Am. Chem. Soc.*, 1990, **112**, 8190.

---

[1] Strictly speaking, a 1s orbital in a hydride ligand and a 1s orbital of H in a H_2 molecule are not completely spherical because they are polarized to some extent. However, it can be said that their directionality is very low compared to that of sp^x orbitals.

Chapter 7

Catalysis by Organometallic Complexes

Hiroshi Nakazawa[a]

[a] Osaka City University Osaka, Japan
Email: nakazawa@sci.osaka-cu.ac.jp

7.1   Introduction

The characteristic reactions of organometallic complexes are described in Chapter 6. By combining these elementary reactions, transformations catalyzed by organometallic complexes can be constructed. In order for the catalyst to work effectively, certain system conditions need to be considered. Careful selection of the following are particularly important:

1) Transition metal
2) Supporting ligands bound to transition metal
3) Substrate reagent
4) Reaction conditions (solvent, temperature, order of reaction, concentration *etc.*)

It is not easy to determine the optimal conditions, but many excellent catalytic systems have been discovered and industrialized. This chapter introduces representative reaction systems catalyzed by organometallic complexes, and outlines the reactions occurring.

7.2   Olefin Polymerization[1,2]

7.2.1   Ziegler Catalysts

The olefin polymerization catalysis created by Ziegler is very useful because the reactions occur at room temperature and under normal pressure.

Although Ziegler catalysts are prepared from tetrachlorotitanium ($TiCl_4$) and alkylaluminium reagents ($AlEt_3$ or $AlEt_2Cl$), the exact nature of the active species has not been completely elucidated. It is clear, however, that the alkylaluminium ethylates Ti to form a complex with a Ti–Et bond, which plays an important role in the olefin polymerization. The currently accepted catalytic mechanism is shown below.

1) Polymerization initiation
Ethylene π-coordinates to a complex with a Ti–Et bond, and then inserts into the Ti–Et bond (eqn (7.1)) forming a butyl-coordinated Ti complex.

$$\text{Ti—Et} \quad + \quad \text{═} \quad \longrightarrow \quad \overset{\underset{\raisebox{0.2em}{$\vdots$}}{\text{═}}}{\text{Ti—Et}} \quad \longrightarrow \quad \text{Ti—CH}_2\text{CH}_2\text{—Et} \qquad (7.1)$$
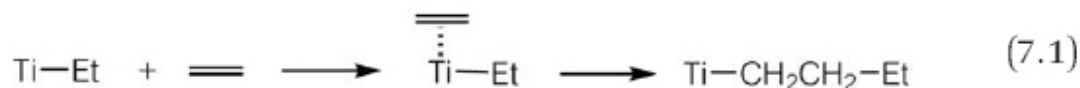
2) Propagation
Another ethylene molecule subsequently π-coordinates to the butyl Ti complex formed in eqn (7.1), and then inserts into the Ti–Bu bond. These steps of ethylene coordination and insertion into the Ti–C σ bond are repeated and the alkyl chain grows (eqn (7.2)).

$$\text{Ti—CH}_2\text{CH}_2\text{—Et} \xrightarrow{+ \text{═}} \overset{\underset{\raisebox{0.2em}{$\vdots$}}{\text{═}}}{\text{Ti—CH}_2\text{CH}_2\text{—Et}} \longrightarrow \text{Ti}\left(\text{CH}_2\text{CH}_2\right)_2\text{Et}$$

$$\xrightarrow{+ \text{═}} \cdots \cdots \xrightarrow{+ \text{═}} \text{Ti}\left(\text{CH}_2\text{CH}_2\right)_n\text{Et} \qquad (7.2)$$
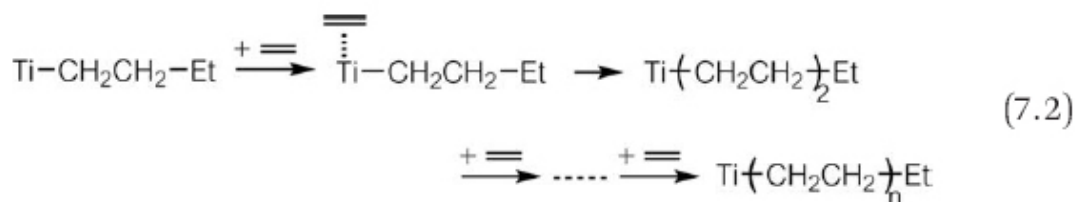
3) Chain transfer
The Ti complex formed by the ethylene insertion always has β hydrogens, so during the ethylene polymerization process, β hydride elimination occurs with a certain probability, liberating a long chain terminal olefin, and generating a Ti–H complex (eqn (7.3)).

$$\text{Ti}\left(\text{CH}_2\text{CH}_2\right)_n\text{Et} \longrightarrow \text{Ti—H} \quad + \quad \text{H}_2\text{C=CH}\left(\text{CH}_2\text{CH}_2\right)_{n-1}\text{Et} \qquad (7.3)$$
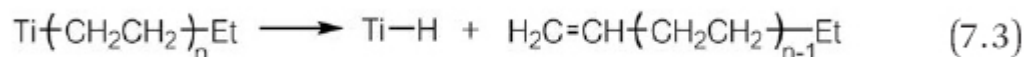
Ethylene π-coordinates to the Ti–H complex formed in eqn (7.3), and then inserts into the Ti–H bond to form a Ti–Et complex (eqn (7.4)). Since this is identical to the starting complex in eqn (7.1), the ethylene polymerization cycle starts again.

$$\text{Ti—H} \quad + \quad \text{═} \quad \longrightarrow \quad \overset{\underset{\raisebox{0.2em}{$\vdots$}}{\text{═}}}{\text{Ti—H}} \quad \longrightarrow \quad \text{Ti—Et} \qquad (7.4)$$
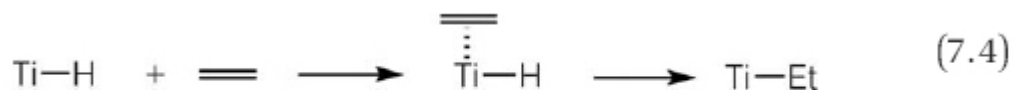
7.2.2 Natta Catalysts

Ziegler catalysts are very effective for ethylene polymerization, but not for propylene polymerization. Natta used alkylaluminium with crystalline $TiCl_3$ instead of $TiCl_4$ to prepare a catalyst and succeeded in propylene polymerization.

Propylene is a compound in which one hydrogen of ethylene is replaced with a methyl group. In the case of propylene polymerization, it is necessary to consider the following points, which do not arise in ethylene polymerization.

1) Regioselectivity

There are two possibilities when propylene inserts into a Ti–R bond: 1,2-insertion and 2,1-insertion, as shown in Figure 7.1.

If 1,2-insertion (or 2,1-insertion) occurs repeatedly, the resulting polymer has head-to-tail connectivity. However, if a 2,1-insertion occurs after a 1,2-insertion, or conversely a 1,2-insertion occurs after a 2,1-insertion, then the conjunction becomes either tail-to-tail or head-to-head (Figure 7.2).

2) Stereoselectivity

When an olefin bearing a substituent is polymerized, an asymmetric carbon is generated. The relative arrangement of the asymmetric carbons is called "tacticity". When the main chain carbons in polypropylene are arranged in the same plane, say horizontal, a polymer in which the methyl groups are all on the same side (*i.e.* either above or below the plane) is *isotactic*, while a polymer in which adjacent methyl groups alternate above and below the plane is *syndiotactic*. A polymer in which the methyl groups are completely randomly configured is *atactic* (Figure 7.3). The physical properties of polypropylene depend greatly on its tacticity. For example, atactic polymers are waxy compounds and less useful, whereas isotactic polymers are easily moldable crystalline solids and thus have a wide range of applications.
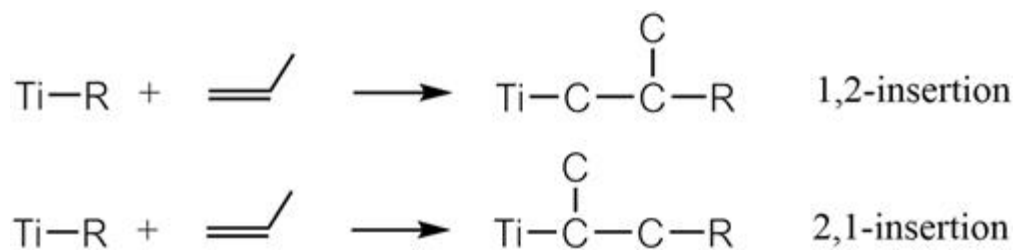
Figure 7.1   1,2-Insertion and 2,1-insertion of propylene.
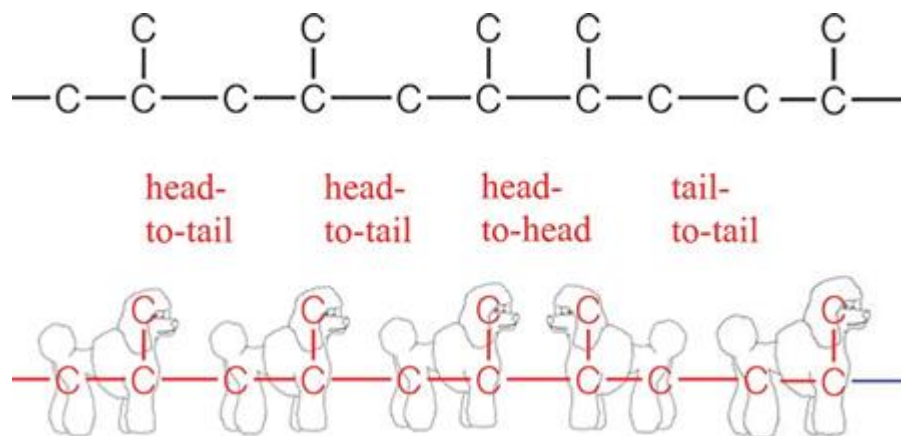
Figure 7.2 Conjunction part of polypropylene.
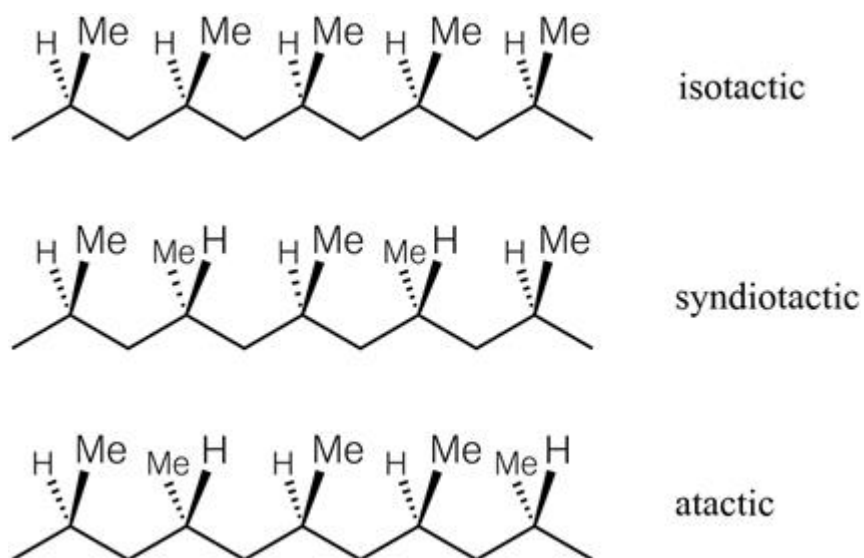
Figure 7.3 Tacticity of polypropylene.

   The Natta catalyst, reported in 1954, is excellent for the regioselective and stereoselective polymerization of propylene, and the process was industrialized in 1957. Until the middle of the 20th century when the Natta catalyst was developed, it was thought that only complicated and precisely constructed enzymes with molecular weights in the hundreds of thousands of Daltons produced by biological systems could control asymmetric carbon. $TiCl_3$, however, has a formula weight of less than 200 and is extremely simple, and just a blend of this with an alkylaluminium can control the asymmetry of thousands of carbon atoms. People at the time

were amazed at this, and Ziegler and Natta received the Nobel Prize in Chemistry in 1963 for their discoveries in the field of the chemistry and technology of high polymers (see Chapter 12).

With Natta catalysts, isotactic polymers are obtained. The detailed mechanism is still not fully elucidated, but it has been clarified to some extent in various studies. The most widely accepted mechanism at present is shown in Figure 7.4. The catalytically active site is at a Ti atom in a chloride-bridged polynuclear complex. The growing polymer exists at the far right of Figure 7.4. This figure shows how the monomer (propylene) π-coordinates *via* the C=C double bond to the Ti from above. The presence of the relatively large Cl ligands in three directions of the reaction face, and smaller methylene at the coordinated end of the polymer chain, results in the least steric hindrance when the approaching propylene methyl group is oriented on the coordinated methylene group side. The C=C double bond of propylene then inserts into the Ti–C bond such that the methyl group is directed below the plane of the paper, and when repeated for each subsequent insertion, affords the isotactic polymer.
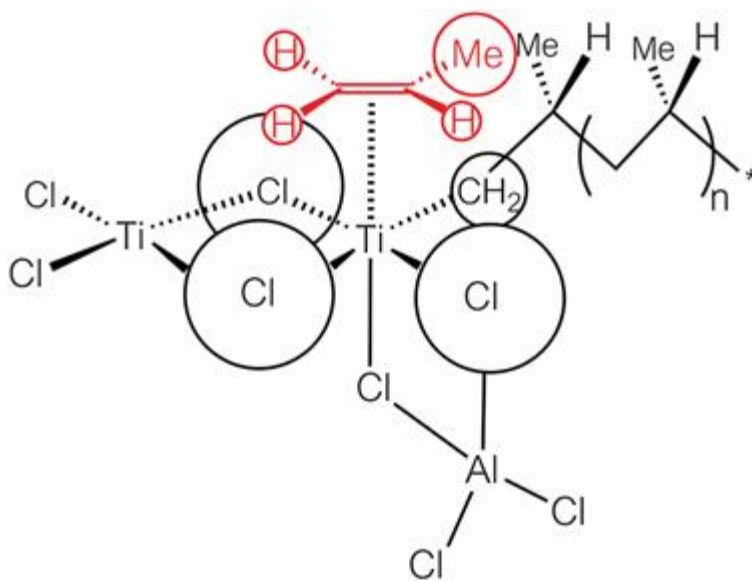
Figure 7.4   Stereoselective polymerization mechanism by the Natta catalyst.

Since the catalytic systems developed by Ziegler and Natta use $TiCl_4$ and $TiCl_3$ as catalyst precursors, respectively, catalysts prepared from titanium

chloride and an alkylaluminium are collectively called Ziegler–Natta catalysts.

7.3 Olefin Isomerization

The combination of an olefin insertion into a metal–hydride bond and β hydride elimination allows the olefin double bond to migrate within the molecule. Figure 7.5 shows an example of the isomerization of 1-butene. Since several hydride complexes serve as catalysts, the catalytically active species is shown here as M–H.
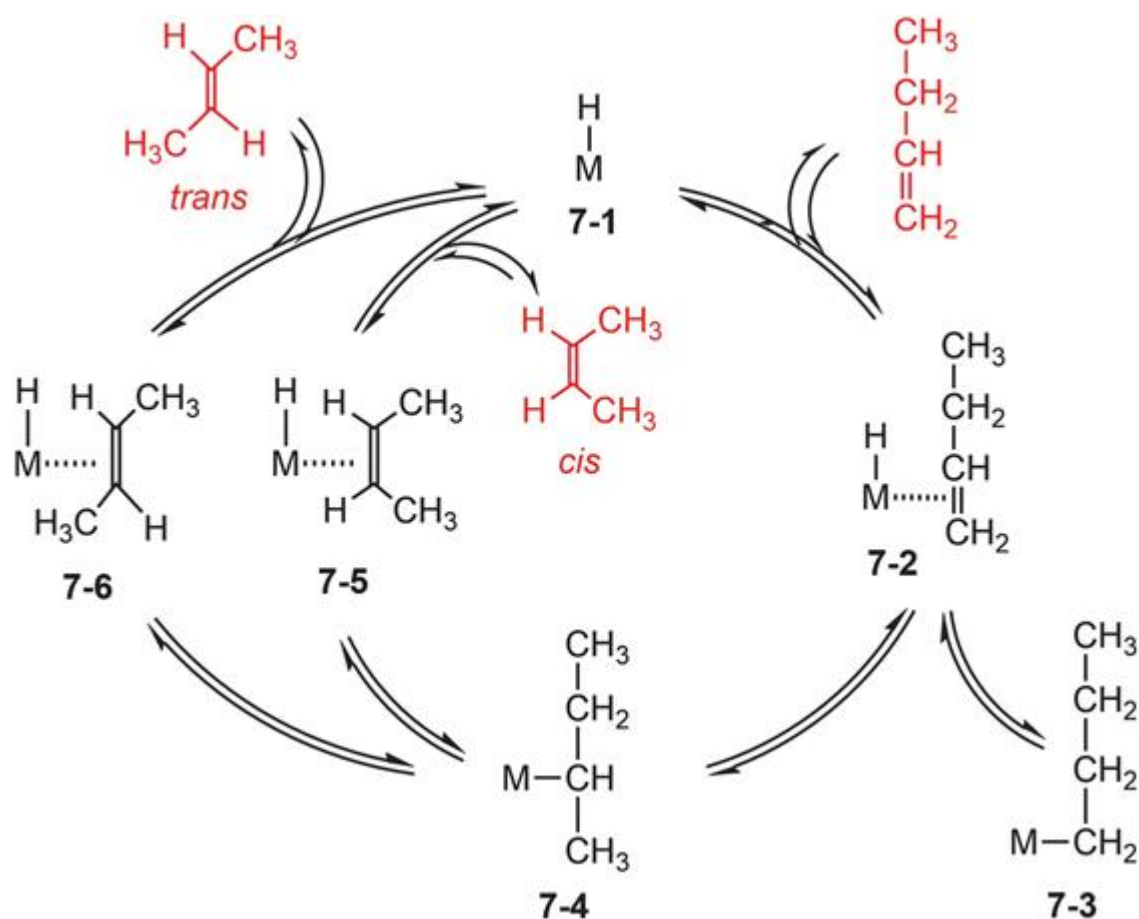
Figure 7.5   Olefin isomerization catalyzed by a hydride complex.

The reaction starts from the point where the olefin π-coordinates to the M–H complex (**7-1**) to form **7-2**. Depending on how the insertion of the olefin into the M–H bond occurs, either **7-3** or **7-4** may be formed. If β hydride elimination occurs from **7-3**, **7-2** is regenerated. Complex **7-4**,

however, has two kinds of β hydrogens, so two different β hydride eliminations are conceivable. When a methyl hydrogen is eliminated by M, **7-2** is regenerated, but when a methylene hydrogen is eliminated, **7-5** or **7-6** is formed. If dissociation of the olefin occurs at this point, *cis*-2-butene and *trans*-2-butene are obtained, and in the presence of additional 1-butene substrate, **7-2** is formed. Because all of the reactions shown in Figure 7.5 are reversible, 1-butene, *cis*-2-butene and *trans*-2-butene are ultimately distributed in a ratio based on thermodynamic stability. [Rh(H)(CO)(PPh$_3$)$_3$] is known to exhibit catalytic activity according to this mechanism.[3] Since this complex is an 18e species, PPh$_3$ dissociation firstly takes place to form the catalytically active 16e species, [Rh(H)(CO)(PPh$_3$)$_2$], and then olefin coordination and isomerization occur.

Transition metal complexes other than hydride complexes are also known to catalyze olefin isomerization (double bond migration). In such cases, the π allyl complex is an important intermediate. Figure 7.6 shows such a catalytic cycle.
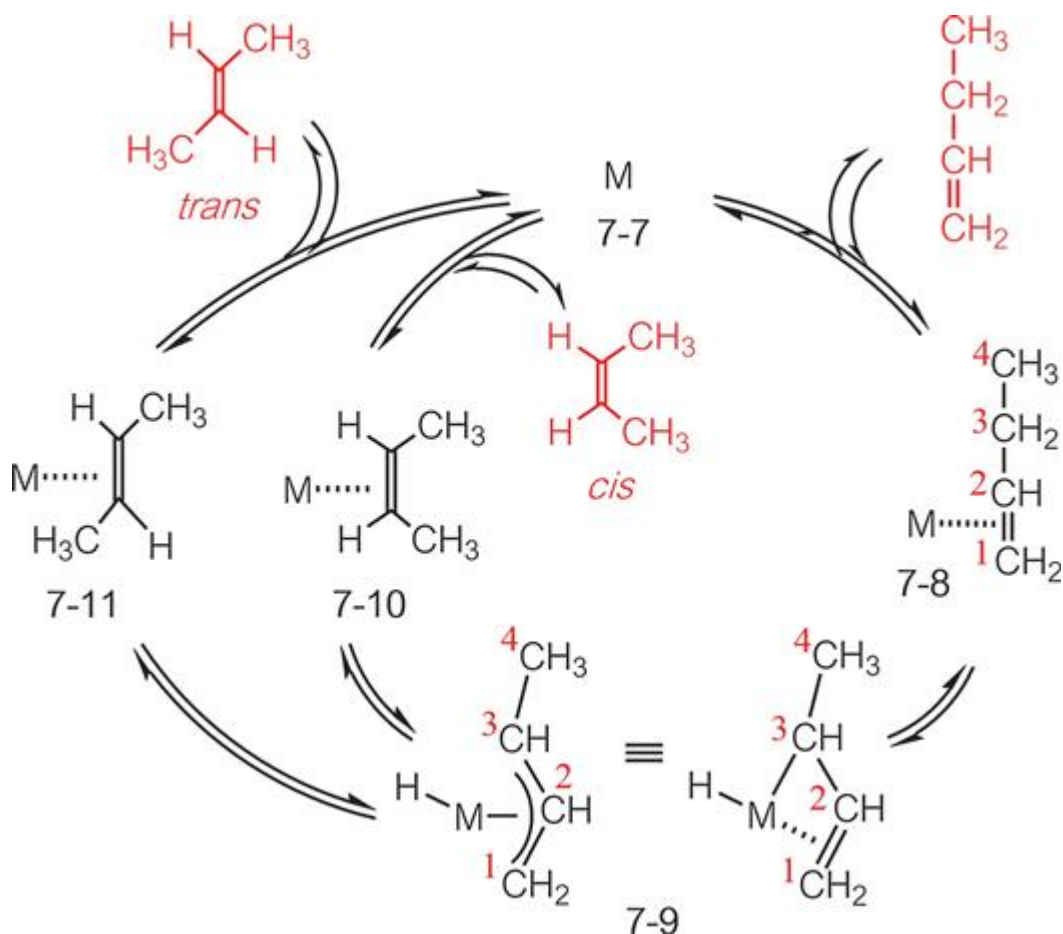
Figure 7.6   Olefin isomerization catalyzed by initially non-hydride complexes.

When an olefin π-coordinates to **7-7**, **7-8** is generated. Next, the C–H bond on C^3 oxidatively adds to the metal to form **7-9**, which has both π-allyl and hydride ligands. If the C^3 carbon and hydride are reductively eliminated, **7-8** is regenerated. However, if the C^1 carbon and hydride are reductively eliminated, then **7-10** or **7-11** is formed. Dissociation of olefin from these generates *cis* and *trans* 2-butene, respectively, simultaneously reforming catalytically active M again. This catalytic cycle consists of π-coordination and dissociation of olefin and oxidative addition and reductive elimination of C–H bonds, each step of which is reversible. Since **7-7** is expected to be a 14e species, the precursor should be a complex which readily forms a 14e species. $Fe_3(CO)_{12}$ is known as a precursor complex that catalyzes *via* this mechanism.[4,5] $Fe(CO)_3$ formed from this complex is thought to be the real catalytically active species.

7.4 Olefin Hydroformylation

The reaction of olefin, carbon monoxide and hydrogen molecules in the presence of a catalyst generates an aldehyde. This reaction is referred to as hydroformylation because it corresponds to the addition of hydrogen and a formyl group to an olefin (eqn (7.5)).

$$
RCH{=}CH_2 \;+\; CO \;+\; H_2 \xrightarrow{\text{cat.}}
\begin{array}{c}
\text{H} \quad \text{H} \\
\text{R}{-}\overset{\displaystyle |}{\text{C}}{-}\overset{\displaystyle |}{\text{C}}{-}\text{H} \\
\text{H} \quad \text{C}{-}\text{H} \\
\quad\;\; \text{O}
\end{array}
\;+\;
\begin{array}{c}
\text{H} \quad \text{H} \\
\text{R}{-}\overset{\displaystyle |}{\text{C}}{-}\overset{\displaystyle |}{\text{C}}{-}\text{H} \\
\text{H}{-}\text{C} \quad \text{H} \\
\quad\; \text{O}
\end{array}
\tag{7.5}
$$
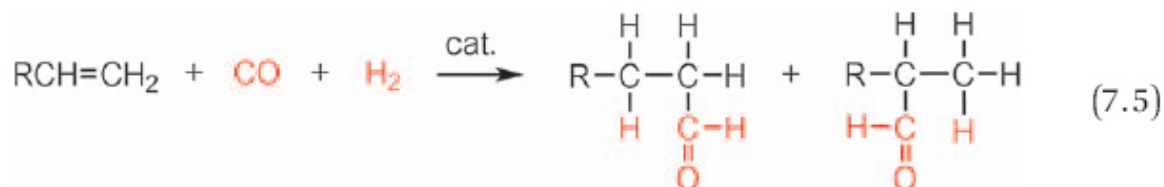
This reaction, also called the oxo method, is an industrially important reaction, and millions of tons of aldehyde are produced annually by this method. Co and Rh compounds have been used as catalysts.[6]Figure 7.7 shows the catalytic cycle when $[Co_2(CO)_8]$ is used.
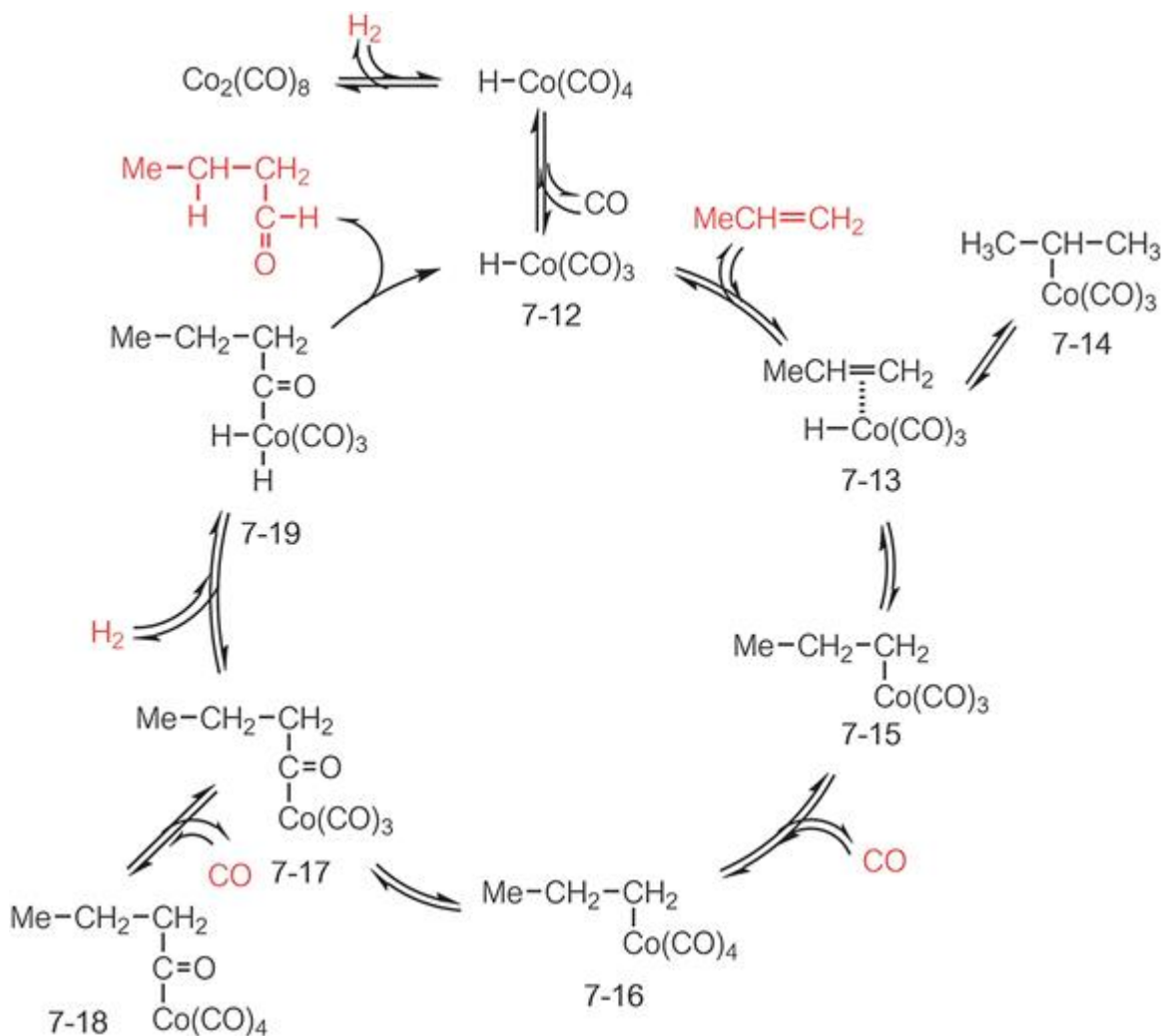
Figure 7.7 Olefin hydroformylation.

The dinuclear catalyst precursor $[Co_2(CO)_8]$ reacts with H_2 to form mononuclear $[Co(H)(CO)_4]$. Dissociation of a CO (and dissolution into the solution) from this complex forms the 16e complex $[Co(H)(CO)_3]$ (**7-12**). This is the catalytically active species and its formation starts the catalytic cycle. An olefin (propylene in this case) then π-coordinates to **7-12** forming **7-13**. The coordinated propylene then inserts into the Co–H bond in one of two ways, producing either **7-14** or **7-15**. Since **7-15** is a 16e species, it recaptures CO from the solution to form the 18e species **7-16**. Since this has alkyl and carbonyl ligands, CO insertion may occur to generate **7-17**, a 16e species. Coordination of CO to **7-17** forms **7-18**, but in the presence of hydrogen, H_2 adds oxidatively to **7-17** forming **7-19**. The reactions up to

this point are all reversible. However, when reductive elimination of the acyl group and hydride ligand from **7-19** occurs, an aldehyde is irreversibly eliminated (since it does not react with **7-12**) with the regeneration of the catalytically active **7-12**. The catalytic cycle thus rotates clockwise in the figure.

As explained above, when olefin insertion occurs in **7-13**, two different complexes, **7-14** or **7-15**, may be formed. Complex **7-15** undergoes reactions leading to the primary aldehyde, but similar reaction pathways from **7-14** lead to the secondary aldehyde. Thus, if it is possible to control the reaction at this stage, selective aldehyde synthesis is possible. Although primary aldehydes have higher industrial utility and value, the $[Co_2(CO)_8]$-based catalyst system does not have very high selectivity for controlling aldehyde formation (primary *vs.* secondary). How can this selectivity be improved? Complex **7-15** has a *n*-propyl ligand, whereas **7-14** has an *i*-propyl ligand, which is bulkier. Therefore, if a supporting ligand is replaced by a ligand bulkier than CO, **7-14** becomes less favorable, resulting in higher selectivity for **7-15** formation. In fact, the addition of $P(n\text{-Bu})_3$ to this catalyst and reaction system improved the selectivity of primary aldehyde formation and also improved the activity of the catalyst.[7] Thus, drawing a catalytic cycle may provide some insights into improving the catalyst system.

Olefin hydroformylation consists of the combination of olefin π-coordination, olefin insertion into an M–H bond, CO coordination and insertion, H_2 oxidative addition and reductive elimination of the acyl and hydride ligands. Although each individual step comprises a fundamental reaction, these elementary reactions maintain an exquisite balance. For example, CO coordinates to the 16e complex **7-15**, but there is a possibility that instead H_2 present in the system oxidatively adds to **7-15** to form $[Co(CO)_3(H)_2(C_3H_7)]$ and then for the propyl and hydride ligands to reductively eliminate producing propane. In fact, with careful selection of the transition metal and supporting ligands, this reaction does not occur and hydroformylation results. Such metal and ligand selection to achieve a desired outcome is difficult, and trial and error, inspiration, luck, the researcher's knowledge and intuition, *etc.* often play a large part. The development of a new catalyst is usually a difficult, but also very interesting part of chemical research and application.

7.5   The Wacker Process (Höchst–Wacker Process)[8]

The Wacker process (sometimes referred to as the Höchst–Wacker process) employs a transition metal catalyst in the production of acetaldehyde by ethylene oxidation. The catalytic cycle is described below.

It was already known at the end of the 19th century that acetaldehyde was formed by bubbling ethylene into aqueous palladium chloride ($PdCl_2$) solution. However, in this reaction, Pd^{2+} is reduced to Pd^0 in stoichiometric amounts, losing its catalytic activity (eqn (7.6)), and hence it was far from practicable. If the Pd formed were to be converted into Pd^{2+} by air oxidation, the palladium could be used as a catalyst in a practical level process, but such a reaction does not actually occur.

$$H_2C{=}CH_2 + PdCl_2 + H_2O \rightarrow CH_3CHO + Pd^0 + 2HCl \qquad (7.6)$$

Researchers at the Wacker company, however, addressed and solved this problem. The key point is to use $CuCl_2$. When Pd and $CuCl_2$ coexist, a redox reaction occurs to form Pd^{2+} and CuCl (eqn (7.7)). This reaction converts Pd^0 back to Pd^{2+}, and results in the stoichiometric reduction of Cu^{2+} to Cu^+. However, CuCl is easily oxidized by air in aqueous hydrochloric acid to $CuCl_2$ (eqn (7.8)). That is, addition of the Cu compound rendered possible the indirect air oxidation of Pd^0 to Pd^{2+}, although direct oxidation does not normally occur. The H_2O produced in eqn (7.8) is used in eqn (7.6), and the HCl produced in eqn (7.6) is used in eqn (7.8), so that the stoichiometric quantities are in perfect agreement.

$$Pd^0 + 2CuCl_2 \rightarrow PdCl_2 + 2CuCl \qquad (7.7)$$

$$2CuCl + 2HCl + \frac{1}{2}O_2 \rightarrow 2CuCl_2 + H_2O \qquad (7.8)$$
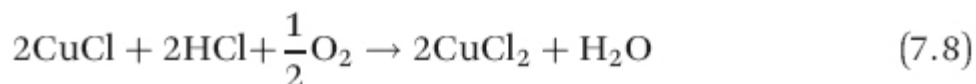
Eqn (7.9) shows the combination of eqn (7.6)–(7.8) after cancellation of compounds appearing on both the left and right sides. Although this

reaction does not usually occur, it proceeds due to catalytic action by $PdCl_2$ and $CuCl_2$.

$$H_2C=CH_2 + \frac{1}{2}O_2 \rightarrow CH_3CHO \tag{7.9}$$

A closer look at the proposed catalytic cycle of the Wacker process is shown in Figure 7.8, although the details are unclear. Chloride anions are omitted for simplicity. Ethylene coordinates to the initially added Pd^{2+} (**7-20**) to form **7-21**. Since this complex has a $2+$ charge, the ethylene carbons are highly electrophilic and nucleophilic attack by OH^- generated from water forms **7-22**. [An alternative mechanism involving H_2O coordination to **7-21** to form an aqua complex, subsequent deprotonation to form a hydroxo complex (Pd–OH), and olefin insertion into the Pd–O bond to give **7-22** is also conceivable for this step, but is not currently supported.] Since **7-22** has β hydrogens, β hydride elimination occurs to give **7-23**. Dissociation of the enol hydroxyethylene and proton from this complex generates a Pd^0 complex (**7-24**). The unstable enol rearranges to the stable tautomer, acetaldehyde, while the Pd^0 formed and Cu^{2+} present in the reaction system undergo a redox reaction to form Pd^{2+} (**7-20**) and Cu^+. Cu^+ is subjected to air oxidation in hydrochloric acid solution to regenerate Cu^{2+}, completing the full catalytic cycle. The H_2O formed at this time is used in the reaction generating **7-22** from **7-21**, and $2H^+$ used in the oxidation of Cu^+ is supplied by the reactions from the same reaction and also that generating **7-24** from **7-23**.
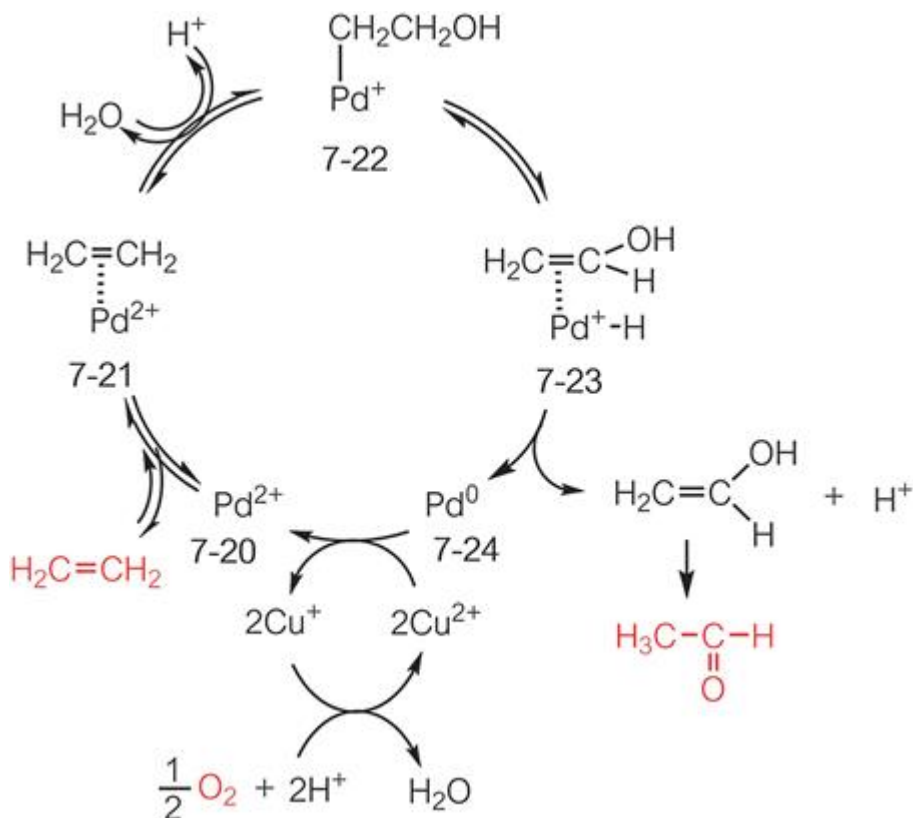
Figure 7.8   Catalytic cycle of the Wacker process.

In this catalytic system, two kinds of transition metals show individual and different catalytic activity without inhibiting each other. In addition, the product of one catalytic cycle is the reactant in the other catalytic cycle. This is a chemically very beautiful catalytic cycle, incurring minimal waste.

7.6   The Monsanto Process for the Synthesis of Acetic Acid[9]

Acetic acid is an industrially important raw material. Acetic acid can be obtained by acetaldehyde oxidation, and, as described above, acetaldehyde can be obtained by oxygenation of ethylene in the Wacker process. Thus, acetic acid could be obtained starting from ethylene, a product of the petrochemical industry, as a raw material. The Monsanto process, on the other hand, is a method of synthesizing acetic acid from methanol and carbon monoxide, and is industrially important since it does not depend on the petrochemical industry (eqn (7.10)).

$$\text{MeOH} + \text{CO} \xrightarrow{\text{cat.}} \text{MeCOOH} \tag{7.10}$$

The catalyst used in the Monsanto process is a Rh complex. In the 1960s a Co complex discovered by the BASF company was used to catalyze the synthesis of acetic acid from methanol and carbon monoxide, but the Rh complex discovered in the 1970s by the Monsanto company showed higher catalytic activity at lower temperature and pressure. Over 8 million tons of acetic acid are produced annually by the Monsanto method.

The proposed catalytic cycle is shown in Figure 7.9. Although $RhCl_3$ and HI are used as catalysts in this reaction, $[Rh(CO)_2(I)_2]^-$ formed in this system is the actual catalytically active species. In order to construct an acetyl group from methanol and CO, it is necessary to coordinate a methyl group to Rh. However, Rh–Me species cannot be generated from methanol because C–O activation does not occur under the reaction conditions. A catalytic amount of HI plays an important role here: MeOH and HI are in equilibrium with MeI and H_2O (eqn (7.11)). As **7-25** is a 16e species, MeI produced in the equilibrium noted above adds oxidatively to it in a *trans* configuration (see Section 6.2.1) forming **7-26**. Since **7-26** has both methyl and carbonyl ligands, CO insertion occurs to give **7-27**. A further molecule of CO coordinates to the 16e species **7-27** to give **7-28**, from which the acetyl and iodide ligands are reductively eliminated to form MeC(O)I, at the same time regenerating **7-25** to complete the catalytic cycle. The MeC(O)I produced reacts with H_2O formed in eqn (7.11) to generate the target compound, acetic acid, while the concomitantly formed HI is used in eqn (7.11). This is a sophisticated catalytic reaction with minimal waste.

$$\text{MeOH} + \text{HI} \rightleftharpoons \text{MeI} + \text{H}_2\text{O} \tag{7.11}$$
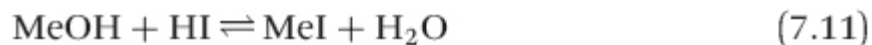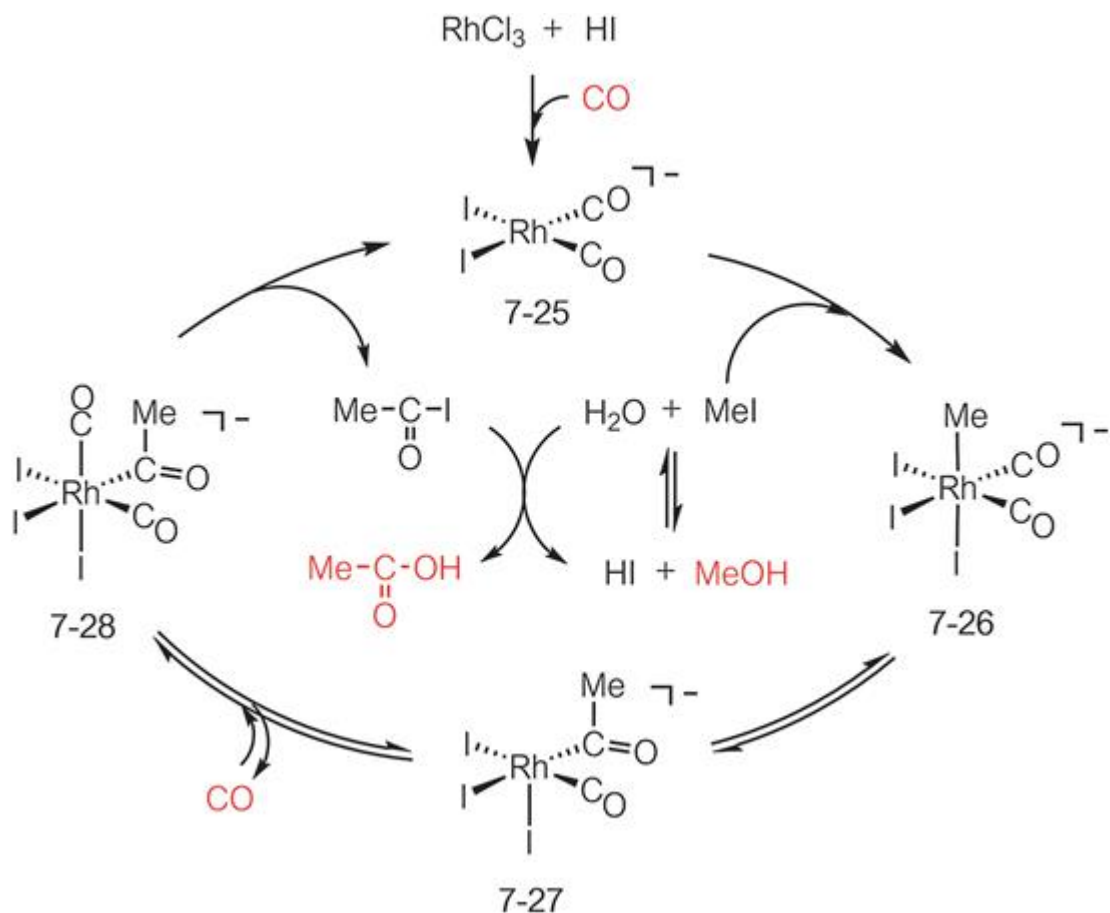
Figure 7.9 Catalytic cycle of the Monsanto process.

References

1. G. Odian, *Principles of Polymerization*, Wiley, 4th edn, 2004.
2. V. Chandrasekhar, *Inorganic and Organometallic Polymers*, Springer, 2005.
3. (a) D. Evans, J. Osborn and G. Wilkinson, *J. Chem. Soc. A*, 1968, 3133; (b) S. Krompiec, M. Pigulla, M. Krompiec, B. Marciniec and D. Chadyniak, *J. Mol. Catal. A*, 2005, **237**, 17.
4. C. P. Casey and C. R. Cyr, *J. Am. Chem. Soc.*, 1973, **95**, 2248.
5. D. Seyferth, *Organometallics*, 2003, **22**, 2.
6. (a) R. L. Pruett, *Adv. Organomet. Chem.*, 1979, **17**, 1; (b) *New Syntheses with Carbon Monoxide*, ed. J. Falbe, Springer, 1980.
7. L. H. Slaugh and R. D. Mullineaux, *J. Organomet. Chem.*, 1968, **13**, 469.
8. J. M. Takacs and X. T. Jiang, *Curr. Org. Chem.*, 2003, **7**, 369.
9. C. M. Thomas and G. Suss-Fink, *Coord. Chem. Rev.*, 2003, **103**, 283.

Section 2: Advanced

Chapter 8

Chemistry of Transition Metal Complexes with Group 14 Elements: Transition Metal Complexes with Silicon, a Heavier Carbon Group Element

Masaaki Okazaki[a]

[a] Graduate School of Science and Technology, Hirosaki University, Japan
mokazaki@hirosaki-u.ac.jp

8.1 Introduction

Group 14 in the periodic table contains carbon, silicon, germanium, tin and lead, although lead will not be addressed in this chapter. Each element has four valence electrons of the type $n\text{s}^2n\text{p}^2$ and tends to adopt oxidation states of +2 and +4 (Table 8.1). Due to the low electronegativity of the E atom (E = silicon, germanium and tin) compared with hydrogen, the E–H bond is polarized $E(\delta^+)$–$H(\delta^-)$, which is opposite to the polarization in the C–H bond. Accordingly, hydrogen compounds of silicon, germanium and tin, *i.e.* silanes, germanes and stannanes, exhibit high reactivity and undergo E–H oxidative addition to transition metals to give transition metal-group 14 element complexes.

Table 8.1 Electronegativities of selected elements.

Element	Electronic configuration	Allred–Rochow electronegativity
H	1s^1	2.20

C	$[He]2s^22p^2$	2.50
Si	$[Ne]3s^23p^2$	1.74
Ge	$[Ar]3d^{10}4s^24p^2$	2.02
Sn	$[Kr]4d^{10}5s^25p^2$	1.72

Silyl, germyl and stannyl groups (ER_3) derived from these electropositive elements act as electron-donating ligands and due to their lower electronegativity result in metal centers that are more electron-rich. This is a significant difference from the situation with carbon-based ligands. The low energy level of the d orbital and/or antibonding E–R σ* orbital enable efficient π-back donation from the metal dπ orbital, leading to a rich variety of chemistries of heavier group 14-transition metal complexes.

In the case of divalent species, a methylene is relatively stable in the triplet state, while the silicon, germanium and tin analogues, *i.e.* silylene, germylene and stannylene, favor the singlet state. The difference of the electronic states can be rationalized by the greater tendency of the ns^2 valence electrons of the heavier group 14 elements to form a lone pair of electrons due to their spatially spread valence orbitals and greater s–p energy gap.[1]

This chapter surveys the most widely investigated silicon-containing transition metal complexes.

8.2 Transition Metal Silyl Complexes

The first transition metal silyl complex, possessing a single bond between a transition metal and a silicon atom, was $[CpFe(CO)_2SiMe_3]$ (**1**) (Cp = η^5-C_5H_5), prepared by Wilkinson in 1956,[2] but research on silyl complexes made little progress until the 1970s. Silyl complexes were then recognized as key intermediates in the metal-catalyzed hydrosilation of unsaturated organic compounds, an important preparative route in modern organic synthesis, and the chemistry of silyl complexes then rapidly developed. Transition metal silyl complexes may be synthesized by a wide variety of methods. This section firstly describes the main synthetic routes to silyl complexes, then outlines the bonding mode between the transition metal and silicon, followed by the effects of the ligating silicon atom on the metal center and finally the reactivity of silyl complexes.

8.2.1 Synthetic Routes to Transition Metal Silyl Complexes

There are four main synthetic routes to transition metal silyl complexes, as shown in Figure 8.1:

1. Salt elimination using anionic metal complexes and halosilanes (A)
2. Oxidative addition of hydrosilanes to metal complexes (B)
3. Salt elimination using silyl anion and transition metal halides (C)
4. σ-bond metathesis (D)

$$L_nM^- \;+\; X—SiR_3 \longrightarrow L_nM—SiR_3 \qquad \textbf{A}$$

$$L_nM \;+\; H—SiR_3 \longrightarrow \underset{\displaystyle L_nM—SiR_3}{\overset{\displaystyle H}{|}} \qquad \textbf{B}$$

$$L_nM—X \;+\; R_3Si^- \longrightarrow L_nM—SiR_3 \qquad \textbf{C}$$

$$L_nM—E \;+\; H—SiR_3 \longrightarrow \begin{matrix} L_nM\text{---}E \\ \vdots \qquad \vdots \\ R_3Si\text{---}H \end{matrix} \longrightarrow L_nM—SiR_3 \qquad \textbf{D}$$
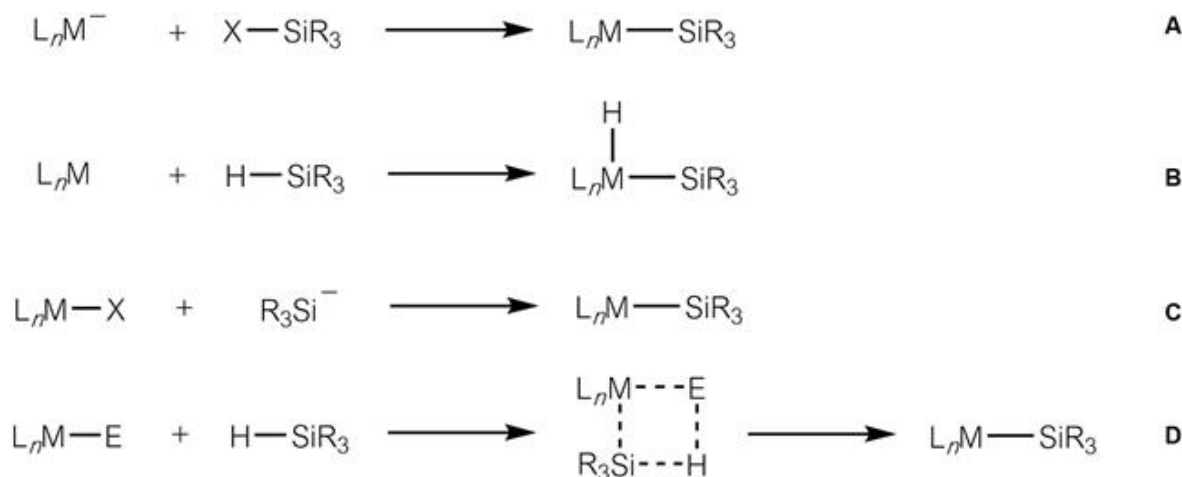
Figure 8.1 Synthetic routes to transition metal silyl complexes.

Route (A). Complex **1**, $[CpFe(CO)_2SiMe_3]$ (see above), was synthesized by the reaction of $Na[CpFe(CO)_2]$ (freshly prepared by reduction of $[Cp_2Fe_2(CO)_4]$ with Na/Hg amalgam) with chlorosilane in tetrahydrofuran (THF) (eqn (8.1)).[2] The solvent has to be considered carefully, as it is known that the positively charged silicon atoms in silyl complexes sometimes undergo nucleophilic attack by ethers leading to cleavage of the metal–silicon bond. An example, in which THF undergoes ring-opening, is illustrated in eqn (8.2).[3] Due to the instability of the anionic metal precursors, this salt-elimination method of silyl complex formation is limited to first row transition metal silyl complexes.

$$\text{Na}^+ \left[\underset{\text{OC}}{\overset{}{\text{Fe}}}{}_{\text{CO}} \right]^{-} + \text{Me}_3\text{SiCl} \xrightarrow[\text{-NaCl}]{\text{THF}} \underset{\text{OC}}{\overset{}{\text{OC}}}{}^{\text{...}}\text{Fe} - \text{SiMe}_3 \qquad (8.1)$$

1

$$\text{K}^+ \left[\underset{\text{OC}}{\overset{}{\text{Fe}}}{}_{\text{CO}} \right]^{-} \xrightarrow[\substack{\text{THF} \\ \text{-KCl}}]{+\text{ClSiMe}_2\text{NPh}_2} \underset{\text{OC}}{\overset{}{\text{OC}}}{}^{\text{...}}\text{Fe} \diagdown\diagup\diagdown\diagup^{\text{O}}\diagdown \text{SiMe}_2\text{NPh}_2 \qquad (8.2)$$

2
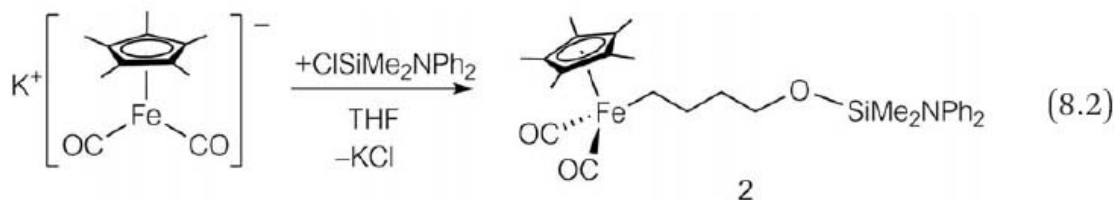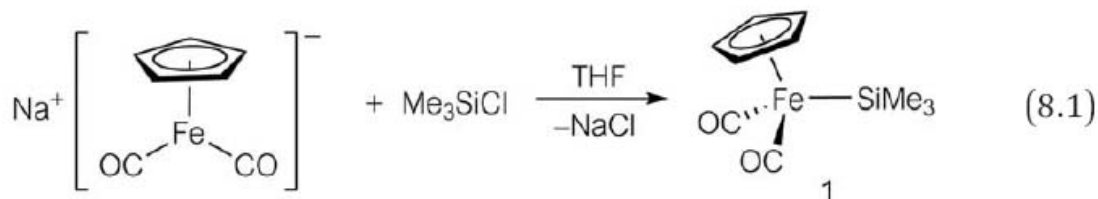
Nevertheless, *in situ* generation of the anionic metal precursor may be possible. Bergman and coworkers reported the synthesis of silyliridium complex **3** by the reaction between an anionic complex, generated *in situ* by deprotonation of a hydridoiridium complex with *t*-BuLi, and Me$_3$SiCl (eqn (8.3), *pmdeta = N,N,N',N'',N''*-pentamethyldiethylenetriamine).[4] Since this finding, a variety of anionic organometallic complexes have been reported and applied to the synthesis of electron-rich silyl complexes (eqn (8.4) and (8.5)).[5]

$$\underset{\text{H}\,\underset{\text{H}\,\text{H}}{}}{\overset{}{\text{Ir}}} \xrightarrow[\text{pmdeta}]{t\text{-BuLi}} \left[\underset{\text{H}\,\underset{\text{H}}{}}{\overset{}{\text{Ir}}}_{\text{H}} \right]^{-} \text{Li}^+(pmdeta) \xrightarrow[\text{-LiCl}]{\text{Me}_3\text{SiCl}} \underset{\text{H}\,\underset{\text{H}\,\text{H}}{}}{\overset{}{\text{Ir}}}_{\text{SiMe}_3} \qquad (8.3)$$

3

$$\underset{\text{Me}_3\text{P}\,\underset{\text{OC}\,\text{CO}}{}}{\overset{}{\text{W}}}_{\text{H}} \xrightarrow{n\text{-BuLi}} \left[\underset{\text{Me}_3\text{P}\,\underset{\text{CO}}{}}{\overset{}{\text{W}}}{}^{\text{...}}\text{CO} \right]^{-} \text{Li}^+ \xrightarrow[\text{-LiCl}]{\text{Me}_2\text{SiHCl}} \underset{\text{Me}_3\text{P}\,\underset{\text{OC}\,\text{CO}}{}}{\overset{}{\text{W}}}_{\text{SiHMe}_2} \qquad (8.4)$$

4

$$(8.5)$$
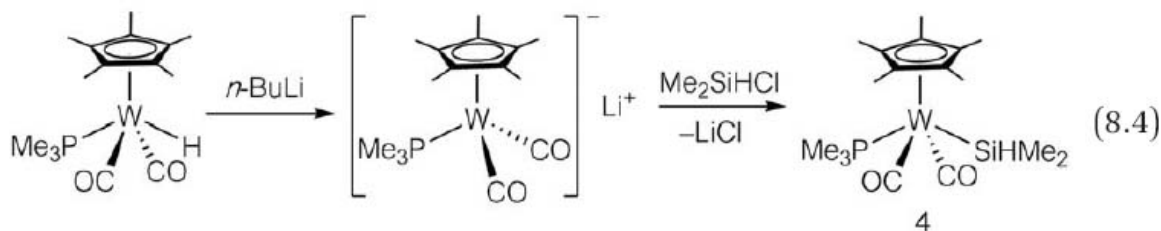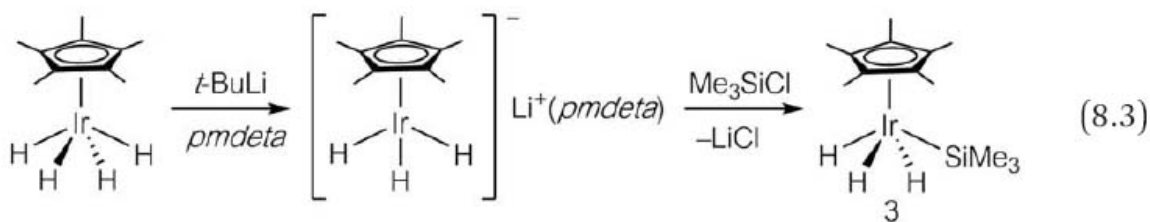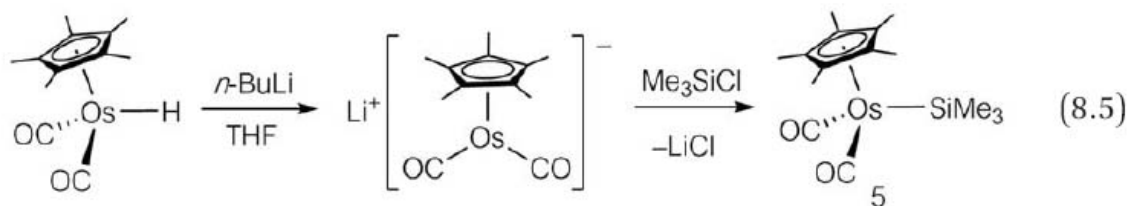
Route (B). The Si–H bond in hydrosilanes is polarized Si (δ^+)–H (δ^-). Compared with the oxidative addition of a C–H bond, the energy of the transition state for oxidative addition of an Si–H bond is located closer to that of the reactant, and thus the activation energy is lower than that for the oxidative addition of a C–H bond. In general, Si–H bonds are weaker than C–H bonds, while M–Si bonds are stronger than M–C bonds. Thus, from a thermodynamic viewpoint, oxidative addition of hydrosilanes is preferential to that of alkanes. Indeed, in most unsaturated metal complexes, the oxidative addition of Si–H is energetically downhill.

A wide variety of silyl complexes has been synthesized *via* the kinetically and thermodynamically favorable oxidative addition of hydrosilanes. In this method, the metal complex should be coordinatively unsaturated or substitutionally labile. Wilkinson's complex, [RhCl(PPh$_3$)$_3$] (a 16e complex), reacts with HSiCl$_3$ and loses a PPh$_3$ ligand to afford a 16e hydrido(silyl)rhodium(iii) complex **6** (eqn (8.6)). As indicated by this reaction, the oxidative addition of Si–H is more favorable than that of Si–Cl, which can be rationalized by considering the directionality of the atomic orbitals (Section 6.3.1).[6]

$$(8.6)$$
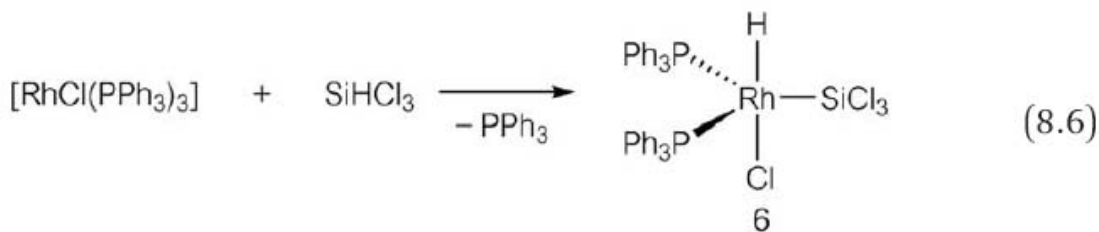
Oxidative addition of hydrosilanes is generally a reversible process. In order to isolate silyl complexes in stable forms, a subsequent irreversible step, such as reductive elimination of an alkane, might be required (eqn (8.7)).[7]

$$[\text{Rh}(\text{CH}_3)(\text{PMe}_3)_n] \;\; \underset{}{\overset{\text{HSiPh}_3}{\rightleftharpoons}} \;\; \left[\begin{array}{c} \text{CH}_3 \\ \text{Me}_3\text{P}_{\prime\prime\prime\prime}\!\!\overset{|}{\underset{|}{\text{Rh}}}\!\!^{\prime\prime\prime\prime\prime}\text{H} \\ \text{Me}_3\text{P}^{\diagup} \quad \diagdown \text{SiPh}_3 \\ \text{PMe}_3 \end{array} \right] \;\; \overset{-\text{CH}_4}{\longrightarrow} \;\; \begin{array}{c} \text{Me}_3\text{P}_{\prime\prime\prime}\!\!\overset{}{\underset{}{\text{Rh}}}\!\!^{\prime\prime\prime\prime}\text{SiPh}_3 \\ \text{Me}_3\text{P}^{\diagup} \quad \diagdown \text{PMe}_3 \\ \mathbf{7} \end{array}$$

$n = 3, 4$

$$(8.7)$$
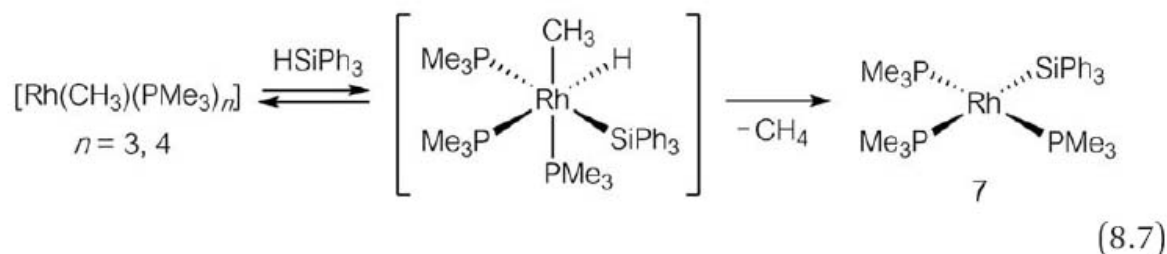
Route (C). The salt elimination reaction between a transition metal halide and a silyl anion is another synthetic route to silyl complexes: treatment of a dichloroplatinum(ii) complex with LiSiMePh_2 allowed the introduction of two silyl ligands to give **8** (eqn (8.8)).[8] Whereas the use of alkyl lithium or Grignard reagents is an established and versatile synthetic method in the preparation of alkyl complexes, the greater instability of silyl anions means that this type of salt elimination reaction is rather limited. Nevertheless, the use of silylanion reagents is particularly appropriate for d^0 transition metal complexes since for these, even if they are coordinatively unsaturated, oxidative addition (of a hydrosilane) is not possible. d^0 transition metal silyl complexes are thus synthesized by the salt elimination reaction using silyl anions (eqn (8.9) and (8.10)).[9]

$$\begin{array}{c} \text{PhMe}_2\text{P}_{\prime\prime\prime\prime}\!\!\overset{}{\underset{}{\text{Pt}}}\!\!^{\prime\prime\prime\prime}\text{Cl} \\ \text{PhMe}_2\text{P}^{\diagup} \quad \diagdown \text{Cl} \end{array} \;\; \underset{-2\text{LiCl}}{\overset{+2\text{LiSiMePh}_2}{\longrightarrow}} \;\; \begin{array}{c} \text{PhMe}_2\text{P}_{\prime\prime\prime\prime}\!\!\overset{}{\underset{}{\text{Pt}}}\!\!^{\prime\prime\prime\prime}\text{SiMePh}_2 \\ \text{PhMe}_2\text{P}^{\diagup} \quad \diagdown \text{SiMePh}_2 \\ \mathbf{8} \end{array}$$

$$(8.8)$$

$$1/2\,[\text{Cp}_2\text{ScCl}]_2 \;+\; (\text{THF})_3\text{LiSiPh}_3 \;\; \underset{-\text{LiCl}}{\overset{-2\text{THF}}{\longrightarrow}} \;\; \begin{array}{c} \overset{}{\underset{}{\text{Sc}}}\!\!^{\prime\prime\prime\prime}\text{SiPh}_3 \\ {}^{\diagdown}\text{O} \\ \mathbf{9} \end{array}$$

$$(8.9)$$

$$[Cp_2ZrCl_2] + Al(SiMe_3)_3 \longrightarrow \text{10} \qquad (8.10)$$
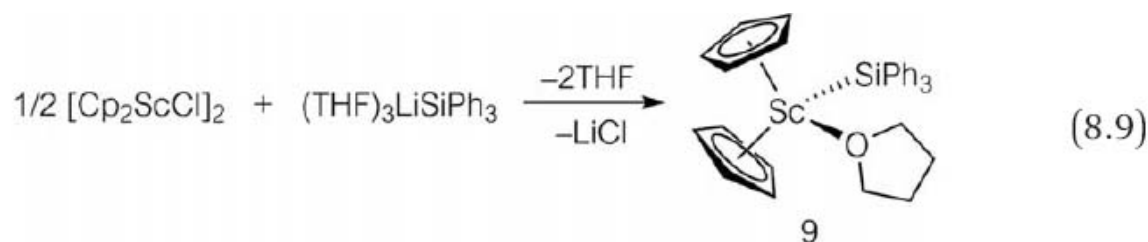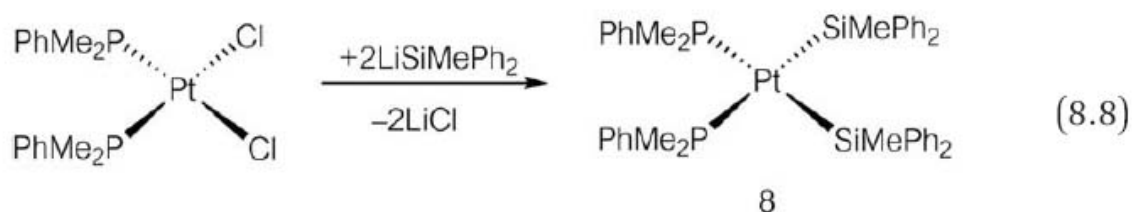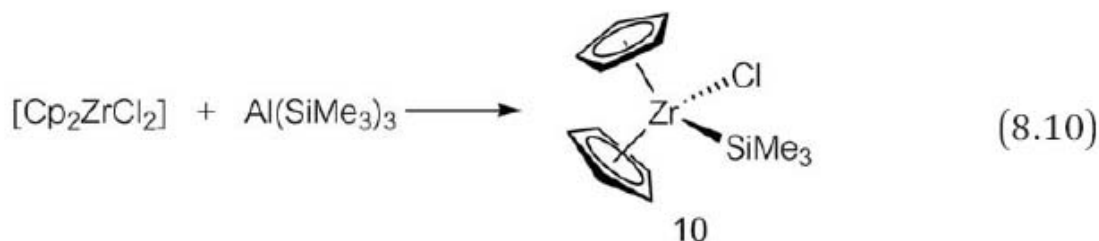
Route (D). The silylscandium(iii) complex **11** is formed by reaction of the methylscandium(iii) complex with $PhSiH_3$ *via* elimination of methane (eqn (8.11)).[10] Taking the d^0 electronic state of Sc(iii) into account, the oxidative addition/reductive elimination pathway can be ruled out. The reaction is presumed to proceed *via* a σ-bond metathesis mechanism. The synthetic strategy *via* σ-bond metathesis is commonly used in the synthesis of early transition metal silyl complexes.

$$[Cp^*_2ScMe] + PhSiH_3 \longrightarrow \left[Cp^*_2Sc \cdots \right]^{\ddagger} \xrightarrow{-CH_4} \text{11} \qquad (8.11)$$
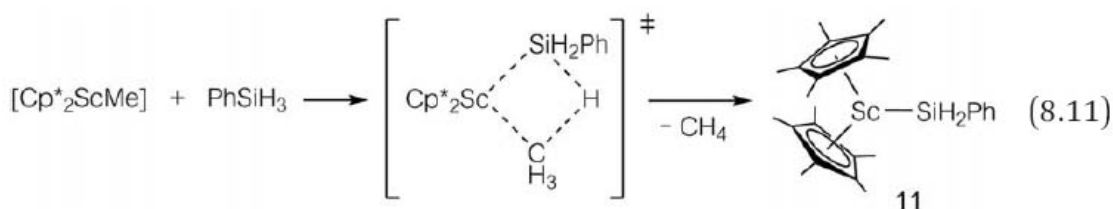
8.2.2 Bonding in Transition Metal Silyl Complexes

It is known that M–Si bond lengths in late transition metal–silyl complexes are significantly shorter than those expected for a single σ-bond.[11] Spectroscopic analysis and extended Hückel calculations of $[Co(SiR_3)(CO)_4]$ suggested π-back donation from the metal dπ orbitals to the silicon dπ orbitals, leading to multiple bond character between the metal and silicon atoms (Figure 8.2(a)).[12] However, Lichtenberger *et al.* measured the photoelectron spectra of $[CpFe(CO)_2(SiCl_3)]$ and concluded that the π-back donation occurred to the Si–Cl σ* orbital (Figure 8.2(b)) and not the Si dπ orbitals.[13] It has been recently accepted that compared to the Si–X σ* orbital, the silicon d orbital is higher in energy and does not interact efficiently with the filled metal dπ orbital.[11c] In $[RhH(Cl)(SiCl_3)(PPh_3)_2]$, the observed Rh–Si bond length is 2.203(4) Å and considerably shorter than that expected for a single bond.[11b] This shortening is explained by three

factors, *i.e.* the inductive effect of the three chloro groups, π-back donation from the Rh(iii) $d\pi$ orbital to the energetically low-lying Si–Cl σ^* orbital, and the absence of a competing π-accepting ligand at the opposite side of the transition metal to the silyl ligand.
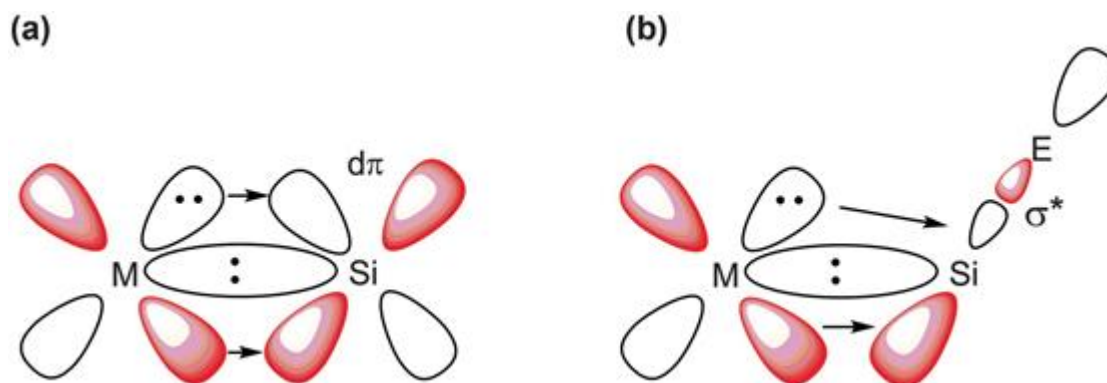
Figure 8.2 π-Back donation in transition metal–silyl complexes.

In contrast to the late transition metal–silyl complexes, the M–Si bond lengths in d^0 early transition metal–silyl complexes are in the range expected for a single bond of pure σ type.[11]

8.2.3   Effect of Silyl Ligands on Metal Centers

It has been demonstrated that there is a good correlation between the electronegativity of the coordinating atom and the *trans* influence of the ligand by measurement of the Pt–Cl bond length in square-planar *trans*-chloroplatinum(ii) complexes (Figure 8.3).[14] Accordingly, the *trans* influence of the electropositive silyl ligands is expected to be larger still than hydrido and alkyl ligands, which are recognized to be strongly *trans*-influencing ligands.
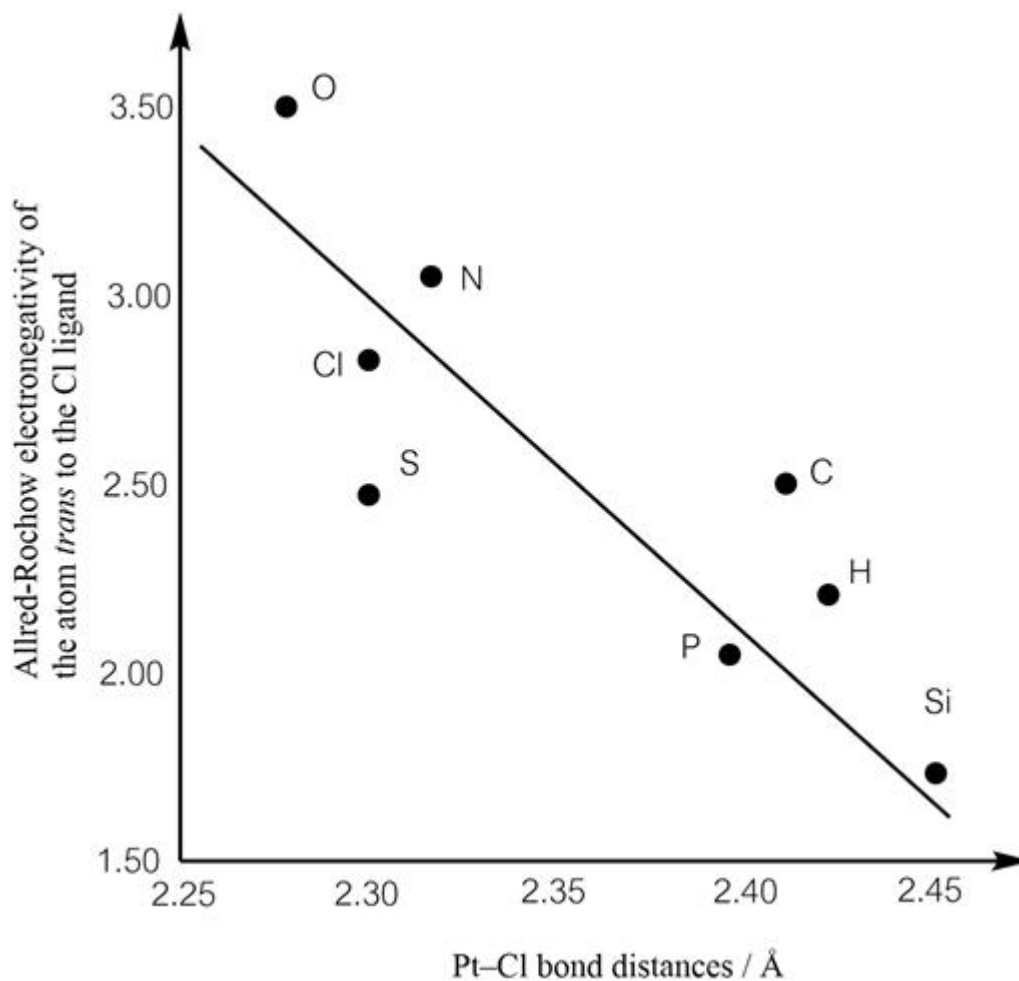
Figure 8.3 Relationship between Pt–Cl bond distances and Allred–Rochow electronegativity of the atom *trans* to the Cl ligand.[14]

Haszeldine *et al.* measured the $v(M-Cl)$ values in the infrared spectra of octahedral iridium complexes $[IrCl(H)(ER_n)(CO)(PPh_3)_2]$ and square-planar platinum complexes *trans*-$[PtCl(ER_n)(PPh_3)_2]$ to obtain a quantitative estimate of the *trans*-influence of the silyl ligands and concluded that the *trans*-influence of silyl ligands is exceptionally strong (Table 8.2).[14b]

Table 8.2 Frequency of M–Cl stretching vibration as a function of *trans* ligand, **L** (M = Ir, Pt).[14b]
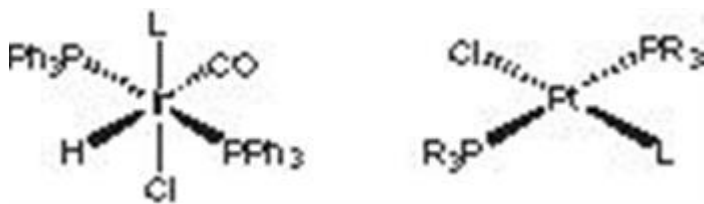
L	ν(Ir–Cl), cm^{-1}	ν(Pt–Cl), cm^{-1}
Halogen	315–330	325–340
CO	300–315	
PR$_3$, AsR$_3$	260–290	275–300
Alkyl	255–270	245–280
Hydrido	245–265	270–280
Silyl	228–272	238–275

The strength of the *trans*-influence is also known to correlate with the σ-donor ability of a ligand. Indeed, Lichtenberger *et al.* measured the photoelectron spectrum of [CpFe(CO)$_2$L] (L = SiMe$_3$, CH$_3$, H) and found that σ-donor ability is in the following order: SiMe$_3$ > CH$_3$ > H.[13]

Although the *trans* effect of silyl ligands has not yet been quantified, a strong *trans* influence and strong σ-donor ability should lead to a strong *trans* effect. Thus, introduction of silyl ancillary ligands should generate a coordinatively unsaturated and electron-rich metal center, leading to high catalytic activity. However, as mentioned in Section 8.2.1, the metal–silicon bond is easily cleaved through nucleophilic attack, insertion and reductive elimination reactions. To suppress these side reactions, chelate-type silyl ancillary ligands have been developed. In 1999, Tobita and Ogino reported the synthesis of ruthenium(ii) complexes possessing a bis(silyl) chelating ligand, "xantsil", and observed facile arene exchange at the Ru(ii) center (eqn (8.12)). They suggested that the arene exchange should be facilitated by the strong *trans*-effect of the two *cis*-silyl groups and/or pre-coordination of the bridging oxygen atom to the ruthenium center.[15]

$$(8.12)$$

12a   12b
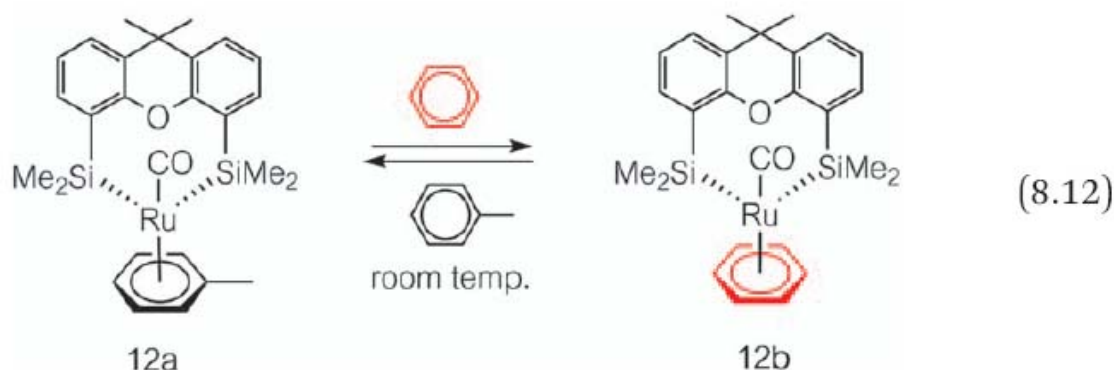
8.2.4   Reactivity of Transition Metal–Silyl Complexes

Transition metal–silyl complexes are considered to be key intermediates in the metal-catalyzed hydrosilation of unsaturated organic compounds, and much effort has been focused on their reactivity. This section deals with the mechanism of catalytic hydrosilation and the related reactivity of silyl complexes.

8.2.4.1   *Mechanism of Catalytic Hydrosilation*

Addition of hydrosilane to the unsaturated bond in an alkyne, alkene or ketone, *i.e.* hydrosilation, is an essential C–Si bond formation reaction in organic synthesis. Since the discovery of $[H_2PtCl_6]$-catalyzed hydrosilation in 1957,[16a] the field has attracted vigorous global research attention. A possible mechanism for the hydrosilation of alkenes was proposed by Chalk and Harrod (Figure 8.4)[16b] and involves coordination of ethylene and oxidative addition of hydrosilane to give a hydrido(silyl)(ethylene) complex. Subsequent insertion of ethylene into the metal–hydrogen bond generates an (ethyl)(silyl) complex from which Si–C reductive elimination affords the hydrosilation product. As research on hydrosilation progressed, some results inexplicable by the Chalk–Harrod mechanism were observed. For example, alkyl(silyl) complexes are generally inert to Si–C reductive elimination under moderate conditions, and furthermore, vinylsilane was detected as a by-product in the catalytic hydrosilation of ethylene.
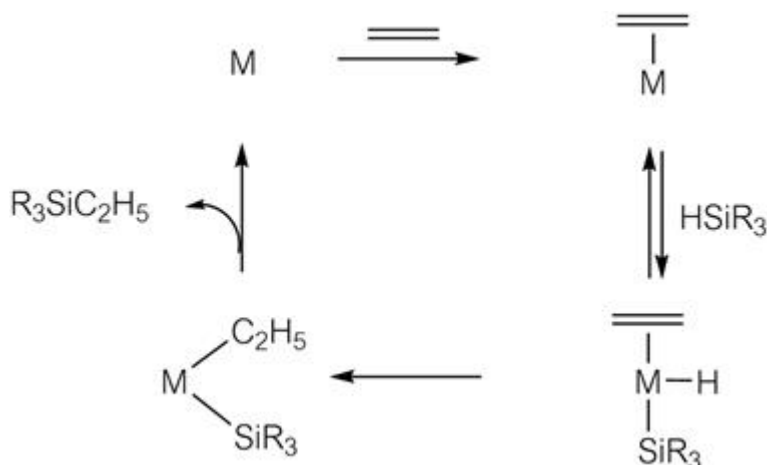
Figure 8.4 Chalk–Harrod hydrosilation mechanism.

In keeping with these experimental results, a modified Chalk–Harrod mechanism was proposed for the mainly cobalt and rhodium catalytic systems (Figure 8.5).[17] In this modified mechanism, a hydrido(silyl) (ethylene) intermediate undergoes insertion of ethylene into the metal–silicon bond to give a hydrido(silylethyl) intermediate. C–H reductive elimination affords the hydrosilation product, while β-hydrogen elimination leads, *via* a couple of steps, to vinylsilane. The activation barrier for the C–H reductive elimination is lower than that for the Si–C reductive elimination. Insertion of unsaturated organic moieties into metal–silicon bonds is well documented.
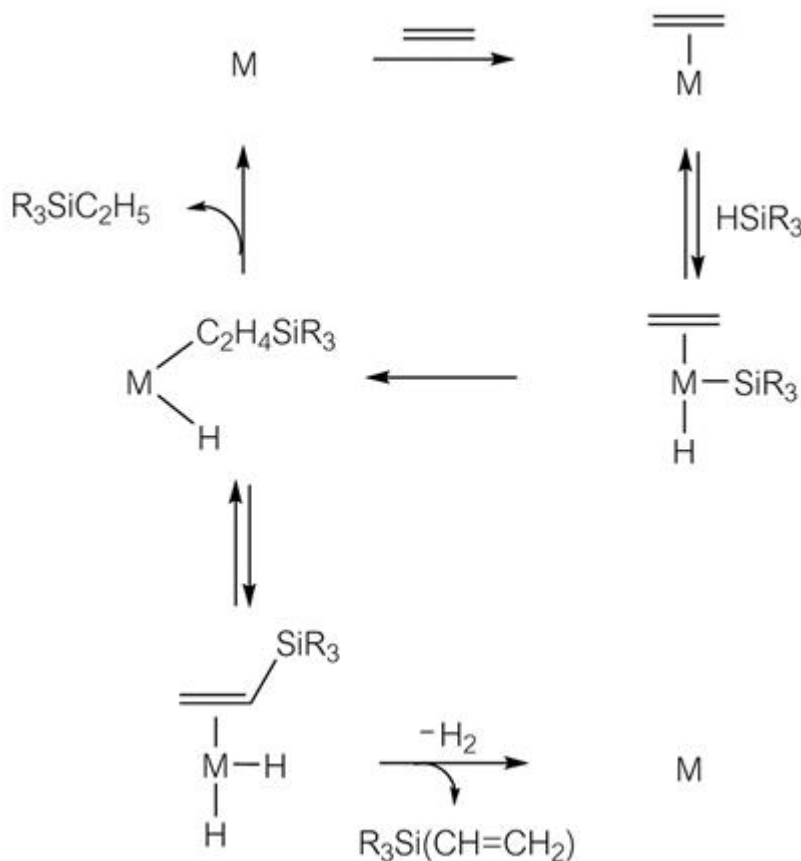
Figure 8.5 Modified Chalk–Harrod mechanism.

8.2.4.2 Reactivity of Silyl Complexes

The reactivity of transition metal–silyl complexes has attracted much attention in relation to the catalytic hydrosilation reaction mentioned above. Reductive elimination from the metal center is one of the most important elementary processes in organometallic chemistry. The transition state was calculated in a computational study.[6] Based on the principle of microscopic reversibility, research on the reductive elimination process gives insight into the reverse process, *i.e.* oxidative addition. The activation energy for the reductive elimination of H_2 is small due to the spherical nature of the hydrogen 1s orbital and the process is reversible in most cases. In contrast, the reductive elimination of silane and methane reaches the transition state late due to the directionality of the sp^3 orbitals used in silyl and methyl groups and their activation energy is larger than that for H_2 (Section 6.3.1). Additionally, the Si–H bond is weaker than the C–H bond, while the M–Si

bond is stronger than the M–C bond. These trends are consistent with the observation that reductive elimination of methane is irreversible, but that of silane is reversible. Exploiting these properties, silyl complexes can be synthesized *via* the selective reductive elimination of methane as illustrated in eqn (8.7).

Si–C bonds are formed by combination of two sp^3 hybrid orbitals of silicon and carbon atoms. Their activation energies towards reductive elimination and oxidative addition are thus larger than those of Si–H and C–H bonds, as these also include the spherical 1s orbital of the H atom. As mentioned above, the Chalk–Harrod mechanism, which explains catalytic hydrosilation, involves the generation of an alkyl(silyl) intermediate, followed by reductive elimination of the Si–C bond. Such a process has been reported in an octahedral iron(ii) system at room temperature (eqn (8.13)).[18]

$$
\begin{array}{c}
\text{13 } \xrightarrow{\text{room temp.}} \text{RSiMe}_3 \quad + \quad [\text{Fe}] \\
\text{R} = \text{CH}_3, \text{CH}_2\text{Ph}
\end{array}
\tag{8.13}
$$
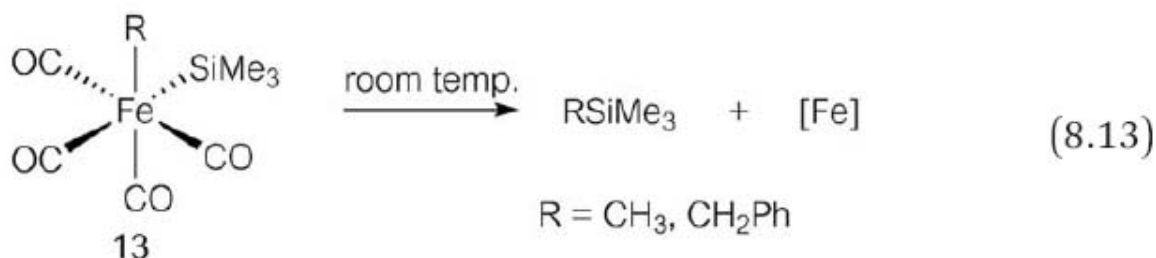
In a rhodium system, frequently employed in actual catalytic reactions, it was reported that Si–C reductive elimination proceeded at 80 °C *via* the transient formation of the octahedral iodo(methyl)(silyl)rhodium(iii) complex (eqn (8.14)).[7]

$$\tag{8.14}$$
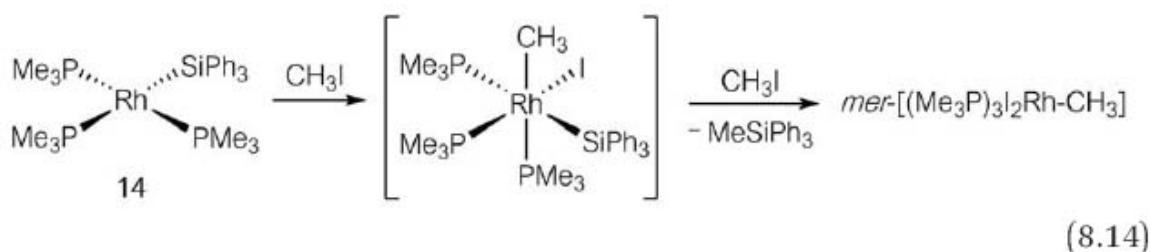
Regarding some (silyl)iridium(iii) complexes, Milstein *et al.* reported that the hydrido(methyl)(silyl)iridium(iii) complexes underwent competitive C–H and Si–C reductive elimination in the ratio 4 : 1 (eqn (8.15)).[19] The ratio

is dependent on the substituent on the silyl ligand: electron-withdrawing substituents strengthen the metal–silicon bond by enhancing π-back donation from the metal, resulting in selective reductive elimination of methane, followed by the formation of metallacycles to give **16a** and **16b** (eqn (8.16)).

$$(8.15)$$

$$(8.16)$$
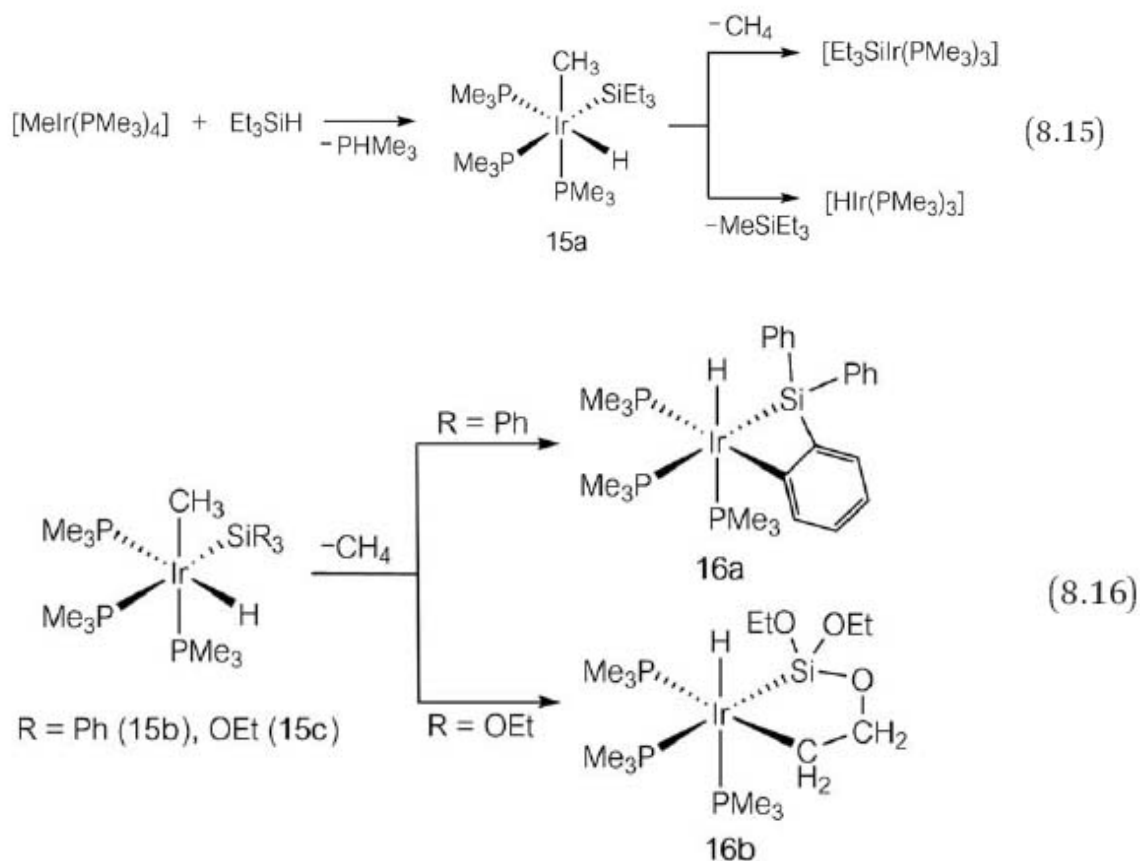
The modified Chalk–Harrod mechanism involves the insertion of an alkene into the metal–silicon bond. To verify the validity of this elementary reaction, much effort has been devoted to investigating the reactivity of silyl complexes towards unsaturated organic molecules. Three selected findings are presented:

(i) Silylmanganese(ɪ) complex **17** reacted with tetrafluoroethylene to give the insertion product **18** (eqn (8.17)).[20]

(ii) Bubbling of ethylene gas into a solution of silyliridium(ɪɪɪ) complex **19** resulted in SiEt$_4$ and Et$_3$Si(CH=CH$_2$), hydrosilation and β-H elimination products, respectively (eqn (8.18)).[21] This observation is consistent with the generation of a silyl(hydrido)(ethylene) intermediate, followed by the insertion of ethylene into the Ir–Si bond.

(iii) UV-irradiation of $[(\eta^5\text{-}C_5Me_5)Fe(CO)_2(SiMe_3)]$ (**20**) in the presence of ethylene gave **21**, which on heating in the presence of CO gave the ethylene insertion product **22** (eqn (8.19)).[22]

$$[(CO)_5MnSiMe_3] \xrightarrow{F_2C=CF_2} [(CO)_5MnCF_2CF_2SiMe_3] \qquad (8.17)$$
$$\text{17} \qquad\qquad\qquad\qquad \text{18}$$

$$[IrH_2(SiEt_3)(cod)(PPh_3)] \xrightarrow[-[Ir]]{C_2H_4} Et_3SiCH_2CH_3 + Et_3Si(CH=CH_2) \qquad (8.18)$$
$$\text{19}$$

$$(8.19)$$
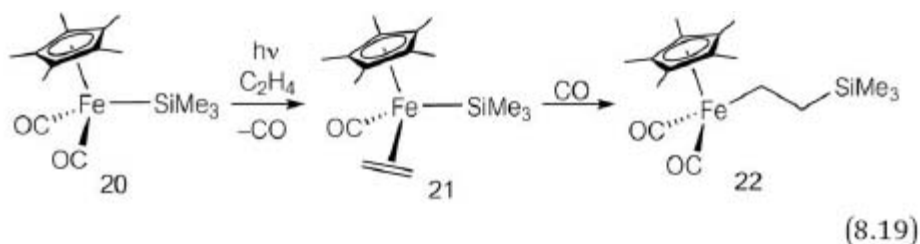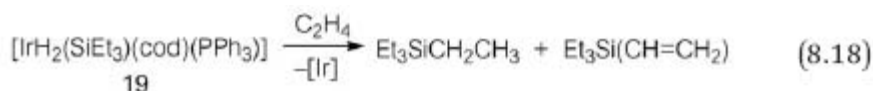
The metal-catalyzed hydrosilation of alkynes also proceeds through the insertion of the alkyne into the metal–silicon bond. Under mild conditions, the square-pyramidal silylruthenium(ii) complex **23** undergoes insertion of acetylene into the Ru–Si bond (eqn (8.20)) to give (silylethenyl)ruthenium(ii) complex **24**.[23] Two factors are important:

(1) Complex **23** is coordinatively unsaturated and is initially coordinated by acetylene.
(2) Coordination of Ru by electron-donating phosphine and silyl ligands results in an electron-rich metal center, which enhances the insertion reaction.

The key point is that the electron-donating ability of the silyl ligand is stronger than that of the alkenyl ligand and so the driving force for the insertion reaction is the reduction of electron density at the ruthenium center.

$$(8.20)$$
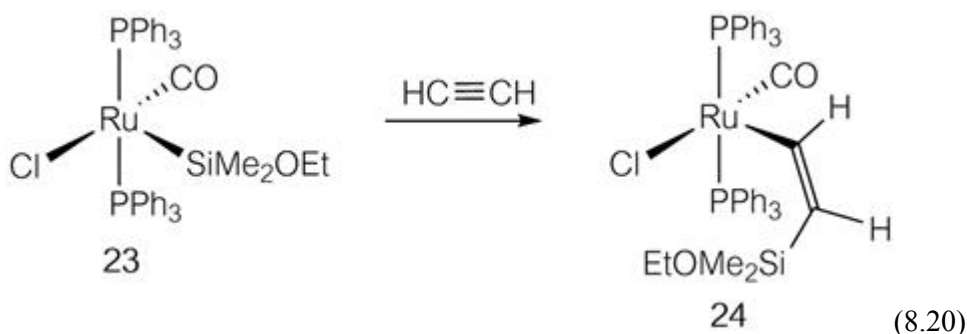
The hydrosilation of aromatic compounds in the presence of a homogeneous catalyst was reported by Harrod. Reaction of pyridine and PhMeSiH$_2$ in the presence of a catalytic amount of a titanium complex ([Cp$_2$TiMe$_2$]) afforded the hydrosilation product (eqn (8.21)).[24] The proposed mechanism starts from the titanium hydride **25**, formed *in situ* upon decomposition of [Cp$_2$TiMe$_2$] (Figure 8.6). Coordination of pyridine, followed by insertion of the N=C double bond into the Ti–H bond gives **26**. The silicon–nitrogen bond is formed by σ-bond metathesis with silane.
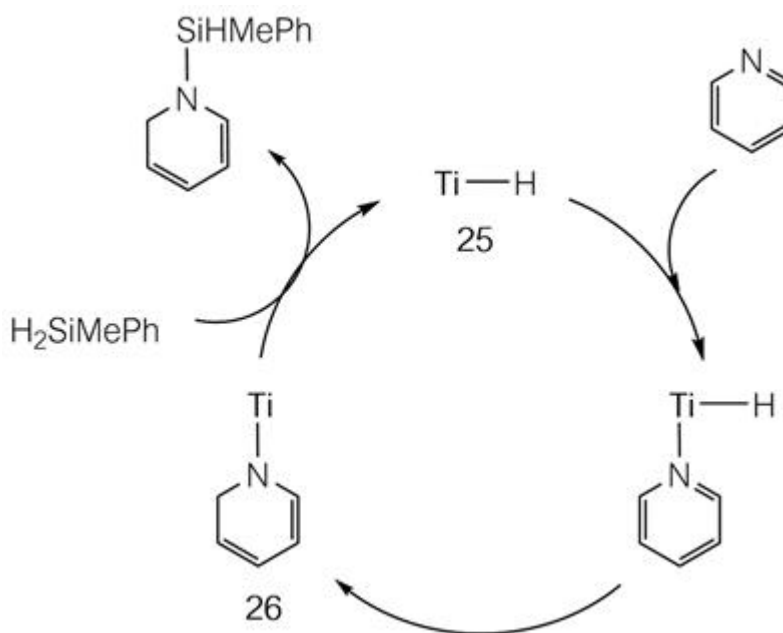
Figure 8.6   Postulated mechanism for hydrosilation of pyridine (**Ti** = Cp$_2$Ti).

The insertion of pyridine into the metal–silicon bond, leading to the formation of the silicon–nitrogen bond was reported by Tobita (Figure

8.7).[25] The mechanism involves the initial formation of an $\eta^2(N,C)$-pyridine complex, which undergoes migratory insertion of the pyridine into the Fe–Si bond, accompanied by coordination of the terminal nitrogen atom. The resulting η^1-allyl complex isomerizes to the η^3-allyl complex on dissociation of the amino part.

$$(8.21)$$
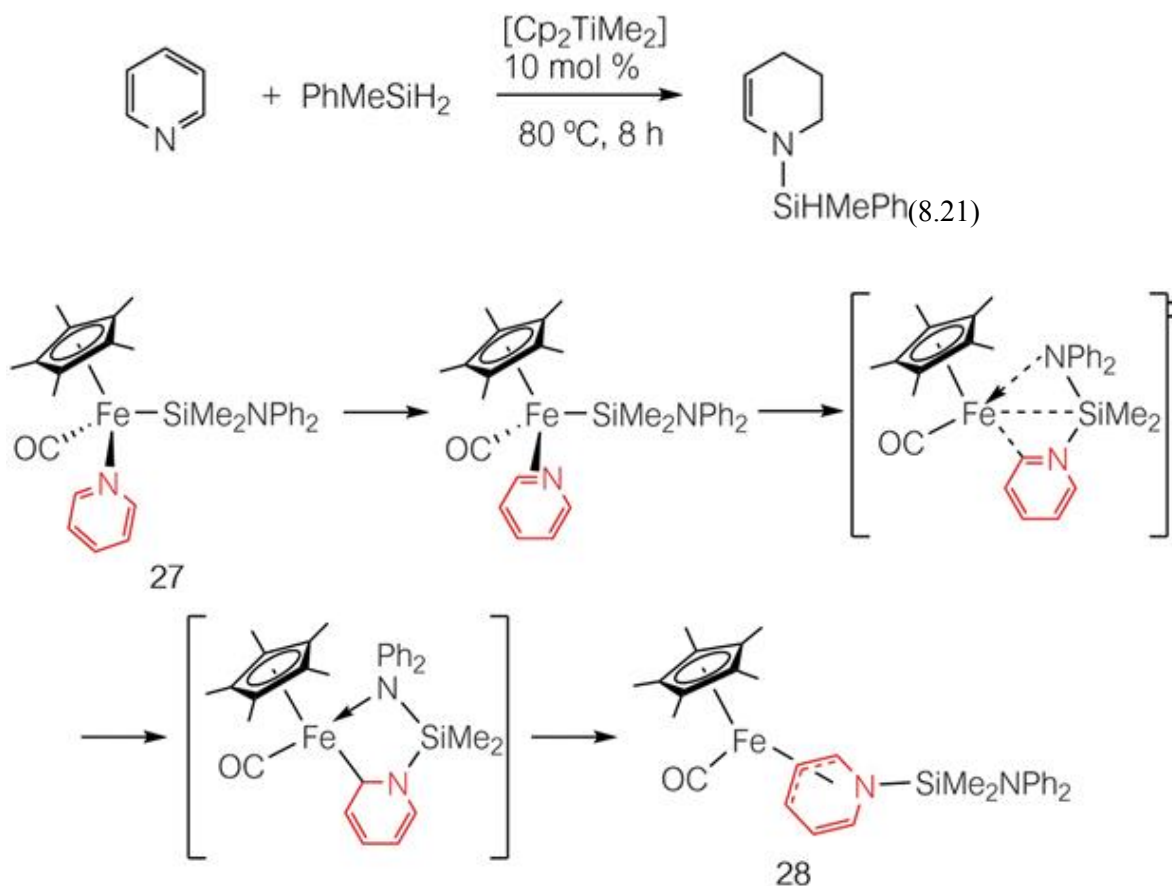
Figure 8.7   Insertion of pyridine into an Fe–Si bond.

Bergman and Brookhart,[26] and independently, Nakazawa and Koga[27] reported the insertion of nitriles into metal–silicon bonds, followed by the cleavage of the carbon–carbon bond. In the rhodium system investigated by Bergman and Brookhart, the three-membered metallacycle derived from insertion of the nitrile into the Rh–Si bond was isolated and characterized by single crystal X-ray diffraction (Figure 8.8).[26]
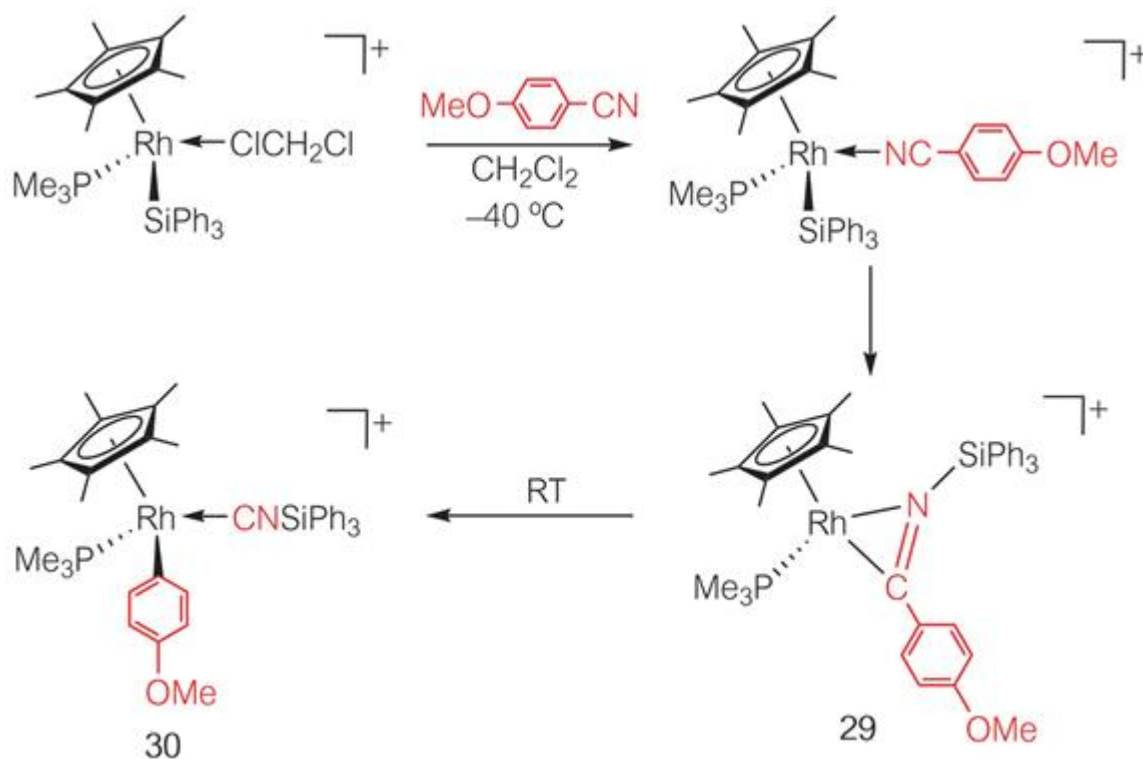
Figure 8.8 Insertion of nitrile into a Rh–Si bond and cleavage of the C–C bond.

Nakazawa and Koga reported that photochemical dissociation of one of the CO ligands in $[(\eta^5\text{-}C_5H_5)Fe(CO)_2(SiMe_3)]$ in the presence of acetonitrile afforded $[(\eta^5\text{-}C_5H_5)Fe(CO)(CN\text{-}SiMe_3)Me]$. Based on DFT calculations, the mechanism in Figure 8.9 was proposed, in which nucleophilic attack by the η^2-acetonitrile on the positively charged silyl Si plays a crucial role in the insertion of acetonitrile into the metal–silicon bond (Figure 8.9). This stoichiometric reaction was applied to the related catalytic reaction (eqn (8.22)).[27]

$$Et_3SiH + R-CN \xrightarrow[h\nu,\ THF]{cat.\ [Fe]} Et_3Si^-CN + RH \tag{8.22}$$
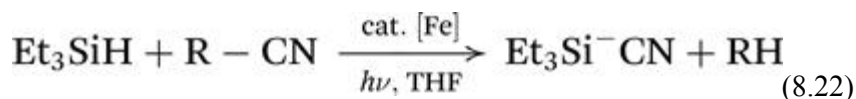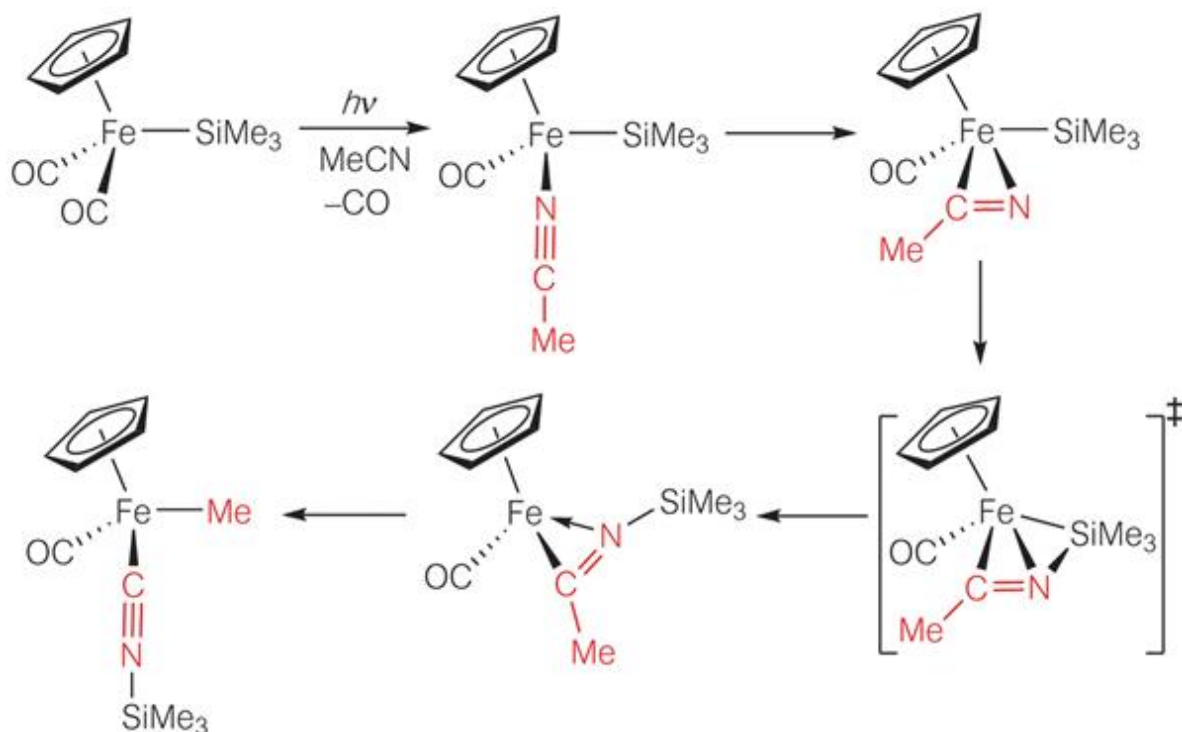
Figure 8.9   A plausible mechanism for the insertion of nitrile into an iron–silicon bond and cleavage of the carbon–carbon bond.

Although there are numerous examples of the insertion of CO into metal–carbon bonds affording acyl complexes, little is known about their silicon analogues, *i.e.* silaacyl complexes. In one example, the η^2-silaacyl complex **32** is formed on reaction of silylzirconium(iv) complex **31** with CO and was characterized by an X-ray diffraction study (eqn (8.23)).[28] The insertion of CO into the Zr–Si bond is reversible, and the heating of **32** in toluene in a stream of N_2 results in regeneration of **31**.

(8.23)
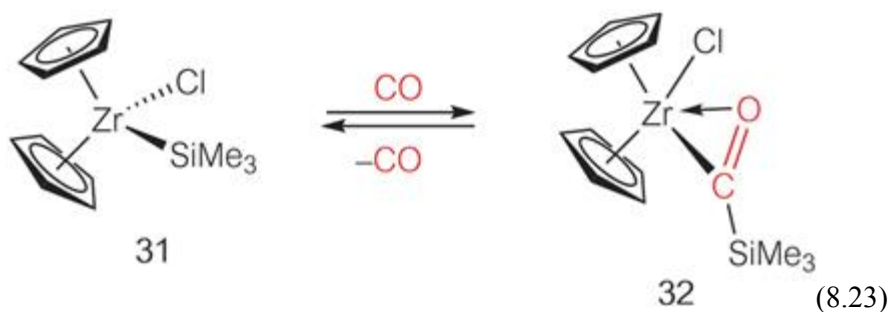
The insertion of an isonitrile into a metal–silicon bond was reported for the scandium system (eqn (8.24)).[9a]

$$Xyl = 2,6\text{-}Me_2C_6H_3$$

(8.24)
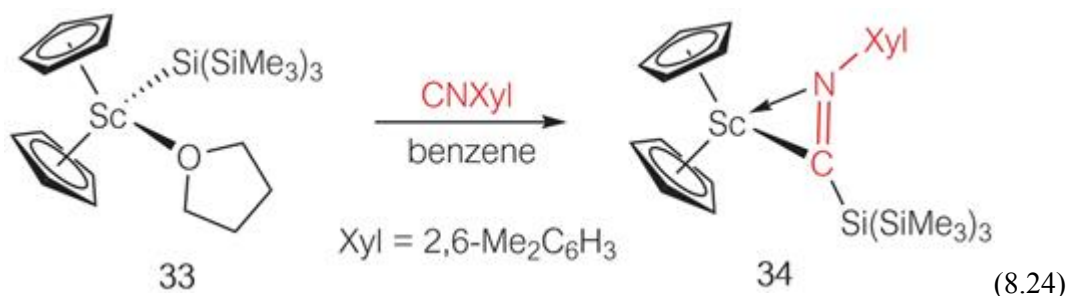
Coordination of the electropositive silicon atom to late transition metals results in an $M(\delta^-)$–$Si(\delta^+)$ polarized bond. Accordingly, cleavage of the metal–silicon bond occurs when the silyl silicon atom undergoes nucleophilic attack. As mentioned above, insertion of a polar unsaturated molecule into the metal–silicon bond thus starts with nucleophilic attack at the silicon atom.

Reaction of $[Cp^*RhH_2(SiEt_3)_2]$ (**35**) with $LiBEt_3H$, followed by treatment with MeOH, gave monodesilylated $[Cp^*RhH_3(SiEt_3)]$ (**37**) (eqn (8.25)). The formation of **37** can be explained by assuming the generation of **36** *via* nucleophilic attack of hydride on the silyl silicon atom.[29]

(8.25)
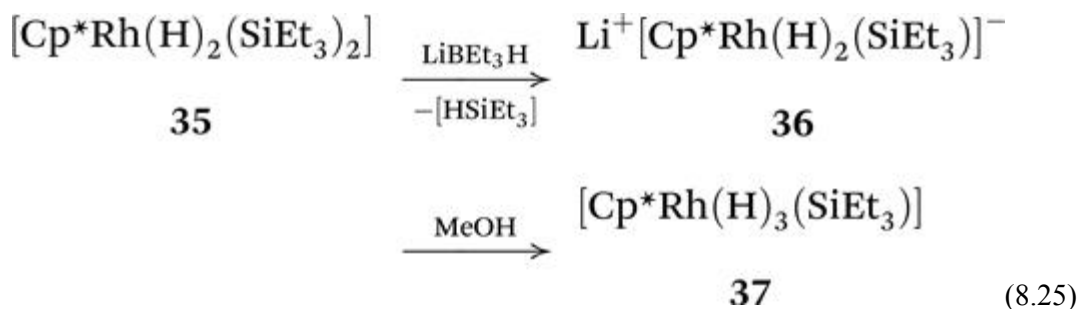
In the reaction of the silyliron(ii) complex **38** with *n*-BuLi and MeI in this order, complex **39** was formed *via* migration of the silyl group from the iron center to the cyclopentadienyl carbon atom (eqn (8.26)).[30] The proposed mechanism consists of the deprotonation of the cyclopentadienyl ligand by *n*-BuLi and intramolecular nucleophilic attack by the C_5H_4 anionic species on the silyl silicon atom, followed by methylation by MeI.

(8.26)
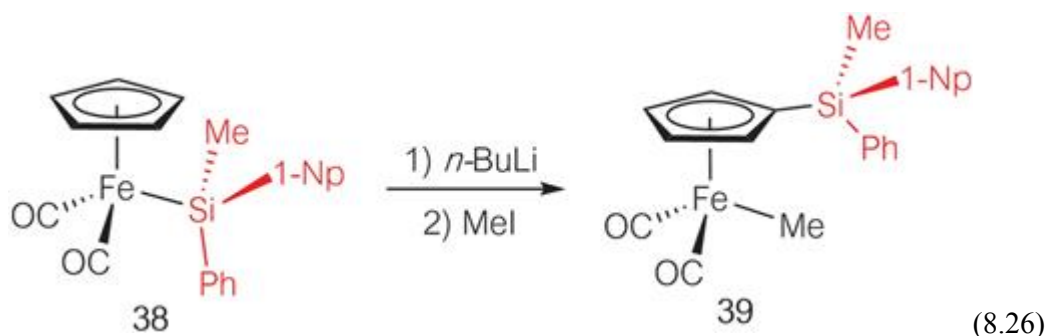
8.3 η^2-Silane Complexes

η^2-Silane complexes, in which Si–H σ bond electron density is donated to the metal center, are known for mononuclear[31] and dinuclear complexes.[32] These complexes have attracted much attention, because they can be regarded as intermediates in the oxidative addition of hydrosilanes and as models for η^2-alkane complexes.

(8.27)

(8.28)
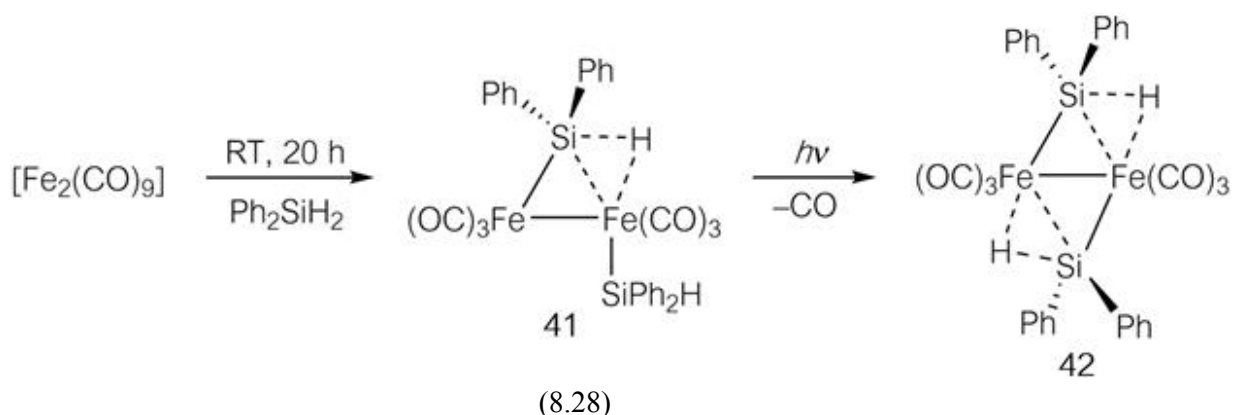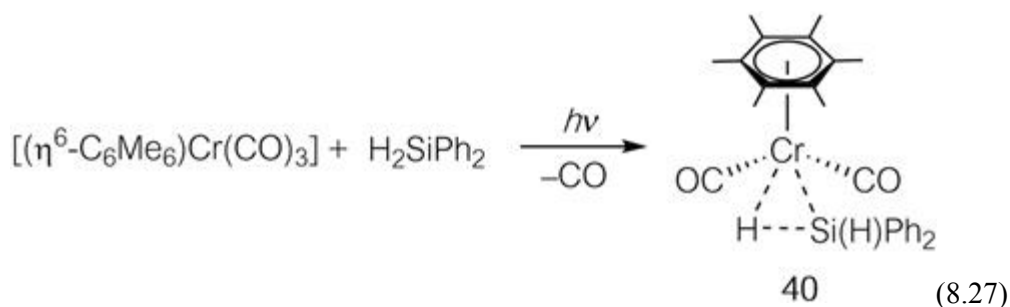
8.3.1 Bonding in η^2-Silane Complexes

The electronic states of η^2-silane complexes have been discussed with reference to the extended Hückel calculations of $[(\eta^5\text{-}C_5H_5)(CO)_2Mn(\eta^2\text{-}$

SiH$_4$)] as a model compound.[33] The overlap population of the η^2-Si–H bond is small (0.24), compared to 0.72 (av.) for other Si–H bonds, which can be explained by two types of interaction:

1. Donation of σ electron density from the η^2-Si–H bond via a σ interaction with a d orbital of Mn reduces the bond order of the η^2-Si–H bond, decreasing the overlap population of the Si–H bond.
2. π-Back donation from a filled metal d orbital to the Si–H antibonding orbital via a π interaction also reduces the bond order of the η^2-Si–H bond and decreases the overlap population of the Si–H bond.

In this model, σ-electron donation is the major interaction. The minor π-back donation causes no change to the oxidation state, and the formal oxidation state of Mn is regarded as +1.

Based on the photoelectron spectra and Fenske–Hall calculations for a series of [Cp$'$(CO)(L)Mn(HSiR$_3$)] (Cp$'$ = C$_5$H$_5$ and substituted cyclopentadienyls), counterarguments were made against this bonding scheme around H, Si and Mn.[34] The photoelectron spectrum of [(η^5-C$_5$H$_5$)(CO)$_2$Mn(HSiCl$_3$)] suggested considerable π-back donation from the Mn d orbital to the Si–H σ^* orbital via a π interaction. This observation indicates that the complex is best described as a hydrido(silyl)manganese(iii) complex, which is supported by the MO calculations. In contrast, however, it was revealed that [(η^5-C$_5$H$_4$Me)(CO)$_2$Mn(H$_2$SiPh$_2$)] exhibits relatively little π-back donation and is best described as an η^2-SiH manganese(i) complex. This issue, as to whether the complex should be regarded as a hydrido(silyl) or as an η^2-Si–H complex, depends not only the electron-richness of the metal center but also the steric environment, including the substituents on the silyl ligand. Indeed, electron-rich [(η^5-C$_5$Me$_5$)(CO)$_2$Mn(H$_2$SiPh$_2$)] exists as an η^2-silane complex, where the steric hindrance between the C$_5$Me$_5$ ligand and the substituents on the silicon atom would prevent the oxidative addition of H$_2$SiPh$_2$.

The $^1J_{\mathrm{SiH}}$ value in NMR is useful to distinguish between η^2-silane and hydrido(silyl) complexes. The $^1J_{\mathrm{SiH}}$ value of free hydrosilane is in the range

of 150–220 Hz. In η^2-silane complexes, the value falls in the range of 40–70 Hz, while in hydrido(silyl) complexes, the value reduces to 10–22 Hz.[35]

8.3.2 Reactivity of η^2-Silane Complexes

In η^2-silane complexes, the silicon atom is expected to be positively charged due to donation of the Si–H σ electron density to the metal. In the alcoholysis of a hydrosilane mediated by the cationic iridium complex, $[IrH_2S_2(PPh_3)_2]SbF_6$ ($\mathbf{S}$ = solvent), Crabtree proposed a mechanism involving nucleophilic attack by the alcohol on the positively charged silicon atom of the η^2-silane complex (Figure 8.10).[36]
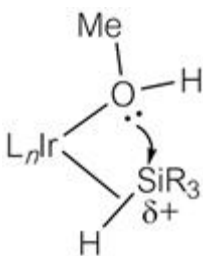
Figure 8.10 Alcoholysis of hydrosilanes on metals.

8.4 Silylene Complexes

Silylene complexes, possessing metal–silicon double bonds, are heavier analogues of carbene complexes. Silylene complexes have been regarded as key intermediates in the homogeneously metal-catalyzed dehydrogenative coupling of hydrosilanes and redistribution of substituents on organosilicon compounds. This section deals with stoichiometric and catalytic reactions involving silylene complexes as key intermediates and the bonding, synthesis and reactivity of silylene complexes.

8.4.1 Stoichiometric and Catalytic Reactions Involving Silylene Complexes as Key Intermediates

In the 1970s, Yamamoto and Kumada reported the monomerization and oligomerization of $HSiMe_2SiMe_3$ catalyzed by *trans*-$[PtCl_2(PEt_3)_2]$, leading to the formation of HSi_nMe_{2n+1} (n = 1–6). Trapping experiments using an alkyne provided evidence of the existence of a silylene complex as an

intermediate.[37] A possible mechanism is shown in Figure 8.11. This mechanism starts with the oxidative addition of $HSiMe_2SiMe_3$ to the Pt(ii) center to give a hydrido(disilanyl)platinum complex. A subsequent 1,3-shift of the $SiMe_3$ group, followed by reductive elimination of $HSiMe_3$ affords the intermediate (but not isolated) silylene complex. Oxidative addition to this of HSi_nMe_{2n+1}, a 1,2-shift of the Si_nMe_{2n+1} moiety, and Si–H reductive elimination affords $HSi_{n+1}Me_{2(n+1)+1}$.
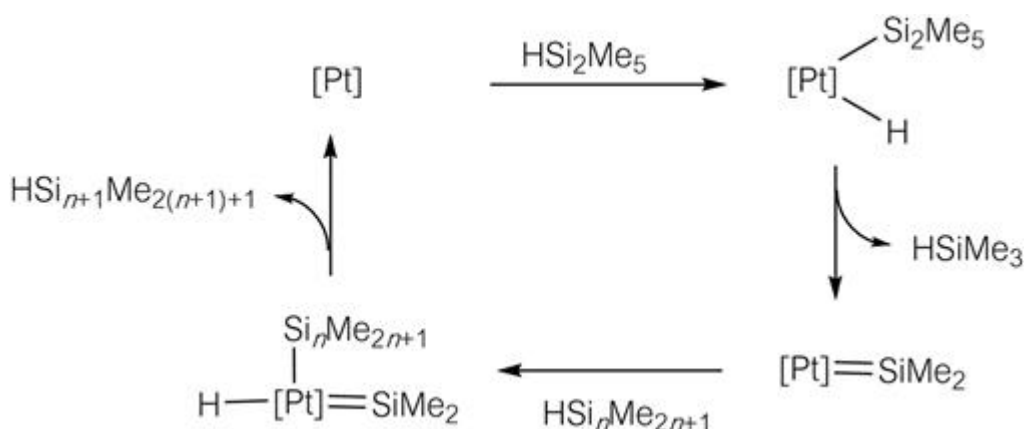
Figure 8.11 A possible mechanism for metal-mediated monomerization and oligomerization of hydrosilanes.

In relation to the reaction of Figure 8.11, Ojima reported the $[RhCl(PPh_3)_3]$-mediated dehydrogenative coupling of $H_2SiPhMe$. It should be noted that the catalytic reaction also yielded products derived from redistribution of substituents on the silicon atom (eqn (8.29)).[38a] A possible mechanism is illustrated in Figure 8.12.[38b] This mechanism involves the formation of a silyl(silylene) complex intermediate. If the silyl(silylene) complex undergoes a 1,2-shift of the silyl group, then Si–H reductive elimination affords the dehydrogenative coupling product. However, if the silyl(silylene) complex undergoes a 1,3-shift of substituents followed by Si–H reductive elimination, redistribution of substituents on the silicon atom is observed.

$$H_2SiPhMe \xrightarrow[\text{70 °C, 1 h}]{[RhCl(PPh_3)_3]} SiPh_3Me + HSiPh_2Me + \underset{\underset{Me \ Me}{|\ \ |}}{H-Si-Si-H} + \underset{\underset{Me \ Me \ Me}{|\ \ \ |\ \ \ |}}{H-Si-Si-Si-H}$$

<div align="center">(8.29)</div>
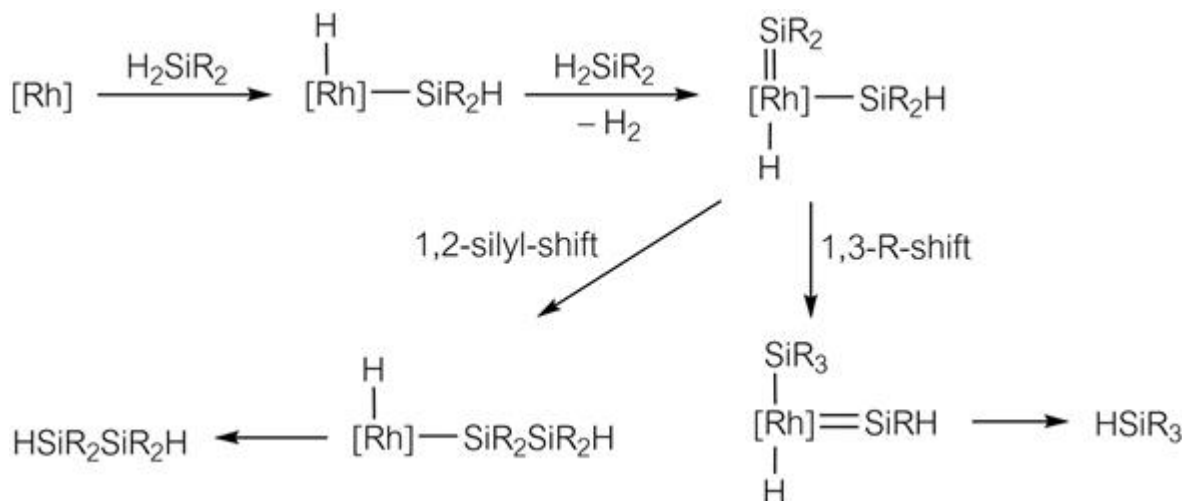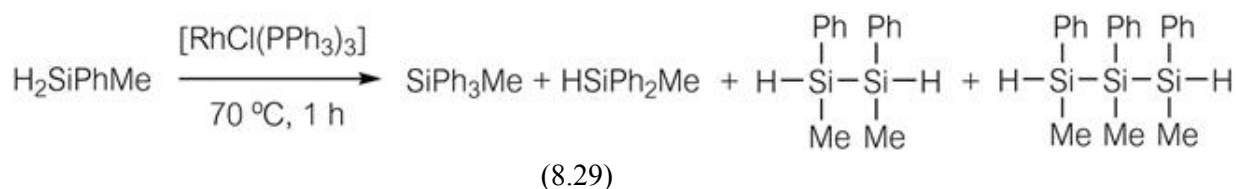
Figure 8.12 A mechanism for the metal-mediated redistribution of substituents on organosilicon compounds.

8.4.2 Bonding in Silylene Complexes

Nakatsuji *et al.* reported the SCF-MO calculation of $[(CO)_5Cr=SiH(OH)]$ as a model silylene complex.[39] The metal–silicon bond interaction consists of σ-donation of the lone pair of electrons on the silylene to the metal and π-back donation from a filled metal dπ orbital to the empty 3p orbital of the silylene moiety (Figure 8.13). The bond dissociation energy of Cr=Si is 124 kJ mol^{-1}, indicating that a silylene complex is thermodynamically stable enough to exist. The LUMO of the silylene complex is the π* orbital of the Cr–Si bond and has an energy of 2.12 eV, with a coefficient for Si of 0.85 so that it is localized to the Si side. The carbene complex, $[(CO)_5Cr=CH(OH)]$, in contrast, has an energy of 3.86 eV and a C coefficient of 0.66. This theoretical study suggests that due to inefficient π-back donation in silylene complexes, the silylene silicon atom should undergo nucleophilic attack by polar molecules. Thus, the synthetic strategy for stable silylene complexes is as follows:

- Use of an electron-rich metal center to stabilize the LUMO

- Introduction of bulky ligands or groups leading to kinetic stabilization
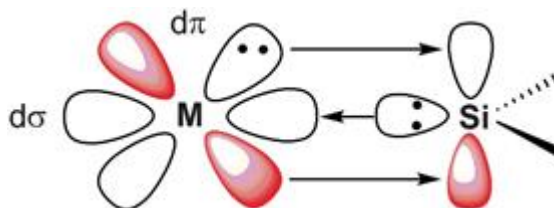
Figure 8.13 MO interactions in silylene complexes.

8.4.3 Synthesis of Silylene Complexes

In 1977, the first silylene complex, **43**, was synthesized by photolyzing a mixture of the 18e complex $[Fe(CO)_5]$ and $HSiMe_2NEt_2$ (eqn (8.30)).[40] Photoirradiation causes dissociation of a carbonyl ligand to generate a 16e intermediate, which undergoes Si–H oxidative addition and 1,2-elimination of NEt_2H. The resulting silylene complex is stabilized by coordination of NEt_2H to the electron-deficient silylene silicon atom. Since complex **43** is unstable above −20 °C, the complex was not characterized by X-ray diffraction and its reactivity was not explored.

$$[Fe(CO)_5] + HSiMe_2NEt_2 \xrightarrow[-CO]{h\nu} (OC)_5Fe = SiMe_2$$

43 (8.30)
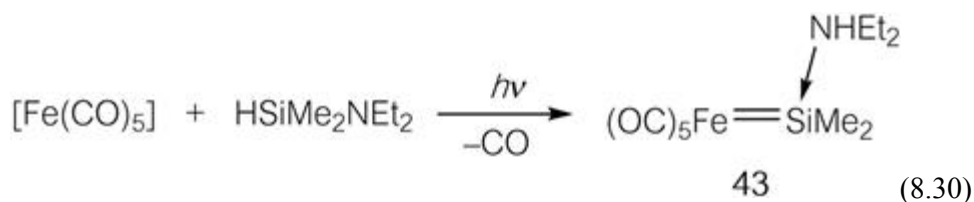
In 1987, Tilley[41] and Zybill[42] independently reported the synthesis and X-ray characterization of base-stabilized silylene complexes. Since then, a variety of base-stabilized and base-free silylene complexes have been reported and the chemistry of silylene complexes has made rapid progress. In order to synthesize silylene complexes, it is important how the electron-deficient silylene moiety is stabilized. In complex **44**, use of the 4d metal Ru and strongly electron-donating η^5-C_5Me_5 and PMe_3 ligands leads to stabilization *via* π-back donation (eqn (8.31)). In complex **45**, use of the strong base, hexamethylphosphoric triamide (HMPA), and two bulky *tert*-butoxy groups compensates for the low electron density of the silicon atom directly through σ and π interactions, respectively (eqn (8.32)).

$$[Cp^*(Me_3P)_2RuSiPh_2(OTf)] \ + \ NaBPh_4 \xrightarrow[-NaOTf]{MeCN} \quad \mathbf{44}$$

(8.31)

$$(^tBuO)_2SiCl_2 \ + \ [Na_2Fe(CO)_4] \xrightarrow[-2NaCl]{HMPA} \quad \mathbf{45}$$

(8.32)
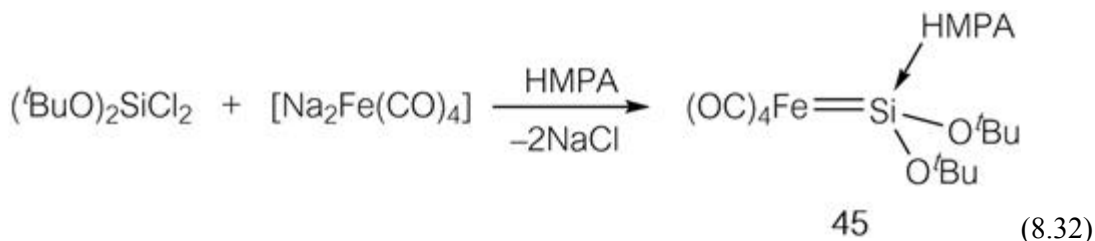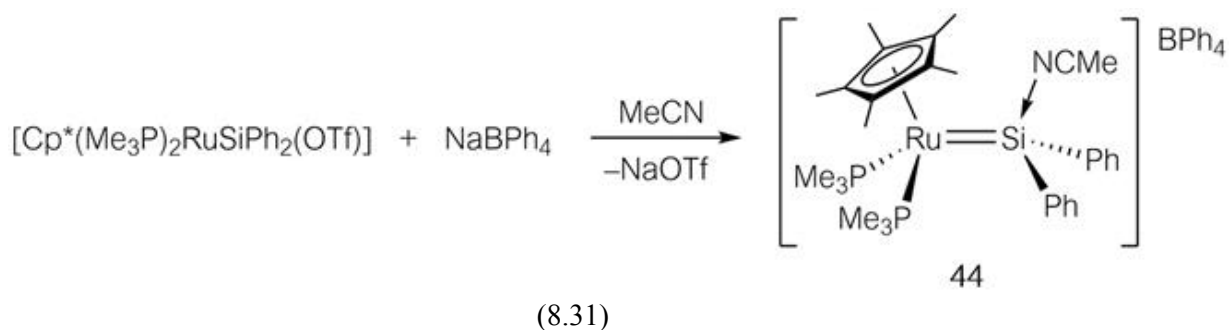
In the homogeneously catalyzed dehydrogenative coupling and redistribution of substituents on organosilicon compounds, silyl(silylene) complexes have been postulated as key intermediates. Ueno, Tobita, and Ogino succeeded in the first synthesis and X-ray characterization of a silyl(silylene) complex **46** stabilized intramolecularly by coordination of a bridging methoxy group (eqn (8.33)).[43]

(8.33)
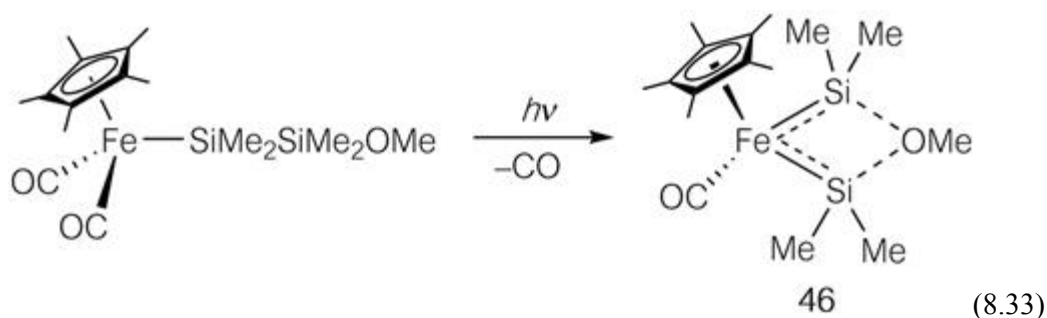
According to the X-ray structural analysis, the metal–silicon bonds even in base-stabilized silylene complexes are still shorter than those expected for metal–silicon single bonds, indicating the unsaturated character of the metal–silicon bonds. In the bonding scheme of the base-stabilized silylene complexes, the filled metal $d\pi$ electrons are π-back-donated to the antibonding orbital between the metal–base σ bond (Figure 8.14).
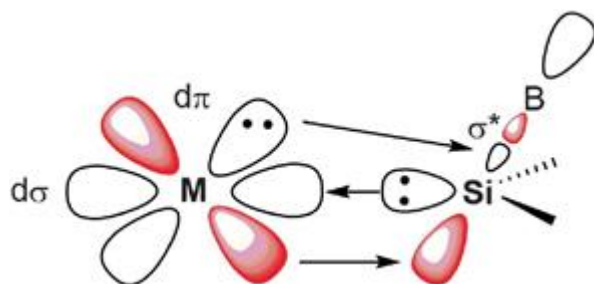
Figure 8.14   MO interactions in base-stabilized silylene complexes.

The main synthetic routes to silylene complexes are shown below. Zybill *et al.* synthesized silyleneiron complex **45** by salt-elimination between dianionic iron and dichlorosilane (eqn (8.32)). Due to the instability of dianionic metal species, this method is of limited application.

Tilley *et al.* synthesized a cationic silyleneruthenium complex **44** by abstraction of a substituent on a silyl silicon atom (eqn (8.31)). This method has been widely adopted, and base-free silylene complex **47** was synthesized based on this strategy (eqn (8.34)).[44] The Ru–Si bond length in **47** is 2.238(2) Å, which is significantly shorter than that in the base-stabilized silylene complex **44** (2.328(2) Å), indicating greater double bond character between the Ru and Si atoms in **47**.

(8.34)
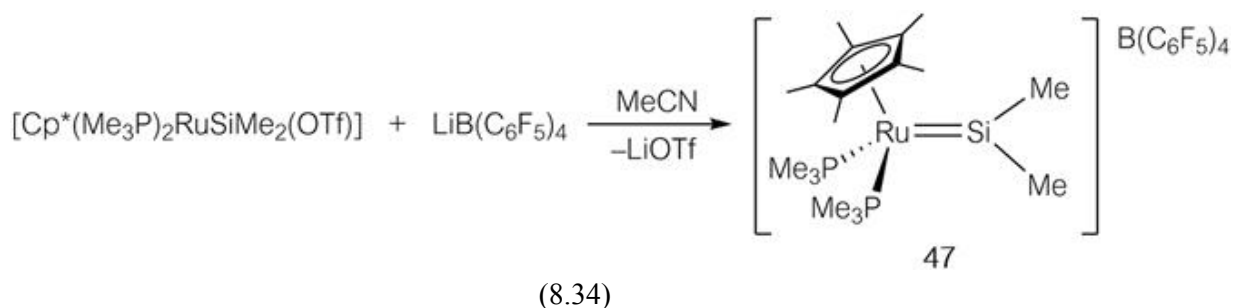
In relation to the strategy mentioned above, Ueno and Ogino synthesized the cationic silyleneiron complex **49** by hydride abstraction from a coordinated H-bearing silyl group by the trityl cation (eqn (8.35)).[45]

(8.35)
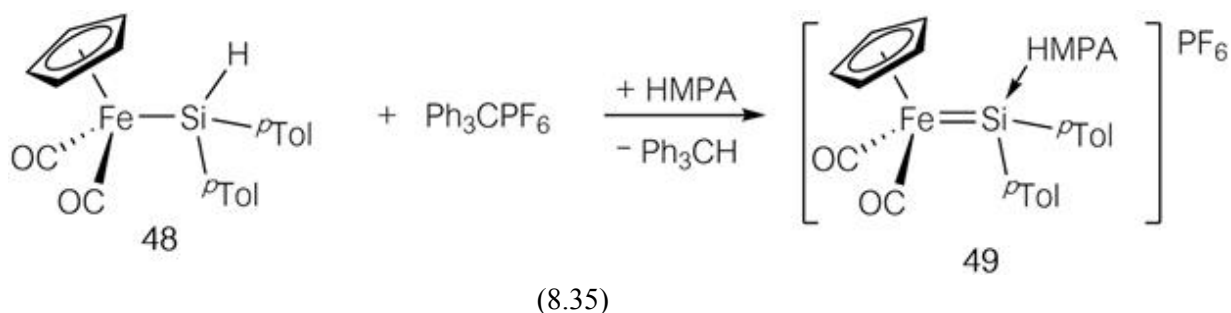
In real catalytic cycles, silylene complexes would be formed as a result of 1,2-dihydrogen elimination from hydrido(hydrosilyl) complexes. By following this process, Corriu *et al.* synthesized the silyleneiron complex **50** (eqn (8.36)).[46] The hydrido(hydrosilyl)iron(ii) intermediate undergoes 1,2-elimination of H_2 to give **50**. The methyl(hydrosilyl)platinum(ii) complex **51** smoothly forms the cationic hydrido(silylene) complex **52** on reaction with $B(C_6F_5)_3$ (eqn (8.37)).[47] In the proposed mechanism, abstraction of the methyl ligand by $B(C_6F_5)_3$ results in the coordinatively unsaturated cationic species, which is further converted to **52** *via* a 1,2-H shift.

(8.36)

(8.37)
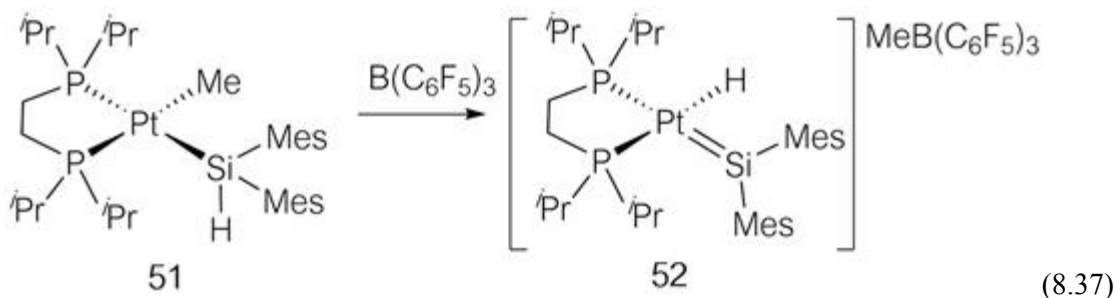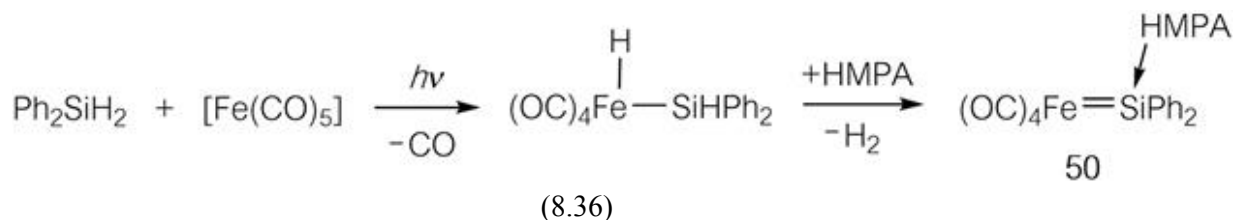
A direct and simple synthesis of silylene complexes would be the reaction between free silylenes and coordinatively unsaturated metal complexes. Two examples in eqn (8.38)[48] and (8.39)[49] contain the photoinduced generation of silylene species, which were trapped by osmium and platinum fragments respectively giving **53** and **54**. Starting from the stable N-heterocyclic silylenes, nickel and platinum silylene complexes **55** and **56** were synthesized (Figure 8.15).[50]

$$(8.38)$$

$$(8.39)$$
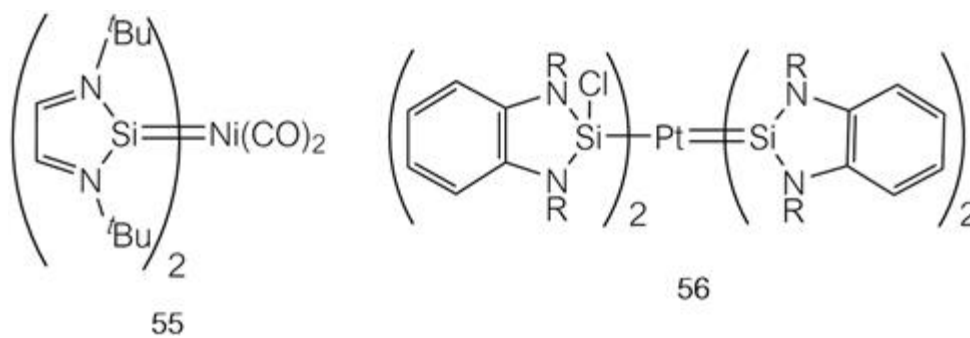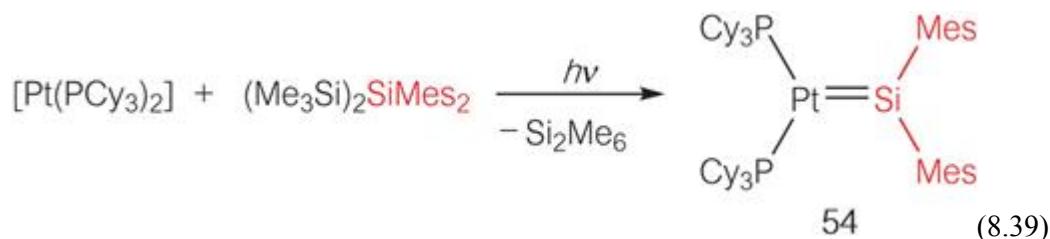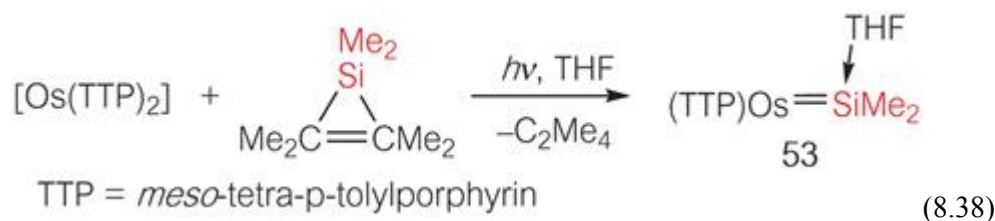
Figure 8.15   Complexes possessing N-heterocyclic silylenes as ligands.

The photoreaction of $[(\eta^5\text{-}C_5H_5)(CO)_2FeSiMe_2SiMe_3]$ was examined by DFT calculation (eqn (8.40)).[51] The photo-induced dissociation of one carbonyl ligand gives $[Cp(CO)FeSiMe_2SiMe_3]$, which can be considered to be a transition state. The subsequent 1,3-silyl-shift is downhill and affords a silyl(silylene)iron complex. Based on this strategy, a wide variety of base-stabilized and base-free silyl(silylene) complexes has been synthesized so far.

$$(8.40)$$
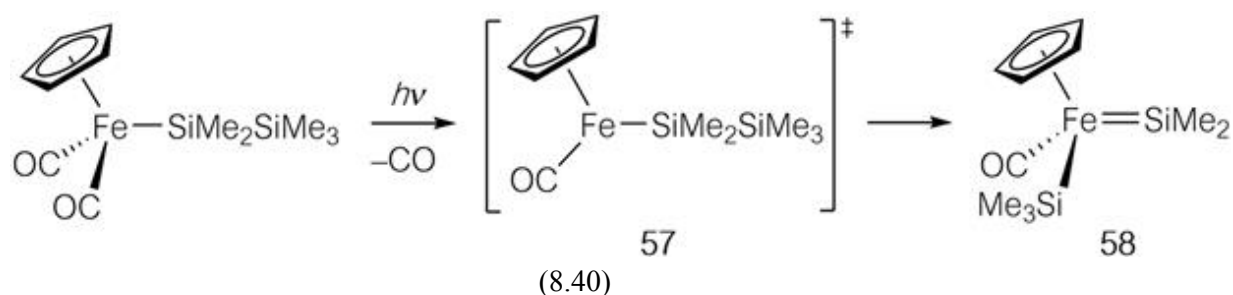
8.4.4 Schrock-type Silylene Complexes

The late transition metal silyl complexes, mentioned above, were classified as Fischer-type silylene complexes, in which the metal–silicon bond is polarized $M(\delta^-)$–$Si(\delta^+)$. Nakatsuji *et al.* computationally examined the MOs of $[(CH_3)H_2Nb=SiR_2]$ (**59**) as model Schrock-type silylene complexes.[52] Although there were no examples of Schrock-type silylene complexes at the time, the theoretical studies revealed that Schrock-type silylene complexes should be more stable than the Fischer-type, and that **59** should undergo nucleophilic attack not only at the silicon atom but also at the niobium atom and that electrophilic attack at niobium should also be possible. In 2005, the first early transition-metal silylene complex, **60**, was reported for tantalum, but its reactivity was not explored (eqn (8.41)).[53] In 2006, a hafnium silylene complex was synthesized by reaction of hafnium chloride with dilithiosilane (eqn (8.42)).[54] MO calculations (NPA) indicated that the hafnium–silicon bond is polarized $Hf(\delta^+)$–$Si(\delta^-)$, indicating that **61** can be regarded as a Schrock-type silylene complex.

(8.41)

(8.42)
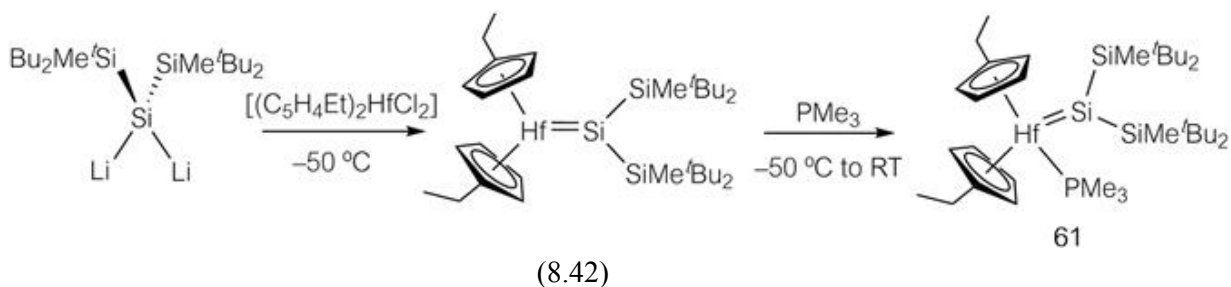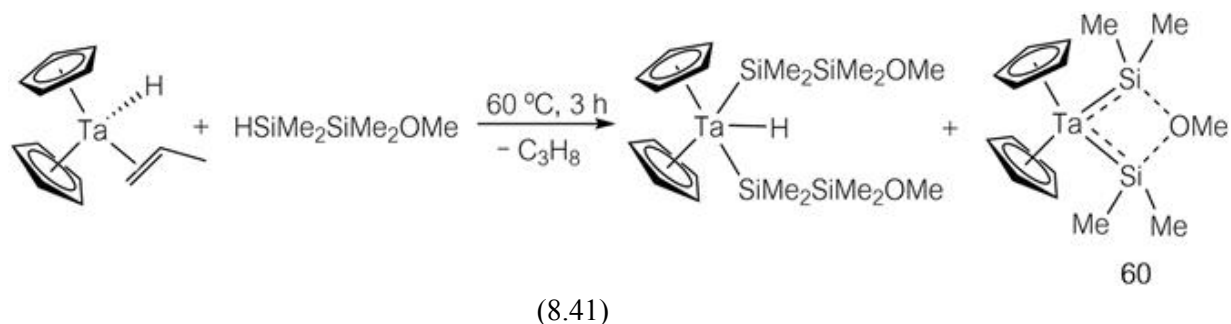
8.4.5 Reactivity of Silylene Complexes

All the reactivity studies were carried out on Fischer-type silylene complexes, in which the metal–silicon bond is formed by σ-donor/π-back donation interactions. Compared with carbene complexes, π-back donation from the filled metal $d\pi$ orbital to the empty 3p Si orbital is not efficient,

and the metal–silicon bond is significantly longer than expected for a metal–silicon double bond. Thus, the metal–silicon bond is polarized $M(\delta^-)$–$Si(\delta^+)$, with a large dipole moment, and together with the existence of the low-lying empty Si 3p orbital, leads to the high reactivity of silylene complexes.

Silylene complexes, in general, are highly reactive toward polar molecules such as alcohols, which are thus used as trapping reagents for silylene complexes. Reaction of cationic ruthenium complex **44** with alcohol afforded **64** and alkoxysilane (Figure 8.16).[55] An alcohol molecule replaces the acetonitrile molecule to give the alcohol-stabilized silylene complex **62**. 1,2-addition of alcohol to the Ru–Si unsaturated bond then affords **63**. Si–H reductive elimination and recoordination of acetonitrile yield **64** and alkoxysilane.

$$[Cp^*L_2Ru=SiPh_2(NCMe)]^+ \underset{+NCMe}{\overset{-NCMe}{\rightleftharpoons}} [Cp^*L_2Ru=SiPh_2]^+$$

44

L = PMe$_3$

$$\text{--ROH} \big\Updownarrow \text{ROH}$$

$$[Cp^*L_2Ru]^{+\diagdown^H}_{\diagdown SiPh_2OR} \longleftarrow [Cp^*L_2Ru=SiPh_2(ROH)]^+$$

63

62

R = Me, Et, ^{t}Bu

$$\text{NCMe} \Big\downarrow$$

$$[Cp^*L_2Ru(NCMe)]^+ \;+\; HSiPh_2OR$$

64
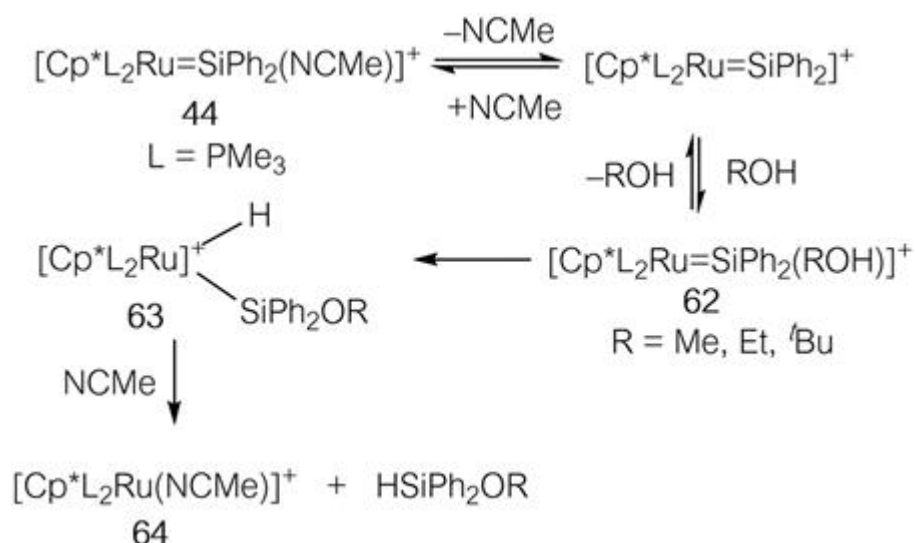
Figure 8.16 Reaction of cationic (silylene)ruthenium complex **44** with alcohol.

Complex **44** reacts with acetone to give **64** and a silyl enol ether (eqn (8.43)).[55] The reaction starts with nucleophilic attack by acetone on the electron-deficient silicon atom. In another example, the base-free silylene complex **47** reacts with isocyanate to afford the [2 + 2] cycloaddition product **65** (eqn (8.44)).[56] This reaction is also considered to proceed *via* initial nucleophilic attack by isocyanate on the silicon atom.

(8.43)

(8.44)
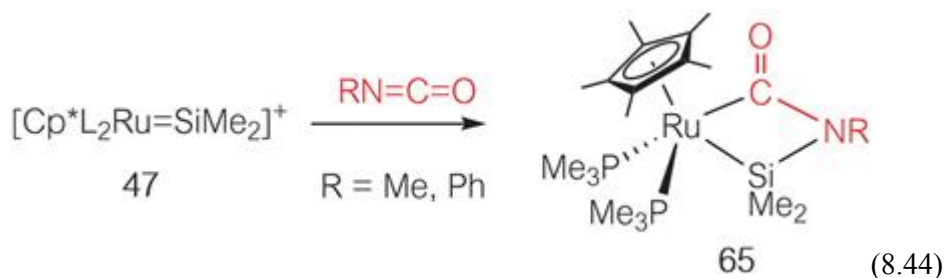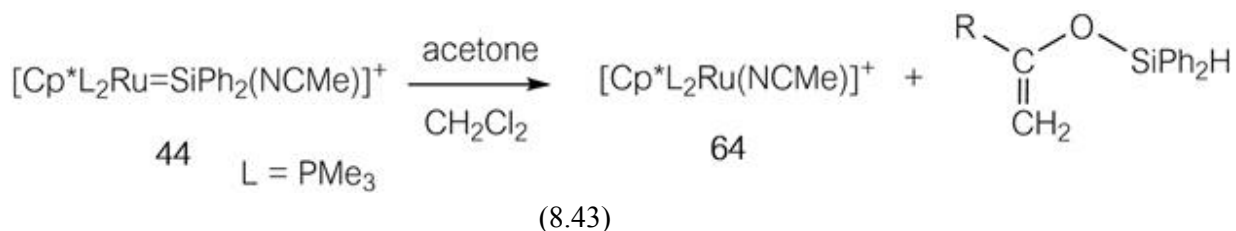
Reaction of **47** with a phosphorus ylide gave **66**, in which the negatively charged ylide carbon atom is bonded to the electron-deficient silylene silicon atom (eqn (8.45)).[57]

(8.45)
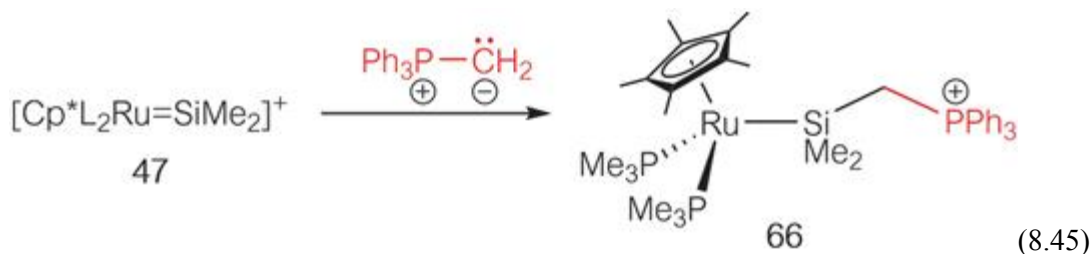
Some silylene complexes, upon heating or photolysis, afford free silylenes. Thermolysis of **45** at 120 °C resulted in $[Fe_3(CO)_{12}]$ and oligosilanes (eqn (8.46)).[58] Furthermore, irradiation of **45** in the presence of PPh_3 also yielded oligosilanes (eqn (8.47)). The free silylene generated upon irradiation was confirmed by trapping experiments using 2,3-dimethylbutadiene and alkynes.[58]

(8.46)

(8.47)
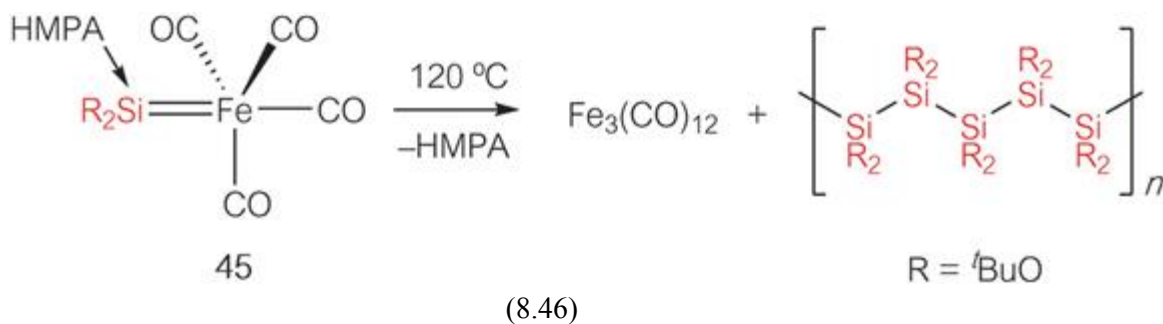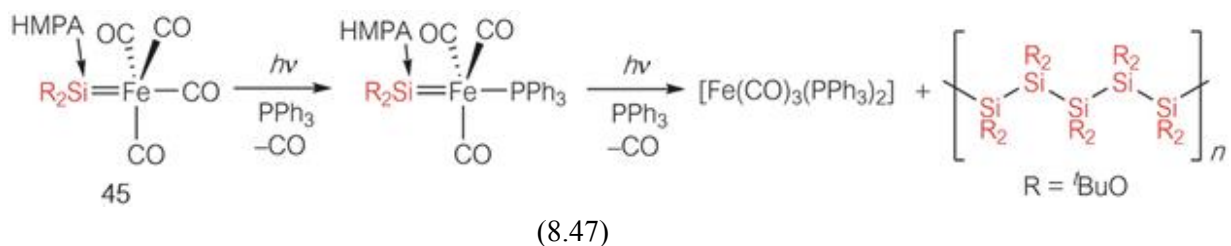
The 16e valence electron (silylene)platinum complex **54** reacts with dihydrogen to give hydrido(hydrosilyl)platinum(ii) complex **67** (eqn (8.48)).[49] Two possible mechanisms can be considered: one involves initial oxidative addition of H_2 to the platinum center, followed by a 1,2-H-shift, while the other involves the direct 1,2-addition of H_2 across the Pt–Si double bond. There are no experimental results to distinguish between the two mechanisms.

(8.48)
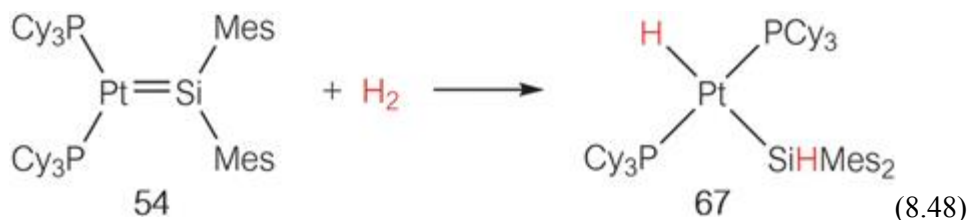
The *tert*-butoxy-bridged silyl(silylene)iron complex **68** reacts with hydrosilane to give **69** (eqn (8.49)).[59] Since the iron center is coordinatively saturated, the reaction is considered to proceed *via* the direct 1,2-addition of hydrosilane across the iron–silicon double bond.

(8.49)
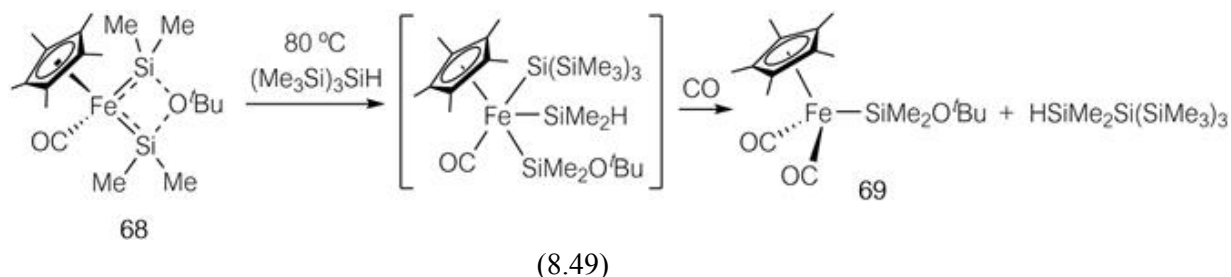
Heating of the methoxy-bridged silyl(silylene)ruthenium complex **70** in solution results in the insertion of the Ru=Si unit into a C–H bond of PPh_3 to give **71** (eqn (8.50)).[60] This unusual reaction is considered to proceed *via* the electrophilic, intramolecular attack by the electropositive silylene silicon atom on the *ortho*-carbon atom of the phenyl group.

70

(8.50)
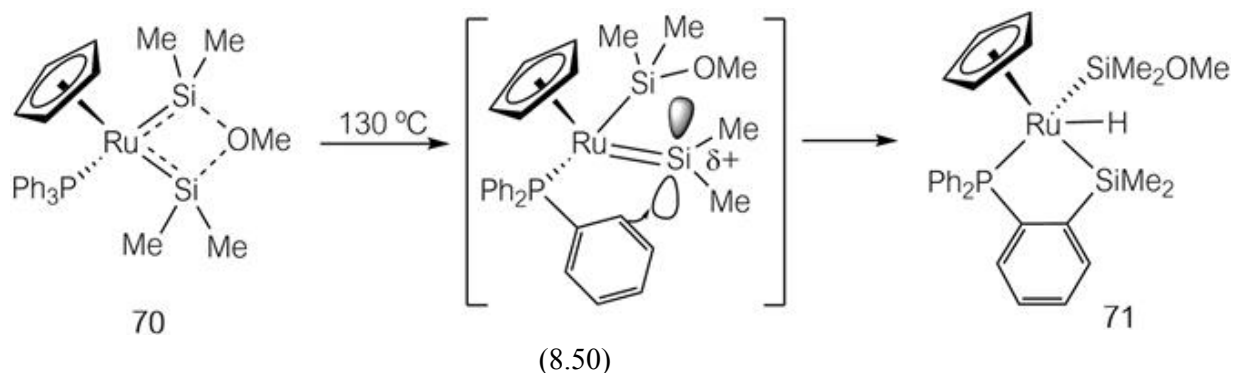
One characteristic reaction of silylene complexes is intramolecular rearrangement, which has been observed in the catalytic redistribution of substituents on the silicon atom for a long time. In particular, silyl(silylene) complexes are believed to undergo 1,2- and 1,3-shifts under mild conditions. In 2004, Tobita *et al.* reported direct evidence for 1,2- and 1,3-shifts in silyl(silylene) complexes under moderate conditions (eqn (8.51) and Figure 8.17).[61]

(8.51)
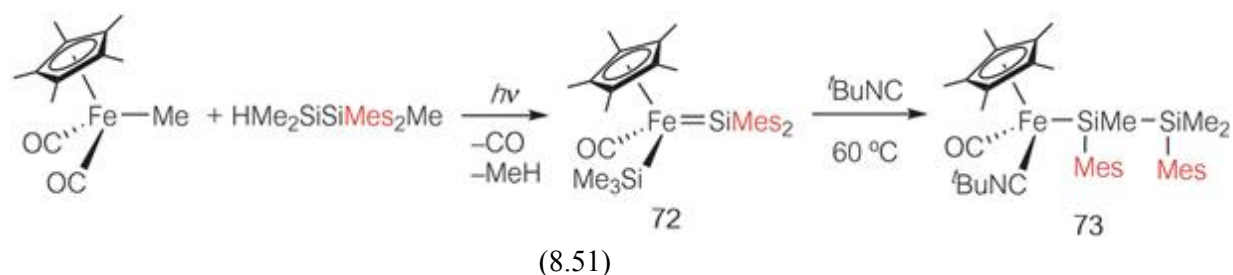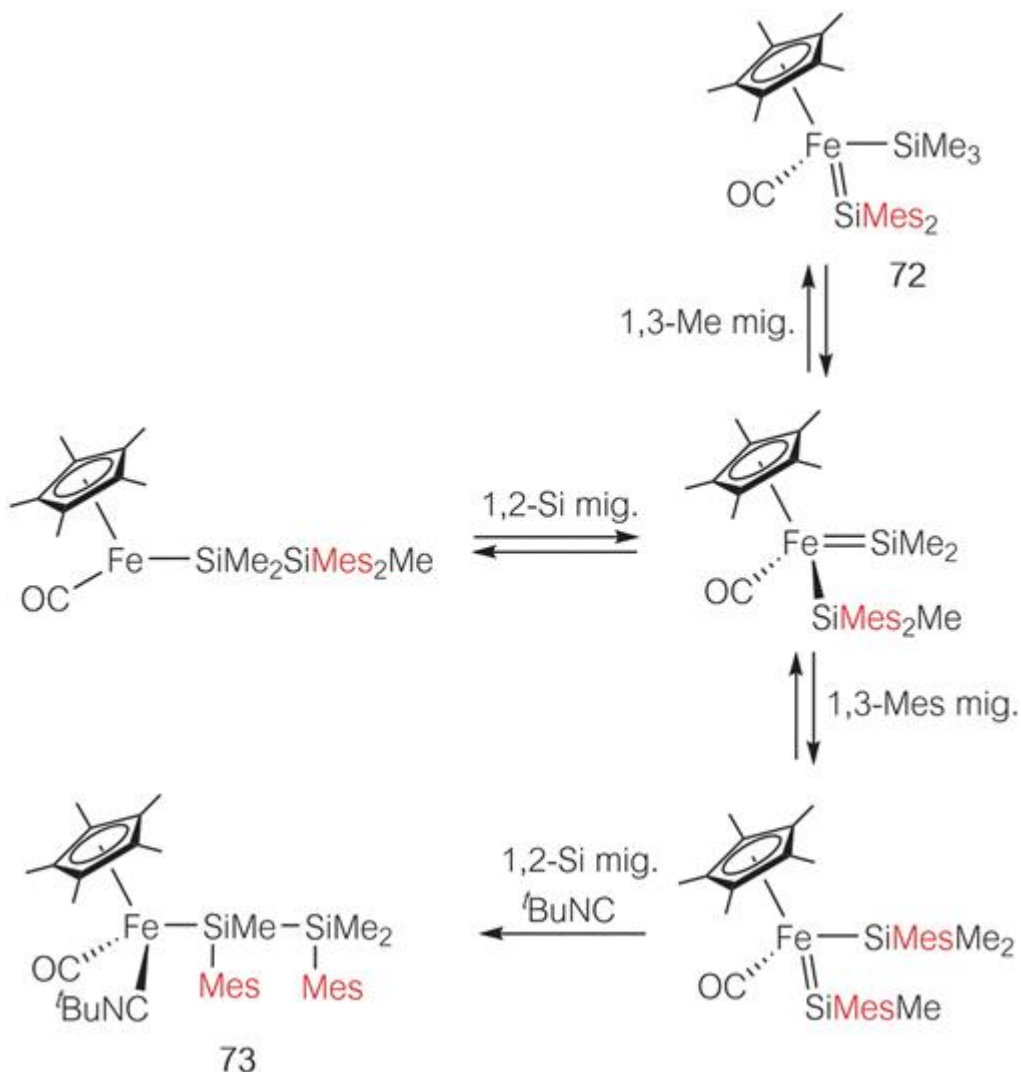
Figure 8.17 1,2- and 1,3-shifts in silyl(silylene) complexes.

Related rearrangements (Figures 8.18[62] and 8.19[63]) have been observed in other silylene complexes. A methyl(silylene)iridium(ɪɪɪ) complex, proposed as an intermediate, undergoes a 1,2-Me-shift to give a (methylsilyl)iridium(ɪɪɪ) complex. The reverse process was also reported for a cationic silyliridium(ɪɪɪ) complex, which undergoes a 1,2-Ph-shift to give the phenyl(dimethylsilylene) complex as an intermediate exclusively. This selectivity is attributable to the relative stability of the resulting silylene complexes, where the electron-donating methyl groups stabilize the silylene complex better than the phenyl group.
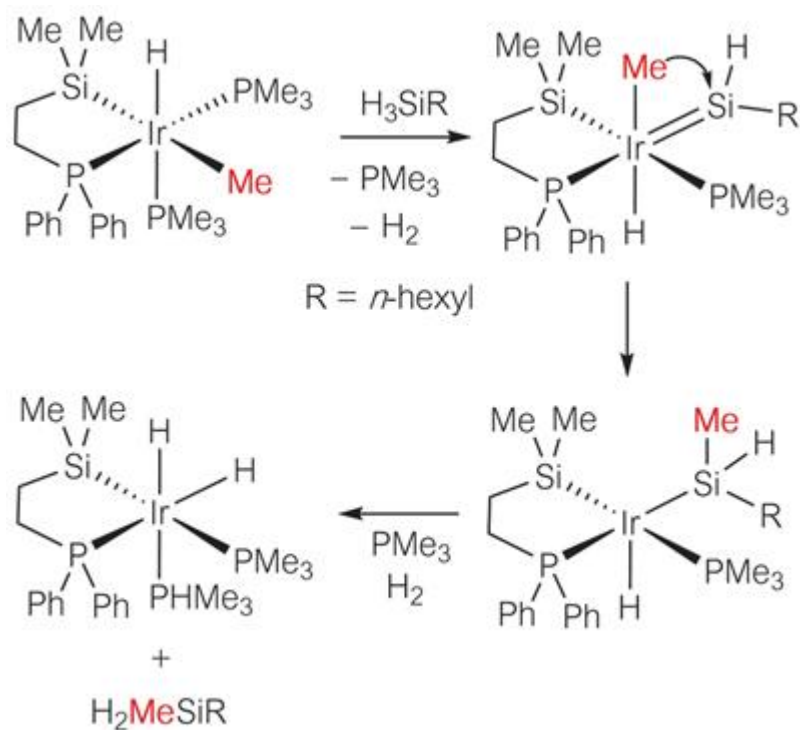
Figure 8.18   1,2-Me-shift in a silylene complex.
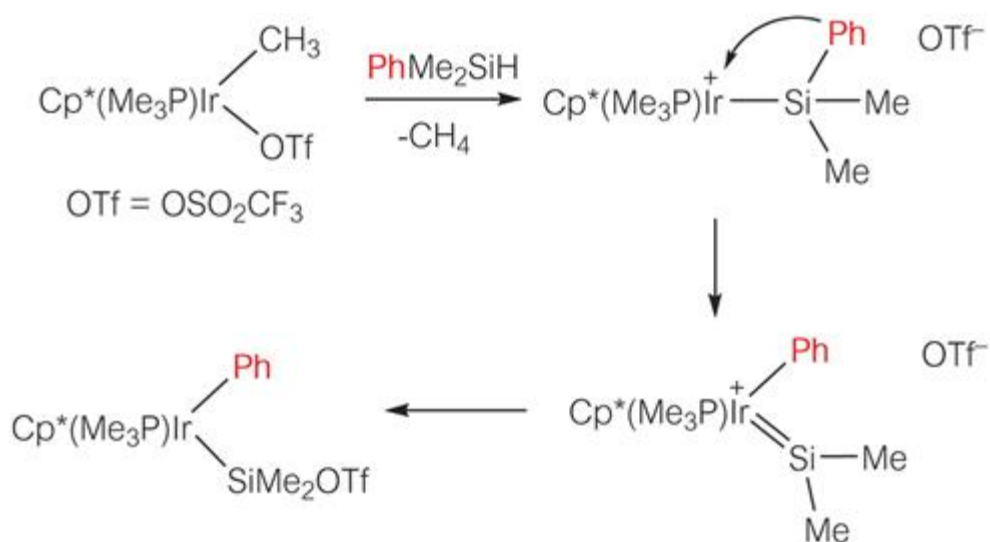
Figure 8.19   1,2-Ph-shift in a silyl complex, affording a silylene complex.

8.5   Three-membered Silametallacycles

Three-membered silametallacycles are classified into two categories (Figure 8.20). One is a metal complex with unsaturated organosilicon moieties such as silene, disilene, and silaimine, in which two π-electrons are donated to the metal center. The other is a metal complex with the η^2-heteroatom-substituted silyl ligand, in which three electrons are donated to the metal center (the latter is similar to the metallacycle derived from the intramolecular C–H bond activation of a PMe$_3$ ligand). The reactivities of these two types of silametallacycles are very different.

ER$_n$ = CR$_2$, SiR$_2$, NR   ER$_n$ = PR$_2$, SR, TeR
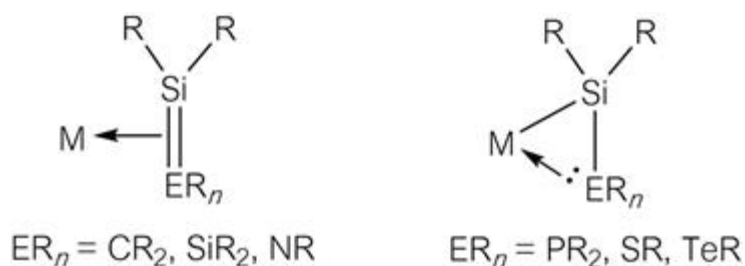
Figure 8.20   Three-membered silametallacycles.

8.5.1   Silene Complexes

Silenes are organosilicon compounds possessing a silicon–carbon double bond. In a silene complex, the silene is coordinated to the metal center by donation of two double bond π-electrons. The bonding in silene complexes is similar to that in alkene complexes, and there is considerable contribution from the silametallacyclopropane canonical form (Figure 8.21).
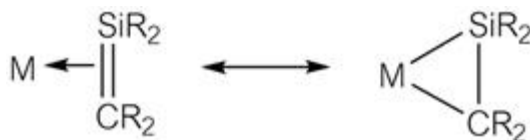
Figure 8.21   Canonical structures of silene complexes.

Silene complexes have attracted much attention in relation to the intermediates postulated in the metal-catalyzed redistribution of organosilicon compounds. In 1998, Tilley *et al.* reported the synthesis and full characterization of sileneruthenium complex **74a** (eqn (8.52)).[64] The Si–C bond length of the silene moiety is 1.78(2) Å, which is longer than

that in the isolated silene, $Me_2Si=C(SiMe_3)(SiMe^tBu_2)$ (1.702(5) Å), but shorter than that expected for a carbon–silicon single bond (1.87–1.91 Å). The sum of the bond angles around the silicon atom except for the ruthenium atom is 344°, which is between the values of sp^2 (360°) and sp^3 (329°) hybridization. These structural features suggest the considerable unsaturated character of the silicon–carbon bond.

(8.52)
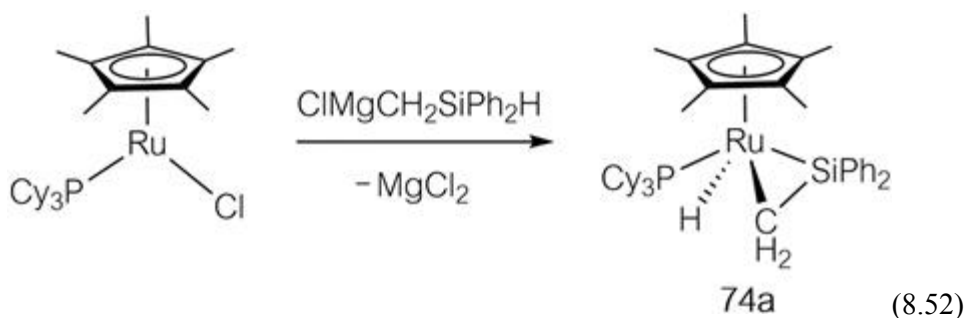
Berry *et al.* succeeded in the synthesis of **75** through C–H oxidative addition of a silyl methyl group, similar to the real catalytic pathway (eqn (8.53)).[65]

(8.53)
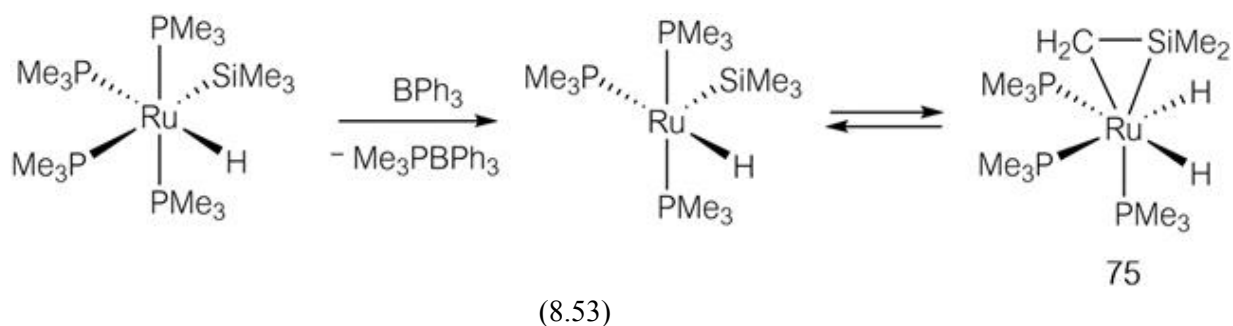
Although little is known about the reactivity of silene complexes, it was reported that **74b** reacts with methanol to give the 1,2-addition product **76** (eqn (8.54)).[66]

(8.54)
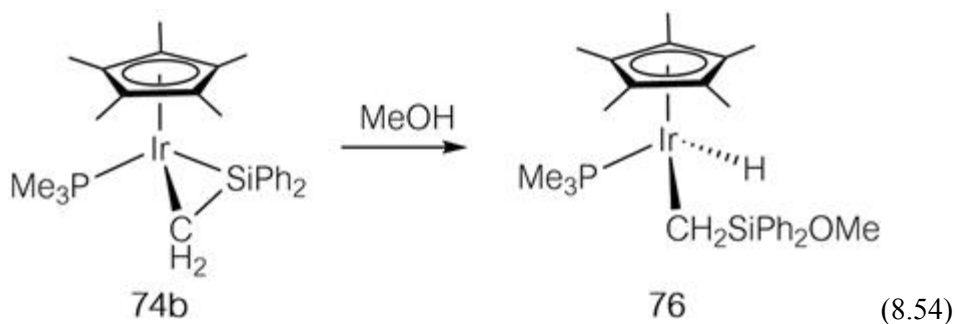
8.5.2 Disilene Complexes

The first complex containing a coordinated disilene, **77**, was synthesized in 1989 by West *et al.* by reaction of a platinum(0) complex with dihydrodisilane with evolution of H_2 (eqn (8.55)).[67]

In a different approach, treatment of a chloro(chlorodisilanyl)tungsten complex with Mg led to the formation of the disilene-coordinated complex **78** (eqn (8.56)).[68] According to the X-ray structural analysis of **78**, the Si–Si bond length is 2.260(2) Å, which is between the values expected for single (2.35 Å) and double bonds (2.14 Å). The sum of the bond angles around the silicon atom except for the tungsten atom is 348.3°, which is between the values expected for sp^2 and sp^3 hybridization, indicating unsaturation in the Si–Si bond.

$$(8.55)$$

$$(8.56)$$
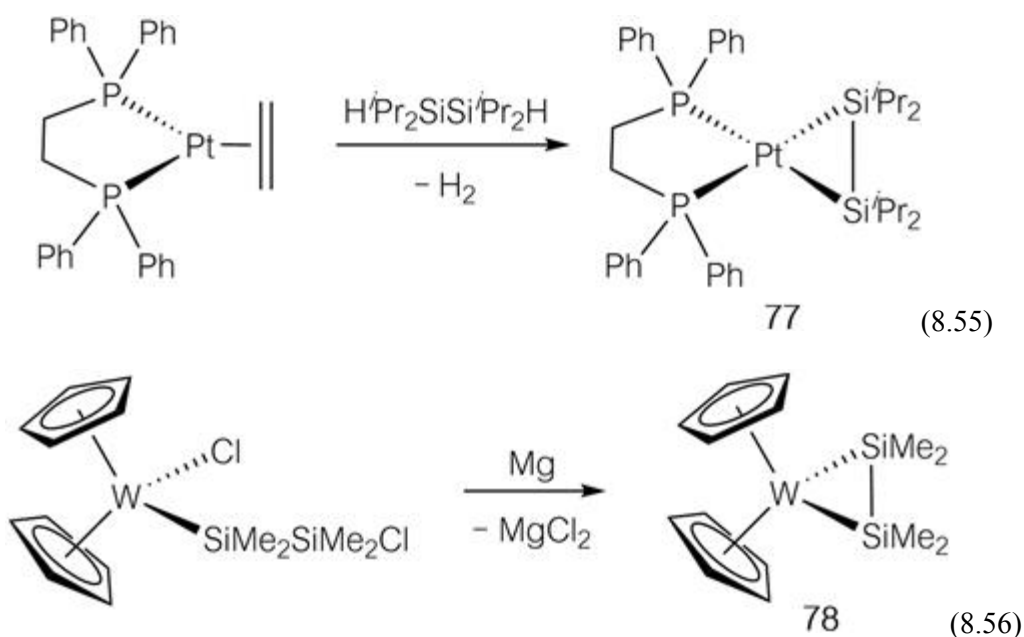
Since the first discovery of a free disilene by Fink and West in 1981,[69a] a wide variety of disilenes have been synthesized. The simplest and most promising strategy for the synthesis of disilene complexes is the direct reaction between the transition metal complex and the free disilene (Figure 8.22). This approach has been suitable in certain cases and a number of disilene complexes have been synthesized this way.[69b]
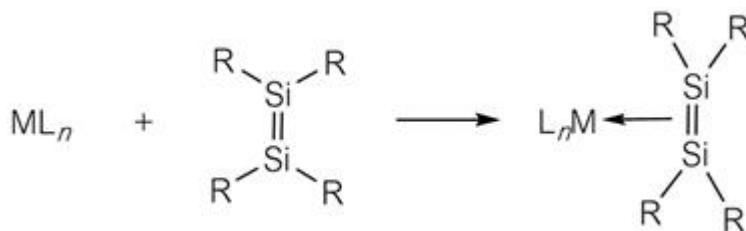
Figure 8.22 Synthesis of disilene complexes by the reaction of free disilenes with metal complexes.

Reactions of disilene complexes have been well documented. A typical reaction is the insertion of small molecules into the silicon–silicon bond (Figure 8.23).[68]

M = Mo, W
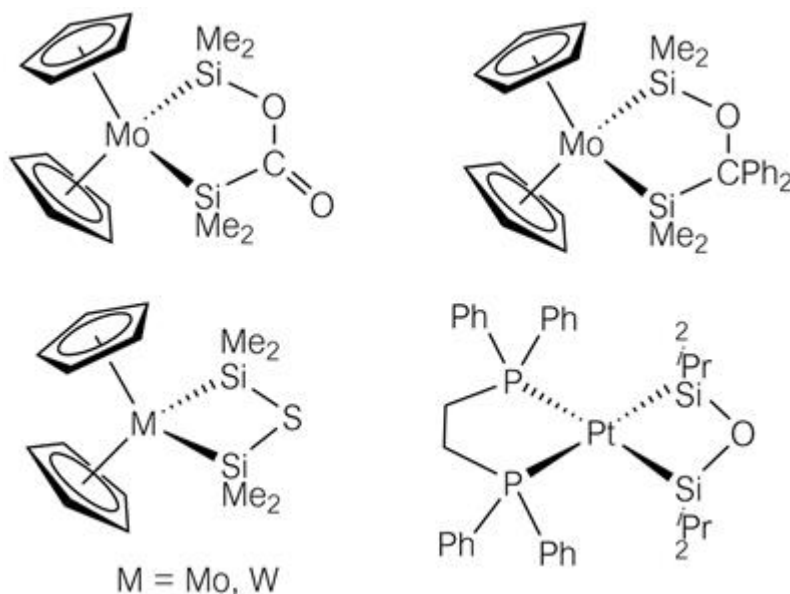
Figure 8.23 Insertion products derived from disilene complexes and small molecules.

8.5.3 Silaimine Complexes

A silaimine, the silicon analog of an imine, possesses a Si–N double bond. There exist only a few examples of η^2-silaimine-coordinated complexes.[70] The first silaimine-coordinated complex **79** was reported by Berry for a zirconium system (eqn (8.57)).[70a] According to the X-ray diffraction study, the Si–N bond length (1.687(3) Å) is much longer than that in ^{t}Bu$_2$Si=NSi^{t}Bu$_3$ (1.568(3) Å) and is in the range expected for Si–N single

bonds (1.64–1.80 Å). The Zr–Si bond length (2.654(1) Å) is shorter by 0.10–0.16 Å than Zr–Si bonds in silylzirconium complexes. In contrast to silene and disilene complexes, silaimine complexes exhibit a considerable contribution by the silametallacyclopropane canonical form. The reactivity of silaimine complexes towards unsaturated molecules has been examined, with insertion occurring into the metal–silicon bond, consistent with the structural properties of silametallacyclopropanes.

$$(8.57)$$
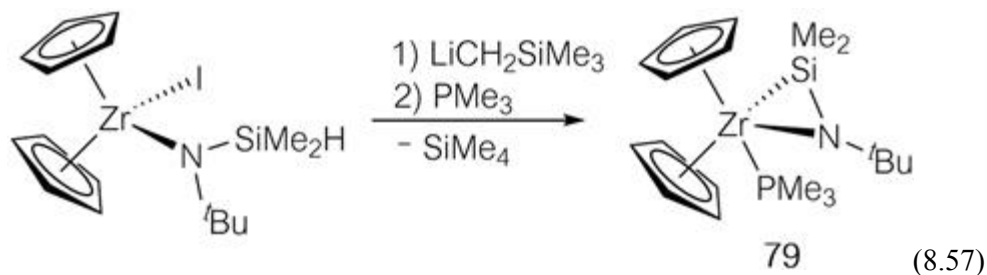
8.5.4   Phosphasilametallacyclopropanes

Phosphasilametallacyclopropanes possess a considerable contribution of the intramolecularly base-stabilized silylene canonical form and exhibit extremely high reactivity (Figure 8.24). The silicon–phosphorus bond reacts with polar molecules[71] with the silicon and phosphorus atoms cooperating as a Lewis acid and base, respectively. The reactions of **80** with methanol, acetone, and N,N-dimethylaminopyridine (DMAP) are illustrated in Figure 8.24.
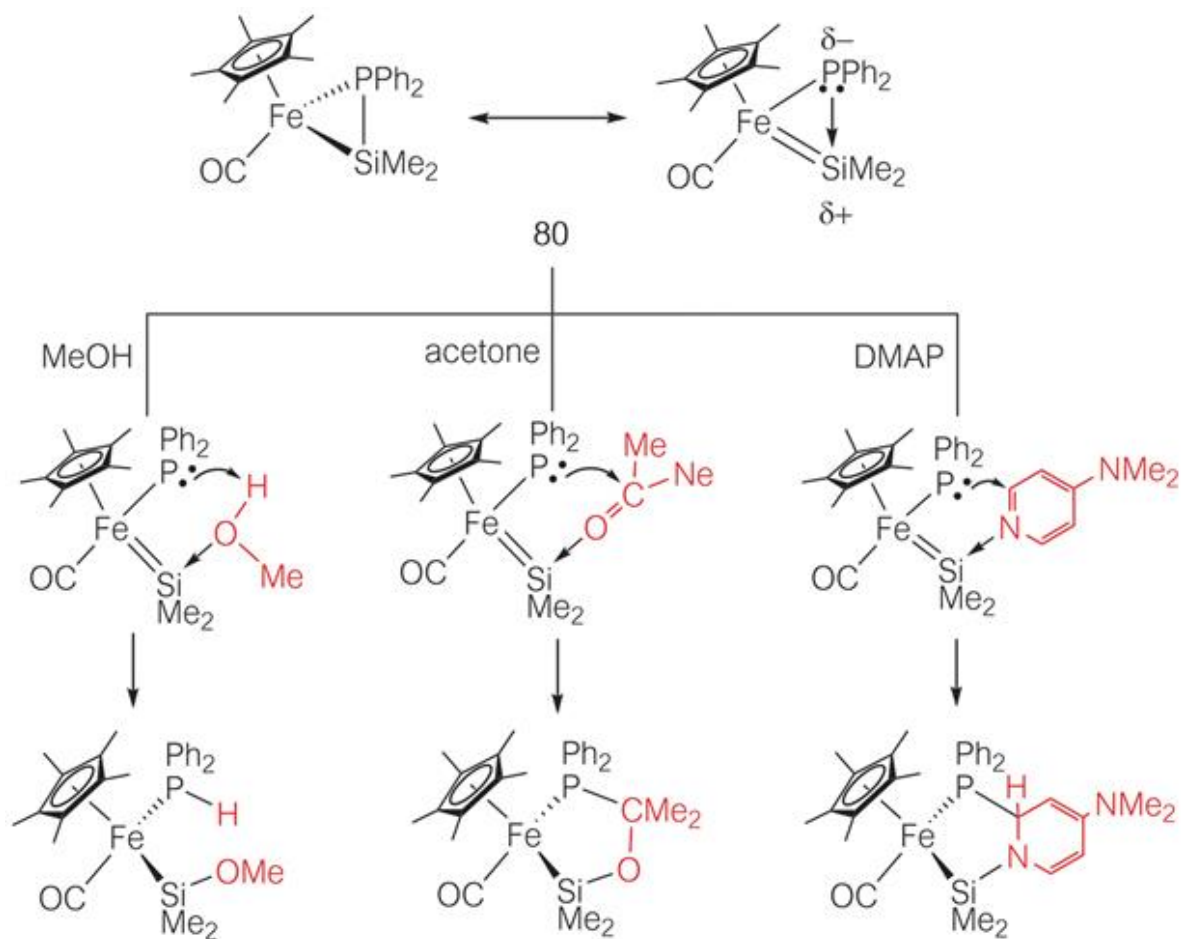
Figure 8.24 Reactions of phosphasilametallacyclopropane **80** with small molecules.

8.6 Silicon-bridged Dinuclear Complexes

Silicon-bridged dinuclear complexes may be classified into two categories, **A** and **B**, depending on whether a metal–metal bond exists or not (Figure 8.25). Spectroscopic data indicate that silicon atoms of type **A** are sp^3 hybridized and the complex can be regarded as a dimetallasilane, with reactivity similar to mononuclear silyl complexes. Type **B** complexes are regarded as silylene-bridged dinuclear complexes. The bonding, synthesis and reactivity of type **B** complexes are discussed in this section.
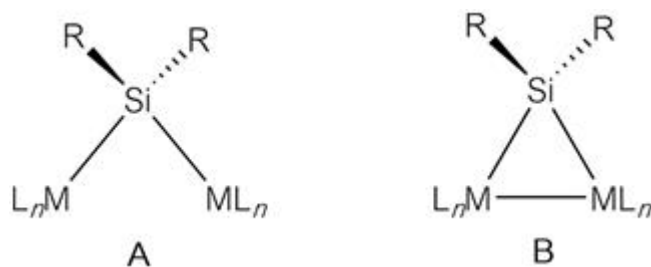
Figure 8.25   Silicon-bridged dinuclear complexes.

In type **B** complexes, the sp^2 orbital of silicon interacts with the bonding orbitals of two metal atom d_{xy} orbitals in a σ mode (Figure 8.26).[72] Furthermore, the p orbital of silicon interacts with the antibonding orbital of two metal atom d_{xy} orbitals in a π mode.
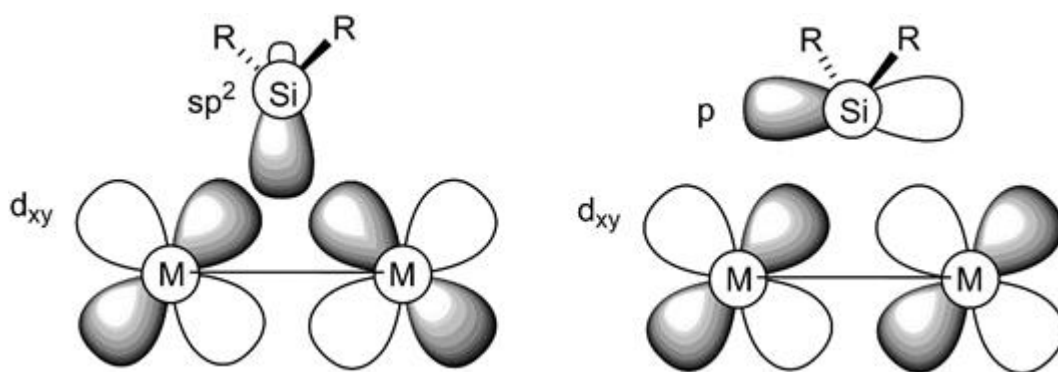
Figure 8.26   MO interactions in silylene-bridged dinuclear complexes.

Silylene-bridged dinuclear complexes are relatively stable due to efficient π-back donation from two metal centers and a variety of complexes have been reported. Irradiation of $[(\eta^5\text{-}C_5H_5)(CO)_2FeSiMe_3]$ in the presence of $^tBuSiH_3$ gave silylene-bridged diiron complex **82** *via* reductive elimination of $HSiMe_3$ (eqn (8.58)).[73a] The $^{29}Si\{^1H\}$ NMR spectrum shows a signal at δ 254.4. Such a low-field chemical shift is characteristic of an sp^2 silylene ligand. The hydrogen atom on the bridging silicon atom was substituted by iodine by reaction with CH_2I_2 (eqn (8.58)).[73b] Further treatment of **83** with *N,N*-dimethylaminopyridine (DMAP) gave the DMAP-stabilized silylyne-bridged diiron complex **84** on dissociation of the iodide anion (eqn (8.59)).

It is considered that DMAP is coordinated to the sp hybridized silicon atom by interaction with the vacant silicon 3p orbital.

(8.58)

(8.59)
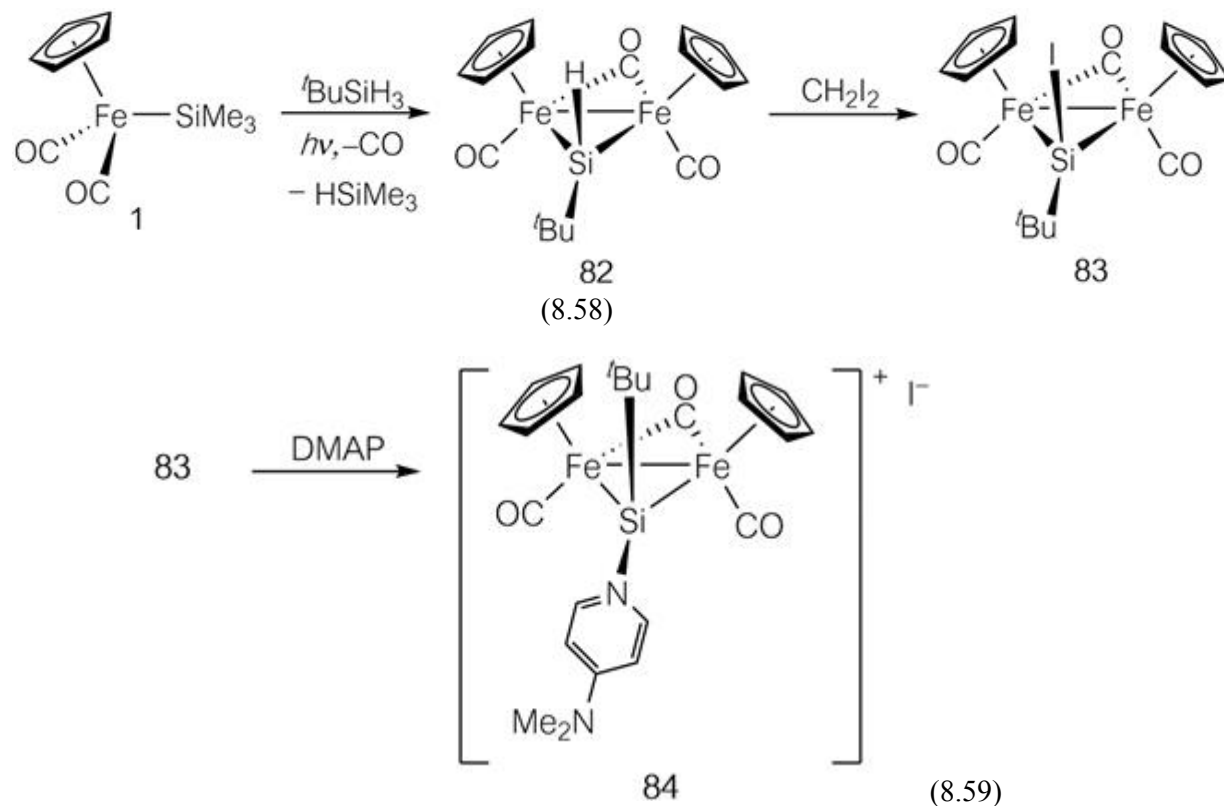
References

1. (a) S. Koseki, *Chemistry and Chemical Industry*, 1990, **43**, 619; (b) Y. Apeloig, R. Pauncz, M. Karni, R. West, W. Steiner and D. Chapman, *Organometallics*, 2003, **22**, 3250.
2. T. S. Piper, D. Lemal and G. Wilkinson, *Naturwissenschaften*, 1956, **43**, 129.
3. M. Okazaki, M. Iwata, H. Tobita and H. Ogino, *Dalton Trans.*, 2003, 1114.
4. T. M. Gilbert, F. J. Hollander and R. G. Bergman, *J. Am. Chem. Soc.*, 1985, **107**, 3508.
5. (a) S. Schmitzer, U. Weis, H. Kaeb, W. Buchner, W. Malisch, T. Polyzer, U. Posset and W. Kiefer, *Inorg. Chem.*, 1993, **32**, 303; (b) Y. Kawano, H. Tobita and H. Ogino, *Organometallics*, 1994, **13**, 3849.
6. S. Sakaki and M. Ieki, *J. Am. Chem. Soc.*, 1993, **115**, 2373.
7. D. L. Thorn and R. L. Harlow, *Inorg. Chem.*, 1990, **29**, 2017.
8. J. Chatt, C. Eaborn, S. D. Ibekwe and P. N. Kapoor, *J. Chem. Soc. (A)*, 1970, 1343.
9. (a) B. K. Campion, R. H. Heyn and T. D. Tilley, *Organometallics*, 1993, **12**, 2584; (b) T. D. Tilley, *Organometallics*, 1985, **4**, 1452.
10. A. D. Sadow and T. D. Tilley, *J. Am. Chem. Soc.*, 2005, **127**, 643.
11. (a) T. D. Tilley, in *The Chemistry of Organic Silicon Compounds*, ed. S. Patai and Z. Rappoport, Wiley, New York, 1989, ch. 24, pp. 1415–1470; (b) K. W. Muir and J. A. Ibers, *Inorg. Chem.*, 1970, **9**, 440; (c) M. S. Eisen, in *The Chemistry of Organic Silicon Compounds*, ed. Z. Rappoport and Y. Apeloig, Wiley, New York, 1998, **vol. 2**, ch. 35, pp. 2037–2128.

12. (a) A. P. Hagen and A. G. MacDiarmid, *Inorg. Chem.*, 1969, **6**, 686; (b) O. Kahn and M. Bigorgne, *J. Organomet. Chem.*, 1967, **10**, 137; (c) A. D. Berry, E. R. Corey, A. P. Hagen, A. G. MacDiarmid, F. E. Saalfeld and B. B. Wayland, *J. Am. Chem. Soc.*, 1970, **92**, 1940.
13. D. L. Lichtenberger and A. Rai-Chaudhuri, *J. Am. Chem. Soc.*, 1991, **113**, 2923.
14. (a) F. R. Hartley, *Chem. Soc. Rev.*, 1973, **2**, 163; (b) R. N. Haszeldine, R. V. Parish and J. H. Setchfield, *J. Organomet. Chem.*, 1973, **57**, 279.
15. H. Tobita, K. Hasegawa, J. J. G. Minglana, L.-S. Luh, M. Okazaki and H. Ogino, *Organomtellics*, 1999, **18**, 2058.
16. (a) J. L. Speier, J. A. Webster and G. H. Barnes, *J. Am. Chem. Soc.*, 1957, **79**, 974; (b) A. J. Chalk and J. F. Harrod, *J. Am. Chem. Soc.*, 1965, **87**, 16.
17. F. Seitz and M. S. Wrighton, *Angew. Chem., Int. Ed.*, 1988, **27**, 289.
18. K. C. Brinkman, A. J. Blakeney, W. Krone-Schmidt and J. A. Gladysz, *Organometallics*, 1984, **3**, 1325.
19. M. Aizenberg and D. Milstein, *J. Am. Chem. Soc.*, 1995, **117**, 6456.
20. H. C. Clark and T. L. Hauw, *J. Organomet. Chem.*, 1972, **42**, 429.
21. M. J. Fernandez, M. A. Esteruelas, M. S. Jimenez and L. A. Oro, *Organometallics*, 1986, **5**, 1519.
22. C. L. Randolph and M. S. Wrighton, *J. Am. Chem. Soc.*, 1986, **108**, 3366.
23. S. M. Maddock, C. E. F. Rickard, W. R. Roper and L. J. Wright, *Organometallics*, 1996, **15**, 1793.
24. L. Hao, J. F. Harrod, A.-M. Lebuis, Y. Mu, R. Shu, E. Samuel and H.-G. Woo, *Angew. Chem. Int., Ed.*, 1998, **37**, 3126.
25. M. Iwata, M. Okazaki and H. Tobita, *Chem. Commun.*, 2003, 2744.
26. F. L. Taw, P. S. White, R. G. Bergman and M. Brookhart, *J. Am. Chem. Soc.*, 2002, **124**, 4192.
27. (a) H. Nakazawa, T. Kawasaki, K. Miyoshi, C. H. Suresh and N. Koga, *Organometallics*, 2004, **23**, 117; (b) H. Nakazawa, M. Itazaki, K. Kamata and K. Ueda, *Chem. – Asian J.*, 2007, **2**, 882.
28. B. K. Campion, J. Falk and T. D. Tilley, *J. Am. Chem. Soc.*, 1987, **109**, 2049.
29. J. Ruiz, B. E. Mann, C. M. Spencer, B. F. Taylor and P. M. Maitlis, *J. Chem. Soc., Dalton Trans.*, 1987, 1963.
30. S. R. Berryhill and R. J. P. Corriu, *J. Organomet. Chem.*, 1989, **370**, C1.
31. U. Schubert, J. Mueller and H. G. Alt, *Organometallics*, 1987, **6**, 469.
32. R. S. Simons and C. A. Tessier, *Organometallics*, 1996, **15**, 2604.
33. H. Rabaâ, J.-Y. Saillard and U. Schubert, *J. Organomet. Chem.*, 1987, **330**, 397.
34. D. L. Lichtenberger and A. Rai-Chaudhuri, *Organometallics*, 1990, **9**, 1686.
35. J. Y. Corey, *Chem. Rev.*, 2016, **116**, 11291.
36. X. L. Luo and R. H. Crabtree, *J. Am. Chem. Soc.*, 1989, **111**, 2527.
37. (a) K. Yamamoto, H. Okinoshima and M. Kumada, *J. Organomet. Chem.*, 1970, **23**, C7; (b) K. Yamamoto, H. Okinoshima and M. Kumada, *J. Organomet. Chem.*, 1971, **27**, C31.
38. (a) I. Ojima, S. Inaba, T. Kogure and Y. Nagai, *J. Organomet. Chem.*, 1973, **55**, C7; (b) H. Ogino, *Chem. Rec.*, 2002, **2**, 291.
39. H. Nakatsuji, J. Ushio and T. Yonezawa, *J. Organomet. Chem.*, 1983, **258**, C1.
40. G. Schmid and E. Welz, *Angew. Chem., Int. Ed.*, 1977, **16**, 785.
41. D. A. Straus, T. D. Tilley, A. L. Rheingold and S. J. Geib, *J. Am. Chem. Soc.*, 1987, **109**, 5872.
42. C. Zybill and G. Müller, *Angew. Chem., Int. Ed.*, 1987, **26**, 669.
43. K. Ueno, H. Tobita, M. Shimoi and H. Ogino, *J. Am. Chem. Soc.*, 1988, **110**, 4092.
44. D. A. Straus, S. D. Grumbine and T. D. Tilley, *J. Am. Chem. Soc.*, 1990, **112**, 7801.
45. H. Kobayashi, K. Ueno and H. Ogino, *Chem. Lett.*, 1999, 239.
46. R. J. P. Corriu, G. F. Lanneau and B. P. S. Chauhan, *Organometallics*, 1993, **12**, 2001.
47. G. P. Mitchell and T. D. Tilley, *Angew. Chem., Int. Ed.*, 1998, **37**, 2524.
48. L. K. Woo, D. A. Smith and V. G. Young, *Organometallics*, 1991, **10**, 3977.

49. J. D. Feldman, G. P. Mitchell, J.-O. Notle and T. D. Tilley, *J. Am. Chem. Soc.*, 1998, **120**, 11184.
50. (a) M. Denk, R. K. Hayashi and R. West, *J. Chem. Soc., Chem. Commun.*, 1994, 33; (b) B. Gehrhus, P. B. Hitchcock, M. F. Lappert and H. Maciejewski, *Organometallics*, 1998, **17**, 5599.
51. K. Morokuma, private communication; Z. Liu, PhD thesis, Emory University, 2000, chap. 3.
52. H. Nakatsuji, M. Hada and K. Kondo, *Chem. Phys. Lett.*, 1992, **196**, 404.
53. H. Koshikawa, M. Okazaki, S. Matsumoto, K. Ueno, H. Tobita and H. Ogino, *Chem. Lett.*, 2005, **34**, 1412.
54. N. Nakata, T. Fujita and A. Sekiguchi, *J. Am. Chem. Soc.*, 2006, **128**, 16024.
55. C. Zhang, S. D. Grumbine and T. D. Tilley, *Polyhedron*, 1991, **10**, 1173.
56. G. P. Mitchell and T. D. Tilley, *J. Am. Chem. Soc.*, 1997, **119**, 11236.
57. S. K. Grumbine, G. P. Mitchell, D. A. Straus and T. D. Tilley, *Organometallics*, 1998, **17**, 5607.
58. C. Zybill, D. L. Wilkinson, C. Leis and G. Müller, *Angew. Chem., Int. Ed. Engl.*, 1989, **28**, 203.
59. H. K. Sharma and K. H. Pannell, *Organometallics*, 2001, **20**, 7.
60. H. Wada, H. Tobita and H. Ogino, *Organometallics*, 1997, **16**, 3870.
61. H. Tobita, A. Matsuda, H. Hashimoto, K. Ueno and H. Ogino, *Angew. Chem., Int. Ed.*, 2004, **43**, 221.
62. M. Okazaki, H. Tobita and H. Ogino, *J. Chem. Soc., Dalton Trans.*, 1997, 3531.
63. P. Burger and R. G. Bergman, *J. Am. Chem. Soc.*, 1993, **115**, 10462.
64. B. K. Campion, R. H. Heyn and T. D. Tilley, *J. Am. Chem. Soc.*, 1998, **110**, 7558.
65. V. K. Dioumaev, K. Plössl, P. J. Carroll and D. H. Berry, *J. Am. Chem. Soc.*, 1999, **121**, 8391.
66. B. K. Campion, R. H. Heyn and T. D. Tilley, *J. Am. Chem. Soc.*, 1990, **112**, 4079.
67. E. K. Pham and R. West, *J. Am. Chem. Soc.*, 1989, **111**, 7667.
68. D. H. Berry, J. H. Chey, H. S. Zipin and P. J. Carroll, *J. Am. Chem. Soc.*, 1990, **112**, 452.
69. (a) R. West, M. J. Fink and J. Michl, *Science*, 1981, **214**, 1343; (b) S. Ishida and T. Iwamoto, *Coord. Chem. Rev.*, 2016, **314**, 34.
70. (a) L. J. Procopio, P. J. Carroll and D. H. Berry, *J. Am. Chem. Soc.*, 1991, **113**, 1870; (b) M. Okazaki and S. Ebina, *Chem. Lett.*, 2014, **43**, 1089.
71. M. Okazaki, K. A. Jung, K. Satoh, H. Okada, J. Naito, T. Akagi, H. Tobita and H. Ogino, *J. Am. Chem. Soc.*, 2004, **126**, 5060.
72. H. Ogino and H. Tobita, *Adv. Organomet. Chem.*, 1998, **42**, 223.
73. (a) H. Tobita, Y. Kawano, M. Shimoi and H. Ogino, *Chem. Lett.*, 1987, 2247; (b) Y. Kawano, H. Tobita, M. Shimoi and H. Ogino, *J. Am. Chem. Soc.*, 1994, **116**, 8575.

Chapter 9

Chemistry of Transition Metal Complexes with Group 13 Elements: Transition Metal Complexes with Lewis Acidic Ligands

Yasuro Kawano[a] and Keiji Ueno[1,b]

[a] International Christian University, Japan; ykawano@mbh.nifty.com
[b] Gunma University Japan

9.1 Introduction

The elements boron, aluminum, gallium, indium and thallium are members of Group 13. They have four valence orbitals (ns and np), but only three valence electrons. In their chemical compounds, therefore, they would thus appear to be unable to obey the octet rule and thus "electron-deficient". To resolve this electron deficiency, they show characteristics not found for carbon, such as the formation of three-center two-electron bonds and cluster compounds. This tendency has attracted much attention and contributed to the development of chemical bonding theory. Group 13 elements are thus not only "rule breakers", but "rule makers" as well. This chapter outlines the chemistry of transition metal compounds with Group 13 elements as coordination elements.

9.2 Transition Metal Complexes with Boron Coordination

Boron is the first member of the Group 13 elements and thus it has the four valence orbitals, 2s and 2p, and only three valence electrons. In its

compounds, boron thus shows characteristics due to its electron deficiency and its tendency to form apparently strange compounds has attracted much attention.

Metallaborane clusters have been known for a long time and constitute a class of boron-containing transition metal complexes. These compounds may be considered as boron hydride clusters in which one or more vertices have been replaced by isolobal metal fragments. In these compounds, however, the boron–metal interaction is buried in the complex cluster framework so that it is difficult to understand the nature of the bonding.

From around the 1990s, the synthesis of boryl complexes with electron-precise two-center two-electron bonds was actively pursued. These studies revealed the nature of boron–metal bonds and their unique structures and reactivities. In particular, when it became clear that these compounds were key intermediates in the metal-catalyzed hydroboration of olefins, great attention was then focused on their chemistry. In this section, we survey the chemistry of transition metal–boryl complexes and related compounds.

9.2.1 Syntheses of Transition Metal–Boryl Complexes

Transition metal–boryl complexes are the most fundamental boron–metal compounds and contain a boryl group directly bonded to a metal center. There are several typical synthetic methods: (i) salt-elimination between a haloborane and an anionic metal complex; (ii) oxidative addition of a B–H bond or a B–B bond to a low valence metal complex; (iii) oxidative addition of a boron–halogen or boron–Group 14 element (Si, Ge, Sn) bond to an electron-rich metal center. Methods (i) and (ii) are closely related to the routes to metal silyl complexes, a research area which developed before that of metal boryl compounds. Method (iii) has been developed relatively recently and has been applied to the formation of late transition metal–boron bonds. Examples of syntheses of boryl complexes using these methods are shown in eqn (9.1)–(9.5).[1,2]

(9.1)

$$[RhCl(N_2)(P^iPr_3)_2] \ + \ \text{H–B(catechol)} \ \xrightarrow{-N_2} \ \text{(Cl)(H)Rh(P}^i\text{Pr}_3)_2\text{–B(catechol)}$$

(9.2)

$$\text{Cp}_2\text{WH}_2 \ + \ (^t\text{Bu-cat})\text{B–B}(^t\text{Bu-cat}) \ \xrightarrow{-H_2} \ \text{Cp}_2\text{W(B}^t\text{Bu-cat)}_2$$

(9.3)

(9.4)

$$[Pt(PCy_3)_2] \ + \ R\text{–BBr}_2 \ \xrightarrow{\text{benzene}} \ \text{Br–Pt(PCy}_3)_2\text{–B(Br)R}$$

2 (R = Mes, ferrocenyl)

$$\text{(dmpe)PdMe}_2 \ + \ 2\,\text{Me}_3\text{Sn–B(N(Me)CH}_2\text{CH}_2\text{N(Me))} \ \xrightarrow{-\text{SiMe}_4} \ \text{3} \ + \ \text{Me–B(N(Me)CH}_2\text{CH}_2\text{N(Me))}$$

3

(9.5)
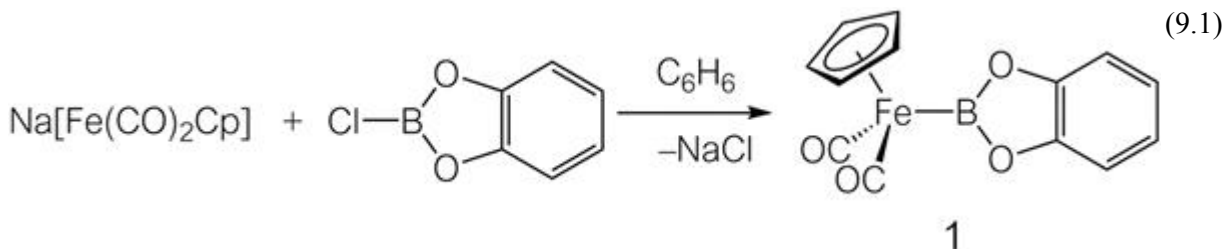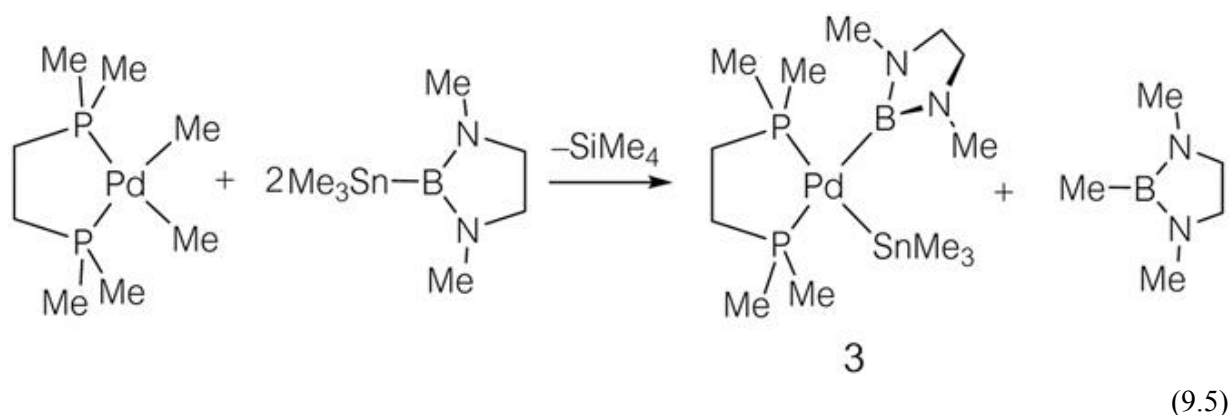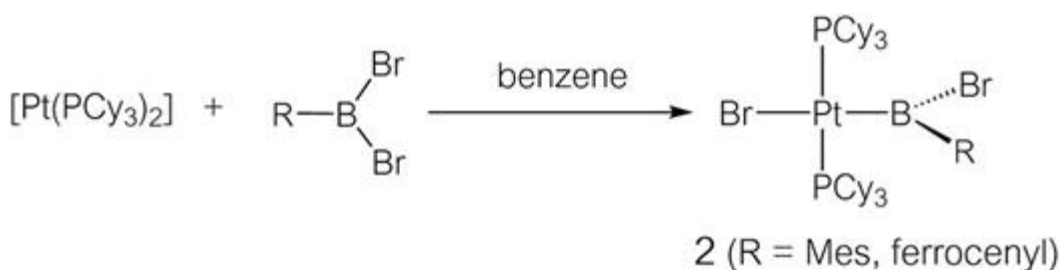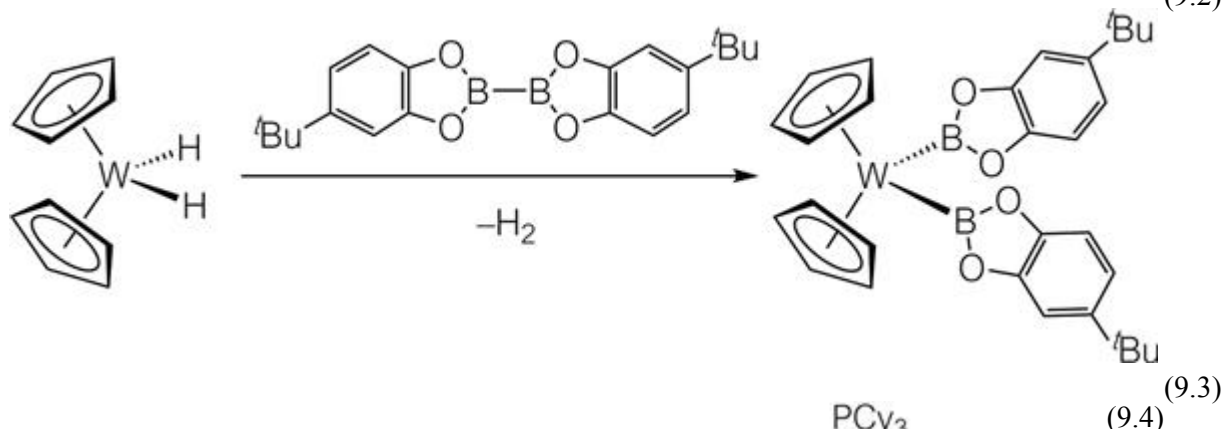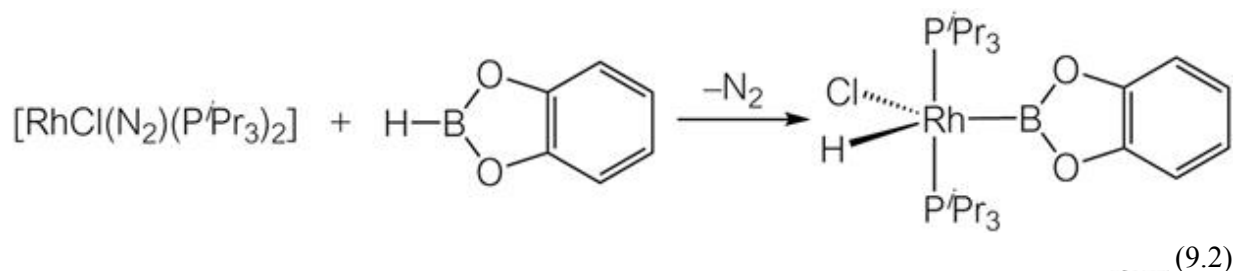
Many boryl complexes possess π-donor substituents on the boron atom (see below and Figure 9.1). In particular, catecholate–boryl complexes played a leading role in the initial development of this field. Since then, many boryl complexes with amino groups or bulky aryl groups have been prepared (eqn (9.4) and (9.5)), while only a small number of simple alkylboryl complexes are known. In complexes bearing a non-substituted

boryl group (BH_2), as shown later, the boron atom is coordinated by a Lewis base and adopts a four-coordinate geometry.
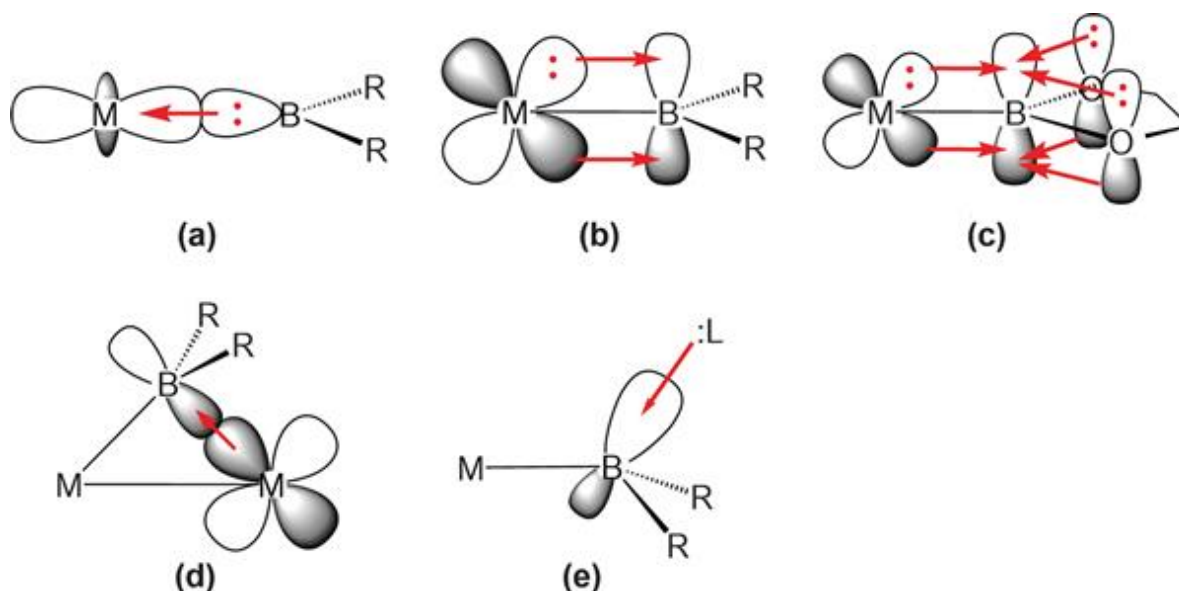
Figure 9.1   Orbital interactions in transition metal boryl complexes: (a) σ-donation, (b) π-back-donation, (c) interaction between π-donating substituents and boron, (d) back-donation from an adjacent metal center, and (e) coordination of a Lewis base to the boryl group.

For preparations of alkyl complexes and silyl complexes, the reaction of a metal halide with an alkyllithium or a silyllithium is frequently employed. However, this methodology cannot normally be applied to the synthesis of boryl complexes because boryllithium is not easily accessible. Boryl anions $[BR_2]^-$ are difficult to prepare because these would be Lewis bases and, at the same time, Lewis acids. Nevertheless, Nozaki and coworkers synthesized a boryllithium, stabilized by a heterocycle, and used this to obtain a boryl hafnium complex, **4** (eqn (9.6)),[3a] which shows catalytic activity toward olefin polymerization. The boryllithium derivative was also employed in the synthesis of the first boryl rare earth complexes.[3b,c]

$$4 \ (\text{Dip} = 2,6\text{-diisopropylphenyl})$$

(9.6)

Boryl ligands have a vacant p orbital into which they can receive π-back-donated electron density from the central metal. Thus, the bonding interaction between a metal atom and a boryl group is related to that in carbene complexes, and has donor–acceptor-type double bond character (Figure 9.1(a)–(e)). When a catecholate or amino group is substituted onto the boron atom, these groups act as π-donors and perturb the metal–boron π-interaction. These types of interactions will be discussed again in Section 9.2.2.

When a boryl group is bound to one of the metal atoms of a dinuclear complex, it occasionally adopts a semi-bridging coordination mode because its vacant p orbital can receive back-donated electron density from the other metal atom (Figure 9.1(d)). In compound **5**, the boryl ligand coordinates to the octahedral Rh(ɪɪɪ) while simultaneously accepting electron density from a filled d orbital of the planar Rh(ɪ). Consequently, it bridges the two metal atoms asymmetrically.[4a] The Rh(ɪɪɪ)–B and Rh(ɪ)–B interatomic distances are 2.057(8) and 2.444(9) Å, respectively. In contrast, in compounds **6** and **7**, the boryl groups symmetrically bridge two metal atoms (Scheme 9.1).[4b,c]

5   **6**   **7**

The p orbital of a boryl ligand can also be coordinated by a Lewis base (Figure 9.1(e)). Dichloroboryl complex **8** undergoes coordination by a pyridine derivative to give a compound bearing a four-coordinate boryl group **9** (eqn (9.7)). In addition, the groups of Shimoi and Nakazawa reported that phosphine- or phosphite-bound tetrahedral boranes react with Group 6 methyl complexes under photolytic conditions to produce four-coordinate boryl complexes **10** (eqn (9.8)). This reaction is thought to proceed through σ-bond metathesis in which a BH hydrogen atom migrates to the methyl carbon atom in the metal coordination sphere.[5]

(9.7)

$M = Mo, W;$
$PR_3 = PMe_3, P(OMe)(NMeCH_2CH_2NMe))$

(9.8)
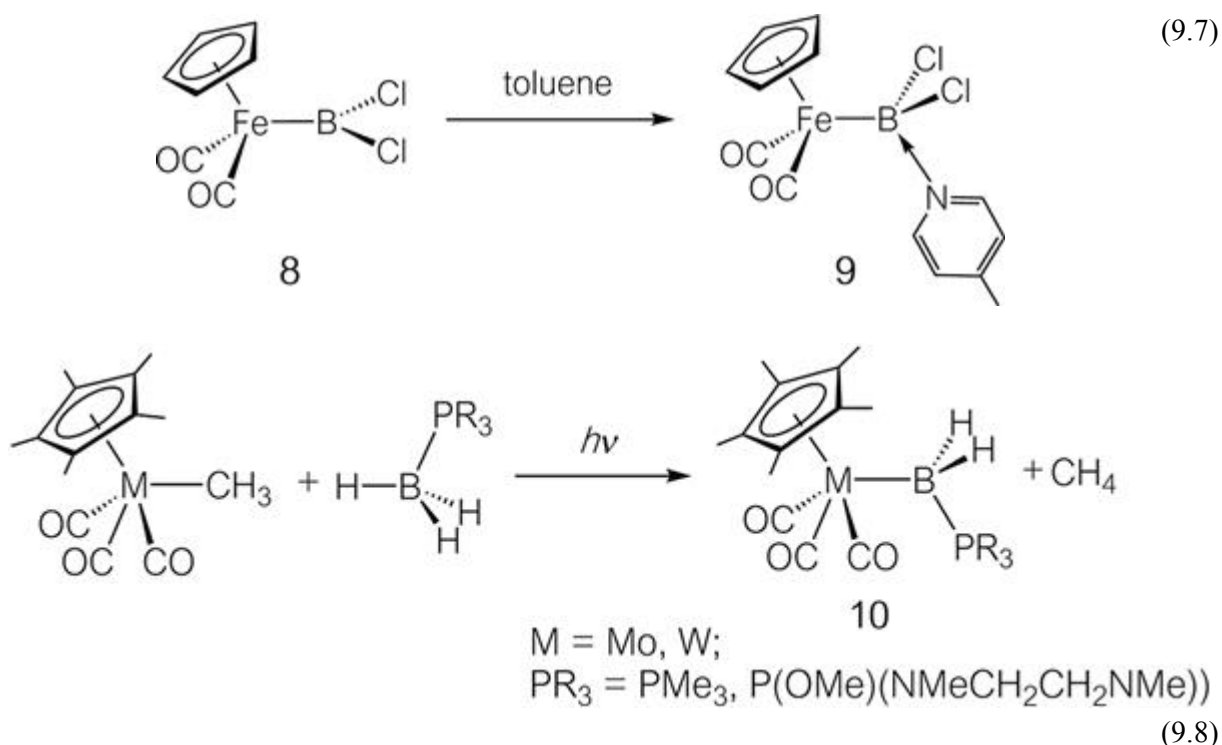
As exemplified in eqn (9.2), oxidative addition of BH is an effective method to obtain boryl complexes. In the reaction of the dimethyl derivative of titanocene with catecholborane, however, BH oxidative addition proceeds only partially and produces borane σ complex **11**, in which the borane coordinates to the metal through a B–H–M three-center two-electron bond (eqn (9.9)). Bonding of the borane ligand with titanium in **11** consists of electron donation from the B–H bonding σ orbital to the metal center, as well as back-donation from Ti(ii) into the empty boron p orbital. This interaction gives rise to pyramidalization around the boron atoms. At the same time, because a three-center bond is formed between the titanium d orbital and the p orbitals of the two boron atoms, the B–B

interatomic distance adopts a value that suggests the existence of a B···B bonding interaction. In ruthenium complex **12**, mesitylborane coordinates to the metal through the two BH bonds (eqn (9.10)). The Ru–B interatomic distance is remarkably short (1.938 Å), indicating strong π-back-donation from the metal to the boron p orbital (Figure 9.2(b)).[6]

(9.9)

(9.10)
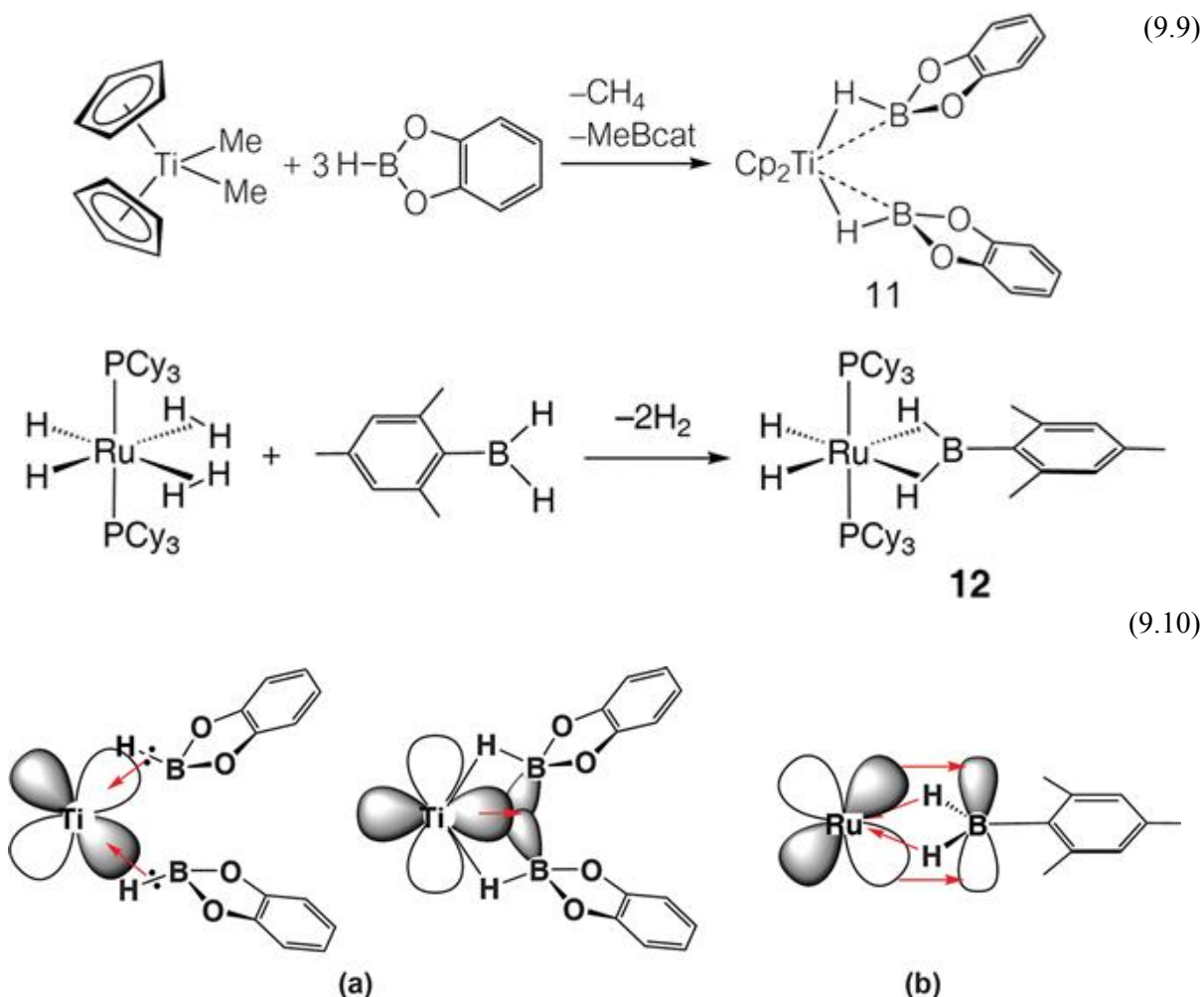
Figure 9.2 Orbital interactions in complex **11** (a) and complex **12** (b).

Four-coordinate borane–Lewis base adducts, which do not have a vacant p orbital, can also form σ complexes. Manganese complexes **13** shown in eqn (9.11) are of interest as analogues of alkane σ complexes since borane–Lewis base adducts are isoelectronic with alkanes. In solution, compounds **13** show dynamic behavior due to fast exchange between the metal-coordinated and terminal BH protons (Figure 9.3). The boron p orbital of **13** is filled due to coordination by the Lewis base and the anti-bonding BH σ*

orbitals are too high in energy to receive any appreciable back-donation from the metal. As a result, their metal···boron interatomic distances (2.573–2.769 Å) are much longer than those of **11** and **12**.[7] Despite the lack of metal-to-borane back-donation, complexes **13** can exist as stable species, mainly because the BH σ orbital can function as a good electron donor due to the high energy of the atomic orbitals of boron.

$$\text{CpMn(CO)}_3 \ + \ \text{BH}_3\text{·L} \ \xrightarrow[- \text{CO}]{h\nu}$$

(9.11)

13

L = PMe$_3$, NMe$_3$, quinuclidine
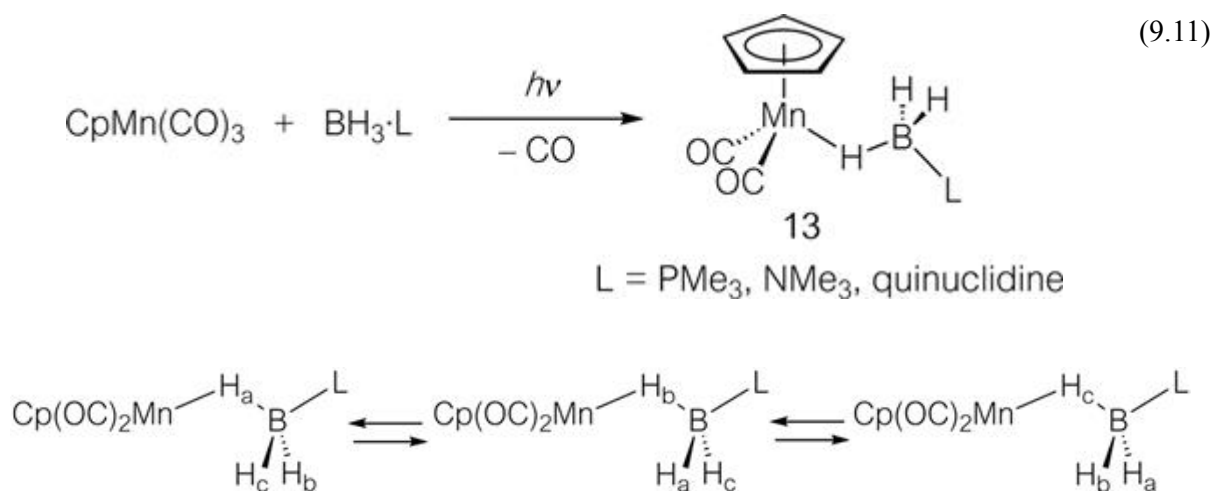
Figure 9.3   Fluxional behavior of manganese complexes **13**.

As noted above, formation of σ complexes *via* incomplete oxidative addition is one of the characteristic features of metal–boron complex chemistry. Stability of the σ complexes and the diverse coordination modes are due to the existence of a vacant p orbital on boron and the high energy of the BH σ orbitals.

Recently, an anionic gold complex with a diboraanthracene-based ligand **14** was reported. In this compound, the two boron atoms act as Lewis acids and accept electron density from the gold atom into the vacant p orbitals to form the gold–boron bonds (Scheme 9.2).[8]

14
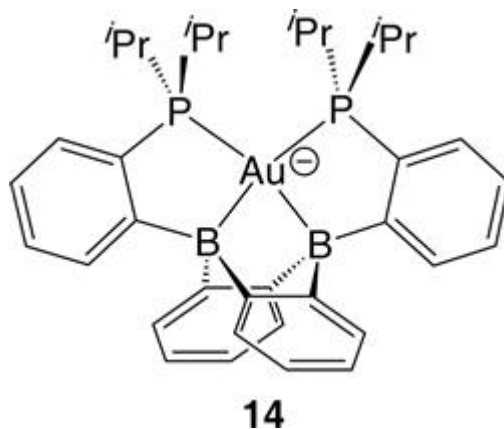
9.2.2 Properties of Boron–Metal Bonds and Structures of Boryl Complexes

Detailed theoretical studies have been carried out on the properties of the metal–boron bonds in iron and osmium boryl complexes.[9] Boryl ligands are stronger σ donors than alkyl groups and carbenes. This is due to the electropositive nature and higher energy of the atomic orbitals of boron. In addition, the M–B bond in boryl complexes is polarized in an $M(\delta^-)$–$B(\delta^+)$ fashion. Also, because of the high energy of the boron p orbital, although a π interaction exists between the metal and boron, it is much weaker in comparison to the metal–carbon π bond in carbene complexes (Figure 9.4). For example, in $[CpFe(CO)_2(Bcat)]$ (**1**) (cat = catecholate), the contributions of the σ and π interactions toward the iron–boron bond are 89% and 11%, respectively.[9a] These values differ considerably from those of the isoelectronic alkylidene complex $[Cp(CO)_2Fe=CH_2]^+$ (64% and 36%). However, when the substituents on boron are changed from catecholate to hydrogen atoms, which do not have π donating ability, the contribution of the metal-to-boron π back-bond increases to 16%. Metal-bound co-ligands also influence the contribution of the metal–boron π interaction. For example, phosphine-substituted $[CpFe(PH_3)_2(Bcat)]$ has a stronger iron–boron π interaction than **1**, and the contributions of σ and π bonds are 85% and 15%, respectively, because of the lack of π-acidic ligands competing with the boryl group. Thus, boryl ligands may be summarized as being strong σ donors and also weak π acceptors. Furthermore, it has been pointed out that electrostatic interaction also contributes about 50% to the metal–boron bond.
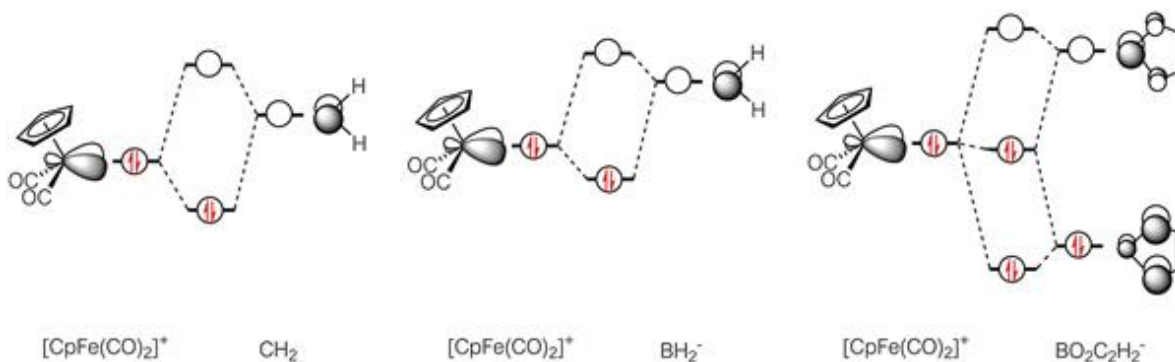
Figure 9.4   π Orbital interactions between iron fragment $[CpFe(CO)_2]^+$ and a carbene or boryl group.

Evidence for the strong σ-donating ability of boryl ligands can be seen in the *trans* influences in the structural data of palladium complexes **3**, **15**, and **16**. In complex **3**, the bond distance between the palladium atom and the phosphorus atom *trans* to the boryl group is 2.338(2) Å. This is longer than that between palladium and the phosphorus atom *trans* to the stannyl group (2.280(2) Å) and the separation between the palladium atom and the phosphorus atom *trans* to the alkyl group in compound **15** (2.2737(9) Å). Furthermore, comparing also the Pd–P bond distances in complex **16**, it is recognized that boryl groups possess a *trans* influence comparable to silyl groups, which are known as one of the strongest *trans* influencing ligands (Section 8.2.3) (Scheme 9.3).[2e,10]
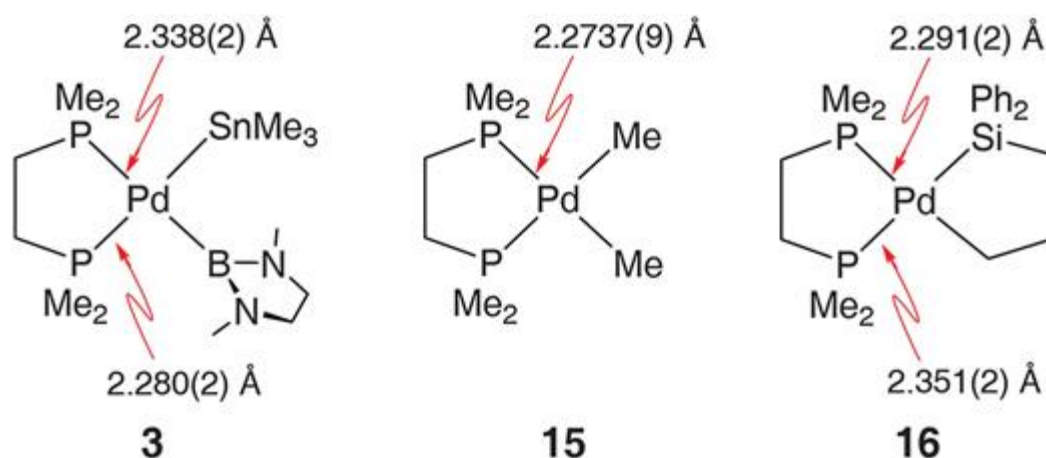
The Fe–B bond distance in **1**, 1.959(6) Å, is shorter than the sum of half the Fe–Fe separation in [CpFe(CO)$_2$]$_2$ (**17**) (2.531(2) Å) and half of the B–B interatomic distance in bis(catecholate)diboron (**18**) (1.678(3) Å), 2.105(3) Å.[2a] This is in contrast to the Fe–C bond distance in alkyl complex **19**, 2.069(10) Å, which roughly accords with the 2.04 Å value expected from the Fe–Fe interatomic distance of **17** and common C–C single bond distances (1.54 Å). Interestingly, in [(η^5-C$_5$Me$_4$Et)Fe(CO)$_2$(BH$_2$ · PMe$_3$)] (**20**), in which the boron p orbital is filled due to coordination by phosphine and cannot accept π-back-donated electron density, the Fe–B bond distance 2.195(4) Å is much longer than that in **1** and slightly longer than the value expected from the Fe–Fe and B–B separations of compound **17** and B$_2$H$_4$ · 2PMe$_3$**21** (2.14 Å).[11] These data clearly indicate that in **1**, the boryl group acts as a π acceptor and that multiple bond character exists between the iron and boron atoms (Figure 9.4) (Scheme 9.4).
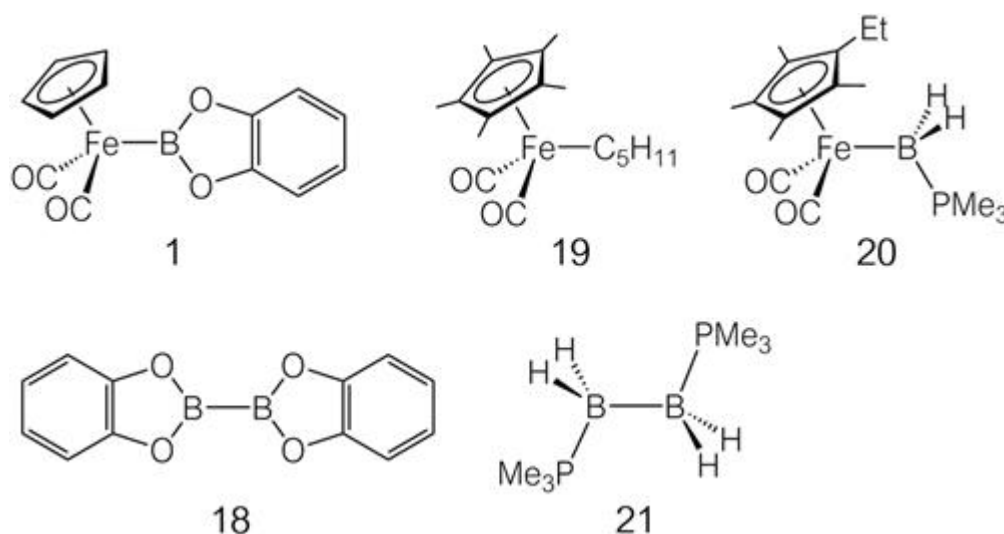
In the IR spectrum of **1**, the ν_{CO} absorption is observed at higher frequency relative to that of **20** because the electron density at the central metal is lowered due to back-donation from iron to the boryl group. On the other hand, the NMR spectra of **1** indicate that the boryl group rotates rapidly even at −90 °C. This is consistent with a weak π interaction. A theoretical study evaluated the barrier for the rotation of the catecholateboryl group to be about 4 kJ mol^{-1}. Even in phosphine-

incorporated [CpFe(PH$_3$)$_2$(Bcat)], it is only 8 kJ mol^{-1}. These values are far smaller than the rotation barrier of the carbene ligand measured for an alkylidene complex [Cp(dppe)Fe=CH$_2$]$^+$ (dppe = PPh$_2$CH$_2$CH$_2$PPh$_2$), 45.1 kJ mol^{-1} (see Chapter 5).

9.2.3 Reactivity of Boryl Complexes

Boryl complexes show remarkable reactivity in contrast to the reactivities of alkyl and silyl complexes, due to the Lewis acidity and electropositive nature of boron. Hartwig and coworkers found that catecholateboryl tungsten complex **22** activates the C–H bond of alkanes under photolytic conditions to borylate the terminal position (eqn (9.12)). Because the resulting alkylboronate esters (borylalkanes) can be converted to various organic compounds including alcohols and carboxylic acids, this reaction is noteworthy as a direct functionalization method for alkanes. A DFT study clarified that this reaction proceeds through σ bond metathesis in the metal coordination sphere. During the course of the process, the vacant p orbital on boron plays an important role (Figure 9.5).[12]
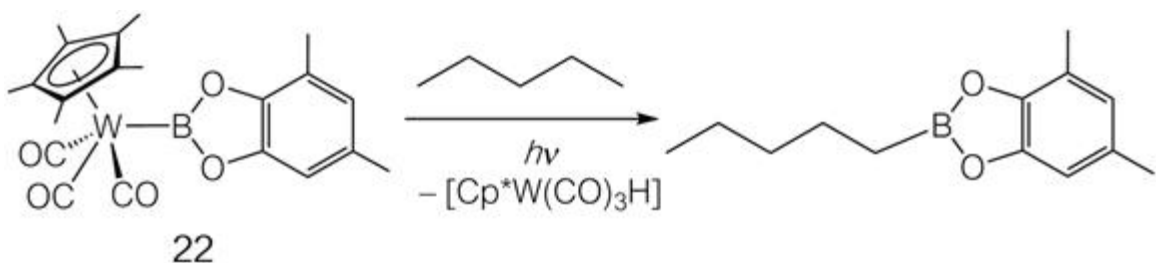
$$(9.12)$$
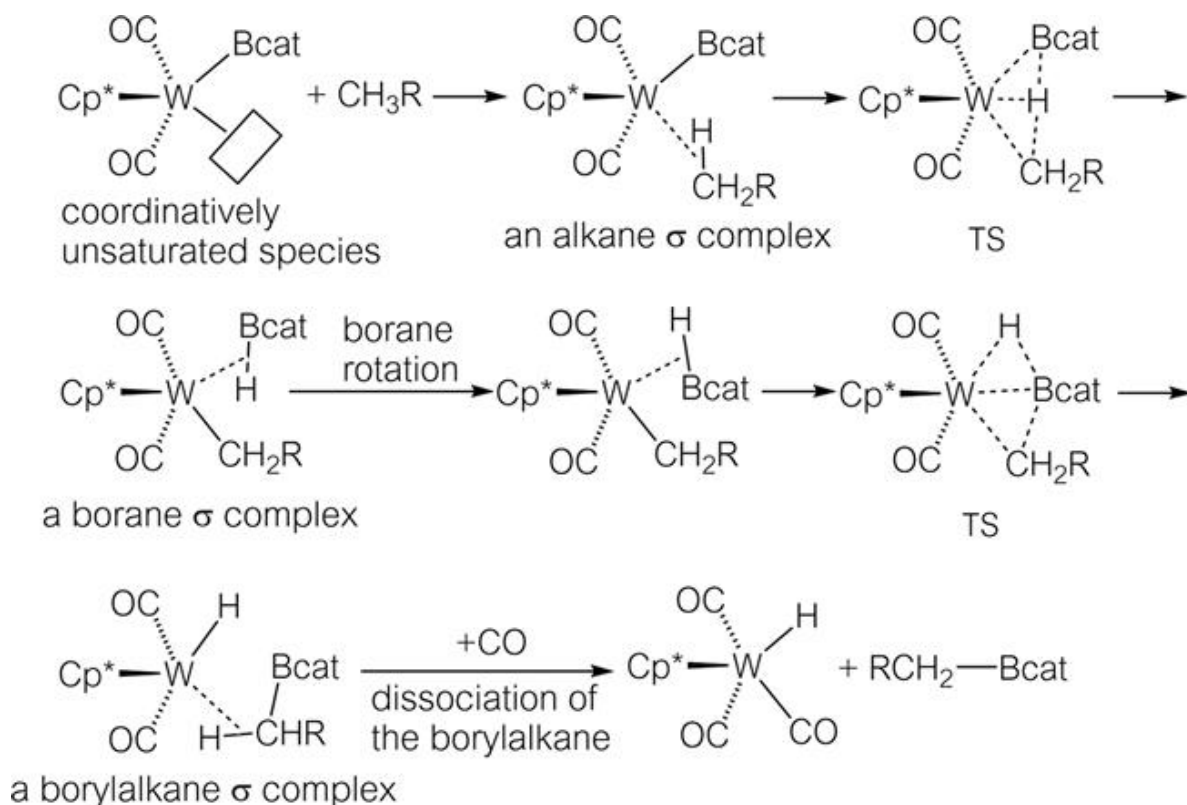
Figure 9.5 Mechanism of regioselective borylation of alkanes mediated by boryl tungsten complex **22**.

Hartwig then succeeded in the catalytic regioselective borylation of alkanes using Re, Ru, and Rh complexes (eqn (9.13)). In these reactions, boryl complexes are thought to be key intermediates. Indeed, in the reaction using a rhodium complex, the precatalyst $[Cp*Rh(\eta^4\text{-}C_6Me_6)]$ reacts with borane faster than with alkanes to produce boryl complexes **23** and **24**, and these react with alkanes on heating to give alkylboronate esters. Activation of inert C–H bonds using metal complexes is an important subject in coordination chemistry and these epoch-making boron-based reactions achieve activation and functionalization of alkanes simultaneously and catalytically (Scheme 9.5).[4c,13]

n-Octane (solvent) (9.13)

catalyst = [Cp*Re(CO)$_3$], [Cp*RuCl$_2$]$_2$, [Cp*Rh(η^4-C$_6$Me$_6$)]

23   24
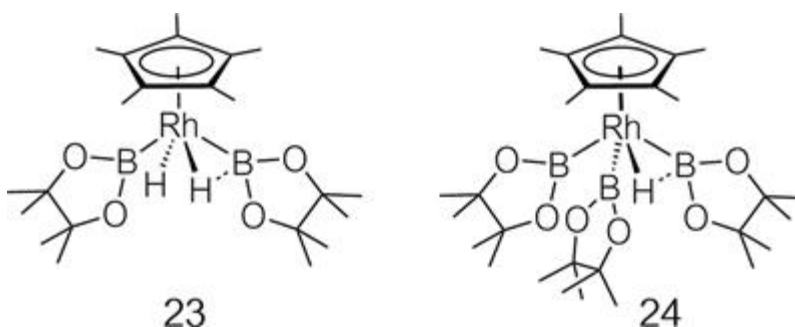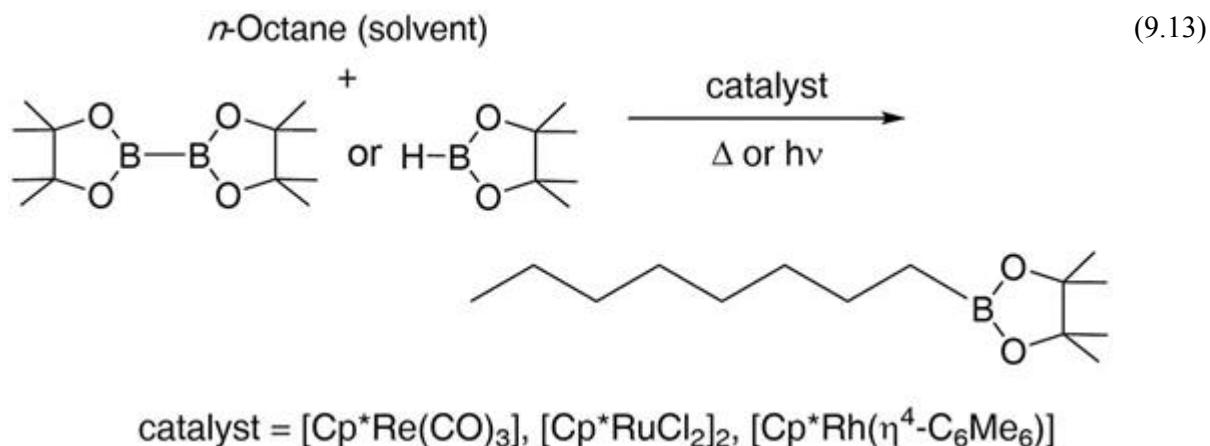
Catalytic hydroboration and diboration of olefins and related compounds are important reactions of metal boryl complexes and have attracted much attention. These reactions were discovered in the 1990s and prompted the rapid development of the chemistry of boryl complexes. Metal-catalyzed hydroboration is very important in synthetic chemistry because the regioselectivity is reversed from non-catalytic reactions (Markovnikov-type hydroboration) and olefins with a functional group (such as a carbonyl group) can be used as substrates.

Figure 9.6 shows the reaction mechanism of the hydroboration of olefins using Wilkinson's catalyst, based on the calculations of Morokuma and coworkers. The catalytic cycle includes:

- Oxidative addition of B–H to the central metal
- Coordination of the olefin
- Olefin insertion into the Rh–B bond
- Reductive elimination of the alkylborane
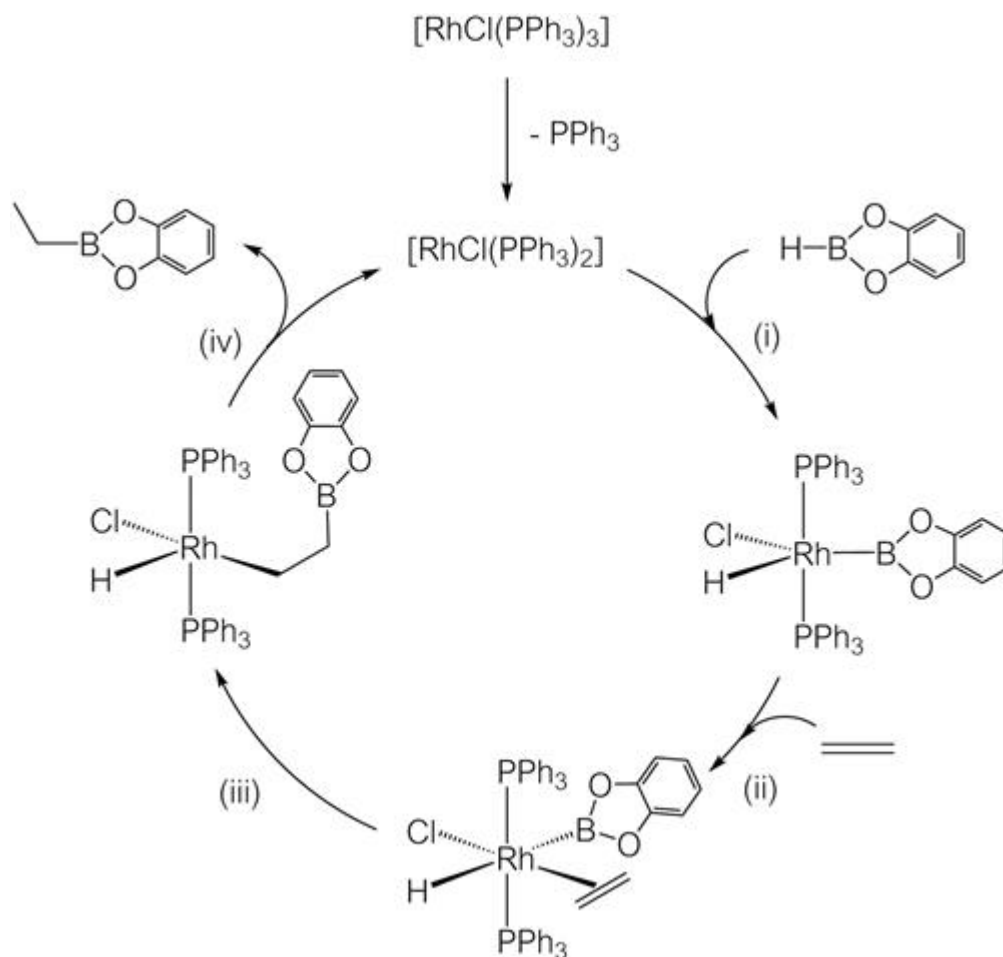
Figure 9.6　Mechanism of olefin hydroboration catalyzed by Wilkinson's complex.

In the reaction pathway, the key step is the olefin insertion into the Rh–B bond. The activation barrier for this step is quite low because at the transition state the vacant p orbital of the boryl group overlaps with the π electron cloud of the olefin. This mechanism is closely related to "the modified Chalk–Harrod mechanism" of metal-catalyzed hydrosilation reactions (Section 8.2.4).[14a]

If diboron compounds, possessing a B–B bond instead of a B–H bond, are used in the reaction with unsaturated hydrocarbons, diboration proceeds *via* a similar mechanism to the hydroboration. Furthermore, when silylboranes and stannylboranes are employed, addition of the corresponding B–Si and B–Sn bonds takes place. An example of silaboration is given in Figure 9.7. Key intermediates in this process are the boryl(silyl) complexes, **25** and **26**, which form on oxidative addition of the

B–Si bond to the metal center. As shown by mechanistic studies, the allene inserts into the Pd–B bond instead of the Pd–Si bond. This is consistent with the facile olefin insertion into the metal–boron bond mentioned above. Suginome *et al.* have shown that silylboranes add to various unsaturated organic compounds with high regioselectivity and they are developing extensive applications of metal-catalyzed silaboration in organic syntheses.[14b]
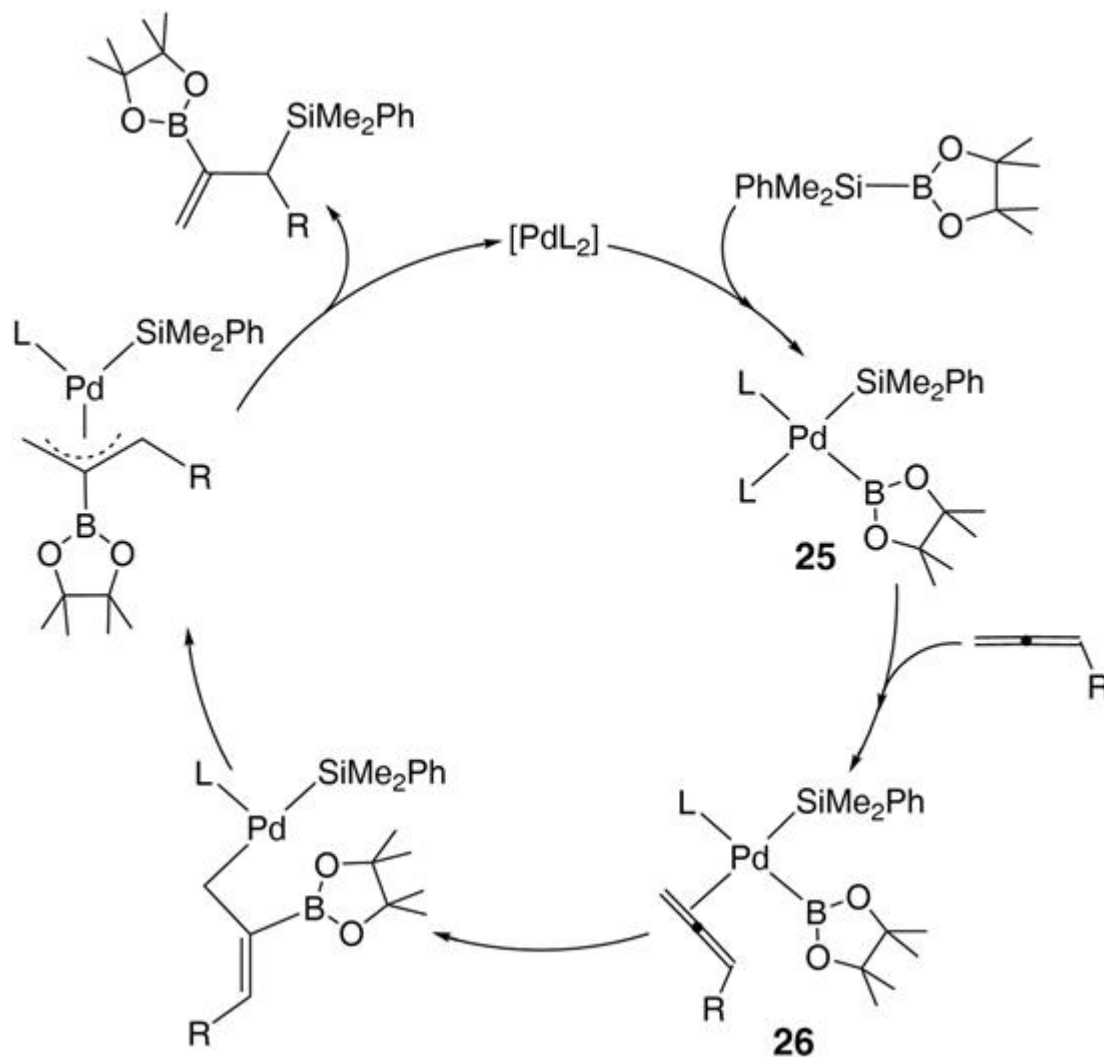
Figure 9.7   Addition of a silylborane to allene *via* a boryl(silyl)palladium complex.

As with complexes bearing a linkage between the metal and other main group elements, boryl complexes show a variety of reactions at the metal center or at the boryl group. Some notable reactions are described below.

When parent boryl–manganese complex **27** is treated with a Brönsted acid, the metal–boron bond is protonated to give a cationic borane σ complex **28** (eqn (9.14)). Compound **28** is thermally unstable and decomposes yielding a hydride complex [MnH(CO)$_4$(PMe$_2$Ph)]. In this process, the metal-coordinated BH bond undergoes heterolytic cleavage.[15]

(9.14)
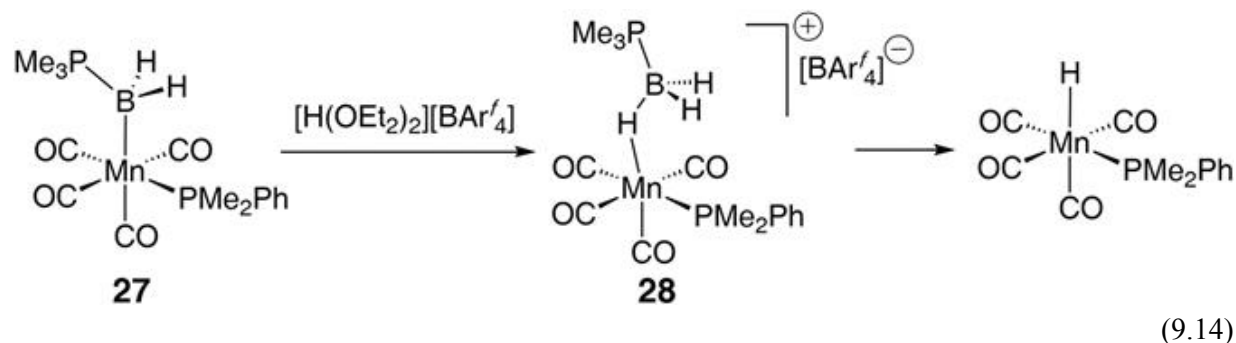
The reaction between bromoboryl–platinum complex **2** and Na[BAr$^f_4$] (Ar^f = 3,5-(CF$_3$)$_2$C$_6$H$_3$) results in bromide abstraction (Figure 9.8). When the substituent is a mesityl group, Br$^-$ is abstracted from the boryl ligand to produce a borylene complex **29**, containing a two-coordinate boron atom (borylene complexes will be discussed later). In the case of the ferrocenylboryl complex, Br$^-$ is abstracted from the metal center, and T-shaped cationic boryl complex **30** is obtained. Compound **30** undergoes complexation by a Lewis base, which causes bromide migration from boron to platinum, affording base-stabilized borylene complex **31**. This is an interesting system, where similar bromide abstractions occur on both the metal center and the boryl group.[16]
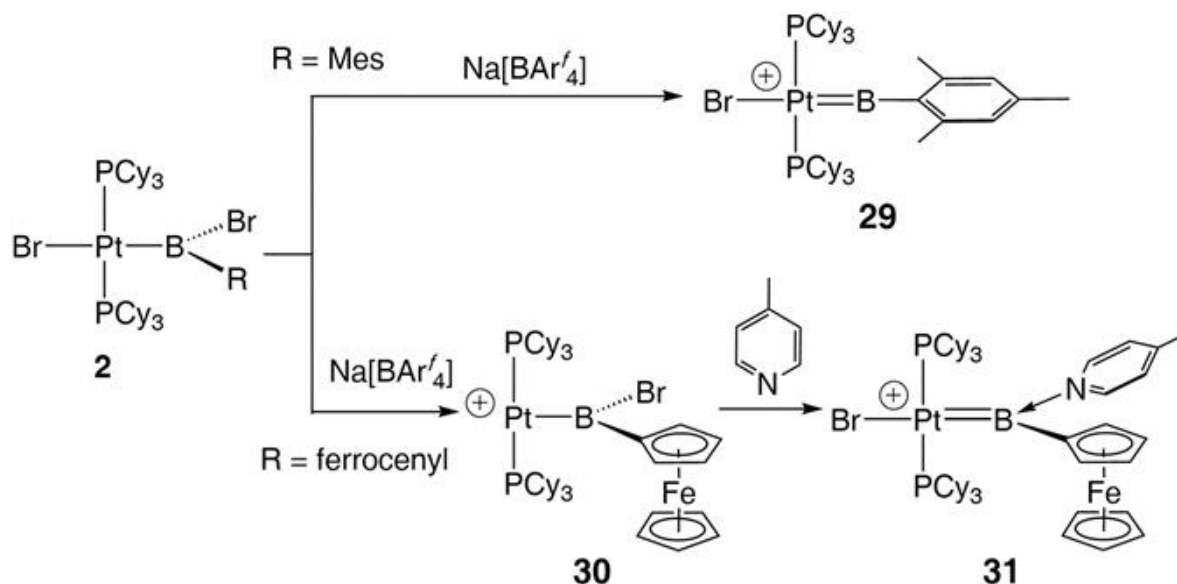
Figure 9.8 Halide abstraction in platinum boryl complexes **2**.

As shown in eqn (9.4), platinum complexes **2** are prepared by oxidative addition of the corresponding dibromoborane $RBBr_2$ (R = Mes, ferrocenyl). If $(Me_3Si)_2NBBr_2$ is used as a dibromoborane, however, the structurally interesting iminoboryl complex **32a** is generated on elimination of Me_3SiBr.[17a] The B–N bond of **32a** is short (1.260(4) Å), indicating the existence of a multiple bond. In addition, use of $Me_3SiOBBr_2$ afforded the first oxoboryl complex **32b**, with the BO^- ligand coordinated to the metal through the boron atom (Figure 9.9).[17b] The BO^- ligand is the boron analogue of carbonyl.
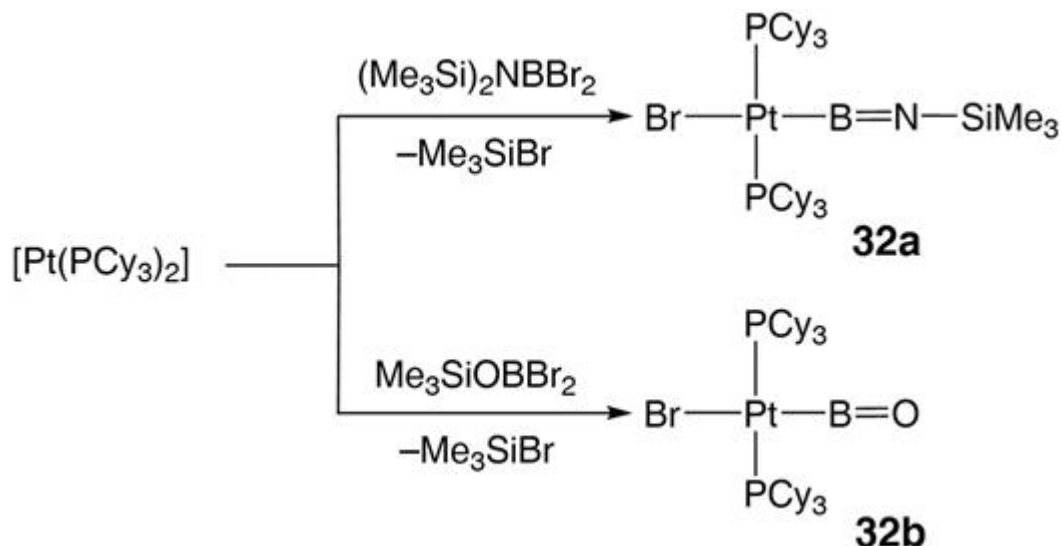
Figure 9.9   Formation of platinum iminoboryl complex **32a**, and oxoboryl complex **32b**.

Furthermore, Braunschweig and coworkers prepared complex **33**, in which the $B_2I_4^{2-}$ ligand is isoelectronic with olefins (eqn (9.15)). DFT calculations show a coordinated olefin-like interaction with donation from, and back-donation to, the $B_2I_4^{2-}$ ligand.[18]
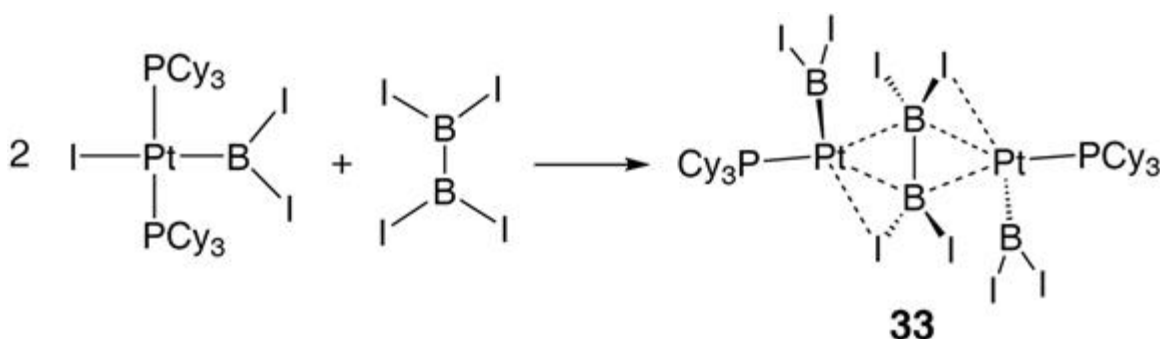
$$(9.15)$$

9.2.4   Borylene Complexes

Borylene complexes include a monovalent boron species BR as a ligand and are of interest for their structure and bonding. They are classified into terminal and bridging borylene complexes.[19]

In terminal borylene complexes, the presence of a double bond is inferred between the central metal and boron atom. Typical synthetic routes to these compounds are halide abstraction from haloboryl complexes and salt

elimination reactions between divalent metal anions and dihaloboranes (eqn (9.16) and (9.17)).

(9.16)

$$Na_2[M(CO)_5] + (Me_3Si)_2NBBr_2 \xrightarrow{-2\ NaBr_2}$$

(9.17)

35 (M = Cr), **36** (M = W)
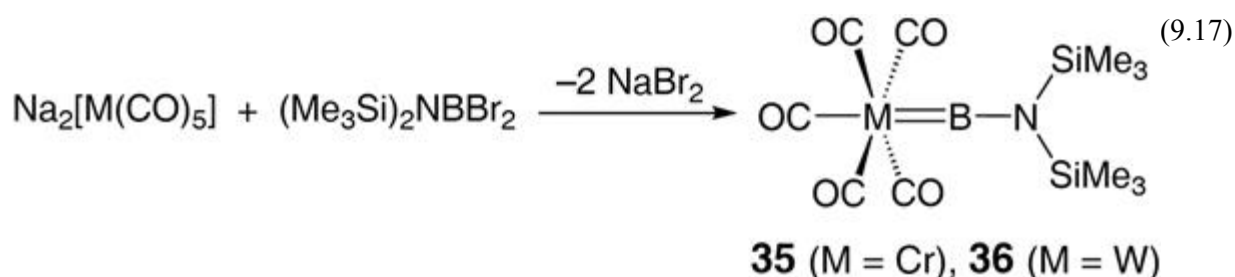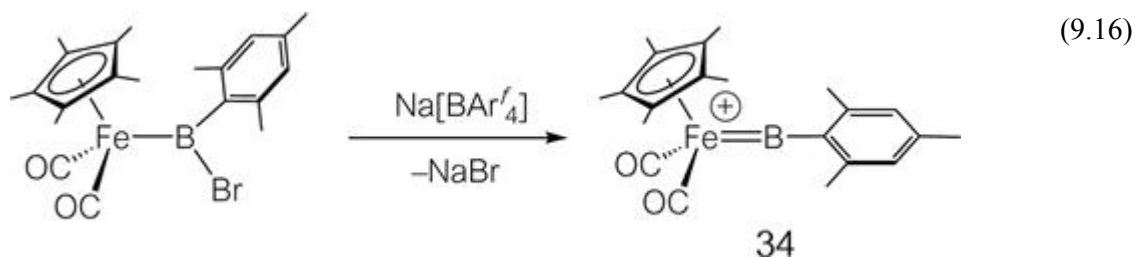
In the cationic borylene complex **34**, the boron atom adopts a linear two-coordinate structure. The Fe–B bond distance 1.792(8) Å is shorter than that in the precursor chloroboryl complex [Cp*Fe(CO)$_2$(BClMes)] (1.985(2) Å), indicating multiple bond character. DFT calculations also show the existence of a π bond between the iron HOMO and boron p_x orbital (Figure 9.10).[20] The boron p_y orbital interacts with the *ipso* carbon atom of the mesityl group rather than with the iron fragment.
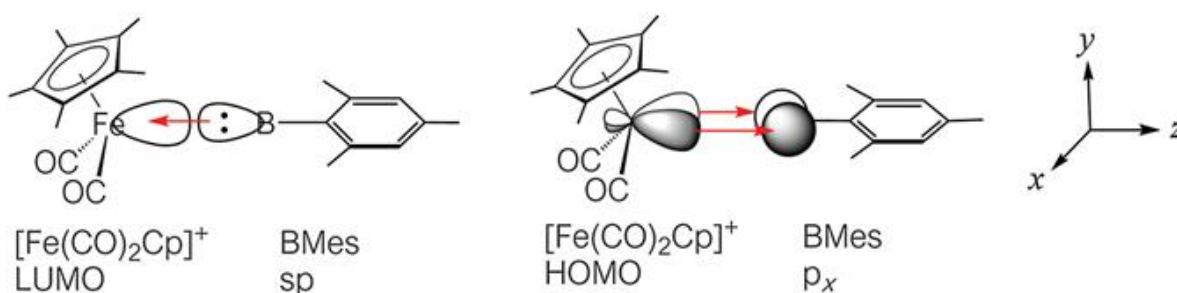
Figure 9.10   Orbital interactions in iron borylene complex **34**.

In the borylene chromium complex **35**, the Cr–B bond distance is 1.996(6) Å, while in silyl-substituted borylene complex **37**, the Cr–B bond is even shorter (1.878(10) Å) because stronger π-back-donation occurs into the boron p orbital since it bears no π donating substituent. The Cr–B bond

distance in **38** is 1.975(2) Å, which corresponds to an intermediate value between those of **35** and **37**, suggesting the presence of weak π–back-donation from the iron fragment to the boron p orbital (Scheme 9.6).[21]

37   38
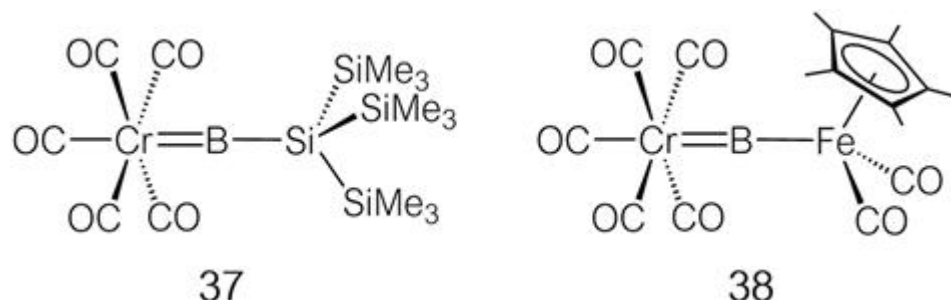
Photoirradiation of **35** results in the dissociation of the borylene ligand. When photolysis is performed in the presence of alkynes, the liberated borylene is captured by the alkyne to produce 2π electron aromatic compounds, boracyclopropene derivatives (eqn (9.18)).

(9.18)

(R = Et, Ph, SiMe₃)
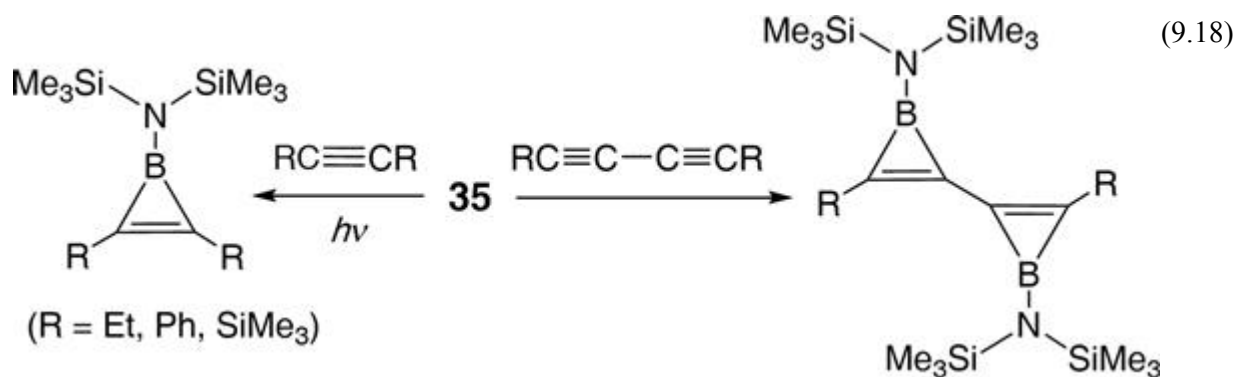
The photo-generated borylene may also coordinate to other metal complexes to afford new borylene species (eqn (9.19)).[21e]

(9.19)

35
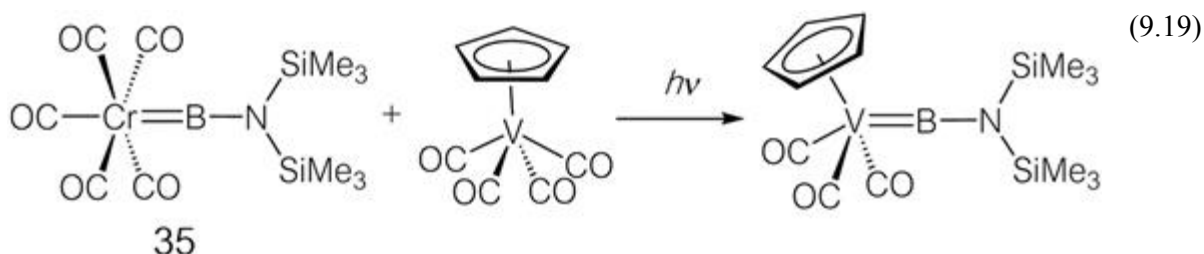
The aminoborylene ligand: B–N(SiMe₃)₂ is isoelectronic with vinylidene: C=CH₂, and with carbonyl. Accordingly, the possibility that

borylene may be a good ligand in transition metal complexes has long been discussed and has been the subject of a number of theoretical studies.[20b,22]

Aminoborylene:B–NH$_2$ (**39**) has a singlet ground state. Its HOMO is the sp hybrid orbital accommodating the electron lone pair that extends from the boron atom, while the LUMO is a boron p orbital lying in the molecular plane. The LUMO + 1 is a BN π* orbital having a large coefficient on boron and is orthogonal to the LUMO (Figure 9.11). The shapes of these orbitals are similar to those of the HOMO and the doubly degenerate LUMO of carbon monoxide. This suggests that the borylene can act as a σ donor/π acceptor. Since the boron atomic orbitals are higher in energy than carbon, the HOMO in borylene **39** is higher in energy than that of CO, and thus it has greater σ donor ability than carbonyl. At the same time, because the LUMO and LUMO + 1 are nearly the same in energy as the π* orbitals of CO, the π acceptor ability of borylene should be similar to that of carbonyl. In fact, the metal–borylene bond dissociation energy of [(OC)$_4$Fe=BNH$_2$] has been evaluated as 367 kJ mol^{-1}, which is greater than the metal–carbonyl bond energy of [Fe(CO)$_5$], 203 kJ mol^{-1}. On the other hand, imbalance between the strong σ-donation and weak π-back-donation and polarization of the B–N bond lowers the kinetic stability of the borylene ligand toward nucleophilic attack. To resolve this problem, steric protection is needed to stabilize borylene complexes.
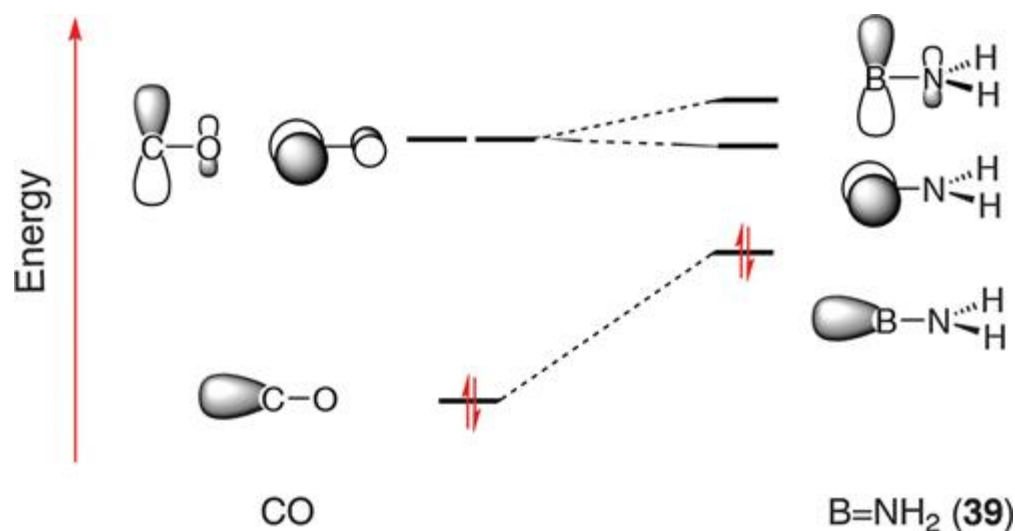
Figure 9.11 Frontier orbitals of carbon monoxide and aminoborylene.

Aldridge and Frenking investigated the nature of metal–borylene bonds in detail, and revealed that this type of bonding is strongly polarized $M(\delta^-)\cdots B(\delta^+)$. They also pointed out the importance of the contribution of electrostatic interactions in metal–borylene bonds. According to their calculations, the covalent contribution to the metal–boron interaction in $[(\eta^5\text{-}C_5R_5)L_2Fe=BR']^+$ (**40**, R = H, Me; L = CO, PMe$_3$) and $[(OC)_4Fe=BN(SiH_3)_2]$ (**41**) is about 40%, with 60% deriving from electrostatic interaction. The contribution of the π bond towards the covalent interaction is around 30–45%. In Aldridge's calculations, the Fe–B Mayer bond orders are 1.24–1.68 for compounds **40**, in accordance with the assumption of "double bonds". In contrast, because of the large electrostatic contribution, the Fe–B Wiberg bond order in **41** was evaluated as 0.65 by Frenking, despite the presence of a π bond. This value is smaller than those for carbene complexes (around 1) and still smaller in comparison to the values calculated for boryl complexes (about 1). However, the same calculation gives a value of 0.62 for the bond order of the iron–carbonyl linkage, which is considered to have multiple bond character. Thus, to precisely understand the nature of transition metal–borylene bonds, further investigation is required, including consideration of the methodology itself (Scheme 9.7).

L = CO, PMe$_3$; R = H, Me;
R' = Mes, H, NMe$_2$, F
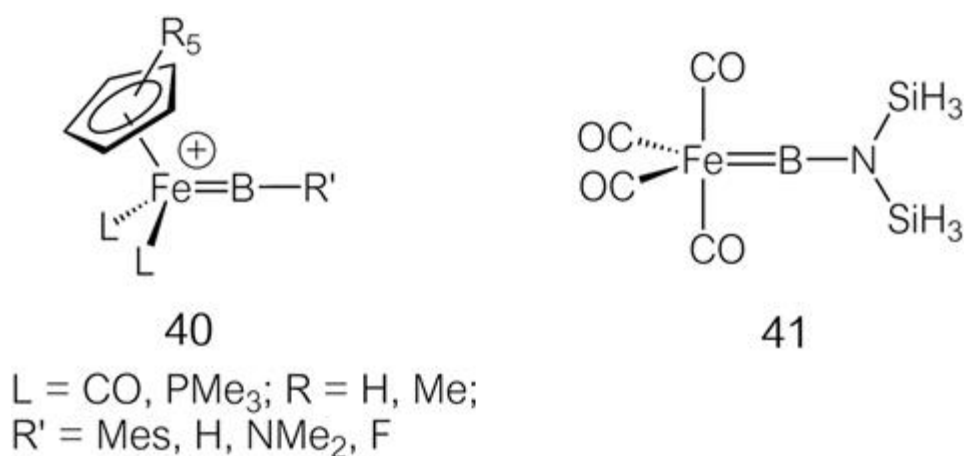
As shown by theoretical calculations, the boron atom of borylene ligands shows enhanced susceptibility towards nucleophilic attack and undergoes coordination by a Lewis base into the p orbital, becoming three-coordinate. One example is the formation of the base-coordinated borylene–platinum

complex, shown in Figure 9.8. In addition, an aminoborylene derivative **42** is converted to an imine-stabilized alkoxyborylene complex **43** on coordination by benzophenone (eqn (9.20)).[23] Such behavior (coordination of a Lewis base) is also observed for silylene complexes.

$$(9.20)$$
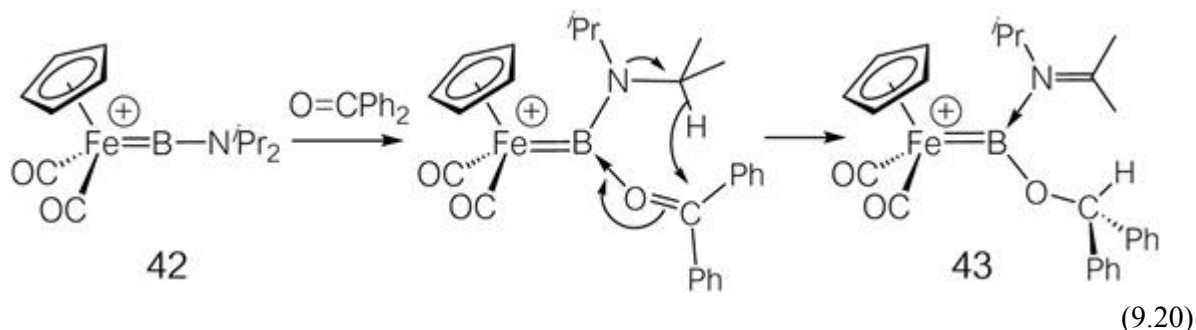
The first example of a bridging borylene complex was manganese dimer **44**, which was synthesized by a salt-elimination reaction using a dichlorodiborane derivative (eqn (9.21)).

$$(9.21)$$
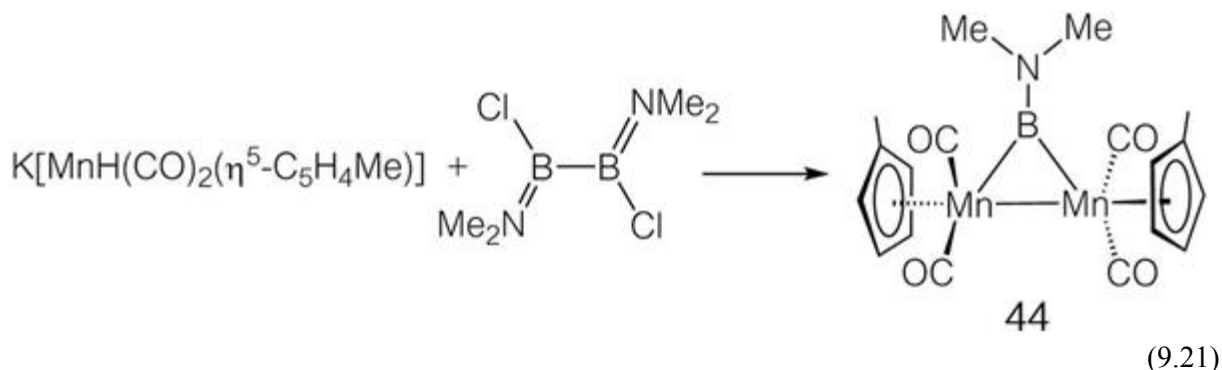
The dimethylamino group on the borylene ligand of **44** can be converted to alkoxy, halogen, and alkyl groups. Chloroborylene derivative **45** undergoes photolysis to produce an electron-deficient metallaborane cluster **46**, probably through the generation and subsequent dimerization of a mononuclear borylene complex (Figure 9.12). The *tert*-butyl derivative **47** is converted to the isolable terminal borylene complex **48** through the action of phosphine. Thus, in this system, the stability of terminal borylene complexes is controlled by the bulkiness of the borylene substituents.
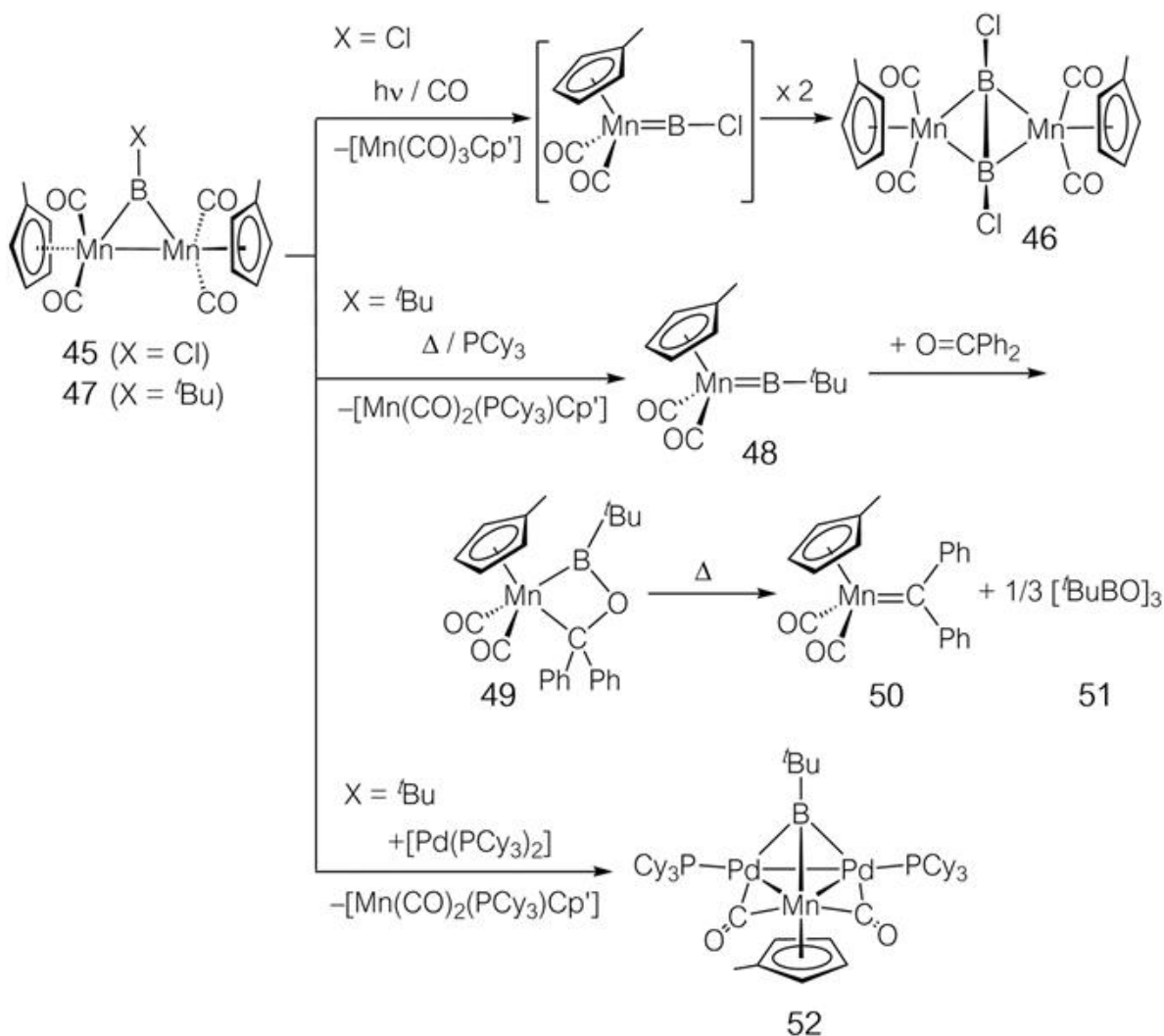
Figure 9.12 Reactivity of bridging and terminal borylene manganese complexes.

Interestingly, the metal–boron double bond of the alkylborylene complex **48** reacts with benzophenone by [2 + 2] cycloaddition, giving **49**. This product decomposes into a carbene complex **50** and a boroxine **51**. This process can be regarded as a metathesis between the Mn=B and C=O double bonds. The formation of a μ³-borylene complex **52** is also notable as a reaction of **47**. This reaction may also be considered as the addition of Pd fragments to the mononuclear species **48**.[24]

Treatment of the terminal borylene complex **35** with [M(PCy₃)₂] (M = Pd, Pt) affords dinuclear complex **53** (eqn (9.22)). In **53** (M = Pd), the borylene ligand bridges the two metal atoms, inclining towards palladium

rather than chromium. Braunschweig described this compound as a semi-bridging borylene complex.[25a]

$$\underset{\textbf{35}}{\text{(OC)}_4\text{Cr}=\text{B}-\text{N(SiMe}_3)_2} + [\text{M(PCy}_3)_2] \longrightarrow \underset{\textbf{53 (M = Pd,Pt)}}{} \tag{9.22}$$
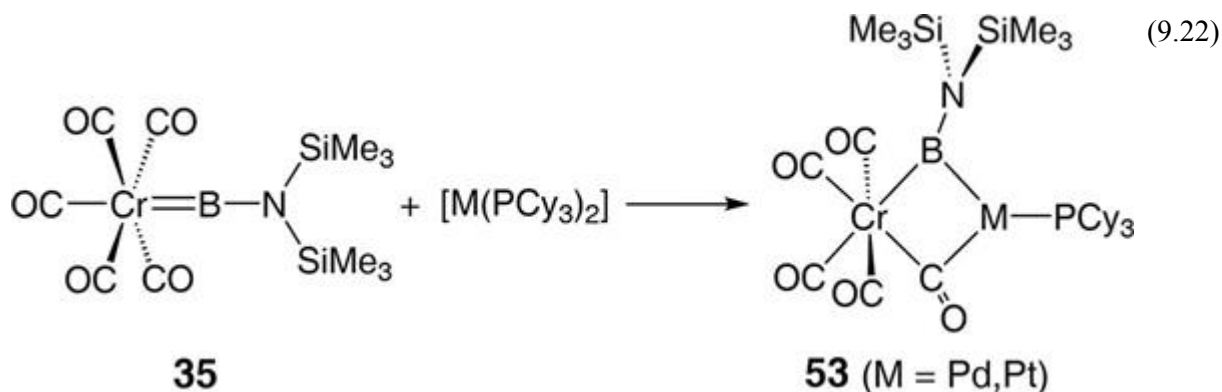
In the dinuclear manganese complex **44**, the aminoborylene ligand BNMe$_2$ is almost coplanar with the BMn$_2$ three-membered ring. This structure can be understood expediently by considering the π interaction between the p orbital of the sp^2 (three-coordinate) boron atom and the electron lone pair on the amino group. In contrast, in **53** the BN(SiMe$_3$)$_2$ ligand plane is orthogonal to the Cr–B–Pd–C four-membered ring. This strongly suggests the occurrence of back-donation from the electron-rich palladium atom into the B–N π^* orbital. This interaction resembles the back-donation into the CO π^* orbital of the semi-bridging carbonyl ligand in this complex, exemplifying an interesting ligand mode similarity between aminoborylene and carbonyl.

The dibromoboryl complex **54** oxidatively adds to a zero valent platinum species, preserving a B–Br bond, to give bridging borylene complex **55**, which further reacts with [Pd(PCy$_3$)$_2$] to produce trinuclear complex **56** (eqn (9.23)). The boron atom in **56** bridges three metal atoms and adopts an extremely peculiar T-shaped planar geometry. For **56**, DFT calculations have shown a bonding model in which the boron atom is sp hybridized, bridging the iron and platinum atoms, and its p orbital is coordinated by the electron-rich palladium atom.[25b]

(9.23)

(i) [Pt(PCy$_3$)$_2$], (ii) [Pd(PCy$_3$)$_2$]
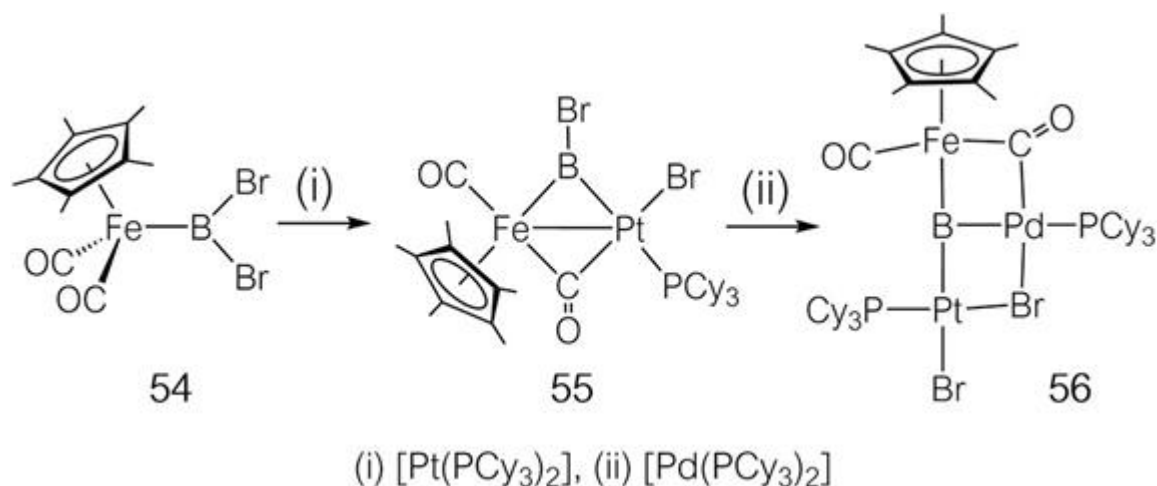
9.2.5 Metal-catalyzed Dehydrocoupling Reactions of Amine–Boranes

Recently, metal-catalyzed dehydrogenation reactions of amine–borane adducts have attracted much attention. Primary and secondary amine–boranes and ammonia–borane have acidic and hydridic protons on the nitrogen and boron atoms, respectively. These protons are readily released as H$_2$ by the catalytic action of metal complexes (Figure 9.13). Because boron–nitrogen covalent bonds are formed during the dehydrogenation (the products are monomeric, dimeric and polymeric aminoboranes, and borazine derivatives), this reaction is called "dehydrocoupling".
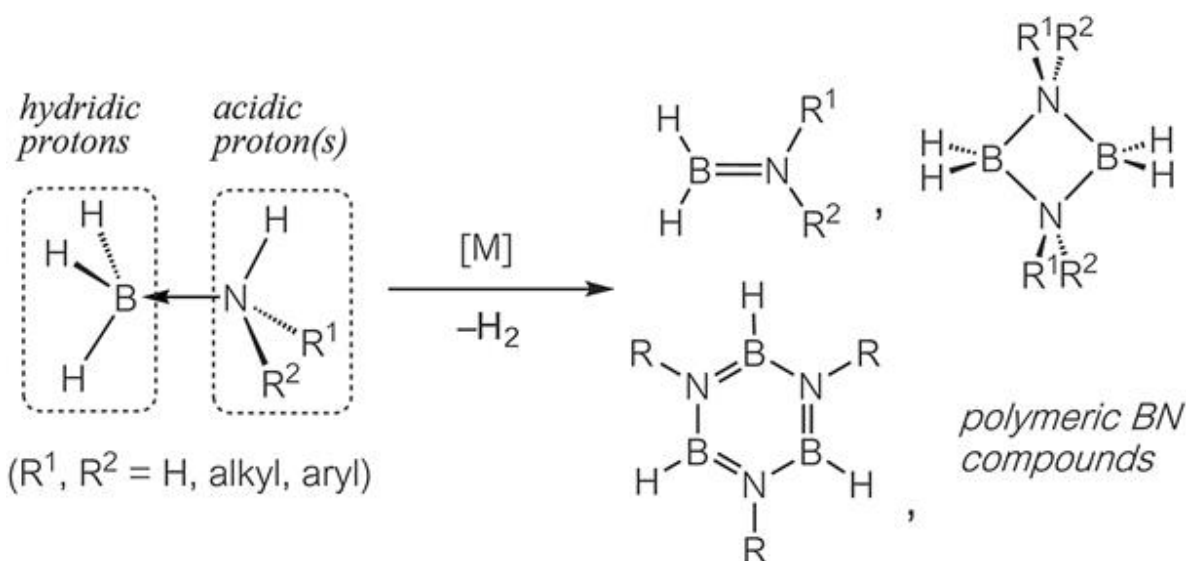
Figure 9.13   Dehydrocoupling of amine–borane adducts.

This research area is now rapidly expanding towards the utilization of amine–boranes as chemical hydrogen storage materials. Since simple amine–boranes (in particular $BH_3 \cdot NH_3$) have a large hydrogen content, they are promising candidates for hydrogen storage materials. Investigation of catalytic dehydrocoupling reactions can thus influence the development of new energy systems such as fuel cells. There are now reports of catalysis by a number of different metals.[26]

In many systems, a borane σ complex acts as a key intermediate in catalytic dehydrocoupling. Figure 9.14 shows the mechanism of the iridium-catalyzed dehydrogenation of ammonia–borane derived from computations by Musgrave.[27] Ammonia–borane coordinates to the iridium atom through a BH hydrogen to generate the σ complex **57**, and then proceeding *via* TS1, the coordinated BH is cleaved concurrently with an NH bond. During this process, a hydride ligand works as an NH proton acceptor. After the BH and NH bond activations, the generated Ir(v) hydride releases H_2. In Shimoi's chromium-catalyzed system, σ complex **58** undergoes stepwise activation of the metal-interacted NH and BH bonds to afford a dihydrogen species and an aminoborane (Figure 9.15).[28] In a related system, Manners has proposed metal nanoparticles generated *in situ* as the active catalyst for the rhodium-catalyzed dehydrocoupling of amine–boranes.[29]
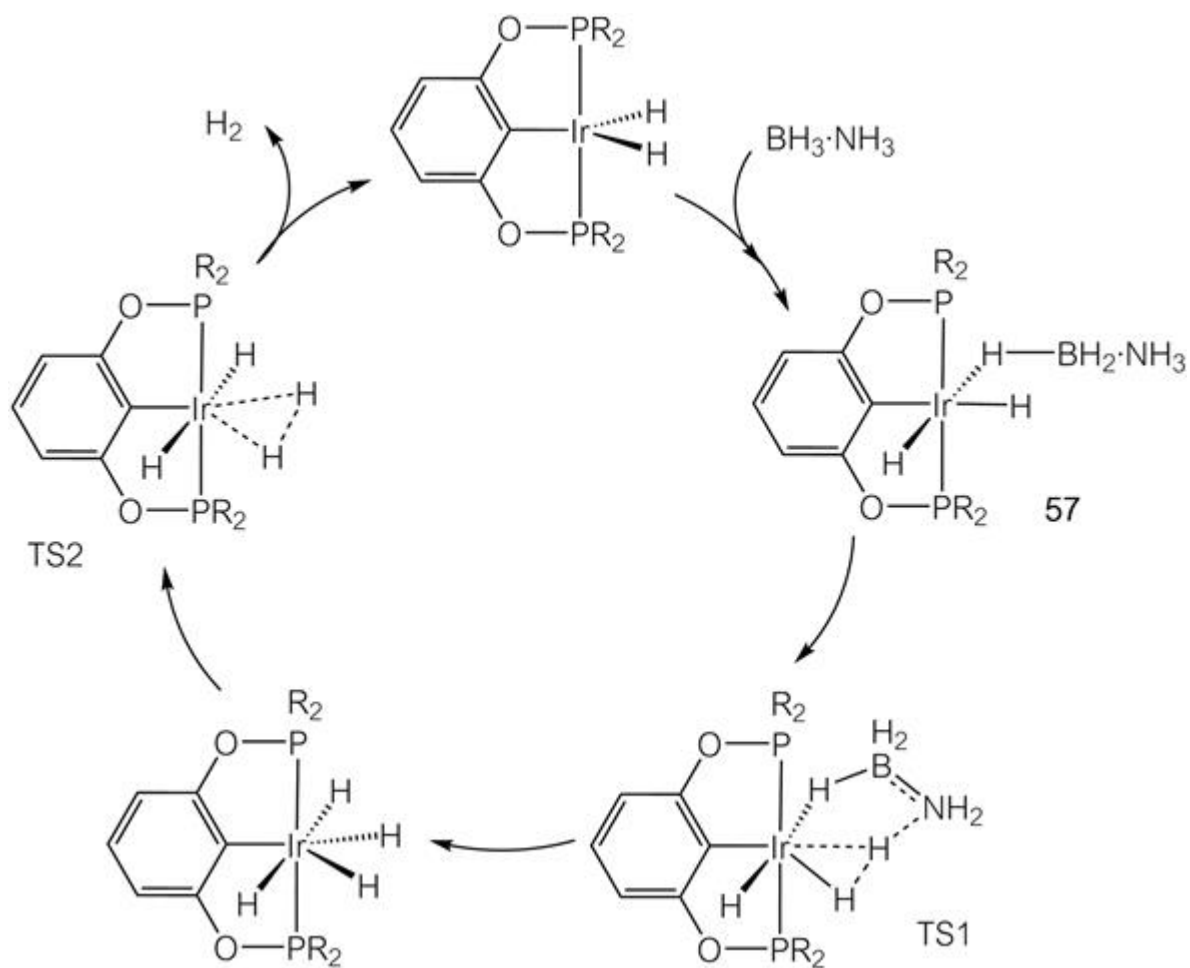
Figure 9.14 Reaction pathway of iridium-catalyzed dehydrocoupling of ammonia–borane.
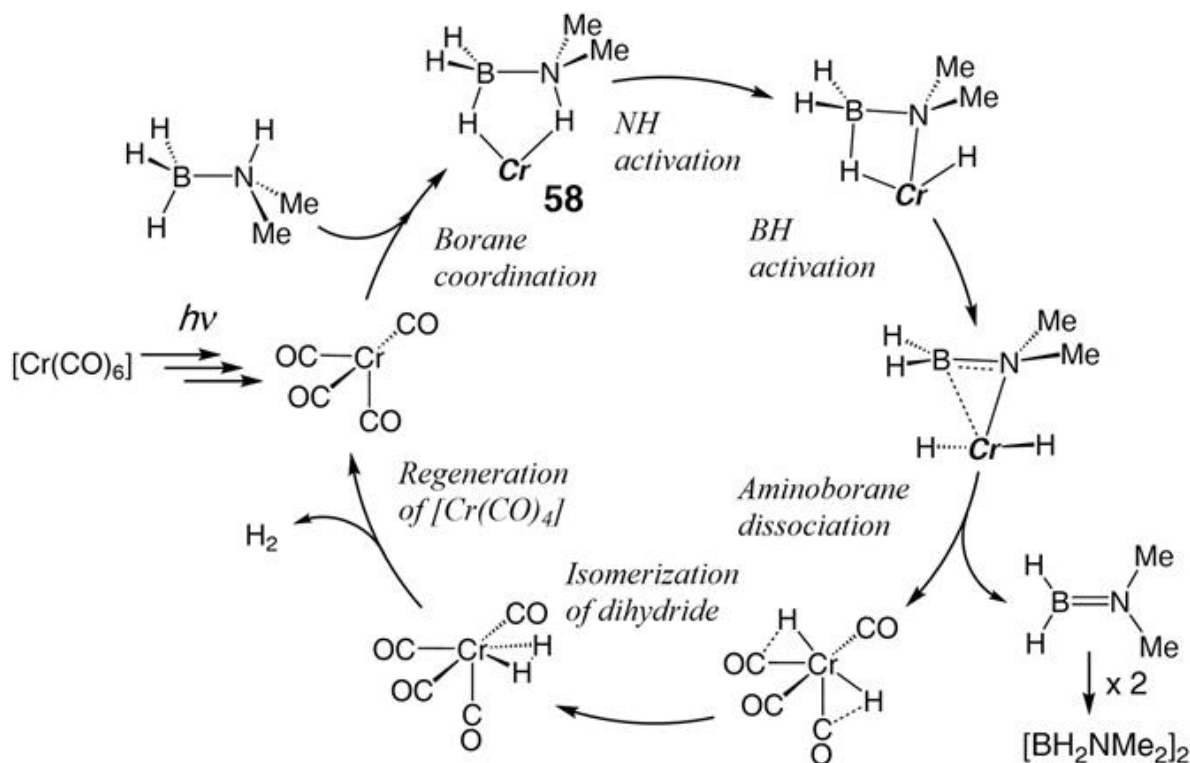
Figure 9.15 Reaction mechanism of chromium-catalyzed dehydrocoupling of dimethylamine–borane. **Cr=Cr(CO)₄**.

Secondary and primary amine–boranes and ammonia–borane can be regarded as containing one, two and three equivalents of H_2, respectively. A nickel–heterocyclic carbene complex is a highly efficient catalyst for the dehydrocoupling of ammonia–borane (eqn (9.24)). In this system, the amount of H_2 released exceeds 2.5 equivalents per equivalent of ammonia–borane.[30]

(9.24)
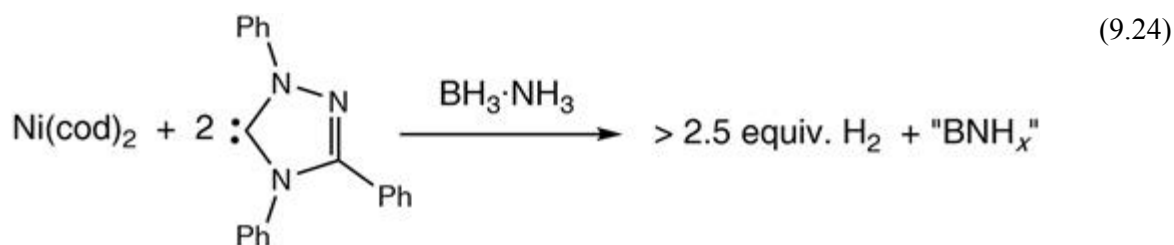
9.2.6   Summary

The chemistry of boron–metal complexes is a relatively new research area, with significant activity starting around the 1990s. Nonetheless, this area

has developed into an active and fruitful research field that can be compared with the preceding investigations of metal complexes of Group 14 elements.

Metal–boron bonds are characterized by the electropositive nature and high energy of the atomic orbitals of boron, as well as its vacant p orbitals. These characteristics result in novel structures for the newly produced complexes and unusually high reactivity, as seen, for example, in the functionalization of organic compounds.

9.3 Transition Metal Complexes with Aluminum, Gallium, Indium and Thallium Coordination

The chemistry of metal–boron complexes was discussed in Section 9.2 above. This section covers complexes with heavier Group 13 element-metal bonding, *i.e.* M-Al, -Ga, -In and -Tl bonds. The properties of the heavier Group 13 elements differ significantly from those of boron. For example, boron is non-metallic while aluminum and the other heavier elements are all metallic. The heavier Group 13 elements have relatively low electronegativities (χ), and the values for B and H are comparable. The chemistry of transition metal complexes with heavier Group 13 element-metal bonding is thus significantly different from that in boron–metal complexes.

9.3.1 Brief History of the Synthesis of M–E Complexes (M = transition metal, E = Al, Ga, In, and Ta)

The chemistry of M–E complexes emerged in the 1940s. Since then, it has expanded continuously, but it is still relatively undeveloped compared to the chemistry of M–C bond-containing complexes. Group 13 elements have three valence electrons, so they can form EM_3-type complexes upon bonding with three metal fragments. The first complex with M–E bonding, $[In\{Co(CO)_4\}_3]$ (**58**), was reported by Hieber *et al.* in 1942 (eqn (9.25)).[31] This complex was synthesized by the reaction of cobalt carbonyl $[Co_2(CO)_8]$ and indium under a carbon monoxide atmosphere. Unfortunately, crystal structure analysis was not carried out at the time and detailed structural information, especially regarding the existence of direct M–In bonds, remained uncertain for another 30 years. In 1973, Robinson *et al.* prepared the same complex *via* a different route, namely the reaction of

$Hg[Co(CO)_4]_2$ with In/Hg, and crystallographically confirmed the structure depicted in eqn (9.25), *i.e.* three Co–In bonds in a trigonal planar arrangement.[32]

$$\text{Co}_2(\text{CO})_8 \ + \ \text{In powder} \xrightarrow{\text{CO 200 atm, 200 °C}} \tag{9.25}$$

58
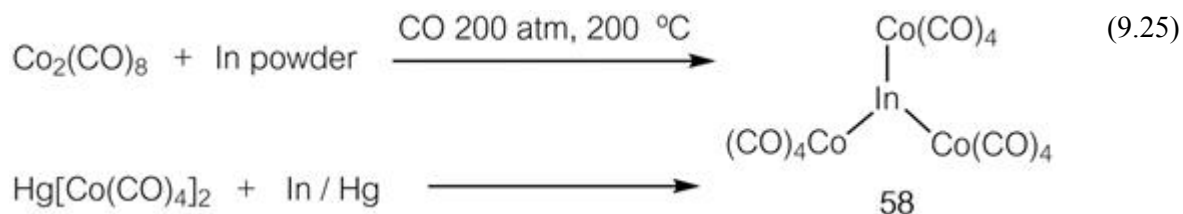
In the 1960s, many compounds containing Ti and Al were prepared, relating to Ziegler–Natta catalysis, although they did not have direct Ti–Al bonds. The first complex containing a direct M–Al bond, $[CpFe(CO)_2AlPh_3]^-$ (**59**), was reported in 1979 and contains a dative bond between the Lewis basic $[CpFe(CO)_2]^-$ and Lewis acidic $AlPh_3$.[33]

$$[\text{NEt}_4][\text{CpFe(CO)}_2] \ + \ \text{AlPh}_3 \longrightarrow \tag{9.26}$$

59
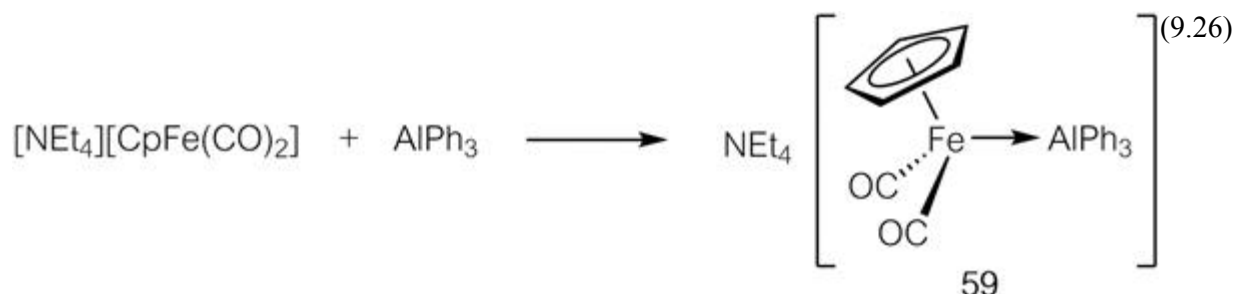
In the 1990s, many transition metal complexes with heavier Group 13 elements, especially gallium, were prepared as possible single-source precursors for MOCVD (metal–organic chemical vapor deposition) applications for the preparation of thin layer films of metal-Group 13 element materials.

Recently, a wide variety of complexes with new types of bonding, such as M–E unsaturated bonds, M–H–E 3-center-2-electron (3c–2e) bonds, M-naked E bonds, *etc.*, have been successfully synthesized. The chemistry of M–E complexes appears set for rapid development and expansion.

9.3.2 Typical Structures of Complexes

Schematic pictures of typical M–E complexes are summarized in Figure 9.16 where all types of bonds, including multiple bonds, are represented by

a single line. Detailed discussions on aspects of M–E bonding will be described in Section 9.3.4.

Complexes with M-E single bonds

M—ER_2
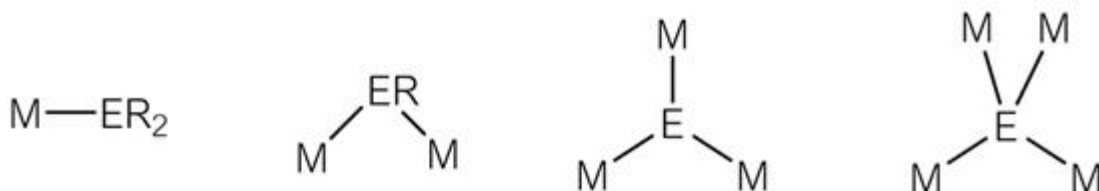
Complexes with M-E multiple bonds

M—ER M—E—M M—E

Complexes stabilized by Lewis base coordination

M—ER_2 M—ER
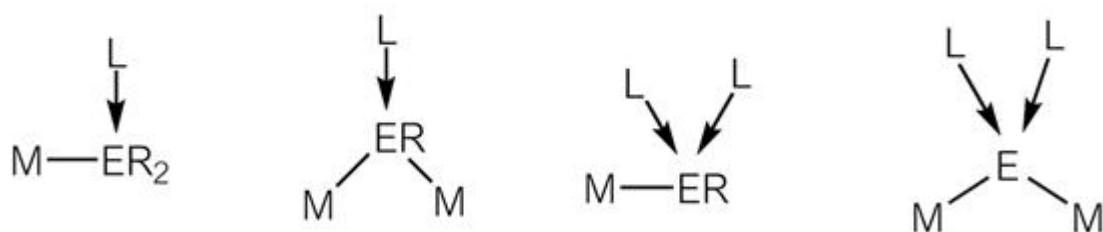
Complexes with metal-to-E dative bonds

$M \longrightarrow ER_3$

Figure 9.16   Schematic representations of metal-Group 13 element complexes.

As noted above, Group 13 elements have 3 valence electrons, and thus an ER_2 fragment behaves as a one-electron donor and formally makes a covalent single bond with a metal fragment. Similarly, an ER fragment behaves as a two-electron donor and would make a dative bond, a covalent double bond, or a M–E–M bridging bond with metal fragments.

M–ER$_2$ and M–ER complexes are isoelectronic/isostructural with cationic silylene [M-SiR$_2$]$^+$ and silylyne complexes [M-SiR]$^+$, respectively. Since the ER$_2$ or ER ligand in the complexes has one or two vacant p-orbital(s) on E (Figure 9.17), respectively, M–ER$_2$ and M–ER complexes can form adducts with Lewis bases such as amines and pyridine. In the solid state, coordination of weak Lewis bases, such as Cl, may also occur. For example, [Fp$_2$GaCl] (Fp = CpFe(CO)$_2$) makes a one-dimensional chain comprising Ga–Cl–Ga bonding (Figure 9.18).
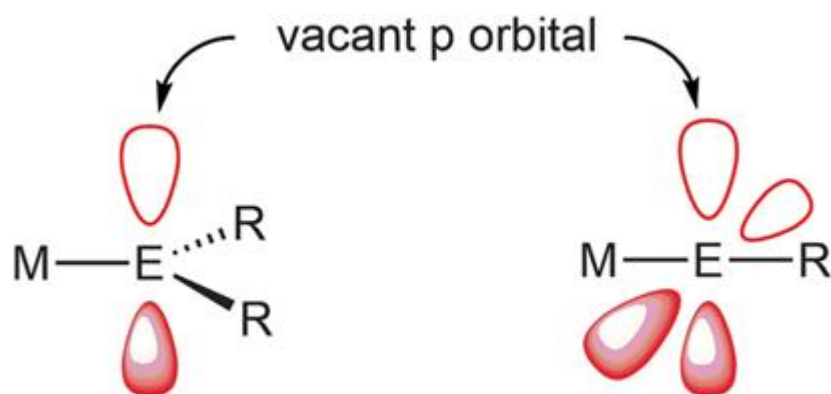
Figure 9.17   [MER$_2$] and [MER].
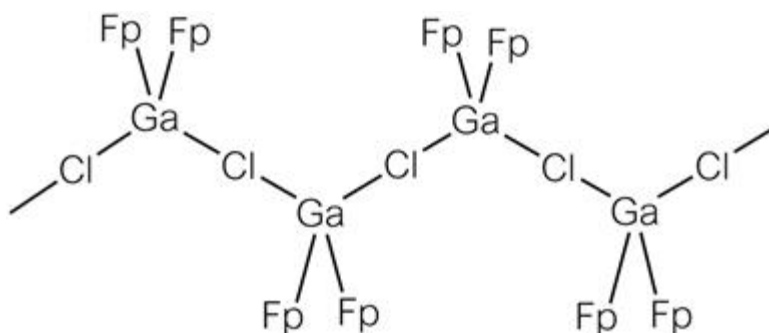
Figure 9.18   One-dimensional chain comprising Ga–Cl–Ga bonding.

ER$_3$ also has a vacant p-orbital on the E atom and can accept an electron pair from a metal fragment to form donor–acceptor complexes such as [Fp-AlPh$_3$]$^-$ (eqn (9.26)). Complexes with M–Cl → E bonds and M–H–E 3c–2e bonds are also known.

9.3.3 Bonding

Bonding between transition metals and heavier main group elements has been discussed based on the well-established ideas of metal–carbon bonding. However, the nature of the M–E (E = Group 13 element) bond differs significantly from that of the M–C bond due to the large electronegativity difference between E and C.

Table 9.1 summarizes the Allred–Rochow electronegativity data of the Group 13 elements. The elements are electropositive and have lower χ values than carbon (2.50). Among the Group 13 elements, boron is exceptional in its relatively high χ (2.01), which approaches that of hydrogen (2.20). In contrast, Al ~ Tl are extremely electropositive and have much lower χ values, lower even than those of silicon (1.74) and germanium (2.02), which are generally recognized as electropositive elements. Thus, EH_4^- (E = Al, Ga) have strongly polarized $E^{\delta +}$–$H^{\delta -}$ bonds compared to BH_4^- and are excellent H^- donors. This consideration can also be applied to M–E bonds, especially in late transition metal complexes, which are strongly polarized $M^{\delta -}$–$E^{\delta +}$ and easily hydrolyzed.

Table 9.1 Allred–Rochow electronegativity data for Group 13 elements.

Element	Electronegativity
B	2.01
Al	1.47
Ga	1.82
In	1.49
Tl	1.44

Due to its highly polar nature, the M–E bond has been considered to be dominated by electrostatic interaction (Coulomb force) between $M^{\delta -}$ and $E^{\delta +}$. On the other hand, the contribution of multiple bonding in the M–E bonds of $M–ER_2$ complexes has also been proposed as an important factor, since $M–ER_2$ complexes have a vacant p-orbital on E which can accept electrons from metal fragments *via* back-donation (Figure 9.19).
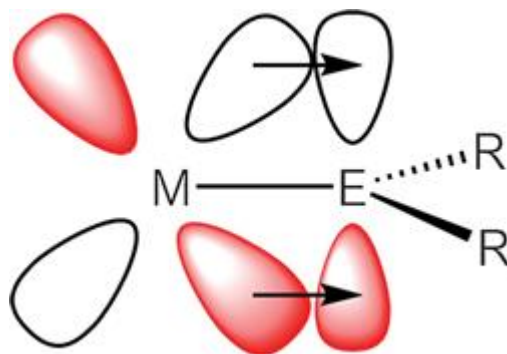
Figure 9.19   Electron density flow from the d orbital of M to the empty p orbital of E.

Deep controversy on the contributions of the electrostatic interaction and multiple bonding modes in the M–E bond broke out when Robinson reported the first gallylene complex **60**, M-GaR, in 1997 (Figure 9.20).[34]

60
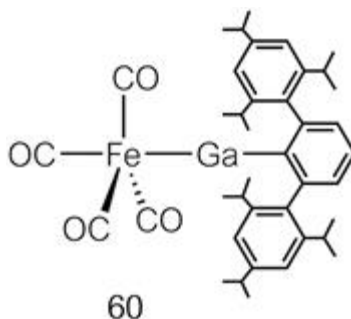
Figure 9.20   The first gallylene complex, reported by Robinson *et al.*[34]

In the following section, we will discuss the nature of the M–ER bond, and note that these discussions are also applicable to the M–ER$_2$ bond.

9.3.4   M–E Bonding in M–ER Complexes

The bonding between metals and main group elements, not limited to Group 13 elements, consists of both electrostatic and covalent interactions. Since the ER ligand (E = Al ~ Tl) takes the singlet ground state with one lone pair of electrons and two empty p orbitals (Figure 9.21), both σ donation from ER to M and π-back-donation from M to ER contribute to covalent interactions.
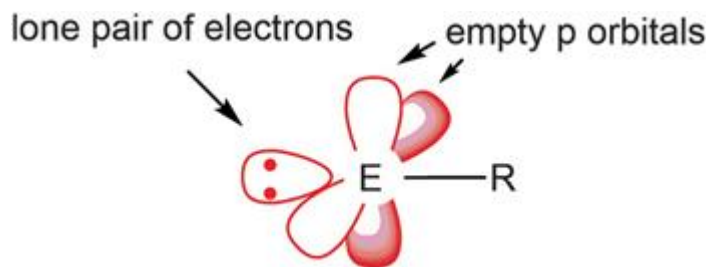
Figure 9.21 ER with one lone pair of electrons and two empty p orbitals.

The nature of M–ER bonds has been investigated extensively based on MO theory and important conclusions are summarized below:

(1) The M–ER bond is strongly polarized $M^{\delta-}$–$E^{\delta+}$.

(2) The M–ER bond is dominated by electrostatic interaction (Coulomb interaction between the negative charge of the lone pair of electrons on ER and the positive charge of the metal nucleus). The covalent contribution to the interaction is 30 ~ 50%.

(3) While σ donation from ER to M (Figure 9.22(a)) is the main contributor in the covalent interaction, the π interaction is not negligible (Figure 9.22(b)). The π contribution to the covalent interaction reaches 30 ~ 50% in some complexes.
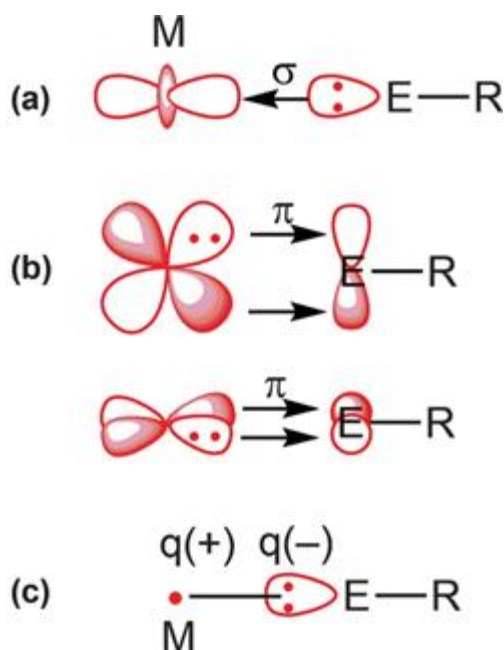
Figure 9.22 Nature of the M–ER bond: (a) σ donation from ER to M, (b) π-back donation from M to RE, and (c) electostatic interaction.

M–ER complexes can thus be understood as Lewis acid–base adducts with strongly polarized M–ER bonds, but π contributions to the covalent interaction cannot be ignored, and so M–ER bonds should be considered to exhibit some multiple bond character.

Frenking evaluated details of the M–E bond energies in M–ER complexes (E = B ~ Tl) using the ETS (Extended Transition State) method.[35]Table 9.2 shows the results of the ETS energy contribution analysis for M–EMe and M–CO bonds at the equatorial position in [Fe(EMe)$_5$] and [Fe(CO)$_5$], respectively. In this table, ΔE terms represent bond energies and are related as follows:$\Delta E = \Delta E_{prep} + \Delta E_{int} \Delta E_{int} = \Delta E_{elstat} + \Delta E_{Pauli} + \Delta E_{orb} \Delta E_{orb} = \Delta E_{\sigma} + \Delta E_{\pi}$

Table 9.2 ETS analysis for M–EMe and M–CO bonds at the equatorial position in Fe(EMe)$_5$ and Fe(CO)$_5$, respectively. All energies are given in J mol^{-1}.

	BMe	AlMe	GaMe	InMe	TlMe	CO
ΔE_{int}	− 498.7	− 364.0	− 280.3	− 248.9	− 226.4	− 215.1
ΔE_{Pauli}	1036.8	586.6	505.4	476.6	472.8	621.2
ΔE_{elstat}	− 955.6	− 566.5	− 482.0	− 451.0	− 434.3	− 462.8
ΔE_{orb}	− 579.9	− 384.1	− 303.8	− 274.5	− 264.9	− 379.5
	(37.8%)	(40.4%)	(38.7%)	(37.8%)	(37.9%)	(45.2%)
ΔE_{σ}	− 312.1	− 230.1	− 190.4	− 174.5	− 179.5	− 182.8
ΔE_{π}	− 267.8	− 154.0	− 113.4	− 100.0	− 85.4	− 196.6
	(46.2%)	(40.1%)	(37.3%)	(36.4%)	(32.2%)	(51.8%)
ΔE_{prep}	56.9	32.6	12.1	8.8	4.6	19.7
ΔE	− 441.8	− 331.4	− 268.2	− 240.2	− 222.2	− 195.4

Here, ΔE_{prep} is the rehybridized energy for ER and the metal fragment required prior to making the M–ER bond, while ΔE_{int} is the interaction energy between ER and the metal fragment. ΔE_{int} is divided into the static interaction ΔE_{elstat}, steric repulsion ΔE_{Pauli}, and orbital interaction ΔE_{orb} factors. The orbital interaction ΔE_{orb} is further divided into a σ bonding interaction ΔE_{σ} and a π bonding interaction ΔE_{π}.

As shown in Table 9.2, all the Fe–EMe bonds are thermodynamically stable compared to the Fe–CO bond. In particular, Fe–BMe has an especially large ΔE. Heavier Group 13 elements have smaller ΔE values, which decrease by *ca.* 170 J mol^{-1} on going from B to Ga but only by *ca.* 40 J mol^{-1} from Ga to Ta.

The contribution ratio of the covalent bond energy ΔE_{orb} in the bonding interaction energy ($\Delta E_{elstat} + \Delta E_{orb}$) is almost constant, *ca.* 40%, for all Group 13 elements. This ratio is smaller than that of the Fe–CO bond (*ca.* 45%) indicating a larger electrostatic contribution in the Fe–EMe bond than in the Fe–CO bond. However, the difference between the ratios for Fe–EMe and Fe–CO is not so large (*ca.* 5%).

The contribution of the π bond interaction ΔE_{π} in ΔE_{orb} decreases on going down Group 13, *i.e.* from 46% in BMe to 32% in TlMe. These ratios are smaller than that for Fe–CO. It is noteworthy that the ΔE_{π} value for Fe–BMe is much larger than that of Fe–CO, which demonstrates that π-back-donation from the metal fragment (the π interaction) is more important in the Fe–BMe bond than in the Fe–CO bond.

Table 9.3 summarizes the ETS analysis data for several types of gallylene complexes. In this table, GaCp and $GaN(SiH_3)_2$ are base-stabilized gallylene complexes. The CpGa and $GaN(SiH_3)_2$ ligands are categorized as $GaRL_2$ (R = one electron donor, L = two electron donor) and GaRL type ligands, respectively, since η^5-Cp donates five electrons to Ga, while the amino substituent $N(SiH_3)_2$ can delocalize its lone pair of electrons on N to Ga.

Table 9.3 ETS analysis for the M–Ga bond in $(OC)_4Fe$–GaR, $Fe(GaMe)_5$, and $Ni(GaMe)_4$.[ae]

	GaCp[b]	GaN(SiH₃)₂[b]	GaPh[b]	GaMe[b]	GaMe[c]	GaMe[d]
ΔE_{int}	− 132.6	− 179.5	− 255.2	− 259.4	− 280.3	− 209.6
ΔE_{Pauli}	292.5	398.3	541.8	558.1	505.4	475.3
ΔE_{elstat}	− 197.1	− 283.3	− 428.0	− 443.9	− 482.0	− 448.9
ΔE_{orb}	− 227.6	− 294.6	− 369.0	− 373.6	− 303.8	− 236.0
	(53.4%)	(50.9%)	(46.3%)	(45.7%)	(38.7%)	(34.5%)
ΔE_{σ}	− 197.5	− 241.0	− 305.4	− 313.8	− 190.4	− 141.8
ΔE_{π}	− 30.1	− 53.6	− 63.6	− 59.8	− 113.4	− 94.1
	(13.2%)	(18.2%)	(17.2%)	(16.0%)	(37.3%)	(39.9%)
ΔE_{prep}	36.4	35.1	36.4	34.3	12.1	14,6
ΔE	− 96.2	− 144.3	− 218.8	− 225.1	− 268.2	− 195.0

[a] All energies are given in J mol⁻¹.
[b] The GaR ligand occupies the axial position in the complexes.
[c] Data for the equatorial Fe–Ga bonds in [Fe(GaMe)₅].
[d] Data for [Ni(GaMe)₄].

^{e} [$(CO)_4Fe$–GaCp] and [$(CO)_4Fe$–GaN$(SiH_3)_2$] are base-stabilized complexes, since η^5-Cp donates five electrons to Ga, while the amino substituent N$(SiH_3)_2$ can delocalize its lone pair electrons on N to Ga.

The data for [$(CO)_4Fe$–GaR] shown in Table 9.3 clarify the following points:

> (1) The order of the Fe–Ga bond energy ΔE is GaPh $\sim$ GaMe > GaN$(SiH_3)_2$ > GaCp. The same tendency is observed in the order of ΔE_{elstat} and ΔE_σ. The ΔE of GaCp is half that of GaMe.
> (2) In the bonding interaction ($\Delta E_{elstat} + \Delta E_{orb}$), the covalent bond ΔE_{orb} contribution is greater than 45% and it is dominated by σ bond interaction. The π contribution to the bond is *ca.* 16%.
> (3) For the base-stabilized gallylene complexes, *i.e.* GaCp and GaN$(SiH_3)_2$, both ΔE_{elstat} and ΔE_{orb} are smaller than those of the GaPh and GaMe complexes. However, ΔE_{elstat} decreases considerably more than ΔE_{orb}. As a result, the contribution of ΔE_{orb} to the bonding interaction ($\Delta E_{elstat} + \Delta E_{orb}$) for the base-stabilized complexes becomes relatively large compared to that in the GaPh and GaMe complexes.

It is noteworthy that the ΔE_π contribution increases to nearly 40% for the homoleptic complexes [Fe$(GaMe)_5$] and [Ni$(GaMe)_4$]. This is attributable to the stronger π acid character of CO compared to GaR. In [$(CO)_4Fe$–GaR], CO and GaR ligands compete for back-donation from the metal. The more π acidic CO ligand accepts more back-donated electron density from the metal, which results in weaker π-back-donation from the metal to GaR. In the homoleptic complexes, no competing π acceptor ligand exists. The good electron releasing ligand GaR increases the electron density on the metal center, which consequently enhances the π-back-donation from the metal to the GaR ligand.

9.3.5 Synthetic Methods

Though the number of reported M–E complexes has increased gradually, they are still rare compared to M–C and M–Si complexes.[36–41] The lack of good and general synthetic routes is a major factor limiting progress in this area. Many of the known M–E complexes contain carbonyl ligands as a supporting ligand because salt elimination reactions between Group 13 halide compounds and anionic metal carbonyl complexes have been widely used for preparing M–E complexes. This situation has changed somewhat since new reactions to form M–E bonds as well as new ligand precursors such as ECp* have been developed recently.

Another factor presenting challenges to the synthesis of M–E complexes derives from the intrinsic nature of Group 13 compounds with small substituents on E. Such compounds tend to disproportionate or redistribute the substituents quite easily. Due to this, M–E complexes generated in the reaction may be converted to different products by disproportionation or substituent redistribution.

Group 13 compounds are easily hydrolyzed due to their Lewis acidity and strongly polarized E–R and E–M bonds. This also makes it difficult to explore the chemistry of M–E complexes. Recent developments in techniques for handling unstable species, such as the use of glove boxes, greatly help to overcome this difficulty.

Typical synthetic routes are described below:

(1) Salt elimination
The most popular synthetic route to M–E complexes is a salt elimination reaction using nucleophilic anionic metal fragments and Group 13 halide compounds EX_nR_{3-n} (X = halogen, n = 1, 2). Eqn (9.27) is a typical example of the synthesis of gallyl complexes. The first gallylene complex **60** as well as gallium and thallium atom-bridged bimetallic complexes (**61** and **62**) were also prepared *via* this route (eqn (9.28)–(9.30)).

(9.27)

$Ar^* = C_6H_3\text{-}2,6\text{-}(2,4,6\text{-}^iPr_3C_6H_2)_2$

60

(9.28)

61

(9.29)

$$2\ K_2[Cr(CO)_5]\ +\ TlCl_3\ \xrightarrow[\text{[2,2,2]-cryptand}]{\text{THF}}\ [K[2,2,2]\text{-cryptand}]\big[(OC)_5Cr-Tl-Cr(CO)_5\big]$$

<div align="center">62</div>

<div align="right">(9.30)</div>
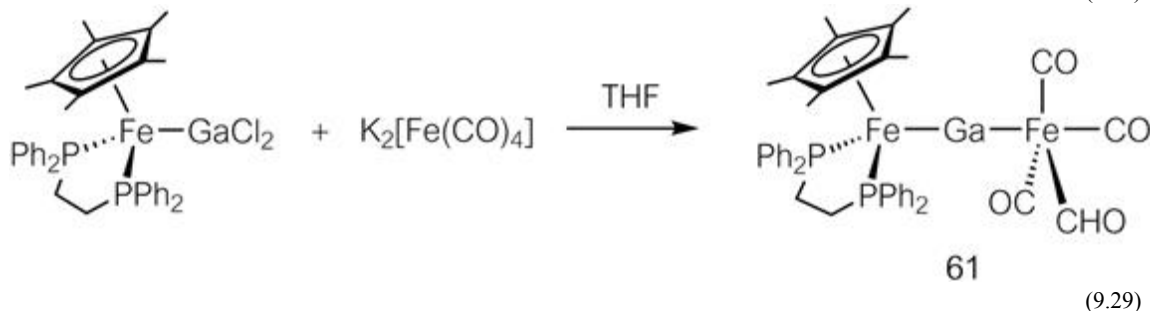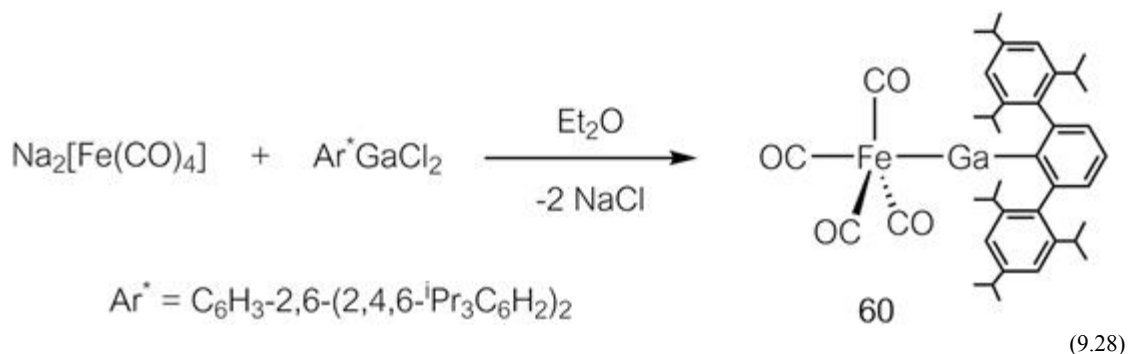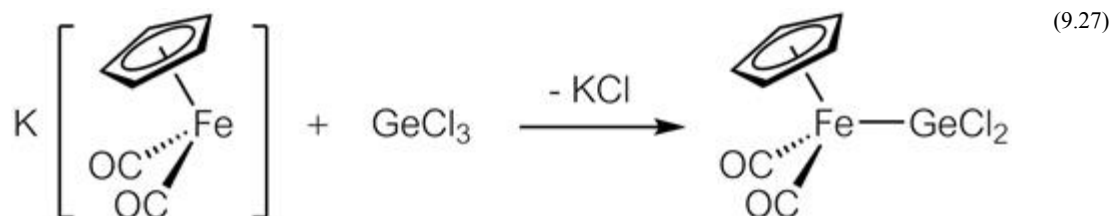
Salt elimination reactions require moderately stable anionic complexes. Metal carbonyl complexes are thus widely used for this reaction. Solvent selection is also important. The anionic complexes are generally prepared in polar solvents such as THF and are used *in situ*. However, the M–E bonds formed by the reaction often cleave heterolytically in polar solvents to give anionic metal fragments and solvated cationic Group 13 species. In such cases, the polar solvent should be replaced with a nonpolar solvent such as toluene before use in the M–E bond-forming reaction.

Reductive coupling between metal halide complexes and Group 13 halide compounds EX_nR_{3-n} using strong reducing agents such as alkali metals has also been used in the preparation of M–E complexes. Eqn (9.31) represents a typical example of a reductive coupling reaction in which dichlorometallocene and dichlorogallane were treated with Na or Mg to give a bis(gallylene)metallocene complex **63**. This method may not be applicable so widely, but is an attractive new synthetic path for making M–E bonds.

<div align="right">(9.31)</div>

$$Cp_2MCl_2\ +\ 2\ Ar^*GaCl_2\ \xrightarrow{\text{Na or Mg}}$$

$$Ar^* = C_6H_3\text{-}2,6\text{-}(2,4,6\text{-}^iPr_3C_6H_2)_2 \qquad\qquad \textbf{63: } M = Zr,\ Ti$$
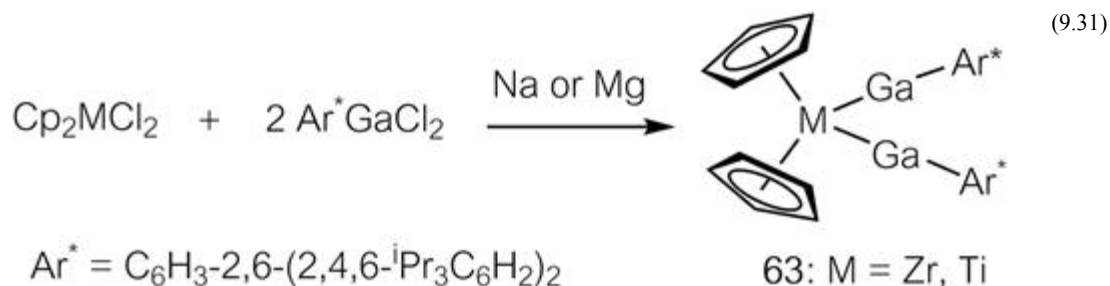
(2) Metallation under CO atmosphere

As shown in eqn (9.25), reaction of elemental indium and metal carbonyls under high-temperature/high-pressure CO conditions (~200 °C, 200 atm) affords products with metal–indium bonds. Ga and Tl complexes were also prepared in a similar manner to that in eqn (9.25). In this method, metal clusters are generally obtained in which more than three metal fragments are connected to one E atom. Reactions using Group 13 halide species are also known instead of elemental E.

(3) Insertion of EX species

Monovalent EX species are very reactive and will insert into M–M and M–X bonds. Eqn (9.32) shows the reaction of monovalent indium halide, InX, with $[\{Cp(CO)_3M\}_2]$ (M = Cr, Mo, W), resulting in the insertion of InX into the M–M bond to afford an InX-bridged bimetallic complex **64**.

<div align="right">(9.32)</div>

$$[\{CpM(CO)_3\}_2]\ +\ InX\ \xrightarrow{\text{THF}}$$

M = Cr, Mo, W   X = Cl, Br, I   64
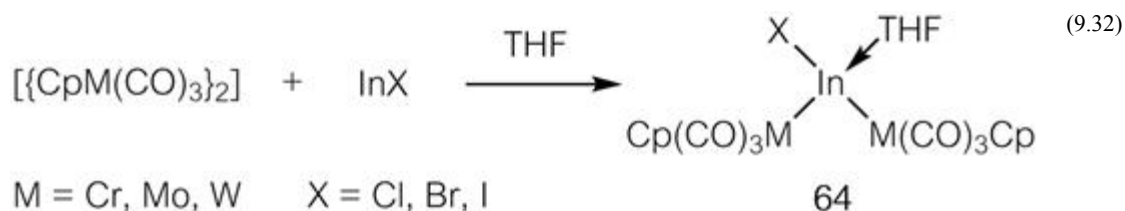
Similarly, EI (E = Ga, In) inserted into the Fe–X bond of $[CpFe(CO)_2X]$ (X = Br, I) to form $[CpFe(CO)_2EXI]$ (**65**) (eqn (9.33)).

$$\text{(9.33)}$$

X = Be, I   E = Ga, In   65
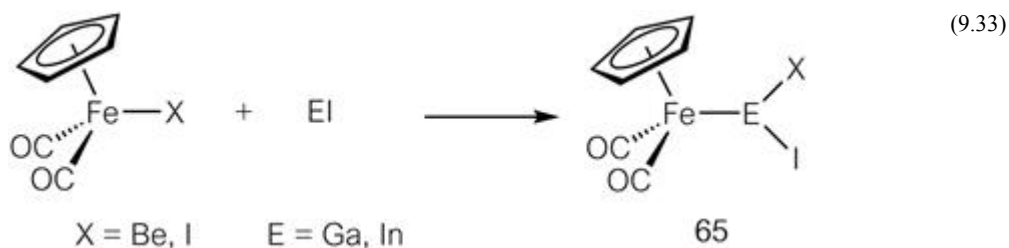
(4) Elimination of alkanes or silanes

Disproportionation readily occurs for ER_3 (E = Al, Ga) with sterically small substituents R. The first gallyl complex, $[Cp(OC)_3W\text{-}GaMe_2]$ (**66**) was synthesized *via* a disproportionation reaction between a tungsten hydride complex and $GaMe_3$ (eqn (9.34)).

$$\text{(9.34)}$$

66
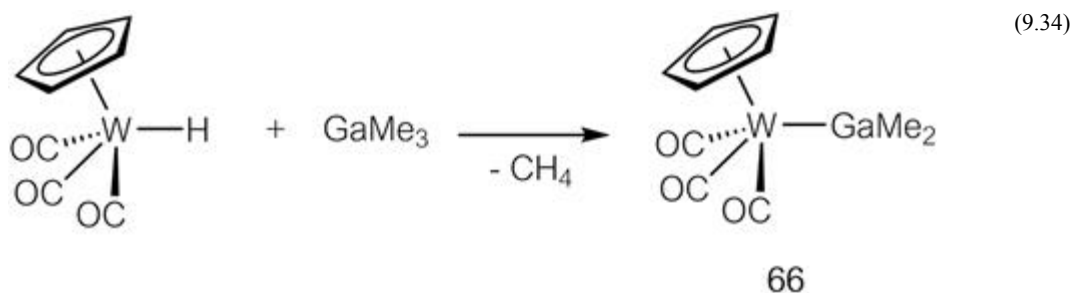
Photolysis of $[\{CpMo(CO)_3\}_2]$ in the presence of InR_3 (R = Et, ^{t}Bu, neopentyl (Np)) afforded $[CpMo(CO)_3InR_2]$ (**67**) (eqn (9.35)). In the case of R = Et, successive disproportionations took place to give $[\{CpMo(CO)_3\}_2InEt]$ and $[\{CpMo(CO)_3\}_3In]$.

$$\text{(9.35)}$$

67
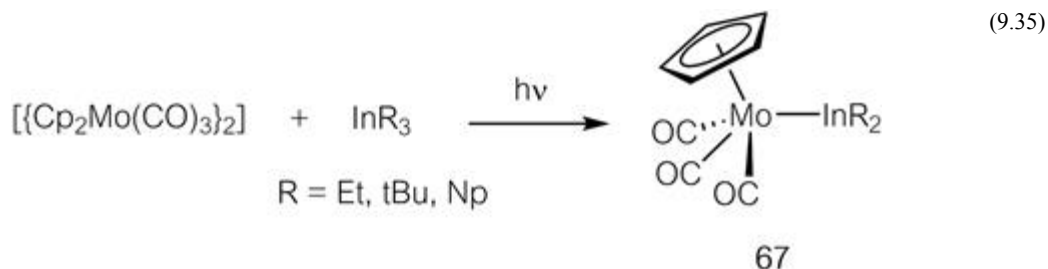
M–Ga bond formation *via* chlorosilane elimination has also been reported recently. Reaction of silyliron complex $[CpFe(CO)_2SiMe_3]$ with $GaCl_3$ afforded the dichlorogallyliron **68** or chlorogallylene-bridged complex **69** quantitatively, depending on the reaction temperature and stoichiometry (eqn (9.36) and (9.37)). Formation of the thermodynamically stable Si–Cl bond is presumably a driving force in these reactions.

$$\text{(9.36)}$$

68

(9.37)
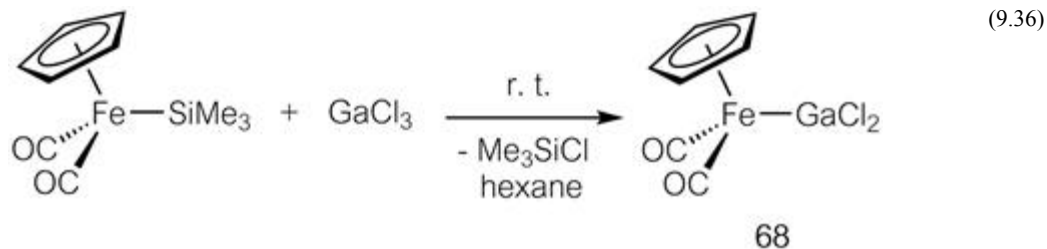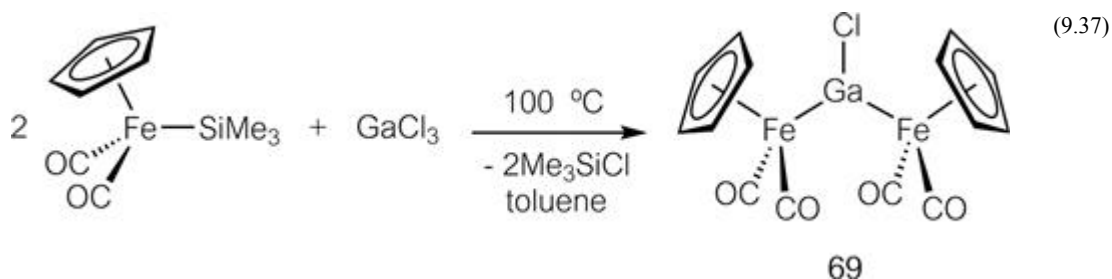
(5) Oxidative addition

Diboryl complexes can be prepared by oxidative addition of the B–B bond of diboranes to unsaturated transition metal fragments. A similar reaction also occurs for digallanes to give digallyl complexes. Eqn (9.38) illustrates the preparation of an anionic digallyl complex **70** obtained by the oxidative addition of a digallane to "Cp$_2$Zr", generated *in situ* from [Cp$_2$ZrCl$_2$] and ^{n}BuLi, followed by reduction with ^{n}BuLi.

70

(9.38)
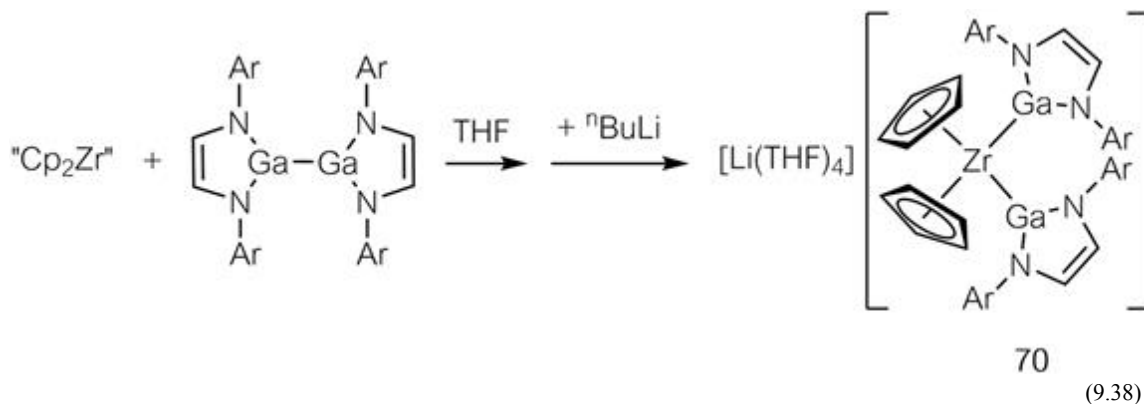
A gallyl platinum complex **71** has also been prepared *via* the oxidative addition of GaX$_3$ (X = Br, I) to [Pt(PCy$_3$)$_2$] (eqn (9.39)).

(9.39)
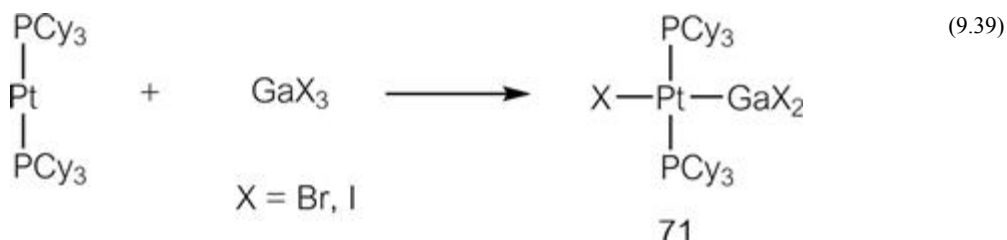
(6) Coordination of metal fragments to Group 13 compounds

Lewis basic metal fragments can coordinate to Lewis acidic Group 13 compounds. As shown in eqn (9.26), reaction of [CpFe(CO)$_2$]$^-$ and AlPh$_3$ afforded the Fe–Al adduct complex, [CpFe(CO)$_2$AlPh$_3$]$^-$ (**59**). Pt–Al complexes **72** have been obtained from AlX$_3$ and [Pt(PCy$_3$)$_2$] (eqn (9.40)). A gallium complex has also been prepared by a similar reaction with GaCl$_3$. It is noteworthy that this reaction differs from that shown in eqn (9.39) only in the halide substituents X, *i.e.* the products depend on the halide X in GaX$_3$.

$$\begin{array}{c}
\text{PCy}_3 \\
| \\
\text{Pt} \\
| \\
\text{PCy}_3
\end{array}
\quad + \quad
\text{EX}_3
\quad\longrightarrow\quad
\begin{array}{c}
\text{PCy}_3 \\
| \\
\text{Pt} \rightarrow \text{EX}_3 \\
| \\
\text{PCy}_3 \\
\textbf{72}
\end{array}
\qquad (9.40)$$

$$E = Al,\ X = Cl,\ Br,\ I$$
$$E = Ga,\ X = Cl$$
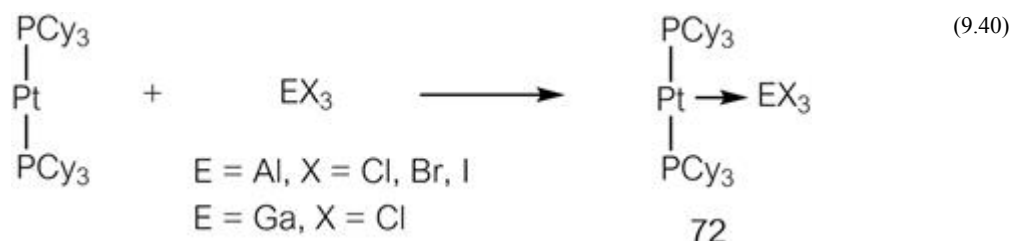
An adduct of Ga^+ and a platinum fragment **73** were obtained by the reaction of $[Cp*Ga_2]BAr^f_4$ ($Ar^f = 3,5\text{-}(CF_3)_2C_6H_3$) and $[Pt(GaCp*)_4]$ (eqn (9.41)). Theoretical investigation revealed that both σ-donation from Ga^+ to Pt and π-back-donation from Pt to Ga^+ are important in the Pt–Ga bonding.

$$Pt(GaCp^*)_4 + [Cp^*Ga_2]BAr^f_4 \longrightarrow \left[\begin{array}{c} Ga \\ \uparrow \\ Cp^*Ga\!-\!Pt\substack{\cdots\cdots GaCp^* \\ \diagdown GaCp^*} \\ | \\ GaCp^* \end{array} \right] BAr^f_4$$

73

(9.41)
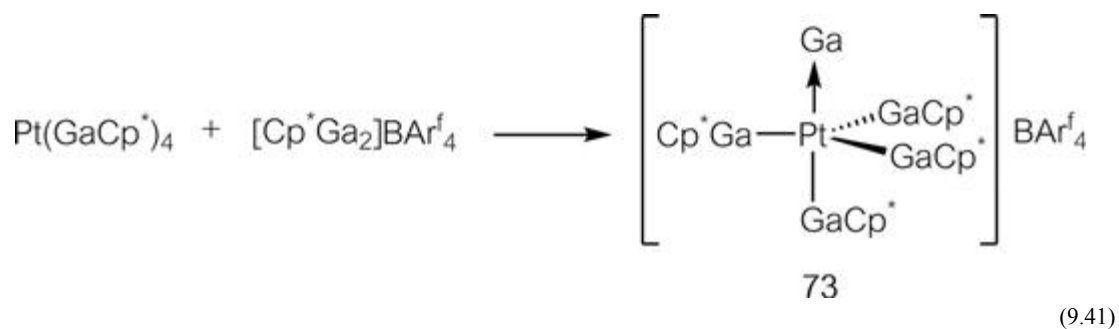
(7) Ligand substitution

A monovalent Group 13 species ER has a lone pair of electrons on E and can substitute a $2e$ donor ligand in the metal complex to form an M–ER bond. In the reaction shown in eqn (9.42), ECp* substituted a cyclooctene ligand.

$$(CO)_5Cr(\text{cyclooctene}) + ECp^* \longrightarrow (CO)_5Cr\!-\!ECp^* \qquad (9.42)$$
$$E = Al,\ Ga,\ In \qquad \textbf{74}$$
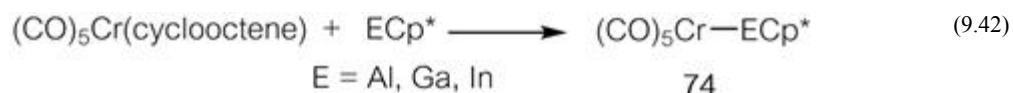
Like the CO ligand, ECp* can behave as a bridging ligand affording bimetallic complexes **75** (eqn (9.43)).

$$Co_2(CO)_8 + ECp^* \longrightarrow (CO)_3Co\underset{\underset{Cp^*}{\overset{|}{E}}}{\overset{\overset{Cp^*}{\overset{|}{E}}}{\diagup\!\!\!\diagdown}}Co(CO)_3$$

75

(9.43)
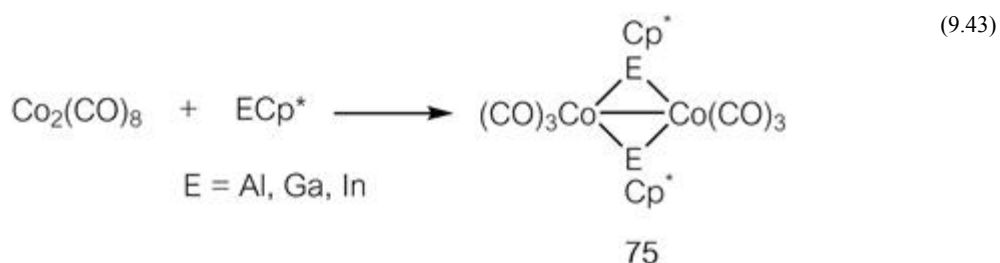
Reaction of $Ni(cod)_2$ and $[\{EC(SiMe_3)_3\}_4]$ afforded the homoleptic four-coordinate complexes $[Ni\{EC(SiMe_3)_3\}_4]$ (**76**) (eqn (9.44)).

(9.44)

E = Ga, In
R = C(SiMe₃)₃
cod = cyclooctadiene
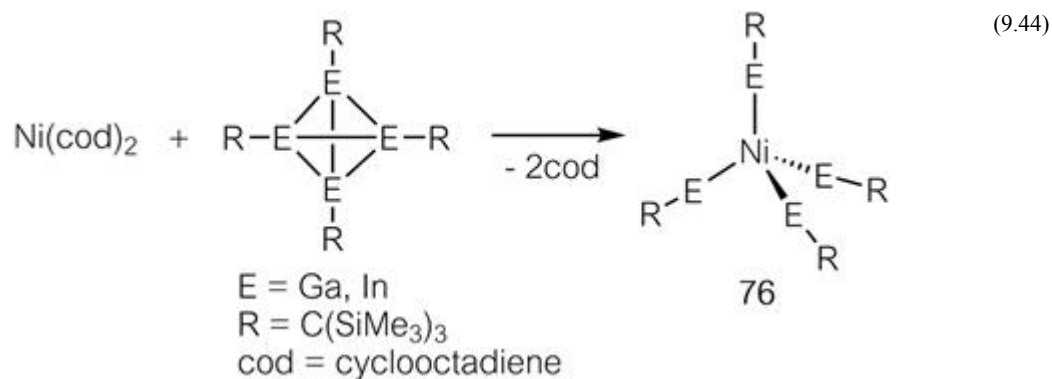
The first gallane σ-complex, [W(CO)₅(H₃Ga · quinuclidine)] (**77**), was synthesized by the ligand substitution reaction between [W(thf)(CO)₅] and gallane-Lewis base adduct H₃Ga · quinuclidine (eqn (9.45)).

(9.45)
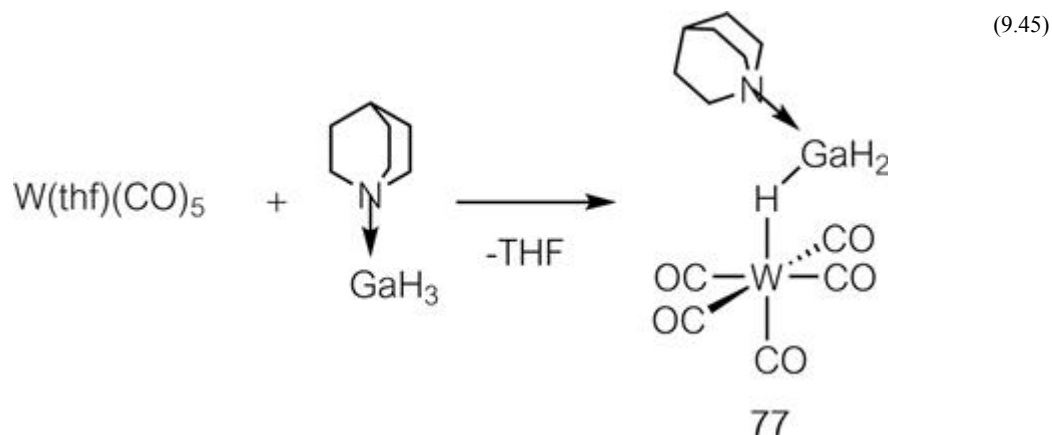
9.3.6 Reactivity

Although the number of reported M–E complexes has increased in recent years, the reactivity and chemistry of M–E complexes has remained largely unexplored. Figure 9.23 illustrates known typical reaction patterns for gallyl complexes.
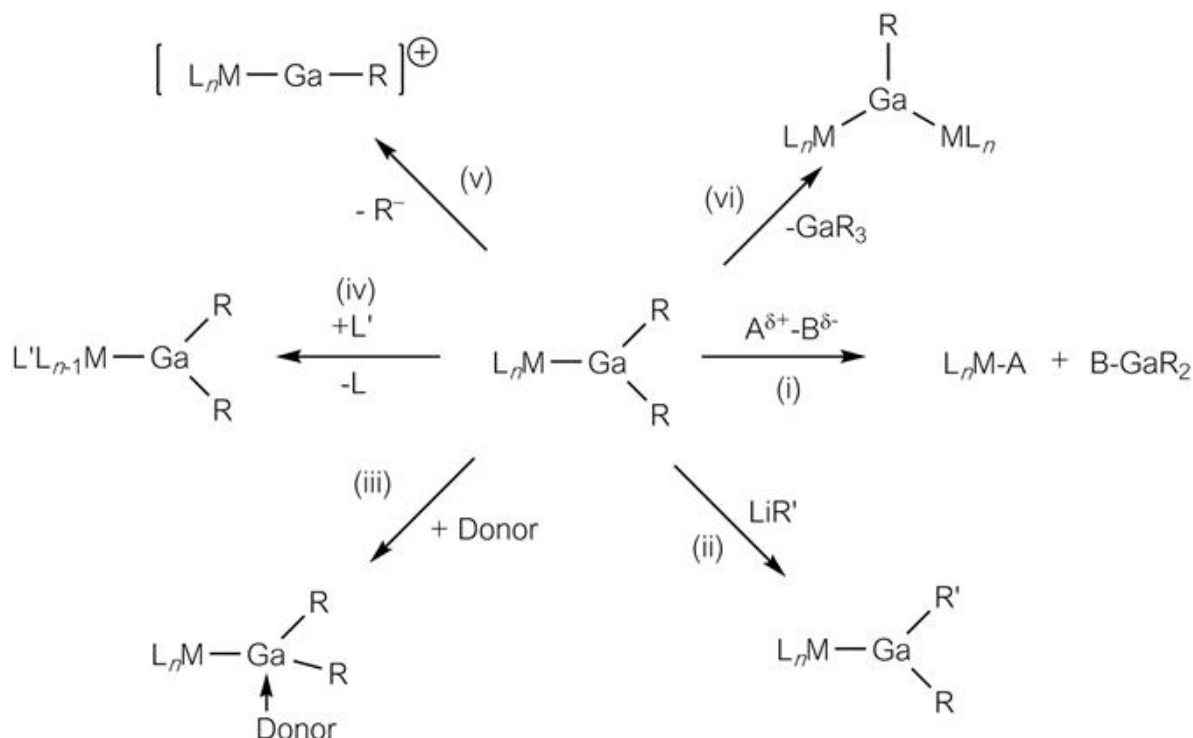
Figure 9.23 Reactivity of $[L_nM\text{-}GaR_2]$.

Due to the strongly polarized M–Ga bonds, protic reagents such as H_2O and HCl smoothly react to cleave the M–Ga bond (path i). Good leaving groups on Ga such as Cl can be replaced by nucleophiles such as alkyl anions (path ii). However, yields of the products are often low since M–Ga cleavage (path i) occurs simultaneously in the reaction system. A typical example of path ii is shown in eqn (9.46). The Fe–Ga bond of the gallyliron complex is stable enough to obtain the (dialkylgallyl)iron complex **78** in 60 ~ 70% yield.

(9.46)
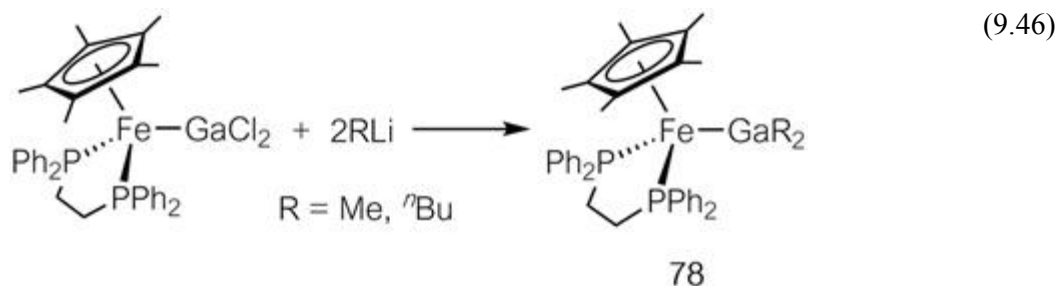
Transmetalation at Ga also occurs, as shown in eqn (9.47), in which reaction of dichlorogallyliron and zirconacycle complexes afforded a

gallacyclopentadienyliron complex **79**.

(9.47)
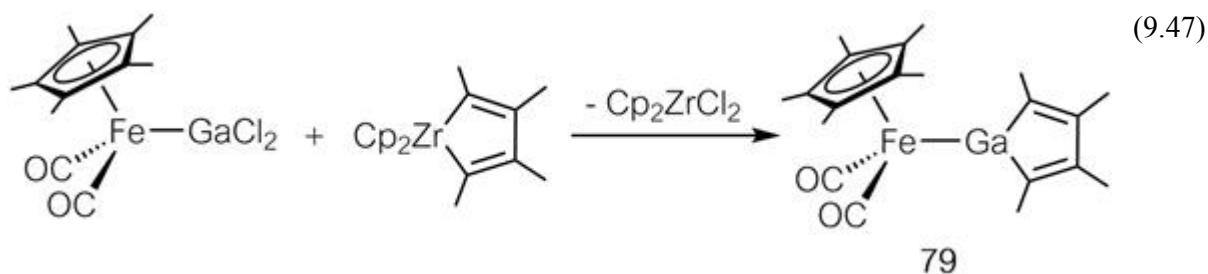
Abstraction of R⁻ from gallyl complexes M-GaR$_2$ affords cationic gallylene complexes [M-GaR]⁺ (path v). Cationic diiron complexes bridged by an E atom (**80**) were prepared by X⁻ abstraction from EX-bridged diiron complexes (eqn (9.48)).

(9.48)

E = Ga, X = Cl
E = In, X = Br, I
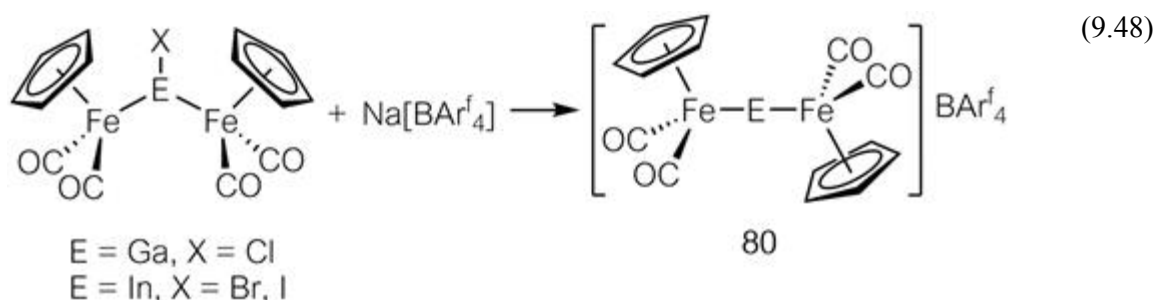
Lewis bases such as pyridine, THF and phosphine can coordinate to the gallium center in gallyl complexes (path iii). Ligand substitution on metal centers occurs when a 2e donor ligand L is labile (path iv).

Gallyl complexes with sterically small substituents on Ga tend to disproportionate to give gallylene-bridged bimetallic complexes and GaR$_3$ (path vi). Further disproportionation affords gallium atom-bridged trimetallic complexes, EM$_3$.

9.3.7 Summary

The chemistry of metal-Group 13 element complexes has grown rapidly since the 1990s. However, examples of such complexes are still limited and in particular the reactivity of such complexes remains largely undeveloped. Since Group 13 elements are electropositive, their compounds might be good electron-donating ligands to metal centers, considerably stronger donors than phosphine. If stable ligands connecting metals with Group 13 elements are developed, unprecedented reactions and catalytic systems may

be discovered. The chemistry of M–E complexes will likely make rapid progress in the near future.

References

1. H. Braunschweig and M. Colling, *Coord. Chem. Rev.*, 2001, **223**, 1.
2. (a) J. F. Hartwig and S. Huber, *J. Am. Chem. Soc.*, 1993, **115**, 4908; (b) S. A. Westcott, H. P. Blom, T. B. Marder, R. T. Baker and J. C. Calabrese, *Inorg. Chem.*, 1993, **32**, 2175; (c) J. F. Hartwig and X. He, *Organometallics*, 1996, **15**, 5350; (d) H. Braunschweig, K. Radacki, D. Rais and F. Seeler, *Organometallics*, 2004, **23**, 5545; (e) S.-Y. Onozawa, Y. Hatanaka, T. Sakakura, S. Shimada and M. Tanaka, *Organometallics*, 2004, **23**, 5545.
3. (a) T. Terabayashi, T. Kajiwara, M. Yamashita and K. Nozaki, *J. Am. Chem. Soc.*, 2009, **131**, 14162; (b) L. M. A. Saleh, K. H. Birjkumar, A. V. Protchenko, A. D. Schwarz, S. Aldridge, C. Jones, N. Kaltsoyannis and P. Mountford, *J. Am. Chem. Soc.*, 2001, **133**, 3836; (c) S. Li, J. Cheng, Y. Chen, M. Nishiura and Z. Hou, *Angew. Chem. Int. Ed.*, 2011, **50**, 6360.
4. (a) S. A. Westcott, T. B. Marder, R. T. Baker, R. L. Harlow, J. C. Calabrese, K. C. Lam and Z. Lin, *Polyhedron*, 2004, **23**, 2665; (b) H. Braunschweig, K. Radacki, D. Rais and G. R. Whittell, *Angew. Chem. Int. Ed.*, 2005, **44**, 1192; (c) J. M. Murphy, J. D. Lawrence, K. Kawamura, C. Incarvito and J. F. Hartwig, *J. Am. Chem. Soc.*, 2006, **128**, 13684.
5. (a) H. Braunschweig, K. Radacki, F. Seeler and G. R. Whittell, *Organometallics*, 2004, **23**, 4178; (b) Y. Kawano, T. Yasue and M. Shimoi, *J. Am. Chem. Soc.*, 1999, **121**, 11744; (c) H. Nakazawa, M. Itazaki and M. Ohba, *J. Organomet. Chem.*, 2007, **692**, 201.
6. (a) C. N. Muhoro, X. He and J. F. Hartwig, *J. Am. Chem. Soc.*, 1999, **121**, 5033; (b) W. H. Lam and Z. Lin, *Organometallics*, 2000, **19**, 2625; (c) G. Alcaraz, E. Clot, U. Helmstedt, L. Vendier and S. Sabo-Etienne, *J. Am. Chem. Soc.*, 2007, **129**, 8704.
7. (a) T. Kakizawa, Y. Kawano and M. Shimoi, *Organometallics*, 2001, **20**, 3211; (b) Y. Kawano, K. Yamaguchi, S.-Y. Miyake, T. Kakizawa and M. Shimoi, *Chem. – Eur. J.*, 2007, **13**, 6920.
8. J. W. Taylor, A. McSkimming, M. E. Moret and W. H. Harman, *Angew. Chem. Int. Ed.*, 2007, **56**, 10413.
9. (a) A. A. Dickinson, D. J. Willock, R. J. Calder and S. Aldridge, *Organometallics*, 2002, **21**, 1146; (b) J. Uddin, C. Boehme and G. Frenking, *Organometallics*, 2000, **19**, 571.
10. (a) W. de Graaf, J. Boersma, W. J. J. Smeets, A. L. Spek and G. van Koten, *Organometallics*, 1989, **8**, 2907; (b) Y. Tanaka, H. Yamashita, S. Shimada and M. Tanaka, *Organometallics*, 1997, **16**, 3246.
11. T. Yasue, Y. Kawano and M. Shimoi, *Chem. Lett.*, 2000, 58.
12. (a) K. M. Waltz and J. F. Hartwig, *J. Am. Chem. Soc.*, 2000, **122**, 11358; (b) C. E. Webster, Y. Fan, M. B. Hall, D. Kunz and J. F. Hartwig, *J. Am. Chem. Soc.*, 2003, **125**, 858.
13. (a) H. Chen and J. F. Hartwig, *Angew. Chem. Int. Ed.*, 1999, **38**, 3391; (b) J. F. Hartwig, K. S. Cook, M. Hapke, C. D. Incarvito, Y. Fan, C. E. Webster and M. B. Hall, *J. Am. Chem. Soc.*, 2005, **127**, 2538.
14. (a) D. G. Musaev, A. M. Mebel and K. Morokuma, *J. Am. Chem. Soc.*, 1994, **116**, 10693; (b) Y. Abe, K. Kuramoto, M. Ehara, H. Nakatsuji, M. Suginome, M. Murakami and Y. Ito, *Organometallics*, 2008, **27**, 1736.
15. T. Yasue, Y. Kawano and M. Shimoi, *Angew. Chem. Int. Ed.*, 2003, **42**, 1727.
16. (a) H. Braunschweig, K. Radacki and K. Uttinger, *Angew. Chem. Int. Ed.*, 2007, **46**, 3979; (b) H. Braunschweig, K. Radacki, D. Rais and D. Scheschkewitz, *Angew. Chem. Int. Ed.*, 2005, **44**, 5651.
17. (a) H. Braunschweig, K. Radacki, D. Rais and K. Uttinger, *Angew. Chem. Int. Ed.*, 2006, **45**, 162; (b) H. Braunschweig, K. Radacki and A. Schneider, *Science*, 2010, **328**, 345–347.

18. H. Braunschweig, R. D. Dewhurst, J. O. C. Jiménez-Halla, E. Matito and J. H. Müssig, *Angew. Chem. Int. Ed.*, 2018, **57**, 412.

19. (a) S. Aldridge and D. L. Coombs, *Coord. Chem. Rev.*, 2004, **248**, 535; (b) H. Braunschweig and M. Colling, *Eur. J. Inorg. Chem.*, 2003, 393.

20. (a) D. L. Coombs, S. Aldridge, A. Rossin, C. Jones and D. J. Willock, *Organometallics*, 2004, **23**, 2911; (b) S. Aldridge, A. Rossin, D. L. Coombs and D. J. Willock, *Dalton Trans.*, 2004, 2649.

21. (a) H. Braunschweig, C. Kollann and U. Englert, *Angew. Chem. Int. Ed.*, 1998, **37**, 3179; (b) H. Braunschweig, M. Colling, C. Kollann, H. G. Stammler and B. Neumann, *Angew. Chem. Int. Ed.*, 2001, **40**, 2298; (c) H. Braunschweig, M. Colling, C. Kollann, K. Merz and K. Radacki, *Angew. Chem. Int. Ed.*, 2001, **38**, 4198; (d) H. Braunschweig, K. Radacki, D. Scheschkewitz and G. R. Whittell, *Angew. Chem. Int. Ed.*, 2005, **44**, 1658; (e) H. Braunschweig, M. Colling, C. Hu and K. Radacki, *Angew. Chem. Int. Ed.*, 2003, **42**, 205.

22. (a) A. W. Ehlers, E. J. Baerends, F. M. Bickelhaupt and U. Radius, *Chem. - Eur. J.*, 1998, **4**, 210; (b) J. Uddin, C. Boehme and G. Frenking, *Organometallics*, 2000, **19**, 571.

23. D. L. Kays, J. K. Day, S. Aldridge, R. W. Harrington and W. Clegg, *Angew. Chem. Int. Ed.*, 2006, **45**, 3513.

24. (a) H. Braunschweig and B. Ganter, *J. Organomet. Chem.*, 1997, **545**, 163; (b) H. Braunschweig, M. Colling, C. Hu and K. Radacki, *Angew. Chem. Int. Ed.*, 2002, **39**, 1415; (c) H. Braunschweig, M. Burzler, T. Kupfer, K. Radacki and F. Seeler, *Angew. Chem. Int. Ed.*, 2007, **46**, 7785; (d) H. Braunschweig, M. Burzler, K. Radacki and F. Seeler, *Angew. Chem. Int. Ed.*, 2007, **46**, 8071; (e) H. Braunschweig, C. Burschka, M. Burzler, S. Metz and K. Radacki, *Angew. Chem. Int. Ed.*, 2006, **45**, 4352.

25. (a) H. Braunschweig, K. Radacki, D. Rais and K. Uttinger, *Organometallics*, 2006, **25**, 5159; (b) H. Braunschweig, K. Radacki, D. Rais and F. Seeler, *Angew. Chem. Int. Ed.*, 2006, **45**, 1066.

26. (a) C. A. Jaska and I. Manners, *Inorganic Chemistry in Focus II*, ed. G. Meyer, D. Naumann and L. Wesemann, Wiley-VCH, Weinheim, 2005, pp. 53–64; (b) C. W. Hamilton, R. T. Baker, A. Staubitzc and I. Manners, *Chem. Soc. Rev.*, 2009, **38**, 279; (c) H. C. Johnson, T. N. Hooper and A. S. Weller, *Top. Organomet. Chem.*, 2015, **49**, 153; (d) A. Staubitz, A. P. M. Robertson, M. E. Sloan and I. Manners, *Chem. Rev.*, 2010, **110**, 4023; (e) A. Staubitz, A. P. M. Robertson and I. Manners, *Chem. Rev.*, 2010, **110**, 4079; (f) A. Rossin and M. Peruzzini, *Chem. Rev.*, 2016, **116**, 8848; (g) J. Choi, A. H. R. MacArthur, M. Brookhart and A. S. Goldman, *Chem. Rev.*, 2011, **111**, 1761; (h) E. M. Leitao, T. Jurca and I. Manners, *Nat. Chem.*, 2013, **5**, 817; (i) R. Waterman, *Chem. Soc. Rev.*, 2013, **42**, 5629.

27. A. Paul and C. B. Musgrave, *Angew. Chem. Int. Ed.*, 2007, **46**, 8153.

28. Y. Kawano, M. Uruichi, M. Shimoi, S. Taki, T. Kawaguchi, T. Kakizawa and H. Ogino, *J. Am. Chem. Soc.*, 2009, **131**, 14946.

29. (a) C. A. Jaska, K. Temple, A. J. Lough and I. Manners, *J. Am. Chem. Soc.*, 2003, **125**, 9424; (b) T. J. Clark, K. Lee and I. Manners, *Chem. – Eur. J.*, 2006, **12**, 8634.

30. R. J. Keaton, J. M. Blacquiere and R. T. Baker, *J. Am. Chem. Soc.*, 2007, **129**, 1844.

31. W. Hieber and U. Teller, *Z. Anorg. Allg. Chem.*, 1942, **249**, 43.

32. W. R. Robinson and D. P. Schussler, *Inorg. Chem.*, 1973, **12**, 848.

33. J. M. Burlitch, M. E. Leonowicz, R. B. Petersen and R. E. Hughes, *Inorg. Chem.*, 1979, **18**, 1097.

34. J. Su, X. W. Li, R. C. Crittendon, C. F. Campana and G. H. Robinson, *Organometallics*, 1997, **16**, 4511.

35. J. Uddin and G. Frenking, *J. Am. Chem. Soc.*, 2001, **123**, 1683.

36. R. A. Fischer and J. Weiss, *Angew. Chem. Int. Ed.*, 1999, **38**, 2830.

37. C. Gemel, T. Steinke, M. Cokoja, A. Kempter and R. A. Fischer, *Eur. J. Inorg. Chem.*, 2004, 4161.

38. G. Linti and H. Schnoeckel, *Coord. Chem. Rev.*, 2000, **206–207**, 285.
39. N. A. Compton, R. J. Errington and N. C. Norman, *Adv. Organomet. Chem.*, 1990, **31**, 92.
40. P. J. Brothers and P. P. Power, *Adv. Organomet. Chem.*, 1996, **39**, 1.
41. T. Muraoka and K. Ueno, *Coord. Chem. Rev.*, 2010, **254**, 1348.

---

[1] Deceased

Chapter 10

Chemistry of Transition Metal Complexes with Group 15 Elements: Transition Metal Complexes with One Lone Pair of Electrons on the Coordinating Atom

Hiroyuki Matsuzaka[a] and Tsutomu Mizuta,[b]

[a] Osaka Prefecture University, Japan matuzaka@c.s.osakafu-u.ac.jp
[b] Hiroshima University, Japan tmizuta@hiroshima-u.ac.jp

10.1 Introduction

Group 15 elements (N, P, As, Sb, Bi) form molecules of the type ER_3 (E = N, P, As, Sb, Bi; R = alkyl, aryl, *etc*.) with one lone pair of electrons on the E atom. These molecules serve as 2e donors to transition metal centers, forming dative bonds ($M–ER_3$). Based on detailed studies of the preparation and properties of a series of transition metal complexes bearing NR_3 ligands, Werner proposed his "coordination theory" at the end of the 19th century.

Much interest has recently been focused on transition metal complexes bearing Group 15 element ligands with a different type of coordination mode. A typical example is $M–ER_2$, in which one of the R groups of an ER_3 molecule is substituted by a transition metal fragment. An ER_2 ligand can serve as a 1e donor to a metal center to form a polar, covalent M–E

bond, as in the case of the isoelectronic alkyl ligands ($-CR_3$) (Section 3.1). This chapter outlines the chemistry of transition metal complexes with amide ($-NR_2$) and phosphide ($-PR_2$) ligands.

10.2 Transition Metal Complexes with Nitrogen Coordination

As noted above, transition metal complexes of the type $M-NR_3$ and $M-NR_2$ exhibit different M–N bonding modes. The former has a dative M–N bond, whereas the latter contains a polar covalent M–N bond. Consequently, these two types of complexes show different reactivity. Before discussing the structure and bonding of $M-NR_2$ type complexes, it is helpful to briefly review the bonding in $M-NR_3$ complexes.

10.2.1 M–N Bond in Transition Metal Amine Complexes

A simple picture of the bonding of NR_3 to a metal center (M) is that the nitrogen atom is a Lewis base by virtue of its ability to σ donate its lone pair of electrons to the metal. A more formal description of M–N bonding can be derived from the orbital interaction between NR_3 and M. The degree of orbital interaction depends on the energy gap between the orbitals and the amount of their net overlap. Interactions between orbitals of different energies become stronger as their energies converge. Also, interactions between orbitals occur more effectively as the amount of their overlap increases. The HOMO of NR_3 is a nonbonding (*i.e.* lone pair) orbital, localized on the nitrogen atom. This lone pair orbital overlaps effectively with the energetically higher nd, $(n + 1)$s, and $(n + 1)$p orbitals of M to form an M–N dative σ-bond (Section 2.4.2 (2)). Figure 10.1 shows an example of such an interaction, in which NR_3 serves as a 2e σ-donor to a metal center.
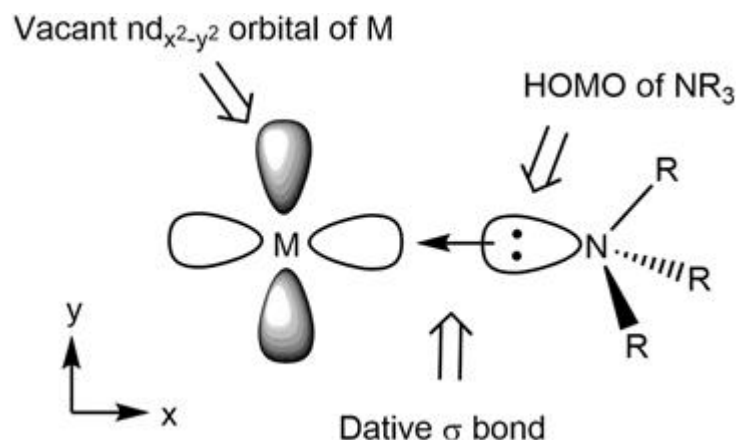
Figure 10.1 Formation of an M–NR$_3$ σ-bond.

Oxidation of a metal center lowers the energies of its orbitals. As a result, the energy gap between the HOMO of NR$_3$ and the metal nd, $(n + 1)$s and $(n + 1)$p orbitals decreases (ΔE in Figure 10.2, right), which leads to more effective interaction between these orbitals to form a stronger M–N bond. NR$_3$ is a σ-donor ligand and tends to form stronger M–N bonds with metals in higher oxidation states. This is in sharp contrast to CO, which prefers low valent transition metal centers. CO acts both as a σ-donor and as a π-acceptor when coordinating to metals, and forms a stronger M–C bond with electron-rich metals (Section 3.2.2).

10.2.2 M–N Bond in Transition Metal Amide Complexes[1]

It was noted above that NR_3 serves as a 2e σ-donor to M to form a dative M–N bond. In contrast, an amide ligand ($-NR_2$) serves as a one-electron σ-donor to M to form a polar covalent M–N bond, as in the case of the isoelectronic alkyl ligands ($-CR_3$) (Section 3.1). Considering the Allred–Rochow electronegativity of N (3.1) and C (2.5), given inside the cover of this book, the M–N bond in amide complexes is expected to be more polar than the M–C bond in alkyl complexes. The M–N bond of amide complexes of metals in Groups 1 to 3 has been reported to be highly polar (ionic), whereas the M–N bond of many transition metal amide complexes has been found to be polar covalent.

    The most important feature of an amide ligand is the presence of a lone pair orbital on the nitrogen atom, which can contribute to form a M–N π-bond. When an empty d_π orbital is available in the valence shell of M, the lone pair orbital on N overlaps with the empty d_π orbital to form a M–N π-bond (Figure 10.3) in addition to the M–N σ-bond described above. Consequently, the M–N bond possesses multiple bond character. The π overlap between the lone pair orbital on N and the empty d_π orbital on M is facilitated by a planar coordination geometry at $N(sp^2)$. For the π-bonding case, the amide ligand thus behaves as a 3e donor (*i.e.* 1e σ-donor and 2e π-donor; Section 2.4.2 (3)).
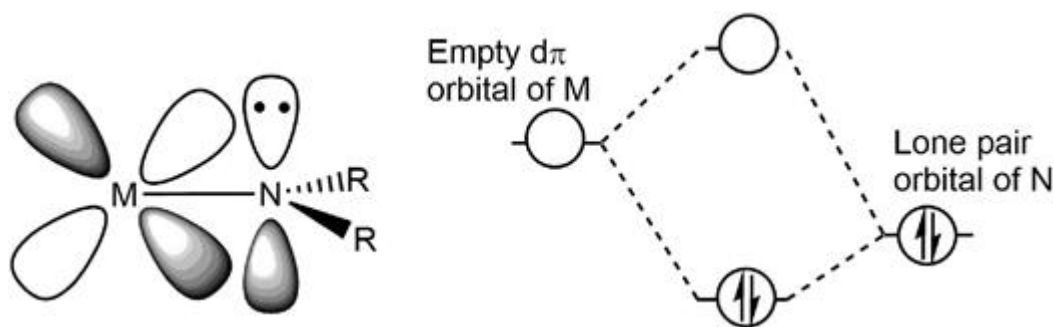
Figure 10.3   Formation of a M–N π-bond. An amide ligand behaves as a 3e donor (*i.e.* 1e σ-donor and 2e π-donor).

Similar π-type interaction has been found in organic amides (RCONR′$_2$), in which a lone pair orbital on N with planar geometry overlaps with an empty π* orbital of an adjacent carbonyl group (Figure 10.4).
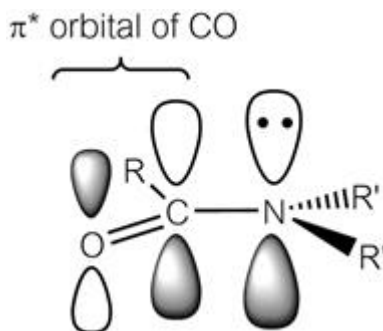
π* orbital of CO

Figure 10.4   π-Type interaction in organic amides (RCONR′$_2$) in which a lone pair orbital on N with planar geometry overlaps with an empty π* orbital of an adjacent carbonyl group.

In complexes containing early transition metals, the metal center is often d^0, and there are fewer than 18 electrons in the metal valence electron shell. There are therefore empty d$_\pi$ orbitals available to form a M–N π-bond. Amide complexes of early transition metals constitute the largest body of well-characterized thermally stable amide complexes. An easy decomposition route exists for isoelectronic complexes with alkyl ligands (–CR$_3$), involving β hydride elimination to give hydride(alkene) complexes (Section 6.4.3). The analogous decomposition pathway for amide complexes of early transition metals forming a hydride(imine) complex is clearly not a dominant characteristic of their chemistry, presumably due to the strong M–N bond in these species (Section 10.2.4). Formation of M–N π-bonds in these complexes is supported by photoelectron spectroscopy and thermodynamically measured M–N bond energies as well as by computational studies.

X-ray diffraction analysis of [W(NMe$_2$)$_6$] (**1**) revealed a regular octahedral WN$_6$ structure in which the W–NC$_2$ units are all planar and arranged in three mutually perpendicular planes involving *trans*-C$_2$N–W–NC$_2$ units. The d$_\pi$–p$_\pi$ overlap in **1** based on these structural data is shown Figure 10.5. The molecular orbital energy level diagram generated by d$_\pi$–p$_\pi$ overlap in **1** is depicted in Figure 10.6. In this configuration, tungsten

attains an 18e valence shell as a result of forming six W–N σ-bonds and three W–N π-bonds (see Chapter 3). The latter are completely delocalized over the WN_6 moiety, leading to an average W–N bond order of 1.5. There is also a triply degenerate, essentially nonbonding, molecular orbital arising from the remaining six NMe_2 π electrons.[2] Photoelectron spectroscopy of **1** supports this bonding scheme (Scheme 10.1).
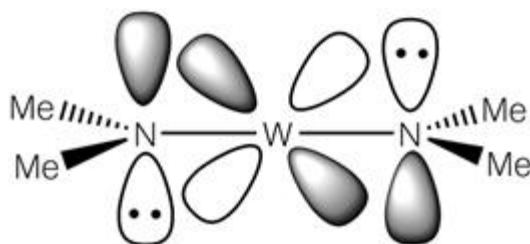
Figure 10.5 d_π–p_π interaction in $[W(NMe_2)_6]$ (**1**). Orbital overlap in one of the three mutually perpendicular planes involving *trans*-C_2N–W–NC_2 units is shown.
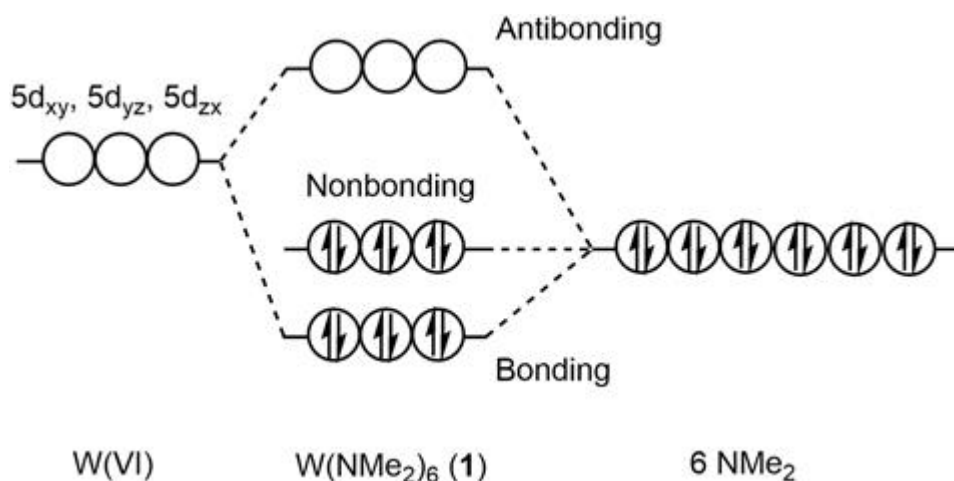
Figure 10.6 Molecular orbital energy level diagram generated by d_π–p_π interaction in $[W(NMe_2)_6]$ (**1**) and the ground state electronic configuration.

W-N, 2.03 Å
N-C, 1.51 Å
C-N-C, 104.9 deg

1
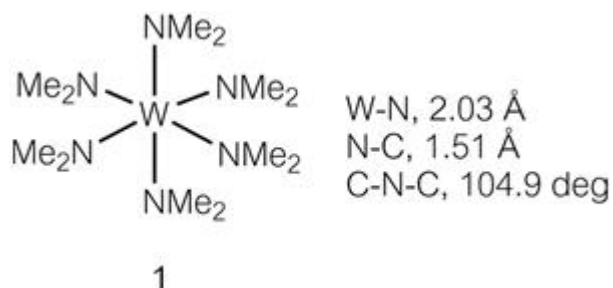
In the past, there were relatively few reports of well-characterized amide complexes of late transition metals compared to those of early transition metals. Since an amide ligand may serve as a 3e hard Lewis base donor (1e σ- and 2e π-donor), it was considered that strong bonding to electron-rich late transition metals (soft Lewis acids) would not be as favorable as for the early transition metals (hard Lewis acids). However, the number of well-characterized amide complexes of late transition metals has been increasing rapidly due to growing interest in the potential catalytic application of these complexes, especially of the second and third row metals. An amide ligand can form a M–N π-bond with a late transition metal center, stabilizing the complex, if there is an empty d_π orbital of suitable energy available. This is generally the case in 16e metal complexes with low coordination numbers (≤6). In contrast, if a metal center attains an 18e valence shell (*i.e.* it is coordinatively saturated; see Section 2.1 to 2.4), d_π–p_π overlap does not take place since such interaction would destabilize the system (Figure 10.7). Instead, a nucleophilic/basic nitrogen center with pyramidal geometry (Figure 10.8), in which the amide ligand serves as a 1e σ-donor to M, results.
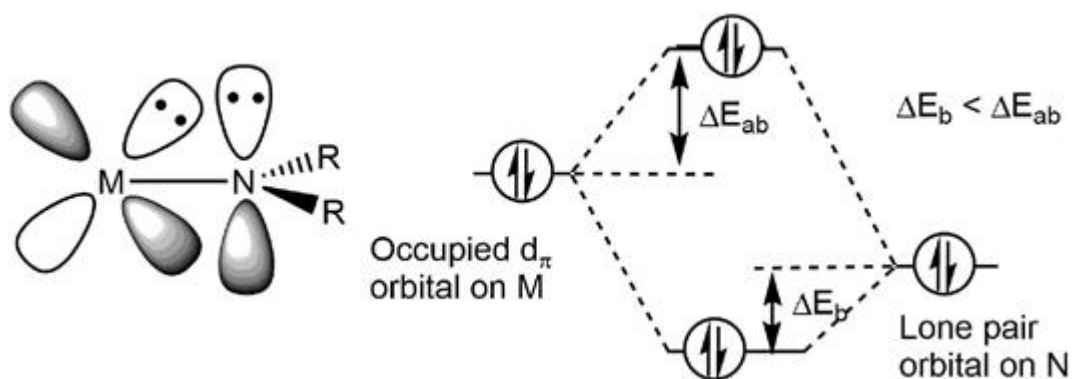
Figure 10.7 Overlap between an occupied d_π orbital on M and a lone pair orbital on N destabilizes the system since $\Delta E_b < \Delta E_{ab}$.
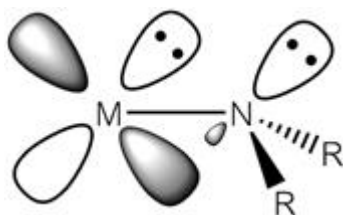
Figure 10.8 Amide ligand as a 1e σ-donor to M containing a nucleophilic/basic nitrogen center with pyramidal geometry.

X-ray diffraction studies of iron and ruthenium amide complexes **2a** and **2b** revealed pyramidal nitrogen atoms in these complexes, in which the parent amide ligand (NH_2) serves as a 1e σ-donor. It is recommended that readers confirm for themselves that the metal centers in **2a** and **2b** attain 18e valence shells. Complex **2b** was found to be strongly basic, similar to the amide compounds of alkali metals, and deprotonates alkynes and ketones (Section 10.2.4). This strong basicity is considered to be due to the lone pair of electrons localized on the pyramidal N^3 (Scheme 10.2).

Fe-N, 2.068 Å
Ru-N, 2.191 Å
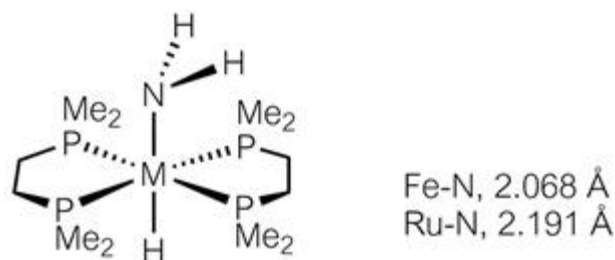
2a, M = Fe; 2b, M = Ru

As noted above, an amide ligand can serve as a π-donor and stabilize a coordinatively unsaturated 16e metal center. Table 10.1 shows the $\Delta H^\ddagger$ values observed for the phosphine dissociation reaction of a series of 18e $[Cp^*Ru(PMe_3)_2X]$ (**3**, $Cp^* = \eta^5\text{-}C_5Me_5$; eqn (10.1)) complexes. The decrease in $\Delta H^\ddagger$ down the series is consistent with the increasing π-donor ability of X to Ru. The NHPh ligand serves as a 1e donor in **3f** and a 3e donor in **4f**.[4]

$$[Cp^*Ru(PMe_3)_2X] \longrightarrow [Cp^*Ru(PMe_3)X] + PMe_3 \qquad (10.1)$$

$$\mathbf{3} \qquad\qquad\qquad\qquad \mathbf{4}$$
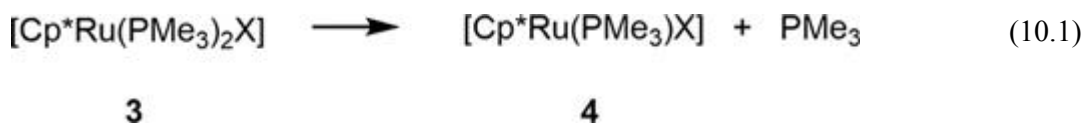
Table 10.1 $\Delta H^{\ddagger}$ values observed for the phosphine dissociation reaction (eqn (10.1)).

Complex	X	$\Delta H^{\ddagger}$ (kJ mol^{-1})
3a	H	> 196
3b	CH$_3$	167
3c	I	150
3d	Cl, SH	138
3e	OH	121
3f	NHPh	117

Treatment of a five-coordinate Ru complex, $[Ru\{1,2\text{-}(NH)_2C_6H_4\}(PPh_3)_3]$ (**5**), with L (L = CH$_2$=CH$_2$, CO and P(OMe)$_3$) did not afford a six-coordinate adduct, but instead yielded the five-coordinate substitution product $[Ru\{1,2\text{-}(NH)_2C_6H_4\}(PPh_3)_2(L)]$) (**6**) (Figure 10.9). Ligand substitution with an excess of the strongly coordinating PMe$_3$ afforded $[Ru\{1,2\text{-}(NH)_2C_6H_4\}(PMe_3)_3]$ (**7**).[5] These results suggest that effective π-donation from the 1,2-(NH)$_2$C$_6$H$_4$ ligand stabilizes the Ru center of **5** to attain a coordinatively saturated 18e structure.
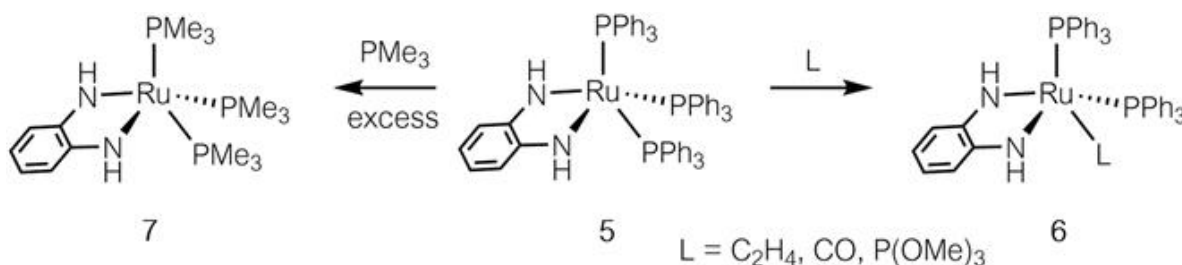
Figure 10.9 Substitution instead of addition has been found to proceed in **5** (L = C$_2$H$_4$, CO, P(OMe)$_3$).

Structural analysis of the 18e complex [Re(*bpy*)(CO)$_3$(NHPh)] (**8**, *bpy* = 2,2′-bipyridine) revealed the planar geometry of the nitrogen atom in the NHPh ligand. In this case, the lone pair orbital on N is considered to overlap not with a filled Re d$_\pi$ orbital, but with an empty π orbital of the Ph group, which leads to multiple bond character in the N–C bond in the NHC$_6$H$_5$ moiety[6] (Scheme 10.3).

8
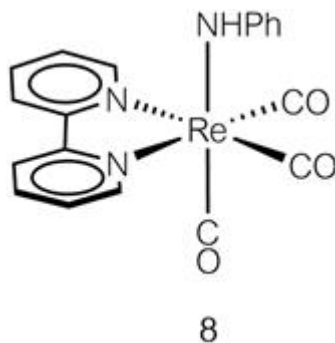
In square planar 16e complexes with d^8 metal centers, all d_π orbitals in the valence shell (d_{xy}, d_{yz}, d_{zx}) are filled. Thus, an amide ligand in such complexes serves as a 1e σ-donor to M. For example, the NMePh ligand in [Pt(*dmpe*)(NMePh)(Me)] (**9**, *dmpe* = $Me_2PCH_2CH_2PMe_2$) is considered to be a 1e donor to the Pt(ii) center. X-ray diffraction of **9** revealed the planar geometry of the nitrogen atom in the NMePh ligand with a dihedral angle between that plane and the Pt(ii) square plane of 68°. The bond distances around the nitrogen atom are given below. These structural data suggest that the lone pair orbital on N overlaps with an empty π orbital of the Ph group, leading to an N–C_{ipso} multiple bond in the $NMeC_6H_5$ moiety[7,8] (Scheme 10.4).

Pt-N, 2.080 Å
N-C(sp^2), 1.361 Å
N-C(sp^3), 1.455 Å

9
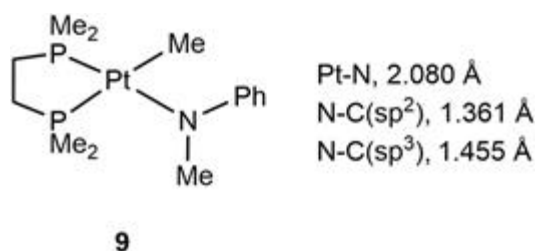
An amide ligand can serve as a 3e donor bridging two metal centers to form a dinuclear structure (Figure 10.10), being a 1e σ-donor to one metal center and a 2e σ-donor to the other, with tetrahedral geometry at the nitrogen atom. This bridging coordination mode of an amide ligand has been frequently found in low valence late transition metal complexes. One such example is [Cp*Ru(μ-NHPh)$_2$RuCp*] (**10**; Cp* = η^5-C_5Me_5).[9] X-ray diffraction analysis of **10** confirmed the dinuclear structure, in which two

Cp*Ru units are bridged by two NHPh ligands with tetrahedral geometry at the nitrogen atoms (Scheme 10.5).
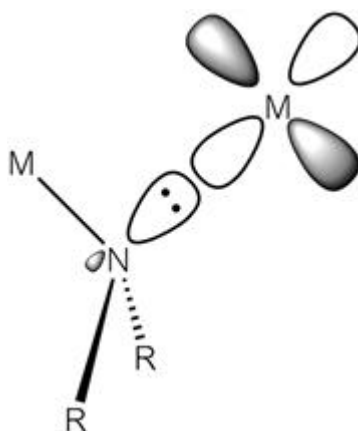
Figure 10.10 An amide ligand as a 3e donor bridging two metal centers.

10
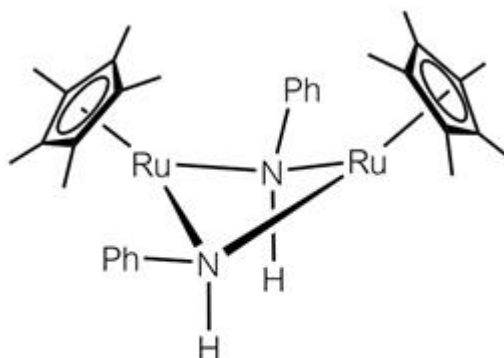
    The ranking of electron donating ability (*i.e.* σ-donation and π-donation) of a series of ligands X has been experimentally established by monitoring v_{CO} values for the square-based pyramidal [RuH(X)(CO)(PBu$^t_2$Me)$_2$] (**11**).[10] Complex **11** would be unsaturated if X were a purely σ-bonded 1e donor to the Ru(ii) center. The presence of the CO ligand in the "16e" species serves as a probe of X → Ru electron donation: a more electron-rich ruthenium center will result in a lower v_{CO} stretching wavenumber due to back donation from the filled Ru d_π orbitals into the CO LUMO (π* orbital)

(Chapter 3.2.2 and 4.2). In order of increasing $X \rightarrow Ru$ electron donation: $H < I < Br \sim C{\equiv}CPh < Cl \sim SPh < OPh \sim NHPh < OBAr_2 \sim OH < OCH_2CF_3 \sim F < OSiPh_3 < OSiMe_3 < OCPh_3 < OEt$ (Scheme 10.6).

11
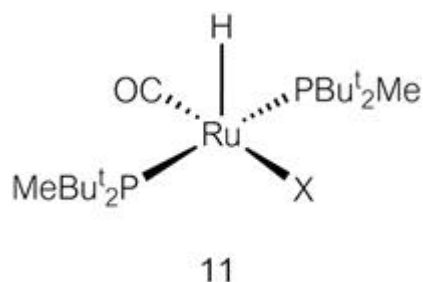
10.2.3 Preparation of Transition Metal Amide Complexes

The general synthetic route to transition metal amide complexes has been treatment of transition metal chlorides with alkali metal amides, most commonly those of lithium (eqn (10.2) to (10.5)) under inert atmosphere conditions.[2,7,9,11]

$$WCl_6 + 6LiNMe_2 \longrightarrow \quad + 6LiCl \qquad (10.2)$$

$$+ LiNHBu^t \longrightarrow \quad + LiCl \qquad (10.3)$$

$$+ LiNMe(Ph) \longrightarrow \quad + \quad LiCl \qquad (10.4)$$
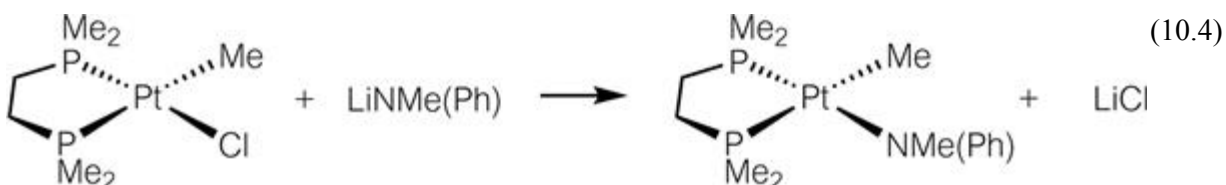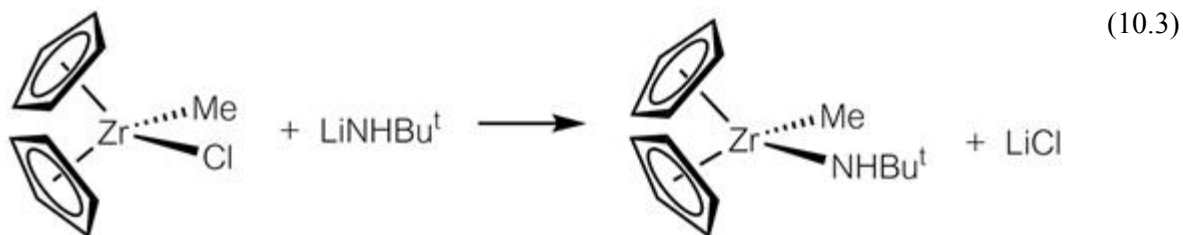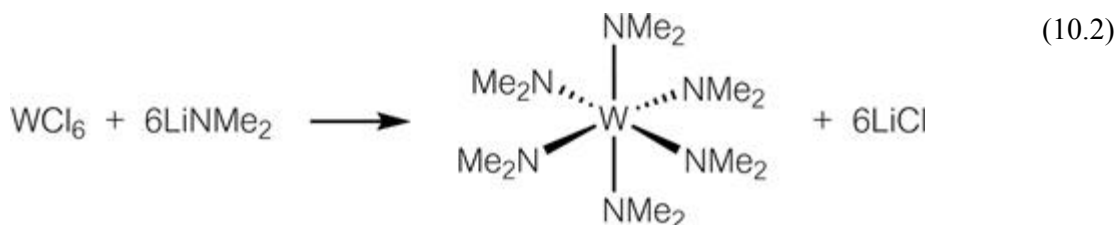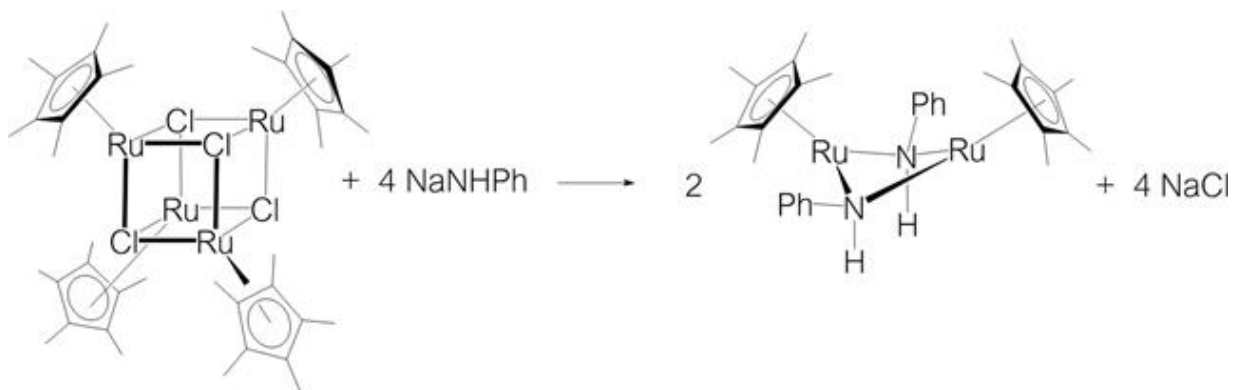
$$(10.5)$$

Displacement of a weakly coordinating OSO_2CF_3 ligand is also a useful approach (eqn (10.6)).[12]
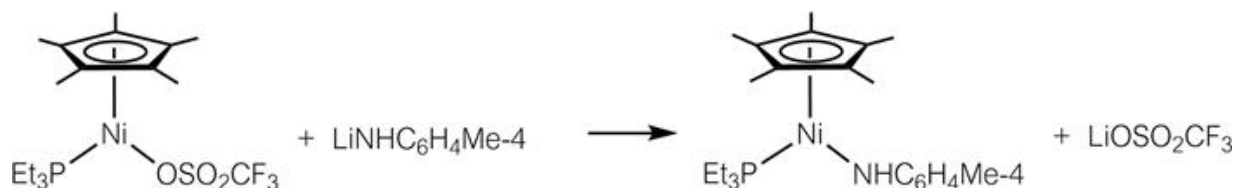
$$(10.6)$$

Additionally, a variety of transition metal amide complexes have been obtained by deprotonation of an amine ligand coordinated to a cationic or neutral metal center (eqn (10.7) to (10.9)).[13,14,15]

$$(10.7)$$

$$(10.8)$$

$$2 \left[\begin{array}{c} \text{H}_{\cdots}\text{Pt}^{\cdots\cdots\text{PPh}_3} \\ \text{Ph}_3\text{P} \quad \text{NH}_3 \end{array} \right] \text{ClO}_4 + 2\,\text{NaNH}_2 \longrightarrow$$

$$\text{H}_{\cdots}\text{Pt} \overset{\text{H}_2}{\underset{\text{H}_2}{\overset{\text{N}}{\underset{\text{N}}{\cdots}}}} \text{Pt}^{\cdots\cdots\text{PPh}_3} + 2\,\text{NH}_3 + 2\,\text{NaClO}_4 + 2\,\text{PPh}_3$$
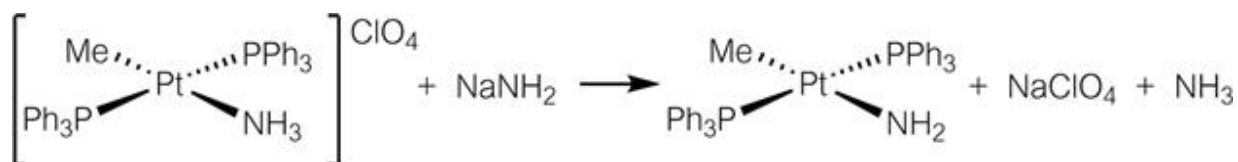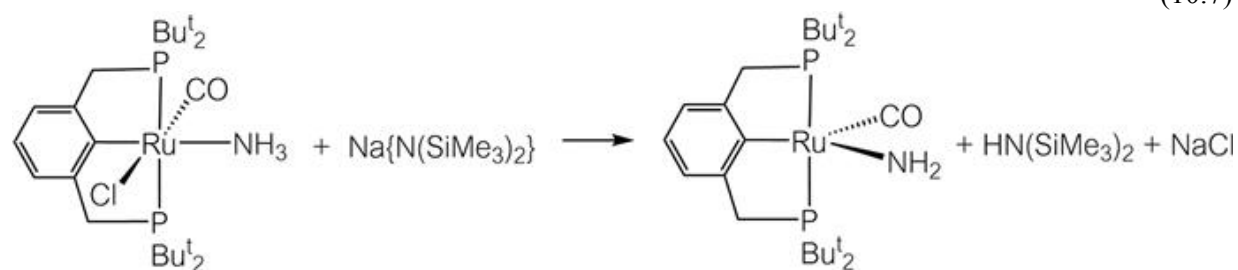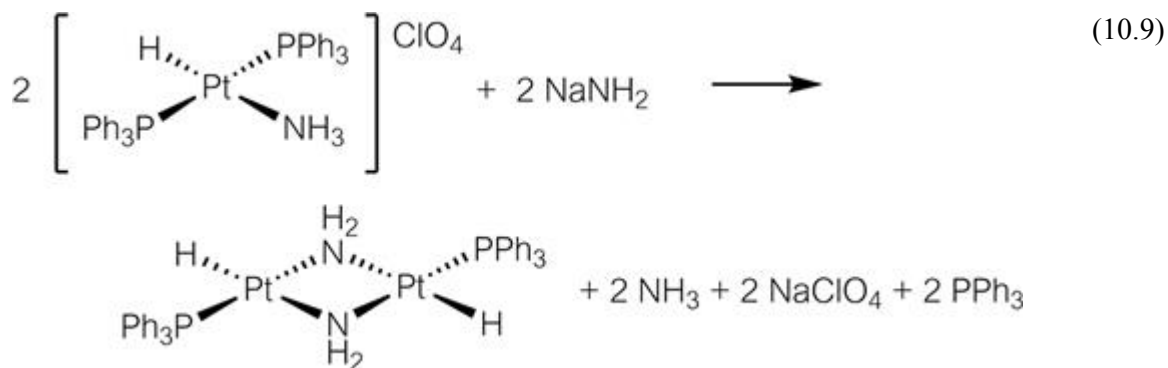
A further route is the oxidative addition of amine N–H bonds to low valence late transition metal centers bearing a labile ligand such as an alkene, which produces amide hydride complexes (eqn (10.10) and (10.11)). Although this approach is not so common compared to the earlier developed synthetic routes described above, the simple oxidative addition of N–H bonds to metal centers is considered to be an essential step in the development of catalytic cycles for hydroamination of alkenes and alkynes, and appears to be of growing importance.[16,17]
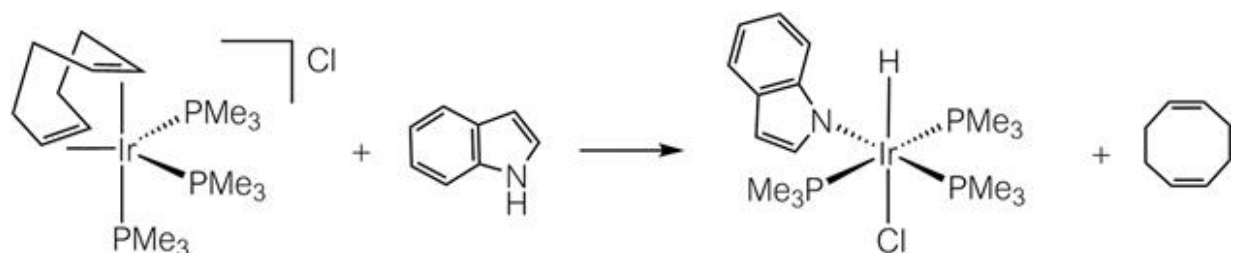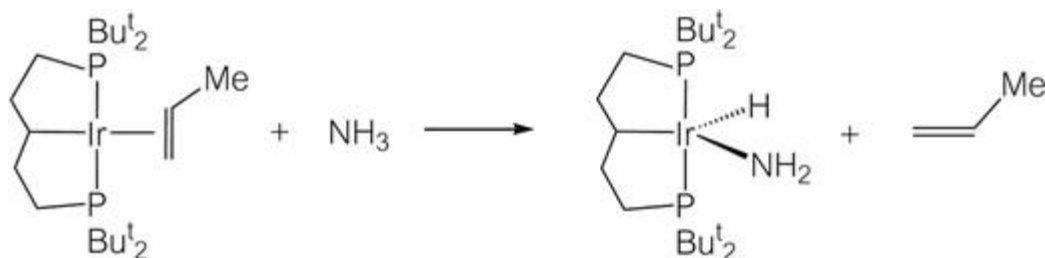
10.2.4 Reactivity of Transition Metal Amide Complexes

Transition metal amide complexes containing pyramidal N atoms act as bases due to the lone pair of electrons localized on the sp^3 hybridized, pyramidal N. Complex **2b**, with a pyramidal N, completely deprotonated fluorene to give the stable cationic ammine complex **12**. Similar deprotonation of cyclobutanone by **2b** initially afforded the corresponding

ammine complex (**13**), from which NH$_3$ slowly dissociated to yield the final product (**14**). Deprotonation of phenyl acetylene and benzyl nitrile readily proceeded to give **15** and **16**, respectively (Figure 10.11).[3]
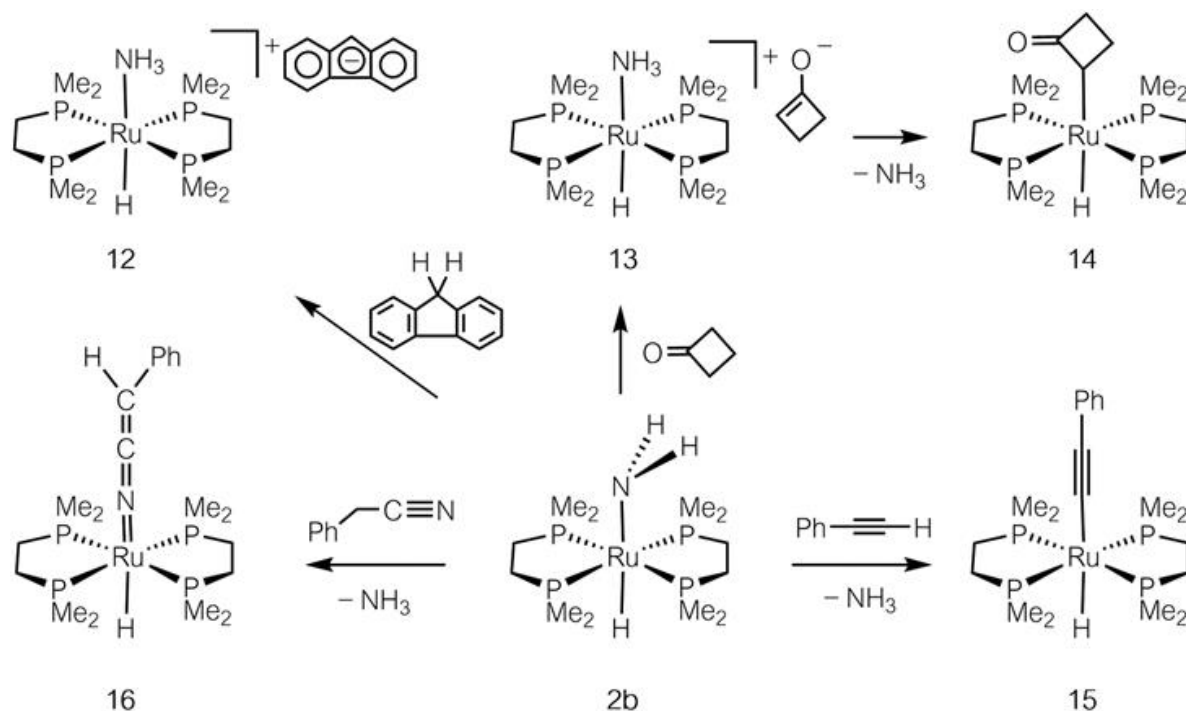
Figure 10.11 Deprotonation of organic substrates by **2b** (stoichiometric reactions).

A stereoselective carbon–carbon bond formation reaction catalyzed by a transition metal amide complex has been developed (Figure 10.12). A ruthenium complex bearing a chiral bis-amide ligand (**17**) deprotonated dimethyl malonate and methyl acetoacetate to form the corresponding amide(amine) complex (**18**), which readily underwent a stereoselective C–C bond formation reaction with cyclopentenone to yield a chiral cyclopentanone derivative and regenerated **17**. Ready interconversion between **17** and **18** is considered to be a key factor in this process.[18]
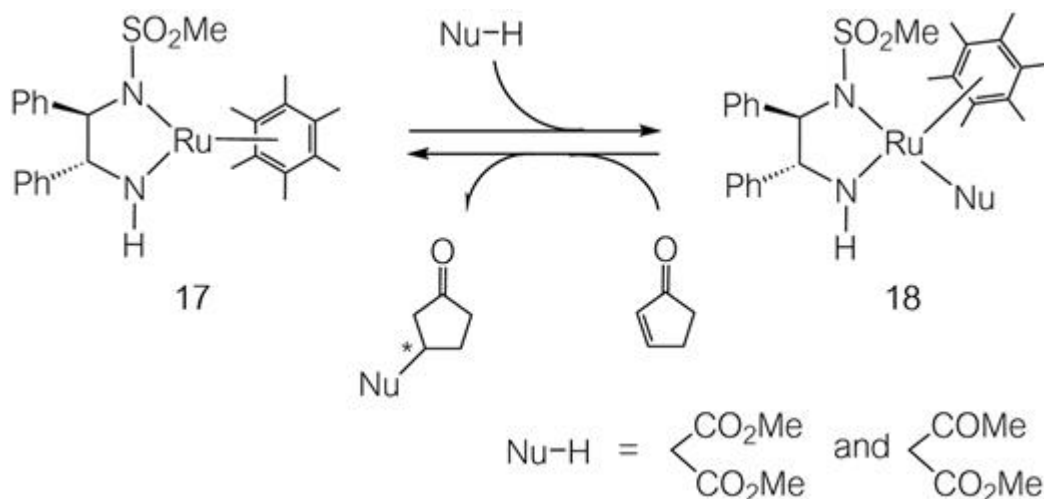
Figure 10.12 Stereoselective carbon–carbon bond formation reaction catalyzed by a Ru complex bearing a chiral bis-amide ligand.

As noted earlier, amide and alkyl ligands are isoelectronic. Insertion of CO into the M–C bond of an alkyl complex L_nM–R to give an acyl complex L_nM–C(O)R is a well-established procedure, and an elementary process in transition metal-catalyzed carbonylation reactions of various organic substrates (Sections 6.4.1, 7.4, and 7.6). In contrast, examples of CO insertion into the M–N bond of an amide complex L_nM–NR_2 to yield a carbamoyl complex L_nM–C(O)NR_2 are still limited (eqn (10.12)).[19]

$$(10.12)$$
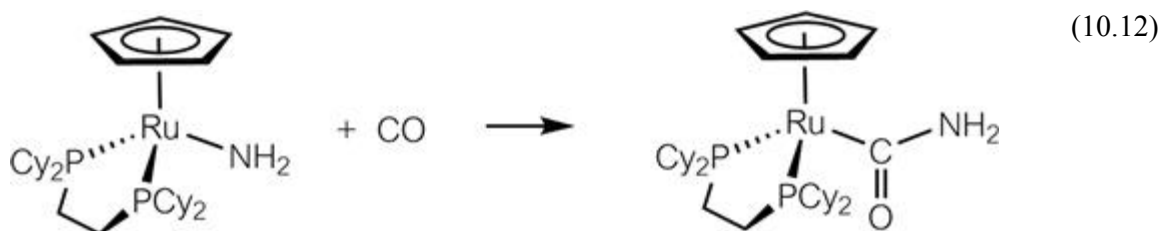
Insertion of CO and CO_2 into the Ru–C, Ru–N and Ru–O bonds in the isoelectronic alkyl (**19a**), amide (**19b**) and alkoxide (**19c**) complexes has been investigated (Figure 10.13).[20] CO exclusively inserted into the Ru–C(sp^2) bonds to yield aroyl complexes (**20** to **22**). On the other hand, CO_2 insertion was observed into the Ru–C(sp^2) bonds for **19a** and **19c**, giving carboxylate complexes **23** and **25**, respectively, but into the Ru–N bond in **19b** to give carbamate complex **24**. Based on kinetic studies and NMR

monitoring of these reactions, insertion of CO_2 into the Ru–C(sp^2) bond of **19c** was proposed to proceed *via* initial coordination of CO_2 to the metal center followed by migration of the aryl substituent. In contrast, a different mechanism was proposed for the CO_2 insertion into the Ru–N bond of **19b**, involving direct attack of the anilide nitrogen atom on CO_2. The high nucleophilicity of the anilide nitrogen atom relative to the aryloxide oxygen atom could account for the mechanistic and selectivity differences between **19b** and **19c**.
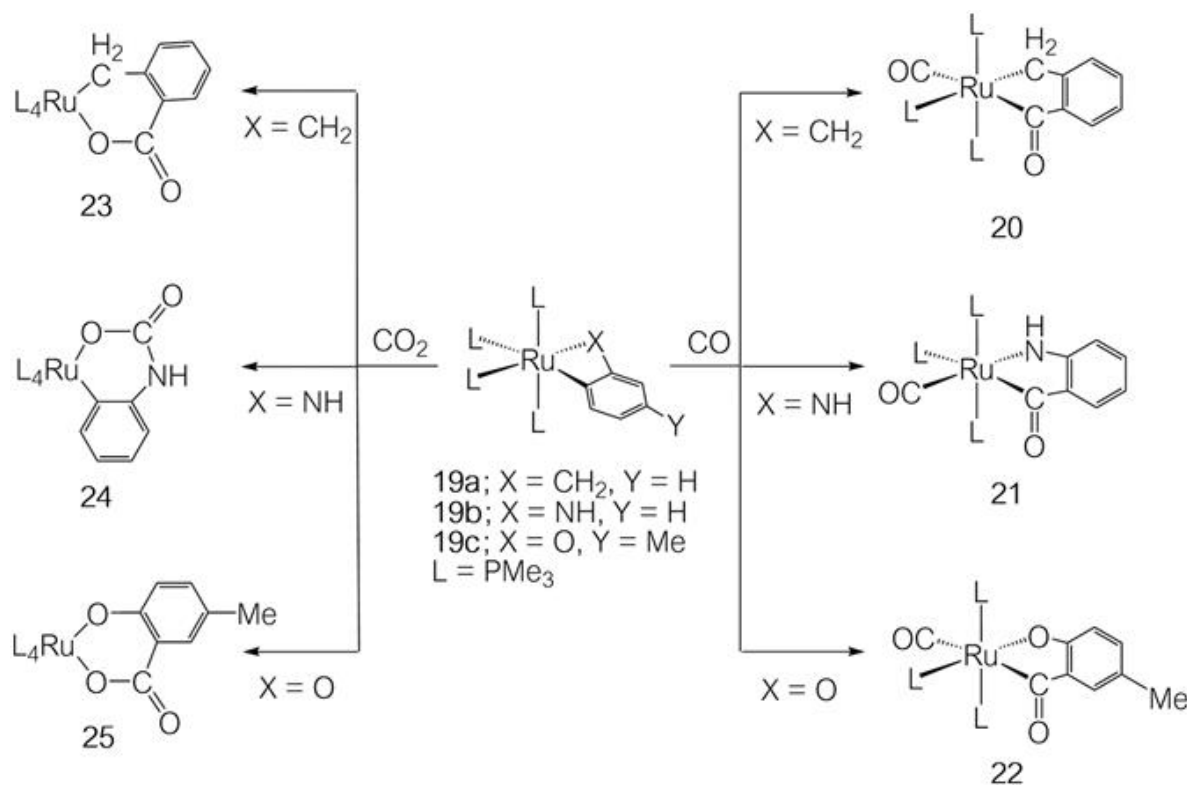
Figure 10.13 Selective insertion of CO and CO_2 into the Ru–C, Ru–N, and Ru–O bond in isoelectronic Ru complexes.

Insertion of alkenes into M–N bonds is considered to be a key step in the hydroamination of alkenes catalyzed by complexes of lanthanide metals (eqn (10.13)). The proposed mechanism is shown in Figure 10.14. Initial aminolysis of alkyl complex **26** generates amide complex **27** as the active catalyst. Coordination and subsequent insertion of the alkene into the M–N

bond gives alkyl intermediate **29**, which undergoes aminolysis to afford the product and regenerate **27**.[21]

$$[Cp^*_2LnCH(SiMe_3)_2]$$

(10.13)

(Ln = La, Nd, Sm, Y, Lu)

$$[Cp^*_2La{-}CH(SiMe_3)_2]$$
26

$$CH_2(SiMe_3)_2$$

27

28

29
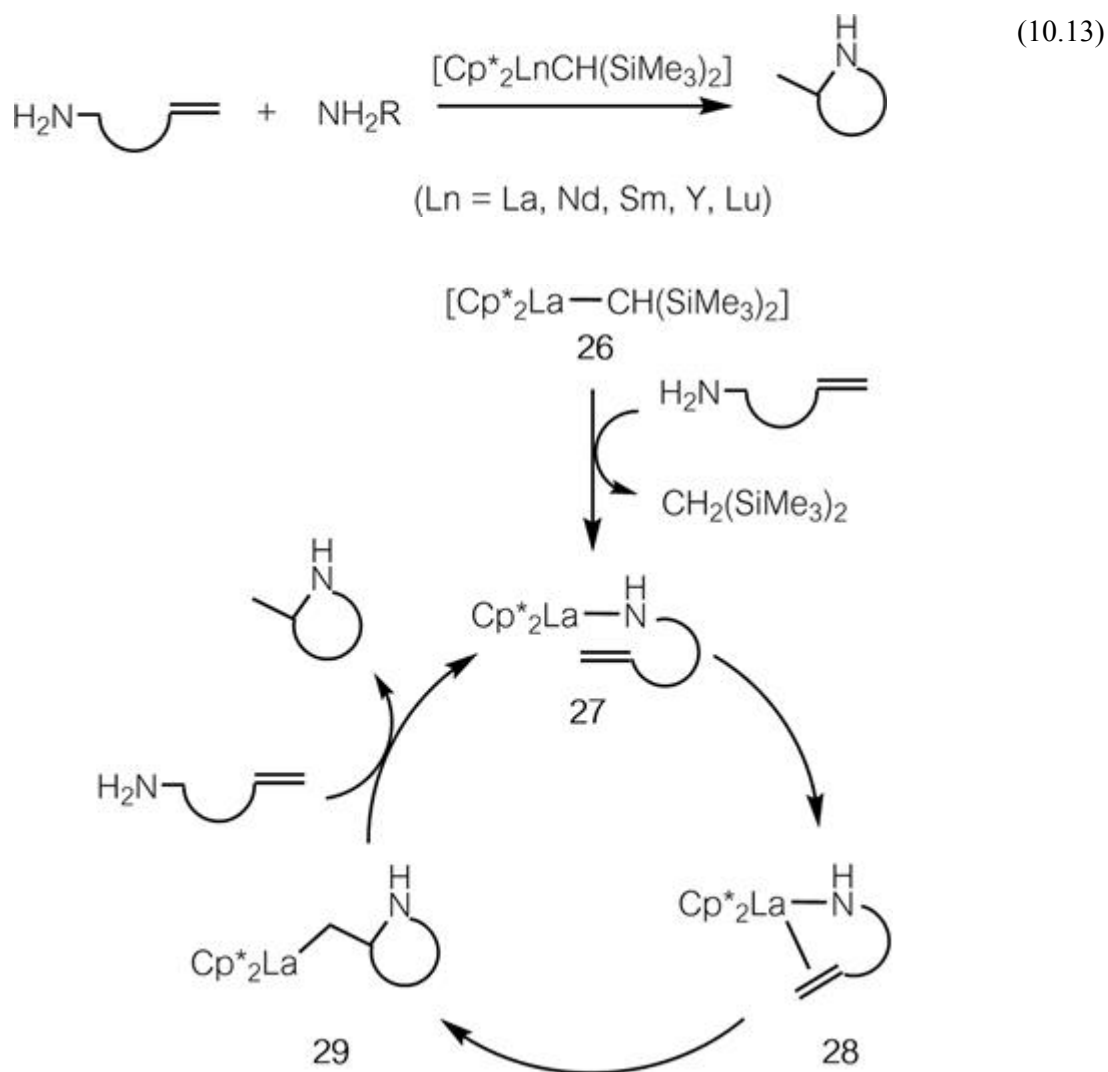
Figure 10.14 Proposed mechanism for cyclohydroamination of an α–ω aminoalkene by using **26** as a catalyst precursor.

β-Hydride elimination in transition metal alkyl complexes affords hydride(alkene) complexes, from which the alkene readily dissociates to afford hydride complexes (Section 6.4.3). Similar β-hydride elimination was reported for the isoelectronic amide complex to initially form a hydride(imine) complex (**32**), which readily liberates the imine to produce a hydride complex (**33**, Figure 10.15).
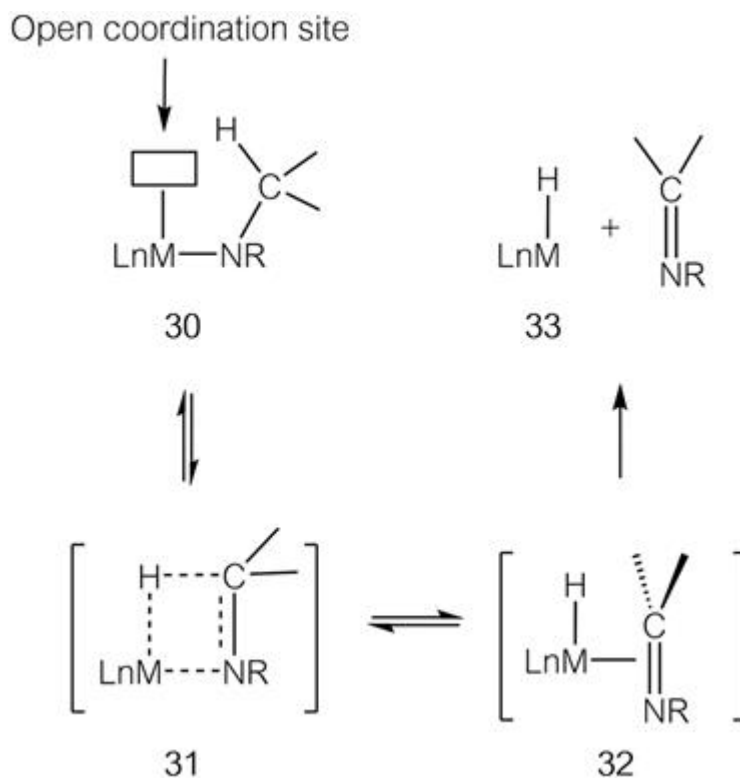
Figure 10.15 Formation of a hydride complex and imine *via* β hydride elimination in an amide complex.

Whether β hydride elimination from amide complexes proceeds readily or not is considered to depend on the M–N bond strength. As noted earlier, amide ligands serve both as σ- and π-donors to electron-deficient early transition metal centers with empty d_π orbitals, and consequently the M–N bond possesses multiple bond character. In this case, β hydride elimination may be effectively suppressed and thermally stable amide complexes have been obtained (for example, eqn (10.2)). On the other hand, β hydride elimination proceeds more easily in the purely σ bonded amide complexes of low valence late transition metals with filled d_π orbitals (Figure 10.16).[22]
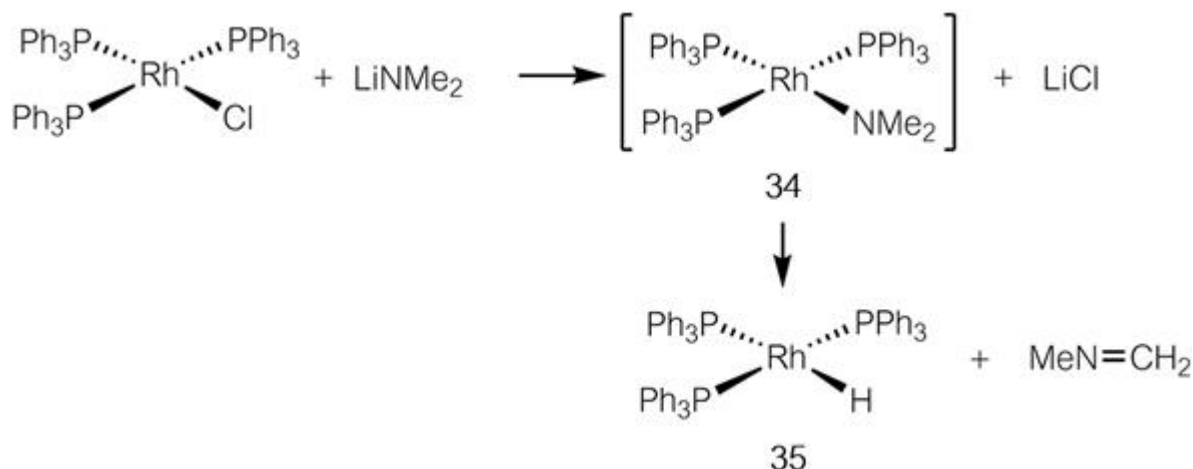
Figure 10.16 Formation of a hydride complex from a transient amide complex *via* β hydride elimination.

10.3 Transition Metal Complexes with Phosphorus Coordination

10.3.1 M-P Bond in Transition Metal Phosphide Complexes

Two types of coordination mode are possible when phosphide ligands (PR_2) form transition metal phosphide complexes, as shown in Figure 10.17(a) and (b).
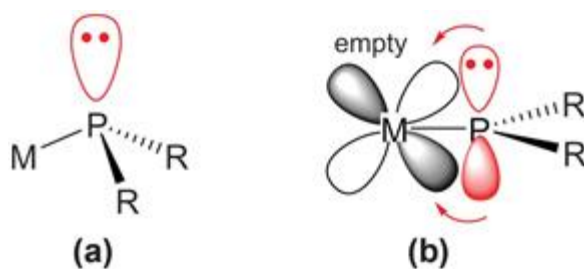
Figure 10.17 Two PR_2 coordination modes, affording (a) trigonal pyramidal and (b) trigonal planar complexes.

These complexes are related to transition metal amide complexes (see Section 10.2.2). The phosphide ligand in type (a) mode is trigonal pyramidal, with an intact, free lone pair of electrons remaining, while in type (b) mode, the lone pair is in a non-hybridized p orbital and also

donates to the metal, forming a π-bond (see Section 2.4.2). Type (a) coordination mode is often observed for both early and late transition metal complexes. However, only some of the early transition metals exhibit type (b) mode, accepting phosphorus p_π electrons into their empty d orbitals. This contrasts with the amide ligands, which have a much stronger preference for the trigonal planar geometry. This is because the second row nitrogen atom can form a strong $p_\pi d_\pi$ bond by effective orbital overlap, while the corresponding interaction of the phosphorus 3p orbital is significantly weaker owing to decreased overlap with the metal d_π orbital. As a result, type (b) phosphide complexes readily dimerize to form bis(phosphide)-bridged binuclear complexes, as shown in eqn (10.14). To avoid dimerization, stereochemical shielding of type (b) P=M bonds through the use of bulky substituents on the phosphorus and/or sterically demanding ligands on the metal is necessary. The lone pair in trigonal pyramidal type (a) species is more basic than a typical PR_3 lone pair because the phosphide ligand has negative formal charge. This high nucleophilicity can induce the dimerization reaction shown in eqn (10.15), where two phosphide complexes with weakly coordinating ligands such as Cl, mutually attack each other's metal centers to form a phosphide-bridged binuclear complex.

$$2\ L_nM{=}P \longrightarrow L_nM \overset{P}{\underset{P}{\diamond}} ML_n \tag{10.14}$$

$$2\ L_nM\overset{P}{\underset{Cl}{}} \longrightarrow \left[L_nM \overset{P}{\underset{P}{\diamond}} ML_n\right]^{2+} 2Cl^- \tag{10.15}$$
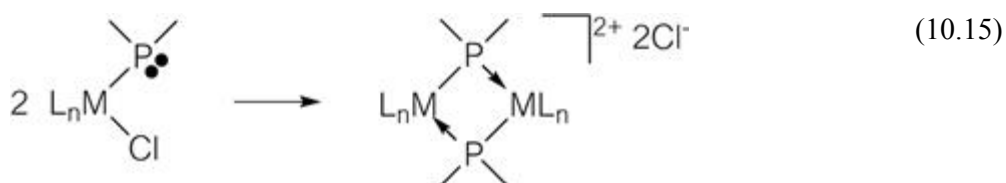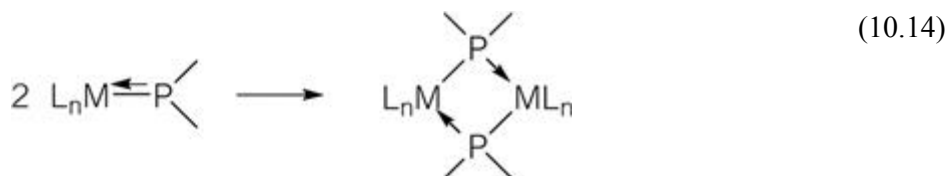
A tertiary phosphine has a high pyramidal atomic inversion barrier, around 125–145 kJ mol^{-1}, which prevents stereoinversion (see Section 4.4) at room temperature. Type (a) phosphide complexes adopt trigonal pyramidal structures like tertiary phosphines, but they readily undergo inversion of the configuration, owing to a much smaller barrier of 25–63 kJ mol^{-1}.[23] In principle, two mechanisms are possible for the inversion, as

shown in Figure 10.18: in (a), inversion takes place with preservation of the M–P bond. In route (b), dissociation and re-coordination of the phosphide ligand occurs.
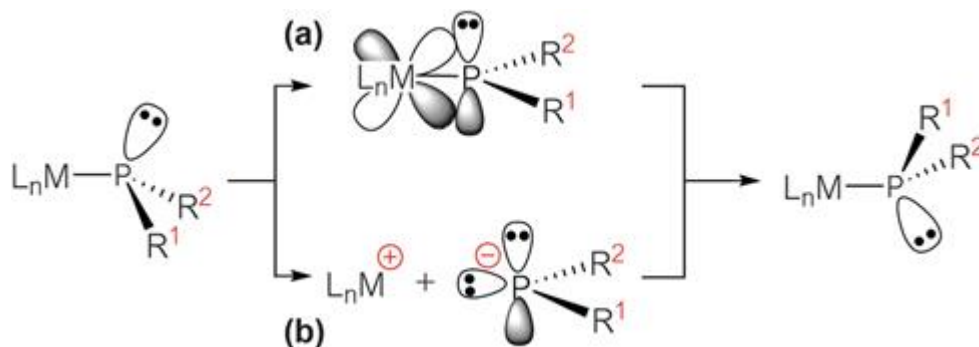
Figure 10.18 Inversion mechanisms of L_nMPR_2 *via* (a) a trigonal planar transition state with p_π–d_π interaction and (b) dissociation and re-coordination processes.

Theoretical calculations indicate that the above-mentioned facile inversion proceeds *via* the former unimolecular mechanism, (a).[24] In the pyramidal structure of a usual tertiary phosphine, the lone pair of electrons are stabilized by hybridization of the p orbitals with the lower energy s orbital. This stabilization is lost in the trigonal planar transition state, because the orbital of the lone pair of electrons becomes a pure p orbital, resulting in a higher energy transition state. However, in the phosphide complex shown in route (a), the p-type lone pair of electrons can be more effectively stabilized by p_π–d_π interaction with an empty d_π metal orbital than can the σ-type lone pair of the starting trigonal pyramidal phosphide complex.

10.3.2 Preparation and Reactivity of Transition Metal Phosphide Complexes

Phosphide complexes can be prepared by metathetical substitution (salt metathesis) of MX with $LiPR_2$, or deprotonation of a secondary phosphine coordinating to a metal fragment as shown in eqn (10.16).

(10.16)
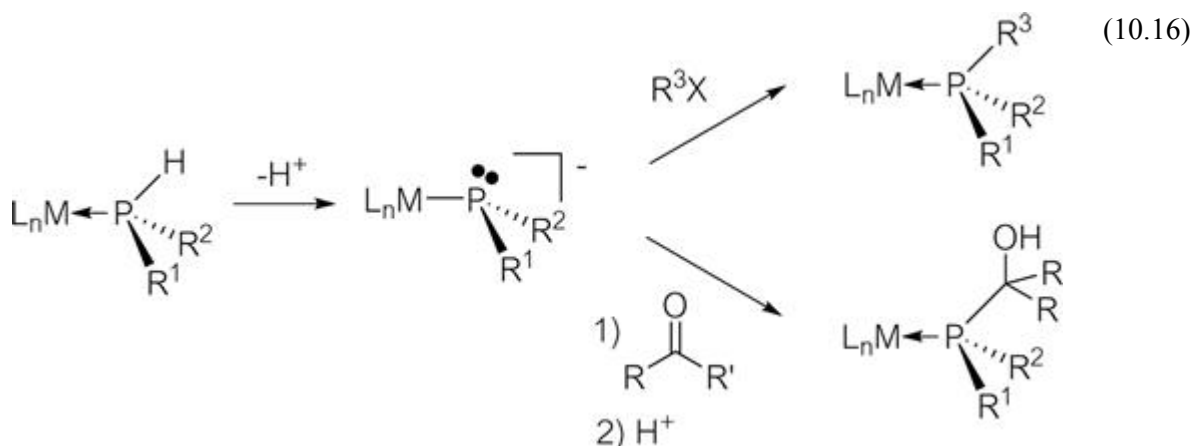
The lone pair of electrons of the phosphide complex is highly nucleophilic and can react with alkyl halide or carbonyl compounds such as aldehydes or ketones to form a P–C bond. Combining this P–C bond formation reaction with the facile steric inversion of the phosphide complex, catalytic conversion of asymmetric secondary phosphines to optically active tertiary phosphines can be achieved as shown in Figure 10.19, if the metal fragment has an axially chiral ligand.[25]
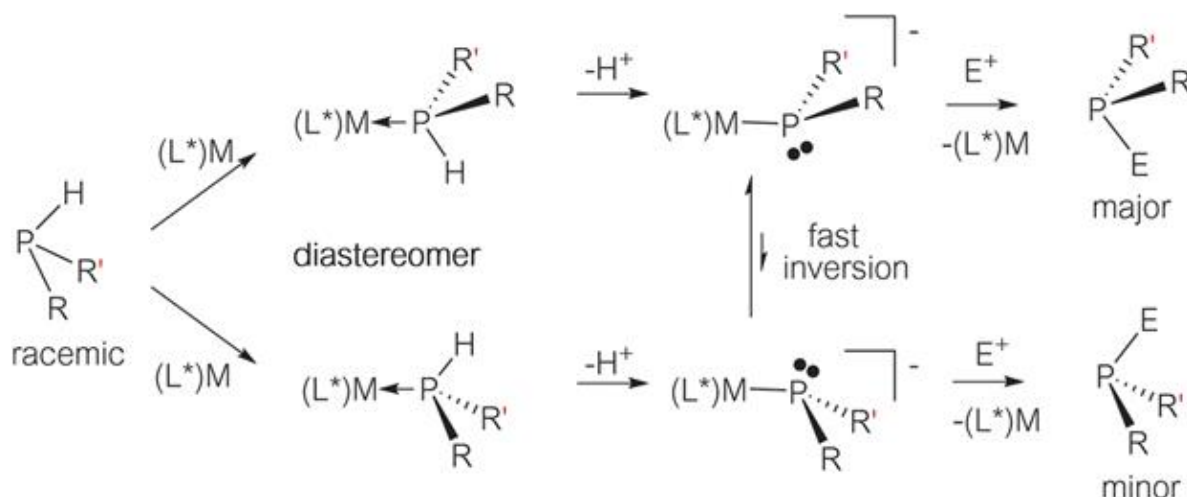
Figure 10.19 In the catalytic synthesis of optically active phosphine, fast equilibrium of inversion is necessary before the electrophilic attack of E^+.

P–C bonds are also formed by reductive elimination when alkyl or aryl groups are present on the metal, since the phosphide–metal bond can be formally regarded as a covalent bond. Olefins can also insert into the M–P

bond. The reaction mechanisms for the reductive elimination and insertion are broadly summarized in Figure 10.20.[25]
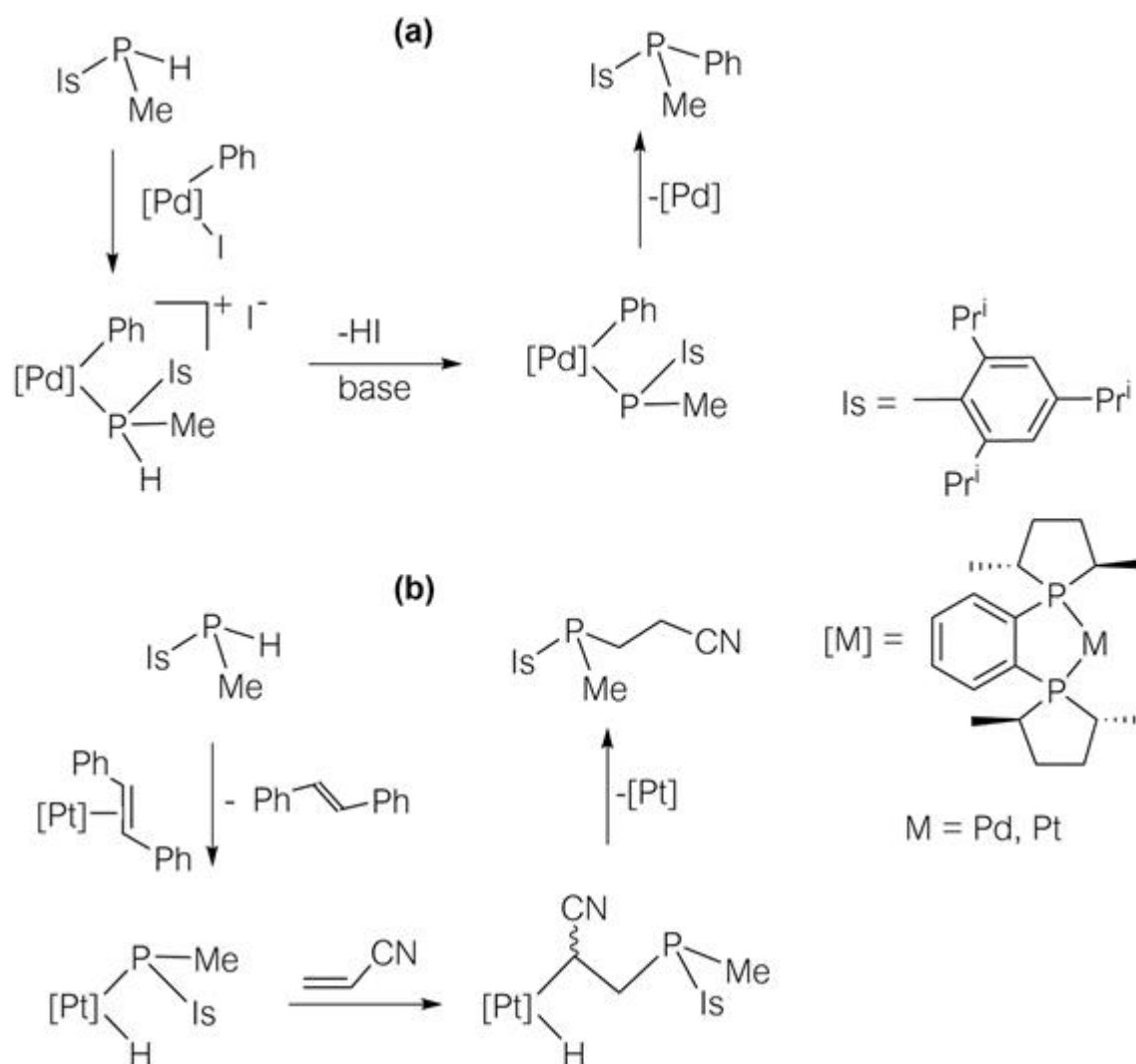
Figure 10.20 (a) Reductive elimination of PR_2 and (b) insertion of a reactive olefin into the Pt–P bond.

10.3.3 Other Types of Phosphorus Ligand

In addition to oxidation state +III, phosphorus may also exhibit the +V oxidation state, resulting in greater diversity as regards structure and bonding for phosphorus ligands compared to N-based ligands. Figure 10.21 summarizes the types of phosphorus ligands reported so far. Types **ii**, **iii**, and **v** have already been mentioned. Here, the unique trivalent mode of **vii**

and the pentavalent modes **i** and **iv** are additionally depicted. The coordination modes of **viii–xii** show phosphorus ligands with a low coordinate phosphorus center (small number of substituents). Such species are relatively new and exciting and in a still expanding realm of chemistry, but due to space limitations, the interested reader is referred to some excellent reviews.[26,27]
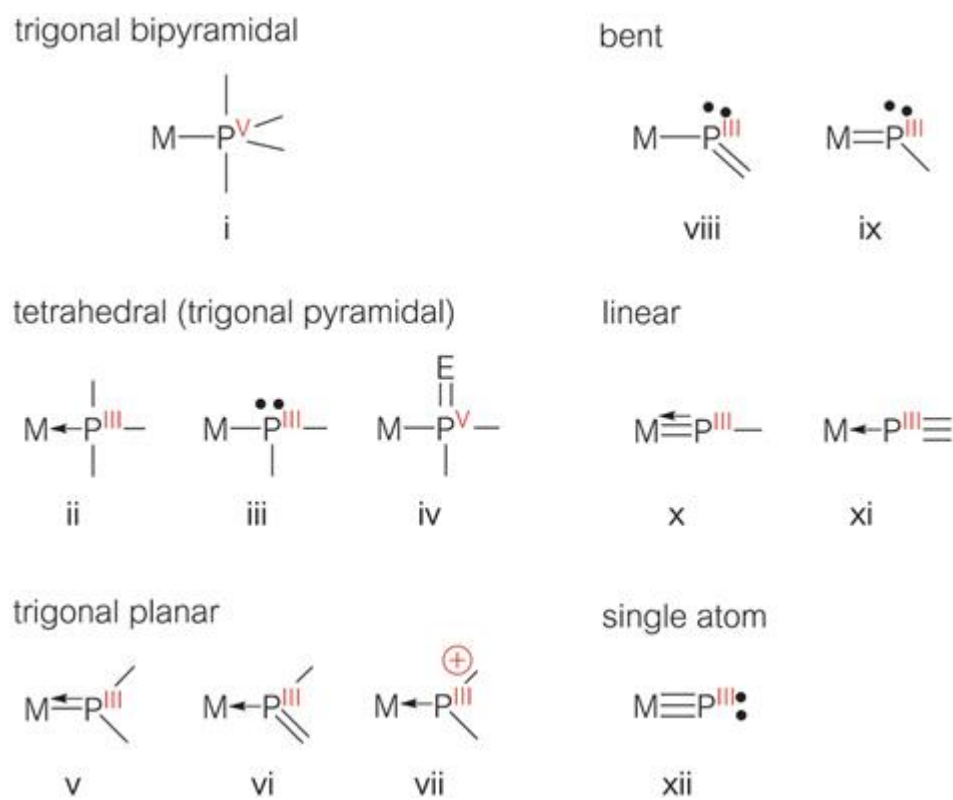
Figure 10.21 Phosphorus ligand types.

10.3.3.1 *Phosphenium Ligand*

The phosphorus center in cationic **vii** has two substituents in addition to the metal such that a trigonal planar structure is adopted. Although the structure is the same as that of **v**, these two types of bonding modes are quite different from an electronic point of view. To distinguish **vii** and **v**, the ligand in **vii** is called "phosphenium" and it bears a formal cationic charge, while **v** (called "planar phosphide") is classified as an anionic ligand. Some literature sources persist in treating planar phosphide **v** as a phosphenium complex, by regarding **v** as containing a bond between L_nM^- and PR_2^+.

Here, to avoid confusing **vii** with **v**, the latter is simply assigned as a PR_2^- anion.[28,29]

The first example of a phosphenium complex was reported in 1978 (eqn (10.17)).[30] A typical synthetic method is the abstraction of X^- from a PR_2X ligand coordinating to a neutral metal fragment by using a Lewis acid. The free cationic ligand may also be isolable, such as when the two R substituents on the phosphorus center are amino (NR_2) groups (eqn (10.18)).[31] In this case, it is noteworthy that the H on the secondary phosphine is removed as hydride. The frontier orbitals of the free $P(NR_2)_2^+$ are depicted in Figure 10.22. The molecular orbitals are closely related to those of the N-heterocyclic carbene (NHC) and the structure corresponds to an analog in which C is replaced by P.

$$(10.17)$$

$$(10.18)$$

$$R^1 = Bu^t, Mes$$
$$R^2 = H, Cl$$
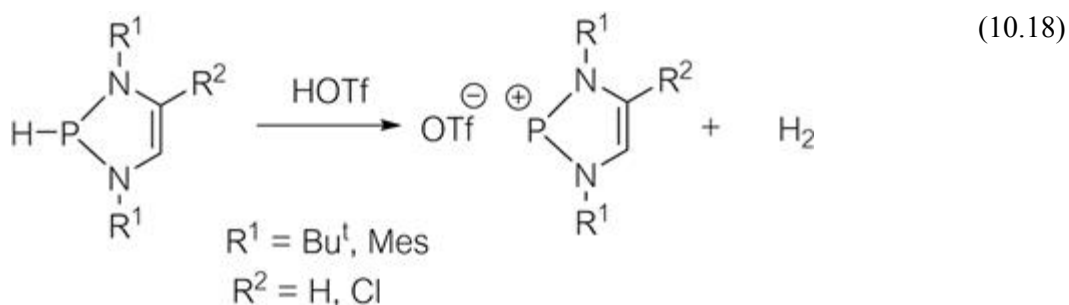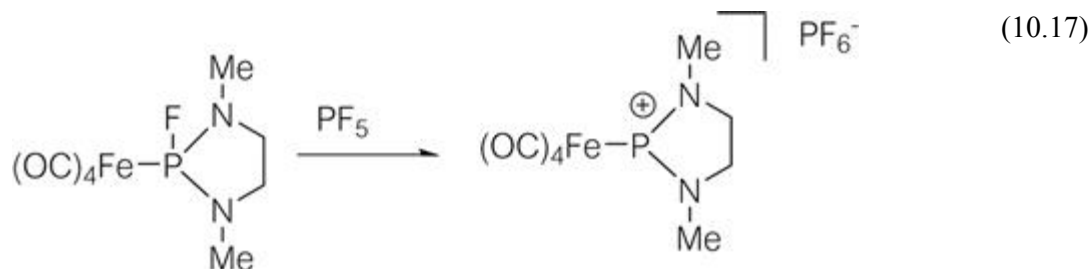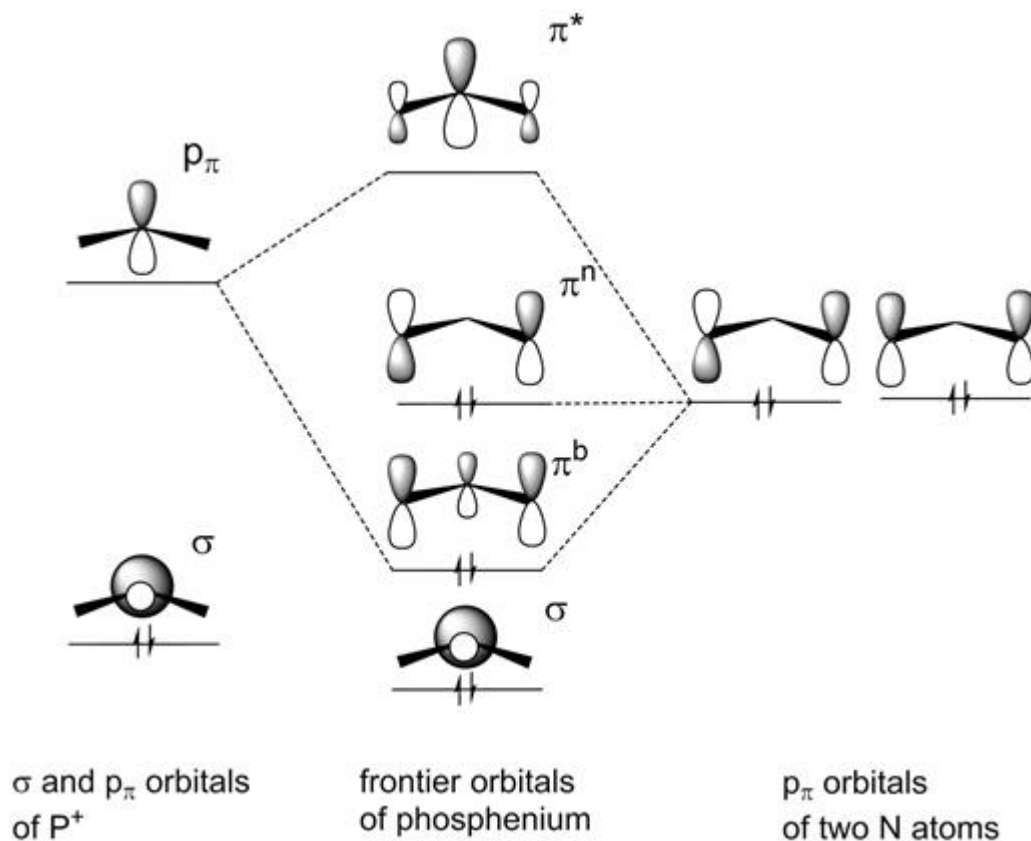
Figure 10.22 Frontier orbitals of the phosphenium ligand: from the bottom, lone pair (σ), bonding orbital (π^b), non-bonding orbital (π^n), and anti-bonding orbital (π^*).

There is, however, a remarkable difference between $P(NR_2)_2^+$ and NHC in the π-acceptor ability at the central atoms. In the NHC, orbital interactions between the $2p_\pi$ orbitals of N and C are strong, resulting in a high π^* orbital energy. As a result, the π-acceptor ability of the carbon center is very weak. On the other hand, in $P(NR_2)_2^+$, the significantly weaker $3p_\pi$–$2p_\pi$ interaction lowers the energy level of the π^* orbital of $P(NR_2)_2^+$, making this ligand a strong π-acceptor. In addition, the phosphorus center is susceptible to external nucleophilic attack, owing to the formal positive charge. This is in sharp contrast to the nature of the phosphide ligand, which may be attacked by electrophiles. Eqn (10.19) is one of the few examples in which an external nucleophile attacks the phosphenium ligand, in this case, with concomitant isomerization from *mer* to *fac*.[32]

$$(10.19)$$

M = Cr, Mo, W
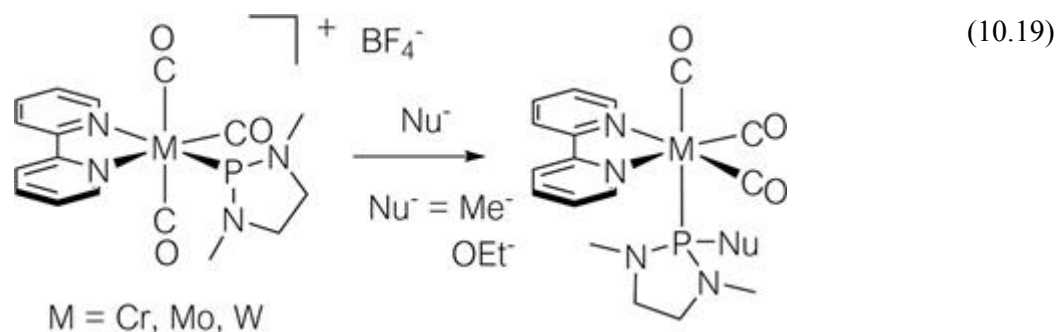
10.3.3.2 P(E)R₂ Ligand

The most common pentavalent phosphorus ligands are P(E)R$_2$ (type **iv** in Figure 10.21) in which E is a Group 16 (E = O, S, Se), Group 15 (E = NR) or Group 14 (E = CR$_2$) moiety. Such ligands have been known since the 1940s, but from 2001, they have attracted significant interest, because Pd complexes bearing P(O)Bu$^t_2$ have found use as Suzuki–Miyaura coupling catalysts that can activate an Ar–Cl bond.[33] The P(O)Bu$^t_2$ ligand is anionic, and is considered to be a better electron donor than neutral phosphines, making the metal center sufficiently electron-rich to activate the Ar–Cl bond. The protonated form of the anionic P(E)R$_2$ ligand is the neutral pentavalent species shown in Figure 10.23(a), which is a tautomer of the trivalent species shown in Figure 10.23(b). These two tautomeric forms are in equilibrium in solution. The dominant form depends on the substituents on the E and P centers to which H$^+$ is bound. When E is the very electronegative O, the equilibrium shifts considerably to the form (a) side. For R groups on the phosphorus with greater electron-withdrawing properties, the contribution of form (b) increases. For example, when R = CF$_3$, the basicity of O becomes higher than P, resulting in a dominant form (b). In contrast, when E = NR or CR$_2$, the major form is (b), except when the R groups of CR$_2$ are the electron-withdrawing CN and COOR functions. In these cases, form (a) is more stable.
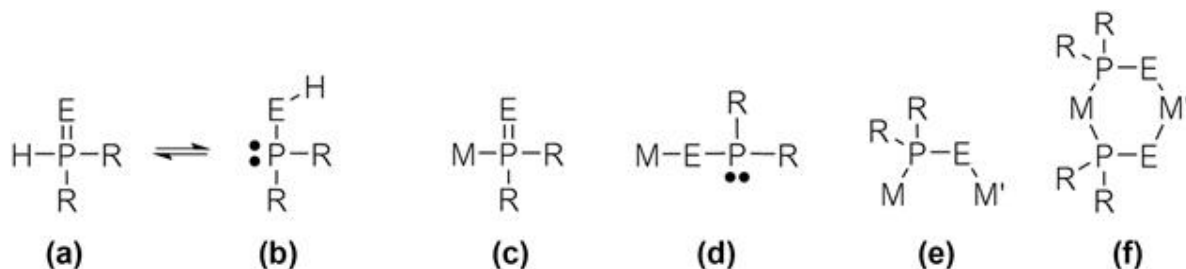
Figure 10.23 Tautomers (a) and (b) of $HP(E)R_2$, and their coordination modes (c)–(f).

   Transition metal complexes corresponding to the protonated forms (a) and (b), are shown as (c) and (d), respectively. The more stable tautomeric form is determined not only by the substituent on P and the type of E, but also by the properties of the metal fragment. Hard metals having π-acceptor properties prefer to bond to E (O and NR) with form (d), while soft metals with π-back-donating ability bond to P with form (c). Examples of the former type are well known for tetravalent Group 4 metal centers, while late transition metal centers prefer the latter coordination mode.
   It is possible for both the P and E donor sites of the $P(E)R_2$ ligand to be simultaneously occupied by metal centers. In this case, the $P(E)R_2$ ligand bridges two metals as shown in (e). In particular, when E prefers early transition metals, the ligand is useful to prepare early-late heterobimetallic complexes. In most examples with bridging $P(E)R_2$ ligands, the two metal centers are multiply bridged by $P(E)R_2$ ligands, as shown in (f) or have a metal–metal bond. The reason for the scarcity of singly bridged examples (e) is probably the poor coordinating ability of the E donor for maintaining a bridging structure.[34]
   $P(E)R_2$ complexes may be synthesized as follows:

1. Salt metathesis using M^+ salt (M^+ = alkali metal).
2. Abstraction of H^+ by a base from M-coordinated $P(EH)R_2$ as shown in eqn (10.20).
3. Arbuzov-type dealkylation reaction as shown in eqn (10.21).
4. Oxidative addition of the H–P bond of $HP(E)R_2$.

$$\text{(10.20)}$$

$$\text{(10.21)}$$
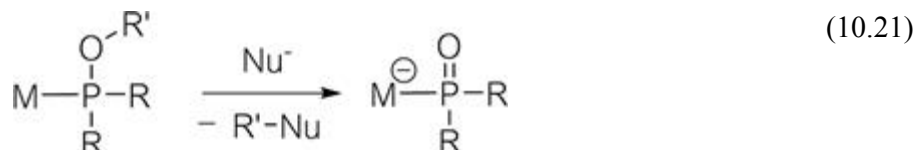
Reactions in which the $P(E)R_2$ ligand itself participates are known. The M–P bond between the metal and the $P(E)R_2$ ligand is a covalent bond, which permits reductive elimination with alkyl and aryl groups to form a P–C bond. Examples of applications to catalytic reactions are the decarbonylation of α-ketophosphonates (eqn (10.22)) and the hydrophosphinylation (or hydrophosphorylation) of H–P(E)R$_2$ (eqn (10.23)).[35,36]

$$\text{(10.22)}$$

$$\text{(10.23)}$$
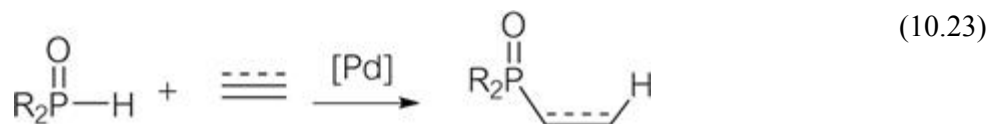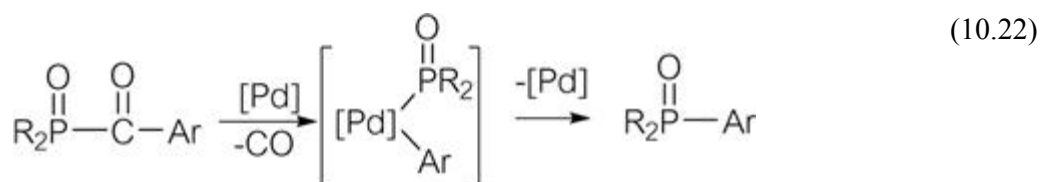
10.3.3.3 Phosphoranide Ligand

Metallaphosphorane (MPR$_4$) is a 5-coordinate phosphorus(v) ligand which adopts a trigonal bipyramidal structure in most cases. Since the first example reported in 1981, the chemistry of coordination compounds bearing ligands with "expanded octets" has attracted interest, especially in the field of hypervalent main group chemistry.[37]

The syntheses are classified into two major methods as shown in Figure 10.24. One is the nucleophilic attack on a trivalent phosphine coordinating to a metal fragment to expand the coordination number. The other is one in which a stable PR$_4^-$ (phosphoranide ligand) prepared in advance is allowed to react with a metal fragment. Most phosphorane complexes prepared so far employ linked phosphorus substituents to stabilize the phosphorane by

the chelate effect. Without stabilization by the chelate effect, phosphorane complexes are generally unstable and only a few examples, spectroscopically identified *in situ*, have been prepared, when the phosphorus has more than three F or Cl atoms.
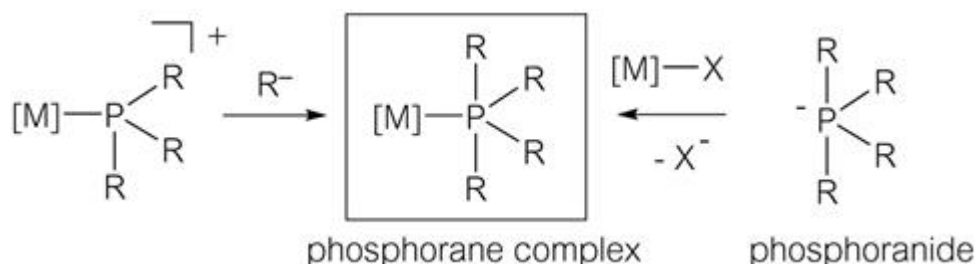
Figure 10.24 Major synthetic methods for phosphorane complexes.

A widely accepted description of the bonding in trigonal bipyramidal phosphoranes is that the phosphorus atom adopts sp^2 hybridization to form three equatorial σ bonds. The remaining p_z orbital and the two axial substituents combine to form a three-center-four-electron (3c–4e) bond. The molecular orbitals of the 3c–4e bond are depicted in Figure 10.25. The bond order of the 3c–4e bond can be regarded as 0.5 *per* P-axial bond, and therefore the axial bond is weaker than the equatorial bond. Of the equatorial and axial groups in the trigonal bipyramidal phosphorane, the electronegative groups have a tendency to occupy the axial positions (Bent's Rule). This trend is called *apicophilicity*. The axial non-bonding orbital in Figure 10.25 localizes its electrons around the apical substituent. Electron-withdrawing groups such as F or OAr can effectively stabilize the localized electrons, and therefore they have greater apicophilicity. On the other hand, since the equatorial groups can form stronger σ bonds than the axial group, electron releasing groups prefer the equatorial sites (*equatophilicity*). The metal center is an electropositive group, since one electron formally transfers to phosphorus to form M^+ and PR_4^-, so it is considered to be equatophilic, and the metals in the examples reported do indeed occupy equatorial positions.
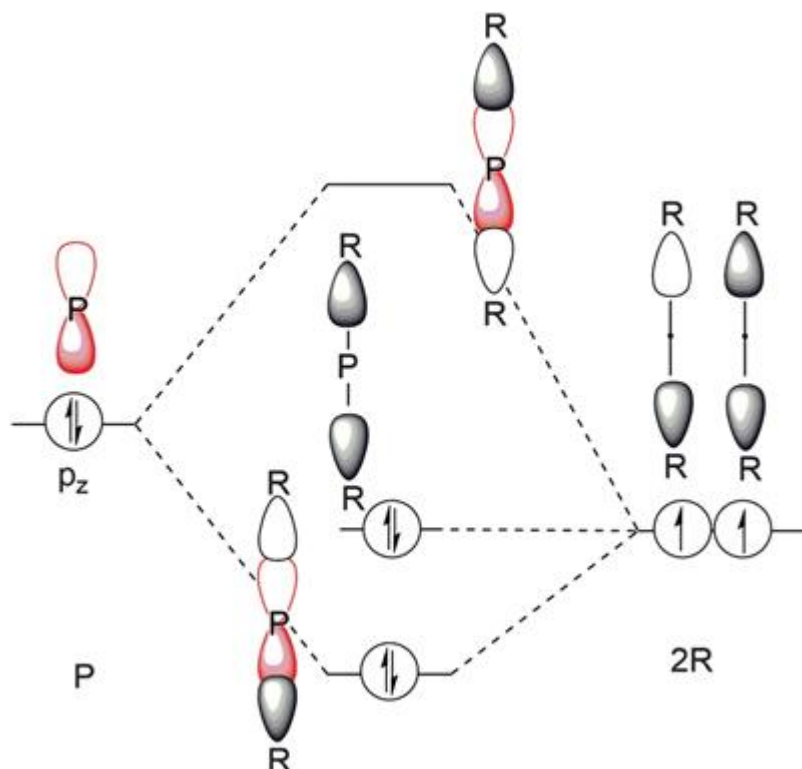
Figure 10.25 Molecular orbitals of the three-center-four-electron bond between P and axial groups.

As for the remaining four substituents on the phosphorus, bidentate chelate-type substituents comprising both electron-withdrawing and -releasing groups are suitable for stabilizing the phosphorane. Two sets of such chelate-type substituents afford isolable spiro-phosphorane complexes, in which the phosphorus atom is a stereogenic center. Such species are expected to be chiral auxiliary ligands, if facile racemization *via* pseudorotation and/or P-to-M migration of the substituent are suppressed. In eqn (10.24), the phosphoranide reacts with a Rh–porphyrin complex to give a Rh–phosphorane complex, which has been found to be the most stable species against racemization among phosphorane complexes reported so far.[38]

(10.24)
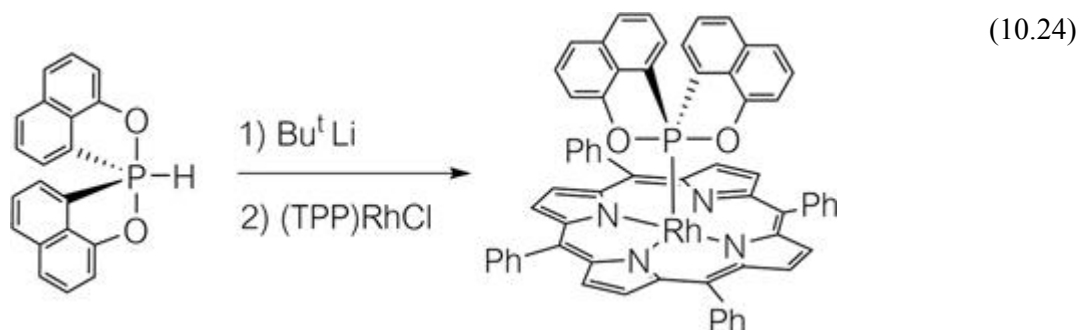
Tertiary phosphines are widely used as auxiliary ligands in transition metal-based catalysts. In general, the ligand is stable on the metal. In some reactions, however, detailed examination of the decomposition process of the catalyst indicates that P–C bond cleavage of the tertiary phosphine takes place during the reactions. For example, the reaction in eqn (10.25) takes place under mild reaction conditions because of its low transition state energy of 84 kJ mol^{-1}. In this case, intramolecular migration of F to the phosphorus center affords a phosphorane complex as an intermediate species.[39]

(10.25)
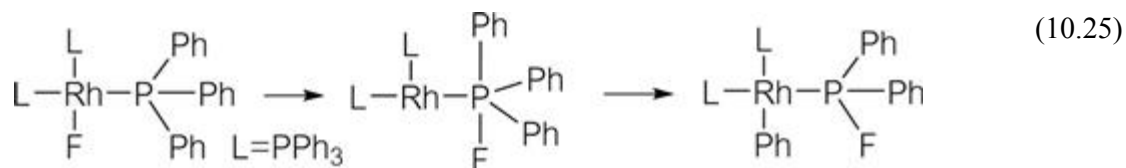
The M–P bond of the phosphorane complex is formally a covalent bond. It is possible that the phosphoranide ligand and R group on the metal form a P–C bond by reductive elimination. Although there is no example of such a simple reductive elimination due to the limited stability of the phosphorane, the spirophosphorane stabilized by chelate-type substituents in eqn (10.26) migrates from the metal to form a P–C bond.[40]

(10.26)

M=Fe,Ru E=O, NMe
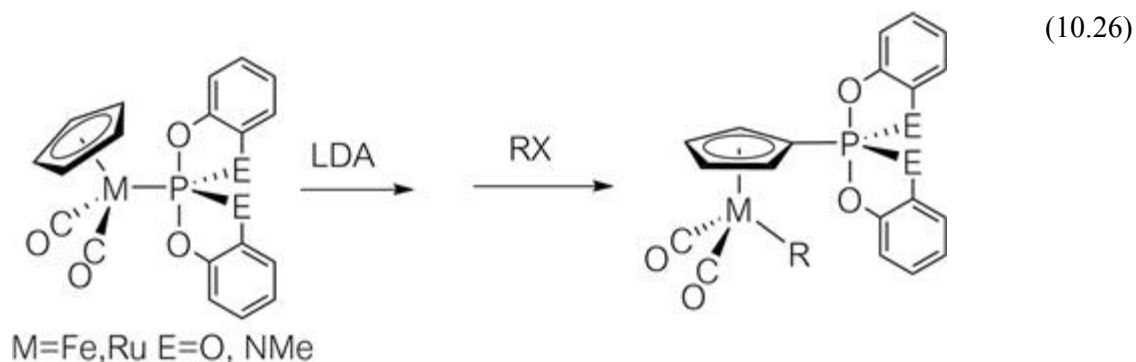
10.4 Summary

Amide ligands and phosphide ligands are related to each other in that both contain two substituents and one lone pair of electrons and form a σ-bond with transition metals. The reactive lone pair of electrons of these Group 15 ligands affords a variety of structures and reactions. These ligands tend to work as an intramolecular Lewis base site and can form bridging structures resulting in multinuclear complexes. These fascinating properties still attract much interest and are expanding the chemistry of the amide and phosphide complexes.

References

1. M. Lappert, P. Power, A. Protchenko and A. Seeber, *Metal Amide Chemistry*, Wiley, West Sussex, 2008.
2. D. C. Bradley, M. H. Chisholm and M. W. Extine, *Inorg. Chem.*, 1977, **7**, 1791.
3. (a) A. W. Kaplan, J. C. Ritter and R. G. Bergman, *J. Am. Chem. Soc.*, 1998 **120**, 6828; (b) J. R. Fulton, M. W. Bouwkamp and R. G. Bergman, *J. Am. Chem. Soc.*, 2000, **122**, 8799; (c) J. R. Fulton, S. Sklenak, M. W. Bouwkamp and R. G. Bergman, *J. Am. Chem. Soc.*, 2002, **124**, 4722; (d) D. J. Fox and R. G. Bergman, *Organometallics*, 2004, **23**, 1656.
4. H. E. Bryndza, P. J. Domaille, R. A. Paciello and J. E. Bercaw, *Organometallics*, 1989, **8**, 379.
5. A. Anillo, C. Barrio, S. Garcia-Granda and R. Obeso-Rosete, *J. Chem. Soc., Dalton Trans.*, 1993, 1125.
6. E. Hevia, J. Perez, V. Riera and D. Miguel, *Orgnometallics*, 2002, **21**, 1966.
7. H. E. Bryndza, W. C. Fultz and W. Tam, *Organometallics*, 1985, **4**, 939.
8. Coordination of strong π-acceptor ligand such as CO at the *trans* position to an amide ligand in a square planar 16e complex may encourage some π-donation from the amide ligand to a d^8 metal center.
9. R. E. Blake, Jr.R. H. Heyn and T. D. Tilley, *Polyhedron*, 1992, **11**, 709.
10. (a) J. T. Poulton, K. Folting, W. E. Streib and K. G. Caulton, *Inorg. Chem.*, 1992, **31**, 3190; (b) K. G. Caulton, *New J. Chem*, 1994, **18**, 25.
11. P. J. Walsh, F. J. Hollander and R. G. Bergman, *J. Am. Chem. Soc.*, 1988, **110**, 8729.
12. P. J. Holland, R. A. Andersen, R. G. Bergman, J. Huang and S. P. Nolan, *J. Am. Chem. Soc.*, 1997, **119**, 12800.
13. S. Park, D. M. Roundhill and A. L. Rheingold, *Inorg. Chem.*, 1987, **26**, 3972.
14. D. Conner, K. M. Jayaprakash, T. R. Chundari and T. B. Gunnoe, *Organometallics*, 2004, **23**, 2724.
15. S. Park, A. L. Rheingold and D. M. Roundhill, *Oranometallics*, 1991, **10**, 615.
16. F. T. Ladipo and J. S. Marola, *Inorg, Chem*, 1990, **29**, 4172.
17. J. Zhao, A. S. Goldman and J. F. Hartwig, *Science*, 2005, **307**, 1080.
18. T. Ikariya and I. D. Gridnev, *Chem. Rec.*, 2009, **9**, 106.
19. F. L. Joslin, M. P. Johnson, J. T. Mague and D. M. Roundhill, *Organometallics*, 1991, **10**, 2781.
20. J. F. Hartwig, R. G. Bergman and R. A. Andersen, *J. Am. Chem. Soc.*, 1991, **113**, 6499.
21. M. R. Gagne, C. L. Stern and T. J. Marks, *J. Am. Chem. Soc.*, 1992, **114**, 275.
22. S. E. Diamond and F. Mares, *J. Organomet. Chem.*, 1977, **142**, C55.
23. M. A. Zhuravel, D. S. Gluck, L. N. Zakharov and A. D. Rheingold, *Organometallics*, 2002, **21**, 3208.

24. J. R. Rogers, T. P. S. Wagner and D. S. Marynick, *Inorg. Chem.*, 1994, **33**, 3104.
25. D. S. Gluck, *Synlett*, 2007, **17**, 2627.
26. K. Lammertsma, *Top. Curr. Chem.*, 2003, **229**, 95.
27. B. P. Johnson, G. Bálazs and M. Scheer, *Coord. Chem. Rev.*, 2006, **250**, 1178.
28. H. Nakazawa, *Adv. Organomet. Chem*, 2004, **50**, 107.
29. L. Rosenberg, *Coord. Chem. Rev.*, 2012, **256**, 606.
30. R. G. Montemayor, D. T. Sauer, Sr.S. FlemingD. W. BennettM. G. Thomas and R. W. Parry, *J. Am. Chem. Soc.*, 1978, **100**, 2231.
31. D. Gudat, A. Haghverdi and M. Nieger, *Angew. Chem., Int. Ed.*, 2000, **39**, 3084.
32. H. Nakazawa, M. Ohta, K. Miyoshi and H. Yoneda, *Organometallics*, 1989, **8**, 638.
33. G. Y. Li, *Angew. Chem., Int. Ed.*, 2001, **40**, 1513.
34. B. Walther, *Coord. Chem. Rev.*, 1984, **60**, 67.
35. H. Nakazawa, Y. Matsuoka, I. Nakagawa and K. Miyoshi, *Organometallics*, 1992, **11**, 1385.
36. F. Alonso, I. P. Beletsukaya and M. Yus, *Chem. Rev.*, 2004, **104**, 3079.
37. J. Wachter, B. F. Mentzen and J. G. Riess, *Angew. Chem., Int. Ed. Engl.*, 1981, **20**, 284.
38. K. Kajiyama, T. K. Miyamoto and K. Sawano, *Inorg. Chem.*, 2006, **45**, 502.
39. S. A. Macgregor and T. Wondimagegn, *Organometallics*, 2007, **26**, 1143.
40. H. Nakazawa, K. Kubo and K. Miyoshi, *Bull. Chem. Soc. Jpn.*, 2001, **74**, 2255.

Chapter 11

Chemistry of Transition Metal Complexes with Group 16 Elements: Transition Metal Complexes with Two Lone Pairs of Electrons on the Coordinating Atom

Kohtaro Osakada[a]

[a] Tokyo Institute of Technology, Japan kosakada@res.titech.ac.jp

11.1 Introduction

Chapters 8 to 10 covered the chemistry of transition metal complexes in which the ligating atoms are boron, silicon, nitrogen, phosphorus and their heavier elements. The coordination bonds of these complexes are highly covalent in character and show reactivity similar to complexes with metal–carbon bonds. This chapter deals with complexes containing Group 16 elements, oxygen and sulfur, as the ligating atoms. The Allred–Rochow electronegativities of oxygen and sulfur are 3.50 and 2.44, respectively, and are greater than those for the other elements in the second and third rows of the Periodic Table, such as boron, carbon, nitrogen and phosphorus. Metal complexes with alkoxide (M–OR) and thiolate (M–SR) ligands are considered to show reactivity due to the ionic character of the coordination bonds. Late transition metal alkoxide complexes, however, undergo associative, not dissociative, exchange of the alkoxide group upon adding alcohol. Thiolate complexes of late transition metals react with alkynes to

form alkenyl complexes *via* migratory insertion of the unsaturated molecule into the M–S bond. α-Elimination of the alkyl group of the thiolato complex forms a complex with alkyl and sulfide (=S) ligands. This reaction is involved in the hydrodesulfurization of organosulfur compounds catalyzed by transition metal complexes.

Transition metal complexes with oxo (M=O) and sulfide (M=S) ligands are of significant interest from the viewpoints of bioinorganic chemistry and material science. They are not, however, discussed here due to the large number of books that have been published relating to these topics. This chapter describes the fundamental bonding, structures and chemical properties of transition metal complexes with alkoxide and thiolate ligands.

11.2   Synthesis of M–OR and M–SR Complexes

Late transition metal complexes with alkoxide or thiolate ligands are mostly prepared by metathesis-type reactions of the alkali metal salts of the alcohols or thiols, such as NaOR or LiSR, with transition metal halogeno and triflate complexes (Figure 11.1). Thallium alkoxide is another convenient synthetic material for preparing metal alkoxides. The reactions resemble the transmetalation reaction that provides alkyltransition metal complexes from organolithium and -magnesium reagents and transition metal halogeno complexes. This synthetic approach to metal alkoxide complexes is advantageous as regards the availability and facile handling of the lithium and sodium salts of the alkoxide and thiolate and in the smooth and selective reactions due to the high basicity of the alkoxide and thiolate anions. Another convenient route is the direct reaction of thiols with transition metal halogeno complexes in the presence of NEt_3, which scavenges the hydrogen halides produced (Figure 11.1(ii)).

(i) $\quad$ M–Cl $\quad + \quad$ Li–E–R $\quad \longrightarrow \quad$ M–E–R $\quad + \quad$ LiCl

(ii) $\quad$ M–Cl $\quad + \quad$ H–S–R $\quad \xrightarrow[\text{- NHEt}_3\text{Cl}]{\text{+ NEt}_3} \quad$ M–S–R

(iii) $\quad$ M–O–R $\quad + \quad$ H–S–R' $\quad \longrightarrow \quad$ M–S–R' $\quad + \quad$ H–O–R

(M: transition metal, E: O, S)
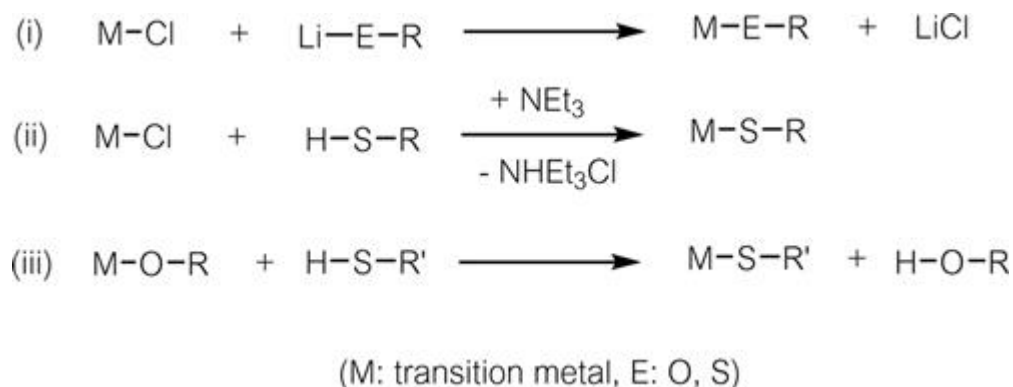
Figure 11.1 Common synthetic routes to M–OR and M–SR transition metal complexes.

Figure 11.2 summarizes the reaction of lithium thiolate with Pt(ii) complexes having square-planar structures.[1] The reaction products are influenced by the structure and chemical properties of the starting complexes. Addition of pyridine influences the *cis/trans* stereochemistry of the square-planar complexes.
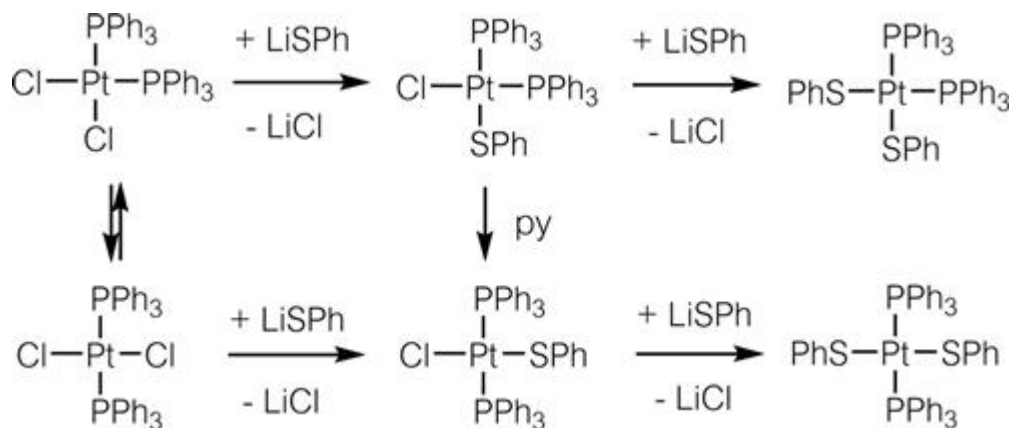
Figure 11.2 Synthesis of *cis*- and *trans*-bis(thiolate)platinum(ii) complexes.

Ligand exchange reactions of transition metal alkoxides with phenols and thiols also produce complexes with new M–O and M–S bonds, as shown in Figure 11.1(iii). The reactions occur reversibly and the equilibrium is influenced by the relative stability of the M–O and M–S bonds of the complexes and H–O and H–S bonds of the other materials. This type of ligand exchange, accompanied by hydrogen transfer in late transition metal complexes, is proposed to be closely related to the bond energy of the

conjugate acids, H–OR and H–SR.[2] Such synthetic reactions usually involve the use of an excess of the added compound, and the absence of side reactions means that by-products are not formed.

Synthesis of alkoxide transition metal complexes starting from organotransition metal complexes has also been reported. Bennett and Yoshida obtained alkyl(methoxide)platinum(ii) complexes **1** (R = Me) from the reaction of methanol with Pt(0) complexes containing π-coordinated strained cyclic alkynes (Figure 11.3).[3] Use of water instead of methanol results in isolation of the corresponding platinum(ii) hydroxide complex.
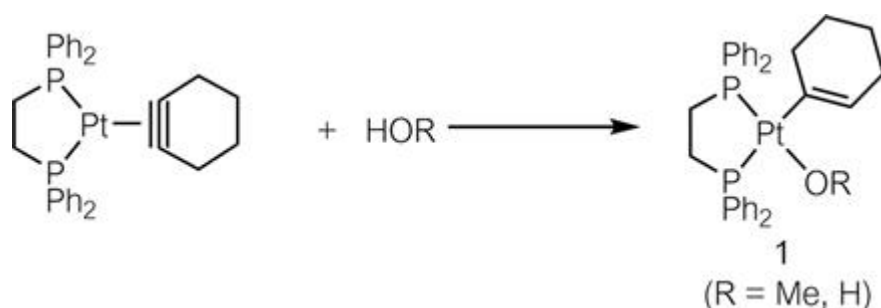
Figure 11.3 Synthesis of Pt(ii) complexes with alkoxide and hydroxide ligands.

Hydride and alkyl complexes of transition metals react with acidic alcohols, resulting in cleavage of the M–C bond. Fluorinated alcohols and phenols are employed as the starting materials for the alkoxide and aryloxide complexes. Komiya reported the reaction of phenols with [FeEt$_2$(bpy)] (bpy = 2,2′-bipyridine) to form the corresponding aryloxide iron(ii) complexes, **2** (Figure 11.4). The complexes are thermally stable but extremely air-sensitive. Similar reactions with aliphatic alcohols also proceed at room temperature, but the alkoxideiron(ii) complexes produced were not isolated due to their thermal instability.[4]
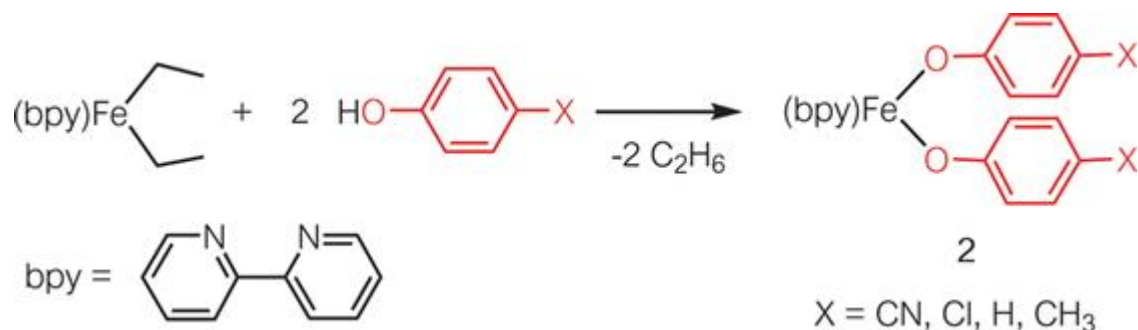
Figure 11.4 Synthesis of bis(aryloxide)iron(ii) complexes.

Hydride complexes of cobalt and rhodium also react with fluorinated alcohols and phenols to form the corresponding alkoxide complexes (**3, 4**) (Figure 11.5).
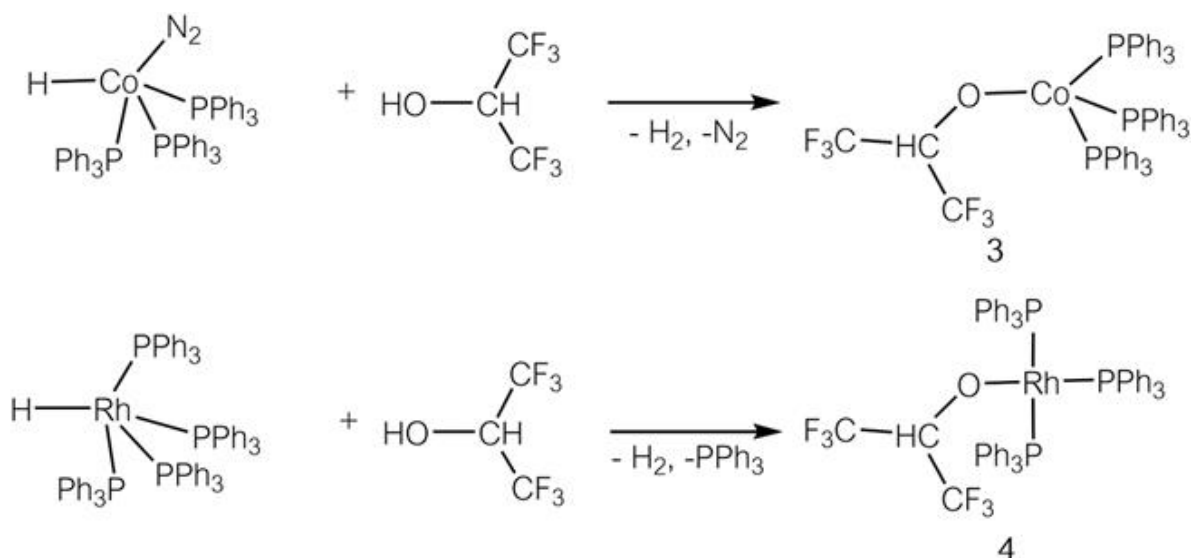
Figure 11.5 Synthesis of alkoxide cobalt and rhodium complexes.

As shown in Figure 11.6, the ruthenium dihydride complex reacts with a fluoroketone by insertion of the C=O bond into a Ru–H bond, forming ruthenium alkoxide complex **5**.[5] Such insertion of C=O bonds into the M–H bond of metal hydride complexes and the reverse process, β-hydrogen elimination of the carbonyl compound from the alkoxide complex, is proposed in the mechanism of reduction of carbonyl compounds and oxidation of alcohols promoted by transition metal catalysts.
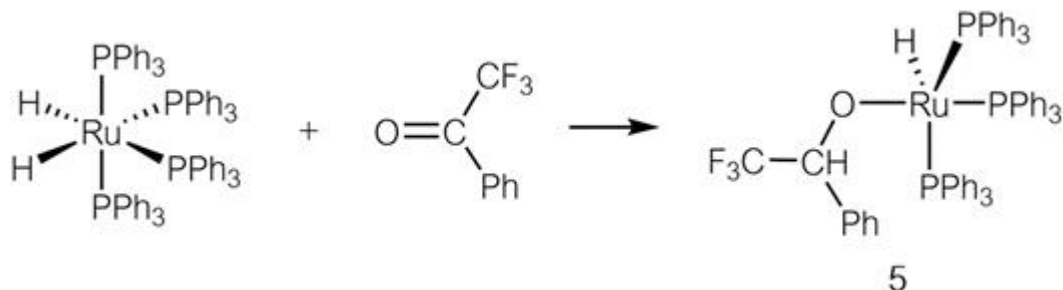
Figure 11.6 Formation of a ruthenium alkoxide complex *via* insertion of C=O into a M–H bond.

Reaction of 2-butenyl(phenyl)carbonate with the ruthenium dihydride complex causes decarboxylation of the substrate to form a mixture of butenes and the ruthenium phenoxide complex **6** (Figure 11.7).[6]
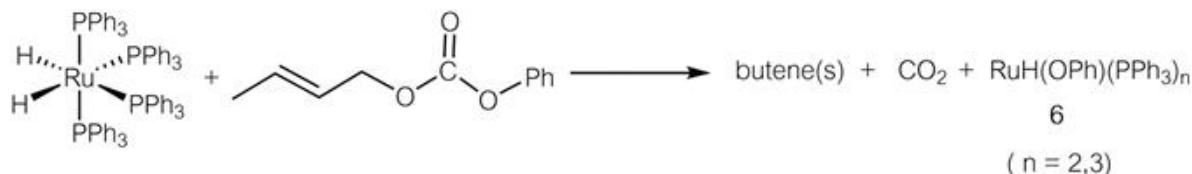
Figure 11.7 Formation of a ruthenium phenoxide complex from 2-butenyl(phenyl)carbonate and a ruthenium dihydride complex.

A similar reaction of allyl(phenyl)sulfide with a rhodium(i) hydride complex forms a dirhodium complex with bridging thiolate ligands, **7**. A deuterium labelling study of the reaction revealed that the mechanism involves insertion of the C=C double bond of the substrate into the Rh–H bond, followed by β-elimination of the thiolate group from the alkylrhodium intermediate (Figure 11.8).[7]
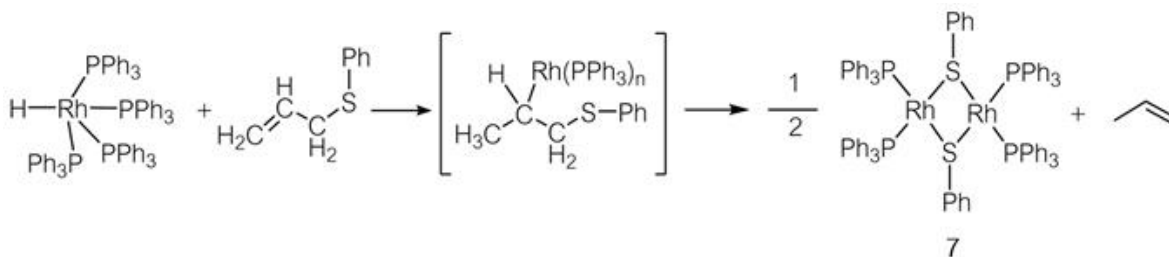
Figure 11.8 Formation of a rhodium(i) thiolate complex formed *via* C–S bond cleavage of the allyl(phenyl)sulfide.

Hillhouse reported the reaction of nitrous oxide (N_2O) with alkylnickel-bipyridine complexes to form alkoxide complexes (Figure 11.9).[8,9] This reaction involves the insertion of nitrous oxide into a Ni–C bond and elimination of the stable dinitrogen molecule, affording the alkoxide complexes **8** and **9**. Complexes of early transition metals such as Zr and Hf also undergo similar insertion of an oxygen atom into the M–C bond.[10] Methyl(trioxo)rhenium, $MeReO_3$ reacts with aqueous hydrogen peroxide to form MeOH. The proposed reaction mechanism involves the initial formation of an intermediate containing an O_2 ligand. One of the oxygens of the dioxygen ligand inserts into the Re–C bond to form a complex having methoxide, hydroxide and oxo ligands, **10** (Figure 11.10).[11]
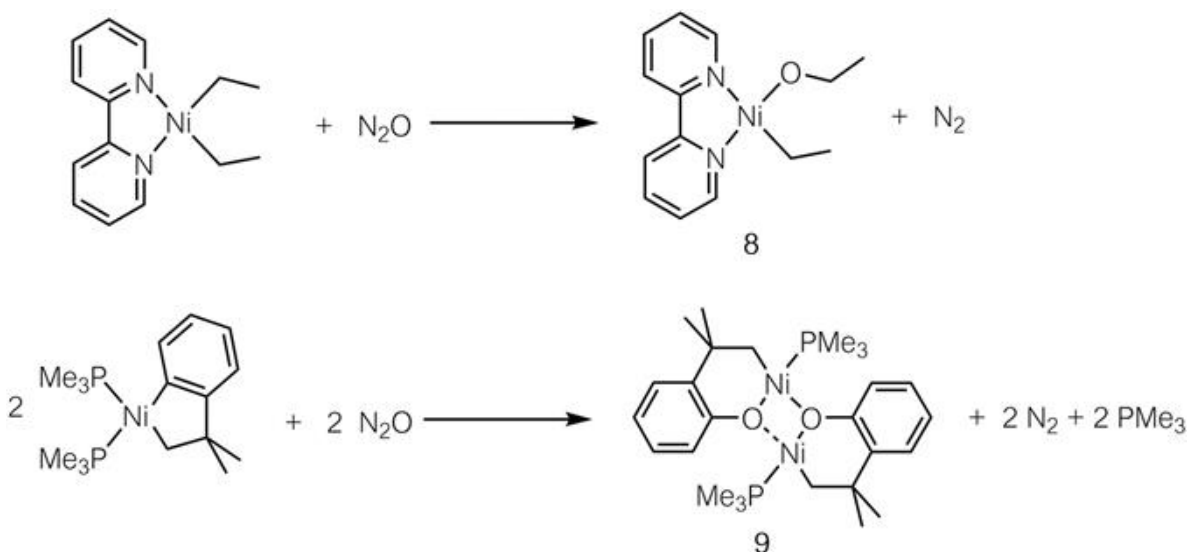
Figure 11.9 Synthesis of nickel alkoxide complexes by insertion of oxygen into Ni–C bonds.
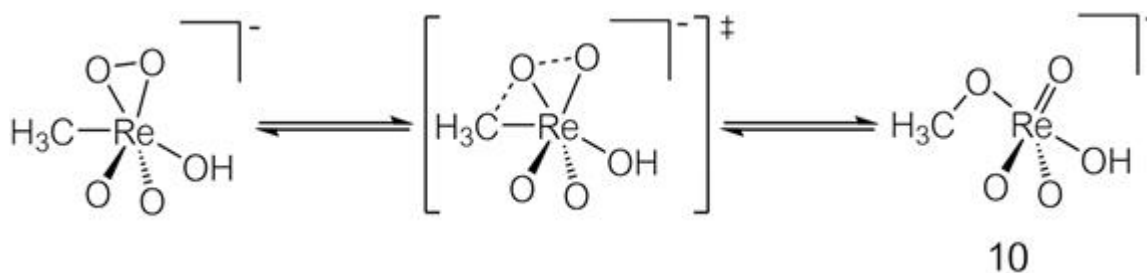
Figure 11.10 Rearrangement and insertion of oxygen into a Re–C bond.

Reaction of sulfur (S_8) with a cyclic alkylnickel complex was reported to result in the insertion of a sulfur atom into the M–C bond, forming a nickelacycle with a Ni–S bond.[12] Kajitani reported the reaction of S_8 and alkynes in the presence of $[Co(Cp)(CO)_2]$ (Cp = η^5-cyclopentadienyl) to form a cyclic metalladithiolene **11** (Figure 11.11).[13] Similar dithiolene complexes were obtained for late transition metals, such as Rh and Ni. These metal-containing π-conjugated compounds exhibit unique electrochemical properties and can be transformed into various derivatives.
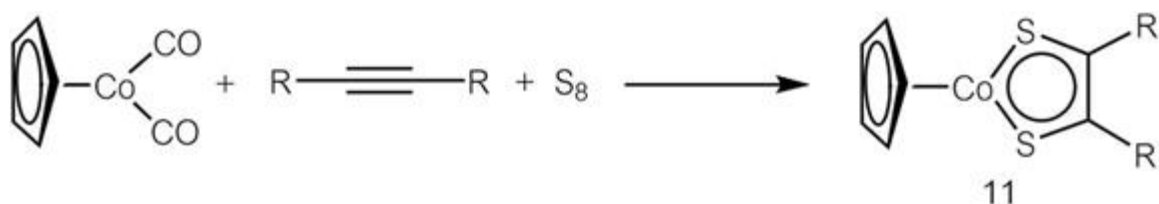
Figure 11.11 Synthesis of cobaltadithiolene starting from sulfur and alkyne.

DuBois reported that a dinuclear molybdenum complex with bridging sulfide (S^{2-}) ligands undergoes a nucleophilic reaction with organohalogen compounds to yield a new complex, **12**, with thiolate ligands (Figure 11.12).[14]
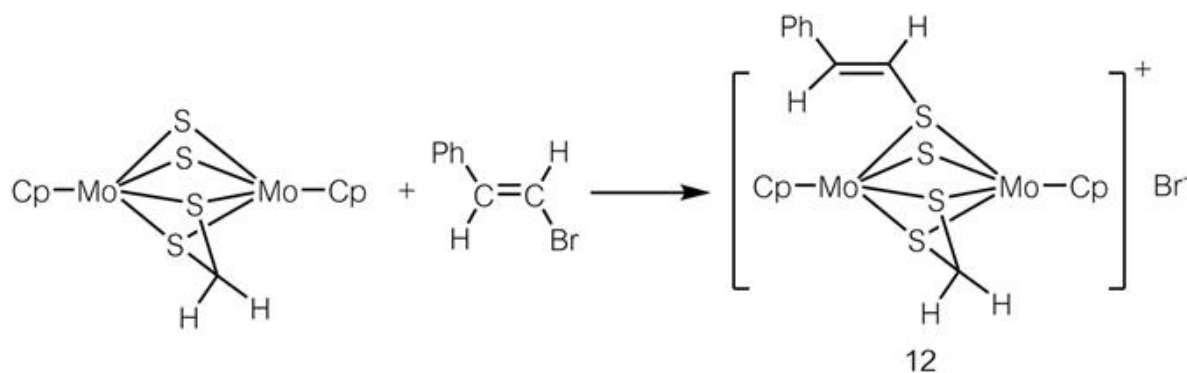
Figure 11.12 Formation of thiolate ligands *via* nucleophilic reaction of a dinuclear molybdenum complex with sulfide ligands.

The ligating Group 16 atom has two lone pairs of electrons and high basicity and can thus form various multinuclear complexes with bridging OR and SR ligands, depending on the coordination number and valency of

the metal centers. Use of the permethylcyclopentadienyl (Cp*) ligand enables formation of di- and tetranuclear Ru complexes with bridging OMe ligands (Figure 11.13).
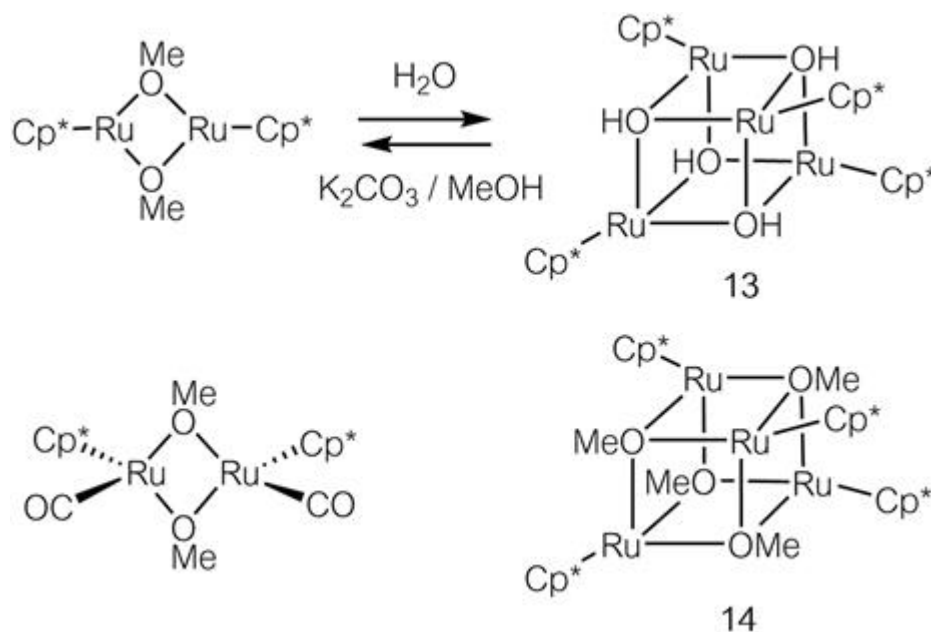
Figure 11.13 Multinuclear Ru–Cp* complexes with bridging OH and OR ligands.

Addition of water to the diruthenium complex with bridging alkoxide ligands results in the formation of hydroxo complexes, which dimerize giving tetraruthenium complexes with bridging OH ligands **13**. The reaction proceeds reversibly, and addition of MeOH in the presence of a base regenerates the dinuclear Ru complex with bridging OMe ligands. An intermediate tetraruthenium complex with OMe ligands **14** was obtained *via* an independent reaction.[15]

The stable bridging coordination of the thiolate ligands affords multinuclear transition metal complexes with new structures. Konno reported the synthesis of various multinuclear complexes by linking metal centers, as in **15** and **16**, *via* chelating amino group-containing thiolate ligands (Figure 11.14).
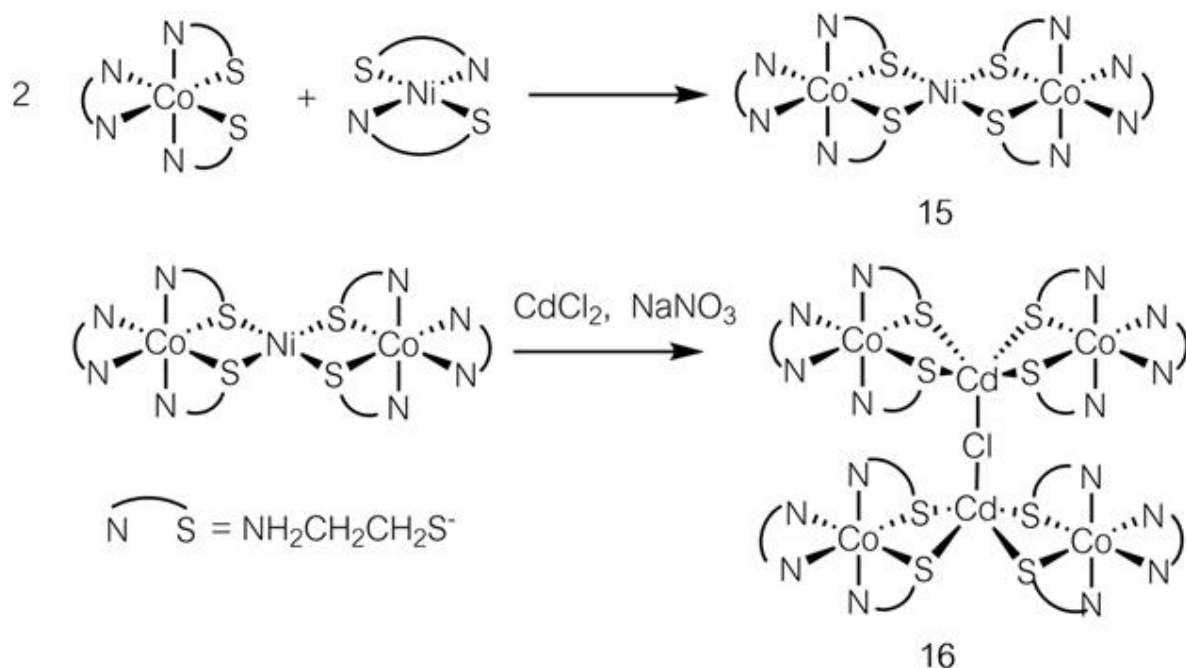
Figure 11.14 Multicobalt complexes with bridges incorporating additional metal centers.

The low spin d^6 transition metals, Co(iii) and Rh(iii), are stabilized by amine-containing thiolate ligands, and coordinating sulfur atoms are employed in the formation of their aggregates *via* intermolecular coordination of the sulfur atom with the metal center of the other complexes. Many transition metals can be employed in this strategy, which can lead to complexes with supramolecular structures.[16]

Since mononuclear units with three chelating ligands have molecular chirality, assembly of the complexes in a stereochemically controlled manner affords chiral assemblies composed of a number of the metal complex units **17** and **18** (Figure 11.15).
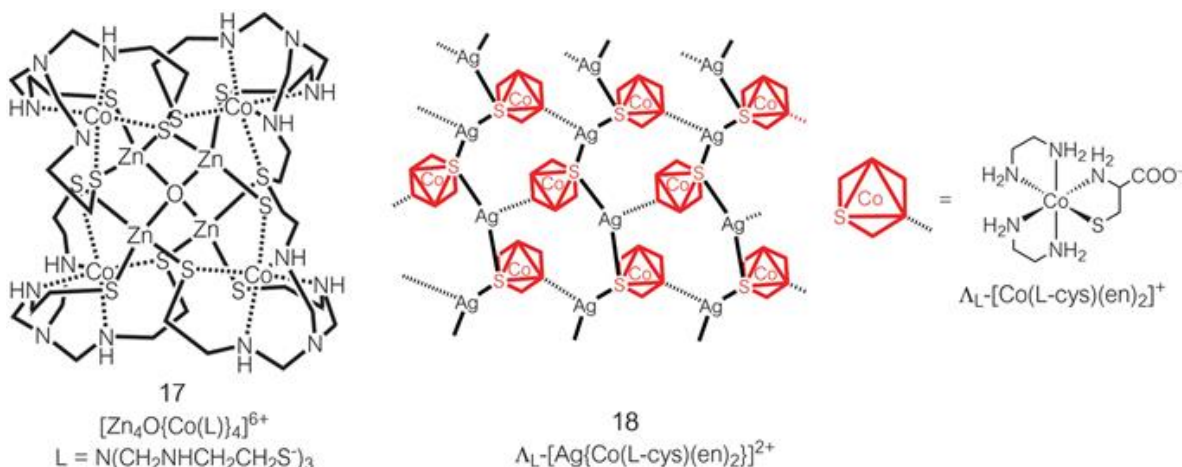
Figure 11.15 Ordered assembly of multinuclear transition metal complexes.

11.3 Bonding and Properties of M–OR Complexes

As shown in Figure 11.16(a), d electron-deficient early transition metals form bonds with oxygen, involving not only σ-bonds but also π-bonds between the filled p orbital of the oxygen atom and an empty d orbital of the transition metal. Thus, M–O bonds in the alkoxide complexes of early transition metals exhibit some double bond character. This is reflected in the more open M–O–C bond angles in the alkoxide complexes of Ti(iii) and Zr(iv) (Figure 11.16(a)), and some complexes even have linear M–O–C bonds.
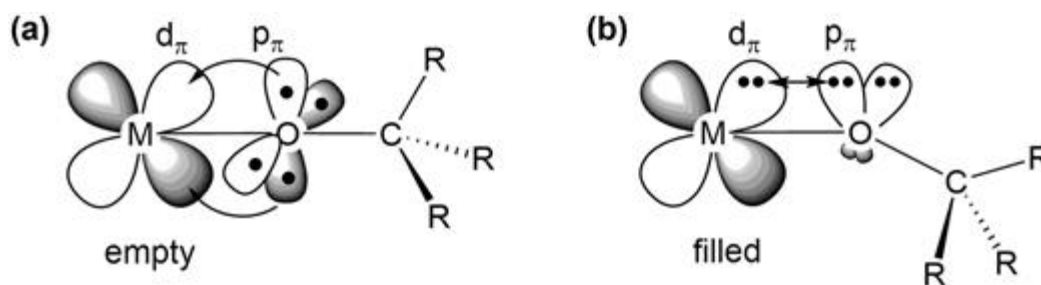
Figure 11.16 Schematic drawing of the bonding and orbitals in transition metal alkoxide complexes: (a) multiple bond character in early transition metals and (b) electronic repulsion between filled orbitals in late transition metals.

The alkoxide ligand may be regarded formally as a neutral 1e donor ligand or as an anionic 2e donor ligand, but in early transition metal

complexes, the ligand actually functions as a neutral 3e or anionic 4e donor ligand due to π-donation from the ligating oxygen atom, as mentioned above. Homoleptic alkoxide complexes of Ti(ɪᴠ) and Zr(ɪᴠ), formulated as $M(OR)_4$ with tetrahedral structures, are common and commercially available. Alkoxide complexes of early transition metals often have metal coordination spheres, the valence electron count of which is less than 18.

Wolczanski compared the orbitals relating to the coordination bonds between the metal and alkoxide to those between a metal and cyclopentadienyl ligand, as shown in Figure 11.17.[17] The metal center and oxygen atom form a σ-bond accompanied by the formation of two π bonds between two p orbitals perpendicular to the M–O bond and two d orbitals of the metal center. The M–O bond caused by such (σ + 2π) interaction suggests an alkoxide ligand with neutral 5e (anionic 6e) donor ligand character. Figure 11.17 suggests that the ligand orbital is comparable with that of the cyclopentadienyl (Cp) ligand. The coordination bond of the Cp ligand comprises the ψ_1 orbital, which corresponds to the σ-bond of the alkoxide ligand, and the ψ_2 and ψ_3 orbitals, with nodes, which correspond to the two pπ orbitals of the alkoxide ligand. The degree of such π-coordination of alkoxide ligands to early transition metal centers is influenced by the number of d electrons of the metal center, the electron-donating or -accepting properties of the R group of the alkoxide (OR) ligand, and the ligand *trans* to the alkoxide ligand.
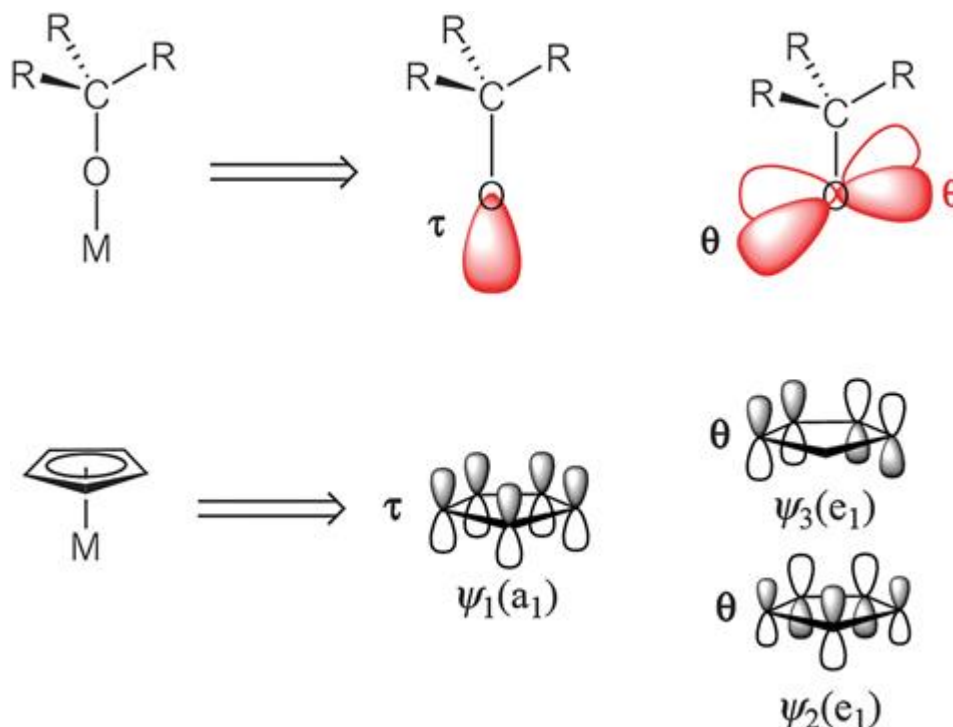
Figure 11.17 Schematic drawing comparing coordination of alkoxide and Cp ligands.

Low valent late transition metals, on the other hand, contain a larger number of d electrons which are in the d_{xy}, d_{yz} and d_{zx} orbitals. The ligating alkoxide ligand is destabilized by electronic repulsion between the lone pair of electrons on the oxygen atom and the d electrons of the metal center (Figure 11.16(b)). Such repulsion tends to make the M–O–C angle smaller and many alkoxide complexes of late transition metals show angles around 120°.

Aryloxide complexes of late transition metals are more stable than the corresponding alkoxide complexes. π-Conjugation between the lone pair of electrons of the oxygen atom and π-electrons of the aryl group (Figure 11.18) reduces the pπ–dπ repulsion mentioned above.

Figure 11.18 Stabilization of aryloxide complexes of late transition metals.

The ligand *trans* to the M–O bond influences the stability of the M–O bond. For example, having two alkoxide ligands in mutually *trans* positions destabilizes both ligands due to interaction of the pπ orbitals of the two ligating oxygen atoms with the same metal d orbital. Electron-withdrawing (π-acid) ligands, such as the carbonyl ligand, stabilize the alkoxide ligand when *trans* to it.

Si-bonded analogues of alkoxide complexes with an M–O–Si bond are named silanolates, and their coordination bond may be compared with the M–O–C bond of the alkoxide complexes. The Allred–Rochow electronegativity of silicon is 1.74, so it is considerably more electropositive than carbon, and the acidity of HOSiPh$_3$ (pK_a = 16.57) is slightly greater than that of the corresponding alcohol (HOCPh$_3$, pK_a = 16.97).[18] This is consistent with a stronger O–M bond for silanolate complexes of late transition metals compared to the analogous alkoxide complexes.

Molecular silsesquioxanes having OH groups are regarded as model compounds of the surface of solid silica. Silsesquioxane complexes of early transition metals, such as Ti and Zr (**19**), have complete cage structures due to the high affinity of the metals for oxygen and large M–O–Si angles (Figure 11.19).[19] Late transition metals, such as Pd and Pt (**20**), also form silsesquioxane complexes, but these contain free OH groups in the ligand and bent M–O–Si bonds.[20]

R = c-C$_6$H$_{11}$

19

Zr-O-Si = 146(1)°

R = *i*-C$_4$H$_9$,

20

Pt-O-Si = 130.2(2)°
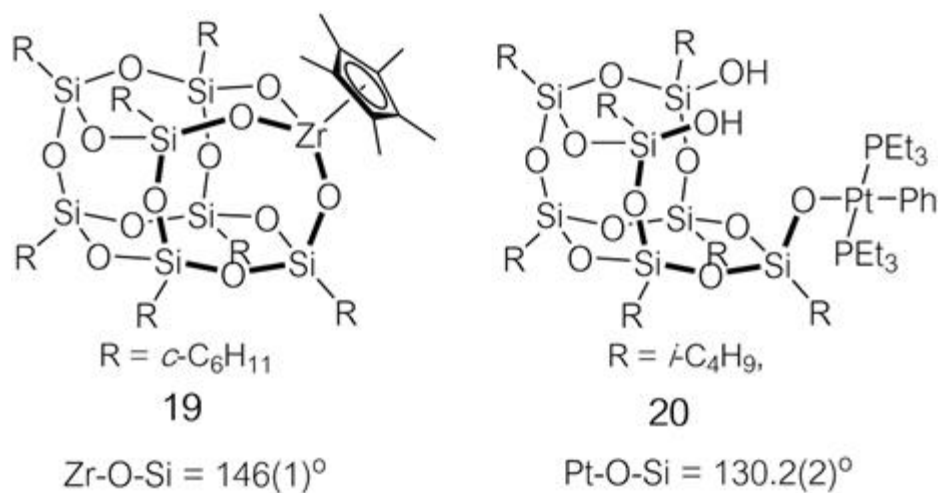
Figure 11.19 Structures of early and late transition metal complexes with silsesquioxane ligands.

Stable coordination of alkoxide ligands to early transition metals hinders reactions of the ligating oxygen atom with added reagents. Chisholm employed sterically bulky alkoxide ligands and reported new reactions of the complexes formed, such as **21** (Figure 11.20).[21] Multinuclear complexes in which the alkoxide ligand operates in a bridging mode have been studied as model molecular compounds of solid metal–oxide surfaces.

21
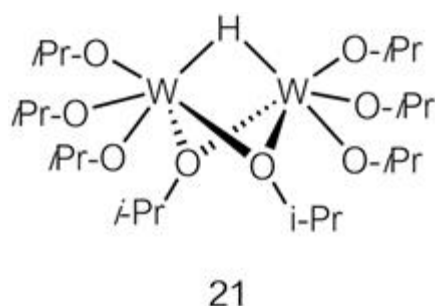
Figure 11.20 Structure of dinuclear tungsten complexes containing alkoxide ligands.

Early transition metal alkoxides are used in catalysts. A Mo-imide complex **22**, shown in Figure 11.21(i), catalyzes olefin metathesis with high activity. The carbene ligand bonded to the Mo center reacts directly with olefin molecules to complete the catalytic cycle. The two alkoxide and one imide supporting ligands also play roles in the catalysis. The imide ligand is highly electron-donating, increasing the electron density on the metal center to enhance the catalysis. The alkoxide ligands, on the other hand, are less electron-donating, and lower the LUMO level of the metal complex, inhibiting deactivation of the catalyst caused by dimerization of the complex. The Mo complex with bulky aryloxide ligands having axial chirality, **23**, is known as a Schrock–Hoveyda catalyst and promotes asymmetric olefin metathesis reactions (Figure 11.21(ii)).[22]
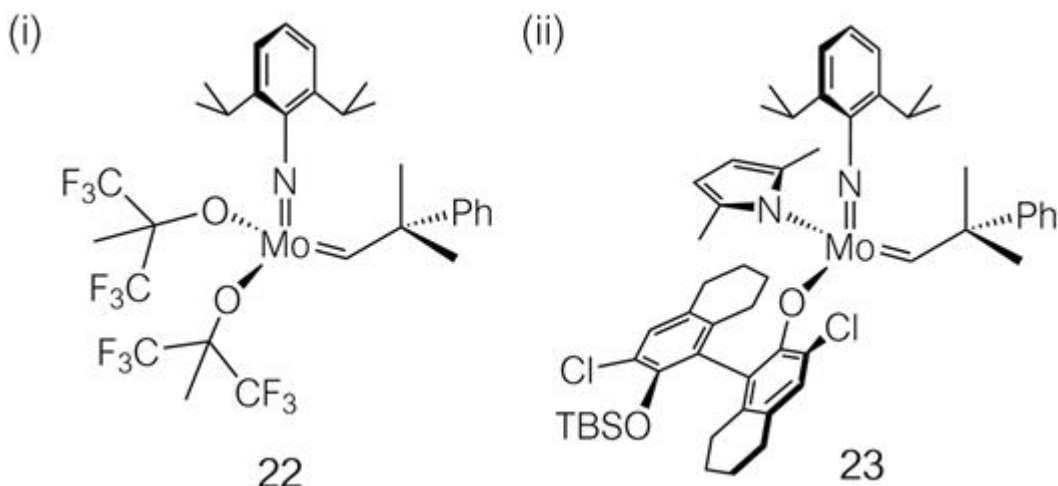
Figure 11.21 Catalysts for olefin metathesis: (i) Schrock catalyst; (ii) Schrock–Hoveyda catalyst.

Ti(iv) complexes with two chelating alkoxyamine ligands were found to catalyze olefin polymerization, as reported by Coates and by Mitsui Chemical Co. (**24** and **25**, Figure 11.22).[23,24] The activity of the catalyst established a new (and thus far, unbeaten) record for molecular catalysis in olefin polymerization, and enables a variety of polymerization reactions. A mechanistic study of the reactions revealed that the ligated structures of the catalysts are retained during the reaction. Related Zr complexes were also reported and used as olefin polymerization catalysts. Addition of alkoxides to the lanthanoid salts results in the formation of the corresponding alkoxide complexes of the metals: bulky alkyl anions and t-butoxide react with YCl_3 to form -ate complexes, formulated as $[Y(CH(SiMe_3)_2)_2(O^tBu)_4]^-$ (**26**). The complexes are further stabilized by coordination of the two alkoxide ligands to the Li cation (Figure 11.22).[25]
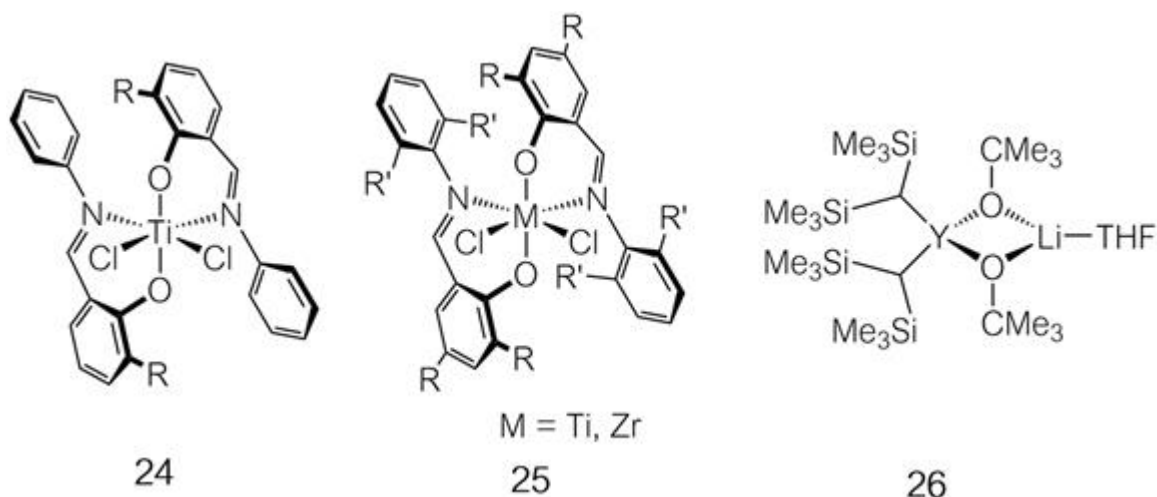
Figure 11.22 Metal complex catalysts for ethylene polymerization and related complexes.

Triaryloxide, composed of three aryloxides bonded to a CH group and calixarene, formed by four aryloxy groups bonded by CH_2 groups in the 2- and 6-positions, function as chelating ligands in Nb complexes **27** and **28** (Figure 11.23).[26] Niobium complexes having these ligands activate a dinitrogen molecule by scission of the triple bond between the nitrogen atoms to form complexes with bridging nitride ligands. In such reactions, π-donation of the multiple Nb–O bond of the alkoxide ligand increases electron density at the metal center, resulting in the six-electron reduction of the dinitrogen molecule, and complete scission of the triple bond.
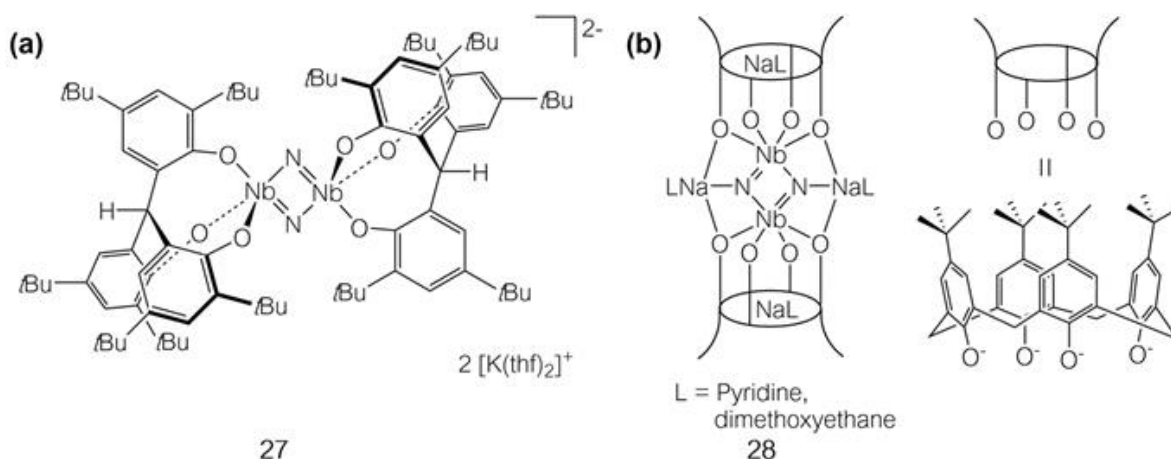
Figure 11.23 Niobium complexes with aryloxide and nitride ligands formed *via* activation of a dinitrogen molecule.

Insertion of small molecules into the M–O bond in late transition metal alkoxide complexes has been studied for several decades. An alkenyl(alkoxide)platinum(ii) complex was reported to undergo insertion by CO into the Pt–O bond under mild conditions to form a platinum(ii) complex containing an ester function (**29**, Figure 11.24(i)).[27] The analogous reaction of CO with the Pt–OH complex also proceeds, and the product further reacts with CO, resulting in the formation of an acyl(hydroxycarbonyl)platinum(ii) complex (**30**, Figure 11.24(ii)). The complexes undergo insertion of CO into the Pt–O bond rather than into the Pt–C bond. Further reaction of CO with complex **30** produces the acylplatinum complex *via* insertion of CO into the Pt–C$_{alkenyl}$ bond. Reaction of MeOH with the carboxyl ligand forms the methoxycarbonyl complex.[28]
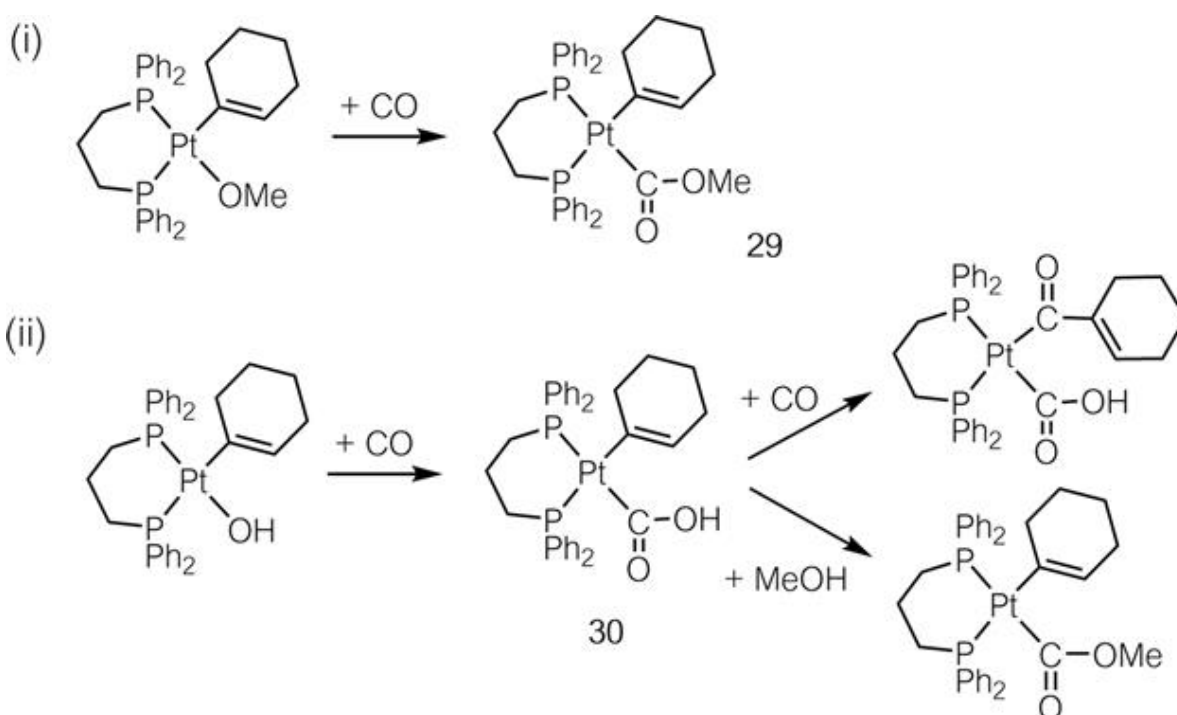
Figure 11.24 Insertion of CO into Pt–O bonds of alkoxyplatinum(ii) complexes.

Figure 11.25 shows possible mechanisms of the reaction. Migratory insertion of a coordinated CO molecule into the Pt–O bond forms the complex with an alkoxycarbonyl ligand, as shown in Figure 11.25(i). Initial dissociation of the alkoxide ligand and coordination of carbon monoxide

generates a cationic intermediate with the alkoxide as a counter anion. Subsequent nucleophilic reaction of the alkoxide ligand to the carbonyl ligand also yields the alkoxycarbonyl complex as the product (Figure 11.25(ii)). Concerted insertion of a CO molecule into the Pt–O bond *via* an intermediate with the OMe group in the coordination sphere can be considered as a pathway for the formation of the complex with an alkoxycarbonyl ligand (Figure 11.25(iii)).

Figure 11.25 Possible mechanisms for insertion of CO into M–O bonds.

Palladium complexes with fluorinated alkoxide ligands were reported to undergo insertion of CO into the Pd–O bond to form complexes containing an alkoxycarbonyl ligand (**31**, Figure 11.26).[29] The reaction exhibits temperature-dependent reversibility, probably *via* an associative pathway (Figure 11.25(i)).

Figure 11.26 Reversible insertion of CO into a Pd–O bond.

A Vaska-type square-planar Ir complex with an alkoxide ligand reacts with MeI generating a hexacoordinate Ir(iii) complex, which undergoes insertion of CO into the Ir–O bond to form an alkoxycarbonyl iridium(iii) complex (**32**, Figure 11.27). Atwood proposed a reaction mechanism involving initial dissociation of the methoxide ligand to form an ion pair intermediate, and nucleophilic attack of MeO⁻ on the new carbonyl ligand, based on the results of isotope labeling experiments.[30]
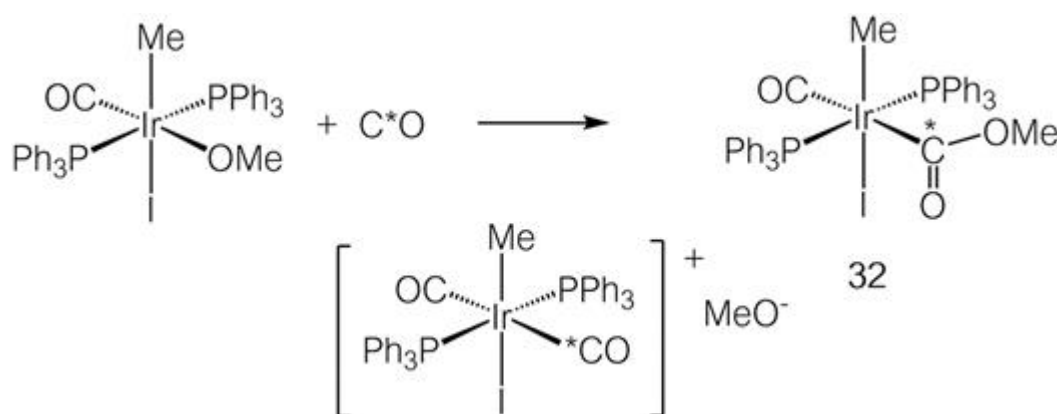
Figure 11.27 Insertion of CO into an Ir–OMe bond.

Bryndza investigated details of the insertion of CO into the Pt–O bond of [PtMe(OMe)(dppe)] (dppe = 1,2-bis(diphenylphosphino)ethane).[31] The results indicate that a mechanism involving dissociation of the OMe ligand (Figure 11.25(ii)) is less plausible than the concerted insertion of CO into the Pt–OMe bond (Figure 11.25(i)). The author also states that an alternative mechanism, involving an intermediate with the OMe group in the coordination sphere, cannot be excluded (Figure 11.25(iii)).

In an attempt to understand the experimental results of the reaction, including kinetics, deuterium-labelling reactions and NMR observations of the intermediates, and to clarify the mechanism further, Macgregor carried out molecular orbital calculations[32] on a mononuclear model complex with PH₃ ligands, cis-[M(Me)(OMe)(PH$_3$)$_2$] (M = Ni, Pd, Pt). The M–Me bond dissociation energy increases in the order, Ni (170 kJ mol⁻¹) < Pd (208 kJ mol⁻¹) < Pt (261 kJ mol⁻¹). The difference of the dissociation energies of the M–OMe bonds is smaller among the Ni (253 kJ mol⁻¹), Pd (246 kJ mol⁻¹), and Pt (279 kJ mol⁻¹) complexes. Thus, the influence of the

metal on the insertion rate is less significant for CO insertion into the M–O bond than into the M–C bond. This observation is related to the experimental results for carbonylation of [NiMe(OPh)(phosphine)$_2$]. The Ni complex undergoes preferential insertion of CO into the Ni–C bond to form an acetylnickel(ii) complex *via* a pentacoordinate intermediate formed by associative coordination of a CO molecule.[33]

The carbonylation of Pt complexes with monodentate phosphine ligands is initiated by dissociation of a phosphine ligand to form a methyl(methoxy)(phosphine)carbonylplatinum(ii) intermediate (Figure 11.28(A)). Insertion of CO into the Pt–C or Pt–O bond is governed by the geometry of the intermediates.

Pt-O insertion   Pt-C insertion   ion-pair intermediates (or transition state)
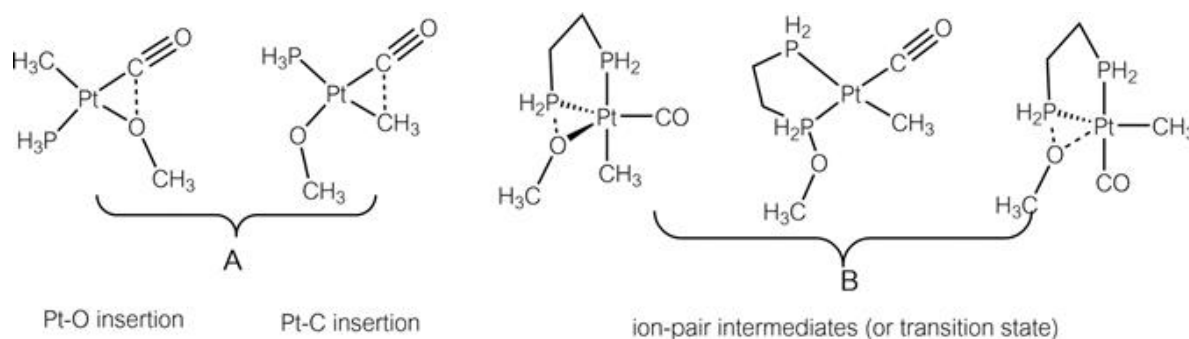
Figure 11.28   Proposed intermediates (or transition states) of reactions involving insertion of CO into a Pt–O bond obtained from computational studies.

Theoretical calculations for insertion of CO into the Pt–O bond of the Pt complex bearing the diphosphine ligand $H_2PCH_2CH_2PH_2$ suggest the involvement of intermediates with interactions between the alkoxide group and a P atom or between the alkoxide group, a P atom and the Pt atom, as shown in Figure 11.28(B).

A rhenium methoxide complex undergoes insertion of CO_2 and CS_2 into the Re–O bond to yield **33**, as shown in Figure 11.29.[34]
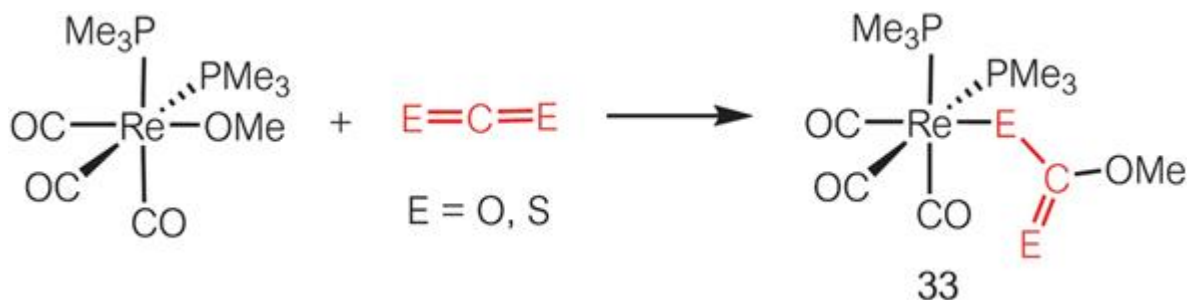
Figure 11.29 Insertion of CO_2 and CS_2 into a Re–O bond.

There have also been several reports on the insertion of alkenes and alkynes into M–oxygen bonds: alkoxide complexes of Mn and Re undergo insertion of dimethyl acetylenedicarboxylate into the M–O bond, forming an alkenyl metal complex (**34**, Figure 11.30).[35]
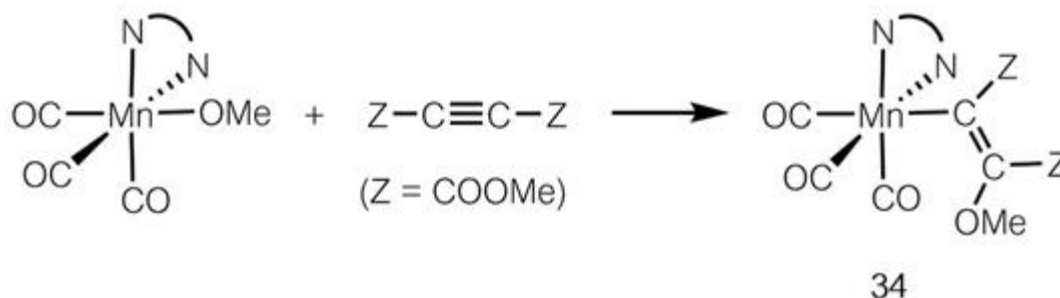
Figure 11.30 Insertion of an alkyne into a Mn–O bond.

Bryndza and Bercaw investigated the thermal decomposition reactions of the methoxyplatinum(ii) complexes and reported much higher reactivity of the methoxide ligands than the ethyl ligands.[36] These are summarized in Figure 11.31.
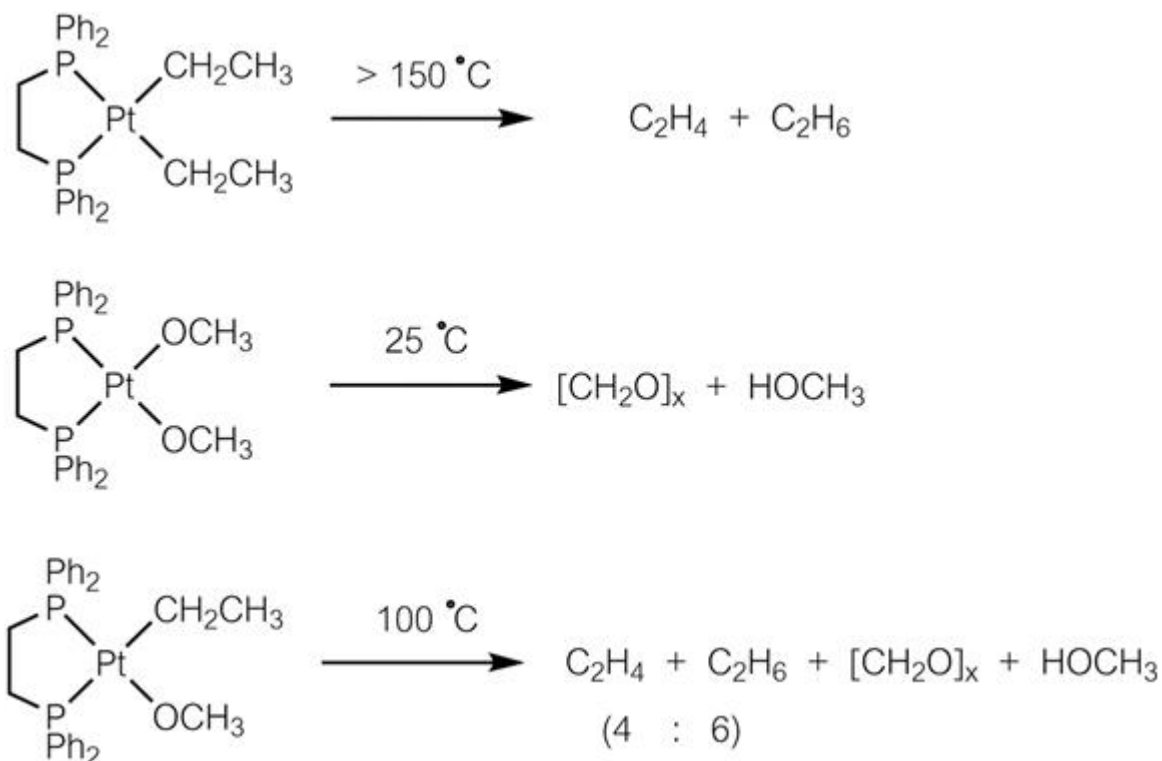
Figure 11.31 Thermal decomposition of complexes with Pt–C and Pt–O bonds.

The diethylplatinum(ii) complex undergoes β hydride elimination to release ethylene above 150 °C, while the bis(methoxide)platinum(ii) complex undergoes elimination of formaldehyde at room temperature. The complex having both ethyl and methoxide ligands decomposes at 100 °C, giving a 4 : 6 mixture of ethane and ethylene. The OMe ligand undergoes β hydride elimination of formaldehyde much more easily than the ethyl ligand. In the complexes having both ethyl and methoxide ligands, the OMe ligand enhances β hydride elimination of the *cis* ethyl ligand.

Bergman investigated an aryloxyrhodium(i) complex with three phosphine ligands, which is associated with phenol *via* a stable O–H–O hydrogen bond in both solid and solution states (**35**, Figure 11.32). The association constants are comparable with that between phenol and pyridine.[37]
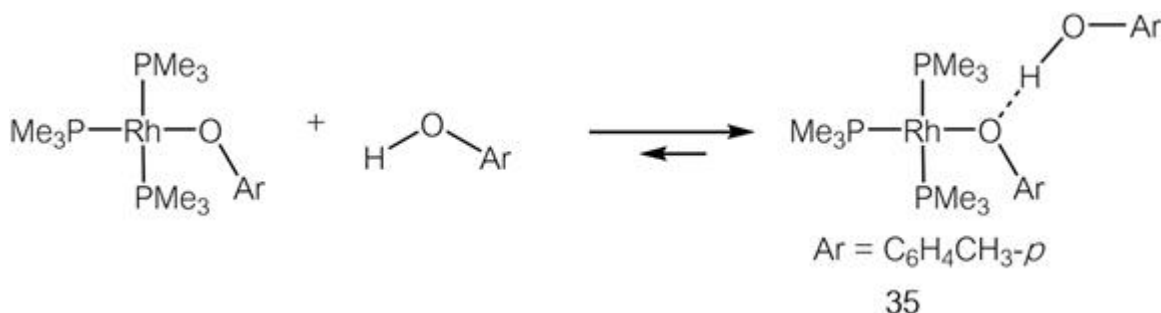
Figure 11.32 Association of phenol with a rhodium(I) phenoxide complex.

Formation of similar association complexes *via* hydrogen bonding were reported also for fluoroalcohols and phenols with Pd and Pt complexes containing N- and P-ligands, as well as rhenium aryloxy complexes having carbonyl ligands.[38,39]

The alcohol-alkoxide (aryloxide) associated complexes of late transition metals undergo a 1,3 M–O shift on the NMR time scale, as shown in Figure 11.33. A four-membered cyclic intermediate is suggested, although it is not detected in the NMR spectra of the solution.
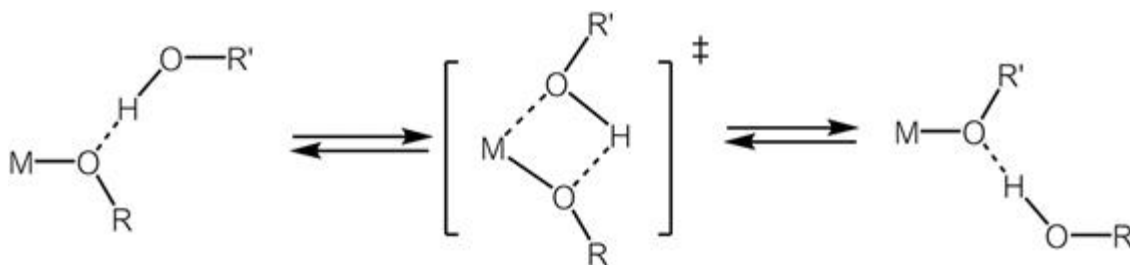
Figure 11.33 Proposed mechanism of ligand exchange of an alcohol-alkoxide adduct.

A palladium complex with a fluoroalkoxide ligand reacts with phenol and phenyl acetate to form a complex with a phenoxide ligand (**36**, Figure 11.34). The C–O bond of the fluoroalkoxide complex undergoes metathesis-type exchange with the O–H and C–O bonds of phenol and phenyl acetate, respectively. The Pd–O σ-bond of the phenoxide complex formed is more stable than that of the fluoroalkoxide complex, thus favoring the formation of phenoxide for thermodynamic reasons. The reaction is applied to the transesterification of ester and phenol catalyzed by Pd complexes.
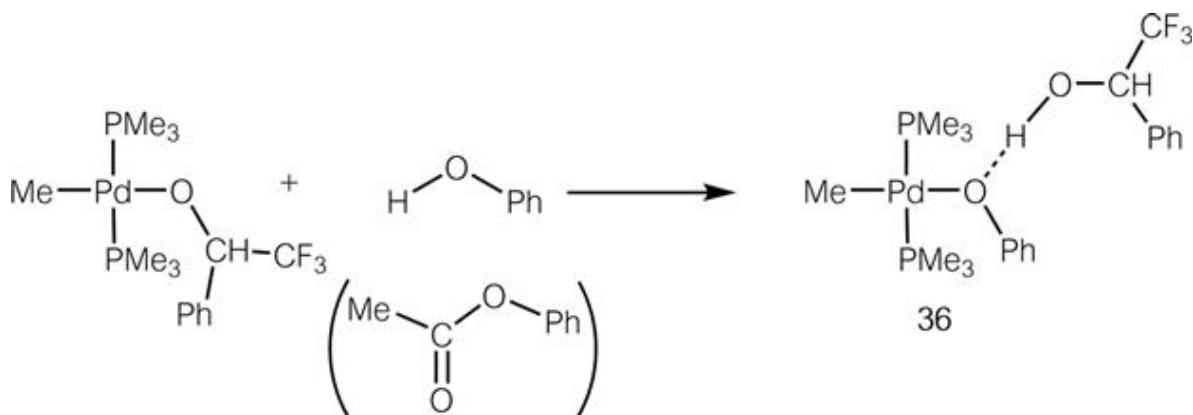
Figure 11.34 Exchange of coordinated fluoroalkoxide with phenol.

The silsesquioxane complexes of late transition metal complexes undergo intramolecular exchange between OH and O–M groups. Figure 11.35 shows a Pd-silsesquioxane complex **37** that undergoes an M–O shift: two SiO–H groups and a SiO–Pd bond undergo exchange rapidly on the NMR timescale.[40] X-ray crystallography of the complex revealed hydrogen bonds between the non-bonded OH group and the ligating oxygen atom. This intramolecular exchange of the siloxide ligand with silanol occurs rapidly and reversibly.
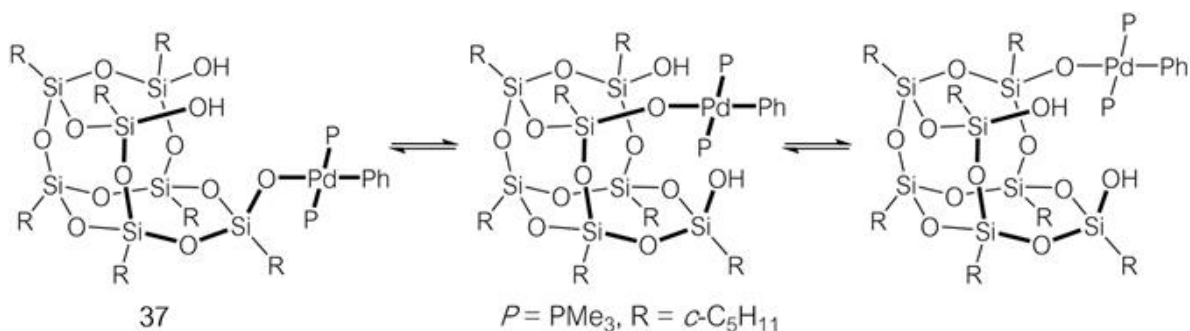
Figure 11.35 Dynamic behavior of silsesquioxane-coordinated Pd complex.

11.4 Properties of M–SR Complexes

Thiolate groups form stable complexes with early and late transition metals due to their high basicity. Late transition metal complexes with thiolate ligands have longer coordination bonds than the alkoxide complexes, and do not suffer unfavorable interaction between the filled orbitals (Figure

11.16(b)). Complexes with thiolate ligands have long been studied as model compounds of the active sites of metalloenzymes. This section, as mentioned in the introductory part, is focused on the fundamental structure and reactivity of transition metal complexes bearing thiolate ligands.

Figure 11.36 summarizes details of the reaction of alkynes with a thiolate–platinum(ii) complex involving insertion of the alkyne into the Pt–S bond.
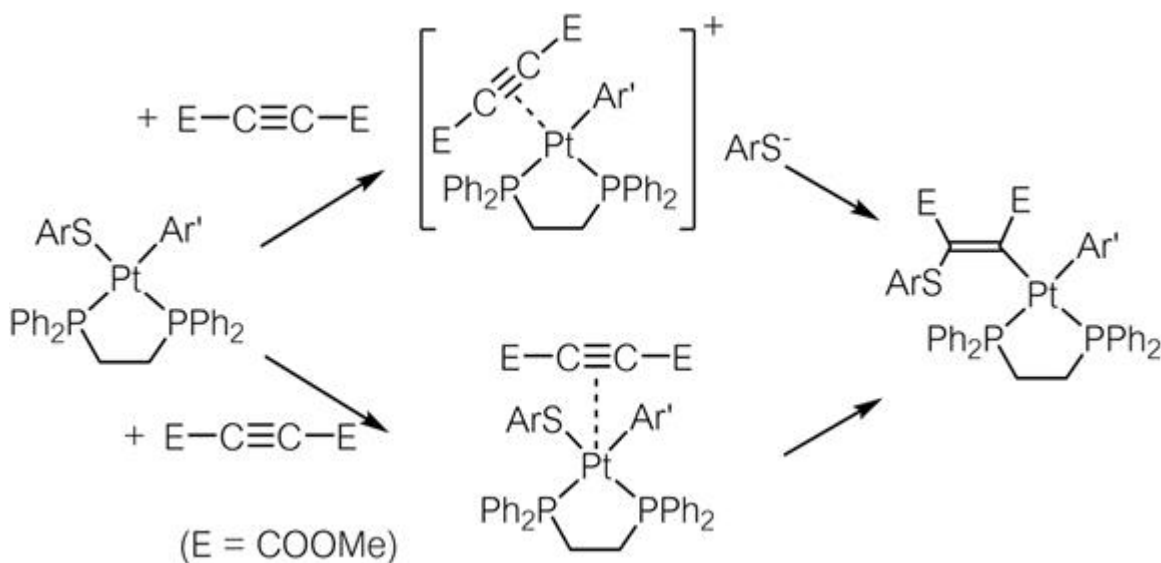
Figure 11.36   Insertion of an alkyne into a Pt–S bond.

Aryl(thiolate)platinum(ii) complexes with chelating diphosphine ligands undergo insertion of alkynes into the Pt–S bond to form alkenyl-platinum(ii) complexes. Two pathways are possible, as shown in Figure 11.36. The upper route involves dissociative substitution of the thiolate ligand to form a tetracoordinate intermediate with the alkyne ligand, while the lower route proceeds *via* associative coordination of the alkyne, forming a pentacoordinate intermediate, followed by intramolecular insertion of the alkyne. The geometry of the starting complex and results of the reaction favor the latter mechanism.[41] The C–S bond-forming reaction above is considered to be important and relevant to the Pt-catalyzed addition of disulfides to alkynes.

Hydrosulfide complexes (M–SH) are regarded as analogues of thiolate complexes, but show unique reactivity owing to the lability of the S–H bond. A dinuclear Mo complex with two bridging hydrosulfides and two

bridging sulfides reacts with two equivalents of alkyne giving **38**, as shown in Figure 11.37.[42]
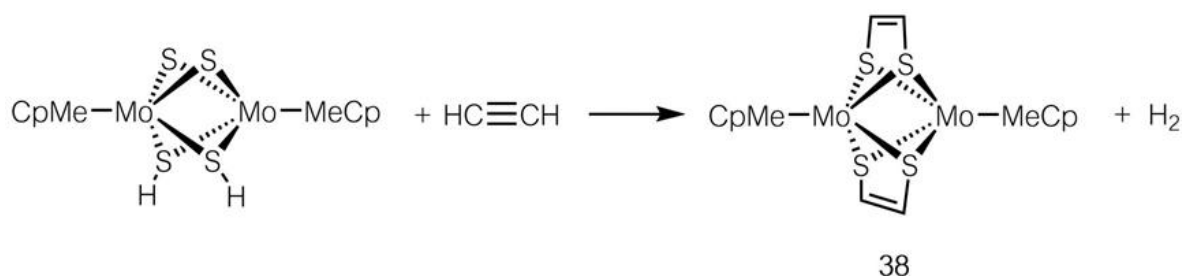
Figure 11.37 Reaction of an alkyne with a dinuclear Mo complex with bridging sulfide and hydrosulfide ligands.

A dinuclear Rh complex with two terminal hydrosulfide ligands undergoes insertion of alkynes into the S–H bonds, forming a bis(thiolate) complex **39**, as shown in Figure 11.38.[43]
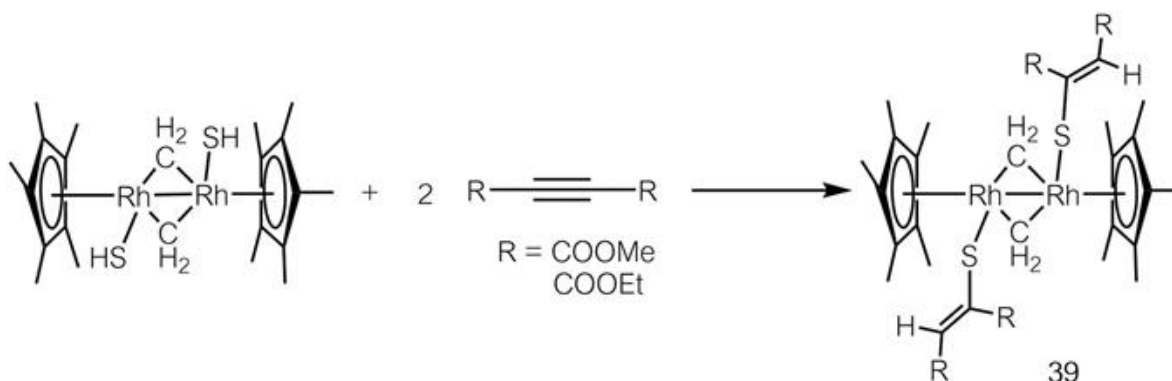
Figure 11.38 Insertion of an alkyne into the S–H bonds of a hydrosulfide ligand.

Compared to M–OR complexes, α-alkyl elimination is more common in M–SR complexes. Such reactions involve migration of the alkyl group from the sulfur atom to the metal center, forming a sulfide complex (M=S), although they have not been studied in detail. The process is considered to be involved in the hydrodesulfurization of organo-sulfur complexes during heterogeneous catalysis.

Eisch used a Ni(0) complex formed from Ni(cod)$_2$ and bipyridine, and observed the desulfurization of dibenzothiophene to form biphenyl.[44] He

compared the reactivity of various substituted dibenzothiophenes and proposed a mechanism involving a radical species. The low-valent Ni complex **40** with bidentate diphosphine ligands cleaves the C–S bond of thiophene at room temperature, as shown in Figure 11.39. The S-containing hydrocarbon formed is rapidly and easily exchanged by the thiophene derivative in the reaction mixture.[45]
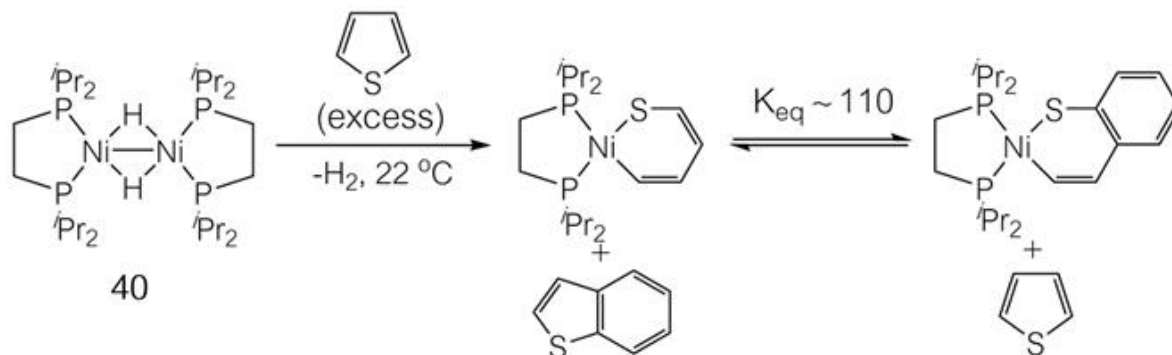
Figure 11.39 Activation of the C–S bond of thiophenes by a dinuclear Ni complex.

$[Ni_2(\mu\text{-}H)_2\{(^iPr)_2PCH_2CH_2P(^iPr_2)\}_2]$ catalyzes the methylative desulfurization of dibenzothiophene in the presence of two equivalents of MeMgBr (Figure 11.40). The reaction forms the solid formulated as $MgSBr_2$, probably by reduction of initially formed NiS by the Mg reagents to regenerate the catalytically active Ni(0) complex.[46] Alper reported desulfurization of thiols to yield hydrocarbons using catalytic amounts of Mo and Co carbonyl complexes.[47]
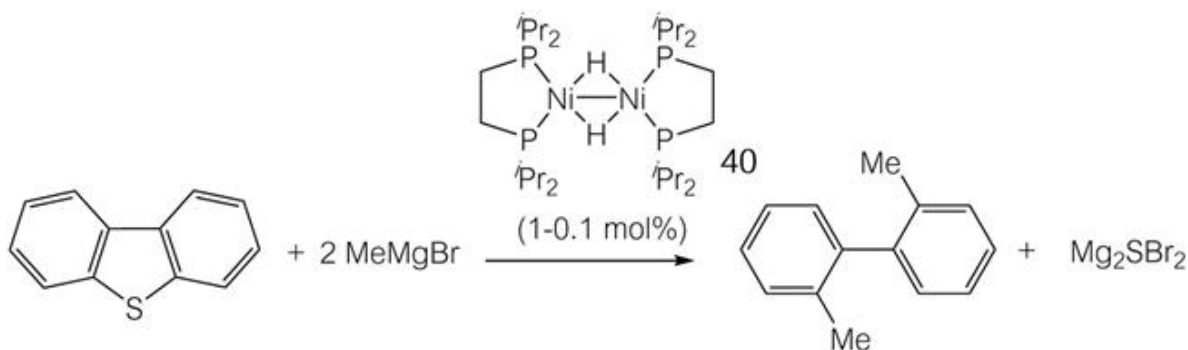
Figure 11.40 Desulfurization of dibenzothiophene catalyzed by a Ni complex.

The controlled synthesis of metal sulfides and their deposition on solid surfaces are of importance in material science and technology. The C–S bond (259 kJ mol^{-1}) is weaker than the C–O bond (360 kJ mol^{-1}). This enhances α-elimination of the alkyl groups in thiolate complexes (M–SR), forming new M–R and M=S bonds. Concerted α-elimination of alkyl groups from the alkoxide ligands of late transition metal complexes has not been reported so far. A tris(ethanedithiolate)niobium complex reacts with weak protonic acids resulting in cleavage of the C–S bonds and forming a complex having sulfide, thiolate and thioether ligands **41**, as shown in Figure 11.41.[48]
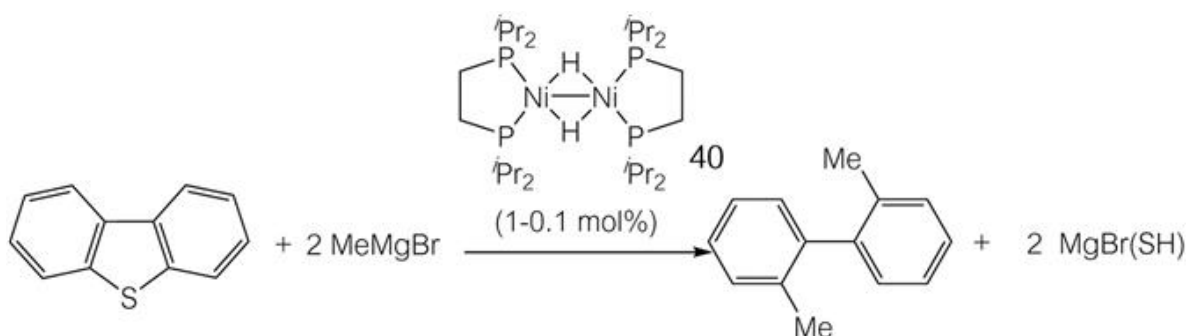
Figure 11.41 C–S bond cleavage reactions of a thiolate-Nb complex.

Benzenthiolate complexes of Ni and Pd also undergo thermal decomposition to generate diphenyl sulfide (Figure 11.42). In this case, the phosphine ligand forms sulfur adducts, which renders characterization of the metal-containing products difficult.[49]
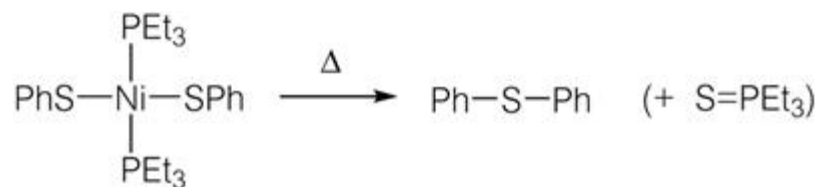
Figure 11.42 C–S bond formation by thermal decomposition of a nickel thiolate complex.

Thermal decomposition of M(SR)$_n$ type complexes without auxiliary ligands is expected to cause C–S bond cleavage in the ligand, forming metal sulfides. Neutral thiolate complexes of zinc and cadmium, [Zn(SR)$_2$]$_n$ and

$[Cd(SR)_2]_n$, have polymeric structures with bridging thiolate ligands.[50] Thermal reactions of the complexes release dialkylsulfides to form the corresponding metal sulfides. Thermal reaction of the selenolate Cd complex with phosphine ligands, $[Cd(SePh)_2]_2[Et_2PCH_2CH_2PEt_2]$, forms CdSe, similarly.[51]

11.5 Summary

Group 16 elements have high electronegativity and can be expected to react more as ionic complexes, rather than those with more covalent character. However, complexes with OR and SR ligands show properties more consistent with coordination bonds with covalent character. This chapter discussed the insertion of small molecules into M–O and M–S bonds, and coupling of thiolate ligands with organic ligands, reactions which are considered favorable from the perspective of atom-economy. On the other hand, alkoxide and thiolate groups are important as functional groups of organic compounds, and so their complexes will attract the attention of organic chemists for new synthesis applications.

References

1. F. Yamashita, H. Kuniyasu, J. Terao and N. Kambe, *Inorg. Chem.*, 2006, **45**, 1399.
2. H. E. Bryndza, L. K. Fong, R. A. Paciello, W. Tam and J. E. Bercaw, *J. Am. Chem. Soc.*, 1987, **109**, 1444.
3. M. A. Bennett and T. Yoshida, *J. Am. Chem. Soc.*, 1978, **100**, 1750.
4. S. Komiya, S. Tane-ichi, A. Yamamoto and T. Yamamoto, *Bull. Chem. Soc. Jpn.*, 1980, **53**, 673.
5. Y. Hayashi, S. Komiya, T. Yamamoto and A. Yamamoto, *Chem. Lett.*, 1984, 1363.
6. Y. Hayashi, S. Komiya, T. Yamamoto and A. Yamamoto, *Chem. Lett.*, 1984, 977.
7. K. Osakada, K. Matsumoto, T. Yamamoto and A. Yamamoto, *Organometallics*, 1985, **4**, 857.
8. (a) P. T. Matsunaga and G. L. Hillhouse, *J. Am. Chem. Soc.*, 1993, **115**, 2075; (b) K. Koo and G. L. Hillhouse, *Organometallics*, 1998, **17**, 2924.
9. K. Koo, G. L. Hillhouse and A. L. Rheingold, *Organometallics*, 1995, **14**, 456.
10. G. A. Vaughan and G. L. Hillhouse, *J. Am. Chem. Soc.*, 1988, **110**, 7215.
11. J. M. Gonzales, R. Distasio Jr., R. A. Periana, W. A. Goddard III and J. Oxgaard, *J. Am. Chem. Soc.*, 2007, **129**, 15794.
12. R. Han, G. L. Hillhouse, R. T. Lum, S. L. Buchwald and A. L. Rheingold, *J. Am. Chem. Soc.*, 1998, **120**, 7657.
13. A. Sugimori, T. Akiyama, M. Kajitani and T. Sugiyama, *Bull. Chem. Soc. Jpn.*, 1999, **72**, 879.
14. R. T. Weberg, R. C. Haltiwanger, J. C. V. Laurie and M. R. DuBois, *J. Am. Chem. Soc.*, 1986, **108**, 6242.
15. (a) U. Koelle, B. S. Kang and U. Thewalt, *Organometallics*, 1992, **11**, 2893; (b) A. Hörnig, U. Englert and U. Koelle, *J. Organomet. Chem.*, 1993, **453**, 255; (c) H. Suzuki, T. Kakigano, M. Igarashi, A. Usui, K. Noda, M. Oshima, M. Tanaka and Y. Moro-oka, *Chem. Lett.*, 1993, 1707.

16. (a) T. Konno, *Bull. Chem. Soc. Jpn.*, 2004, **77**, 627; (b) K. Tokuda, K. Okamoto and T. Konno, *Inorg. Chem.*, 2000, **39**, 333; (c) T. Konno, T. Yoshimura, K. Aoki, K. Okamoto and M. Hirotsu, *Angew. Chem. Int. Ed.*, 2001, **40**, 1765.

17. P. T. Wolczanski, *Polyhedron*, 1995, **14**, 3335.

18. O. W. Steward and D. R. Fussaro, *J. Organomet. Chem.*, 1977, **129**, C28.

19. (a) F. J. Feher, *J. Am. Chem. Soc.*, 1986, **108**, 3850; (b) F. J. Feher, D. A. Newman and J. F. Walzer, *J. Am. Chem. Soc.*, 1989, **111**, 1741.

20. N. Mintcheva, M. Tanabe and K. Osakada, *Organometallics*, 2006, **25**, 3776.

21. (a) M. H. Chisholm, J. C. Huffman and C. A. Smith, *J. Am. Chem. Soc.*, 1986, **108**, 222; (b) M. H. Chisholm, K. Folting, J. C. Huffman, J. A. Klang and W. E. Streib, *Organometallics*, 1989, **8**, 89.

22. (a) R. R. Schrock, *Acc. Chem. Res.*, 1990, **23**, 158; (b) R. R. Schrock, *Pure Appl. Chem.*, 1994, **66**, 1447; (c) S. J. Malcolmson, S. J. Meek, E. S. Sattely, R. R. Schrock and A. H. Hoveyda, *Nature*, 2008, **456**, 933; (d) E. S. Sattely, S. J. Meek, S. J. Malcolmson, R. R. Schrock and A. H. Hoveyda, *J. Am. Chem. Soc.*, 2009, **131**, 943.

23. (a) J. Tian and G. W. Coates, *Angew. Chem. Int. Ed.*, 2000, **39**, 3626; (b) J. Tian, P. D. Hustad and G. W. Coates, *J. Am. Chem. Soc.*, 2001, **123**, 5134.

24. (a) S. Matsui, Y. Tohi, M. Mitani, J. Saito, H. Makio, H. Tanaka, M. Nitabaru, T. Nakano and T. Fujita, *Chem. Lett.*, 1999, 1065; (b) H. Makio, N. Kashiwa and T. Fujita, *Adv. Synth. Catal.*, 2002, **344**, 477; (c) T. Matsugi and T. Fujita, *Chem. Soc. Rev.*, 2008, **37**, 1264; (d) J. Saito, M. Mitani, J. Mohri, Y. Yoshida, S. Matsui, S. Ishii, S. Kojoh, N. Kashiwa and T. Fujita, *Angew. Chem. Int. Ed.*, 2001, **40**, 2918; (e) M. Mitani, J. Mohri, Y. Yoshida, J. Saito, S. Ishii, K. Tsuru, S. Matsui, R. Furuyama, T. Nakano, H. Tanaka, S. Kojoh, T. Matsugi, N. Kashiwa and T. Fujita, *J. Am. Chem. Soc.*, 2002, **124**, 3327.

25. W. J. Evans, R. N. R. Broomhall-Dillard and J. W. Ziller, *Organometallics*, 1996, **15**, 1351.

26. (a) A. Caselli, E. Solari, R. Scopelliti, C. Floriani, N. Re, C. Rizzoli and A. Chiesi-Villa, *J. Am. Chem. Soc.*, 2000, **122**, 3652; (b) H. Kawaguchi and T. Matsuo, *Angew. Chem. Int. Ed.*, 2002, **41**, 2792; (c) F. Akagi, T. Matsuo and H. Kawaguchi, *Angew. Chem. Int. Ed.*, 2007, **46**, 8778.

27. M. A. Bennett and A. Rokicki, *J. Organomet. Chem.*, 1983, **244**, C31.

28. M. A. Bennett and A. Rokicki, *Organometallics*, 1985, **4**, 180.

29. Y. J. Kim, K. Osakada, K. Sugita, T. Yamamoto and A. Yamamoto, *Organometallics*, 1988, **7**, 2182.

30. K. A. Bernard and J. D. Atwood, *Organometallics*, 1989, **8**, 795.

31. H. E. Bryndza, *Organometallics*, 1985, **4**, 1686.

32. S. A. Macgregor and G. W. Neave, *Organometallics*, 2003, **22**, 4547, ; 2004, **23**, 891 .

33. S. Komiya, Y. Akai, K. Tanaka, T. Yamamoto and A. Yamamoto, *Organometallics*, 1985, **4**, 1130.

34. R. D. Simpson and R. G. Bergman, *Oragnometallics*, 1992, **11**, 4306.

35. E. Hevia, J. Pérez, L. Riera, V. Riera and D. Miguel, *Organometallics*, 2002, **21**, 1750.

36. H. E. Bryndza, J. C. Calabrese, M. Marsi, D. C. Roe, W. Tam and J. E. Bercaw, *J. Am. Chem. Soc.*, 1986, **108**, 4805.

37. S. E. Kegley, C. J. Schaverien, J. H. Freudenberger, R. G. Bergman, S. P. Nolan and C. D. Hoff, *J. Am. Chem. Soc.*, 1987, **109**, 6563.

38. (a) Y.-J. Kim, K. Osakada, A. Takenaka, T. Yamamoto and A. Yamamoto, *J. Am. Chem. Soc.*, 1990, **112**, 1096; (b) Y.-J. Kim, K. Osakada, A. Yamamoto and S. Ishiguro, *Bull. Chem. Soc. Jpn.*, 1989, **62**, 964; (c) K. Osakada, Y. Oshiro and A. Yamamoto, *Organometallics*, 1991, **10**, 404; (d) G. M. Kapteijn, A. Dervisi, D. M. Grove, H. Kooijman, M. T. Lakin, A. L. Spek and G. van Koten, *J. Am. Chem. Soc.*, 1995, **117**, 10939.

39. R. D. Simpson and R. G. Bergman, *Organometallics*, 1993, **12**, 781.

40. M. Tanabe, K. Mutou, N. Mintcheva and K. Osakada, *Organometallics*, 2008, **27**, 519.

41. H. Kuniyasu, K. Takekawa, F. Yamashita, K. Miyafuji, S. Asano, Y. Takai, A. Ohtaka, A. Tanaka, K. Sugoh, H. Kurosawa and N. Kambe, *Organometallics*, 2008, **27**, 4788.
42. C. J. Casewit and M. R. Dubois, *J. Am. Chem. Soc.*, 1986, **108**, 5482.
43. Y. Kaneko, N. Suzuki, A. Nishiyama, T. Suzuki and K. Isobe, *Organometallics*, 1998, **17**, 4875.
44. J. J. Eisch, L. E. Hallenbeck and K. I. Han, *J. Org. Chem.*, 1983, **48**, 2963.
45. D. A. Vicic and W. D. Jones, *J. Am. Chem. Soc.*, 1997, **119**, 10855, *;* J. Am. Chem. Soc., 1999, **121**, 7606 .
46. (a) J. Torres-Nieto, A. Arévalo, P. García-Gutiérrez, A. Acosta-Ramírez and J. J. García, *Organometallics*, 2004, **23**, 4534; (b) J. Torres-Nieto, A. Arévalo and J. J. García, *Organometallics*, 2007, **26**, 2228.
47. (a) H. Alper and C. Blais, *J. Chem. Soc., Chem. Commun.*, 1980, 169; (b) S. Antebi and H. Alper, *Organometallics*, 1986, **5**, 596.
48. K. Tatsumi, Y. Sekiguchi, A. Nakamura, R. E. Cramer and J. J. Rupp, *J. Am. Chem. Soc.*, 1986, **108**, 1358.
49. (a) T. Yamamoto and Y. Sekine, *Inorg. Chim. Acta*, 1986, **83**, 47; (b) K. Osakada, H. Hayashi, M. Maeda, T. Yamamoto and A. Yamamoto, *Chem. Lett.*, 1986, 597.
50. (a) I. G. Dance, *J. Am. Chem. Soc.*, 1980, **102**, 3445; (b) K. Osakada and T. Yamamoto, *J. Chem. Soc., Chem. Commun.*, 1987, 1117; (c) K. Osakada and T. Yamamoto, *Inorg. Chem.*, 1991, **30**, 2328.
51. J. G. Brennan, T. Siegrist, P. J. Carroll, S. M. Stuczynski, L. E. Brus and M. L. Steigerwald, *J. Am. Chem. Soc.*, 1989, **111**, 4141.

Chapter 12

Nobel Prizes Relating to Organometallic Chemistry

Kohtaro Osakada[a]

[a] Tokyo Institute of Technology, Japan kosakada@res.titech.ac.jp

12.1 Introduction

This chapter presents six Nobel Prizes for chemistry relating to the field of organometallics: olefin polymerization catalysts (1963), sandwich compounds (1973), electrically conductive polymers (2000), asymmetric catalysis (2001), olefin metathesis (2005), and Pd-catalyzed cross-coupling reactions (2010). These most prestigious prizes were awarded for achievements in organometallic chemistry or those closely related to this research area. Another, concerning boron- and phosphorus-containing compounds in 1979, can also be classified as relating to the organometallic chemistry of main group elements.

The study of organometallic chemistry started in the middle of the last century, expanded rapidly and achieved a number of pioneering and important scientific milestones, including those noted above. Organometallic chemistry has a strong relationship with other research areas, including inorganic, organic, polymer and catalysis chemistry. It also relates to material science and bio-inorganic chemistry, although these topics are not included in this chapter. The initial successes of organometallic chemistry encouraged many talented scientists to enter the field, which resulted in the further increase of knowledge and progress, expanding the influence of this research field to related sciences and technologies. Many books and articles have already described certain details regarding these Nobel Prizes, but this chapter will focus on the

relationship of the discoveries to organometallic chemistry, the initial progress of the related science, and the influence of the research on industry and human society.

12.2 Olefin Polymerization Catalysts, Nobel Prize for Chemistry 1963, Karl Ziegler and Giulio Natta

Karl Ziegler and Giulio Natta discovered high mass polymerization catalysts for ethylene and propylene, the basis of modern life, science and technology, and won the Nobel Prize for chemistry in 1963, *"for their discoveries in the field of the chemistry and technology of high polymers"*.

The 1963 Nobel ceremony speech of that year includes the following sentences: "Towards the end of his life, Alfred Nobel was thinking of the manufacture of artificial rubber. Since then, many rubber-like materials have been produced, but only the use of Ziegler catalysts enables us to synthesize a substance that is identical with natural rubber".[1]

As mentioned in Chapter 7, Ziegler catalysts ($TiCl_4$ + $AlEt_3$) and Natta catalysts ($TiCl_3$ + AlR_3) are the original olefin polymerization transition metal catalysts. The catalysts, modified by using solid supports and added donor compounds, increased polyolefin productivity and still occupy positions as the major olefin polymerization catalysts in industry seven decades after their initial discovery. A number of related catalysts using transition metals and alkylating reagents (co-catalysts) have been investigated for the purposes of increasing the productivity and selectivity of olefin polymerization and, together with the use of new monomers and copolymerization techniques, have expanded the scope of the polymerization. Before their discovery, commercial production of polyethylene had required the use of oxygen as the radical initiator and high temperature and pressure. The polyethylene obtained from this catalysis had low density due to its branched structure (LDPE, low density polyethylene, density = 0.91–0.93 g cm^{-3}). Polymerization using the Ziegler catalyst, however, resulted in high density (HDPE, high density polyethylene, density >0.942 g cm^{-3}). Figure 12.1 compares the structures of the two types of polyethylene. HDPE is obtained as a much harder solid than LDPE due to its higher linear : branched chain ratio, which affects the physical properties and commercial utility of the polymers.
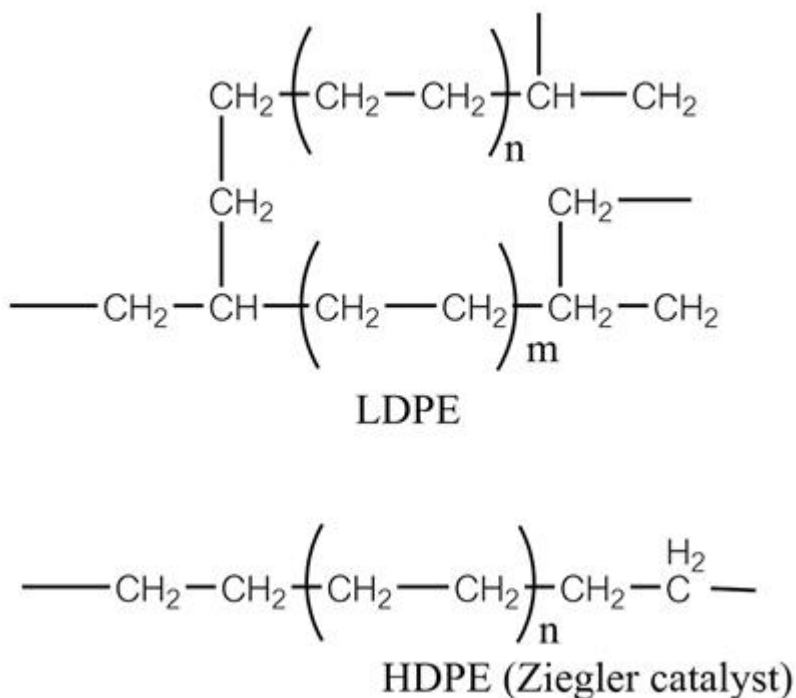
Figure 12.1 Typical structures of polyethylene.

The discovery of the Ziegler catalyst is famous.[2] In 1953, Dr Ziegler (Max-Planck-Institute for Coal Research, Germany) was conducting a study of the oligomerization of ethylene using organoaluminum reagents and encountered selective butene formation under certain conditions. A detailed study of the reaction conditions revealed that a small amount of Ni impurity remaining on the surface of the autoclave enhanced the dimerization of ethylene in the presence of the aluminum reagents. His entire research group started the search for a new binary catalyst composed of transition metal salts and organometallic compounds of non-transition metals. They attempted the catalytic conversion of ethylene using all of the possible transition metals of the Periodic Table and found that the commercial high-mass polymerization of ethylene was best catalyzed by a mixture of $TiCl_4$ and $AlEt_3$, now named after the discoverer.[3] Natta, in 1954 at the Milano Technical University Italy, found that a combination of $TiCl_3$ and AlR_3 catalyzed the polymerization of propene to produce crystalline polypropylene (the polypropylene reported to that point had not been crystalline). He analyzed the polymer by X-ray diffraction, and proposed stereoselective polymerization to form isotactic polypropylene.[4]

The discovery of Ziegler–Natta catalysis stimulated research in related fields of science and technology. Cossee proposed the mechanism for smooth olefin polymerization by transition metal catalysts (the Cossee mechanism), recognizing the transition metal as the main component of the catalyst, and the non-transition metal alkyls as a co-catalyst. The proposed pathway involved the coordination of ethylene to the transition metal and subsequent migratory insertion of the olefin into the metal-polymer bond, as shown in Figure 12.2(i).[5]
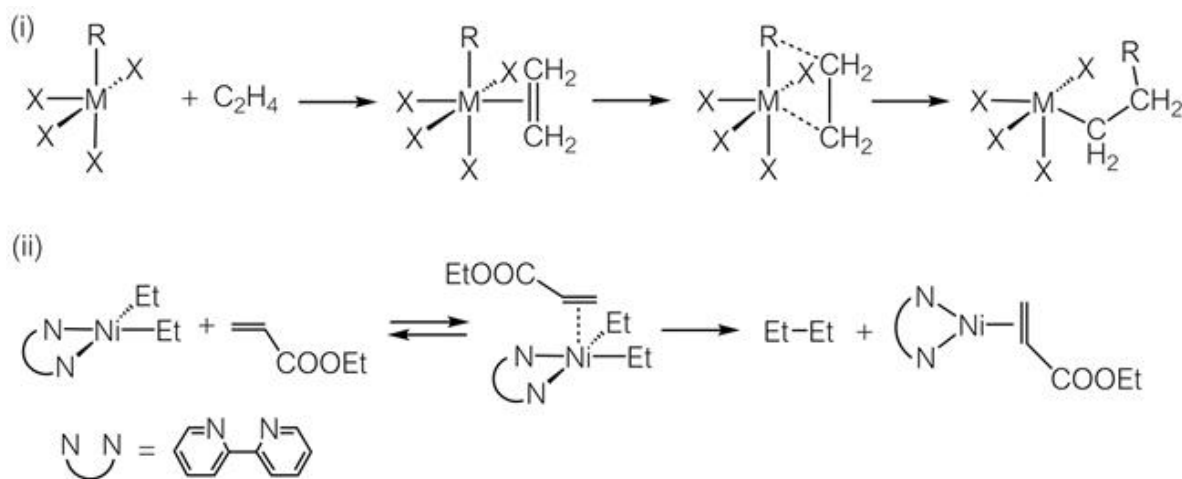
Figure 12.2   (i) The Cossee mechanism of coordination polymerization of ethylene; (ii) activation of the Ni–C bond of an alkylnickel complex caused by coordination of olefins.

It should be noted that, at the time, transition metal complexes of alkyl ligands were quite uncommon, and the proposal was significant due to the novel intermediates and fundamental reactions of transition metal compounds described. The original report by Cossee rationalized the reaction using ligand field theory, then a new topic in inorganic and physical chemistry, but did not include sufficient experimental or theoretical evidence for the proposed mechanism. Nevertheless, it stimulated further discussion on the olefin polymerization mechanism among many scientists, advancing the field of organotransition metal chemistry.

Cis-insertion of an olefin into a M–C bond, involved in the Cossee mechanism, was proven by a study on the polymerization of partially deuterated ethylene using a Ziegler-type catalyst.[6] Yamamoto succeeded in the preparation of alkyl complexes of Ni and Fe bearing the 2,2′-bipyridine

ligand from the reaction between the metal acetylacetonate and alkylaluminums.[7] These complexes were thermally more stable than anticipated and exhibited new properties. For example, π-coordination of an olefin to the metal center activates metal–carbon bonds and induces reductive elimination of the coupling products (Figure 12.2(ii)).[8] The results proved the coordination of an olefin molecule to nickel, its consequent activation of M–C bonds in the complex and subsequent migratory insertion of the olefin into the M–C bond, as proposed by Cossee. Studies on the Fe complexes revealed similar olefin activation of, and insertion into, the metal–carbon bond, converting acrylic esters to the corresponding polymers.

As mentioned above, nickel was the metal that led to the discovery of olefin polymerization catalysis by transition metals. Nickel was soon recognized as an important transition metal, enabling the isolation of stable alkyl complexes. The catalytic activity of many Ni complexes, however, was known to be much lower than the other early transition metal compounds. Reaction of ethylene in the presence of Ni complexes and co-catalysts yielded low molecular weight oligomers rather than polymers. However, 40 years after the initial discovery, nickel complexes bearing diamine ligands were found to promote high-mass polymerization of ethylene and α-olefins.[9] The polymerization differs from the heterogeneous Ziegler catalyst but is effective in solution, affording branched chain polyethylene (LDPE), and also copolymers of ethylene with other acrylic monomers. Thus, organotransition metal chemistry was stimulated significantly by the discovery of ethylene polymerization using the Ziegler catalyst, which has also provided insights into new kinds of homogeneous catalysis for ethylene polymerization over the years.

Other homogeneous catalysts for ethylene polymerization were studied in order to clarify the actual structures of the active sites of the Ti catalysts and the reaction mechanism. Dichloro{bis(cyclopentadienyl)}titanium(ɪᴠ) did not achieve ethylene polymerization in the presence of organoaluminum compounds such as trialkylaluminum, although a catalyst composed of the molecular Ti complex and methylalumoxane (MAO), formed by partial hydrolysis of $AlMe_3$, was found to be effective. A similar zirconocene-MAO catalyst, named after its discoverer, Kaminsky, produces polyethylene with higher efficiency.

A Ziegler catalyst contains various active transition metal sites on the surface of the solid support, and hence yields polymers with more varied structures as a result of reaction at metal centers with different environments. On the other hand, metallocene catalysts in solution contain identical active sites and thus form molecular weight-regulated polyethylene or even living polyethylene. Introduction of substituents on the catalyst cyclopentadienyl (Cp) ligands and a spacer linking the two Cp groups improves the polymerization, providing more structural control. Metallocenes with C_2-symmetry, **2**, produce isotactic propylene. The stereochemistry of the polymer chain growth is considered to be a result of the stereochemically controlled migratory insertion of prochiral olefin molecules. Studies of molecular metallocene catalysts for olefin polymerization thus enabled the synthesis of molecular weight-controlled polyethylene and living and block copolymerization of olefins, and provided mechanistical insights for olefin polymerization. Further studies resulted in molecular catalysts with one Cp ligand (half-metallocene catalyst, **5**) or without Cp ligands (non-metallocene or post-metallocene catalyst **6-9**). The molecular structures of major molecular catalysts for olefin polymerization are summarized as **2-9** in Figure 12.3.
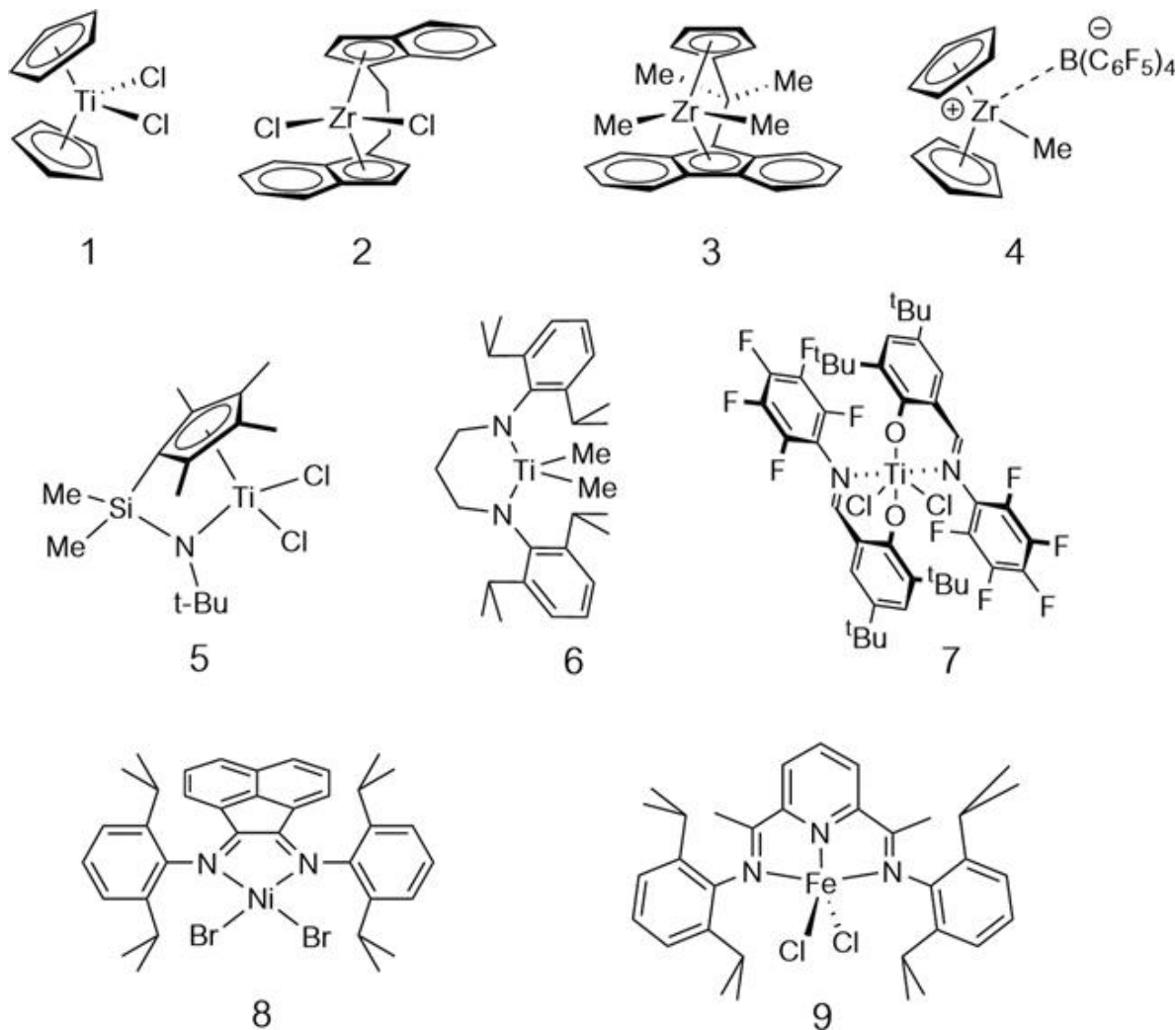
Figure 12.3 Metallocene, half-metallocene and non-metallocene olefin polymerization catalysts (in most cases a cocatalyst such as MAO is required).

As mentioned above, the heterogeneous and homogeneous olefin polymerization catalysts based on early transition metals have various functions, and permit considerable control over polymerization, such as of product molecular weight, the stereochemistry of polymers from α-olefins and copolymerization including block copolymerization.

Ziegler–Natta catalysts can polymerize other unsaturated molecules, such as 1,3-butadiene and acetylene, affording *cis*-polybutadiene and polyacetylene, respectively (Figure 12.4). The synthesis of electroconductive polymers and olefin metathesis polymerization mentioned later have their origins in the research on the polymerization of unsaturated monomers by Ziegler–Natta catalysis.

cis-1,4-polybutadiene   *trans*-polyacetylene
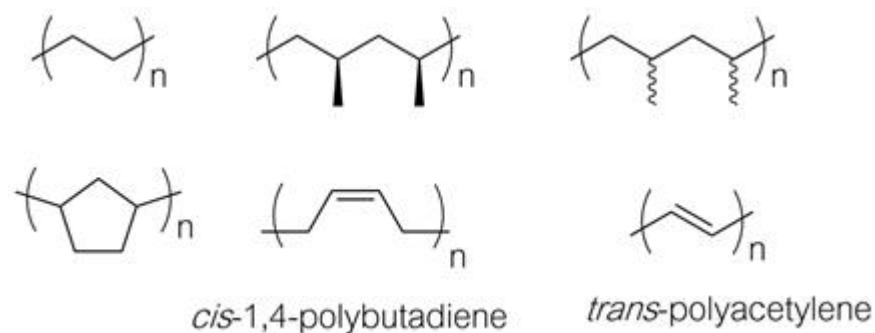
Figure 12.4 Polymers accessible *via* Ziegler–Natta catalysis.

Polyolefin synthesis, initiated by the contributions of research on Ziegler–Natta catalysis, has profoundly influenced human life and society, providing access to "hard plastics" such as high density polyethylene and isotactic polypropylene. The former can be molded and colored and copolymerization with 1-butene and other comonomers allows further tuning of product properties, including hardness. Such materials and their properties caused a revolution in classic material technology in which the product was made from single source substances or the combination of a few. Polyolefin materials, accessible at low cost from petroleum, have thus replaced in large part materials based on natural or inorganic materials. From start to finish, energy consumption is considerably lower for the manufacture of items from polyolefins compared to those made from metal or glass. People worldwide in all areas of life have thus benefitted from the cheap and ready availability of these convenient and economically favorable materials. Nevertheless, these same advantages have ironically also become a double-edged sword, since due to their low cost, robustness and ubiquity, their use has out-paced human insight and ability to deal with the resulting environmental disaster which now threatens ecosystems globally.

12.3 Sandwich Compounds, Nobel Prize for Chemistry 1973, Ernst Otto Fischer and Geoffrey Wilkinson

Ernst Otto Fischer and Geoffrey Wilkinson discovered transition metal complexes of unsaturated hydrocarbon ligands and won the Nobel Prize for chemistry in 1973, "*for their pioneering work, performed independently, on the chemistry of the organometallic, so-called sandwich, compounds.*"

Co(iii) complexes are regarded as typical transition metal complexes, having a definite coordination number of six and octahedral geometry in most cases. The ligands at each vertex coordinate to the metal center *via* σ-bonds, such as Co–O, Co–N and Co–Cl. The alkyl complexes of transition metals mentioned in the previous section are also considered to have σ-bonds between the carbon atom of the alkyl ligand and the metal center. On the other hand, $K[PtCl_3(C_2H_4)] \cdot H_2O$, Zeise's salt, has long been known as a compound containing an ethylene molecule as a ligand. The structure and properties were such that the bonding was suggested to be different to that in transition metal complexes with σ-bonds around the metal center. Elucidation of the structure of ferrocene, described in this section, provided the key to understanding the bonding and structures of transition metal complexes of π-coordinating ligands, including ferrocene and Zeise's salt.

During a 1951 study of the coupling reactions of organic halides, Pauson isolated an orange crystalline compound from a reaction mixture containing an iron salt and the cyclopentadienyl anion in a 1 : 2 ratio.[10] Soon after that, the group of Fischer in Germany, and a joint research team combining the groups of Wilkinson and Woodward in the USA, started independent studies on the structure of the new compound. Within a year, both research teams had reached the same conclusion about the sandwich structure of the compound, shown in Figure 12.5, based on their respective experimental evidence.[11,12]
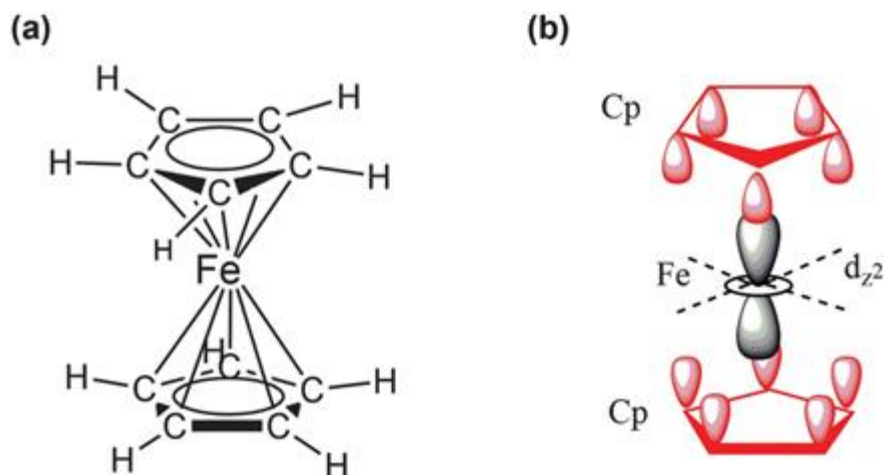
Figure 12.5   (a) Ferrocene sandwich structure and (b) interaction of the d_{z^2} orbital of the iron center and π-orbitals of two cyclopentadienyl ligands.

Initial grounds for considering the sandwich structure were all indirect: the chemically stable nature of the compound, the absence of a dipole moment for the molecule and oxidation reactions affording paramagnetic compounds, *etc.* To prove the proposed structure, NMR (which was in its infancy and the newest analytical method for compounds at the time) and IR spectroscopic data were obtained. Final definitive evidence was provided by a single crystal X-ray crystallographic study, reported in 1956.[13] The molecule is highly symmetrical, containing ten equivalent C–H bonds both in the solid state, as shown by the crystallography, and in solution, as evidenced by NMR and IR. The original crystallographic paper contains a drawing of the electron density map obtained by Fourier analysis of the data, and it must have given a strong impression to many readers. The beautiful and symmetrical molecular structure was pictured on later editions of the front cover of Linus Pauling's famous book on the chemical bond.[14] Zeise's salt, with a platinum center and π-coordinated ethylene ligand, was characterized by X-ray diffraction in 1969, more than 10 years after the structural determination of ferrocene.[15]

Further details of the structure and bonding of ferrocene are now understood more precisely by considering the interaction of metal center d-orbitals with the orbitals of the two cyclopentadienyl fragments. Figure 12.5(b) depicts the orbital interaction that stabilizes the coordination bond.

The report of the structural study of ferrocene announced not only its unique molecular structure but also the new bonding mode of such π-ligands. Ni and Co analogs of the sandwich compounds were then obtained by similar procedures. The cyclopentadienyl (Cp) ligand is now recognized as a major C-ligand in transition metal complexes. The ligand is anionic and belongs to the family of aromatic compounds with six π electrons, similar to benzene. Related complexes of transition metal centers sandwiched by arenes were then reported, such as bis(benzene)chromium. This stable compound has a molecular structure composed of a Cr(0) center sandwiched by two parallel arene ligands.

There are now many examples of unsaturated hydrocarbon ligands, similar to the Cp ligand. As shown in the basic part of this book, the coordination bonds of olefin ligands and π-allyl ligands are often stabilized by back-donation from the metal to the ligand. As described in Chapter 3, the Dewar–Chatt–Duncanson (DCD) model explains the stable coordination of olefin ligands with late transition metal centers. Complexes with other

unsaturated hydrocarbon ligands, such as π-allyl and arene ligands, also contain similar coordination bonds. Thus, cyclobutadiene with four π-electrons (and hence not aromatic) cannot be not isolated due to its thermal instability. However, its Co complex may be obtained as a crystalline compound due to bonding between the carbon atoms and the metal center. Figure 12.6 summarizes representative transition metal complexes of unsaturated π-hydrocarbon ligands. It is not easy to determine a definite coordination number for the metal centers of such complexes, as distinct from the Werner-type transition metal complexes. Thus, in discussions of molecular structure, it is the number of electrons involved in the coordination from both the transition metal and the ligands (the valence electron count – see Chapter 2) which is important. Molecules that satisfy the 18e rule are stable and are often now studied with the aid of molecular orbital calculations.
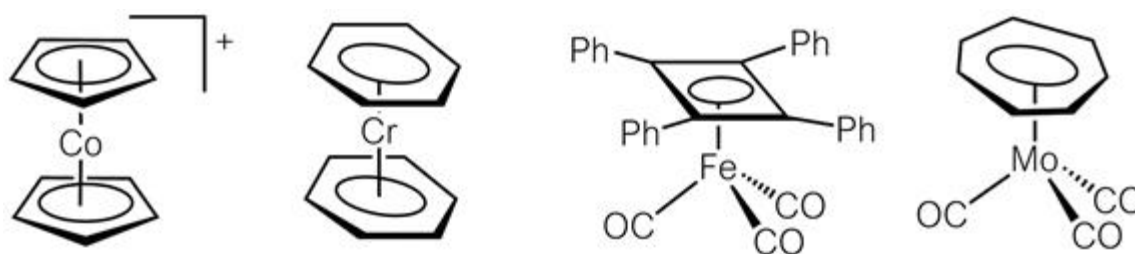
Figure 12.6 Organotransition metal complexes with π-conjugated cyclic compounds as ligands.

Ferrocene and its derivatives have unique and important chemical properties. The highly reversible redox properties of the metal center of ferrocene make it useful as a standard reference material in electrochemical measurements. The aromatic ligands of ferrocene can be converted into various derivatives by substitution of the hydrogen atoms by functional groups. Their rigid and unique structures enhance the use of the derivatives as materials and also as reagents for organic synthesis.

12.4 Electrically Conductive Polymers, Nobel Prize for Chemistry 2000, Alan J. Heeger, Alan G. MacDiarmid, and Hideki Shirakawa

Alan J. Heeger, Alan G. MacDiarmid and Hideki Shirakawa discovered that polyacetylene, upon doping, becomes an electroconductive material, and

won the Nobel Prize for chemistry in 2000, "*for the discovery and development of conductive polymers*."

Electrically conductive substances require free and mobile electrons, similar to metals, and no such properties are expected for common organic compounds, since the bonding orbitals are usually all filled and the anti-bonding orbitals are usually all empty. Materials can be rendered electrically conducting, however, in a number of ways. Graphite shows electrical conductivity due to its planar π-conjugated system with mobile electrons within the planes. Akamatsu, in a study to realize an electrically conducting organic compound, exposed perylene to Br_2 vapor, and observed electrical conductivity of the product up to 1 S cm^{-1} in 1954.[16] The electrical conductivity, however, is temporary, and lost in a short time due to the further conversion of the material into dibromoperylenes, which have no conductivity.

Polymerization of acetylene by a Ziegler–Natta catalyst was known to form a polymer, which should have a π-conjugated linear structure, and was thus expected to be an electrically conducting hydrocarbon polymer.[17] However, the polymer obtained by the usual procedure was a hard and insoluble solid from which films suitable for the estimation of the material's physical properties could not be prepared. Shirakawa conducted a fundamental study of the synthesis and properties of polyacetylene using Ziegler–Natta catalysts and discovered a method to obtain the polymer as a film.[18] In his lectures, Shirakawa frankly introduced his discovery as a serendipitous event. The Nobel Prize committee cited it precisely as, "a visiting researcher in the laboratory added more catalyst than written in the experimental instructions: actually one thousand times too much. Instead of the expected black polyacetylene powder normally obtained, which was of no use, a beautifully lustrous silver-colored film resulted".[1b] Further refining of the synthetic procedure eventually afforded a tough, large area polyacetylene film. MacDiarmid and Heeger invited Shirakawa to Pennsylvania and started collaborative work investigating the efficient doping of the polymer film with iodine. Introduction of acetylene gas into a flask containing a large surface area solution of the catalyst in high concentration results in growth of a polyacetylene film by contact of gaseous acetylene with the catalyst solution. The film thickness can be controlled in the range 10^{-5}–0.5 cm and the films can be spectroscopically

analyzed, doped by addition of iodine *etc.*, and their electrical conductivity can be measured. The electrical conductivity of polyacetylene films reaches 40 S cm^{-1} on doping with iodine and 560 S cm^{-1} on doping with AsF_5. The values correspond to ten million and a billion times increase in conductivity of the polymer compared to pre-doping levels. Figure 12.7 plots the increase of electrical conductivity per repeat unit with increase of the dopant.
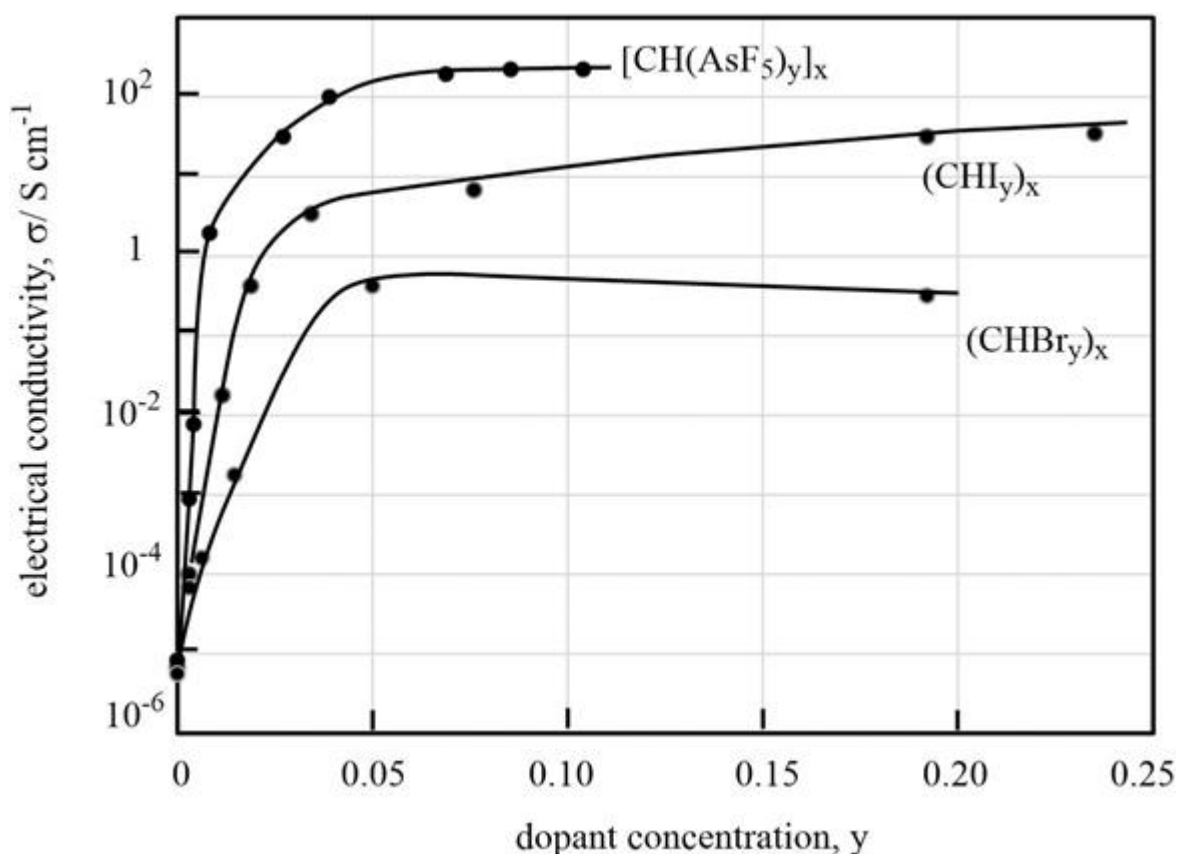
Figure 12.7   Change of electrical conductivity of polyacetylene upon doping (from ref. [18](b)).

Figure 12.8 shows the simplified structure of doped and undoped polyacetylene (all-*trans* structure). The doping of polyacetylene by iodine leads to oxidation of the polymer chain, forming positively charged carbon atoms (holes) along the polymer chain and I_3^-. Hole transport occurs easily along the polyacetylene chain due to the delocalization of the alternating σ and π bonds in the π-conjugated system of the polymer main chain.
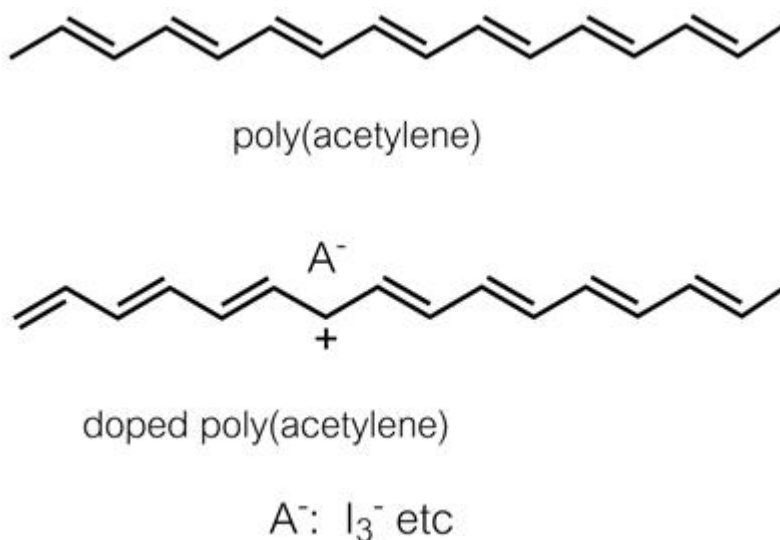
Figure 12.8 Polyacetylene and electrically conductive I_2-doped polyacetylene.

Polyacetylene had been theoretically predicted to show electroconductive properties.[17] Actual electroconductivity was realized after the unexpected discovery of the polyacetylene film caused by the misdirected experiment. The ceremony speech of the Nobel Prize summarized it thus: "Perhaps the development of new knowledge in chemistry, more than any other science, has been characterized as a sparkling interplay between theory on one hand, the safe and predictable, and, on the other hand, the explosive and surprising reality. When we by chance discover something that may become valuable, we talk about serendipity."[1b]

Polyacetylene shows typical physical properties as an organic conductor, but is rather unstable even after doping. This prevented application of the polymer as a common conductor, but the discovery of polyacetylene paved the way for other organic electroconductors based on π-conjugated polymers and oligomers.

Figure 12.9 shows the structures of three additional typical aromatic polymers with π-conjugation in which the repeat units are stabilized by aromaticity. These polymers were prepared by coupling reactions catalyzed by transition metal complexes or oxidative electrochemical polymerization, and form electrically conducting polymers on suitable doping. Polythiophene and polypyrrole are p-type conductors, while polypyridine is an n-type conductor.
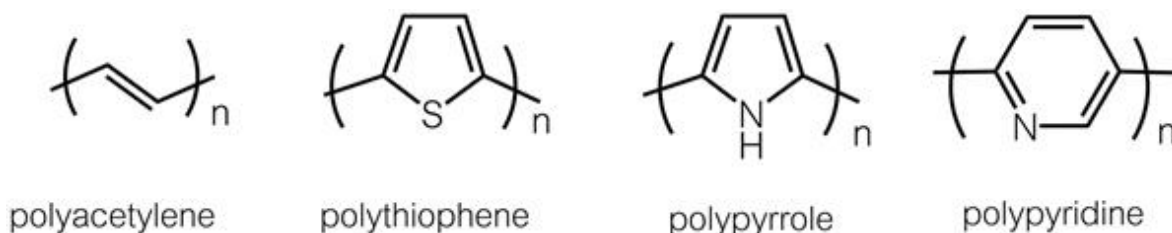
Figure 12.9 π-Conjugated polymers.

The polymers were applied in the positive electrodes of batteries: in 1981, Yamamoto reported a Zn–I_2 battery using polythiophene as the positive electrode, while Heeger and MacDiarmid reported batteries whose negative and positive electrodes were made of polyacetylene.[19,20] Such plastic batteries are of low weight due to the use of the light element Li as the negative electrode. In 2000, the year of the Nobel Prize award, cellular phones equipped with Li-polymer batteries were produced. Further application of π-conjugated polymers to electrical and optical materials is a competitively active worldwide field of research.

12.5 Asymmetric Catalysis, Nobel Prize for Chemistry 2001, William S. Knowles, Ryoji Noyori and K. Barry Sharpless

William S. Knowles, Ryoji Noyori and K. Barry Sharpless pioneered the methodology to form optically pure compounds from achiral molecules by using a small amount of a chiral catalyst, opening the door to many important organic synthesis reactions, and were awarded the Nobel Prize for chemistry in 2001, "*for their work on chirally catalysed hydrogenation reactions (Knowles and Noyori)" and "for his work on chirally catalysed oxidation reactions (Sharpless).*"

Since Pasteur's successful separation of the two optical isomers of tartaric acid in 1848, the artificial synthesis of optical isomers of chiral organic compounds has been a central goal in organic chemistry and its relevance to the chemistry of natural compounds is clear. The most challenging among the former reactions are those converting molecules without chirality into optically active compounds, termed asymmetric or enantioselective reactions, and which have revolutionized synthetic organic reactions, particularly in the drug industry. The first work on asymmetric reactions not involving natural substances but using an artificial catalyst was reported by

Akabori. He designed a solid catalyst whose surface was functionalized by optically active silk and reported the results in a paper in which he used the term "asymmetric catalyst."[21] This was followed by research using a RANEY®-nickel catalyst functionalized by sugar and by tartaric acid.

Asymmetric reactions using homogeneous transition metal complex catalysts have advantages in elucidation of the reaction mechanism and logical design of the catalyst because the molecular catalyst has a single structure and can be characterized by NMR spectroscopy, X-ray crystallography, *etc.* In 1966, Wilkinson found that $[RhCl(PPh_3)_3]$ (Wilkinson's catalyst) homogeneously catalyzes the hydrogenation of terminal olefins under mild conditions.[22] This reaction involves migratory insertion of a coordinated olefin ligand into an Rh–H bond (formed during the cycle) as the key step. Similar hydrogenation of olefins with two different substituents on the same sp^2 carbon would form products having new asymmetric center(s). Olefin hydrogenation using Rh complexes with optically active phosphine ligands to form chiral products is based on these concepts.

Figure 12.10 summarizes the initial studies on this topic. In 1968, Knowles prepared a new chiral phosphine and from this, an enantiopure analog of Wilkinson's catalyst. Subsequent catalytic hydrogenation of a prochiral olefin afforded a non-racemic product mixture of enantiomers with 15% ee (enantiomeric excess; a mixture of enantiomers in the ratio 57.5 : 42.5).[23]
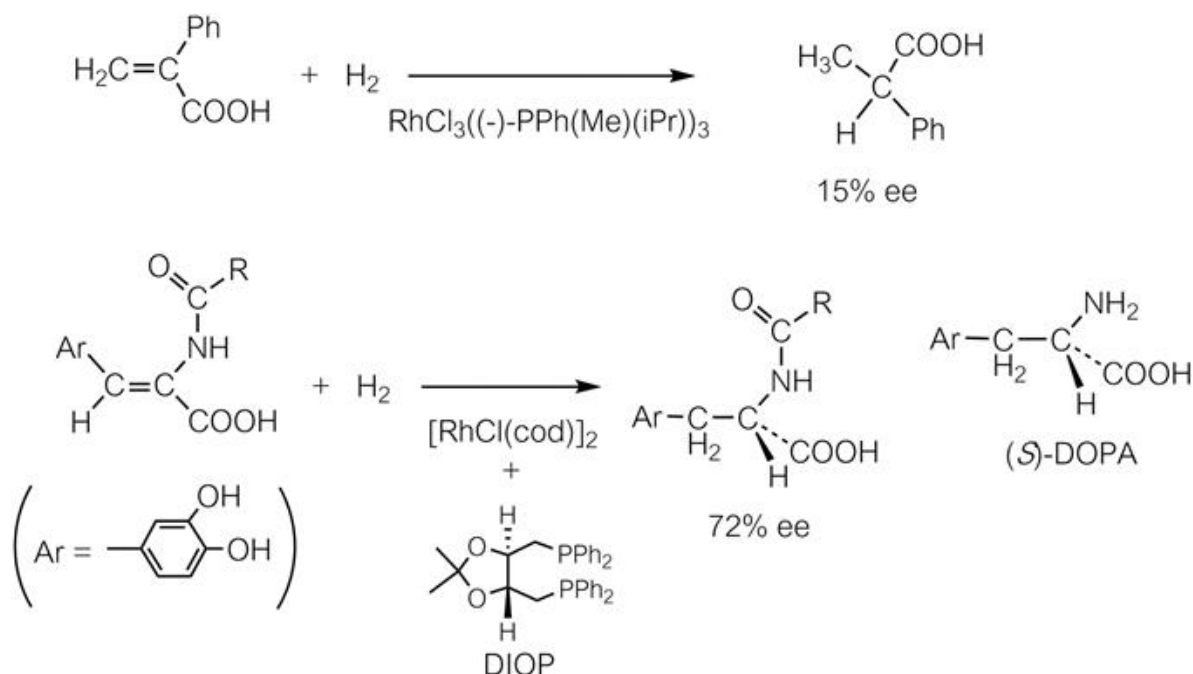
Figure 12.10 Asymmetric hydrogenation of olefins using Rh complex catalysts.

Kagan designed an optically active diphosphine, DIOP (see Figure 12.11), which can be prepared easily from (ₗ)-tartaric acid, and used its Rh complex as a catalyst for the hydrogenation of prochiral olefins. Use of acetamidoacrylic acid as the substrate resulted in the formation of the amino acid derivatives with 72% ee.[24] The higher optical yield of the product compared to the previous asymmetric hydrogenation studies is partly ascribed to an attractive interaction between the functional group of the substrate and the metal center of the catalyst in the transition state or an important intermediate of the catalytic cycle. Hydrogenation of acetamidoacrylic acid was adopted as the standard reaction to check the performance of chiral ligands in many subsequent studies on asymmetric hydrogenation. An optically active phenylalanine derivative, DOPA, was obtained by this reaction, and has been used as a medicine to treat Parkinson's disease. Many optically active diphosphine ligands were designed and tested in order to achieve absolute asymmetric hydrogenation with an optical yield of 100% ee. The standard Gibbs energy difference between the two enantiomer-yielding transition states of the reaction, to afford the products with 95% ee, is estimated as 7.5 kJ mol^{-1}, while that for 99.9% ee corresponds to an energy difference of 17.6 kJ mol^{-1}. Thus,

reactions affording absolute asymmetric synthesis are much harder to achieve than reactions to produce products with high optical yields, such as 90 or 95% ee. Figure 12.11 summarizes representative chelating diphosphines bearing chiral center(s). Knowles used diPAMP in the Rh-catalyzed hydrogenation of acetamidoacrylic acid and obtained the product in 95% ee.[25]
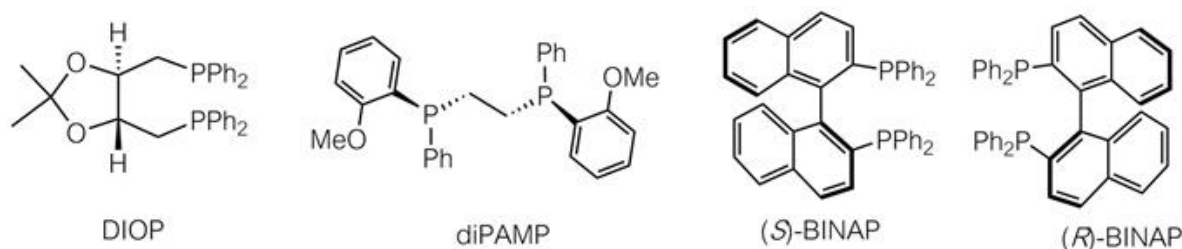
Figure 12.11 Optically active chelating diphosphines for asymmetric olefin hydrogenation.

Noyori designed and synthesized a new chelating diphosphine ligand, BINAP, which has axial chirality due to steric stereochemical locking of the conformation between the two neighboring naphthyl groups. Bidentate coordination of the ligand to a transition metal center restricts the complex to a molecular structure with C_2 symmetry. Thus, a Rh complex of BINAP was expected to behave as an ideal asymmetric catalyst. The initial catalytic hydrogenation attempt, however, yielded a product with insufficient optical purity (38% ee). The catalyst was prepared by addition of the BINAP ligand to $[Rh(\mu\text{-}Cl)(nbd)]_2$ (nbd = norbornadiene) with expectation of the formation of a Rh species bearing the BINAP ligand. However, detailed studies on the active species of the catalyst revealed the formation of two complexes, mononuclear complex A and dinuclear complex B (Figure 12.12) by the above procedure. Dinuclear complex B catalyzed the hydrogenation, but with reduced stereoselectivity of the reaction, and so a mixture of the two complexes afforded products with only moderate optical yield. Mononuclear complex A, isolated from the mixture, catalyzed asymmetric hydrogenation of acetamidoacrylic acids to produce amino acid derivatives with high enantiomeric purity. The reaction of benzoylamido(phenyl)acryclic acid afforded the product with 100% ee.[26]
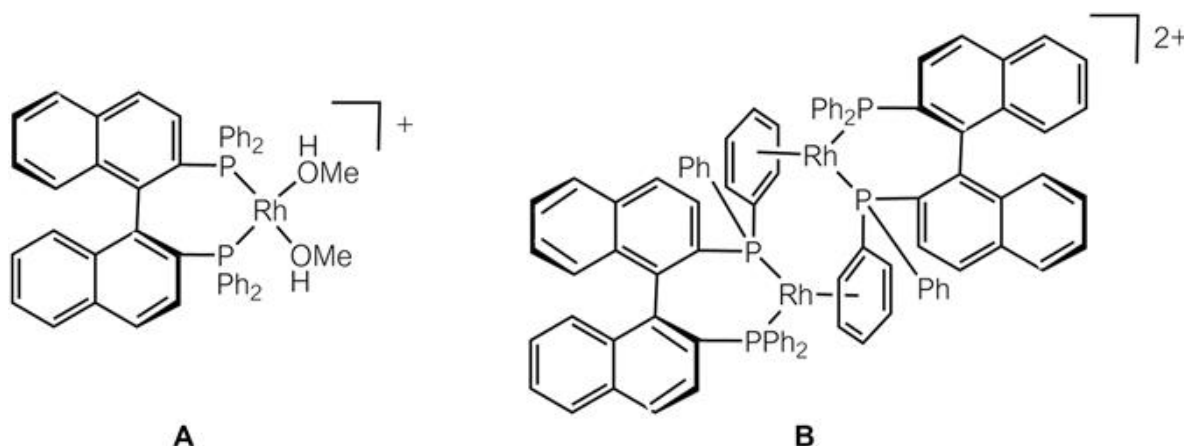
Figure 12.12 Two Rh complexes formed by the reaction of BINAP with Rh(i) precursor: mononuclear complex, A and dinuclear complex, B.

Coordination of BINAP to Rh(i) forms a square planar cationic complex with a metal of d^8 electron configuration, as shown in Figure 12.12(A). The complex [Ru(OAc)$_2$(BINAP)], with octahedral coordination around a d^6 metal center, also catalyzes asymmetric hydrogenation of acetamidoacrylic acids with high enantioselectivity. Interestingly, the absolute configuration of the product is opposite to that obtained using the Rh catalyst bearing the same BINAP ligand.[27]

Figure 12.13 depicts the intermediates for both reactions. Two isomeric intermediates are generated in each reaction, the structure depending on which of the olefin faces of the prochiral substrate is coordinated. The more stable intermediates in the Ru- and Rh-catalyzed reactions have similar structures around the metal center. In the Ru-catalyzed reaction, the more stable intermediate is generated preferentially in the reaction mixture and then undergoes rapid hydrogenation to form the major product. For the Rh-catalyzed reaction, however, the hydrogenation of the intermediate is the rate-determining step of the total reaction, and the more stable intermediate reacts with dihydrogen much more slowly than the less stable intermediate. The less stable intermediate in the Rh-catalyzed reaction is responsible for the major reaction product, whose absolute configuration is opposite to that of the major product of the Ru-catalyzed reaction. The relative stability of the intermediate cannot always be correlated with the stereochemistry of the total reaction, as often explained by the Curtin–Hammett principle.[28] Thus, homogeneous catalysis for asymmetric hydrogenation enabled not only

high stereoselectivity of the reaction but also clear elucidation of the mechanism based on the detailed structures of the intermediates and reaction kinetics.
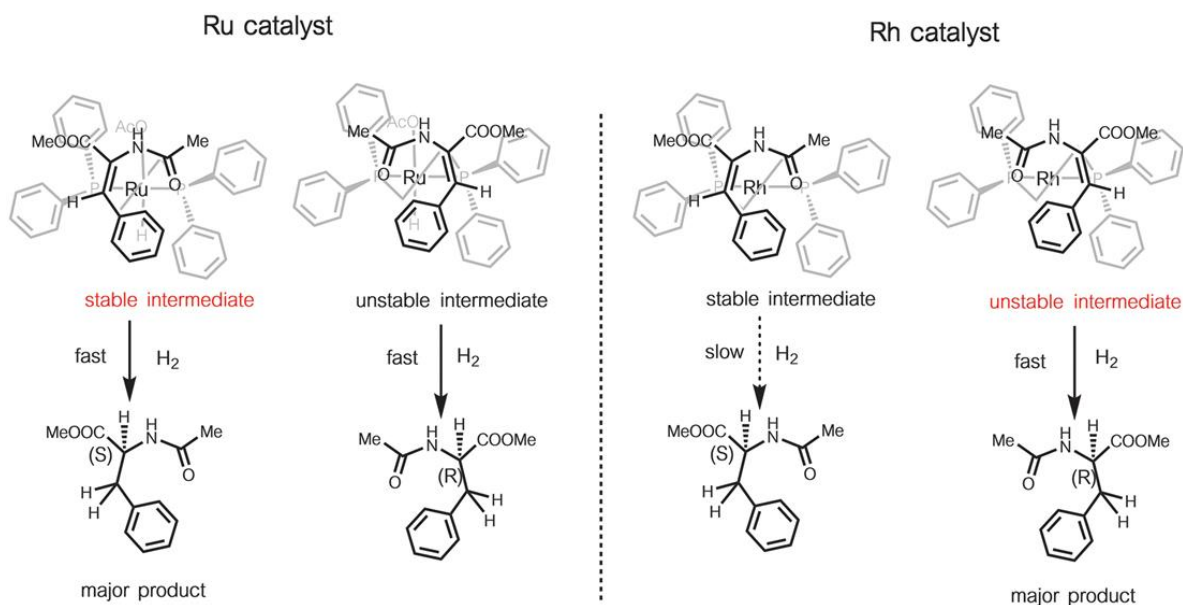
Figure 12.13 Asymmetric hydrogenation of an acetamidoacrylic acid using Ru- and Rh-BINAP complexes as catalysts.

The first discovery of asymmetric hydrogenation using a homogeneous catalyst was by Knowles in 1968.[23] Prior to that, though, in 1966, Noyori and Nozaki reported the asymmetric cyclopropanation of styrene derivatives catalyzed by chiral Cu complexes.[29] The report of the former was extended to research activities by a number of scientists on this subject. The latter work formed the practical insecticide that has been used on a worldwide scale. Comparison of the priority and achievements of both pioneering works probably has no meaning. Knowles predicted in his first report, "we are hopeful that our current effort will result in real progress towards complete stereospecificity," and it was realized by Noyori who synthesized BINAP, incorporated it as the ligand and the crucial part of asymmetric catalysts, and using these, investigated catalytic hydrogenation. Transition metal complexes are employed as catalysts in many other reactions. BINAP is also employed in a Rh catalyst for the asymmetric isomerization of allylic amines, as shown in Figure 12.14.[30]
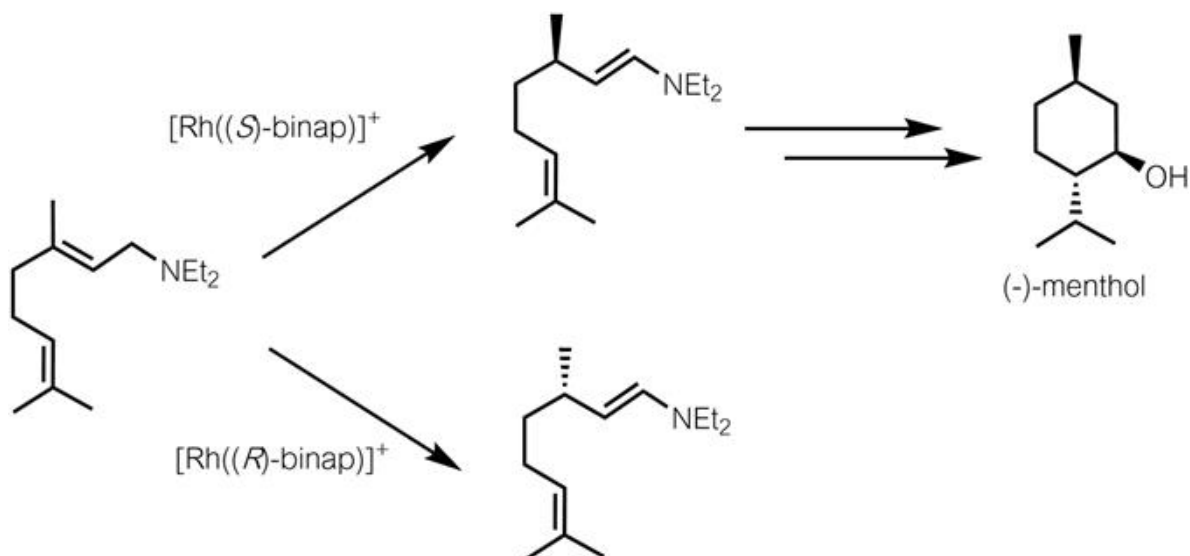
Figure 12.14 Enantioselective synthesis of (−)-menthol by using asymmetric isomerization of a racemic allylic amine catalyzed by Rh-BINAP complexes.

Asymmetric reactions involving oxidation were also achieved by using transition metal complex catalysts. Sharpless and Katsuki found that a mixture of diethyl tartrate and $[Ti(Oi\text{-}Pr)_4]$ catalyzes the asymmetric epoxidation of olefins, as shown in Figure 12.15.[31]
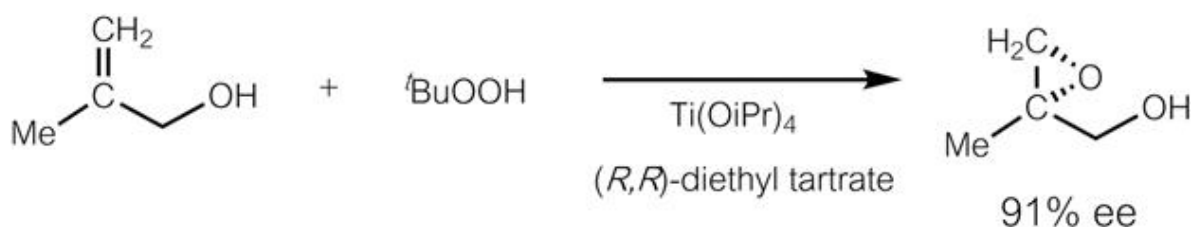
Figure 12.15 Asymmetric epoxidation of olefins by Sharpless *et al.*

For this reaction, there is less evidence concerning the detailed structures of the intermediates and reaction mechanism than the asymmetric hydrogenation of olefins, mentioned above. The stereoselectivity of the reaction is influenced more by the substrate backbone than the substituents on the olefinic carbon and the absolute configuration of the product depends on which face of the olefinic group is oxidized, as shown in Figure 12.16.
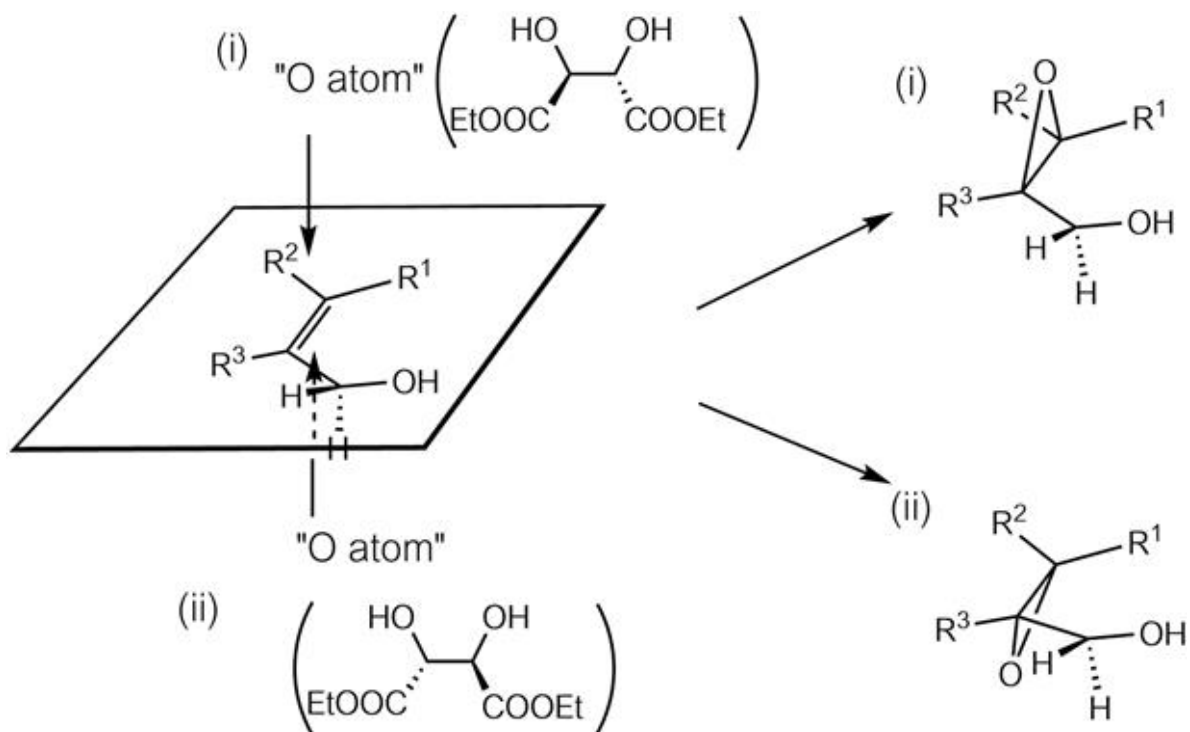
Figure 12.16 Stereoselectivity of asymmetric epoxidation by Sharpless *et al.*

The catalyst is effective not only for asymmetric epoxidation of prochiral allylic alcohols but also the kinetic resolution of allylic alcohols with chiral carbon atoms.[32] As shown in Figure 12.17, crotyl(cyclohexyl)carbinol with the (*S*) configuration undergoes epoxidation using the Ti catalyst more rapidly than does the (*R*) substrate.
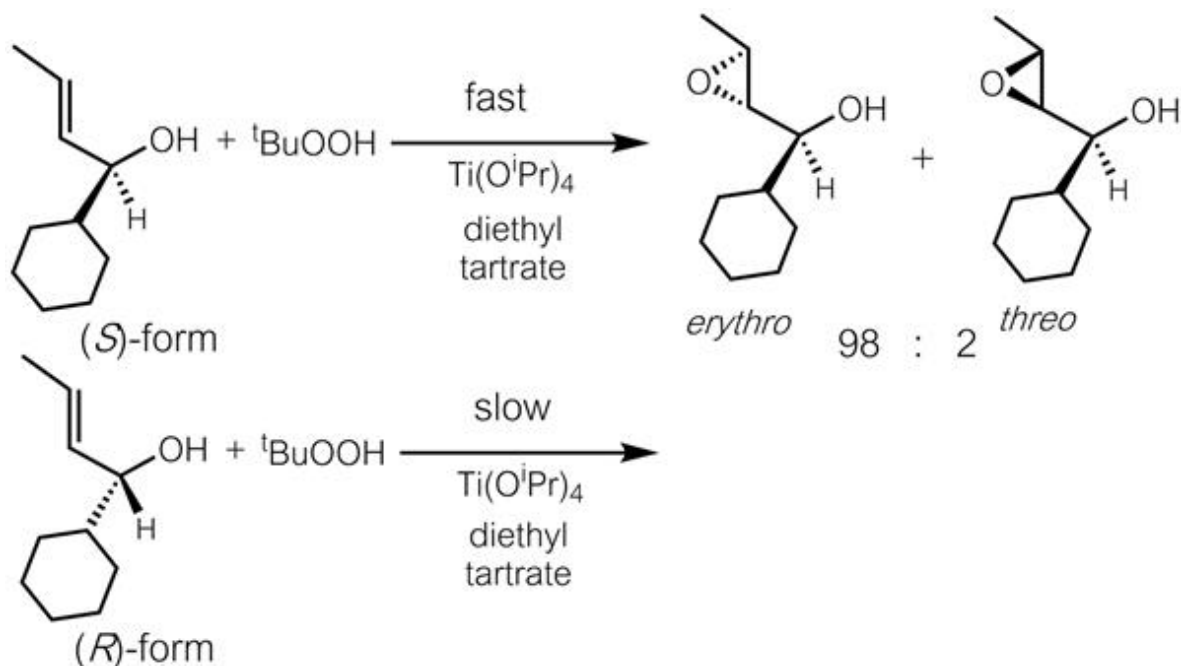
Figure 12.17 Kinetic resolution in epoxidation of allylic alcohol.

The reaction, terminated at a suitable point, yields the optically active epoxide by reaction of the (S) enantiomer as the product, while the (R) enantiomer remains as unreacted alcohol. Figure 12.18 depicts the relationship between the optical purity of the unreacted substrate and the conversion of the reaction. When the relative reaction rates have a difference larger than 25 : 1, the recovered allylic alcohol should have enantiomer purity higher than 80% ee.
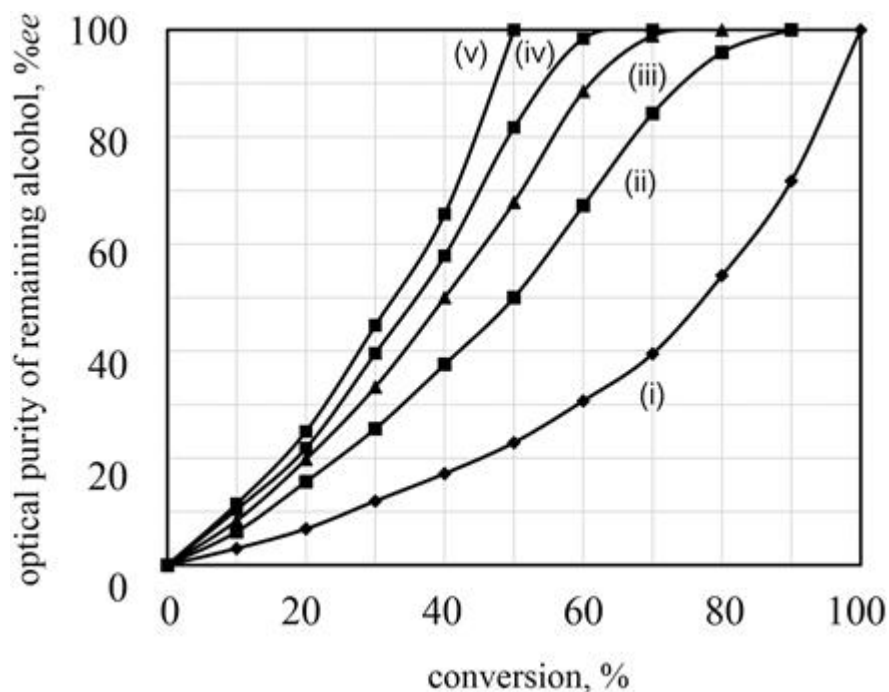
Figure 12.18 Calculated relationship between epoxidation conversion and optical purity of the remaining alcohol. Reaction rate ratios of the two enantiomeric substrates, (i) 2.0, (ii) 5.0, (iii) 10.0, (iv) 25.0, (v)∞.Data were taken from ref. [32].

When the catalyst prepared from the Ti salt and diethyl tartrate was used in the epoxidation of the allyl alcohol, the unreacted substrate was recovered with optical purity greater than 96% ee, and the epoxide product was formed with high diastereomer selectivity (98 : 2). The experimental stereoselectivity is greater than those calculated (Figure 12.17), suggesting that the reaction rates for the two stereochemical pathways are significantly more different from each other.

Asymmetric reactions using molecular metal-containing catalysts are of interest due to the high efficiency of the synthetic reactions and relative ease of elucidation of the asymmetric induction mechanism and relate to the challenging topic of the origin of biomolecular chirality on earth, as proposed by Soai.[33] On the other hand, olefin metathesis reactions, as described in the coming section, were long considered as unsuited for asymmetric reactions due to the high freedom of the intermediate structures. Rapid progress in catalysis research, however, enabled the asymmetric version of olefin metathesis.

12.6 Olefin Metathesis, Nobel Prize for Chemistry 2005, Yves Chauvin, Robert H. Grubbs and Richard R. Schrock

Yves Chauvin, Robert H. Grubbs and Richard R. Schrock discovered organotransition metal catalysts for metathesis reactions, opening the door to their application for the synthesis of organic compounds and materials, and won the Nobel Prize for chemistry in 2005, *"for the development of the metathesis method in organic synthesis."*

Olefin metathesis reactions are now recognized as the exchange of the vinylidene groups of two olefins, as shown in Figure 12.19. Propene is reversibly converted into an equimolar mixture of ethylene and 2-butene.
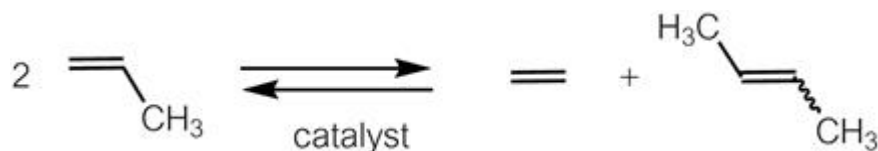
Figure 12.19 Metathesis of 2-butene, ethylene and propene.

The discovery of olefin metathesis was triggered by unexpected results in a study of propene polymerization using Ziegler–Natta catalysts. A researcher at the DuPont company, Esteruelas, was studying the preparation of polypropylene using a Mo catalyst supported on aluminum and found incorporation of ethylene units in the polymer chain. Careful investigation of the results led him to conclude that ethylene was generated in the reaction mixture. He reported the results in a patent, rather than in a scientific journal, and described the details in a review in 1991.[34]

The first olefin metathesis paper in a scientific journal was also from a polymerization study. Norbornene polymerizes in the presence of a Ziegler-type catalyst to afford two types of polymers, depending on the catalyst used, as shown in Figure 12.20.[35] One polymer is formed *via* normal addition polymerization of the cycloolefin and contains norbornane-diyl units. The other type of polymer contains vinylene groups in each repeat unit and has a ring-opened structure. The latter reaction was pioneered by several research groups, including Natta's, and was the first example of ring-opening metathesis polymerization (ROMP). Similar reactions were observed for cyclobutene.
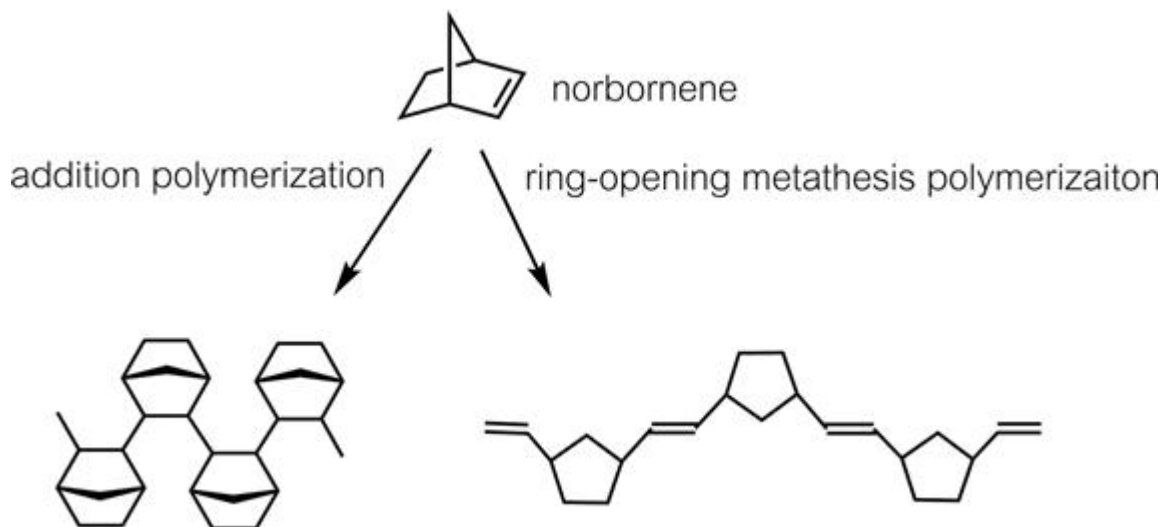
Figure 12.20 Norbornene polymerization *via* addition polymerization and ring-opening metathesis polymerization.

At the time of discovery, olefin metathesis was not properly understood because of its novelty. Classic organic and inorganic chemistry concepts do not explain the reaction well. One proposed mechanism involved cleavage of C–C single bonds of the substrate rather than of the more stable C=C double bonds, which would cause exchange of the substituents of the olefins. It was not clear for several years following the initial discovery whether disproportionation of propene to give ethylene and 2-butene, and ring-opening polymerization of cycloolefins should be categorized in the same class of reactions or not.

Figure 12.21(i) shows the initially proposed mechanism of olefin metathesis: the [2 + 2] cycloaddition of olefins, which is allowed under photoirradiation conditions, but occurs with transition metal catalysts. In 1971, Chauvin proposed a novel mechanism for the olefin metathesis: a transition metal complex having a C=M double bond undergoes addition of olefin, to produce a metallacyclobutane intermediate, which undergoes elimination of a new olefin product and generates a new carbene complex (Figure 12.21(ii)).[36] His original 1971 paper summarizes and discusses the complicated experimental results of the polymerization clearly and his proposed reaction mechanism.
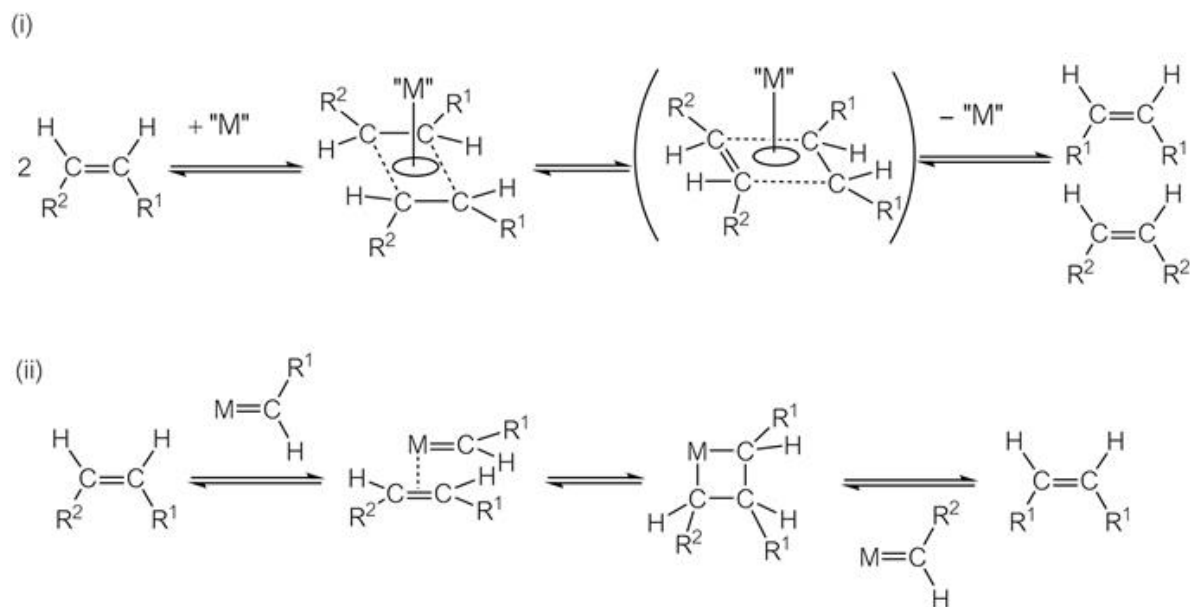
Figure 12.21 (i) Initially proposed mechanism for olefin metathesis; (ii) mechanism proposed by Chauvin.

Fischer, one of the discoverers of ferrocene, had already reported carbene complexes of transition metals, such as Fe.[37] The complexes do not show the chemical properties expected in Chauvin's mechanism nor olefin metathesis. Many other transition metal complexes with carbene ligands and metallacyclobutanes were studied in order to reveal the mechanism of catalysis. Katz and Schrock studied the ring-opening metathesis polymerization of strained cyclic monomers and found that their tungsten–carbene complexes catalyze metathesis polymerization. Grubbs investigated titanacyclobutanes and showed that such species were involved in the metathesis reaction as an important intermediate. These results clarified and confirmed the plausibility of the Chauvin mechanism, in which both carbene complexes and metallacycles are involved as intermediates.

Schrock synthesized thermally stable Mo and W complexes with neopentylidene ligands and demonstrated their high catalytic activity for intra- and intermolecular metathesis reactions. The complexes are air-sensitive and cannot be used for the reaction of olefin substrates with functional groups such as carbonyl groups.

Grubbs synthesized a Ru catalyst having a carbene ligand and bulky supporting ligands. The 1st and 2nd generation Grubbs catalysts in Figure 12.22 catalyze olefin metathesis efficiently, although the productivity is

slightly lower than that of the Mo and W catalysts. The Ru complexes are advantageous in terms of their easy handling and applicability to olefins having functional groups in the molecule. A useful organic reaction involving olefin metathesis using these catalysts is the ring-closing metathesis of terminal dienes. Certain organic compounds are synthesized in high selectivity because they undergo cyclization more easily than intermolecular coupling with other substrates and because ethylene, formed in the reaction, can easily be removed from the equilibrium mixture.

| Ta catalyst by Schrock | Schrock catalyst | Schrock-Hoveyda catalyst |

| Grubbs catalyst (1st generation) | Grubbs catalyst (2nd generation) | Grubbs-Hoveyda catalyst (2nd generation) |
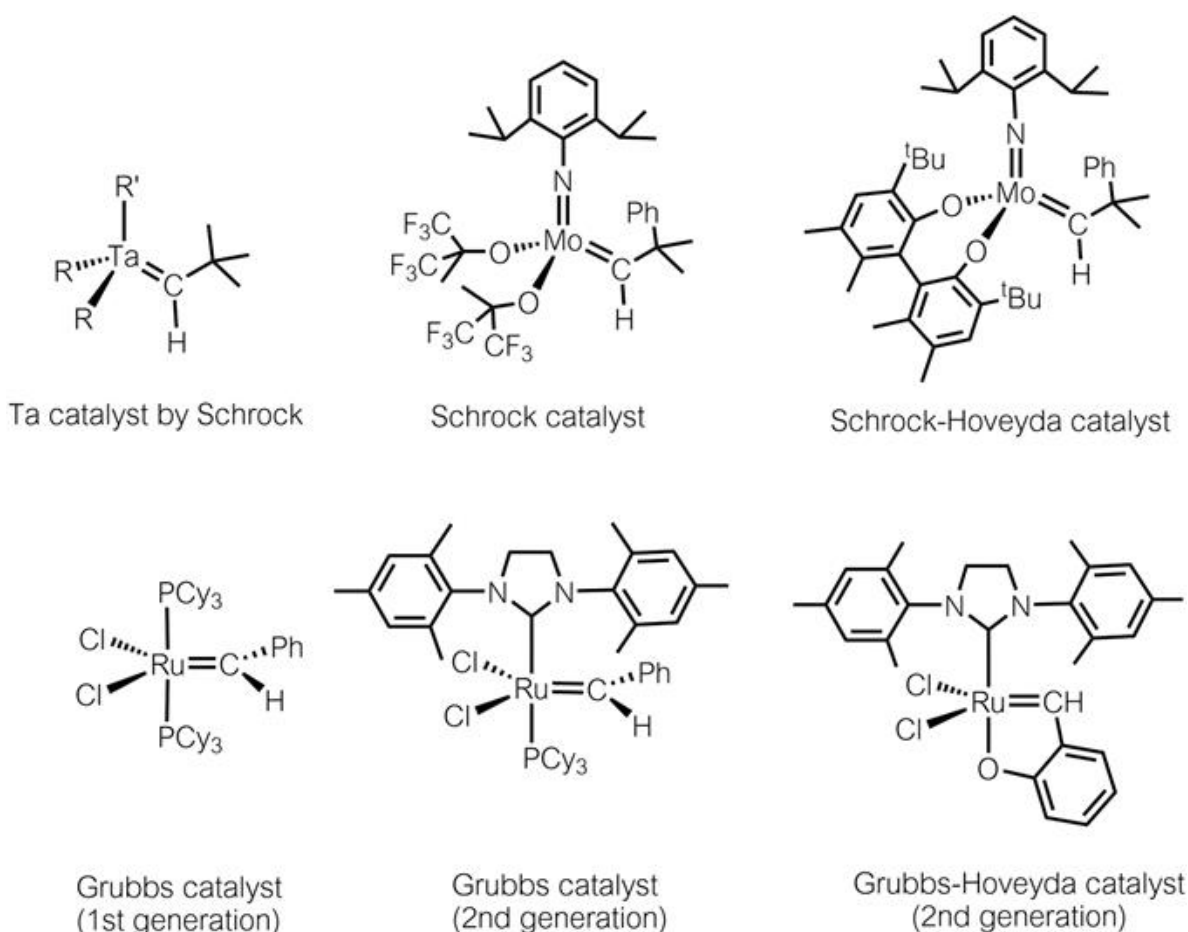
Figure 12.22 Catalysts for olefin metathesis.

Figure 12.23 summarizes mechanistic details of the olefin metathesis reaction using a Grubbs catalyst. Dissociation of a phosphine ligand from the catalyst and coordination of the olefin substrate forms a ruthenacyclobutane intermediate, which undergoes elimination of the olefin product. In the case of 2nd generation catalysts, the N-heterocyclic carbene

ligand is highly electron-donating, enhancing elimination of the *trans* phosphine ligand. Overall, the reaction proceeds more smoothly because of the more favorable dissociation of the supporting phosphine ligand.
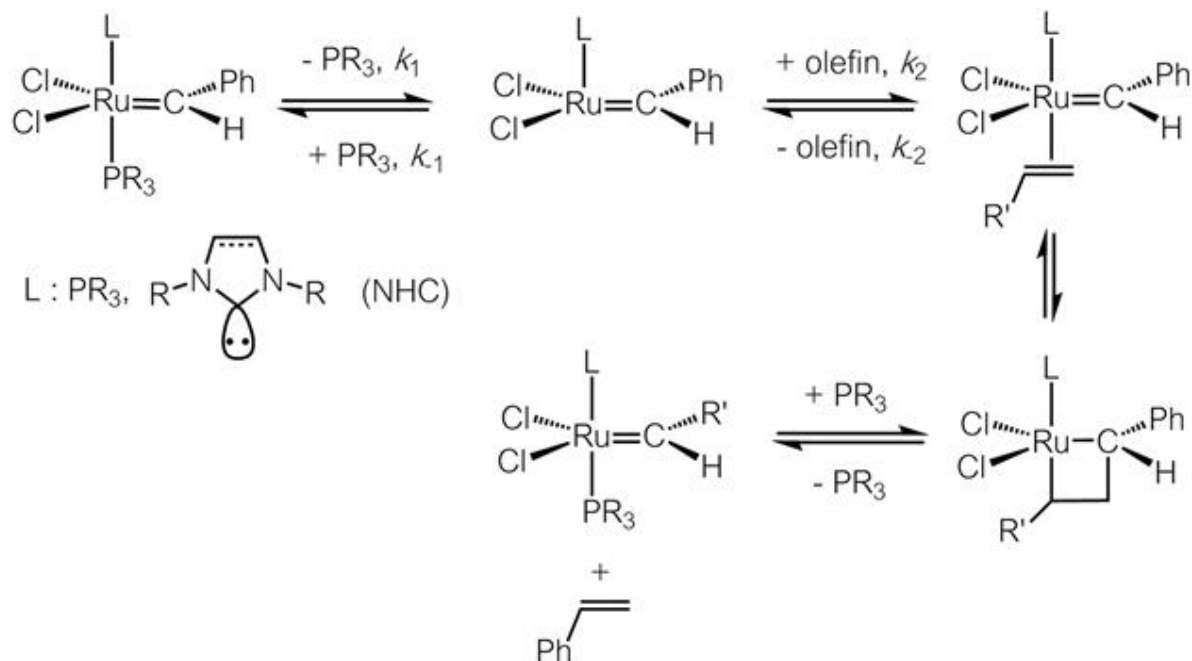
Figure 12.23 Mechanism of olefin metathesis catalyzed by Ru complexes.

Olefin metathesis methodology is now employed to synthesize natural products with macrocyclic structures, including multicyclic supramolecular compounds. Metathesis polymerization, including ROMP, has long been an important synthetic route to polymer materials. Norbornene polymers have high optical transparency and are used as lens materials. Hard polymers with uses in the bulk state, such as car parts, are prepared on an industrial scale using an injection molding system. Metathesis reactions use accessible olefins as the substrate with high atom economy and can be classified as environmentally friendly reactions. Applications have now expanded into asymmetric metathesis reactions, metathesis polymerization of acyclic dienes and metathesis of C–C single bonds.

12.7 Cross-coupling Reactions Using Pd Catalysts, Nobel Prize for Chemistry 2010, Richard F. Heck, Eiichi Negishi and Akira Suzuki

Richard F. Heck, Eiichi Negishi and Akira Suzuki investigated C–C bond forming reactions using Pd catalysts, changing the methodology of the synthesis of organic compounds by their reactions, and won the Nobel Prize for chemistry in 2010, "*for palladium-catalyzed cross couplings in organic synthesis.*"

Carbon–carbon single bonds comprise the basic structural unit of almost all organic compounds and maintain their three-dimensional structure and high thermal stabilities. C–C bond formation before 1970 relied on the reaction of highly reactive species, such as alkyl radicals or alkyl ions, and on concerted reactions with π-bond-containing molecules. These C–C bond-forming reactions are limited as to the substrates, conditions and target molecules that are accessible. Cross-coupling reactions catalyzed by transition metal complexes were reported in the 1970s and considerably extended the scope of C–C bond forming reactions over several decades.[38] A typical cross-coupling reaction is shown in eqn (12.1), in which use of a catalytic amount of a transition metal (such as Ni or Pd) complex results in C–C bond formation between halogeno or pseudo-halogeno (triflate, acetate, *etc.*) compounds and organometallic compounds of main group electropositive elements (B, Mg, Zn *etc.*).

$$\text{Ar} - \text{X} + \text{R} - \text{M} - \text{Y} \xrightarrow[\text{Ni, Pd catalyst}]{} \text{Ar} - \text{R} + \text{M(X)(Y)}$$

$$(\text{X, Y} = \text{Br, I, OTf} ; \ \text{M} = \text{Mg, Li, Al, Zn, Si, Sn etc}) \quad 12.1$$
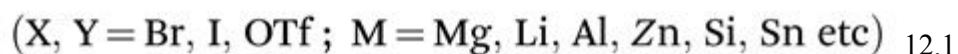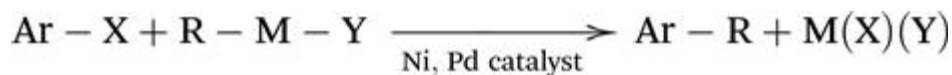
In 1971, Kochi reported the coupling reaction of a Grignard reagent with organic halides in the presence of a catalytic amount of an Ag salt.[39] Cross-coupling reactions as a methodology in organic synthesis were reported in 1972 by two research groups: that of Kumada and Tamao in Japan, and that of Corriu in France (Kumada–Tamao–Corriu coupling).[40] They established the use of various substrates such as aryl halides, alkenyl halides, and many Grignard reagents as the precursors to the C–C bond. The mechanism for the catalytic cycle, comprising successive concerted reactions of organotransition metal complexes, was proposed clearly in the original papers (Figure 12.24).
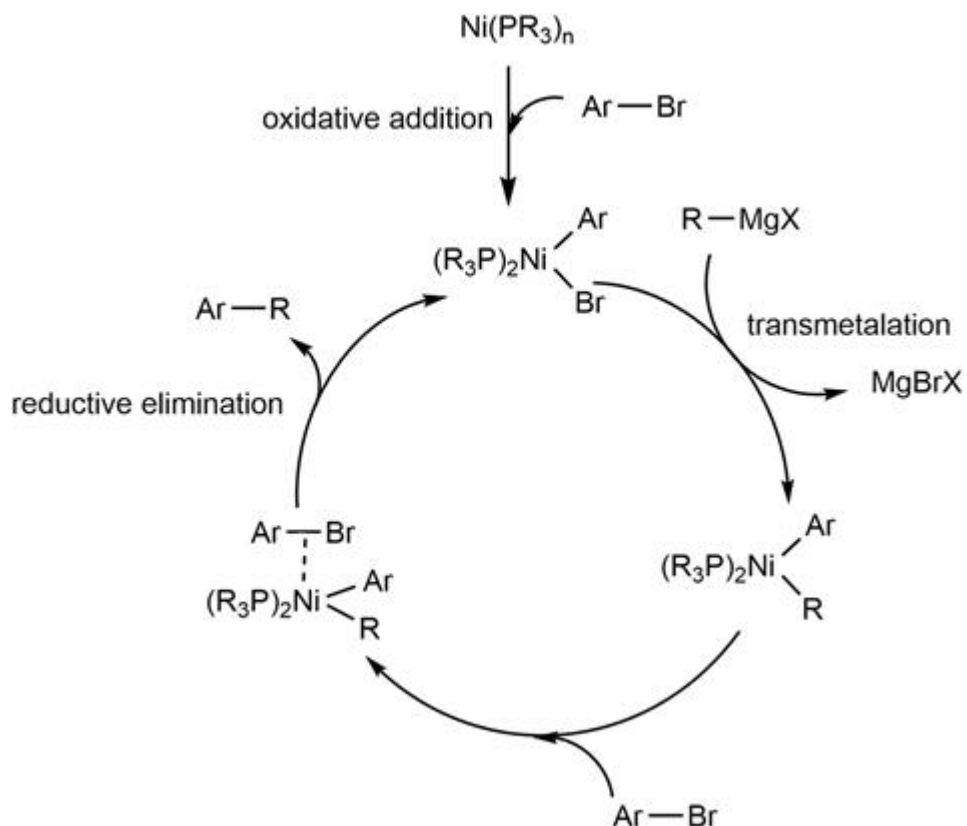
Figure 12.24 Mechanism of cross-coupling reaction catalyzed by a Ni complex.

A Ni(0) intermediate, $[Ni(PR_3)_n]$ in Figure 12.24, is generated by reduction of the Ni(ii) catalyst. Oxidative addition of aryl halide then occurs to form an aryl(halo)nickel(ii) intermediate, which undergoes transmetalation with the Grignard reagent to yield the alkyl(aryl)nickel(ii) intermediate. C–C bond formation occurs with reductive elimination of the C–C-linked aryl-*R* compound from the intermediate. This step is enhanced by coordination of aryl halide to regenerate the Ni(ii) intermediate. The proposed reaction mechanism was shown to be correct and helped further extend the scope of cross-coupling reactions using other substrates and catalysts.

High selectivity and versatility in cross-coupling reactions using Pd catalysts was found and these reactions are now recognized as one of the most important C–C bond formation reactions: Tsuji initiated studies on the Pd-catalyzed allylation (Tsuji–Trost reaction);[41] Murahashi designed cross-coupling reactions using alkyl lithium and Pd catalysts, enabling the selective reaction of alkenyl halides;[42] Negishi studied the cross-coupling

reactions of alkyl compounds of Zn, Al, B and Zr under mild conditions using Pd catalysts (Negishi coupling).[43] Combinations of these coupling reactions with transmetallation and carbometallation provided highly selective synthetic routes to complicated organic molecules and were adopted as key steps in the total synthesis of many natural compounds and their intermediates.

In 1979, Suzuki and Miyaura discovered the cross-coupling of alkenyl boronic acids with alkenyl halides catalyzed by Pd complexes in the presence of a base (Suzuki–Miyaura reaction).[44] The reaction was used in the total synthesis of palytoxin by Kishi. As shown in Figure 12.25, the molecule of palytoxin has a huge and complicated structure containing a hard to prepare (*E,Z*)-dienyene part, since it easily transforms to the (*E,E*) isomer. Because boronic acid derivatives are tolerant to aqueous media, reaction using metal hydroxide as the base was successful in forming the diene part of the hydrophilic target compound.[45]
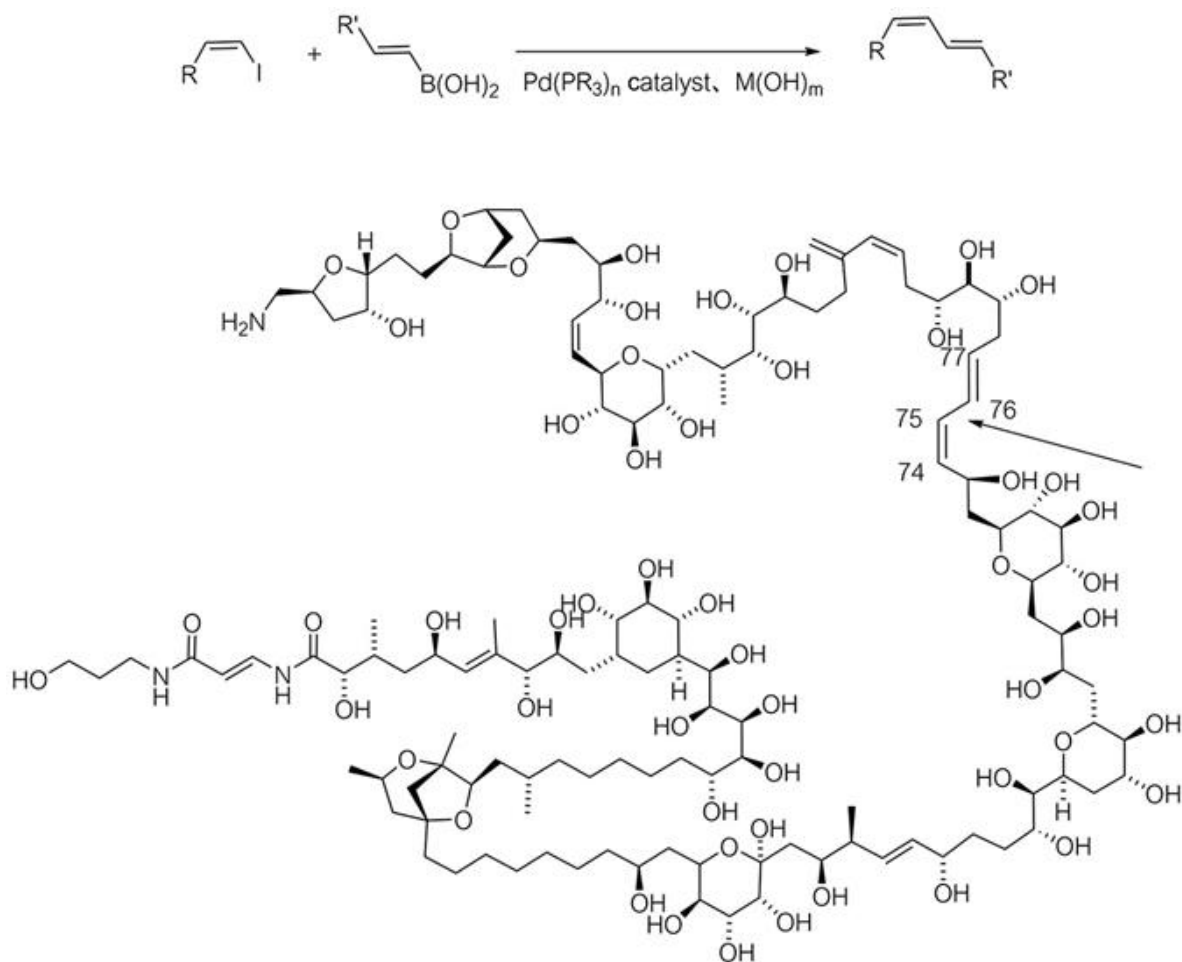
Figure 12.25 Structure of palytoxin and the reaction to form the diene part, indicated by the arrow.

Cross-coupling using organoboronic acids is suitable for aryl substrates and also in the synthesis of π-conjugated organic materials.

Pd complexes catalyze different kinds of cross-coupling reactions, such as coupling using organotin compounds (Migita–Kosugi–Stille coupling)[46] and those using organosilane as the substrate (Hiyama coupling).[47] Pd-catalyzed coupling of terminal alkynes with aromatic halides (Sonogashira coupling) forms a C–C bond between the sp and sp^2 carbon atoms in the presence of a Cu-salt and base.[48] It is understood to involve the formation of a Cu-acetylide and subsequent transmetalation with an arylpalladium complex to form the aryl(alkynyl)palladium intermediate.[49] This is still the most convenient coupling between an alkyne and an arene and the reaction

has been used in the preparation of π-conjugated organic compounds, used as photoactive materials.

In 1971, Mizoroki and Heck discovered Pd-catalyzed reactions of aromatic halides with styrene to yield arylvinylene compounds, accompanied by evolution of hydrogen halide (Mizoroki–Heck reaction).[50] The reaction forms a C–C bond, and resembles the cross-coupling reaction, although the mechanism of the reaction differs from the transmetalation in cross-coupling reactions, and instead involves insertion of the alkene substrate into the Pd–aryl bond, followed by β hydride elimination of the product from the arylethyl–palladium intermediate. Reaction of aryl halides and pseudo halides with olefins has also proved to be a useful tool in the synthesis of organic compounds.

Papers describing cross-coupling reactions using transition metal complexes as the catalyst have been published in huge numbers all over the world. Organic chemists can choose suitable catalysts and substrates from among many candidates, depending on the target compounds. Early investigations in this field have now merged into a new challenging area, including cross-coupling of organic chlorides, NH compounds, arenes without other functionality and reactions using base metals such as Cu and Fe. The reactions are typically named after the initial discoverer, resulting in convenient classification of the reactions and simplicity in searching by reaction name.

12.8 Summary

Several distinguished research fields related to Nobel Prizes for chemistry were introduced in the limited space of this chapter. These studies are closely related to the astonishing launch and advance of organometallic chemistry during the latter half of the last century. Many laureates started their research careers at a time when organometallic chemistry, including its future, was full of ambiguity. The various discoveries and inventions were achieved in spite of this situation, probably due to the rigorous training of the researchers, so that their prepared minds and their courage and conviction to pursue their own ways as scientists, enabled them to explore the unknown. It is clear to us following later that their research in the rapidly progressing field contributed significantly to deepening the core of science and generating new technologies.

References

1. (a) https://www.nobelprize.org/prizes/chemistry/1963/ceremony-speech/; (b) https://www.nobelprize.org/prizes/chemistry/2000/ceremony-speech/.
2. A. Yamamoto, *Organotransition Metal Chemistry – Fundamental Concepts and Applications*, John Wiley, New York, 1986.
3. (a) K. Ziegler, *Ger. Pat.*, DBP973626, 1953; (b) K. Ziegler, E. Holzkamp, H. Creil and H. Martin, *Angew. Chem.*, 1955, **67**, 541.
4. (a) G. Natta, P. Pino and G. Mazzanti, *Br. Pat.*, 810,023, 1954; (b) G. Natta, *J. Polym. Sci.*, 1955, **16**, 143.
5. P. Cossee, *J. Catal.*, 1964, **3**, 80.
6. S. Ikeda, A. Yamamoto and H. Tanaka, *J. Polym. Sci., A1*, 1963, 2925.
7. A. Yamamoto, K. Morifuji, S. Ikeda, T. Saito, Y. Uchida and A. Misono, *J. Am. Chem. Soc.*, 1965, **87**, 4652.
8. (a) T. Yamamoto, A. Yamamoto and S. Ikeda, *J. Am. Chem. Soc.*, 1971, **93**, 3350, and 3360 ; (b) T. Yamamoto, A. Yamamoto and S. Ikeda, *Bull. Chem. Soc. Jpn.*, 1972, **45**, 1111, and 1140 .
9. L. K. Johnson, C. M. Killian and M. Brookhart, *J. Am. Chem. Soc.*, 1995, **117**, 6414.
10. T. J. Kealy and P. L. Pauson, *Nature*, 1951, **168**, 1039.
11. G. Wilkinson, M. Rosenblum, M. C. Whiting and R. B. Woodward, *J. Am. Chem. Soc.*, 1952, **74**, 2125.
12. E. O. Fischer and W. Pfab, *Z. Naturforsch.*, 1952, **B7**, 377.
13. J. D. Dunnitz, L. E. Oroel and A. Rich, *Acta Crystallogr.*, 1956, **9**, 373.
14. L. Pauling, *The Nature of the Chemical Bond and the Structure of Molecules and Crystals; An Introduction to Modern Structural Chemistry*, 3rd edn, 1960, Cornell University Press, New York.
15. M. Black, R. H. B. Mais and P. G. Owston, *Acta Crystallogr., Sect. B*, 1969, **B25**, 1753.
16. H. Akamatsu, *Nature*, 1954, **173**, 168.
17. (a) J. E. Lennard-Jones, *Proc. R. Soc.*, 1937, **A158**, 280; (b) C. A. Coulson, *Proc. R. Soc.*, 1938, **A164**, 383, 1939, **A169**, 413 ; (c) D. L. Beveridge, I. Jano and J. Ladik, *J. Chem. Phys.*, 1972, **56**, 4744; (d) J. E. Falk and R. J. Fleming, *J. Phys. C: Solid State Phys.*, 1975, **8**, 627.
18. (a) H. Shirakawa, E. J. Louis, A. G. MacDiarmid, C. K. Chiang and A. J. Heeger, *J. Chem. Soc., Chem. Commun.*, 1977, 578; (b) H. Shirakawa, *J. Phys. Soc. Jpn.*, 1979, **34**, 313; (c) T. Ito, H. Shirakawa and S. Ikeda, *J. Polym. Sci., Polym. Chem. Ed.*, 1974, **12**, 11; (d) G. E. Wnek, *J. Polym. Sci., Part A: Polym. Chem.*, 1996, **34**, 2531.
19. T. Yamamoto, *J. Chem. Soc., Chem. Commun.*, 1981, 187.
20. D. MacInnes, M. A. Druy, P. J. Nigrey, D. P. Nairns, A. G. MacDiarmid and A. J. Heeger, *J. Chem. Soc., Chem. Commun.*, 1981, 317.
21. (a) S. Akabori, S. Sakurai, Y. Izumi and Y. Fujii, *Nature*, 1953, **178**, 323; (b) Y. Izumi, *Angew. Chem., Int. Ed. Engl.*, 1971, **10**, 871.
22. F. A. Osborn, J. F. Jardine, J. F. Young and G. Wilkinson, *J. Chem. Soc., A*, 1966, 1711.
23. W. S. Knowles and M. J. Sabacky, *Chem. Commun.*, 1968, 1445.
24. (a) T. P. Dong and H. B. Kagan, *J. Chem. Soc., Chem. Commun.*, 1971, 481; (b) H. B. Kagan and T.-P. Dang, *J. Am. Chem. Soc.*, 1972, **94**, 6429; (c) H. B. Kagan, *Pure Appl. Chem.*, 1975, **43**, 401.
25. W. S. Knowles, M. J. Sabackey, B. D. Vineyard and D. J. Weinkauff, *J. Am. Chem. Soc.*, 1975, **97**, 2567.
26. A. Miyashita, A. Yasuda, H. Takaya, K. Toriumi, T. Ito, T. Souchi and R. Noyori, *J. Am. Chem. Soc.*, 1980, **102**, 7932.
27. M. Kitamura, M. Tsukamoto, Y. Bessho, M. Yoshimura, U. Kobs, M. Widhalm and R. Noyori, *J. Am. Chem. Soc.*, 2002, **124**, 6649.

28. (a) J. M. Brown, P. A. Chaloner, G. Descotes, R. Glaser, D. Lafont and D. Sinou, *J. Chem. Soc., Chem. Commun.*, 1979, 611; (b) C. R. Landis and J. Halpern, *J. Am. Chem. Soc.*, 1987, **109**, 1746, and 6217 .
29. H. Nozaki, S. Moriuchi, H. Takaya and R. Noyori, *Tetrahedron Lett.*, 1966, 5239.
30. S. Inoue, H. Takaya, K. Tani, S. Otsuka, T. Sato and R. Noyori, *J. Am. Chem. Soc.*, 1990, **112**, 4897.
31. (a) T. Katsuki and K. B. Sharpless, *J. Am. Chem. Soc.*, 1980, **102**, 5974; (b) E. Rossiter, T. Katsuki and K. B. Sharpless, *J. Am. Chem. Soc.*, 1981, **103**, 464.
32. V. S. Martin, S. S. Woodard, T. Katsuki, Y. Yamada, M. Ikeda and K. B. Sharpless, *J. Am. Chem. Soc.*, 1981, **10**, 6237.
33. (a) K. Soai, T. Shibata, H. Morioka and K. Choji, *Nature*, 1995, **378**, 767; (b) T. Shibata, H. Morioka, T. Hayase, K. Choji and K. Soai, *J. Am. Chem. Soc.*, 1996, **118**, 471.
34. H. S. Eleuterio, *J. Mol. Catal.*, 1991, **65**, 55.
35. W. L. Truett, D. R. Johnson, I. M. Robinson and B. A. Montague, *J. Am. Chem. Soc.*, 1960, **82**, 2337.
36. J.-L. Hérrison and Y. Chauvin, *Makromol. Chem.*, 1971, **141**, 161.
37. E. O. Fischer and A. Maasbol, *Angew. Chem., Int. Ed.*, 1964, **3**, 580.
38. *Applied Cross-Coupling Reactions*, ed. Y. Nishihara, Springer, Heidelberg, 2013.
39. J. K. Kochi and M. Tamura, *J. Am. Chem. Soc.*, 1971, **93**, 1483.
40. (a) K. Tamao, K. Sumitani and M. Kumada, *J. Am. Chem. Soc.*, 1972, **94**, 4374; (b) R. J. P. Corriu and J. P. Masse, *J. Chem. Soc., Chem. Commun.*, 1972, 144.
41. J. Tsuji and H. Takahashi, *J. Am. Chem. Soc.*, 1965, **87**, 3275.
42. M. Yamamura, I. Moritani and S. Murahashi, *J. Organomet. Chem.*, 1975, **91**, C38.
43. (a) E. Negishi and S. Baba, *J. Chem. Soc., Chem. Commun.*, 1976, 596; (b) E. Negishi and S. Baba, *J. Am. Chem. Soc.*, 1976, **98**, 6729.
44. (a) N. Miyaura, K. Yamada and A. Suzuki, *Tetrahedron Lett.*, 1979, **20**, 3437; (b) N. Miyaura, K. Yamada, H. Suginome and A. Suzuki, *J. Am. Chem. Soc.*, 1985, **107**, 972.
45. (a) J. Uenishi, J.-M. Beau, R. W. Armstrong and Y. Kishi, *J. Am. Chem. Soc.*, 1987, **109**, 4756; (b) E. M. Suh and Y. Kishi, *J. Am. Chem. Soc.*, 1994, **116**, 11205.
46. (a) M. Kosugi, K. Sasazawa, Y. Shimizu and T. Migita, *Chem. Lett.*, 1977, 301; (b) D. Milstein and J. K. Stille, *J. Am. Chem. Soc.*, 1978, **100**, 3636, ; 1978, **101**, 4992 .
47. Y. Hatanaka and T. Hiyama, *J. Org. Chem.*, 1988, **53**, 918.
48. (a) K. Sonogashira, Y. Tohda and N. Hagihara, *Tetrahedron Lett.*, 1975, **16**, 4467; (b) S. Takahashi, S. Kuroyama, K. Sonogashira and N. Hagihara, *Synthesis*, 1980, 627.
49. K. Osakada, R. Sakata and T. Yamamoto, *Organometallic*, 1997, **16**, 5354.
50. (a) T. Mizoroki, K. Mori and A. Ozaki, *Bull. Chem. Soc. Jpn.*, 1971, **44**, 581; (b) R. F. Heck and J. P. Nolley, Jr., *J. Org. Chem.*, 1972, **37**, 2320.

Chapter 13

Problem Solutions

Hiroshi Nakazawa[a]

[a] Osaka City University, Japan nakazawa@sci.osaka-cu.ac.jp

To understand the basics and make effective use of the knowledge described in this book, 20 practice problems are dispersed through chapters 2 to 7. In this chapter, model answers to these practice problems are presented to encourage the reader's deeper understanding. In addition to the direct answers, the thinking and logic required to reach the answers are also described, helping readers to establish their knowledge.

Answers to Problem 1 (See Section 2.4.4)

1) $[Cr(CO)_6]$ — $6(Cr) + 2(CO) \times 6 = 18$

2) $[CpFe(CO)_2Me]$ — $5(Cp) + 8(Fe) + 2(CO) \times 2 + 1(Me) = 18$

3) $[Mo(C_6H_6)_2]$ — $6(Mo) + 6(C_6H_6) \times 2 = 18$

4) $[(CO)_5Mn\text{-}Mn(CO)_5]$ — $2(CO) \times 5 + 7(Mn) + 1(Mn(CO)_5) = 18$

5) $[Fe(CO)_3(PPh_3)_2]$ — $8(Fe) + 2(CO)) \times 3 + 2(PPh_3) \times 2 = 18$

6) $[Fe(H)_2(CO)_4]$ — $8(Fe) + 1(H) \times 2 + 2(CO) \times 4 = 18$

7) $[Co(CN)_2(CO)(PEt_3)_2]^-$ — $9(Co) + 1(CN) \times 2 + 2(CO) + 2(PEt_3) \times 2 + 1$ (minus charge) $= 18$

8) $[Pt(C_2H_4)Cl_3]^-$ — $10(Pt) + 2(C_2H_4) + 1(Cl) \times 3 + 1$(minus charge) $= 16$

9) $[CpFe(CO)_2(PMe_3)]^+$ — $5(Cp) + 8(Fe) + 2(CO) \times 2 + 2(PMe_3) - 1$(plus charge) $= 18$

10) $[(\eta^5\text{-}C_5H_5)(\eta^1\text{-}C_5H_5)Ru(CO)_2]$ — $5(\eta^5\text{-}C_5H_5) + 1(\eta^1\text{-}C_5H_5) + 8(Ru) + 2(CO) \times 2 = 18$

11) $[Ni(Ph)_2(PPh_3)_2]$ — $10(Ni) + 1(Ph) \times 2 + 2(PPh_3) \times 2 = 16$

12) $[CpOs(\eta^3\text{-}C_3H_5)(CO)]$ — $5(Cp) + 8(Os) + 3(\eta^3\text{-}C_3H_5) + 2(CO) = 18$

13) $[Cp_2Mo(C_2H_2)]$ — $5(Cp) \times 2 + 6(Mo) + 2(C_2H_2) = 18$

(In this case, the 18-electron rule takes precedence and C_2H_2 acts as a 2e donor ligand.)

14) $[Pd(PEt_3)_2(OMe)_2]$ $10(Pd) + 2(PEt_3) \times 2 + 1(OMe) \times 2 = 16$

15) $[(\eta^3\text{-}C_3H_5)Pd(\mu\text{-}Cl)_2Pd(\eta^3\text{-}C_3H_5)]$ $3(\eta^3\text{-}C_3H_5) + 10(Pd) + 1(\text{one of } (\mu\text{-}Cl)_2)$
     $+ 2(\text{the other } \mu\text{-}Cl) = 16$

16) $[Mn(CO)_5\{C(O)Me\}]$ $7(Mn) + 2(CO) \times 5 + 1(C(O)Me) = 18$

Answers to Problem 2 (See Section 2.4.4)

 1) Since Ni has ten d electrons, coordination of four CO ligands to Ni forms an 18e complex, $[Ni(CO)_4]$.

 2) Since Co has nine d electrons, coordination of one 5e donor Cp and two 2e donor CO ligands forms an 18e complex $[CpCo(CO)_2]$.

 3) Since Mn has seven d electrons, the total valence electron number becomes odd even if some CO ligands coordinate to Mn, and it does not achieve 18e. There are three ways to solve this. The first way is to add one electron to the 17e complex $[Mn(CO)_5]$ to make an anionic complex $[Mn(CO)_5]^-$. The second way is to subtract one electron from the 19e complex $[Mn(CO)_6]$ to make a cationic complex $[Mn(CO)_6]^+$. The last way is to make an Mn–Mn bond between two $[Mn(CO)_5]$ species to give $(CO)_5Mn–Mn(CO)_5$. All of these Mn complexes consist of only Mn and CO, and have been reported.

 4) Since Fe has eight d electrons, coordination of two Cp ligands to Fe forms an 18e species (ferrocene). However, this complex has no CO ligand and thus does not fulfill the criteria. We will therefore make CO coordinate to CpFe, but since CpFe is a 13e species, an 18e species cannot be obtained by simple coordination of CO. When applying the same concept as in 3), 18e complexes such as $[CpFe(CO)_2]^-$, $[CpFe(CO)_3]^+$, and $[Cp(CO)_2Fe–Fe(CO)_2Cp]$ may be obtained. The last complex, however, actually contains two bridging CO ligands, $[Cp(CO)Fe(\mu\text{-}CO)_2Fe(CO)Cp]$ and has an Fe–Fe bond. A dinuclear iron complex having no bridging CO ligands, $[Cp(CO)_2Fe–Fe(CO)_2Cp]$ has been proposed as an intermediate. In any case, the intermediate and final Fe dinuclear complexes have an Fe–Fe single bond.

 5) Since Re has seven d electrons, if one 1e donor H ligand and five 2e donor CO ligands are coordinated to Re, an 18e complex, $[Re(H)(CO)_5]$, is formed. Similarly, $[Re(H)_3(CO)_4]$, $[Re(H)_5(CO)_3]$, $[Re(H)_7(CO)_2]$, and $[Re(H)_9(CO)]$ are also 18e complexes. However, since the coordination numbers of these complexes are 7, 8, 9, and 10, respectively, they become sterically crowded. Actually, these complexes have not been reported as isolable complexes.

Answers to Problem 3 (See Section 2.5.2)

 5) Fe(0).

 6) Fe(ii) (an H ligand increases the oxidation number by 1).

 7) Co(i) (two CN ligands increase the oxidation number by 2, but one minus charge decreases the oxidation number by 1. The final formal oxidation number is 1.)

 8) Pt(ii) (three Cl ligands increase the oxidation number by 3 in total, but one minus charge decreases the oxidation number by 1. The final formal oxidation number is 2).

 9) Fe(ii) (since there is one Cp ligand and one plus charge).

 10) Ru(ii) (both $\eta^5\text{-}C_5H_5$ and $\eta^1\text{-}C_5H_5$ increase the oxidation number by 1).

 11) Ni(ii) (due to the two Ph groups).

 12) Os(ii) (both Cp and $\eta^3\text{-}C_3H_5$ increase the oxidation number by 1).

13) Mo(ii) (acetylene, C_2H_2, does not change the oxidation number).

14) Pd(ii) (due to the two OMe groups).

15) Pd(ii) (this complex has two bridging Cl atoms. In other words, each Pd atom has two Cl atoms. Of the two Cl atoms, one increases the oxidation number by 1, and the other does not affect the oxidation number. This is because each μ-Cl is considered to be covalently bonded to one Pd and coordinatively bonded to the other Pd).

16) Mn(i) (an acetyl group increases the oxidation number by 1).

Answers to Problem 4 (See Section 2.5.3)

(5) d^8, (6) d^6, (7) d^8, (8) d^8, (9) d^6, (10) d^6, (11) d^8, (12) d^6, (13) d^4, (14) d^8, (15) d^8, (16) d^6

Answers to Problem 5 (See Section 2.6)

1) $2(\mu\text{-CO}) + \{4(\eta^4\text{-}C_4H_4) + 8(Fe) + 2(CO)\} \times 2 = 30$

$(36–30)/2 = 3$

This complex has a triple bond between the two Fe atoms and one bridging CO (Scheme 13.1).

2) $2(\mu\text{-CMe}_2) + \{5(Cp^*) + 9(Rh) + 2(CO)\} \times 2 = 34$

$(36–34)/2 = 1$

The complex has a single bond between the two Rh atoms and one CMe_2 bridging ligand between them (Scheme 13.2).

3) $2(\mu\text{-CO}) + 2(\mu\text{-CMe}_2) + \{5(Cp^*) + 9(Rh)\} \times 2 = 32$

$(36–32)/2 = 2$

The complex has a double bond between the two Rh atoms, one bridging CO and one bridging CMe_2 (Scheme 13.3).

4) $3(\mu\text{-Br}) \times 2 + \{7(Mn) + 2(CO) \times 4\} \times 2 = 36$

$(36–36)/2 = 0$

Since the bridging Br ligand acts as a 1e donor ligand to one metal and as a 2e donor ligand to the other metal, each μ-Br is considered to be a 3e donor ligand (Scheme 13.4).

5) $3(\mu\text{-Cl}) + 2(\mu\text{-CH}_2) + 8(Os) \times 3 + 2(CO) \times 10 + 1(\text{minus charge}) = 50$
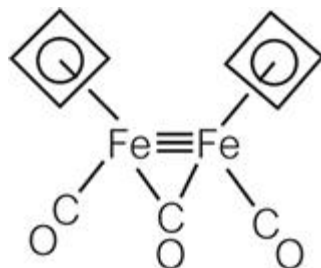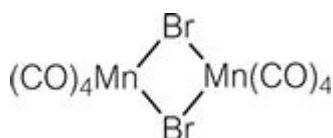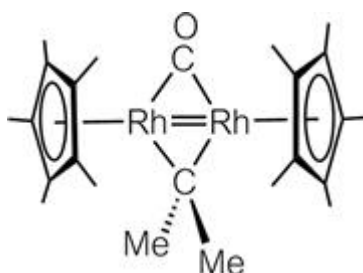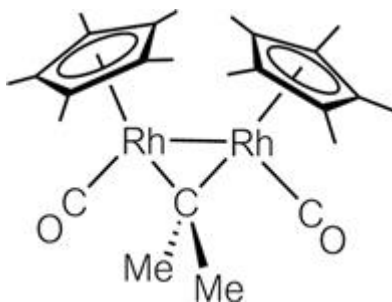
$(54\text{–}50)/2 = 2$

From the above calculation, this complex is estimated to have either two Os–Os single bonds or one Os–Os double bond. There are several possible structures, which are shown below. It is impossible to predict which is the actual structure using only the information given (Scheme 13.5).
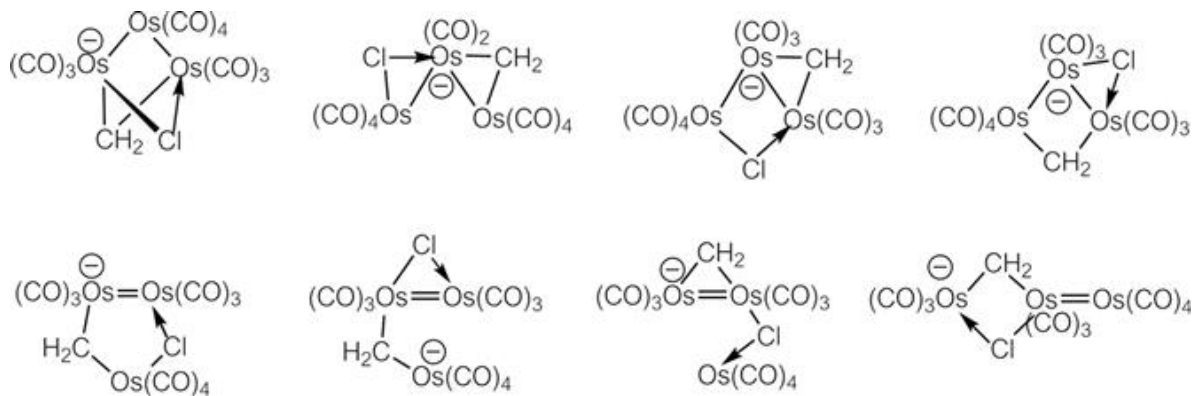
Answers to Problem 6 (See Section 3.4)

The reason why a 4-coordinate compound takes a sterically disadvantageous square planar structure is in the d orbital splitting. BF_4^- is a 4-coordinate compound but does not contain a transition metal. d orbitals are thus not involved in the compound, so it takes a tetrahedral structure. For the same reason, $BeCl_4^{2-}$, AlF_4^-, $ZnCl_4^{2-}$ and $SnCl_4$ also adopt tetrahedral structures.

Among transition metal complexes in which d orbitals are involved, only those with d^8 configurations adopt square planar structures; all the others are tetrahedral. Thus, since $[FeCl_4]^-$ is a d^5 complex, it takes a tetrahedral structure. For the same reason, $[Ni(CO)_4]$ (d^{10}) and $[CoCl_4]^{2-}$ (d^7) also adopt tetrahedral structures. Four coordinate d^8 complexes adopt square planar structures for electronic reasons, but the structure is sterically more crowded than a tetrahedral structure. Thus, when the ligands are sterically bulky or the central metal is small, square planar structures become more unlikely for steric reasons, and tetrahedral structures result. $[PdCl_4]^{2-}$ is a 4-coordinate square planar d^8 complex. $[NiBr_4]^{2-}$ contains the same number of atoms, with elements in the same groups, but the central metal is smaller and the ligands are larger compared to $[PdCl_4]^{2-}$ and a tetrahedral structure results. Similarly for the 4-coordinate d^8 complex $[CoBr(PPh_3)_3]$: the large ligands predicate a tetrahedral geometry.

Answers to Problem 7 (See Section 4.2)

1) Both are d^6 complexes of the type $[M(CO)_5Cl]$, so they are comparable complexes. The answer is $[W(CO)_5Cl]^-$, because $[W(CO)_5Cl]^-$ is anionic while $[Re(CO)_5Cl]$ is neutral.

2) Both are neutral Fe complexes, so they are comparable.
The answer is $[Fe(CO)_5]$, because $[Fe(CO)_5]$ is a d^8 complex but $[Fe(CO)_4Br_2]$ is d^6.

3) Both are neutral d^6 complexes, so they are comparable.
The answer is $[Mo(CO)_4(PPh_3)_2]$, because PPh_3 is a stronger electron donor than CO.

4) Both are neutral d^6 complexes of $[Mo(CO)_4L_2]$ type, so they are comparable.
The answer is $[Mo(CO)_4(PMe_3)_2]$. Comparing the electron-donating ability of PMe_3 and PPh_3, Me is more electron-donating than Ph, so the PMe_3 ligand is considered to be the stronger electron-donor.

5) Both are Fe complexes bearing Cp and CO ligands, so they are comparable.

The answer is $[CpFe(CO)_2]^-$. $[CpFe(CO)_2]^-$ has a negative charge whereas $[CpFe(CO)_2Br]$ is neutral. The charge on the complex ion has a great effect.

Answers to Problem 8 (See Section 4.4)

This problem asked about the trend of equilibrium constants, but many readers will probably be at a loss as to how to answer. When actually conducting research, such problems are normal. In other words, compounds are synthesized, various data are measured and collected, and it is necessary to think about the results oneself. This series of flows is all about research.

Let us return to the problem. The K_d values vary greatly depending on the complex. In order to understand the difference, v_{CO} and θ are helpful but the question is how to utilize these data. Since this reaction concerns CO dissociation from the metal center, it is necessary to consider to what extent the Co–CO bond breaking is due to electronic factors and to what extent the CO ligand is likely to be ejected for steric reasons.

In fact this way of categorizing reaction-controlling factors simply into two factors, electronic and steric, is quite general in chemistry. Considered like this, chemistry may seem simple, but these two factors work differently, and chemistry is indeed not so simple!

Considering in greater depth the steric factor, the intrigue of chemistry can be seen. The steric factor in reactions concerns the shapes of molecules and their relative orientations during approach. Indeed the first question is whether one molecule can approach the reaction active site of the other molecule, considering the steric requirements of both species. The point to note here is that there is no linear relationship between steric bulk and accessibility. The above phrase, "no linear relationship", will be explained by discussing a macroscopic world example.

Consider a room with one entrance through which a person must pass in order to enter the room. There is actually no linear relationship between the weight and the size of a person, but here a linear relationship is assumed. Entering scenarios are as follows: a child and even a 60 kg adult can pass through without problem; an 80 kg adult can enter if that person pulls their stomach in; for a 100 kg adult it is very difficult to enter; and for a *sumo* wrestler it is impossible. From the viewpoint of whether it is possible to enter the room or not, the 5 kg difference between an 80 kg person and an 85 kg person is much more important than the 20 kg difference between a 30 kg child and a 50 kg person, or the 20 kg difference between a 140 kg

sumo wrestler and a 160 kg *sumo* wrestler (for both of whom it is impossible to enter). In other words, a little difference in a certain range can be critical, whereas in other ranges, even a large difference has little or no effect. This is the characteristic of the steric factor. Even in the meter-scale world we see every day and in the world of nanometer and picometer molecules, the situation is quite similar. When molecules are designed by chemists for a particular function, it is thus vital to know where this important range is, and to investigate steric factors in detail in this range, but no useful information will be obtained if steric factors are investigated, even in detail, in other ranges. If this is understood, readers will be more likely to achieve good rewards for their efforts.

Now, back to the subject. In order to understand a chemical reaction by separating the electronic and steric factors, it is necessary to compare systems while varying only one factor. For the dissociation equilibrium reaction of CO in question, complexes with the same steric factor are those bearing phosphines with the same cone angle, θ, that is the systems in runs 2 and 3. $P(n\text{-Bu})_3$ and PEt_2Ph have the same steric bulk, but different basicity (electronic factor). A comparison of these two systems shows that K_d for the PEt_2Ph complex is about twice that of the $P(n\text{-Bu})_3$ complex. Since the v_{CO} value in the IR spectrum of the PEt_2Ph complex is larger than that of the $P(n\text{-Bu})_3$ complex, it is expected that CO binds to Co more weakly in the PEt_2Ph complex than in the $P(n\text{-Bu})_3$ complex. This is interpreted to mean that CO in the PEt_2Ph complex dissociates more readily and shows a larger K_d.

Next, steric factors are compared. Runs 3 and 4 show the same v_{CO} values and are thus considered to have the same electronic factors. It can therefore be said that the degree of π-back donation from Co to CO is the same in both the PEt_2Ph and $PEtPh_2$ complexes. However, θ is 5° greater for $PEtPh_2$ than for PEt_2Ph. The bulkier phosphine causes a more sterically crowded Co coordination sphere, which is considered to result in more facile dissociation of CO. The difference in steric crowding corresponding to the cone angle difference of only 5° increases K_d by a factor of 10. *Steric effects are intense!*

Comparing runs 1 and 2, the CO in the $P(n\text{-Bu})_3$ complex is considered less likely to dissociate for electronic reasons because the $P(n\text{-Bu})_3$ complex

has a lower ν_{CO} value. However, comparing the θ values of these two complexes, that for P(n-Bu)$_3$ is 3° greater than that for PEt$_3$. Thus, on the basis of steric considerations, the CO in the P(n-Bu)$_3$ complex is the more likely to dissociate. The experimental result that the two K_d are almost the same thus indicates that these two opposing effects more or less cancel each other out. Considering runs 4 and 5, the approximately 30 times larger K_d value indicates a synergistic effect resulting from cooperative electronic and steric effects. Even from this table alone, with careful consideration, a considerable amount of useful information can be derived.

Answers to Problem 9 (See Section 5.2)

The complexes in (1) and (2) differ only in the central metal. In the same group in the periodic table, the lower metal forms a more stable complex, so in this case also the complex in (2) has a stronger binding of the methylidene ligand and therefore the rotation barrier also increases.

The difference between complexes in (2) and (3) is the phosphine ligand. Since PEt$_3$ is more strongly electron-donating than PPh$_3$, the metal in the complex in (3) π back-donates more strongly to the methylidene ligand, resulting in a greater rotation barrier.

Answers to Problem 10 (See Section 5.3) (Scheme 13.6)

1) Typical Fischer carbene complex synthesis method (see eqn (5.1)).
2) This is a reaction in which the –OR group on the carbon is abstracted as an anion by a Lewis acid to give a cationic carbene complex.
3) The formal oxidation number of Nb in the starting complex is +5. Thus, the acidity of the hydrogen on the α carbon is high, resulting in its abstraction as a proton by a Lewis base to form the carbene complex.
4) Nucleophilic attack of HSMe on the carbene carbon of the Fischer carbene complex takes place and a substituent exchange reaction eventually takes place (see Figure 5.9).
5) The betaine complex from the Fischer carbene complex and phosphine is in equilibrium with the carbene complex and free phosphine. The reaction of a betaine complex with more basic PMe$_3$ shifts the equilibrium towards a more stable betaine complex.

1)

$(CO)_5W=C\begin{smallmatrix} Ph \\ OEt \end{smallmatrix}$

2)

$\left[Cp(CO)_2Fe=C\begin{smallmatrix} H \\ Ph \end{smallmatrix} \right]^+$

3)

$Cp_2(CH_2SiMe_3)Nb=C(H)(SiMe_3)$

4)

$(CO)_5Cr=C\begin{smallmatrix} Ph \\ SMe \end{smallmatrix}$

5)

$(CO)_4\overset{\ominus}{Fe}-\underset{Ph}{\overset{H}{C}}-\overset{\oplus}{PMe_3}$
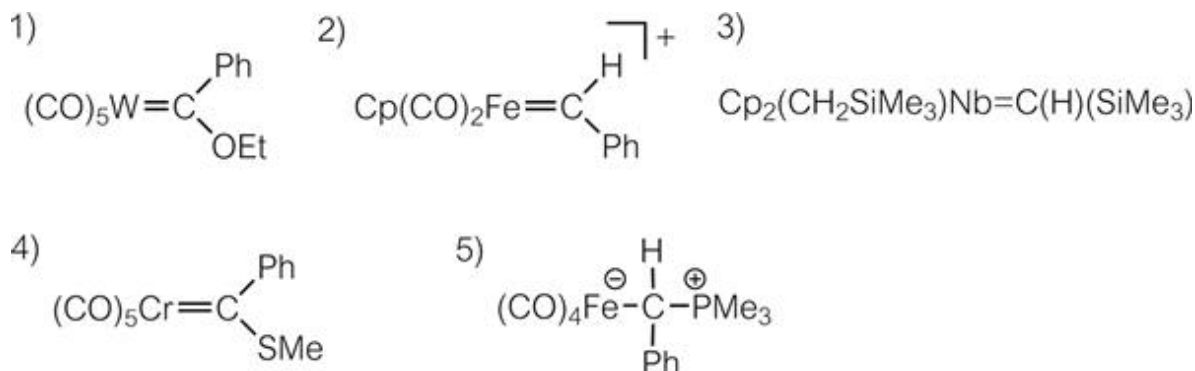
Answers to Problem 11 (See Section 6.2.4)

1) [Ir($dppe$)$_2$]$^+$: all are equal except for the central metal. In such cases, the lower the metal in the periodic table, the more stable the complex formed.

2) [RhCl(PPh$_3$)$_3$]: because PPh$_3$ is more strongly electron-donating than CO.

3) [IrCl(CO)(PPh$_3$)$_2$]: all are equal except for the central metal. In such cases, the lower the metal in the periodic table, the more stable the complex formed.

4) [IrBr(CO)(PPh$_3$)$_2$]: the only difference is the halogen. The electron-withdrawing ability of Br is weaker than that of Cl.

5) [Rh($dmpe$)$_2$]$^+$: because $dmpe$ is more strongly electron-donating than $dppe$.

6) [IrCl(CO)(PPh$_3$)$_2$]: the total charges are different (neutral and cationic) and the oxidation states are different: Ir(i) and Pt(ii).

7) [Os(CO)$_5$]: The answer that the oxidative addition of H$_2$ to *trans*-[Os(PPh$_3$)$_2$(CO)$_3$] is more likely to occur because PPh$_3$ is more strongly electron-donating than CO is incorrect. Here, it is necessary to remember what is important for oxidative addition to occur. Oxidative addition to an 18e complex would result in the formation of a 20e complex. Therefore, no such reaction occurs. Since all starting complexes from (1) to (6) are 16e complexes, H$_2$ is able to oxidatively add directly to them. In contrast, since both starting complexes in (7) are 18e complexes, H$_2$ cannot oxidatively add directly. In order for the oxidative addition of H$_2$ to occur, a 16e complex must first be formed, by dissociation of the CO ligand. Since the conversion of the 18e complex into the 16e complex is more difficult than the reverse reaction, the former reaction is the rate determining step. Since π back donation from the central metal to the carbonyl ligands in *trans*-[Os(PPh$_3$)$_2$(CO)$_3$] is greater than in [Os(CO)$_5$], a carbonyl in the former complex is less likely to be eliminated. Therefore, [Os(CO)$_5$], which is more likely to release the CO ligand than *trans*-[Os(PPh$_3$)$_2$(CO)$_3$], undergoes oxidative addition of H$_2$ more easily.

Answers to Problem 12 (See Section 6.3.4)

1) All reactions are reductive eliminations. (a) is a coupling reaction between sp^3 and sp^2 carbon atoms. (b) is a coupling reaction between sp^3 carbon atoms. Hybridized orbitals with greater p character (*i.e.* sp^3) have higher directionality. Since the coupling in (b) requires a

large amount of energy to change the orbital geometry, reductive elimination is unlikely to occur.

2) Since (c) is a coupling reaction between sp^2 carbons and (d) is a coupling between sp^3 carbons, reductive elimination is more likely to occur in the former. When (b) and (d) are compared, both metals are in Group 10 in the periodic table, but one is a first row transition metal and the other is in the third row. The lower the metal in the periodic table, the more stable the complex. The dimethyl complex of Pt does not undergo reductive elimination, even when heated.

Answers to Problem 13 (See Section 6.3.4) (Scheme 13.7)

1) Since the starting complex is an 18e complex, it does not react directly with CF_3CF_2I. If a reaction takes place, one CO in the starting complex dissociates first to form the 16e [CpRh(CO)] species, which then reacts with CF_3CF_2I. There are three possible bonds which could undergo oxidative addition: C–F, C–I or C–C bonds. The weakest bond is C–I, and it is this which undergoes oxidative addition to the metal.

2) This is an example of an orthometallation reaction. See Section 6.2.3.

3) The starting complex has low reactivity because it is an 18e complex. However, on photoirradiation, one CO ligand dissociates to form the 16e [Cp*Ir(CO)]. Since this complex is highly reactive, the C–H bond of the solvent neopentane oxidatively adds to form a stable 18e complex.

4) Methane is reductively eliminated from the starting complex to form a 16e species [Cp$_2$W]. A reaction is also conceivable in which the C–H bond of methane adds oxidatively to the metal to return to the starting complex, but the solvent benzene molecules are overwhelmingly numerous, and oxidative addition of a benzene C–H bond is thermodynamically favored over that of methane, forming an 18e complex.

5) Since the starting complex is a 16e species, the C–I bond adds oxidatively to the complex. *Trans* addition takes place because of the large polarization of the C–I bond.

6) Since the starting complex is a 16e species, the Si–H bond adds oxidatively to the complex. It is known that the Si–H bond shows reactivity similar to H–H. The *cis* addition product is obtained.

7) First, one CO ligand dissociates to form the 16e complex [CpRe(CO)$_2$]. Then, Br$_2$ adds oxidatively to form the *cis* complex.

8) A hydrogen molecule is reductively eliminated to form the reactive 16e complex [Cp*Ir(PMe$_3$)], which undergoes oxidative addition by a C–H bond of the solvent. Three types of complexes are formed because *n*-pentane has three kinds of C–H bond. The complex formed by the oxidative addition of the C–H bond at the 2-position forms two diastereomers since Ir and the coordinated carbon are asymmetric centers. Four kinds of complexes are formed in total.

1)

Rh
OC
I
CF₂CF₃

2)

Cl
Ph₃P
Ir
PPh₃
H
PPh₂

3)

Ir
OC
H
CH₂CMe₃

4)

W
H
Ph

5)

CF₃
Ph₂MeP
Ir
CO
Cl
PPh₂Me
I

6)

H
Ph₂
P
Ir
CO
P
SiEt₃
Ph₂
Br

7)

Re
OC
CO
Br
Br

8)

Me₃P
Ir
H

Me₃P
Ir
H

Me₃P
Ir
H

Me₃P
Ir
H
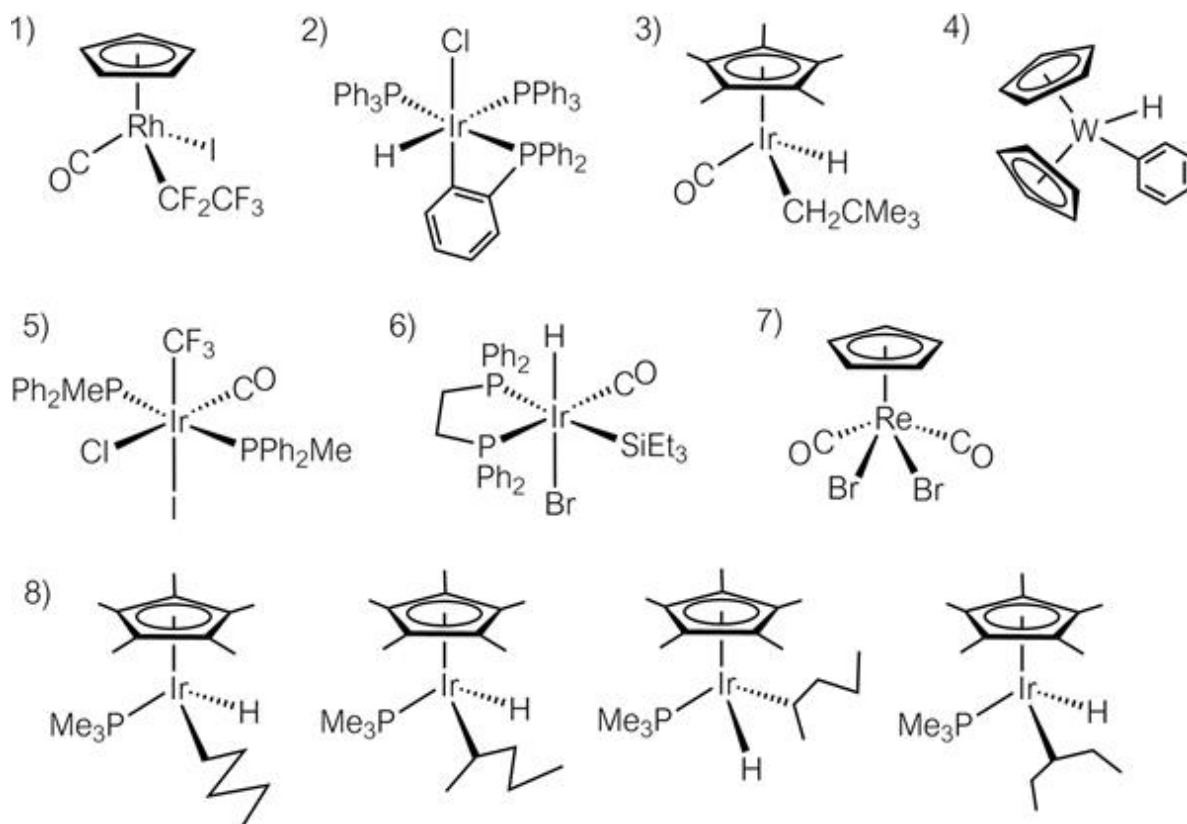
Answers to Problem 14 (See Section 6.3.4) (Scheme 13.8)
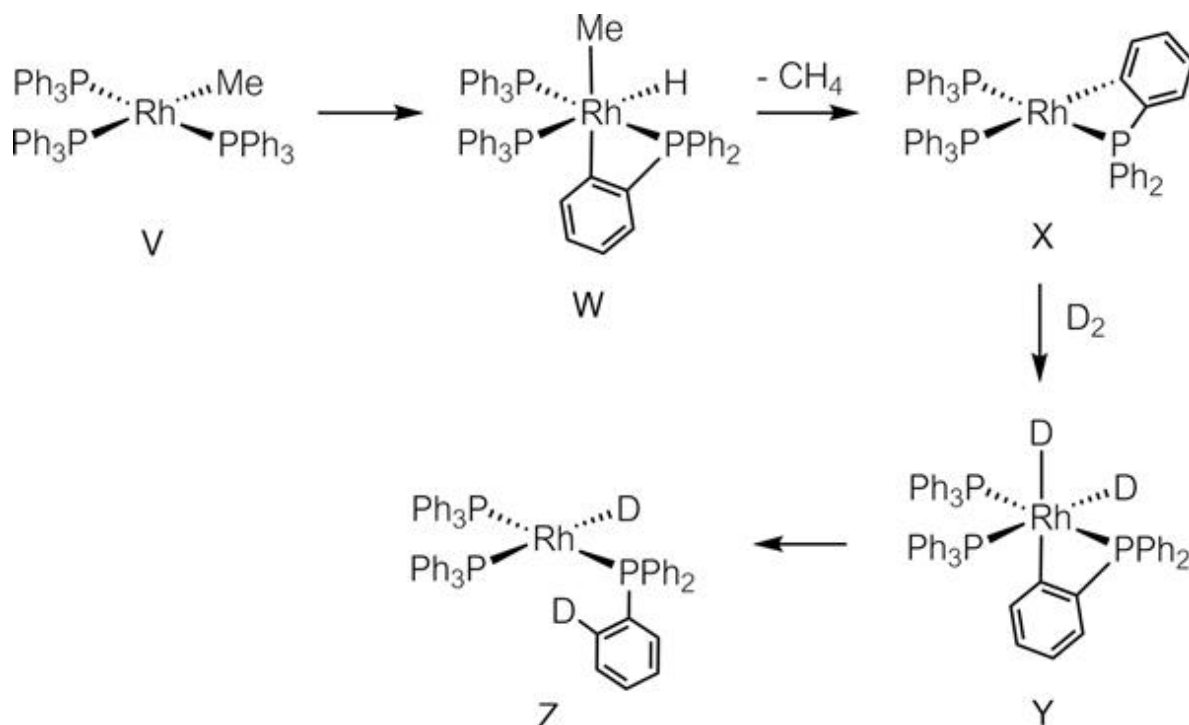
This problem requires deduction of the reaction mechanism by considering the product. Since the starting complex **V** is a 16e complex, it is conceivable that D_2 adds oxidatively to **V** forming $[Rh(PPh_3)_3(Me)(D)_2]$. Consequent reductive elimination of Me and D would result in the evolution of CH_3D. However, since the actual product is CH_4, it can be inferred that a different pathway is taken.

A closer look at the resulting complex, **Z**, shows that D is introduced into a phenyl group of a triphenylphosphine ligand. It is thus expected that an orthometallation reaction takes place, producing complex **W** from **V**, from which CH_4 is reductively eliminated to produce **X**. Since **X** is a 16e species, D_2 can add oxidatively to form **Y**, from which reductive elimination of the phenyl part and D affords the final product **Z**. In sequential order: orthometallation → reductive elimination → oxidative addition of D_2 → reductive elimination.

Answers to Problem 15 (See Section 6.4.1)
All are reactions inserting CO between M and R.

    1) M = Cr: down a group of the periodic table, M–C bonds become stronger, so the Cr–C bond is the weakest. CO insertion is thus most likely to occur for the Cr complex.

2) R = CH₃: since an alkyl group with an electron-donating substituent has a weak M–C bond, CO insertion reactions for such complexes are more likely.

3) In THF: a complex with methyl and carbonyl ligands is in equilibrium with the acetyl complex (the product of the CO insertion reaction). Since this acetyl complex is a 16e complex, the equilibrium is shifted toward the left (18e complex). Coordination of PPh_3 to the 16e complex forms a stable product. Since THF is more Lewis basic than benzene, THF stabilizes the 16e complex by coordination, assisting formation of the final product, $[CpFe\{C(O)Me\}(CO)(PPh_3)]$.

4) R = Et: Et is more strongly electron-donating than Ph.

5) In the presence of $AlBr_3$: the acetyl complex formed after CO insertion is less stable since it is a 16e complex. However, in the presence of $AlBr_3$, the electron-deficient Al site is coordinated by a lone pair of electrons of the acetyl ligand carbonyl oxygen and simultaneously a lone pair of electrons on Br coordinates to the 16e Mn center as shown below, giving an 18e count for the intermediate chelate complex (see structure below). The chelate effect further stabilizes the acetyl complex. CO coordination to the Mn intermediate thus formed and simultaneous dissociation of $AlBr_3$ produce the final product, $[(CO)_5Mn\{C(O)Me\}]$. $AlBr_3$ thus acts as a catalyst (Scheme 13.9).
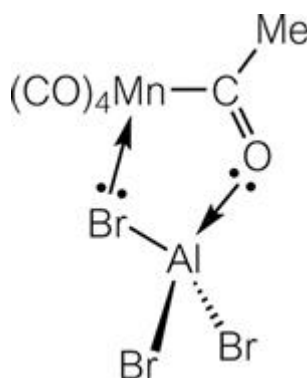
Answers to Problem 16 (See Section 6.4.2)

1) $[Cp_2Mo(Et)(PPh_3)]^+$: Olefin insertion into the Mo–H bond forms the Et complex. Since the latter is a 16e species, the reverse reaction, β hydride elimination, also occurs to reform the starting complex. However, in the presence of PPh_3, the 16e complex is coordinated by PPh_3, forming the stable 18e complex.

2) $[Pt(Et)(OCMe_3)(PEt_3)_2]$: since the starting complex is a 16e complex, ethylene attacks Pt directly, thus inserting into the Pt–H bond to give the ethyl complex.

Answers to Problem 17 (See Section 6.4.3)

Since the metallacycle complex also has a β hydrogen, β hydride elimination followed by reductive elimination of the hydride and alkyl group occurs to give 1-butene. However, it is difficult for the β hydrogen of the metallacycle to approach Pt, and for M–C–C–H to be planar. Therefore,

the β hydride elimination reaction is disfavored, resulting in a slow reaction (Scheme 13.10).
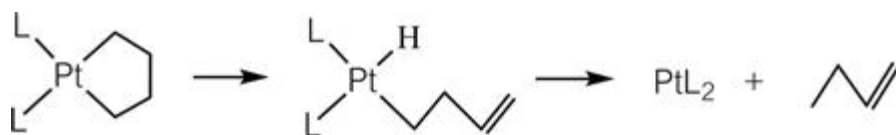
Answers to Problem 18 (See Section 6.4.3)

In the reaction of **6-4** with AgBF$_4$, the Cl on the Pt is abstracted as Cl$^-$ after which π-coordination of the olefin to the empty coordination site occurs to give complex **6-5**. Heating of **6-5** produces **6-6**, in which CH$_2$ and CD$_2$ in the ligand are exchanged. It looks like a very strange reaction, but it can be rationally explained if it is considered as follows.

The carbon atoms in **6-5** will be numbered and the hydrogens on C^1 will be shown for clarity. Complex **6-5** bears an alkyl ligand and a π coordinated olefin, although these two ligands (C^1 and C^4) are connected by a C^2–C^3 portion. Therefore, C^4=C^5 olefin insertion into the Pt–C^1 bond (or to express it another way, addition of Pt–C^1 across the C^4=C^5 double bond) is expected. Although there are two possible modes of addition, the addition where Pt bonds to C^5 and C^1 bonds with C^4 is sterically more reasonable. Complex **A** is formed in this way, but since this complex is a 14e species, it is unstable and there is pressure to become a 16e species. This may be achieved either by β elimination of either hydride or alkyl, since the β carbon (C^4) has both hydrogen and alkyl groups. Usually, β hydride elimination is more likely, but the complex (**B**) formed thereby is not actually observed. Even if **B** is generated temporarily, the olefin may immediately insert into the Pt–H bond, regenerating **A**. If C^1 in **A** migrates to the central metal (β alkyl elimination reaction), **6-5** is formed, and it appears that nothing happens. Since the C^4–C^5 bond in **A** is a single bond, the rotational barrier is very low, and it can easily take the rotameric conformation **A'**. Now when C^3 in **A'** undergoes a β alkyl elimination reaction, **6-6** is formed. In **A** (and equally in **A'**), since C^1 and C^3 are equivalent, it is quite reasonable that **6-5** and **6-6** have a 1 : 1 production ratio. In other words, this seemingly strange reaction consists of a

combination of basic reactions of olefin insertion into a M–C bond and a β alkyl elimination reaction (Scheme 13.11).

6-4   6-5   6-6

B   A   A'
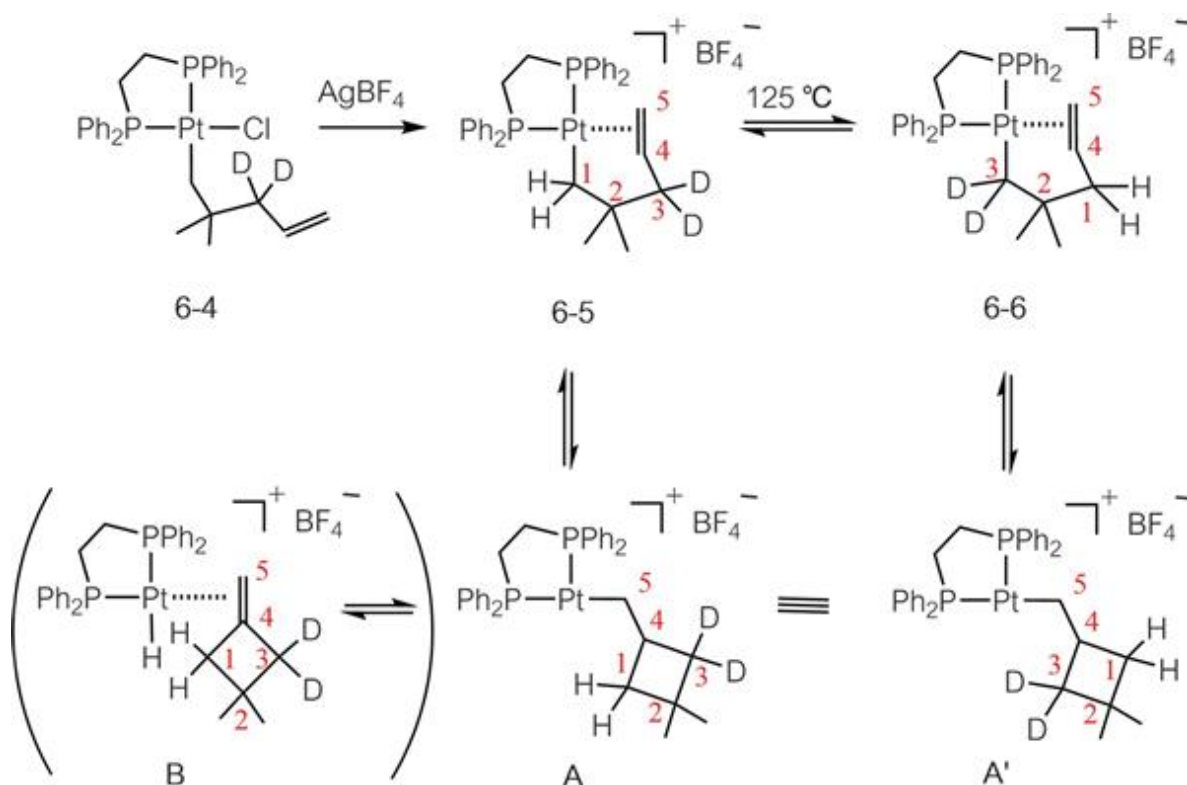
Answers to Problem 19 (See Section 6.4.3)

Consider the reaction pathway for the *trans* complex with reference to the hints (Scheme 13.12).

A   B
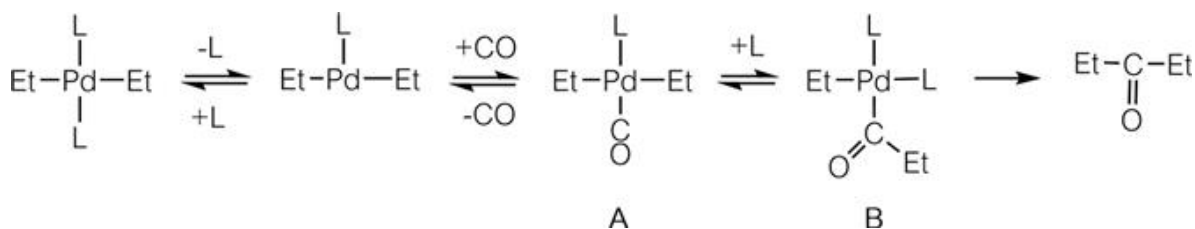
L dissociates from the starting *trans* complex, and CO coordinates to the vacant coordination site. Since the steric environment around the Pd is kept during the reaction, **A** adopts a *trans* structure. Since **A** has both alkyl and carbonyl ligands, an alkyl migration reaction can occur, affording the CO insertion product (the ethyl group migrates to the CO position) containing

an acyl ligand, with a ligand L taking its place to form the 16e complex, **B**. Since the Et and acyl groups are situated *cis* to each other in **B**, reductive elimination occurs to generate diethylketone.

Consider now starting from the *cis* complex: (Scheme 13.13).
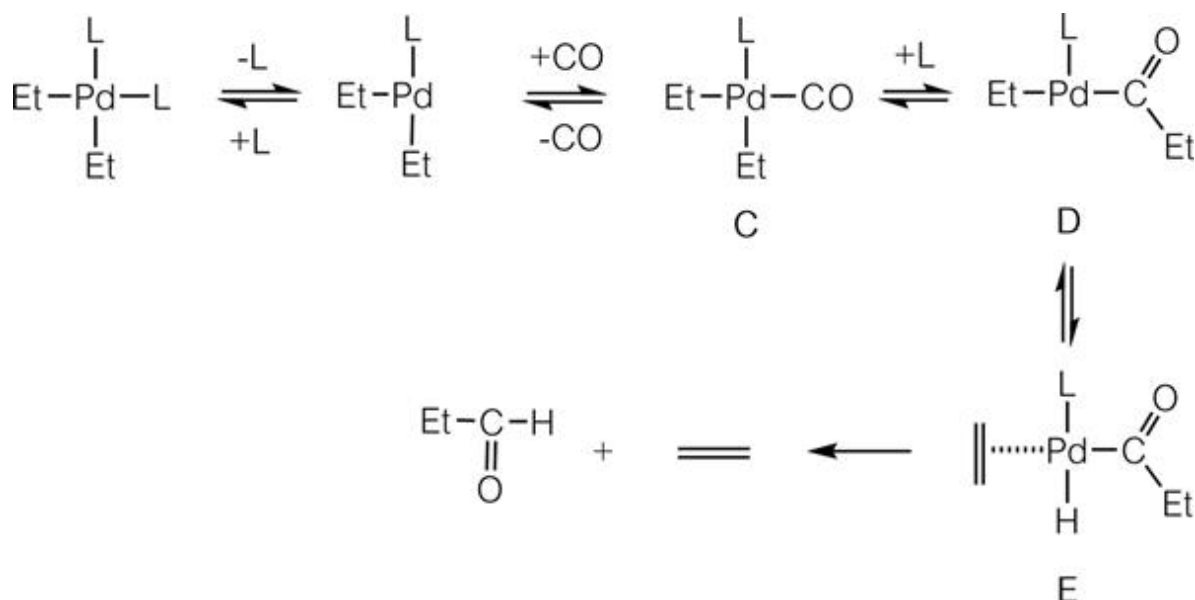
Dissociation of L and coordination of CO forms **C**. Subsequent alkyl migration (CO insertion) results in the formation of **D**. Since the Et and the acyl ligands are situated *trans* to each other in **D**, reductive elimination does not occur. Complex **D** is unstable since it is a 14e complex, and thus the β hydride in the ethyl ligand transfers to the metal to form the relatively stable complex **E**. Since the hydride and the acyl ligands are *cis* to each other in **E**, reductive elimination occurs to form the aldehyde.

Answers to Problem 20 (See Section 6.4.3)

1) First of all, the total valence electron number of the starting complex should be checked. Since this complex is an 18e species, coordination of CO to this complex does not occur. Instead, there is a possibility that reductive elimination between the two methyl groups may occur. However, since ethane is not generated in this reaction, such a reductive elimination may be excluded. Another possibility is the dissociation of PPh_3 followed by coordination of CO. Since **A** formed in this reaction has both alkyl and carbonyl ligands, CO insertion may then occur, followed by coordination of CO to the vacant site to give **B**. Subsequently, reductive elimination of acyl and methyl groups and coordination of CO may occur to form a ketone and the final cobalt complex (Scheme 13.14).

2) Considering similarly to the above, dissociation of PPh_3 and coordination of ethylene take place first to form **C**. Since this complex has both alkyl and olefin ligands, ethylene insertion

takes place to form **D**. Reductive elimination between methyl and butyl ligands is one of the possibilities for the next step, but butane is not formed in this reaction. Instead, β hydride elimination occurs from **D**, forming **E**. Substitution of propylene by ethylene forms **F**, from which reductive elimination of methane accompanied by coordination of PPh₃ forms the final cobalt complex (Scheme 13.15).

Appendix

Period / Group	1	2	3	4	5	6	7	8	9	10	11	12	13	14	15	16	17	18
																		Periodic Table with Allred-Rochow Electronegativity Values
1	H 2.20																	He 5.50
2	Li 0.97	Be 1.47											B 2.01	C 2.50	N 3.07	O 3.50	F 4.10	Ne 4.84
3	Na 1.01	Mg 1.23											Al 1.47	Si 1.74	P 2.06	S 2.44	Cl 2.83	Ar 3.20
4	K 0.91	Ca 1.04	Sc 1.20	Ti 1.32	V 1.45	Cr 1.56	Mn 1.60	Fe 1.64	Co 1.70	Ni 1.75	Cu 1.75	Zn 1.66	Ga 1.82	Ge 2.02	As 2.20	Se 2.48	Br 2.74	Kr 2.94
5	Rb 0.89	Sr 0.99	Y 1.11	Zr 1.22	Nb 1.23	Mo 1.30	Tc 1.36	Ru 1.42	Rh 1.45	Pd 1.35	Ag 1.42	Cd 1.46	In 1.49	Sn 1.72	Sb 1.82	Te 2.01	I 2.21	Xe 2.40
6	Cs 0.86	Ba 0.97	La 1.08	Hf 1.23	Ta 1.33	W 1.40	Re 1.46	Os 1.52	Ir 1.55	Pt 1.44	Au 1.42	Hg 1.44	Tl 1.44	Pb 1.55	Bi 1.67	Po 1.76	At 1.90	Rn 2.06
7	Fr 0.86	Ra 0.97	Ac 1.00															

Subject Index